



SCUOLA DI DOTTORATO  
UNIVERSITÀ DEGLI STUDI DI MILANO-BICOCCA

Department of

**Department of Biotechnology and Bioscience**

PhD program in Chemical, Geological and Environmental Sciences

Cycle XXXIII

Curriculum Chemical Sciences

# **Rational drug design and synthesis of new steroid derivatives for the treatment of chronic heart failure**

Surname Luraghi Name Andrea

Registration number 835523

Supervisor: Prof. Francesco Peri

Tutor: Prof. Marco Orlandi

Coordinator: Prof.ssa Maria Luce Frezzotti

**ACADEMIC YEAR 2019/2020**



# TABLE OF CONTENTS

<b>Abstract</b> .....	<b>III</b>
<b>Acronyms</b> .....	<b>VI</b>
<b>1. Introduction</b> .....	<b>1</b>
1. Circulatory system and the Heart .....	2
2. The heart cycle .....	5
3. The heart electrophysiology .....	7
4. The Na/K-ATPase .....	9
5. The Na/Ca-exchanger .....	11
6. transmembrane cation channel .....	13
7. Sarco-Endoplasmic Reticulum Calcium ATPase (SERCA2a) and the sarcoplasmic reticulum .....	16
8. The action potential .....	20
9. The diseases correlated to circulatory system .....	22
10. Heart failure diseases .....	26
11. Therapy for heart failure diseases .....	28
12. Inotropic agents .....	34
13. Cardiac glycosides .....	35
14. Istaroxime .....	42
15. Electrospun nanofibers for the delivery of cardiac drugs .....	44
16. Electrospinning .....	46
17. Fiber features .....	47
18. Drug loading in the fiber .....	50
19. Electrospun nanofibers for cardiovascular tissue engeneering .....	52
<b>2. Aim of the work</b> .....	<b>54</b>
<b>3. Results and discussion</b> .....	<b>59</b>
1. Design of non-toxic istaroxime analogues .....	61
2. PST3093 derivatives: pure SERCA-2a stimulators .....	64
3. Istaroxime amine derivatives with double targeting. ....	76
4. Towards drug delivery systems based on electrospun nanofibers .....	81

<b>4. Conclusions .....</b>	<b>96</b>
<b>5. Experimental section .....</b>	<b>102</b>
1. General .....	103
2. Design of non-toxic istaroxime analogues.....	103
3. Section 2-Pure SERCA-2a stimulators.....	105
4. Section 3-double target molecules .....	114
5. Section 4-drug delivery platform .....	119
<b>6. Supporting informations.....</b>	<b>123</b>
<b>7. Bibliography.....</b>	<b>167</b>
<b>8. Patent application .....</b>	<b>181</b>

## Abstract

Despite the mortality of heart failure (HF) disease decreased in the last 20-30 years, it remains one of the major causes of death in the world. In the United States, one over four deaths can be attributed to heart failure. Also, due to the aging of the population and uncorrect lifestyle of people, admission in hospital for heart failure are constantly rising, making it one of the most concern in public health.

Patients affected by HF presents a pathophysiological state in which the heart is not capable of pumping the blood efficiently in the body due to a loss of contractility of the myocardium, leading to a chronic condition in which oxygen and nutritional need of the body are not satisfied. Fatigue, breathlessness, and peripheral edema are some of the symptoms of the disease.

Therapy is addressed at reducing symptoms to guarantee survival and better life conditions: vasodilator aims to reduce the vascular resistance and hence the afterload, diuretic and salt restriction aims reduce systemic congestion, but the most important therapy involves inotropic agents, such as digitalis glycosides, efficient in improving the cardiac output.

The first and most known digitalis glycoside is Digoxin extracted from *Digitalis purpurea*. Such compounds act as inhibitors of the  $\text{Na}^+/\text{K}^+$  pump, an active membrane transporter capable of expelling  $\text{Na}^+$  from the cardiac cells introducing  $\text{K}^+$  against the natural gradient. The inhibition causes an accumulation of  $\text{Na}^+$  inside the cell. Sodium is so used from the  $\text{Na}^+/\text{Ca}^{++}$  pump to introduce  $\text{Ca}^{++}$  inside the cell. The high concentrations of  $\text{Ca}^{++}$  accumulated inside cardiac cells induce contraction of the myocardium.

However, despite the improvement of the patient conditions and a lowering hospitalization, digitalis glycosides are not efficient in lowering the mortality of the disease. Also, digitalis compounds have a low therapeutic index, in other words, they present a small gap between the active concentration and the toxic one. In fact, if more than 30% of the pumps are blocked the membrane potential became critically low, leading to spontaneous activity. In addition, the over intracellular accumulation for long periods of  $\text{Ca}^{++}$  leads to arrhythmic situations.

To develop an active compound capable of exploiting the beneficial effect of digitalis drugs but with lower risks associated to the side effects, the research is focused on identifying a class of new

compounds able to exploit inotropic effect by inhibition of  $\text{Na}^+/\text{K}^+$  pump and a lusitropic effect by stimulation of SERCA-2a.

SERCA-2a is a membrane protein located in the sarcoplasmic reticulum within myocytes. The protein, formerly a  $\text{Ca}^{2+}$  ATPase, transfers  $\text{Ca}^{2+}$  from the cytosol of the cell to the lumen during muscle relaxation and releases the calcium during the contraction. SERCA is regulated by a small peptide called phospholamban that acts as an inhibitor.

At present it is known only one compound able to stimulate both inotropic and lusitropic effects, such molecule, called "Istaroxime", was formerly patented and developed by the Italian pharmaceutical company Sigma-Tau. Istaroxime is now under clinical development for the treatment of acute decompensated heart failure by the Taiwanese company CVie Therapeutics. Such compound is still under clinical trials.

Istaroxime shows strong inotropic and lusitropic effects. Detailed studies highlighted that a metabolite of Istaroxime, the so-called "PST3093", acts as a pure activator of SERCA-2a without any action on  $\text{Na}^+/\text{K}^+$  pump. PST3093 is the only example in the literature of a pure SERCA-2a activator, making an interesting case of study and a possible first in class drug.

Despite the promising activity and the unique characteristic of this compound, there is still the main issue due to the genotoxicity of the carboxyl-hydroxylamine formed after oxime degradation by metabolism.

Within this thesis the rational design of non-toxic compounds derived from Istaroxime is described, their synthesis and the development of a new drug delivery systems based on electrospun nanofibers. The work can be divided in three parts.

In the first part the work is focused on the development of hydrolytically stable derivatives of the molecule "PST3093", able to maintain the unique stimulatory effect over Serca-2a but, at the same time, substituting the non-metabolically stable and toxic oxime with a carbon-carbon bond. To achieve the final result, starting from 6-hydroxyandrostane-3-17-dione different approaches like cross metathesis reaction, different Wittig reaction or Horner-Emmons reaction contributed to the synthesis and identification of two new and non-toxic compounds that will be further developed as first-in-class drugs, able to efficiently stimulate the activity of Serca-2a with potential application as anti-arrhythmic drugs.

This section includes also the optimization of the synthetic routes and the scale-up necessary for the *in vivo* characterization of the two and most promising compounds synthesized.

The second section is focused on the creation of compounds with double targeting. Inspired from Istaroxime, we thus decided to develop new compounds able to act as  $\text{Na}^+/\text{K}^+$  inhibitors and Serca-2a stimulator. Here we first applied the knowledge of the optimized synthetic routes developed in the first section to obtain the analogue of Istaroxime, lacking the risks associated to the oxime group. Then, to avoid the rapid degradation by action of cytochrome of the primary amine into a carboxylic acid, we created a library of cyclic-secondary amines derivatives. Such compounds exhibited lower potency respect Istaroxime, but, on the other hand, the toxicity and liability correlated to the oxime group are absent, making a suitable alternative to the original compound.

The third section was developed in the MERLN institute of Maastricht University, under the supervision of Prof. L. Moroni. In this part of the work is described an alternative method to chemical synthesis, able to reduce the risks associated to Istaroxime, boosting its activity at the action site. In particular, were studied the methodologies and the release properties of a drug delivery system based on electrospun polymeric scaffolds. This section is focused on the preliminary development of the model scaffold, leading to the identification of the most promising system for future improvement. Still, the obtained results indicate this approach as a promising alternative for the reduction of drawbacks associated to the continuous intravenous infusion of Istaroxime, and its high first-pass metabolism. Remarkably, for additional future development, this platform could be used as a powerful tool for boosting the activity of the new chemically synthesized derivatives.

## Acronyms

HF - Heart failure  
CHF - Congestive heart failure  
FDA - United States food and drug administration  
ECM - Fibrillary extracellular matrix  
NCX - Na/Ca exchanger  
SR - Sarcoplasmic reticulum  
Serca-2a - Sarco-Endoplasmic Reticulum Calcium ATPase  
Ryr receptors - ryanodine receptor  
A-II - Angiotensin II  
ACE - Angiotensin-converting enzyme  
cAMP - 3'-5'cyclic adenosine monophosphate  
EO - Endogenous ouabain  
SAR- structure-activity relationship  
NBS - *N*-bromosuccinimide  
HG-II - Hoveyda–Grubbs 2<sup>nd</sup> generation catalyst  
EDC - 1-Ethyl-3-(3-dimethylaminopropyl)carbodiimide  
LiHMDS - Lithium bis(trimethylsilyl)amide  
p-TSA - p-Toluene sulfonic acid  
PCC - Pyridinium chlorochromate  
HFIP- Hexafluoroisopropanol  
THF - Tetrahydrofuran  
Py - Pyridine  
t-BuOK - Potassium tert-butoxide  
DCM - Dichloromethane  
TFA - Trifluoroacetic acid  
MeOH - Methanol  
DMSO - Dimethyl sulfoxide  
EtOAc - Ethyl acetate  
ACN - Acetonitrile  
DMF - *N,N*-dimethylformamide  
PEOT - Poly(ethylene oxide) terephthalate  
PBT - poly(butylene terephthalate)  
300PA - 300Polyactive  
1000PA - 1000polyactive  
PCL - Poly( $\epsilon$ -caprolactone)  
NMR - Nuclear magnetic resonance  
SEM - Scanning Electron Microscope  
FIB-SEM - Focused Ion Beam - Scanning Electron Microscope  
TEM - Transmission electron microscopy  
TLC - Thin-layer chromatography

# 1. Introduction

## 1. Circulatory system and the Heart

To guarantee the survival nutrients, like oxygen, carbon dioxide, and sugar, should be efficiently transported to the cells of the entire body. The circulatory system, also called the cardiovascular system, is the apparatus of vertebrates that fulfill the task, providing nourishment. The essential components of the human cardiovascular system are blood vessels that pervade all the body carrying blood, blood composed by a fluid mixture of plasma, erythrocytes, leukocytes, and thrombocytes, and the heart the pump of the entire system. The whole system is divided into two different sub-systems: the pulmonary and systemic circulatory systems. While the pulmonary circulatory system consists of blood vessels that transport deoxygenated blood from the heart to the lungs and return oxygenated blood from the lungs to the heart, the systemic circulatory system, blood vessels transport oxygenated blood from the heart to various organs in the body and return deoxygenated blood to the heart.[1]

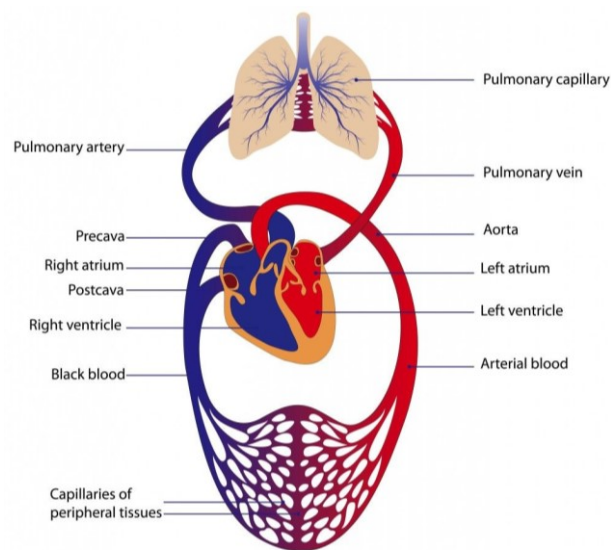


Figure 1: The human circulatory system.

As said, the heart is the main pump of the entire system that permits the blood to flow inside the vessels. The heart is a muscle located in the middle of the thoracic cavity, in a space called the pericardial cavity, and it is supplied by coronary circulation. The heart is divided hermetically into the right part, where venous blood flow and the left part where arterial blood flow. Such division does not allow any exchange of material. Since the venous blood travels on the shorter pulmonary circulatory

system, respect the arterial blood that travels all across the entire body, the shape of the heart is not symmetric: as a reflection of the shorter path the venous blood must flow in, the right part is smaller than the left one.[2,3]

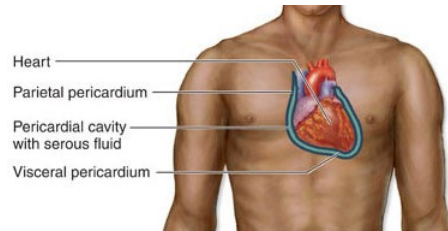


Figure 2: Heart location in the thoracic cavity.

Both the right and the left parts are themselves divided into atria and ventricles: the formers are the upper two chambers of the heart, and the two latter are the lower chambers. While the atria have the only function of receiving blood from the vessels, the ventricles make the real pumping action. In particular, looking at the right side of the heart, the superior vena cava transports deoxygenated blood from the head and the arms while the inferior vena cava transports deoxygenated blood from the lower part of the body back to the heart, where it enters the right atrium and moves to the ventricle through the action of the tricuspid valve. Once in the ventricle, the venous blood is pumped through the pulmonary arteries and into the lungs for re-oxygenation. In the same time frame, the left atrium receives freshly oxygen-rich blood from the lungs via the pulmonary veins; the blood passes through the bicuspid or mitral valve to the left ventricle where it is pumped through the aorta, the principal artery of the body able to transport oxygenated blood to all part of the body. In both cases, the flux of the blood is unidirectional thanks to specific valves, called atrioventricular valves, that only open in one direction, to let blood into the ventricles, and are flapped shut by the pressure of the blood when the ventricles contract. In this way, the valves block the backflow of the blood into the heart. Furthermore, the semi-lunar valves, located at the bottom of the aorta and pulmonary artery, prevent blood from re-entering the ventricles after it has been pumped out of the heart. [2]

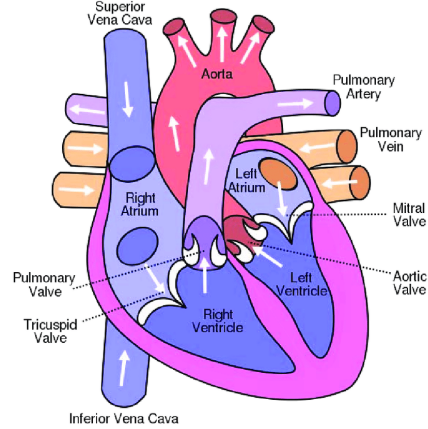


Figure 3: Heart compartments and blood flow through them.

The whole heart is protected by a layer called pericardium, while the principal tissue is composed of three layers: the epicardium, the myocardium, and the endocardium. The inner wall of the heart is composed of the endocardium. The outer by the epicardium. While the middle, thickest, and the fundamental layer of the cardiac muscle is called the myocardium.

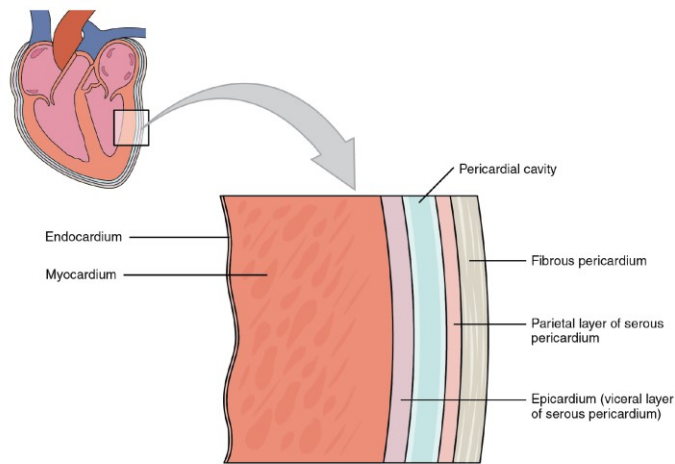


Figure 4: The composition of pericardium.

Within the myocardium, there are several sheets of cardiac muscle cells called cardiomyocytes. These peculiar cells are mainly responsible for heart contraction, which allows the pumping movement. Cardiomyocytes are mononuclear, striated, and elongated cylindrical cells, attached through intercalated discs. The contact between the cells allows them to transmit the contracting and relaxing force from one cell to the other. Another peculiarity of those cells, respect the normal muscle cells, is

their incredible resistance to fatigue, to allow the continuous contraction and relaxation, allowing at the same time the circulation of the blood around the body. Moreover, cardiomyocytes do not require external electric stimuli to contract. Therefore, the heart is capable of contracting without an external stimulus but only thanks to specific myocardial cells called pacemaker cells, able to generate spontaneously the potential required for the contraction.[3]

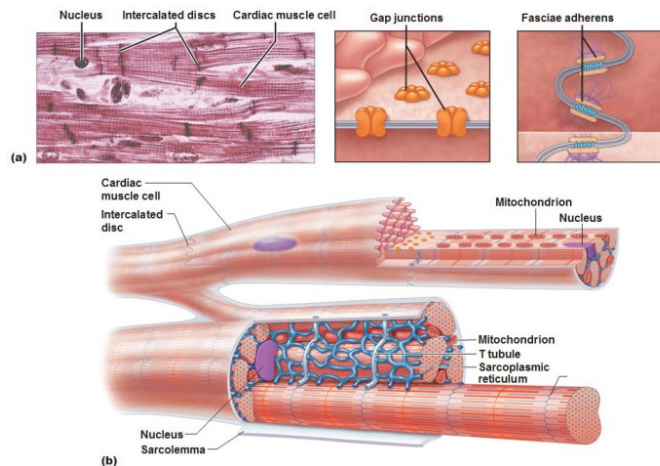


Figure 5: The cardiomyocytes and their composition.

Furthermore, cardiomyocytes contain T-tubules, pouches of the membrane that run from the surface to the cell interior, which helps to improve the efficiency of contraction. Differently from skeletal muscle, T-tubules of cardiomyocytes are bigger and wider but fewer in number. In general, cardiomyocytes go through a contraction-relaxation cycle that enables cardiac muscles to pump blood throughout the body, achieved through a process known as the excitation-contraction coupling that converts action potential into muscle contraction.[4]

## 2. The heart cycle

The pumping action of the heart is exploited through a cyclic movement, known as the heartbeat. The typical frequency of a healthy human heartbeat is approximately 70-75 beats per minute, and consists in two separate steps: the diastole, in which the heart muscle relaxes and refills with blood; and the systole, a period of robust contraction and pumping of blood.[1]

The left and right side of the heart works in concert to repeat the cardiac cycle continuously: the sequence starts with the ventricular diastole in which the heart relaxes and expands while receiving

blood into both ventricles; in the same time frame, the two atria are in the systolic phase, where they begin the contraction, and each pumps blood into the correspondent ventricle. The following stage of the cycle is the exact opposite: while ventricles make a vigorous contraction, called ventricular systole, ejecting the blood from the heart to the lungs or the body, the two atria are relaxed, or atrial diastole, and start to refill with blood. The precise timing and coordination ensure an efficient collection and circulation of the blood through the entire body, maximizing the quantity of fluid pumped out in every cycle.

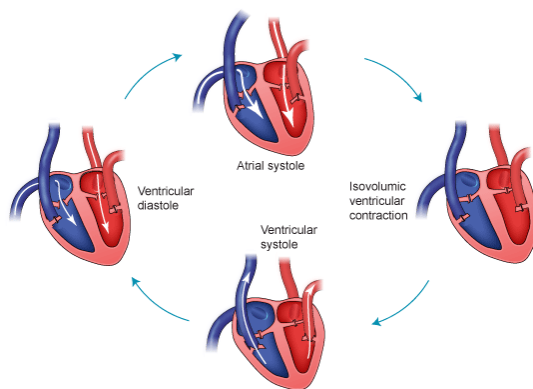


Figure 6: The heart cycle.

The complete cycle is described efficiently with the Wiggers diagram, named after its developer Carl Wiggers, in 1915. This simple diagram gives a comprehensive overview of the various electrical, pressure, volume, and blood flow changes and mechanical temporal relationships throughout a heartbeat, providing essential information on how the normal heart works with a description of pressure changes during phases of diastole and systole.[5]

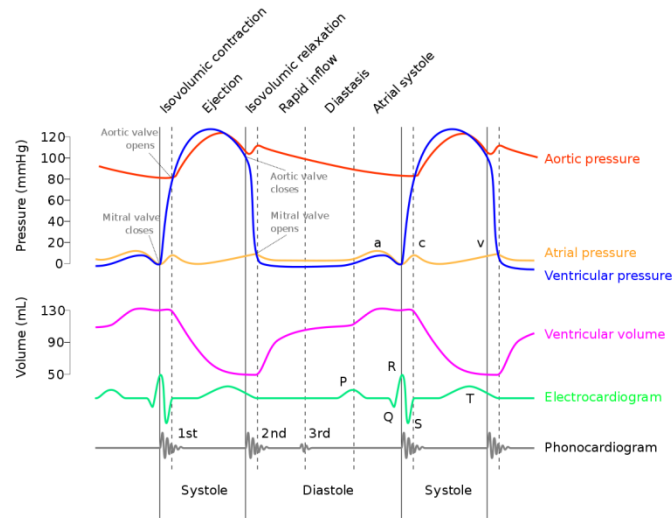


Figure 7: The Wiggers diagram.

Looking at the diagram, can be easily observed that every mechanical event is always preceded by an electric one. In particular, the electrocardiograms describe the voltage change versus time, in other words, the electrical activity of the heart. For example, ventricular depolarization occurs just before the mechanical event of contraction and expulsion of the blood from ventricles.

Electrocardiograms (ECGs) are recorded using electrodes placed over the skin, able to detect electrical changes that are a consequence of cardiac muscle depolarization followed by repolarization during each heartbeat, being the most wide-spread clinical tools for monitoring the heart function and for the determination of heart associated disease. The ECGs track, and the voltage changes observed macroscopically, are just a reflection of what happens at the cellular level during contraction and relaxation of cardiomyocytes.[6]

### 3. The heart electrophysiology

The whole heart cycle is governed at the cellular level by the change of the value of the membrane potential, itself a reflection of the different variations in the distribution of ions in the cardiomyocytes. The primary responsible for the contraction is the rapid increase of concentration of the calcium ions inside the cell, while the  $Ca^{2+}$  concentration is itself dependent on the concentration of sodium and potassium ions.[2]

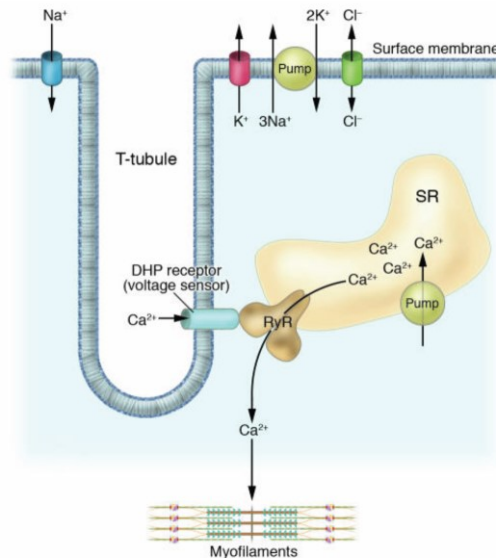


Figure 8: Schematic representation of the events leading to heart contraction.

In physiological conditions, cardiomyocytes possess a resting potential of  $-70\text{mV}$ . The potential is due to the presence of a high difference between  $\text{Na}^+$  and  $\text{K}^+$  concentration, respectively outside and inside the cell. The tendency of the ions to move towards equilibrium is removed by the Na/K-ATPase. The different concentration triggers the trend of  $\text{Na}^+$  to move inside the cell and the one of  $\text{K}^+$  to move outside. Na/K-ATPase works against this natural gradient maintaining stable resting potential.

The cardiac cycle starts when an electrical pulse, generated spontaneously by the pacemaker cells, is transmitted from the cell surface to the cell core by T-tubules, causing a change in polarity of the cell membrane and, subsequently, the activation of voltage-gated channels and the trigger of a cascade of events.

The membrane goes towards a rapid depolarization, allowing the  $\text{Ca}^{2+}$  to enter inside the cell. Calcium can recruit additional calcium, creating a strong gradient that enables muscle contraction. At the same time, the activation of supplementary channels and transporter works for rapidly decrease the calcium concentration inside the cell, allowing the relaxation and the restoration of the resting potential.

The described process involves different channels and transporter, able to actively or passively transport distinct kinds of ions. The principals are the Na/K-ATPase, the Na/Ca exchanger, the Na-

channel, the K-channel placed in the cell membrane; the Ca-channel placed inside the T-tubules; Serca-2a, and the Ryr receptors placed on the sarcoplasmic reticulum.[2]

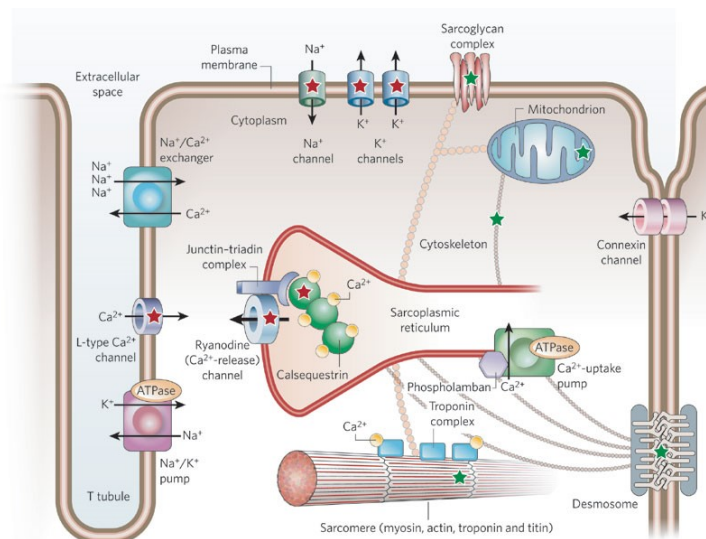


Figure 9: Overview on the different channels, pumps and ions involved in the contraction.

#### 4. The Na/K-ATPase

The Na/K-ATPase, or Na/K pump, is a primary transmembrane transporter belonging to the family of P-type ATPase. The protein is formed by two principal subunits: The  $\alpha$  subunit formed by  $\sim 1020$  amino acids that contain the sequence motifs typical of the P-type family, and the  $\beta$  subunit formed by  $\sim 250$  amino acids with three sites of glycosylation that is required for proper folding and targeting. Some isoforms of the pump has a third subunit called FXYP Subunit, an accessory regulatory protein that regulates the ion pumping.[7]

The protein was discovered by Jens Christian Skou in 1957, the discovery was awarded by the Nobel prize in 1997, marking an important step forward in the understanding of how ions get into and out of cells, particularly important in those cell that respond to stimuli and transmit impulses.[8]

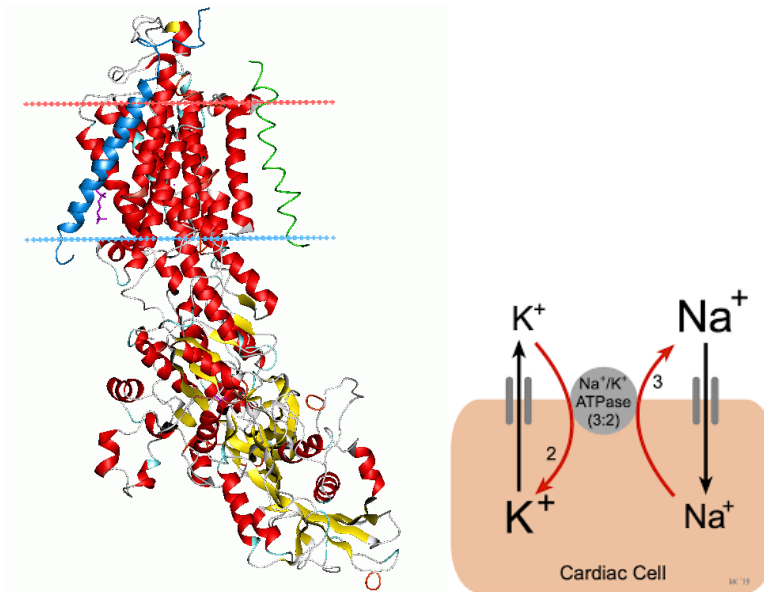


Figure 10: Na/K ATPase from pig (*S.scrofa*) in E<sub>2</sub>-P<sub>i</sub> structure (PDB code 3N23) and its schematic function.

Na-K pump is responsible for maintaining the concentration gradient across the cellular membrane. These gradients provide energy for several cellular functions, including control of membrane potential and cell size, pH homeostasis, and uptake of nutrients and water. The action of the pump can move three Na<sup>+</sup> outside and two K<sup>+</sup> inside the cell against their natural concentration gradients, by balancing energy consumption via the hydrolysis of ATP. The mechanism behind the transport involves two conformations of the protein: E<sub>1</sub> and E<sub>2</sub>. [9] During E<sub>1</sub> state, the cytosolic high affinity Na<sup>+</sup> binding sites are open, and the ATP is bound to the N-terminal domain. Once three Na<sup>+</sup> ions are secured, the protein changes conformation and moves the γ-phosphate of the ATP near the phosphorylation site. ATP phosphorylates the Asp376 causing an additional conformational change and the closure of the Na<sup>+</sup> binding sites, entrapping the three ions in the transmembrane domain and releasing ADP. The protein is now in a state called E<sub>1</sub>-P at high energy that rapidly moves toward the E<sub>2</sub>-P state. The E<sub>2</sub>-P state has a low affinity towards the Na<sup>+</sup>, allowing their release in the extracellular environment. At the same time, two K<sup>+</sup> ions are bound to the high-affinity extracellular domain. When both ions are bound, a conformational change closes the gate, occluding the K<sup>+</sup> and triggering the

dephosphorylation of Asp376. The protein is now in the E<sup>2</sup> state, which requires the binding of an ATP molecule to open the cytosolic K<sup>+</sup> gates and reverting in the E1 state.[10,11]

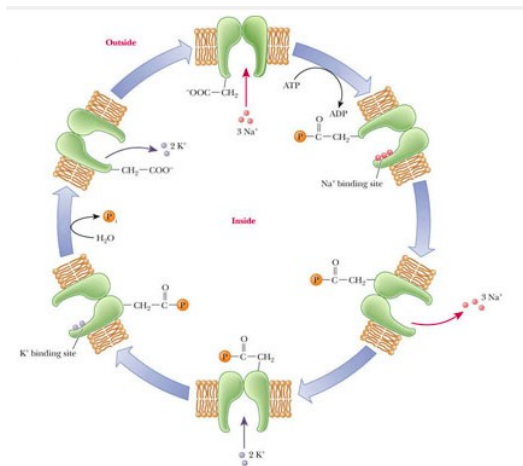


Figure 11: Catalytic cycle of Na/K ATPase.

In cardiomyocytes, the maintenance of the transarcolemmal Na<sup>+</sup> and K<sup>+</sup> gradients is crucial for a variety of electrophysiological processes, including the initiation and propagation of action potentials, as well as for the regulation of secondary transport processes vital for cell function, like the Ca<sup>2+</sup> extrusion via the sodium-calcium exchanger.

### 5. The Na/Ca-exchanger

Na/Ca exchanger, or NCX, is a secondary transporter that catalyzes the counter-transport of three Na<sup>+</sup> and one Ca<sup>2+</sup> using the energy stored in the electrochemical gradient of Na<sup>+</sup> as the driving force. The protein is formed by 10 transmembrane helices, with a total of 302 amino acids.[12]

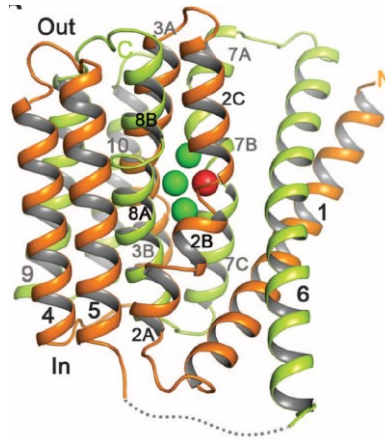


Figure 12: NCX exchanger structure from *M.jannaschii*. PDB code 3V5S. [12]

NCX mechanism of action is characterized by a ping pong mechanism in which one calcium and three sodium ions are sequentially translocated in separate steps across the membrane. Four possible ion binding sites are suspected to reside at the core of the protein, with the  $\text{Na}^+$  ions binding having an antagonistic effect on  $\text{Ca}^{2+}$  binding and vice versa. The complete mechanism is yet to be elucidated. However, there are hypotheses that ligand binding causes conformational changes that induce steric and/or electrical hindrances that alternatively expose or cover the ion-binding sites from the different sides of the membrane.[13]

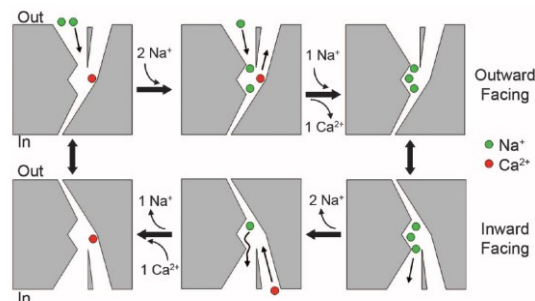


Figure 13: Schematic representation of the catalytic cycle of NCX.

In cardiomyocytes, NCX appears widely distributed within the sarcolemma, and it is the principal cardiac extrusion mechanism for the  $\text{Ca}^{2+}$  that enters via voltage-dependent  $\text{Ca}^{2+}$  channels with each beat. Unlike the  $\text{Na}^+/\text{K}^+$  pump, which utilizes the energy provided by an ATP molecule hydrolysis, the NCX uses the sodium gradient for the  $\text{Ca}^{2+}$  ions transport without the presence of ATP molecules.

Remarkably, the transport is electrogenic. The depolarization of the membrane can reverse the exchanger direction if the cell is depolarized enough. The ability for the  $\text{Na}^+/\text{Ca}^{2+}$  exchanger to invert the direction of flow manifests itself during the cardiac action potential: due to the delicate role that  $\text{Ca}^{2+}$  plays in the contraction of heart muscles, the cellular concentration of  $\text{Ca}^{2+}$  is carefully controlled. During the resting phase, the  $\text{Na}^+/\text{Ca}^{2+}$  exchanger takes advantage of the large extracellular  $\text{Na}^+$  concentration gradient to help pump  $\text{Ca}^{2+}$  out of the cell.[14]

However, the massive influx of  $\text{Na}^+$  ions during the first phase of the contraction causes the reversal of the  $\text{Na}^+/\text{Ca}^{2+}$  exchanger direction pumping  $\text{Na}^+$  ions out of the cell and helping the  $\text{Ca}^{2+}$  influx. This reversal of the exchanger lasts only momentarily: due to the internal influx of  $\text{Ca}^{2+}$  through the calcium channels, the exchanger returns to its forward direction of flow, pumping  $\text{Ca}^{2+}$  out of the cell.[15]

## **6. transmembrane cation channel**

The super-family of cation channels is a class of protein that includes sodium, potassium, calcium channels, and the ryanodine receptor. The proteins are located in the transmembrane domain and have a tetrameric structure. Each channel has at least two transmembrane helices flanking a loop that determines the ion selectivity of the channel pore. Many members of the family present additional control domains able to regulate channel gating and ion conduction.[16]

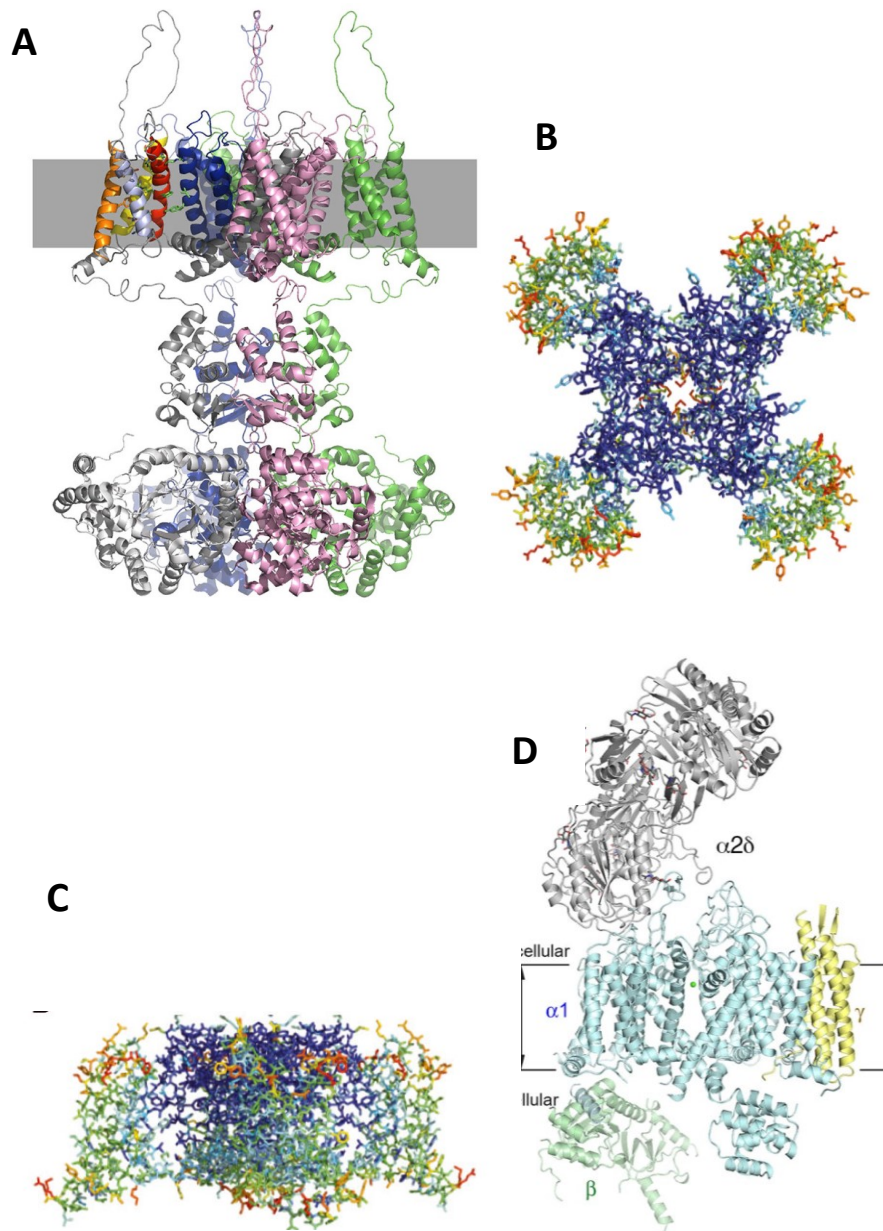


Figure 14: A) the model of Human tetrameric K<sup>+</sup> channel structure in open state. [17] B) Top view of the Na<sup>+</sup> channel structure from *A. butzleri*. (PDB code 4EKW) C) Side view of the Na<sup>+</sup> channel structure from *A. butzleri*. (PDB code 4EKW) [18] D) structure of Human the L-Type Ca<sup>2+</sup> channel. (PDB code 6D7S)

The presence of the voltage-gated channels in cardiomyocytes is crucial for their capacity of contracting.[19] The channels allow the modification of the concentration gradient of the different ions according to the instantaneous membrane potential. For example, the voltage change caused by the electric pulse emitted by pacemaker cells opens the voltage-gated Na channel, allowing Na<sup>+</sup> ions

to enter inside the cytosol prompting the depolarization and the increase of the  $\text{Ca}^{2+}$  gradient. On the other hand, during the depolarization stage of the membrane, the voltage-gated K channel allows the exit of  $\text{K}^+$  ions inducing the re-polarization of the membrane and the decrease of calcium gradient.[20]

Cardiomyocytes, like other excitable muscle cells, can exploit the electric potential as a way of energy storage, and ions transporter behave like selective "on-off" buttons. As said, high  $\text{Na}^+$  concentration in the extracellular fluids and high  $\text{K}^+$  in the cytoplasm are constantly maintained by the action of the Na/K-ATPase. Such system keeps the membrane potential to a negative value and in the resting state.  $\text{Na}^+$  channels behave like an "on" button: when the electric pulse hits the cell, triggering the depolarization of the membrane, is activated the cascade of events that lead to the contraction. Contraction should decay rapidly toward a relaxation. This process is triggered by the K channels that act as an "off" button: when the depolarization occurs, K channels open, enabling the repolarization of cells and the triggers of relaxation cascade.[2]

In other words, the concentration gradients of  $\text{Na}^+$  and  $\text{K}^+$  controls the transient of calcium, the final responsible for the contraction.  $\text{Ca}^{2+}$  transport is regulated by specific channels. In fact, besides the action of the NCX transporter, the influx of calcium is mainly regulated by voltage-gated calcium channels and the ryanodine receptor (Ryr).[16]

Voltage-gated calcium channels are classified into two categories: the L, or low threshold type, and T, or transient-type. While the L-type channels are located in all cardiac cell types, the T-type channels are found principally in pacemaker and atrial cells. These two channels act differently towards voltage changes across the membrane: T-type opens first, at a more negative potential, and remains open for a shorter period, contributing more to the depolarization process. On the other hand, L-type channels behave in the exact opposite, contributing to the plateau phase, when the membrane slowly begins to repolarize.[21]

However, the majority of calcium is not located outside the cell, but in the sarcoplasmic reticulum: a reservoir of calcium located in the cytosol. To induce the elevated increase of  $\text{Ca}^{2+}$  concentration necessary for the binding to troponin/tropomyosin and so for the contraction is essential to release such ions.[22]

Ryanodine receptors are unique calcium channels located across the sarcoplasmic membrane. Differently from Voltage-gated calcium channels, they are not susceptible to voltage changes. Besides, the opening of those channels is triggered by the calcium ions entered through the Voltage-gated calcium channels, in a process known as “calcium-induced-calcium release”. [23]

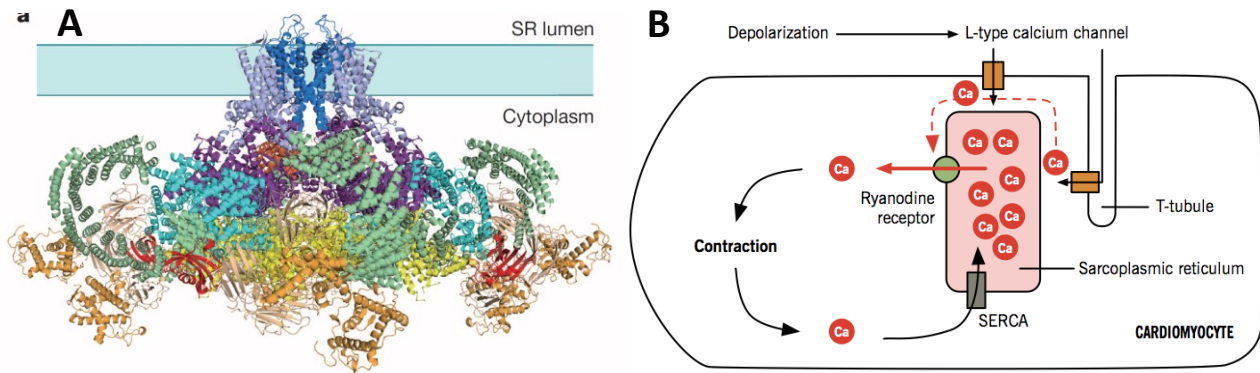


Figure 15: A) Structure of a ryanodine receptor from rabbit (*O. cuniculus*) (PDB code 3J8H). [24] B) schematic representation of the calcium-induced-calcium release.

## 7. Sarco-Endoplasmic Reticulum Calcium ATPase (SERCA2a) and the sarcoplasmic reticulum

Ca<sup>2+</sup> plays a vital role in the contraction by being the triggering element.[1,22] However, calcium accumulation within the cells can lead to calcification or hardening of intracellular structures, such as mitochondria, leading to rapid cell death. This Janus nature of calcium in the cells requires a strict control mechanism that releases and sequester in a highly efficient way the calcium within the cytosol of muscular cells. To control calcium concentration gradients in such effective manner, the best strategy is to store it directly in the cytosol within dedicated compartments. This work is made by the sarcoplasmic reticulum (SR), the organelle dedicated to the storage of intracellular Ca<sup>2+</sup>. The SR is characterized by a membrane-bound structure, similar to the endoplasmic reticulum in other cells, that can store up to millimolar amounts of calcium.[25]

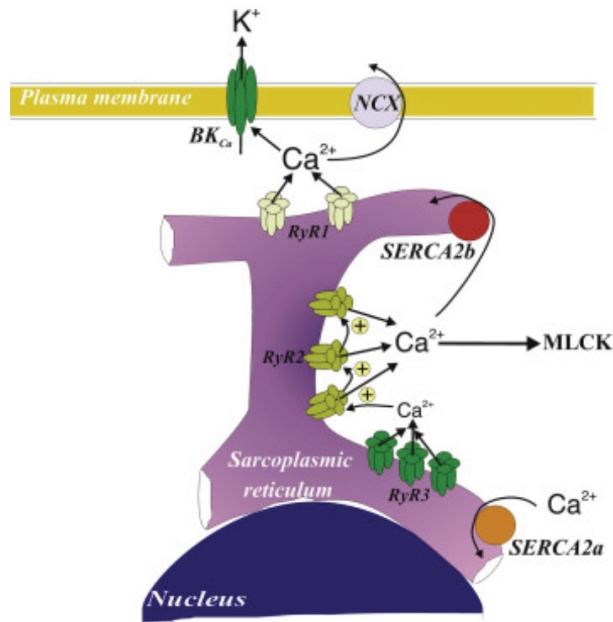


Figure 16: The sarcoplasmic reticulum and its main membrane components.

As already discussed, the release of calcium from the SR is operated by the Ryanodine receptors in a calcium concentration-dependent way. On the other hand, the rapid sequestration of calcium and its removal from the cytosolic ambient is mediated by the Sarco-Endoplasmic Reticulum Calcium ATPase (SERCA).[22]

The SERCA pump has a dual function: cause muscle relaxation by lowering the cytosolic calcium and, at the same time, restore the sarcoplasmic reticulum calcium store, which is needed for muscle contraction.

Among the different isoforms of the protein SERCA, SERCA2a is involved in the calcium cycle of cardiomyocytes, which function is to re-uptake Ca<sup>2+</sup> into the SR to relax the cardiomyocytes, thereby maintaining Ca<sup>2+</sup> homeostasis in cells.[26]

Human SERCA2a structure was clarified in 2019 by Sitsel *et al.* The structure is formed by 997 residues and possesses two possible conformation E1 and E2.[27] E1 has a great affinity for Ca<sup>2+</sup>, while E2 has low affinity; the protein changes between the two conformations after phosphorylation by ATP. In the resting-state SERCA is in the E1 structure, two Ca<sup>2+</sup> ions enter from the high-affinity calcium gate inducing the binding of Mg<sup>2+</sup>-ATP to bind in the N domain. The phosphorylation of Asp351 with

consequent hydrolysis of ATP causes the formation of an occluded  $[Ca^{2+}]E1P$  intermediate. An immediate conformational change allows the opening of the  $Ca^{2+}$  exit gate to the luminal compartment and lowering, at the same time, the  $Ca^{2+}$  affinity. Subsequently, negatively charged residues of the ion-binding sites are temporarily protonated, causing occlusion and triggering the dephosphorylation of the protein, catalyzed by a conserved Glu183 residue. In this way, SERCA is restored and can begin another catalytic cycle.[27,28]

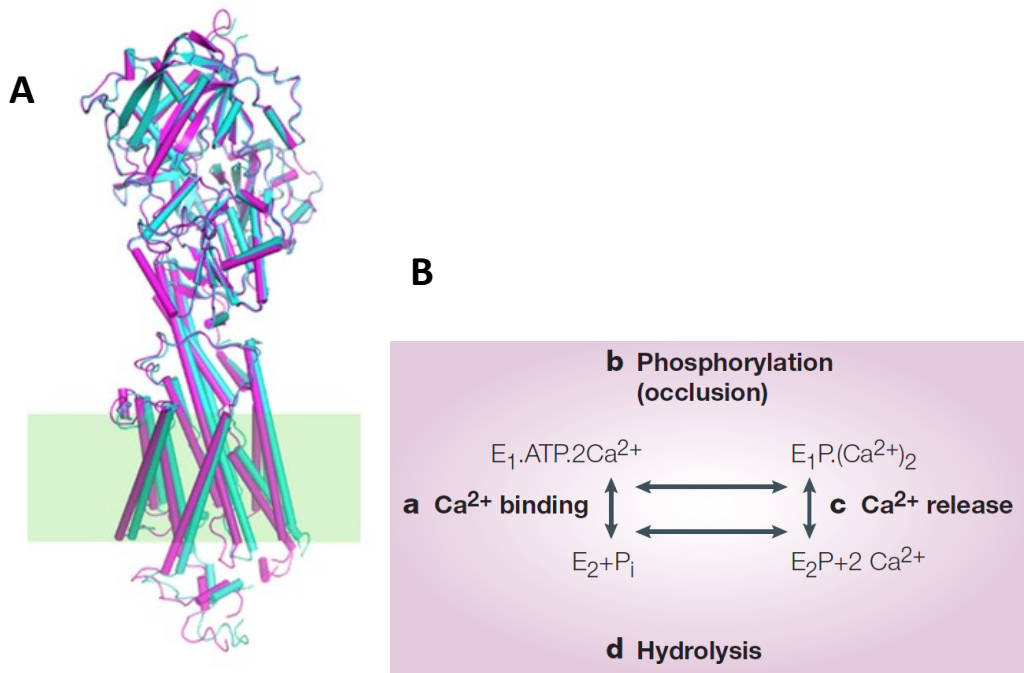


Figure 17: A) Human SERCA2a structure (PDB code 7BT2). [28] B) Scheme of the catalytic cycle of SERCA2a.

SERCA pump activity is additionally regulated by small-molecular-weight proteins, phospholamban (PLB) and sarcolipin, in a tissue-specific manner. The principal regulator of SERCA2a activity is PLB, a peptide formed by 52 residues, located in the transmembrane of SR, which exists as a pentamer.[29] PLB possesses a phosphorylation site that regulates its inhibitory activity: the pentameric aggregate is not active as an inhibitor and it is stabilized by the presence of phosphates. Contrariwise, the non-phosphorylated PLB is a monomer, able to interact and inhibit the activity of SERCA2a. The phosphorylation is mediated by a cAMP-dependent protein kinase (PKA) and by calcium/calmodulin-dependent protein kinase II (CaMKII). PLB monomer can bind in the cytosolic and/or transmembrane domains of SERCA2a since the novelty of the SERCA2a structure the exact binding sites are not yet

characterized.[30] However, some suggestions were made by the observation of the binding between the isoform SERCA1a and PLB. In this case, was observed that in the E2 conformation is present a groove in the lipid-facing surface of the transmembrane domain.[31] The carboxy-terminal helix of PLN can fit into this groove and form interaction. The binding between SERCA and PLB is inhibited, and the activity of SERCA restored, in two cases: the first case is the phosphorylation of PLB while the second case is an increase of calcium concentration.  $\text{Ca}^{2+}$  binding to SERCA2a can relieve PLB inhibition.[32]

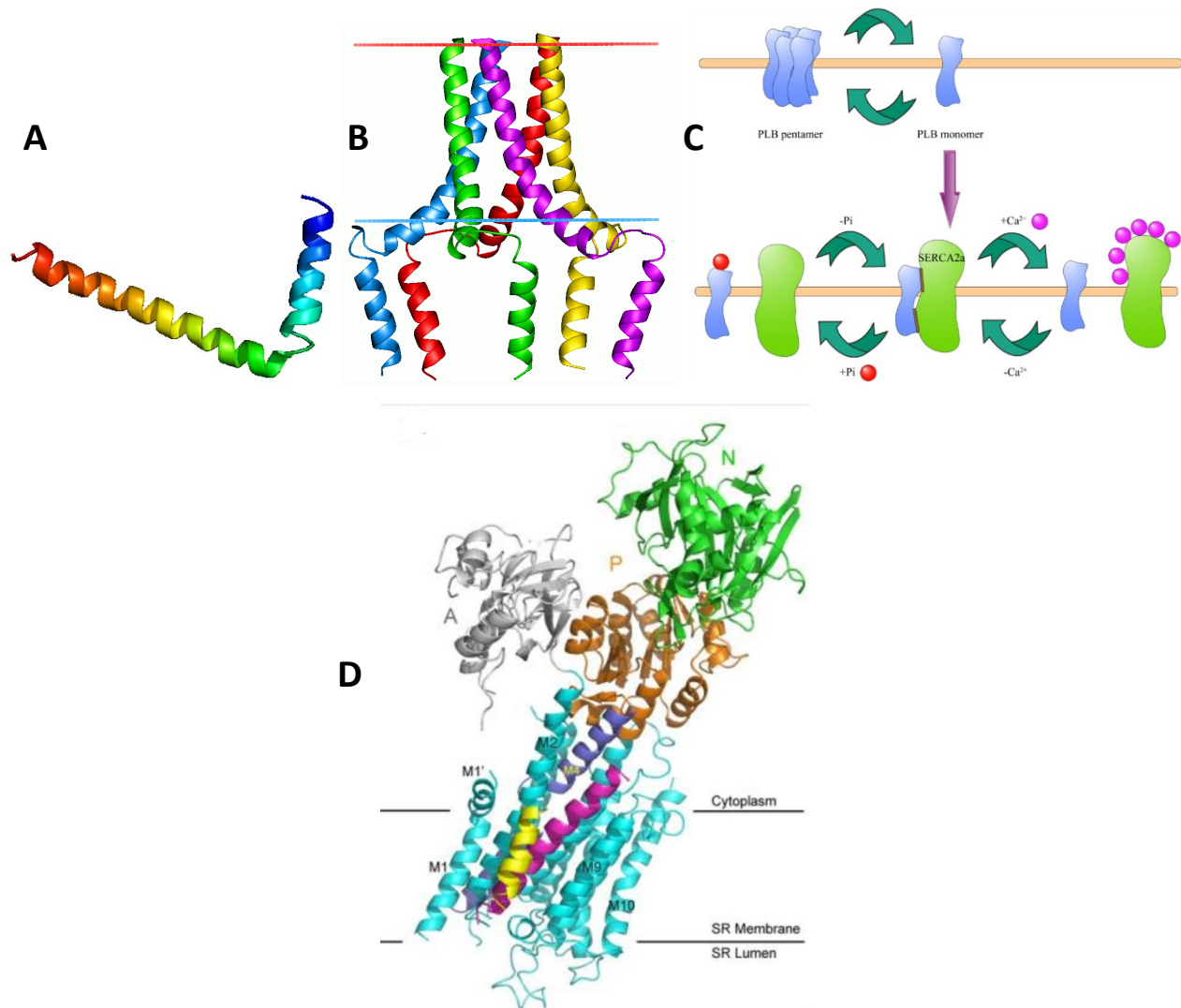


Figure 18: A) Structure of Human phospholamban monomer (PDB code 1plp). B) Human phospholamban pentameric aggregate (PDB code 2kyv). C) Schematic mechanism of the inhibition of SERCA2a and the two possibility to inhibit the interaction with phospholamban. D) Structure of

SERCA2a-phospholamban complex (phospholamban is represented in magenta). The figure was generated by Akin et al. using PyMOL (The PyMOL Molecular Graphics System, version 1.5.0.4, Schrödinger, LLC). [31]

These mechanisms are essential for the keeping of good contractility of the heart: if SERCA does not work correctly,  $\text{Ca}^{2+}$  can accumulate in the cytosol leading first to a series of drawbacks, including cell death; Also, if the sarcoplasmic reticulum is not filled properly, the calcium gradient will be lower, reflecting in a less efficient contraction.

## 8. The action potential

The cardiac action potential describes the series of events that lead to contraction. Their synchronicity, characteristic shape, and length safeguard the heart against the abnormal electrical activity. The final output of these events is to convert the electric stimuli into mechanics ones, which intermediate mediators are the  $\text{Ca}^{2+}$  ions.[33]

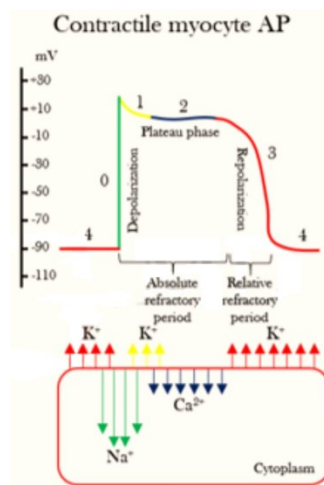


Figure 19: The scheme of cardiac action potential in term of mV change and the ion flow that characterize each phase.

The cardiac potential can be divided into five different phases (from 0 to 4). The whole cycle starts with phase 4 in which the cell is in the resting phase, the membrane potential is around -90mV, and the muscle is in diastole. Here, the membrane potential is maintained constant and the leakage of  $\text{Na}^+$  and  $\text{K}^+$  are maintained by the action of the  $\text{Na}/\text{K}$ -ATPase.[34]

Phase 0 starts when the equilibrium potential is disrupted by the pulse coming from pacemaker cells. The potential firstly reaches the threshold of  $-70\text{mV}$  causing the opening of voltage-gated Na channels. The strong flux of sodium within the cell leads to a depolarization of the membrane that reaches potential around  $+50\text{mV}$  in less than 2ms. Another contribution to the depolarization is given by the opening of calcium channels during this phase, in particular the L-type channels. Finally, the Na<sup>+</sup> channels inactivate almost immediately after opening and will recover from inactivation only at very negative membrane potentials blocking the induction of another action potential within the cell.

Phase 1 is also known as the notch, a brief phase in which the potassium channels open and start to repolarize rapidly the membrane through the outflow of potassium.

When the potential reaches values around  $+20\text{mV}$  begin phase 2, known as the plateau phase. This period is characterized by an almost complete balance between the charges moving towards the membrane, leading to a slightly constant potential. Here exists a balance between the outflow of K<sup>+</sup> ions through the voltage-gated K channels and the inflow of Ca<sup>2+</sup> through the L-type channels. The rising concentration of calcium induces calcium release from the Ryr on the sarcoplasmic reticulum. This mechanism allows the rapid rising Ca<sup>2+</sup> concentration necessary for the contraction. Despite the neat potential remains constant during this phase, a great flux of ions is present: the movement of Ca<sup>2+</sup> opposes the repolarizing voltage change caused by K<sup>+</sup>; also, the increased calcium concentration increases the activity of the sodium-calcium exchanger, and, consequently, the increase in sodium entering the cell increases the action of the sodium-potassium pump. This phase is responsible for the long duration of the action potential and is essential in preventing irregular heartbeat.

The plateau ends with the closure of the Ca<sup>2+</sup> channel, starting phase 3 of the process. At this point, only the voltage-gated K channels are all open, causing a powerful outflow of K<sup>+</sup> from the cell. In this stage, the action of SERCA2a removes the calcium from the cytosol, and the membrane potential is driven back to its original value, and the muscle starts its relaxation. The reset of the pre-pulse concentration of ions is then operated by the Na/K-ATPase and the Na/Ca transporter.[35]

During the action, the potential exists two stages in which the cells became refractory to other stimuli. The first, known as the absolute refractory period, starts during phase 0 and lasts until phase

3. The cause is the closure of Na gates and their lock until the cells reach a negative potential. The second one immediately follows the first, and is called the relative refractory period, during which a stronger-than-usual stimulus is required to produce another action potential, which is caused by the leaking of potassium ions that makes the membrane potential more negative than physiological to reset the sodium channels; opening the inactivation gate, but still leaving the channel closed.[36]

All the overall process mentioned above is necessary for the proper function of the heart: if one of these stages fails, the heart loses its contractility and, therefore, its capacity of pump blood to all the body leading to the appearance of heart failure disease or syndrome.

### 9. The diseases correlated to circulatory system

The circulatory system is vital for the nutrients supply in the entire body, providing nourishment. Diseases that affect the circulatory system, including the heart, could heavily compromise the everyday life and the survival of the individual being one of the principal cause of death in the United States, Europe, and much of Asia.[37,38]

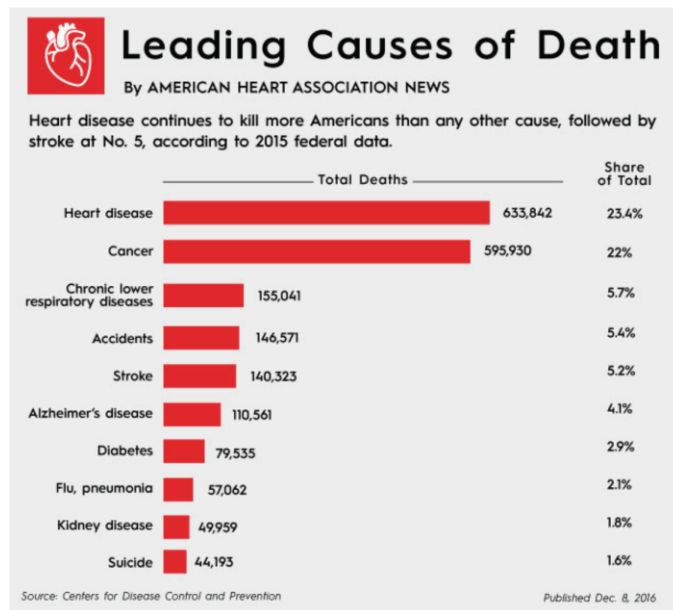


Figure 20: Leading cause of death in the world according to 2015 data.

These complications could arise for different risk factors, including aging, improper lifestyle, and genetics.

High blood pressure or hypertension, for example, is an high frequency medical situation in which the blood pressure within arteries is continually higher than average values.[39] Blood pressure is a reflection of how much force is used to pump blood through arteries and is expressed by two measurements the systolic and diastolic pressures. High values of blood pressure cause extra strain on blood vessels, heart, and other organs, such as the brain, kidneys, and eyes.[40] Usually, this kind of disease does not have symptoms associated and can be managed with physical exercise and dietary changes. However, in long-term periods hypertension is a primary risk factor for more severe diseases like coronary artery disease, stroke, chronic kidney disease, heart failure, and dementia.[41,42]

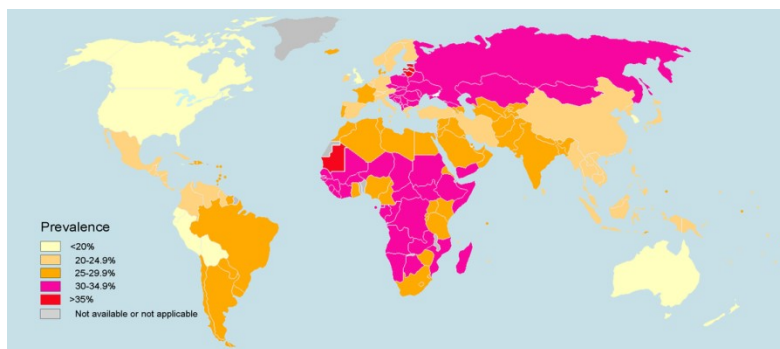


Figure 21: Distribution of patients affected by heart diseases in the world.

Another example is given by atherosclerosis, in which an abnormal accumulation of material in the inner layer of the wall of an artery, called plaque, caused by a chronic inflammation causes the narrowing of the arteries and sometimes so-called “hard event” (myocardial infarction or stroke).[43] Only in recent years was elucidated the whole process and became clearer that atherosclerosis is a chronic inflammatory process. In the first stage, endothelial dysfunction is triggered by exposure to different risk factors, such as LDL cholesterol, free radicals, homocysteine, or chronic infection. This process leads to tissue damage that activates T-lymphocytes, monocytes, and platelets to the injured site. Failure in the reparative process causes permeabilization of the most internal arterial tissue, attracting LDL particles in the site. As the attempt at endothelial repair progresses, macrophages and monocytes involved in the initial reaction begin to die arising in the formation of a necrotic core. In the meanwhile, collagen forms a fibrous cap that entraps the plaque. Small blood vessels (*vasa vasorum*) supplies the plaque, allowing its growth in size and occupying up to 45% of the original vessel.

When the rate of fissuring surpasses the rate of repair, plaque rupture release lipid fragments and cellular debris into the vessel lumen, triggering thrombotic agents at the endothelial surface, resulting in thrombus formation. If the thrombus formed is large enough, luminal occlusion occurs terminating in a “hard event”.[44–46]

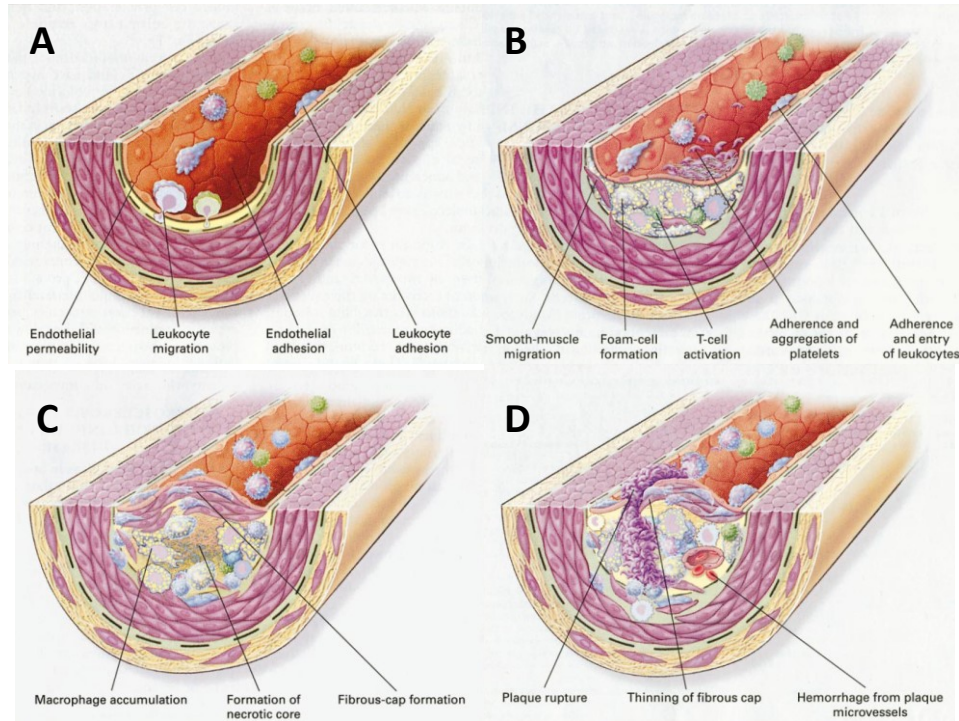


Figure 22: Pathological process of atherosclerosis. A) Risk factors triggers tissue damages B) Failure in the regenerative process leads to a permeabilization of the tissue attracting LDL particles C) Formation of the necrotic core D) Tissue rapture and release of lipid fragments.

If atherosclerosis involves the coronary arteries, the syndrome is called coronary heart disease or ischemic heart disease. This pathology is the most common among cardiovascular diseases.[47] The symptom usually involves chest pain or discomfort occurring most of the time with regularly activity, after eating, or at other predictable times. The narrowing of the coronary causes a non-optimal supply of nutrients on the heart and can precede heart attack, or myocardial infarction.[48]

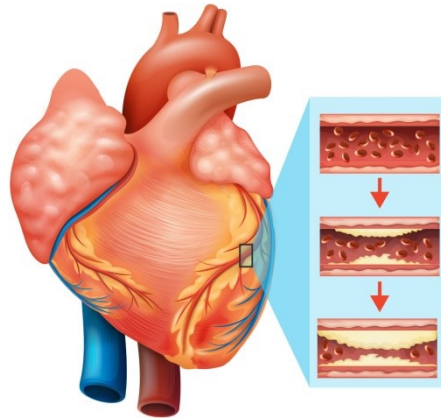


Figure 23: Coronary heart disease causes narrowing of coronary arteries.

The heart muscle itself could be involved in different pathologies, like cardiomyopathies. This large group of diseases can be either confined to the heart or part of a generalized systemic disorder, both involving many factors that contribute to a non-regular beating (arrhythmias) or non-optimal contraction or relaxation. Causes are still to elucidate but sometimes related to genes defect or to environmental or lifestyle associated behavior. Most of the cardiomyopathies can lead to cardiovascular death or progressive heart failure-related disability.[49–52]

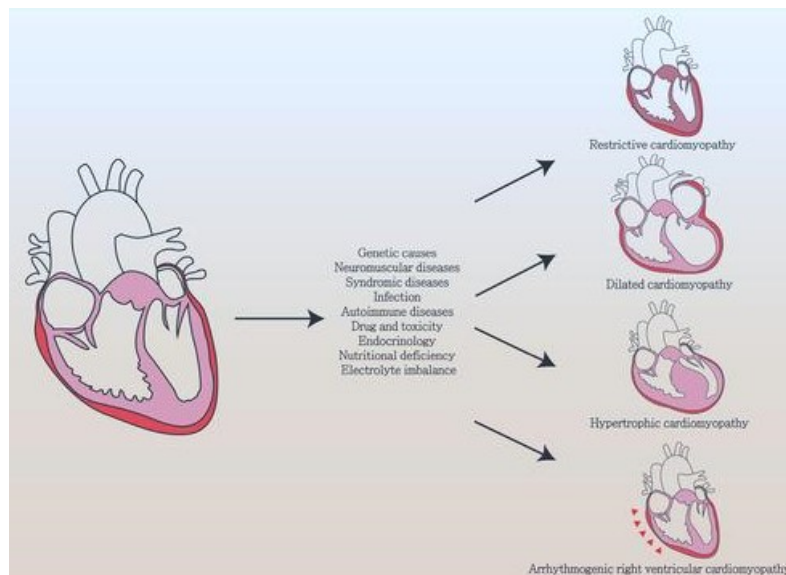


Figure 24: Some example of cardiomyopathies.

The pathological situations presented, along with other medical conditions, can lead to the so-called heart failure. This pathology is characterized by a non-sufficient pumping of the heart that does not allow correct blood flow. Since its medical relevance will be discussed in the following section.

## 10. Heart failure diseases

Heart failure (HF) is the pathophysiological state in which the heart is unable to pump blood at a rate adequate with the requirements of metabolism, due to a loss of cardiac contractile function. The common causes of heart failure are associated with coronary artery disease hypertension, atrial fibrillation, valvular heart disease, improper lifestyle, infection, and cardiomyopathy. The chronic medical condition is known as congestive heart failure (CHF), in which exists congestion of the systemic and pulmonary venous circulation due to ventricular failure. Patients with heart failure display symptoms of fatigue, breathlessness, and peripheral edema, which severely limit their regular activities.[53,54]

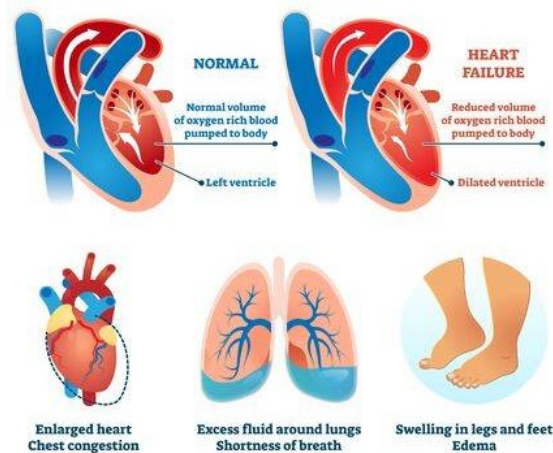


Figure 25: Causes and symptoms of heart failure.

The metabolism can adapt and counteract the diminishing efficiency of the left ventricle, compensating the cardiac output and maintaining the perfusion of vital organs. Some examples are the activation of the renin/angiotensin/aldosterone system and progressive hypertrophy of the ventricles. The output is initially beneficial, but as the chronic condition arises, there is a worsening of the condition due to excessive vasoconstriction. Consequently, heart failure rises with an increase in the preload and afterload, sodium and water retention, and edema formation.[55]

Despite the mortality of heart failure disease decreased in the last 20-30 years, it remains one of the leading causes of death in the world. In the United States, one over four death can be attributed to heart failure. Also, due to the aging of the population and wrong lifestyle of people, admission in hospital for heart failure are constantly rising, making it one of the most concern in public health. [56–59]

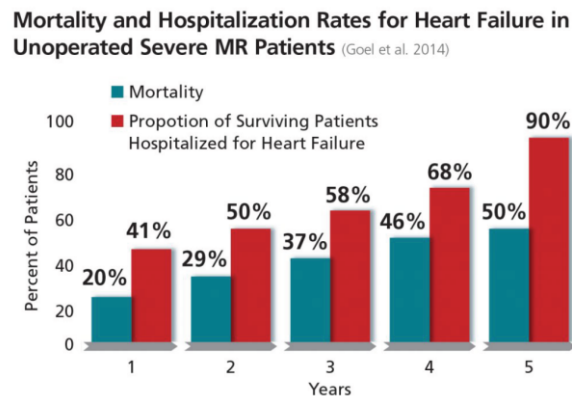


Figure 26: Mortality and hospitalization rate according to Goel *et al.* for patients affected by heart failure.

Medical and pharmacological treatment depends on the severity and cause of the disease. Usually, if symptoms are stable and mild, treatment consists of lifestyle modifications such as stopping smoking, physical exercise, and dietary changes. [60]

On the other hand, in chronic and severe situations, such as CHF, pharmacological treatment is needed to achieve symptomatic relief. The first step is to decrease the congestion and to implement lifesaving therapies. The immediate management of patients with chronic heart failure situations often requires inotropic support.

Therapy is addressed at improving the beating performance of the heart and at reducing the cardiac load. Different pharmacological and medical treatments are available to counteract the decline of the heart pumping. Some examples are diuretics and dietary salt restriction to reduce systemic congestion; vasodilators able to reduce vascular resistance and hence the afterload; finally, inotropic agents, such as digitalis glycosides, to improve cardiac output. [61,62]

However, almost 60% of patients hospitalized for CHF have coronary artery disease, and a sizable proportion of these individuals will suffer from ischemic myocardium.[63] Therefore, the inadequate oxygen supply to heart tissue caused by atherosclerotic coronary damages in the presence of pharmacological inotropic stimulation and vasodilator therapy is detrimental to tissue viability, affecting coronary blood flow, particularly in those patients with a marked decrease in blood pressure.

### **11. Therapy for heart failure diseases**

The objective of treatments is the improvement of symptoms, quality of life, and survival. The therapies consist of two different approaches: the first is addressed at improving the pumping performance of the heart and, on the other hand, at reducing cardiac load by increasing vasodilatation. The different classes of drugs available to counteract the decline of the pump efficiency are inotropic agents, such as digitalis glycosides, diuretics, and vasodilators.

While diuretics can only improve symptoms of CHF by acting on solute and water reabsorption but do not influence the progression of the disease, vasodilators can reduce systemic vascular resistance, thus reducing afterload.[64]

Vasodilation is a process in which the relaxation of smooth muscle cells located in the vessel walls causes a widening of the vessel itself. The process creates a lower vascular resistance, allowing higher blood flow and a higher volume of blood pumped by the heart per time unit, known as cardiac output.[57,65]

The renin-angiotensin-aldosterone system plays a fundamental role in the regulation of arterial blood pressure, electrolyte balance, and blood volume. Such enzymatic-hormonal mixed system consists of two main enzymes, renin, and angiotensin-converting enzyme (ACE), which activity regulates the release of the bioactive octapeptide angiotensin II (A-II). Angiotensin II fulfills its vasoconstrictor task by stimulating the Gq protein in vascular smooth muscle cells and acting on the Na<sup>+</sup>/H<sup>+</sup> exchanger in the proximal tubules of the kidney, stimulating Na reabsorption and H<sup>+</sup> excretion. Also, the octapeptide stimulates the synthesis of aldosterone, which mediates additional sodium retention by acting on the nuclear mineralocorticoid receptors (MR) within the kidney nephron.[66]

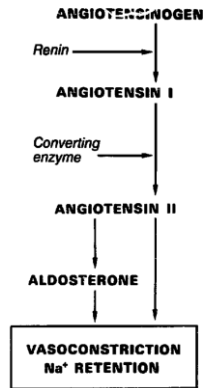


Figure 27: The renin-angiotensin-aldosterone system.

Since the crucial role played by the renin-angiotensin system in vasoconstriction, antagonists of this system are probably the most widely used vasodilators. In this context exists two principal strategies. The first is the use of angiotensin-converting enzyme inhibitors (for example, captopril, enalapril, fosinopril) blocking the generation of A-II from angiotensin I. Besides the direct vasodilation associated with lower levels of A-II, a secondary effect of this drug is the inhibition of the degradation of bradykinin, commonly carried out by ACE. Bradykinin is a small pro-inflammatory peptide, able to cause the enlargement of small arterioles.[67,68]

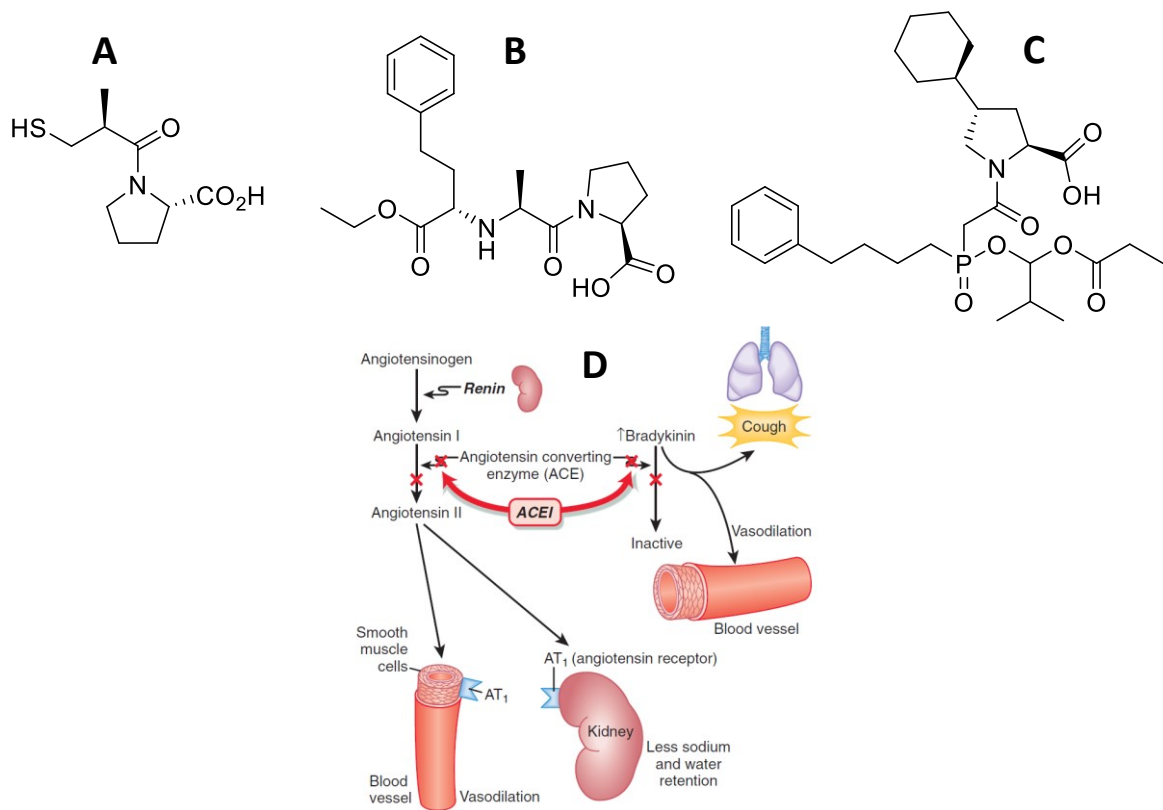


Figure 28: chemical structure of A) Captopril. B) Enalapril. C) Fosinopril. D) Mechanis of ACE inhibitors.

The second strategy involves the use of A-II antagonists (for example, losartan, valsartan), able to act on the A-II (AT<sub>1</sub>) receptors, inhibiting the signaling caused by A-II. Despite both classes of drugs find applicability in the treatment of CHF, the ACE inhibitors are preferred since their extended clinical history; yet, AT<sub>1</sub> antagonists have the advantage of not provoke cough associated with increased levels of bradykinin.[69–71]

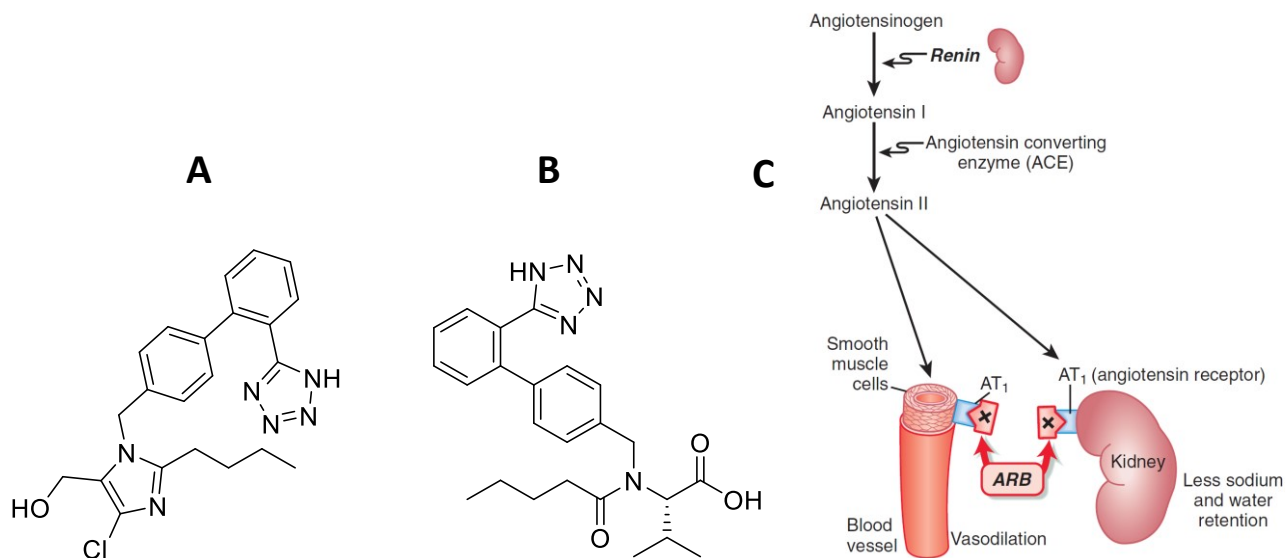


Figure 29: Chemical structure of A) Losartan. B) Valsartan. C) Mechanism of A-II antagonists.

Another class of vasodilators are the nitrovasodilators, which act as sources of nitrogen oxide (NO). This small molecule was identified as the bioactive factor responsible for endothelium-dependent relaxation of blood vessels. The pharmacological activity of these drugs depends on the biotransformation into NO within the blood and vascular tissues. Owing to their vasodilating effects on coronary vessels, organic nitrates (for example, nitroglycerin, isosorbide dinitrate) may improve ventricular function in ischemic cardiomyopathy. Hydralazine reduces ventricular afterload and can be the vasodilator of choice in patients with renal dysfunction who cannot tolerate an ACE inhibitor.[72–74]

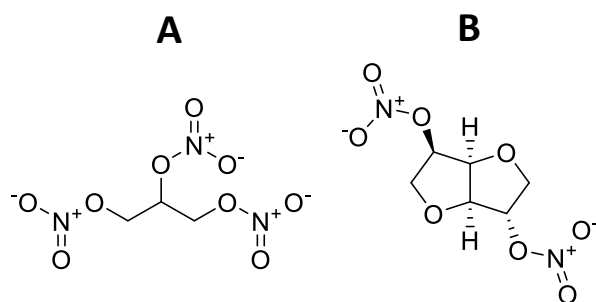


Figure 30: Chemical structure of A) Nitroglycerine. B) Isosorbide dinitrate.

Although calcium channel antagonists are effective vasodilators, none has shown to produce sustained improvement in symptoms in CHF; it may be related to the negative inotropic effects of these drugs. Second-generation drugs (for example, amlodipine, felodipine) appear to have fewer

adverse inotropic effects and are currently under evaluation to determine their impacts on both symptoms and mortality.[75,76]

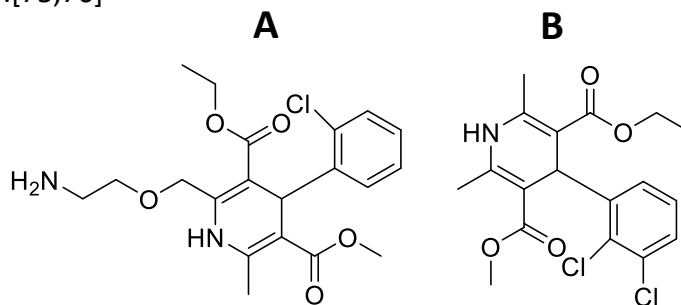


Figure 31: Chemical structure of A) Amlodipine. B) Felodipine.

Another strategy for the improvement of contractile function is to target the adrenergic receptors or adrenoceptors. This class of G protein-coupled receptors are the targets of many catecholamines neurotransmitters like norepinephrine (noradrenaline) and epinephrine (adrenaline) produced by the body, with the generation of sympathetic nervous system (SNS) stimuli. Adrenergic receptors are mainly divided into two principal classes:  $\alpha$  and  $\beta$ , with 9 subtypes in total.[77]

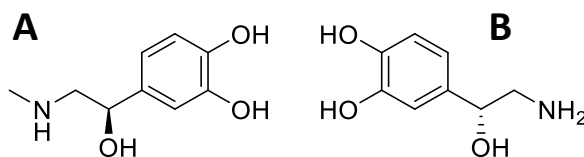


Figure 32: Chemical structure of A) Adrenaline. B) Noradrenaline.

Physiologic and molecular analyses indicate that the  $\beta$ -adrenergic signaling cascade is an essential regulator of myocardial function, and several lines of investigation support alterations in  $\beta$ -adrenergic receptor signal- transduction mechanisms as primary determinants of the natural history of HF. Also, adrenaline can react with both  $\alpha$ - and  $\beta$ -adrenoreceptors, causing vasoconstriction and vasodilation, respectively. The two classes have a different affinity toward adrenaline and still asymmetrical distribution in the body.  $\alpha$  receptors are less sensitive than  $\beta$  ones and are mainly located in the peripheral part of the body, while  $\beta$ -receptors are found principally in coronary arteries. This different distribution and affinity cause that high levels of circulating adrenaline cause peripheral vasoconstriction, and the opposite in the coronary arteries.[78,79]

For example, dobutamine is an adrenergic agonist administered as a racemic mixture, in cases of congestive heart failure to increase cardiac output. It can be used in intravenous infusions in patients refractory to oral medications, up to several days in duration. The racemic mixture stimulates  $\beta_1$  receptors, while the  $\alpha$  agonistic effects of the (-) enantiomer appear to be blocked by the  $\alpha$  antagonistic effects of the (+) enantiomer. The administration of the racemate results in the overall  $\beta_1$  agonism responsible for its activity. Also, (+)-Dobutamine has mild  $\beta_2$  agonist activity, which makes it useful as a vasodilator. Dopamine can also be used in infusions to stimulate dopaminergic receptors; it causes vasodilation of renal arteries and enhances norepinephrine release resulting in increased  $\beta$ -adrenergic receptor activation in the heart.[80,81]

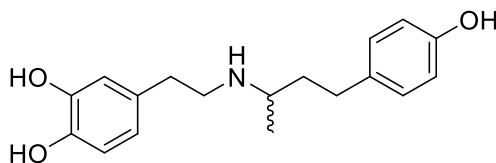


Figure 33: Chemical structure of dobutamine.

From a theoretical point of view,  $\beta$ -adrenergic agonists would improve the contractile function and diastolic relaxation, but clinical trials have demonstrated increased adverse events when administered chronically to heart failure patients. In contrast, in the late 1990s,  $\beta$ -adrenergic antagonists proved to improve symptoms, exercise tolerance, and mortality. However, this is only indicated in cases of compensated, stable CHF; in cases of acute decompensated heart failure, beta-blockers will cause a further decrease in ejection fraction, worsening the patient's current symptoms.[82,83]

Different hypotheses were made on their mechanism of action, including prevention of the excessive and sustained activation of the  $\beta$ -adrenergic system, which appears to be counterproductive because of elevated left ventricular stress or the decrease in renin secretion, which in turn reduces the heart oxygen demand by lowering the extracellular volume and increasing the oxygen-carrying capacity of the blood. Bisoprolol, carvedilol, and sustained-release metoprolol are particularly indicated as adjuncts to standard diuretic therapy in congestive heart failure, although at doses typically much lower than those designated for other conditions.[84,85]

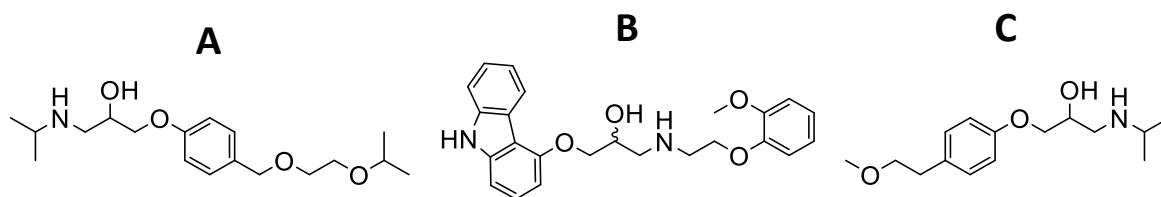


Figure 34: chemical structure of A) Bisoprolol. B) Carvedilol. C) Metoprolol.

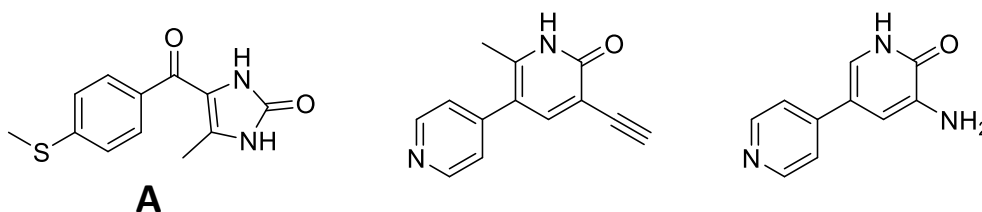
## 12. Inotropic agents

Among the different therapies, agents that alter the force of the muscular contraction find intensive use for the treatment of heart failure. In detail, a positive inotropic agent is a molecule able to increase the strength of heart contraction.[86,87]

In principle,  $\text{Ca}^{2+}$  itself could be considered an inotropic agent, since its variation in concentration in the cardiomyocyte cytosol strongly affects the force of contraction. Many positive inotropic agents act with different mechanisms to raise calcium concentration during the plateau phase of the action potential. The mechanisms are classified in different categories: A) increase 3'-5'cyclic adenosine monophosphate (cAMP) levels; B) interaction with sarcoplasmic reticulum receptors; C) increase of cellular calcium sensitivity; D) combination of the above mechanisms. [88]

For example,  $\beta$ -adrenergic drugs discussed in the previous section, are classified as positive inotropic agents. In fact, besides their activity as vasodilators,  $\beta$ -receptor signaling increases the cyclic adenosine monophosphate (cAMP) levels. cAMP acts as a secondary messenger molecule, able to activate protein kinase A, thus triggering a series of events leading to a release of calcium from the sarcoplasmic reticulum.[89]

Other classes of positive inotropic agents, with a similar mechanism, are the Phosphodiesterase-3 Inhibitors (PDE3), like Enoximone, Milrinone, and Amrinone. cAMP undergoes a physiological degradation to the 5'-adenosine monophosphate by the action of Phosphodiesterase-3. Inhibition of PDE3 increases the cellular levels of cAMP, leading to a higher calcium concentration.[90]



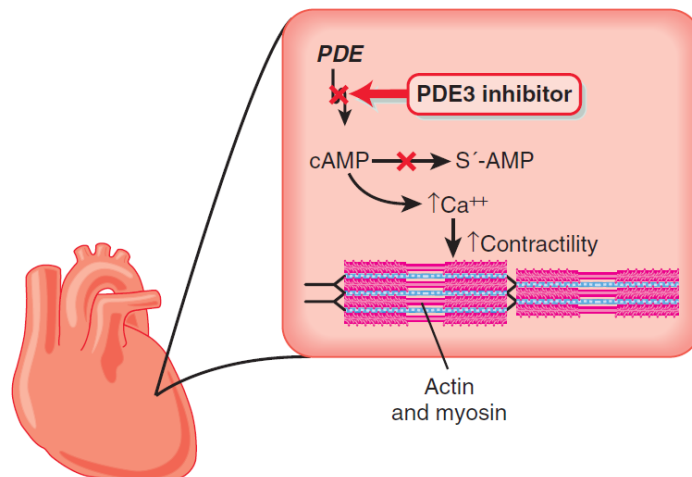


Figure 35: A) Enoximone. B) Milrinone. C) Amrinone. D) Inotropic mechanism of PDE3 inhibitors.

Calcium sensitizers, like Levosimendan, are a rising class of pharmaceuticals for the treatment of HF, able to enhance contractility by sensitizing cardiac myofilaments to the  $\text{Ca}^{2+}$  without raising its intracellular concentrations. In fact, by binding in a calcium-dependent manner to troponin C, these molecules stabilize the conformation of troponin C itself needed to trigger muscle contraction. Remarkably, the great advantage is the achievement of a better contraction without rising calcium levels, which could result in side effects, as will be discussed later on.[91,92]

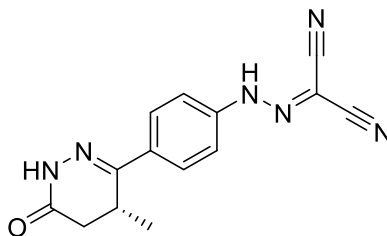


Figure 36: Chemical structure of levosimendan.

### 13. Cardiac glycosides

Cardiac glycosides, or digitalis compounds, are one of the foremost classes of inotropic drugs for the treatment of HF. These compounds share many general features, first among all, the same mechanism of action.[93]

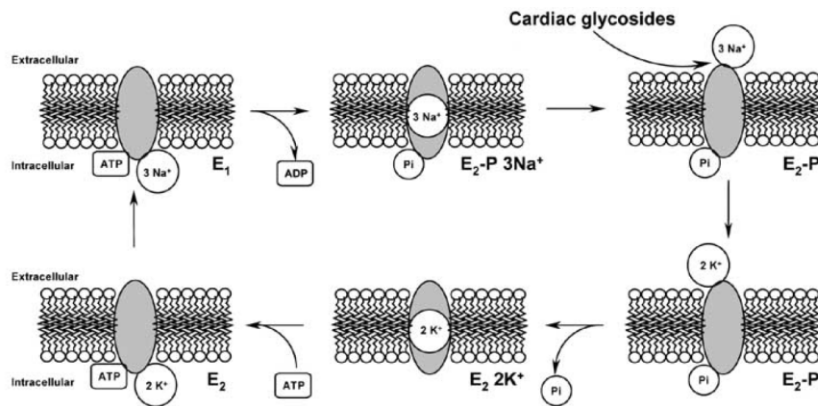


Figure 37: The mechanism of action of the cardiac glycosides

The general chemical structure of these compounds is a classical steroidal core composed of three cyclohexane rings fused with a A/B cis B/C trans junction and a cyclopentane ring fused with a cis C/D junction. The steroids share a hydroxyl group in position 3 glycosylated with a variable number of sugars. Position 17, instead, could bear different functional groups from ketones to furans.[94]

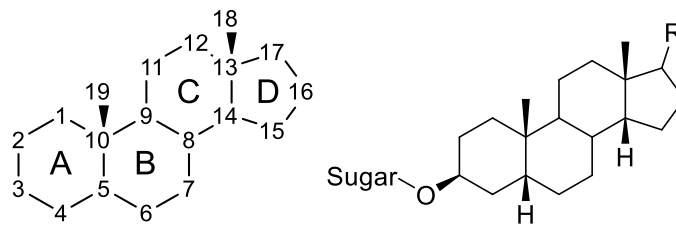


Figure 38:A) Steroidal skeleton with its enumeration. B) General structure of cardiac glycosides.

As said, these compounds have the same mechanism of action, which involves the inhibition of the Na<sup>+</sup>/K<sup>+</sup> ATPase. As stated in the previous section, Na<sup>+</sup>/K<sup>+</sup>-ATPase is a membrane protein involved in the maintenance of cellular homeostasis, keeping constant the Na<sup>+</sup> and K<sup>+</sup> gradients across the membrane by active transport of ions coupled with ATP hydrolysis. Inhibition of the pump causes an accumulation of Na<sup>+</sup> in the cell cytosol triggering a secondary control mechanism of sodium operated by the NCX. The Na/Ca exchanger responds to the rising sodium concentration by starting to expel Na<sup>+</sup> from the cytosol and introducing Ca<sup>2+</sup> instead. The final result is a higher concentration of Ca<sup>2+</sup> available to activate the contraction of the cardiomyocyte.[95,96]

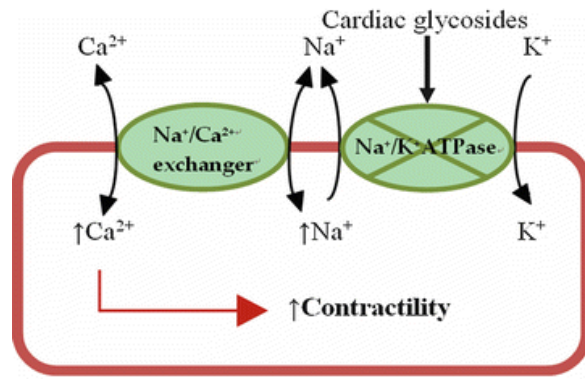


Figure 39: The inotropic effect of cardiac glycosides.

Digitalis compounds were first described back in 1785 by Withering, an English botanist, who observed the therapeutic effects of foxglove in the treatment of edema. Nowadays, digitalis are still the most prescribed drugs for the treatment of congestive heart failure, due to their positive inotropic effect; such therapeutic activity explains their denomination as cardiac glycosides.

Among all the glycosides, Digoxin, sold with the commercial name of Lanoxin, was the first drug for HF approved by FDA in 1954 and is the principal drug used for the chronic treatment of HF, achieving the 168<sup>th</sup> position as the most commonly prescribed medication in the United States, with over three million prescriptions per year.[97,98]

Digoxin is historically obtained by extraction from *Digitalis purpurea* (foxglove) and *Digitalis lanata*. Its structure follows the general cardiac glycosides ones, with a cis/trans/cis steroidal skeleton, an  $\alpha\beta$ -unsaturated lactone in position 17, a 14 hydroxyl group, and the 3-hydroxy group glycosylated to three non-conventional sugar known as D-digitoxose (2,6-Dideoxy-D-Ribopyranose). While the first three moieties are essential for the inotropic activity, the oligo-glycoside is responsible only for the pharmaco-kinetic of the compound. Digoxin can have beneficial effects in alleviating symptoms, improving exercise tolerance, and reducing hospitalization, while performs no impact in reducing mortality.[99]

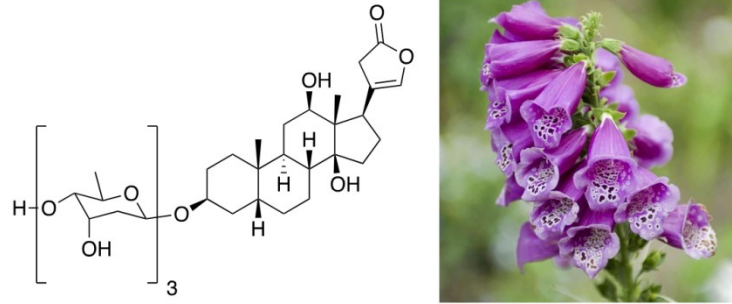


Figure 40:A) Chemical structure of Digoxin. B) *D. purpurea* (foxglove).

Like many other digitalis compounds, digoxin acts as a competitive inhibitor of the sodium-potassium ATPase. Recent studies elucidated the crystal structure of different cardiac glycosides-Na/K ATPase complex, including the one with digoxin. The studies show that the molecule binds to the E2-P state in an extracellular site, with the hydrophobic core located in the pump cavity and the sugar toward the extracellular environment. The binding of the steroid causes a conformational change, stabilizing the E2-P form, thus inhibiting the K<sup>+</sup> dependent dephosphorylation and the course of the catalytic cycle. [95,100,101]

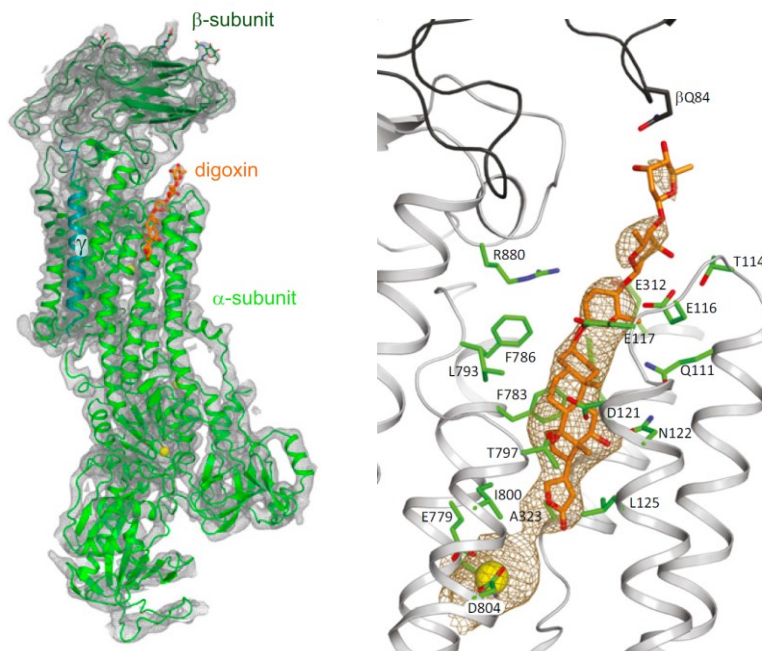


Figure 41: High resolution image of digoxin (orange) in the E2-P state of Na/K ATPase[101]

Another important cardiac glycoside is ouabain. The molecule was first characterized by the French chemist Léon-Albert Arnaud in 1882. Ouabain is extracted from eastern Africa plants, as *Acokanthera schimperi* and *Strophanthus gratus*, and is traditionally used by natives as an arrow poison. The chemical structure is close to the one of digoxin, with cis/trans/cis steroidal skeleton, an ab-unsaturated lactone in position 17, and the 3-hydroxy group glycosylated. Differences are in the number of hydroxyl groups across the steroidal skeleton that are 5 and the sugar glycosylated to position 3, in this case, L-rhamnose. [102,103]

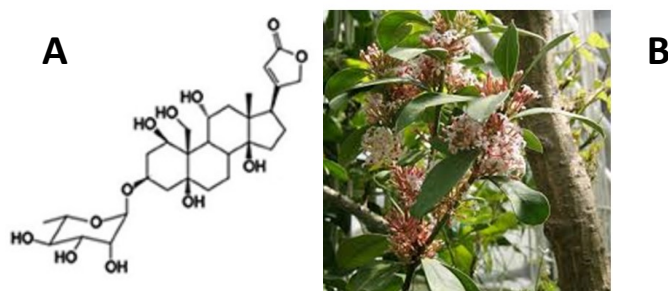


Figure 42: A) Structure of ouabain B) *A.schimperi*.

In lower doses finds application medically to treat hypotension and some arrhythmias, and to control ventricular rate in the treatment of chronic atrial fibrillation. Like digoxin, ouabain inhibits the Na/K ATPase with high potency. Also, acts on the electrical activity of the heart, increasing the slope of the depolarization phase, shortening the action potential duration, and decreasing the maximal diastolic potential. [104] Ouabain, or a closely related isomer, was identified as the endogenous sodium pump inhibitor. This endogenous ouabain (EO) circulates at subnanomolar concentrations and showed implications in hypertension development as well as alterations of sodium reabsorption in the kidney and renal and cardiac complications.[105–107]

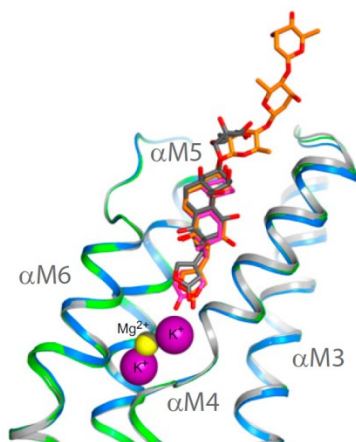


Figure 43: Overlap of digoxin (orange) and ouabain (blue) in the typical digitalis pocket of E2-P state of Na/K ATPase[101]

Remarkably, the two compounds were first characterized as highly poisonous substances. If more than 30% of the Na/K ATPases in the membrane are blocked, the potential is lowered due to the high difference of Na<sup>+</sup> concentration inside the cell and K<sup>+</sup> concentration outside the cell. This condition leads to spontaneous activity. Also, the over intracellular accumulation for long periods of Ca<sup>2+</sup> caused by the reversal action of NCX, could lead to arrhythmic situations, in which the heartbeat is not regular.

The extremely high potency of digitalis drugs reflects in a low therapeutic index, in other words, they have a small gap between the active concentration and the toxic one. Also, despite the improvement of the patient conditions and a lowering hospitalization, digitalis glycosides are not capable of lowering the mortality of the disease. Although the incidence and severity of digitalis intoxication are decreasing, vigilance is necessary to avoid disturbances of conduction and cardiac arrhythmias.

For this reason, some decades ago started the search for safer inotropic digitalis agents, lacking the arrhythmogenic effect typical of this class of compounds. The studies involved the replacement of the unsaturated lactone with different heterocycles,  $\alpha,\beta$ -unsaturated acyclic substituents, or saturated acyclic substituents. These substitutions led to several compounds, which in most cases maintained a satisfying degree of affinity to the Na/K pump, but were usually less potent than the original glycosides.[108–110]

During the years, many efforts were done over the steroidal ring structure. For example, the 14  $\beta$ -hydroxyl groups were replaced. However, this substitution caused a reduction in the binding affinity of about two orders of magnitude.[111] Another example involves the change in the stereochemistry of the junctions between the steroidal rings A/B. The first molecule obtained with a trans junction was the compound called Uzarigenin. Likewise, the compound called Canarigenin was synthesized by the creation of a double bond in position 4, removing the junction stereochemistry. Despite the notable modification of the shape of the molecule, the two compounds maintained the activity of the cardiac glycosides.[112]

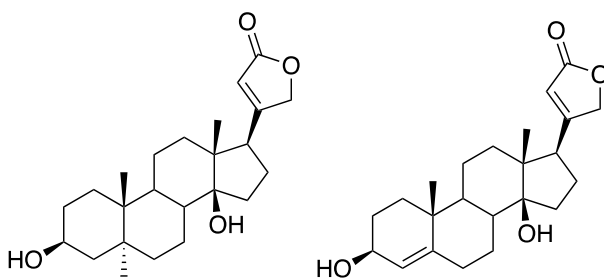


Figure 44. Structures of A) Uzarigenin. B) Canarigenin.

An important step forward was produced by the replacement of the unsaturated  $\gamma$ -butyrolactone moiety with different heterocycles or saturated chains. Indeed, since the early 1970s and long before the X-ray structures, it was generally known that the key functional group for inotropic activity was the unsaturated lactone itself.[113]

One of the most exciting results was the development of a very potent antihypertensive agent with a novel mechanism of action. This molecule known as Rostafuroxin can counteract the effect induced by the endogenous ouabain, discussed above, acting as an antagonist on its receptor, placed on the Na/K ATPase. In this way, the drug counteracts the effects of ouabain on blood pressure regulation. This compound is now in Phase II clinical trials.[114,115]

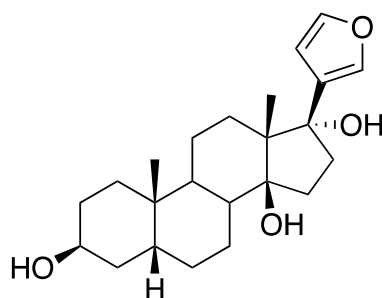


Figure 45: Structure of rostafuloxin.

#### 14. Istaroxime

The great interest in finding new molecules able to induce inotropic effects gave great pulse to the identification of a large number of structures, both natural and synthetic, able to interact with the Na/K ATPase. At the same time, the high toxicity of the cardiac glycosides pushed the research toward the study of new, safer, and more effective mechanisms of action.[116–118]

The Janus role played by calcium at intracellular levels, by stimulating the contraction and causing toxic effects, led to increasing interest over SERCA2a activators. These molecules could be promising drug hits that might improve overall cardiac function in HF with reduced arrhythmogenic risk. [119,120] Various therapeutic approaches that increase the SERCA2a function have been recently investigated. Small-molecule SERCA2a activators drug hits were recently discovered. Pyridone derivatives have been developed that directly bind to PLN, thus displacing it from SERCA2a interaction.[121]

Cassaine, similarly to ouabaine, was discovered in 1935 from the extract of the African plant of *Erythrophleum guineense* used commonly as arrows poison by African tribes.[122] Despite its classification as cardiac glycoside and its typical action of inhibiting Na/K ATPase, cassaine does not have chemical similarity with previously described molecules. In particular, the A/B junction has a trans configuration; the sugar glycosylation in position 3 is absent, and instead of the five-membered D ring is presents an unsaturated ester chain.[123,124]

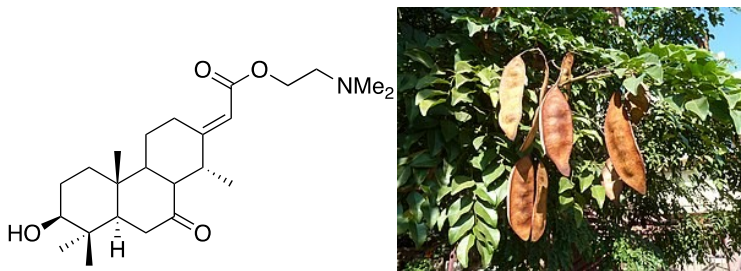


Figure 46: A) Structure of cassaine. B) *E.guineense*

Starting from this unique structure, in 2003, a new molecule was formerly patented and developed by the Italian pharmaceutical company Sigma-Tau. This molecule, called Istaroxime, is a compound capable of exploiting an inotropic effect by Na/K pump inhibition, but, at the same time, stimulates the relaxation of the heart by its lusitropic properties. [125]

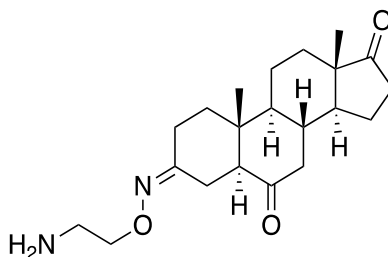


Figure 47: Structure of istaroxime.

Istaroxime was strongly inspired by the structure of cassaine. However, the significant change of many functional groups, like the presence of an oxime group, further reinforces interaction with the enzyme. Despite its inotropic activity is related to the Na/K inhibition, with similar potency of digoxin, this molecule lacks the typical side and toxic effects of that molecule. Istaroxime, in fact, can stimulate SERCA-2a, leading to rapid sequestration of cytosolic calcium into the sarcoplasmic reticulum during diastole and thereby promoting myocardial relaxation.[126] Even though it is still not clear the mechanism of this stimulation, it contributes to increased contractility as the greater calcium uptake in the sarcoplasmic reticulum allows the release of a higher amount of calcium at the subsequent systole with increased contractility. The molecule is now in the clinical phase for the treatment of HF, where proved its desirable safety profile, with no appearance of arrhythmias or ischemic events.[120,127,128]

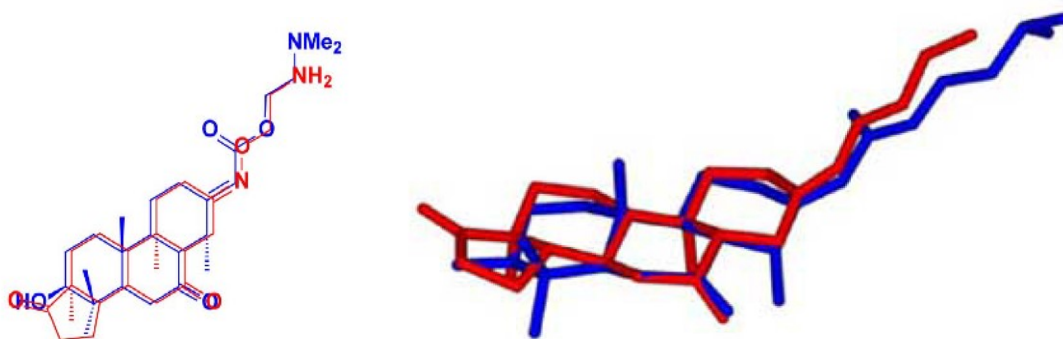


Figure 48: 2D and 3D structure overlap of istaroxime (red) and cassaine (blue).

Since calcium cycling plays a central role in myocardial function and Istaroxime appears to have a favorable effect on calcium cycle modulation, this compound is defined a luso-inotropic agent which is promising for the treatment of HF due to its unique mechanism of action.[96,129]

Despite the excellent pharmacodynamic profile, Istaroxime is not optimal for chronic administration because it has poor gastro-intestinal absorption, high clearance rate and contains the oxime group moiety that might undergo metabolic transformation leading to possible genotoxic moiety (hydroxylamine).[130] Istaroxime therefore, has been developed for intravenous infusion in hospitalized patients with HF only and its administration requires trained medical personnel.[131]

### 15. Electrospun nanofibers for the delivery of cardiac drugs

Pharmaceutical research of new drug candidates is one of the most challenging tasks for academics and industries.[132] It is estimated that in 2018 pharmaceutical industries spent 179 billion dollars globally for research and development of new pharmaceuticals.[133] However, approximately only 11% of new candidates have the probability of reaching the market.[134] The most common failure appears during phase II clinical trials, were most drug candidates show previously unknown toxic side effects or insufficient efficacy to treat the medical condition being tested.[135] For example, despite the unique and promising actions of istaroxime, the success of this drug will be strongly affected by its toxic metabolite and its poor gastro-intestinal absorption.

During the past few decades, it became clear that the method of delivery influences the therapeutic benefit of a drug, affecting numerous factors, including pharmacokinetics, distribution, pharmacodynamics, and metabolism as well as toxicity.[136]

This observation, united at discovery of nanotechnologies, such as nanoparticles, nanofiber, nanogels, micelles, and microspheres, led to the development of new approaches like drug delivery systems. Such systems became a new and promising tool in the pharmaceutical research, and a valuable alternative to development of new molecules.[137] Nanotechnologies can be used to wrap and deliver pharmaceuticals that are too toxic, insoluble, rapidly cleared, or unstable as free molecules by passive or active targeting strategies based on the final formulation.[138,139]

In particular, nanofibers produced with bio-degradable and bio-compatible polymers gained increasing interest due to their broad flexibility, effectiveness and the unique physicochemical properties such as a large surface area, small diameter, and high aspect ratio.[140,141] Also, targeted in-situ application of nanofibrous scaffolds could minimize the disadvantages of systemic perfusion, like the first-pass metabolism, typical of the free drug or other drug delivery system injection, and on the other hand, maximize the action of the active pharmaceutical by a controlled and sustained release directly at the site of action.[142] For instance, a nanofibrous scaffold can reduce the threat of antibiotic-resistant bacteria and multi-drug resistance in cancer therapy by site-specific, dose-specific and timed release of different types of drugs.[143–145]

Another great advantage is given by the similarity of the fibers with the natural fibrillary extracellular matrix (ECM), which facilitates cell attachment and proliferation for biomedical applications.[137,141] During the years, electrospinning proved to be one of the most cost-effective, simple and flexible fabrication technique in the choice of polymer techniques for the production of nanofibers.[146] Electrospinning consists in the application of a high voltage electrostatic field to a suitable polymer solution flowing through a needle. A specific feature of the final electrospun fiber is that structural design parameters such as porosity, morphology and surface area could be tuned easily by modification of the environmental and processing conditions, according to the specific requirements for the delivery conditions.[140]

Drugs can be incorporated in the fiber by different approaches. Starting from a direct blending between the drug and the polymer solution, a surface immobilization after the spinning process, or by using an emulsion, each of them provides a different profile of drug release. A large variety of drugs has been successfully incorporated into electrospun fibers from small molecules to proteins and nucleic acids. More sophisticated devices are also able to deliver multiple drugs with synergistic effects or to selectively tune the release of the incorporated drug in response of specific stimuli.[147]

The purpose of this review is to give an overview of the possible approaches of electrospinning for drug delivery purposes by giving an insight into the different techniques and field applications.

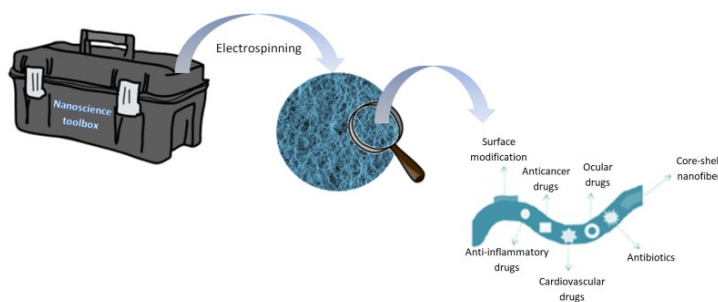


Figure 49: Nanofibers for drug delivery.

## 16. Electrospinning

Electrospinning uses an electrostatic potential characterized by high voltage and very low current for creating ultrafine fibers. Historically, the first observation of an electrospinning process for such purpose was in 1902 by J. F. Cooley who patented the technique with the name of “Apparatus for electrically dispersing fibers”. [148] The popularity of electrospinning raised during the end of the 20th century when many publications started to appear and continue today, where many applications for electrospun fibers, such as drug delivery [149–151], wound healing [152,153], tissue engineering [154,155], textiles [156] as well as sensors [157], cosmetics [158] and food packaging [159] are studied.

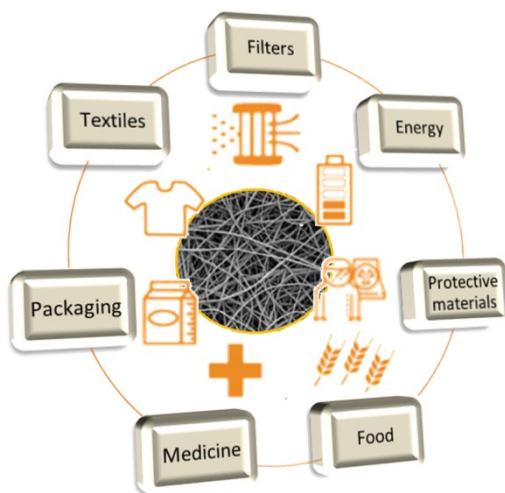


Figure 50: Fields of application for electrospun nanofibers.

The overall process is carried out by using a polymer solution or directly a melted polymer. The polymer must be pumped through a spinneret (usually a syringe needle), to which a high voltage is applied. The applied voltage induces a charge movement in the polymer liquid, disrupting the shape of the pendant drop, normally a sphere formed by the surface tension, into a conical shape known as a Taylor's cone. If enough cohesive force exists in the polymer liquid, a stable jet is ejected from the Taylor's cone, allowing the polymer chains to stretch each other and forming a uniform filament. The process is accompanied by the evaporation of the solvent causing a vigorous whipping of the formed filament.[152,160] Fibers deposition occurs over a grounded metallic collector, usually formed by a simple aluminum foil, placed at optimized distance.[148] In this system, fibers are collected with random orientation.

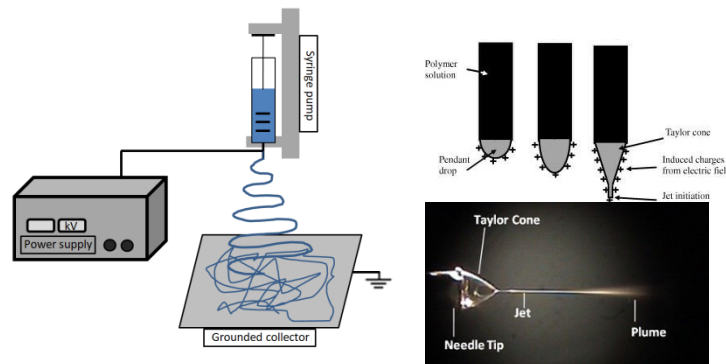


Figure 51: A) Schematic representation of an electrospinning apparatus. B) The formation of the Taylor cone.

## 17. Fiber features

For each different application, nanofibers need to fulfill specific requirements in terms of mechanical properties, hydrophilicity, morphology and biocompatibility. The chemical composition of the fiber, namely the polymer structure, governs most of these features. The polymer, for example, influences the release rate of a loaded drug and the duration of the treatment, due to its: 1) swelling in water, 2) affinity with the drug, and 3) degradation rate. Also, polymer molecular weight influences some of the physical features of the fiber, as for instance its thickness.[150]

The outcome of the electrospinning process is governed by three different categories group the parameters able to influence the formation and the morphology of the final fibers. In most cases, the

desired outcome of the electrospinning process is smooth, uniform, and bead-less nanofibers this result is achieved by a fine-tuning of all the parameters. Indeed, ambient, solution and processing parameters are independent variables capable of cooperating to affect every single feature of the final fibers.

Processing parameters are relative to the mechanical setup of the electrospinning machine, including voltage applied, flow rate, needle-to-collector distance and geometry of the collector. Voltage controls the jet initiation. Usually, at least 6 kV are required to initiate the process. A rise in the voltage causes greater electrostatic interaction in the charged solution leading to thinner fibers.[161] The flow rate of the polymer solution has a great effect on the uniformity of the fibers. Generally thinner fibers production takes place at lower flow rates. An increase in flow can increase the fiber diameter; however, too high flow rates lead to beaded fibers.[162]

Another parameter of great importance is the distance between the needle and the collector. Even though a minimum distance is mandatory for the initiation of the process, an excessive distance gives rise to beads and non-uniform fibers.[161]

Depending on the final application of the fiber, different types of collectors could satisfy different needs. Flat surfaces are the most common and simple collectors, usually, an aluminum foil is used. Varying the geometry in favor of more sophisticated ones enables the production of aligned fibers or 3D structured fibers. Some examples are rotating mandrel, dual collection ring, water bath, moving platform and helical spring.[163]

Solution parameters include concentration, viscosity, volatility and dielectric constant of the solvent. Concentration and viscosity are proportional: higher the concentration, higher the viscosity of the solution.[164] Optimizing concentration and viscosity allows the polymer to flow through the nozzle and being spinnable. Moreover, higher concentration forms greater diameter. [165] Meanwhile, a high viscosity enables the formation of beadless fibers, yet, increasing too much the solution viscosity results in beads formation.[166]

Solvent parameters play a key role in the formation of better fibers; a wise optimization could extremely facilitate the whole process. The dielectric constant and volatility, in particular, strongly contribute to the formation of beadless fibers. Solvents with higher dielectric constant such as acetic

acid, acetone or hexafluoroisopropanol (HFIP) reduce the fiber diameter and increase the deposition area, due to rising in bending instability of the electrospinning jet.[165] Meanwhile, higher volatility is associated with higher fiber porosity.[165]

Ambient parameters are the most complex to control due to their nature. This category includes temperature and humidity. Both parameters contribute to governing of the solvent evaporation rate. At the same time, the temperature affects the viscosity and the dimension of the fibers: higher temperature lowers solution viscosity, causing higher stretching in the process and thinner fibers.[167] Humidity affects the porosity of the final scaffold: in the presence of high humidity rates. The evaporative cooling caused by the solvent leads to the condensation of water over the surface of the fiber contributing to rising the porosity.[168] In the table 1, the effect of the different working parameters on the fiber morphology are summarized.

Table 1: Parameters affecting the electrospinning process.

Parameter		Effect
Processing parameters		
Voltage	↓	No fibers formation
	↑	Fiber diameter decrease
Flow rate	↓	Fiber diameter decrease
	↑	Beaded fibers are formed
Distance needle-collector	↓	No fiber formation
	↑	Non uniform beaded fibers are formed
Collector	Type of the collector controls fiber alignment and 3D structure	
Solution parameters		
Concentration	↓	if too low sputtering can happen Fibers formation with higher diameter and less
	↑	beads. If too high nozzle clogging can be observed

Viscosity	↓	Finer and shorter nanofibers
	↑	Ticker and continuous nanofibers. If too high, beads and nozzle clogging are observed
Solvent parameters		
Volatility	↓	Difficult removal of the solvent
	↑	High porosity and surface area
Dielectric constant	↓	Beaded fiber are formed
	↑	Fiber diameter decrease
Ambient parameters		
Temperature		Temperature affects viscosity and solvent evaporation rate. Higher temperature means lower viscosity and more efficient is evaporation of solvent.
Humidity		Humidity affects solvent evaporation rate. In addition, at higher humidity porosity increases

### 18. Drug loading in the fiber

The incorporation of drugs in the electrospun fibers is carried out by different techniques. Drug loading heavily affects the drug release profile, making the correct choice over the best loading method for the desired application essential.[169] The simplest approach is the direct blending between the polymer and the drug by the dissolution of the two components in a suitable solvent. Blending has the highest loading rate compared to other techniques. The strength of the polymer-drug interaction will govern the release profile together with the drug solubility properties. Balancing hydrophobicity of drug and polymer is a crucial task for constant release over a defined time window.[170] The drawbacks of this technique are associated mainly with the presence of the organic solvent, often capable of denaturing bioactive molecules. Moreover, a burst release of the drug generally is observed.[171]

Emulsion electrospinning gives a possible alternative, enabling the formation of core-shell nanofibers by encapsulation of the drug inside micelles. Usually, the formation of drug-containing micelles occurs by addition of a supernatant to a water solution of the drug itself. Vigorous mixing of the so formed

micelles with an oil solution of the polymer form a stable emulsion suitable for electrospinning. The advantages are mainly two: the first is a minimized contact of the bioactive molecule and the organic solvent, allowing the use of various combinations of hydrophilic drugs and hydrophobic polymers; the second advantage is due to the easy formation of uniform core-shell structure without the use of specific coaxial apparatus. [172,173]

Another alternative for core-shell nanofiber formation is coaxial electrospinning. Despite the other loading methodologies, this technique requires a specific apparatus. However, it does not only give an infinite combination of polymers for the core and the shell, but can be a modular platform for the loading of different drugs in different compartments of the fiber. Also, the coaxial loading of a single drug gives the great advantage of inserting the drug in the core polymer with the presence of the shell acting as a physical barrier preventing a burst release. Disadvantages consist of the difficulty of optimizing parameters and the difficult scalability of the technique. [174,175]

Another approach for drug loading involves surface immobilization of the bioactive molecule after the electrospinning process. Thus, it is possible to avoid every contact between the active molecule and the organic solvent, preventing any undesired degradation. Another advantage is the preservation of the original degradation and mechanical properties of the polymeric matrix. [176,177] However, achieving a longer release over time requires strong non-covalent bonding between the polymer and the drug and usually a cross-linking process. [178]

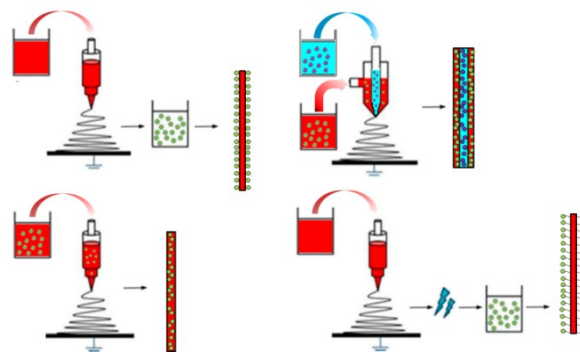


Figure 52: Schematic representation of different approaches for the drug loading. A) Physical absorption after the electrospinning. B) Blend solution between drug and polymer. C) Coaxial electrospinning. D) Chemical surface modification after the electrospinning process.

## 19. Electrospun nanofibers for cardiovascular tissue engineering

As said, nanofibers can be a striking tools for the local delivery of molecules in the heart tissue. Also, this powerful tool could be used for inducing tissue regeneration at the damaged myocardium. For their intrinsic features, electrospun scaffolds have a great affinity with the ECM, which facilitates cell attachment and proliferation for biomedical applications. [135,139].

In general, the biomaterial used for biomedical applications should possess specific features like the biocompatibility of the material, which should not be toxic or cause side effects with its metabolite, being completely biodegradable. To access the possibility of using these tools for repairing the damaged myocardium, the material must possess high mechanical stability. In other words, should be able to withstand stress without failure, to protect and contain the seeded or recruited cells. [179]

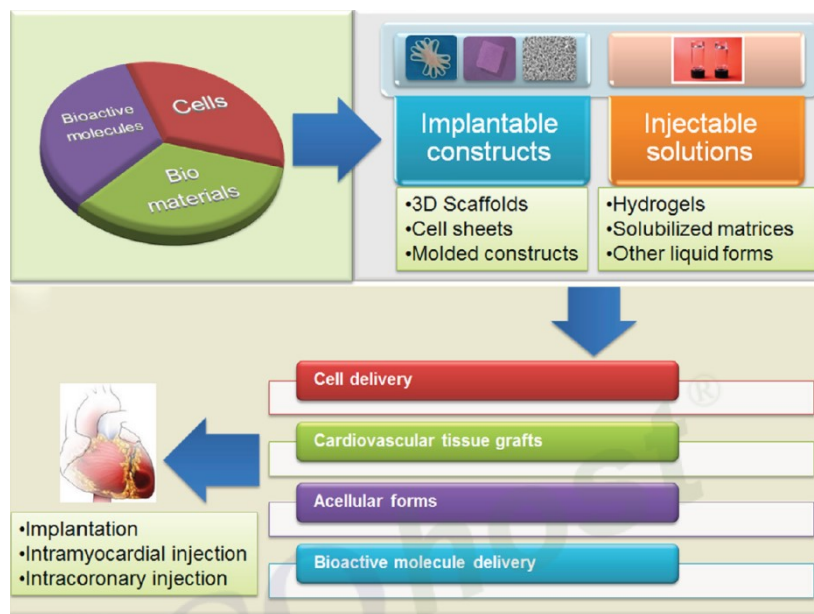


Figure 53: Different application and strategies for the use of biomaterials in cardiac regeneration devices. Electrospun nanofibers are used as implantable constructs, capable of inducing tissue regeneration.

Electrospinning allows the creation of a macroporous structure, which is characterized by a large pore size and matrix porosity. These features affect positively the vascularization of the device after its implantation. Moreover, this architecture is optimal for the cell organization in the tissue.

To induce the regeneration of scar tissue, formed after myocardial infarction, heart patches have to mimic as more as possible the functional and morphological proprieties of the native tissue, to be integrated into the heart and develop systolic force, as well as form electrical and functional syncytium with the host myocardium. In this context, aligned nanofibers could efficiently support the seeding and the regeneration of the tissue.[179]

## 2. Aim of the work

The importance of finding new drugs for the treatment of heart failure remains one of the most challenging tasks of the pharmacological industry. The mortality of this disease and its spreading among the population gives additional pulse toward the identification of new mechanisms of action, able to stimulate an efficient contraction of the cardiac muscle, without the rising of severe side effects.[61,62]

Indeed, istaroxime has the great advantage among other inotropic drugs to act with high potency over the Na/K ATPase, and, at the same time, lacking the common arrhythmogenic and toxic side effects typical of digitalis compounds. Still, the compound has serious drawbacks, mainly related to its metabolites. Also, the fast degradation rate and the low gastrointestinal absorption accentuates those drawbacks.[111]

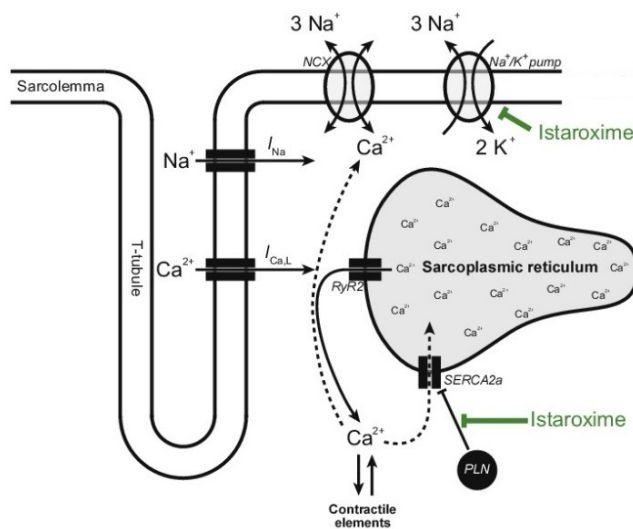


Figure 54: Istaroxime mechanism of action.

To overcome the drawbacks caused by metabolism, required as the first step the identification of the enzymatic reaction involved and their products, making possible the identification of the labile functional groups and their substitution with more stable bioisosteres. Istaroxime is metabolized very likely in the liver. Firstly, the 6-ketone group is reduced by alcohol dehydrogenase. The compound obtained is very similar to the original and still maintains its activity. Then, the molecules undergo oxidation presumably from the cytochrome P450. This reaction transforms the primary amine into a carboxylic acid.

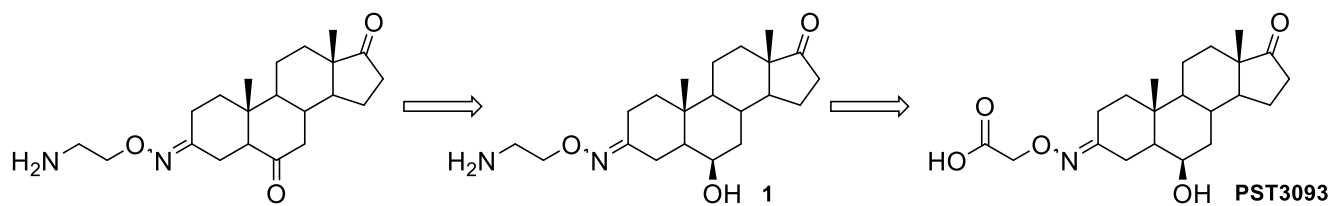


Figure 55: Metabolic transformation leading to PST3093.

Surprisingly enough, the steroid obtained by the two metabolic transformations is still not the toxic derivatives. Although, this molecule, called “PST3093”, does not exhibit any inhibitory action on the Na/K pump, it demonstrated a surprising activity as a pure activator of SERCA-2a. This compound acts as a lusitropy stimulator and is the only example in the literature of a pure SERCA-2a activator, making an interesting case of study and a possible first-in-class drug.

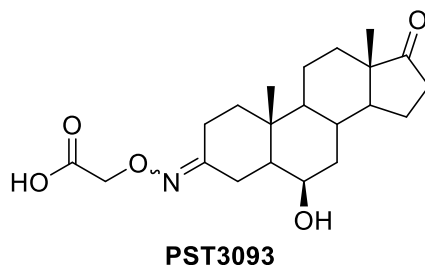


Figure 56: PST3093 structure. The molecule exhibits a pure SERCA2a stimulatory mechanism.

PST3093 is further transformed by metabolism: the oxime moiety is hydrolyzed, resulting in the formation of a carboxyl-hydroxylamine. The latter has high genotoxicity, especially associated with long-term treatment.

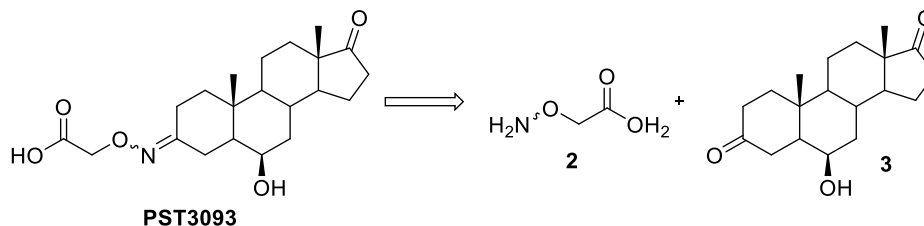


Figure 57: Hydrolysis of the oxime and formation of the toxic metabolite 2.

Istaroxime already proved its potential is being a new and potent tool for the treatment of chronic heart failure, with its incredible potency and unique mechanism of action. Still, various therapeutic

approaches of the past few years identified SERCA2a activators as promising drug hits that might improve the overall cardiac function in HF with reduced arrhythmogenic risk. [180]

Both istaroxime and PST3093, are new and promising candidates for the development of new therapy for improving the survival and the living conditions of patients. For this reason, overcoming the critical limitation associated with the genotoxicity of their metabolite could boost the therapeutical impact and their everyday life application.

Therefore, the aim of this work is divided into three different phases: 1) the identification of metabolically stable PST3093 derivatives with selective activity on the stimulation of SERCA-2a. 2) the creation of new amine derivatives of istaroxime able to retain the double target mechanism lacking metabolic instability. 3) development of a drug delivery system for istaroxime that could reduce the rate of oxidative metabolism, thus improving its therapeutic index.

Our strategy was based on the chemical modification of the labile oxime group in favor of a non-hydrolyzable carbon-carbon bond. To validate our strategy, the first compound synthesized, called CVie209, retaining the exact structure of istaroxime with only the depletion of the metabolically unstable 6-keto and oxime groups. This pilot study demonstrated the retention of the activity of the compound, without the loss of potency.

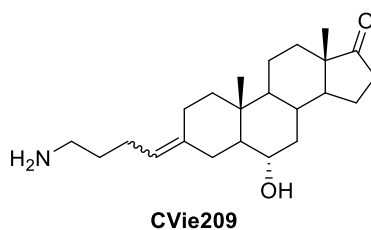


Figure 58: CVie209, the pilot structure of the new class of molecules.

Then, the first task was achieved by chemical modification of PST3093. Since the structure of human SERCA-2a was identified only recently, the approach employed was a structure-activity relationship (SAR) study, to identify the most promising lead compounds.

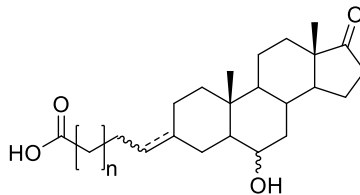


Figure 59: General structure of the PST3093 metabolically stable derivatives.

Similarly, for the amine compounds, retaining the double targeting activity, starting from the structural basis of CVie209 the oxidation of the primary amine into a carboxylic acid was blocked by locking the functional group in a cycle.

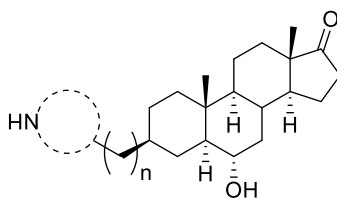


Figure 60: General structure of the istaroxime metabolically stable derivatives.

Still, istaroxime is a phase III investigational drug that showed promising results.[131] For this reason, the improvement of the delivery system could limit the severe side effect caused by the continuous infusion of the drug by a focused release directly at the site of action. The approach adopted was the development of drug delivery devices based on nanofibrous electrospun scaffolds that could combine the advantage of the drug release with an induced regeneration of the damaged myocardium.

## 3. Results and discussion

Despite its promising activity in the treatment of heart failure, Istaroxime, which acts as a lusototropic agent, presents some severe genotoxic side effects due to its final hydroxylamine metabolite. Moreover, his first metabolic transformation leads to the so-called PST3093, which is the only example in the literature of a pure SERCA-2a stimulator.

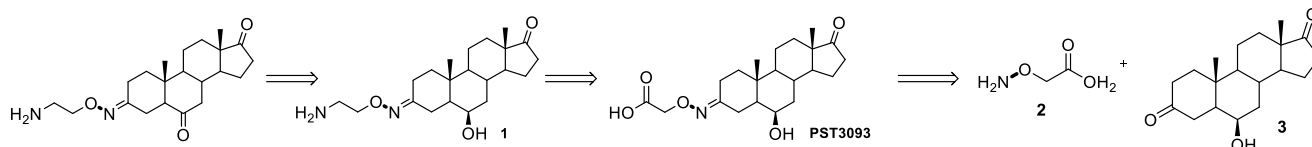


Figure 61: Metabolic transformations of istaroxime.

Istaroxime and PST3093 possess a unique mechanism of action. Our aim was therefore to preserve this unique activity and remove the genotoxicity caused by the oxime metabolite 2. Another target was the possibility of oral administration.

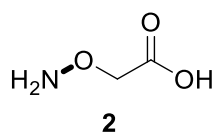


Figure 62: The genotoxic hydroxylamine.

The strategy adopted to avoid the metabolic transformation of istaroxime is based on the chemical modification of the original scaffold, by complete substitution of the oxime functionality with a carbon-carbon double bond (alkene). Istaroxime was originally designed starting from cassaine, in which the oxime group should act as a biological-equivalent to the  $\alpha$ - $\beta$  unsaturated ester of the natural molecule. Moreover, the functionality oxime was found necessary for the activity. [111]

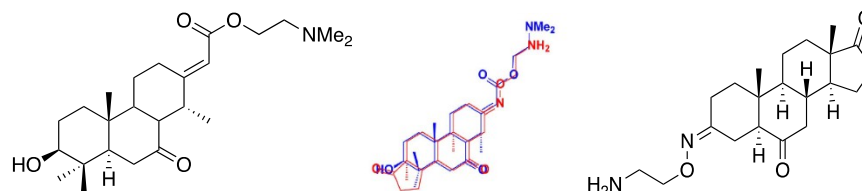


Figure 63: A) Structure of cassaine. B) Superposition of cassaine and istaroxime structures. C) Structure of istaroxime.

On the other hand, the E isomer of istaroxime is 2 times more active than the Z isomer. However, the low rotational energy barrier of oximes leads to the equilibration of the E and Z isomers in a relatively short period. In this case, the presence of a non-isomerizable bond could improve the activity, excluding a possible less-active contaminant. [125]

### 1. Design of non-toxic istaroxime analogues

For this reasons, a pilot study was carried out to validate the strategy chosen, and molecule **4** was synthesized that retains the istaroxime core but the oxime group is substituted by a C-C double bond.

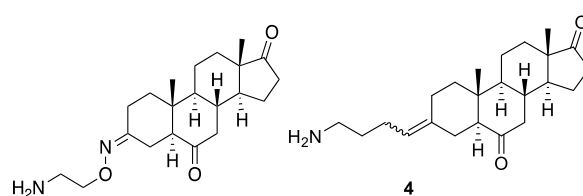
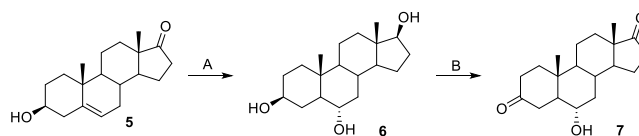


Figure 64: A) Istaroxime. B) The lead structure **4**.

A suitable intermediate to have access to **4**, was identified in the 6- $\alpha$ -3,17 androstenedione **7**, easily obtainable from the dehydroepiandrosterone, commercially called Prasterone **5**. Hydroboration followed by oxidation, as described in De Munari *et al.*, allowed the preparation on a large scale of the desired intermediate.[125]



Scheme 1: Reagents and conditions: A)  $\text{BH}_3$ , THF,  $-20^\circ\text{C}$  then  $\text{NaBO}_3$ ,  $\text{H}_2\text{O}$ . 70%. B) NBS, Dioxane,  $\text{H}_2\text{O}$ , Py. 70%.

The most simple retrosynthetic approach suggests the use of a Wittig reaction, with a suitably protected amine **8**, to obtain the desired C-C double bond of **4**.

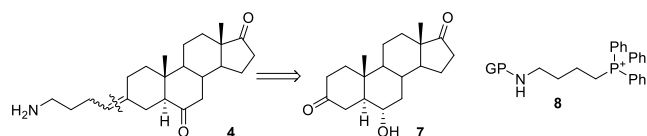


Figure 65: Retrosynthetic approach for the synthesis of the istaroxime follow-on compounds.

However, the intermediate used for the synthesis of the phosphonium salt **8**, tends to cyclise to the protected pyrrolidine derivative **9** in the reaction conditions, forcing us to change the synthetic approach.

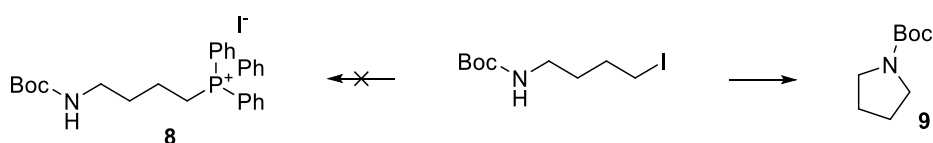


Figure 66: The unwanted cyclization of the intermediate towards **9**.

The second approach involved the use of a cross-metathesis reaction between the suitable protected amine **11** and the exocyclic double bond steroid **10**. **10** can be easily obtained with a Wittig reaction on the diketone **7**, since the 3-keto group of the molecule is less hindered and the more reactive one.

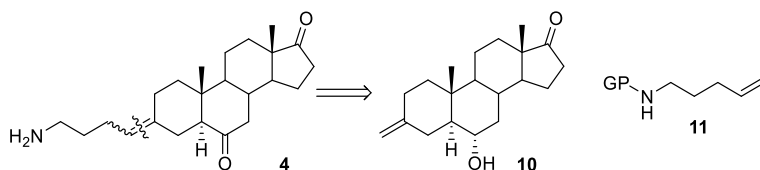
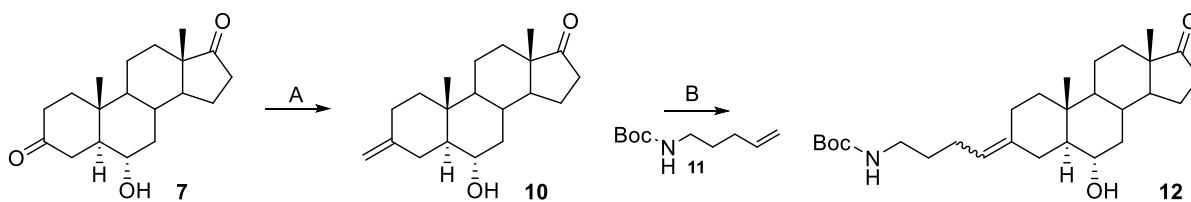


Figure 67: The new retrosynthetic approach.

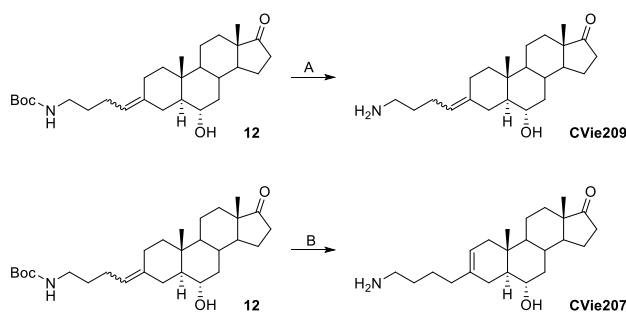
The higher reactivity of mono-substituted double bond respect multi-substituted ones contributed to dramatically drop in the yield over the desired compound **12**. Still, **12** was obtained as a mixture of diastereomers with almost 1:1 ratio.



Scheme 2: Reagents and conditions: A)  $\text{MePPh}_3\text{Br}$ ,  $t\text{-BuOK}$ , THF,  $-10^\circ\text{C}$ . 83%. B) **11**, HG-II, DCM.

For the sake of simplicity, was taken into account the first metabolic transformation, namely the reduction of 6-keto group into alcohol, that gives a derivative with a similar activity of istaroxime itself. For this reason, the intermediate **12** was no further oxidized to its corresponding 6-keto derivatives. **12** exhibited an instability towards acidic treatment, giving the necessity for the identification of a mild protocol for the cleavage of tert-butoxy carbamate.

Two different routes were identified: 1) a rapid treatment with a 1:1 solution of TFA/DCM 2) *in situ* generations of HI by using trimethylsilyl iodide (TMSI) in MeOH. The two procedures proved to be effective in the cleavage without degradation of the products. Still, while the first allowed the isolation of the desired **CVie209** compound, the second cause a migration of the double bond, forming the endo-cyclic double bond derivatives **CVie207**. The different outcomes of the two cleavages can be attributed to the iodine used in the second procedure. Iodine forms reversible bonds with unsaturated compounds; once the interaction is lost, the unsaturation is restored in the more energetic favorable position. In this case, the endo-cyclic bond is more stable than the exocyclic one.



Scheme 3: Reagents and conditions: A) TFA, DCM 1:1. B) TMSI, MeOH.

The preliminary biological test over the two molecules was made only over their inhibitory activity towards the dog renal Na/K-ATPase, to compare the results with istaroxime and validate the approach of the complete depletion of oxime in favor of a carbon-carbon bond.

Table 2: Inhibition of dog renal Na<sup>+</sup>/K<sup>+</sup> ATPase

Compound	IC <sub>50</sub> , μM
Digoxin	0.18
Istaroxime	0.14
CVie209	0.8
CVie207	3.9

Both CVie209 and CVie207 retain their inhibitory activity, even though with lower potency than istaroxime. In particular, while the exocyclic double bond has activity in the same order of magnitude of istaroxime, the endocyclic double bond derivatives lose activity in one order of magnitude. Such experiments highlighted the need of having a chair conformation in the steroidal ring A, instead of a chair-like caused by the endocyclic double bond. At the same time, the data validate the approach chosen.

## 2. PST3093 derivatives: pure SERCA-2a stimulators

The absolute novelty of the mechanism of action of pure SERCA-2a stimulators and their potential impact in the heart failure therapies, suggested the the creation of a chemical library of new compounds derived from the oxidized metabolite PST3093.

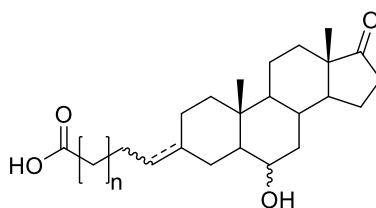


Figure 68: General structures of the PST3093 derivatives.

The cross-metathesis reaction for the synthesis of exocyclic compounds proved to be successful. However, taking into account the low yield caused by the steric encumbrance of the intermediate **9** we decided to explore a different approach for the synthesis of the library. The investigation started with the most simple compounds, retaining the structure of PST3093, but lacking the oxime bond.

Starting from the common intermediate **7**, we decided to employ a Wittig reaction, with the commercial phosphine salt, to obtain the desired products.

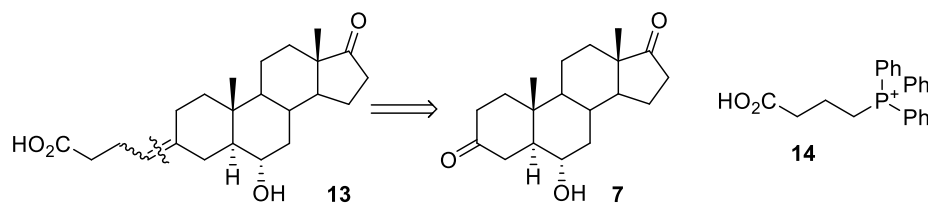


Figure 69: Retrosynthetic approach for the synthesis of the compounds.

In the literature two different possible reaction mechanisms for the Wittig reaction are reported. While the first involves the oxaphosphetane intermediate, the second proceeds through a betaine intermediate. The outcome of these two mechanisms could be extremely different: oxaphosphetane does not allow the rotation of the intermediate; on the other hand, betaine could rotate before the elimination of the phosphine oxide. Thus, two different Wittig reaction-based protocols were developed: 1) by employing the betaine stabilizing system NaH/DMSO 2) by using the LiHMDS and THF through the oxaphosphetane intermediate.[181]

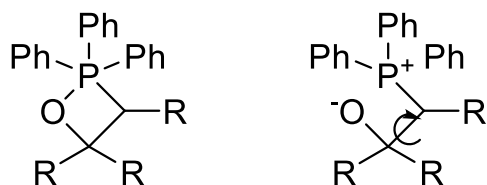
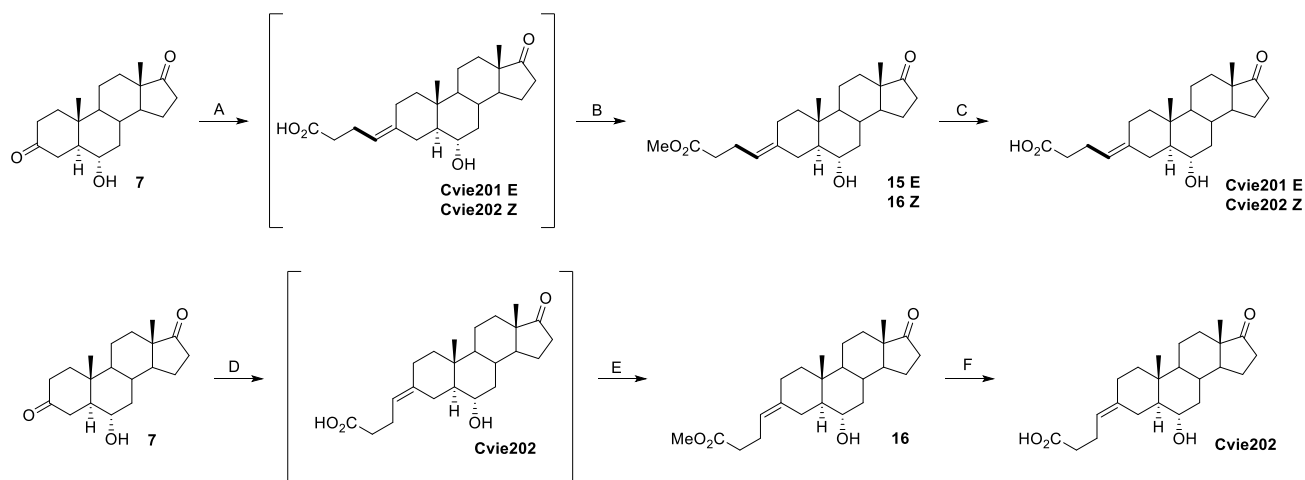


Figure 70: A) The oxaphosphetane intermediate of Wittig reaction. B) The rotatable betaine intermediate of Wittig reaction.

Despite the excellent conversion achieved with the two protocols was necessary transitory derivatization in a carboxylic ester to successfully purify the products from phosphine oxide. Also, such derivatization allowed the separation of different diastereoisomers. As expected, we obtained two different outcomes for the two different conditions used. In particular, the stabilization of oxaphosphetane leads only to the Z diastereoisomer. On the other hand, the presence of a non-cyclic intermediates leads to a mixture of E and Z diastereoisomers in a ratio E/Z 1/2.



Scheme 4: Reagents and conditions: A) NaH, (3-Carboxypropyl)triphenylphosphonium bromide, DMSO. B) EDC, MeOH. 2 step yield 20%, E:Z 1:2. C) aq. LiOH 1M, THF, H<sub>2</sub>O. E 31%, Z 54%. D) LiHMDS, (3-Carboxypropyl)triphenylphosphonium bromide, THF. E) EDC, MeOH. 2 step yield 72%, E:Z 0:10. F) aq. LiOH 1M, THF, H<sub>2</sub>O. 90%.

The two compounds, named **CVie201** and **CVie202**, were isolated, characterized, and the double bond configuration assigned with 2D-NOESY experiments. Biological tests showed no activity over the Na/K-ATPase, still an excellent activity as SERCA-2a stimulators with similar behavior of the original PST3093. Unfortunately, the principal diastereoisomer formed with the Wittig reaction proved to be the less active in the SERCA-2a stimulation, with a potency about half the potency of the more active one.

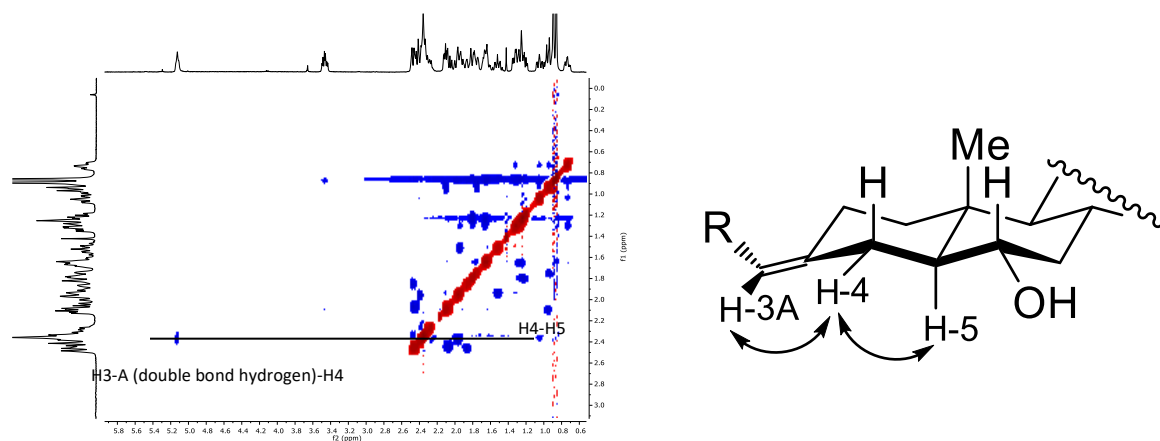


Figure 71: NOESY experiment for the determination of CVie201 configuration.

Table 3: Inhibition of dog renal Na<sup>+</sup>/K<sup>+</sup> ATPase.

<b>Compound</b>	<b>IC<sub>50</sub>, μM</b>
Digoxin	0.18
Istaroxime	0.14
CVie201	> 100
CVie202	> 100

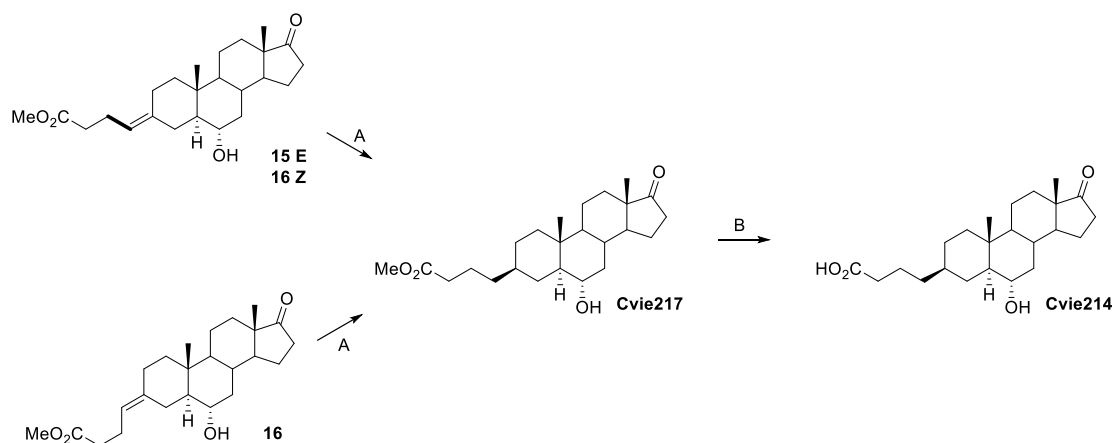
Table 4: Effect of the tested compounds on SERCA2a Kd Ca<sup>2+</sup> in heart-derived SR microsomes from normal guinea pig.

<b>Compound</b>	<b>Concentration nM</b>	<b>% decrease Kd vs control *p&lt;0.05</b>
Istaroxime	0	0
	1 nM	-7%
	10 nM	-18%*
	100 nM	-18%*
CVie201	0	0
	10 nM	-14%*
	100 nM	-15%*
CVie202	0	0
	10 nM	-4%
	100 nM	-7%
	200 nM	-6%

To overcome the stereoselectivity issues of the reaction, giving the less active compound as the main component, guided by the activity observation made with **CVie209** we decided to remove the double bond by hydrogenation, to obtain the saturated compound. Also, in similar literature situations,

authors were able to obtain a single diastereoisomer, thanks to the shielding activity of the upper face made by the methyl-19 group.[182]

Hydrogenation of the mixture **CVie201** and **CVie202**, as well as of **CVie202**, gave **CVie217** as the only product. The absolute configuration of the formed stereogenic center was confirmed by 2D-NOESY experiments. The compound was then hydrolyzed to give the desired compound **CVie214**. Both the two compounds were screened *in vitro* to have information about the pharmacophore. In particular, to confirm the need for a negatively charged group for the activity of the molecule.



Scheme 5: Reagents and conditions: A) H<sub>2</sub>, Pd-C 10%, EtOAc. 93%. B) aq. LiOH 1M, THF, H<sub>2</sub>O. 92%.

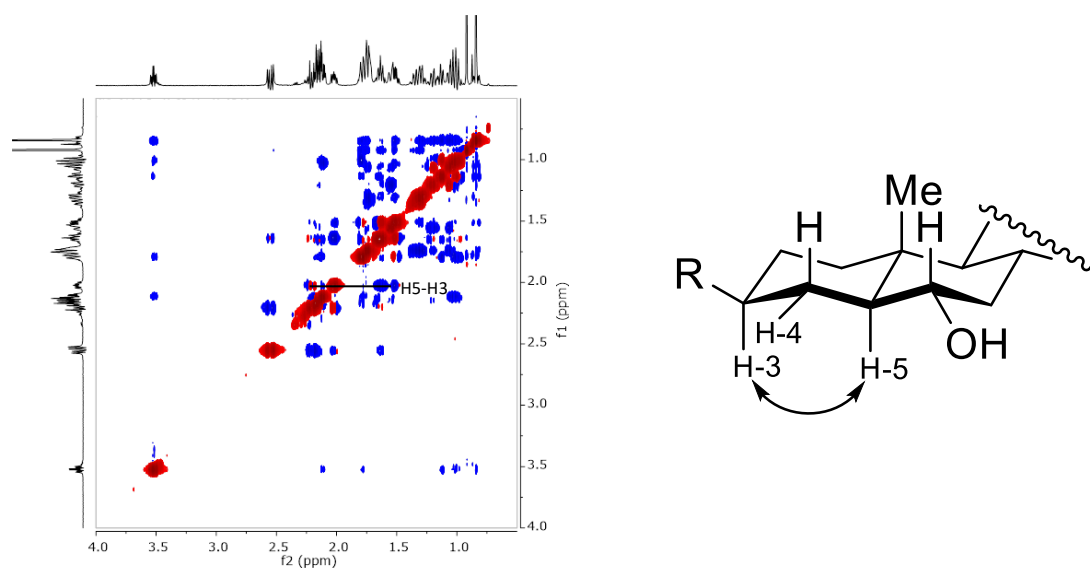


Figure 72: NOESY experiment for the determination of **CVie214** configuration.

Table 5: Inhibition of dog renal Na<sup>+</sup>/K<sup>+</sup> ATPase.

Compound	IC <sub>50</sub> , μM
Digoxin	0.18
Istaroxime	0.14
CVie214	> 100
CVie217	> 100

Table 6: Effect of the tested compounds on SERCA2a Kd Ca<sup>2+</sup> in heart-derived SR microsomes from normal guinea pig.

Compound	Concentration nM	% decrease Kd vs control *p<0.05
Istaroxime	0	0
	1 nM	-7%
	10 nM	-18%*
	100 nM	-18%*
CVie214	0	0
	1 nM	-13%*
	10 nM	-14%*
	100 nM	-21%*
	200 nM	-24%*
CVie217	0	0
	1 nM	-20%
	10 nM	-24.7%*
	100 nM	-20%*

	200 nM	-29.4%*
--	--------	---------

Surprisingly enough, both the compounds demonstrated activity as pure SERCA-2a stimulators. It is unclear if **CVie217** acts as a pro-drug and the ester group is hydrolyzed to carboxylate in situ, or it is active as ester. Still, the mechanism of action remains unknown. To identify the most active drug, starting from the lead compound **CVie214**, we decided to investigate the stereochemistry at the 6-hydroxyl group and the influence of the carboxyl chain length.

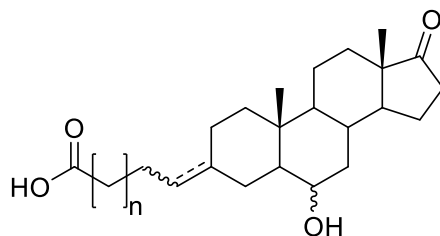
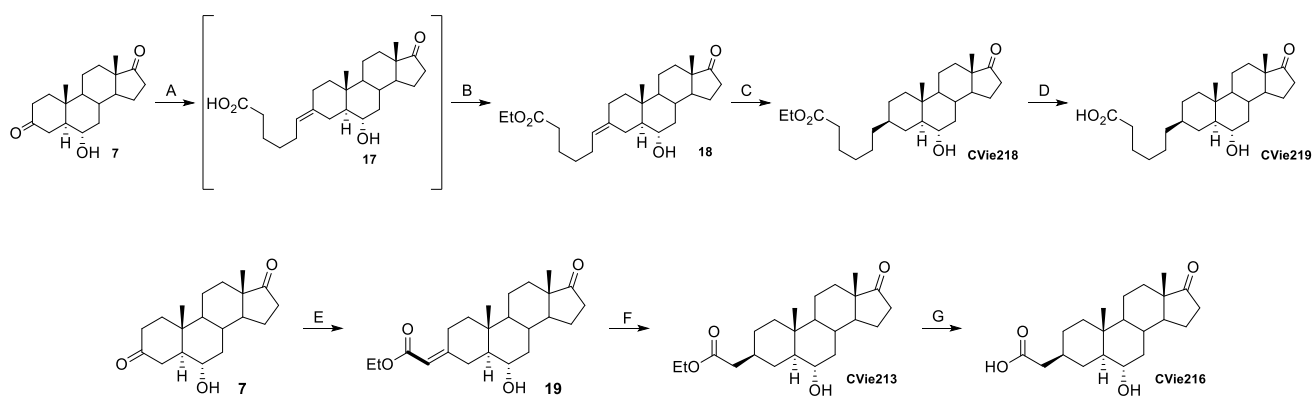


Figure 73: General structures of the PST3093 follow-on compounds.

First, compounds with a longer chain were synthesized, accordingly to the protocol used for the synthesis of **CVie217** and **CVie214**. While compounds with shorter chains were synthesized by a Horner-Emmons reaction with the appropriate phosphonate. In both cases, we tested the free acid as well as the ester compound, to highlight the difference in the activity.



Scheme 6: Reagents and conditions: A) LiHMDS, (5-Carboxypentyl)triphenylphosphonium bromide, THF. B) EDC, MeOH. 2 step yield 69%. C) H<sub>2</sub>, Pd-C 10%, EtOAc. 89%. D) aq. LiOH 1M, THF, H<sub>2</sub>O. 91%. E) Triethyl phosphonoacetate, NaH, DMF. 86%. F) H<sub>2</sub>, Pd-C 10%, EtOAc. 90%. G) aq. LiOH 1M, THF, H<sub>2</sub>O.

86%.

All the compounds synthesized showed similar behavior, with activity as pure SERCA-2a stimulators. **CVie216**, in particular, was identified as one of the most promising compounds due to its higher potency and more accessible synthetic process. Like before, the two esters compound demonstrated to be active, with a potency similar to the acid compounds. This behavior leaves open the possibility that the ester acts as a pro-dug of the acids but does not exclude the possibility that esters are active by themselves.

Table 7: Inhibition of dog renal Na<sup>+</sup>/K<sup>+</sup> ATPase.

<b>Compound</b>	<b>IC<sub>50</sub>, μM</b>
Istaroxime	0.14
CVie213	> 100
CVie216	> 100
CVie218	> 100
CVie219	> 100

Table 8: Effect of the tested compounds on SERCA2a Kd Ca<sup>2+</sup> in heart-derived SR microsomes from normal guinea pig.

<b>Compound</b>	<b>Concentration nM</b>	<b>% decrease Kd vs control *p&lt;0.05</b>
Istaroxime	0	0
	1 nM	-7%
	10 nM	-18%*
	100 nM	-18%*
CVie213	0	0
	10 nM	-12%
	100 nM	-23%*
	200 nM	-17%*

CVie216	0	0
	1 nM	-10%
	10 nM	-21%*
	100 nM	-25%*
	200 nM	-21%*
CVie218	0	0
	1 nM	-3%
	10 nM	-7%*
	100 nM	-19.1%*
	200 nM	-15%*
CVie219	0	0
	1 nM	-10.5%
	10 nM	-16%*
	100 nM	-19.5%*
	200 nM	-17.2%*

The second task was to study the influence of the C-6 hydroxyl group influence of the activity. All the compounds synthesized and tested until now share a configuration at C-6 opposite respect to the original PST3093, due to the syn-addition at the hydroboration step guided by the 19-methyl group.

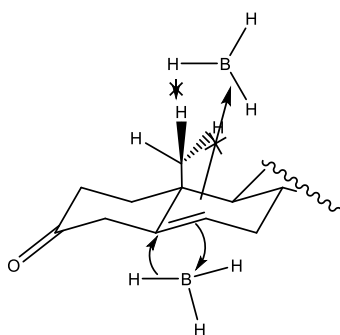
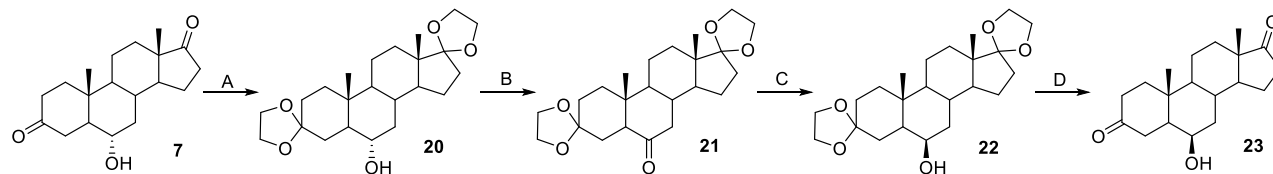


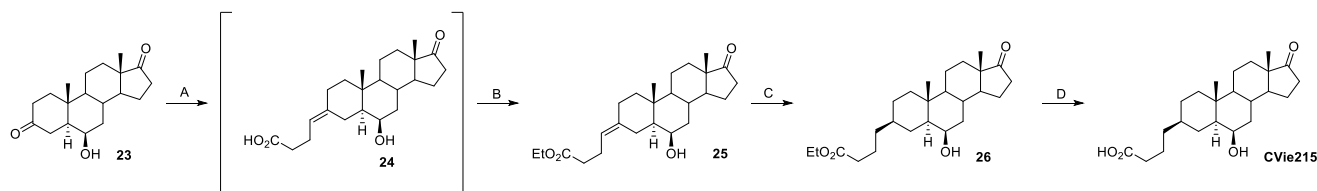
Figure 74: Schematic representation of the 19-methyl shielding effect.

The suitable key intermediate was synthesized by inversion of the stereochemistry of the molecule **7** through an oxidation-reduction protocol, exploiting the shielding activity of methyl-19 to guide the reductive agent in the opposite steroidal face.[125]



Scheme 7: Reagents and conditions: A) ethylene glycol, p-TSA, toluene, reflux. 98%. B) PCC, DCM. 96%. C) NaBH<sub>4</sub>, MeOH, 0°C. 92%. D) p-TSA, acetone. 81%.

The diketone **23** was used as the precursor of the new derivatives, by following the same protocol optimized for the synthesis of **CVie214**.



Scheme 8: Reagents and conditions: A) LiHMDS, (3-Carboxypropyl)triphenylphosphonium bromide, THF. B) EDC, MeOH. 2 step yield 75%. C) H<sub>2</sub>, Pd-C 10%, EtOAc. 94%. D) aq. LiOH 1M, THF, H<sub>2</sub>O. 82%.

**CVie215** retains the pure SERCA-2a stimulator activity like the other compounds. However, with respect to the parent compound **CVie214**, it has a slightly higher potency, suggesting the fundamental contribution of the C-6 hydroxyl group to the biological activity.

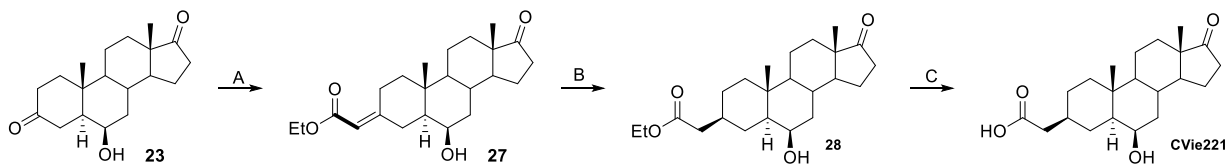
Table 9: Inhibition of dog renal Na<sup>+</sup>/K<sup>+</sup> ATPase.

Compound	IC <sub>50</sub> , μM
Istaroxime	0.14
CVie215	> 100

Table 10: Effect of the tested compounds on SERCA2a Kd Ca<sup>2+</sup> in heart-derived SR microsomes from normal guinea pig.

Compound	Concentration nM	% decrease Kd vs control *p<0.05
Istaroxime	0	0
	1 nM	-7%
	10 nM	-18%*
	100 nM	-18%*
CVie215	0	0
	1 nM	-7%
	10 nM	-19%*
	100 nM	-23%*

With the information gained, we tried to combine the most promising features to achieve the maximum potency for this class of compounds. In particular, the C-6 (R) configuration of **CVie215** was combined with the C-2 chain of **CVie214**.



Scheme 9: Reagents and conditions: A) Triethyl phosphonoacetate, NaH, DMF. 87%. B) H<sub>2</sub>, Pd-C 10%, EtOAc. 97%. C) aq. LiOH 1M, THF, H<sub>2</sub>O. 93%.

Despite the combination of the two features, the molecule obtained presents lower potency with respect to the two other compounds. This result leaves open question marks over the structural requirements that still need clarification.

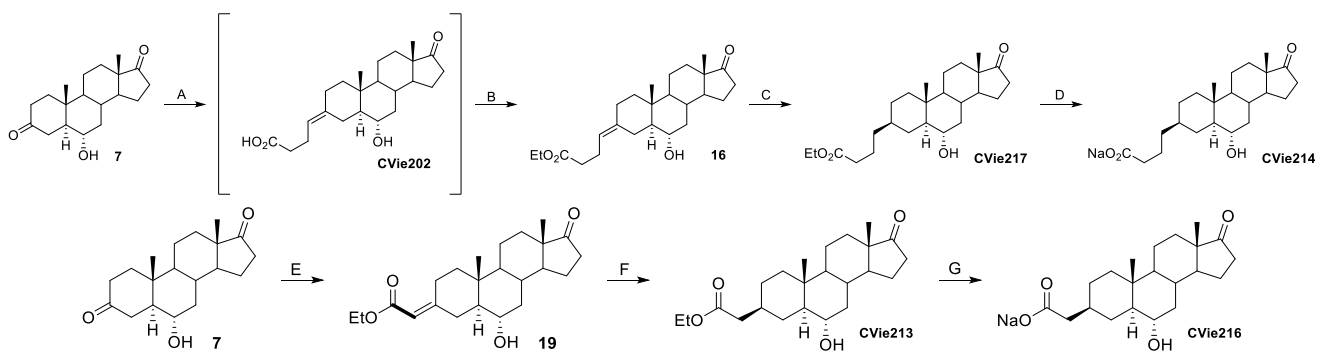
Table 11: Inhibition of dog renal Na<sup>+</sup>/K<sup>+</sup> ATPase.

Compound	IC <sub>50</sub> , μM
Istaroxime	0.14
CVie221	> 100

Table 12: Effect of the tested compounds on SERCA2a Kd Ca<sup>2+</sup> in heart-derived SR microsomes from normal guinea pig.

Compound	Concentration nM	% decrease Kd vs control *p<0.05
Istaroxime	0	0
	1 nM	-7%
	10 nM	-18%*
	100 nM	-18%*
CVie221	0	0
	10 nM	-3%*
	100 nM	-8.5%*

Taking into account the potency of the compounds and their synthetic accessibility, **CVie214** and **CVie216** were chosen as lead compounds. The two molecules were produced in gram-scale for the following *in vivo* tests. The two protocols were optimized in the reaction conditions, as well as the purification procedures. Also, the initial low solubility of the drug in the buffer of the injectable solution forced us to develop a suitable formulation. In this case, the simple salification of the final compound as sodium salt compound solved the problem, giving solubility to the compound with no impact on the activity.



Scheme 10: Reagents and conditions: A) LiHMDS, (3-Carboxypropyl)triphenylphosphonium bromide, THF. B) EDC, MeOH. 2 step yield 89% C) H<sub>2</sub>, Pd-C 10%, EtOAc. 98% D) aq. LiOH 1M, THF, H<sub>2</sub>O then IRA120 Na<sup>+</sup> form, MeOH. 97%. E) Triethyl phosphonoacetate, NaH, DMF. 86%. F) H<sub>2</sub>, Pd-C 10%, EtOAc. 90%. G) aq. LiOH 1M, THF, H<sub>2</sub>O then IRA120 Na<sup>+</sup> form, MeOH. 95%

### 3. Istaroxime amine derivatives with double targeting.

The second task of this thesis, was the creation of metabolically stable amines with double targeting, possessing activity as SERCA-2a stimulators and Na/K inhibitors.

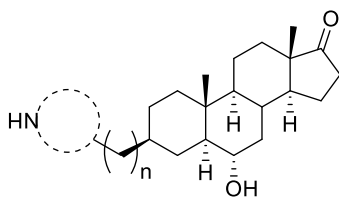


Figure 75: General structures of the istaroxime follow-on compounds.

To achieve this second task, the primary amine of istaroxime was replaced with suitable cyclic amine derivative. Similarly to the SERCA-2a pure stimulators, the synthesis started from compound **7** as the common intermediate, without further oxidation to the correspondent metabolically unstable 6-keto compound. Moreover, to avoid the introduction of additional stereogenic centers were initially chosen symmetric cyclic amines, like 3-substituted azetidines and 4-substituted piperidines.

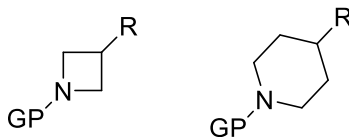
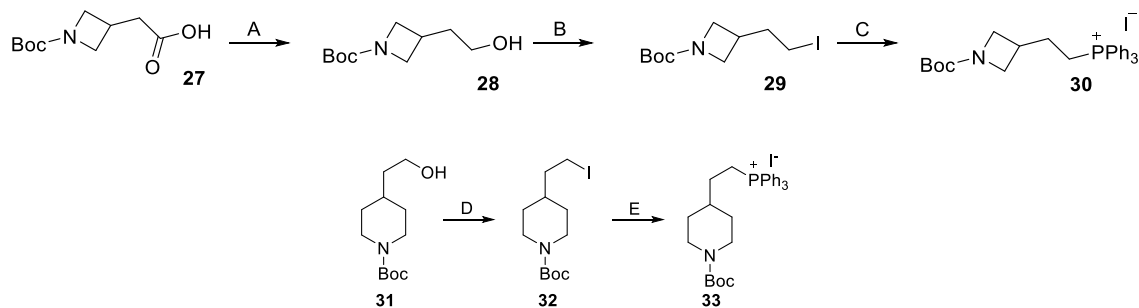


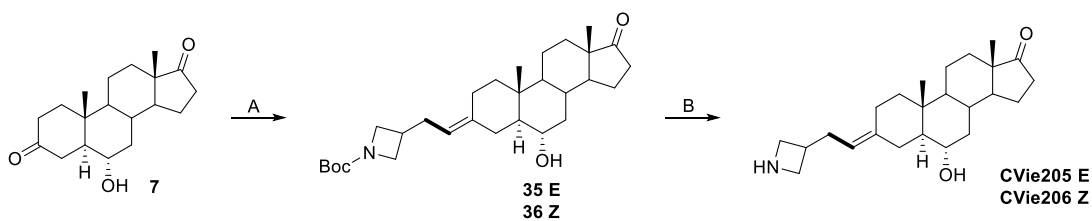
Figure 76: The chosen cyclic amines.

To use the same Wittig protocol of the previous section, as first, the two N-protected phosphonium salts were synthesized.



Scheme 11: Reagents and conditions: A)  $\text{BH}_3$ , THF,  $0^\circ\text{C}$ . q.tive. B)  $\text{I}_2$ ,  $\text{PPh}_3$ , DMF 56%. C)  $\text{PPh}_3$ , ACN, reflux. 83%. D)  $\text{I}_2$ ,  $\text{PPh}_3$ , DMF 91%. E)  $\text{PPh}_3$ , ACN, reflux. 95%.

Starting from the azetidine compound, and to understand the difference with the pure SERCA-2a stimulators, the molecules were synthesized following the ylide stabilizing Wittig protocol, using the NaH/DMSO base/solvent system.



Scheme 12: Reagents and conditions: A) **30**, NaH, DMSO. **35** 15%, **36** 29% B) TFA:DCM 1:1 **CVie205** 97% **CVie206** 98%.

The two diastereoisomers were separated, characterized, cleaved, and tested.

Table 13: Inhibition of dog renal  $\text{Na}^+/\text{K}^+$  ATPase.

<b>Compound</b>	<b>IC<sub>50</sub>, μM</b>
Istaroxime	0.14
CVie205	7
CVie206	5.9

Table 14: Effect of the tested compounds on SERCA2a Kd Ca<sup>2+</sup> in heart-derived SR microsomes from normal guinea pig.

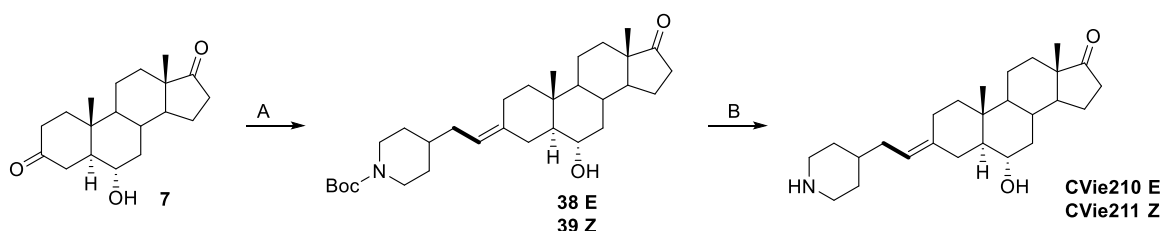
<b>Compound</b>	<b>Concentration nM</b>	<b>% decrease Kd vs control *p&lt;0.05</b>
Istaroxime	0	0
	1 nM	-7%
	10 nM	-18%*
	100 nM	-18%*
CVie205	0	0
	100 nM	-16.7%*
	200 nM	-13.1%*
CVie206	0	0
	100 nM	-13.7%*
	200 nM	-15.1%*

While the activity as stimulators is good, their inhibitory activity over the Na/K ATPase is one order of magnitude less than istaroxime. Also, differently from the pure SERCA-2a stimulators in which is active only the E diastereoisomer, in this case, all the two diastereoisomers, E and Z, showed the desired activity with similar potency, leaving additional question marks over the mechanism and structural requirements.

The unsaturated molecule was then hydrogenated and cleaved, like the SERCA-2a stimulators protocols.



Similarly, the molecules bearing the piperidine as the cyclic group were synthesized and tested.

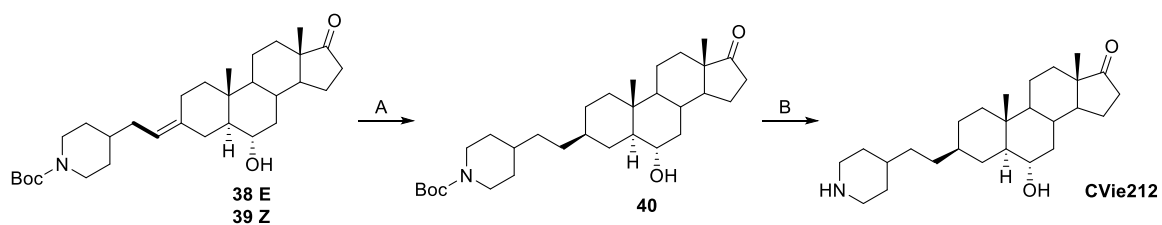


Scheme 14: Reagents and conditions: A) **33**, NaH, DMSO. **38** 8%, **39** 4% B) TFA:DCM 1:1 **CVie210** 67%, **CVie211** 98%.

Table 17: Inhibition of dog renal Na<sup>+</sup>/K<sup>+</sup> ATPase.

Compound	IC <sub>50</sub> , μM
Istaroxime	0.14
CVie210	13.1
CVie211	8.3

In this case, the two diastereoisomers E and Z of the unsaturated compound were not tested as SERCA-2a stimulators, since their initial screening over Na/K ATPase showed non-encouraging results. Contrariwise, the saturated compound not only has a similar inhibitory activity similar to the azetidine compounds but has a promising SERCA-2a stimulatory activity, with a potency comparable with the pure SERCA-2a compound CVie214.



Scheme 15: Reagents and conditions: A) H<sub>2</sub>, Pd-C 10%, EtOAc, 87%. B) TFA:DCM 1:1, 78%.

Table 18: Inhibition of dog renal Na<sup>+</sup>/K<sup>+</sup> ATPase.

Compound	IC <sub>50</sub> , μM
----------	-----------------------

Istaroxime	0.14
CVie212	3.5

Table 19: Effect of the tested compounds on SERCA2a Kd Ca<sup>2+</sup> in heart-derived SR microsomes from normal guinea pig.

<b>Compound</b>	<b>Concentration nM</b>	<b>% decrease Kd vs control *p&lt;0.05</b>
Istaroxime	0	0
	1 nM	-7%
	10 nM	-18%*
	100 nM	-18%*
CVie212	0	0
	10 nM	-19.6%*
	100 nM	-20.2%*

These results show a non-predictable behavior of this class of compounds, with complicated rationalization. Also, the low potency of action over the Na/K ATPase leaves these compounds in a grey area between istaroxime and the pure SERCA-2a stimulators. Also, the synthesis revealed some limitations and dramatic low yields. For these reasons, none of these compounds was chosen for the scale-up and the following in vivo tests.

#### 4. Towards drug delivery systems based on electrospun nanofibers

The striking and unique mechanism of double targeting, typical of istaroxime, and the low potency of cyclic amine derivatives led to the development of new drug delivery systems for istaroxime. Nevertheless, istaroxime is already in phase III clinical, and a new route of administration could improve the activity of the molecule, overcoming its drawbacks. In fact, by changing the route of

administration and encapsulating a drug in an appropriate scaffold changes the pharmacokinetics and the pharmacodynamics of the drug itself.[136]

Among the existing drug delivery systems discovered in the past few years, electrospun nanofibers are gaining interest for their unique features that could combine bio-engineered regenerative behavior with the possibility of a local application directly in the tissue of interest.[143] Also, the electrospinning process for the creation of these platforms is very simple, effective, and scalable.[151] Embedding istaroxime in electrospun nanofibers with a specific composition and morphology could be an adequate tool to improve cardiac functions and induce regeneration of the damaged myocardium. This work was made in collaboration with the group of Prof. L. Moroni of Maastricht University.

Nanofiber composition and morphology influence the release rate of the loaded drug and the duration of the treatment. The main factors playing a role are 1) polymer swelling in water, 2) polymer affinity with the drug, and 3) polymer degradation rate. Also, the chemical composition should be suitable for the application in the body. In other words, the polymer should be highly biocompatible and should act as a seeding point for the cells.[150]

For the specific application in the cardiac field, in which the cardiomyocytes are aligned in a precise direction, nanofiber filament should resemble that particular feature to mimic the tissue in the best possible way. Also, mechanical properties should sustain continuous beating without breaking.[179] Finally, should be optimized the hydrophilic/hydrophobic behavior of the polymer to avoid: A) a too fast release of istaroxime caused by a mismatch with the charged amino group of istaroxime B) a non-compatibility with the hydrophobicity of the cellular membrane.[183]

For these reasons, and based on both previous works and literature, three polymers were identified as the starting point. The first two polymers are known with the commercial name of PolyActive (PA) and are composed of a different ratio between blocks of a soft segment of Poly(ethylene oxide) (PEO) and an hard segment of poly(butylene terephthalate) (PBT).[184]

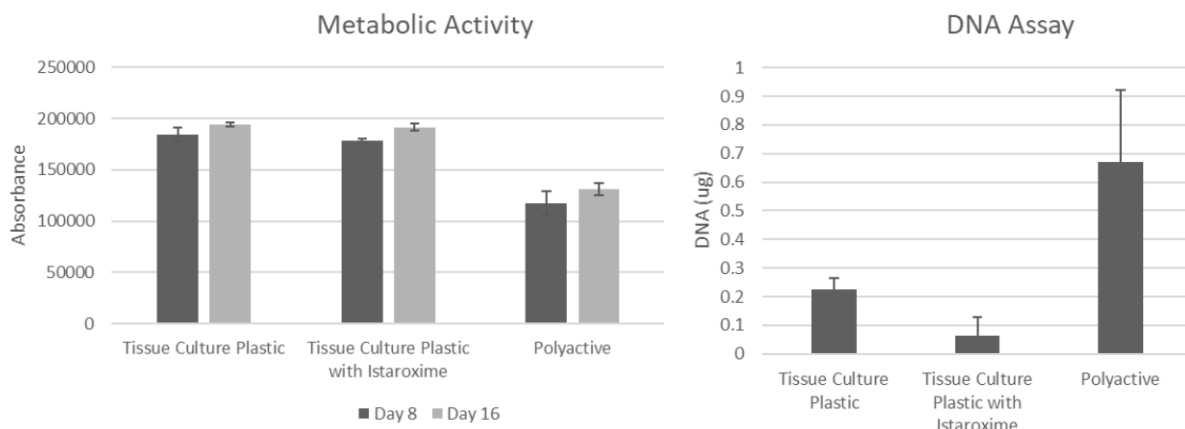


Figure 77: Preliminary results obtained with HL-1 cardiac stem cells. Cardiomyocytes were seeded on tissue culture plastic with and without daily dose of 100nM istaroxime, and on aligned 300PA scaffolds. Metabolic activity was measured at days 8 and 16 with prestoblue assay. DNA assay was made with the provided commercial kit. Results shows lesser metabolic activity in presence of 300PA but higher cell proliferation.

The two blocks are connected with a terephthalate (T) residue. By changing the ratio between the blocks is possible to balance hydrophilicity/hydrophobicity of the surface of the final scaffold, making these polymers striking in tissue engineering.[185] In particular, the two PAs chosen are 300PEOT55PBT45 (300PA) and 1000PEOT70PBT30 (100PA), in which the first number denotes the molecular weight of the incorporated PEO, while the second and third number indicates the ratio of the two blocks PEOT/PBT expressed in wt%. PEO represents the hydrophilic segment, controlling the water uptake of the polymer and its hydrophilic/hydrophobic behavior. Remarkably, the strength of the fiber and elasticity increases with an increase in PBT percentage, while higher water uptake leads to lower tensile strength and stiffness.[186]

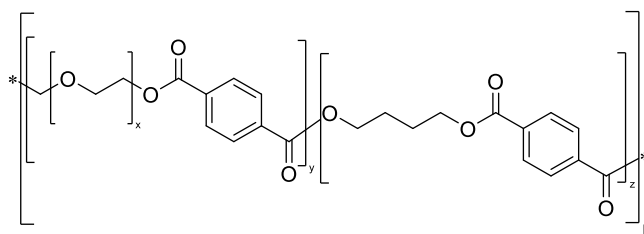


Figure 78: Structure of PolyActive polymers: xPEOTyPBTz, in which x is the molecular weight of PEO, y and z the ratio between the two blocks.

The third polymer chosen was poly( $\epsilon$ -caprolactone) (PCL), one of the most common polymers for long-term biomedical engineering devices, approved by the FDA for usage in the human body.[187] PCL has slow degradation rate and high permeability, exhibiting excellent chemical and solvent resistance, good toughness, and mechanical properties similar to those of other conventional non-biodegradable synthetic polymers.[188]

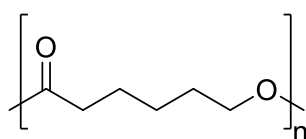


Figure 79: chemical structure of PCL.

Among different techniques existing for the creation of electrospun nanofibers was chosen as the most simple solution electrospinning, in which the polymer is dissolved in a suitable solvent before electrospinning. Solvent influences the outcome of the whole spinning process. By the easy modification of viscosity and conductivity parameters of the liquid is possible to obtain a different kind of morphology in the final fiber. For this purpose, smooth, beadles, and regular nanofibers are desired.[179]

To optimize the working parameters for the creation of the desired morphology, nanofibers composed only by the polymer were created. Electrospinning was made with a custom device, and the fibers were collected over an aluminum foil placed over a fast rotating mandrel to enhance fiber alignment.

Table 20: SEM images of the produced fibers.

300PA	1000PA	PCL

To avoid waste of material and to have a fast and reliable method for studying the kinetics of release from the nanofibers, preliminary experiments were made embedding the fluorescent molecule eosin Y inside the nanofibers. Eosin structure is remarkably different from istaroxime ones, but at the same time, shares the presence of a charged group and a hydrophobic core. The use of eosin gives an idea of the performance of the produced device, allowing a focused choice for the development of the final scaffolds.

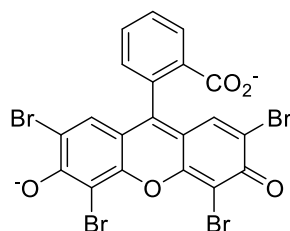
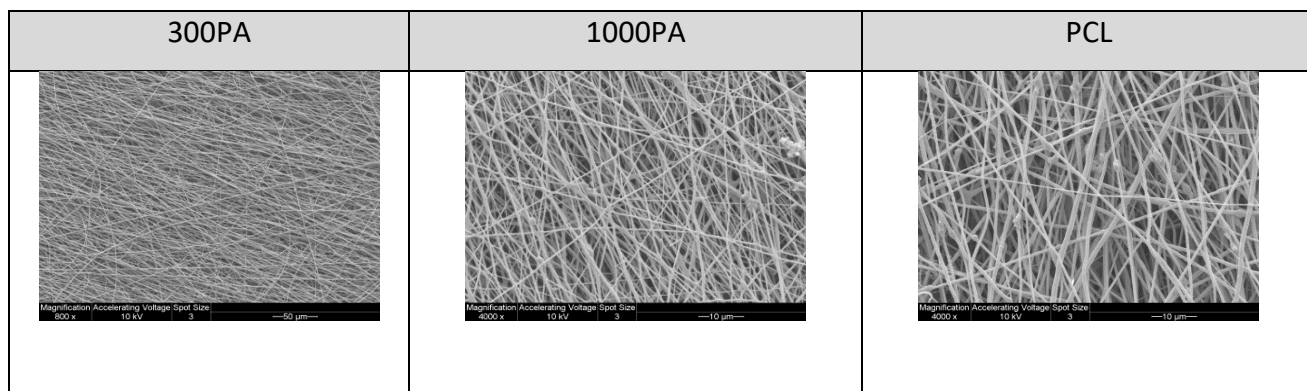


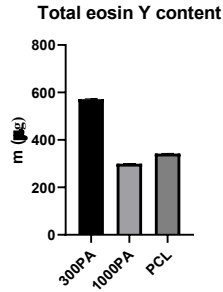
Figure 80: Structure of eosin Y.

Eosin was embedded in the nanofibers through a blending process. Simply, a 2% weight of eosin was added to the polymer solution before electrospinning.

Table 21: SAM images of the eosin Y embedded fibers.

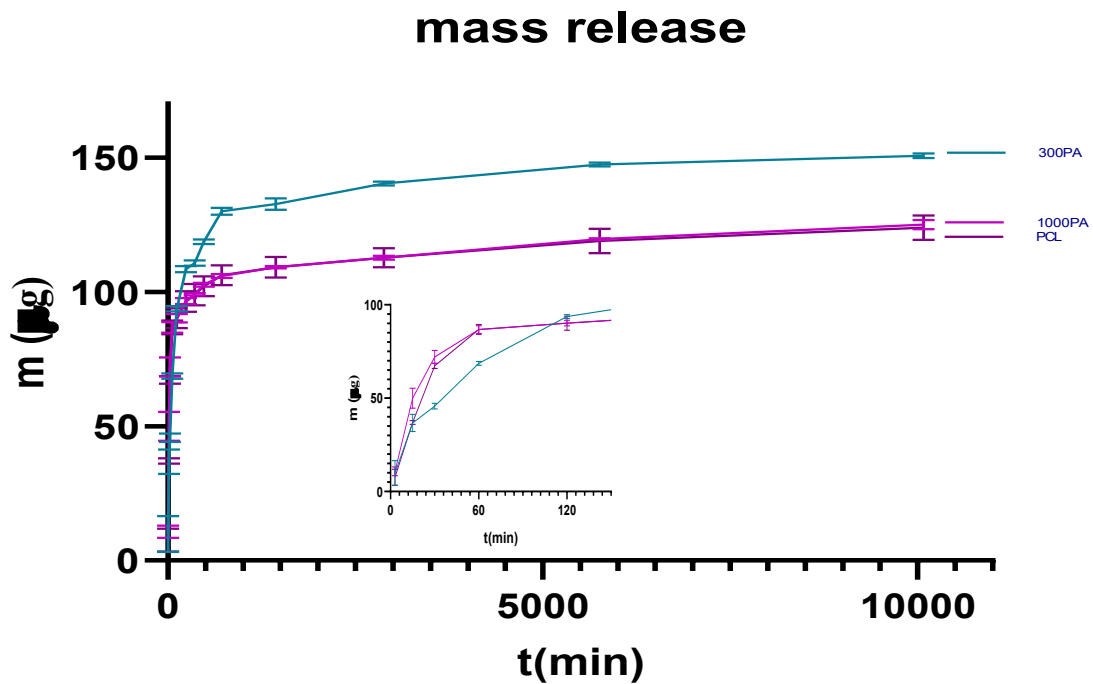


The total amount of eosin contained in the different scaffolds was calculated by dissolving a weight portion of the fibers in a suitable organic solvent and confronting the fluorescence value with a calibration curve.

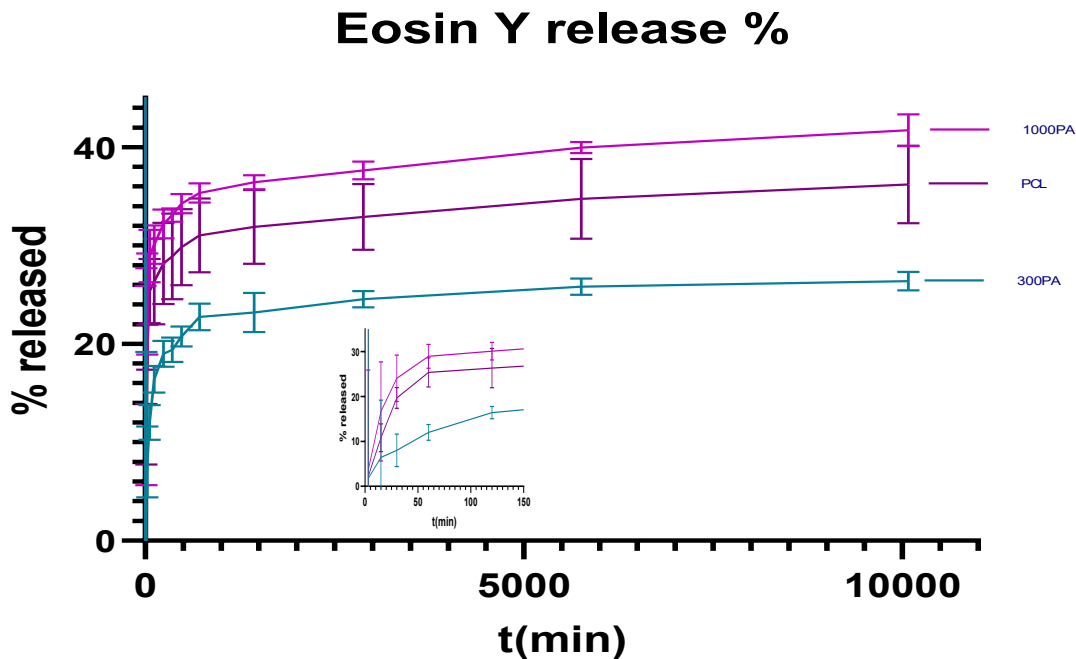


Graph 1: Total eosin Y content in 1mg of the tested fibers.

Release of eosin was studied by immersion of a weighed amount of scaffold in a fixed volume of pH 7.5 PBS buffer and withdraw 100 $\mu$ L of solution at established times, replacing the liquid with 100  $\mu$ L of fresh buffer. Time points were taken at 3, 15, 30 minutes, 1, 2, 4, 6, 8, 12, 24, 48 hours, and 4, 7 days. Fluorescent measure and cumulative calculation gave the amount of eosin released in the medium



Graph 2: Micrograms of eosin Y rereleased in 7 days. The zoom represent the first 150 minutes.

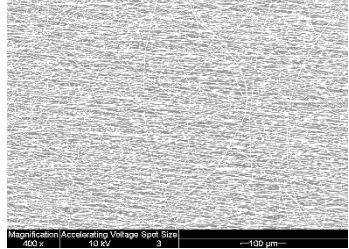
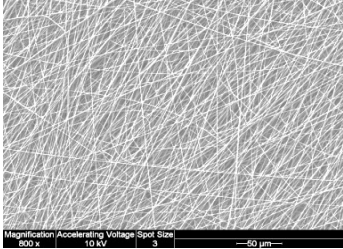
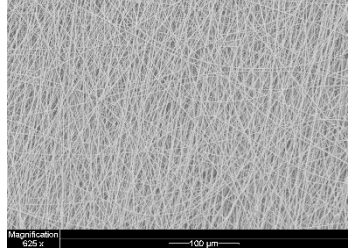


Graph 3: Percentage of eosin Y rereleased in 7 days. The zoom represent the first 150 minutes.

The three polymers release a comparable total amount of eosin over time, but at the same time, looking at the total percentage released, 300PA has the lowest value. The data means that 300PA is capable of incorporating more drug than the other two polymers, and releasing it more slowly in the test media. Remarkably, for all the three polymers the initial slope of the curve, known as “burst phase”, does not lead to a complete or more than half loss of the drug. This means, the majority of eosin remains intact in the fibers and is released in longer periods.

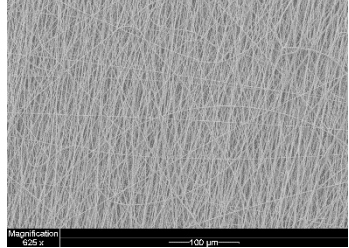
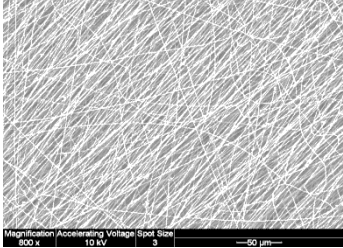
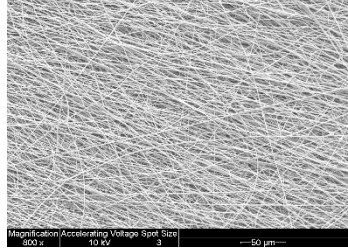
300PA showed exciting results in the preliminary studies. The scaffold exhibited the capability of efficient incorporation of the probe and slower release in the media. To further extend the library of the scaffold, having different possibilities before moving to istaroxime, was decided to extend the variety of the composition of the scaffolds. In particular, The hydrophilic/hydrophobic balance of the nanofibers was changed by blending between 1000PA and 300PA in different ratios. These two polymers are more similar in terms of chemical structure, bypassing problems due to different solubility or several spinning conditions.

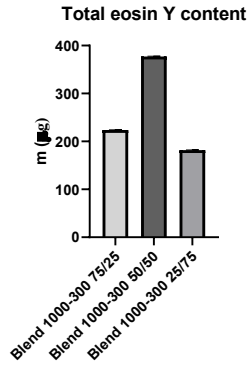
Table 22: SEM images of the produced fibers.

Blend 1000PA-300PA 75/25	Blend 1000PA-300PA 50/50	Blend 1000PA-300PA 25/75
		

Again, once the conditions were optimized, were produced the fibers embedded with eosin. The total amount contained was calculated and the release profile retrieved in the standardized conditions.

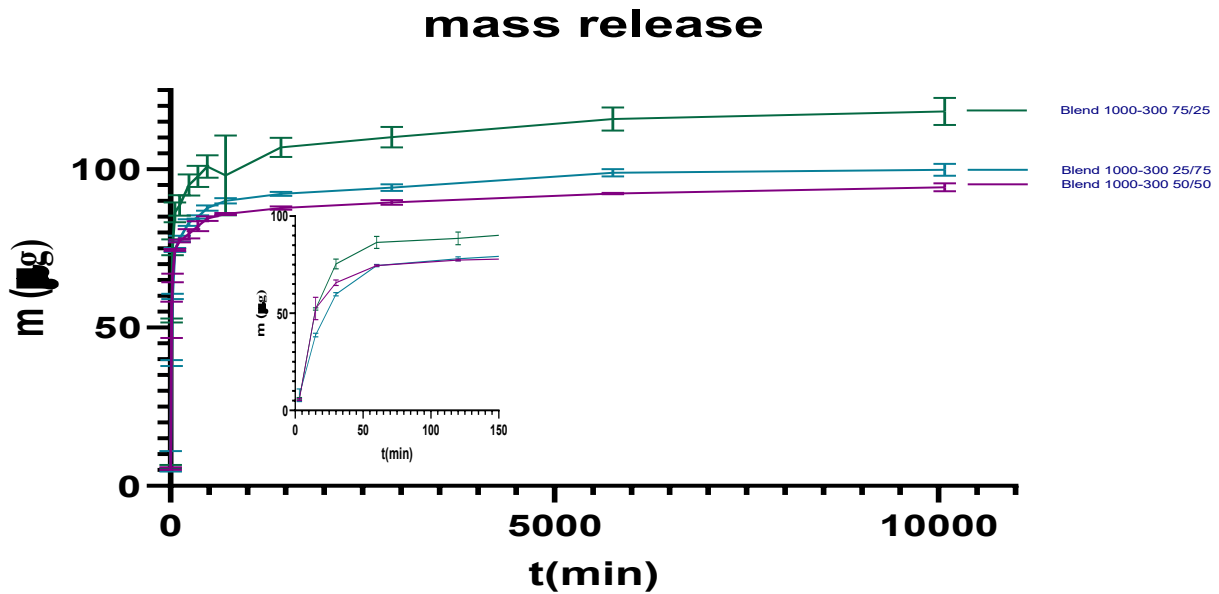
Table 23: SAM images of the eosin Y embedded fibers.

Blend 1000PA-300PA 75/25	Blend 1000PA-300PA 50/50	Blend 1000PA-300PA 25/75
		

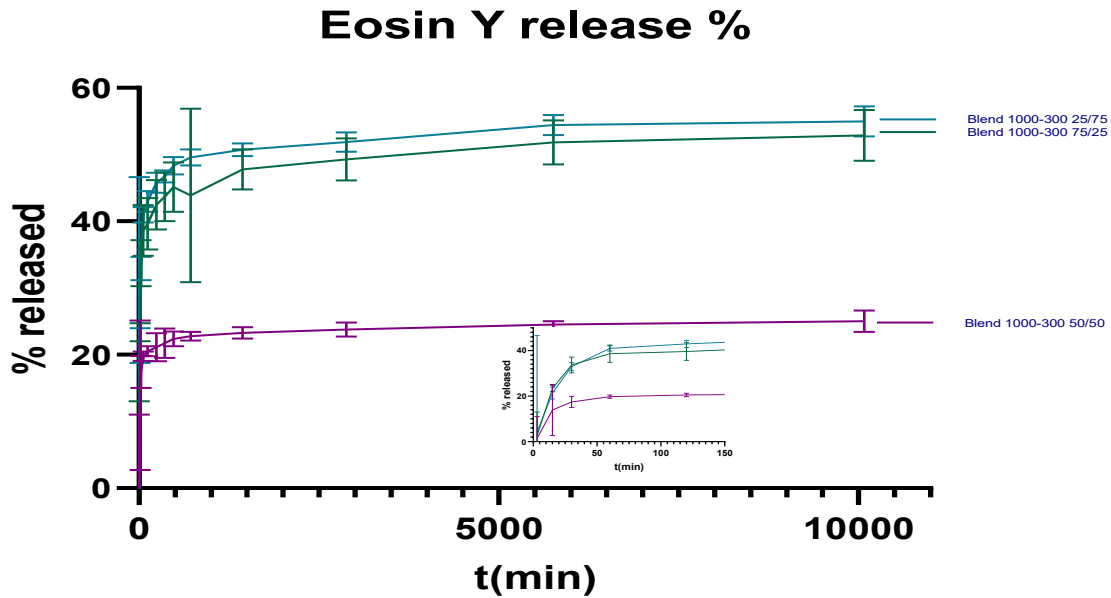


Graph 4: Total eosin Y content in 1mg of the tested the tested fibers.

In this case, all three blends exhibit a similar release profile in terms of micrograms. However, the two blends, 75/25 and 25/75, have the highest percentage among all the tested fibers, reaching around 50% of the drug released in the firsts few hours. On the other hand, the 50/50 blend has a perfectly balanced profile between the two parent fibers.



Graph 5: Micrograms of eosin Y rereleased in 7 days. The zoom represent the first 150 minutes.



Graph 6: Percentage of eosin Y rereleased in 7 days. The zoom represent the first 150 minutes.

Finally, the polymers were combined through the creation of core-shell nanofibers. Hereby, two polymers are not physically mixed together, but coexists in a sort of “fiber in a fiber” system. In this way, the core containing the drug is isolated from the surrounding and protected from the environment, slowing, in principle, its release. 300PA was chosen as shell for its good elasticity and mechanical resistance, together with a good degree of hydrophobicity necessary to improve the cells attachment. PCL and 1000PA was used as the core of the nanofibers, creating two different kind of core/shell nanofibers having respectively an hydrophobic/hydrophobic and a hydrophobic/hydrophilic compositions.

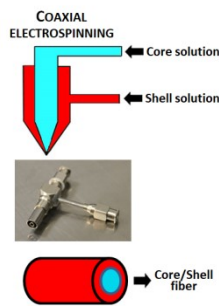
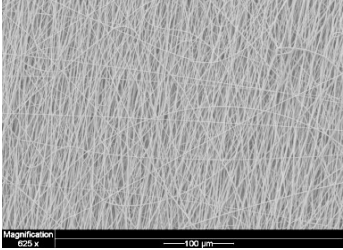
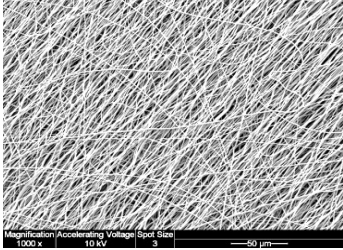
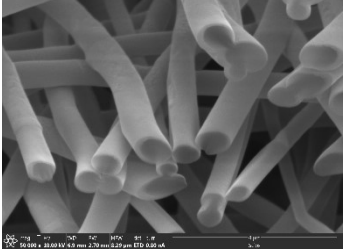
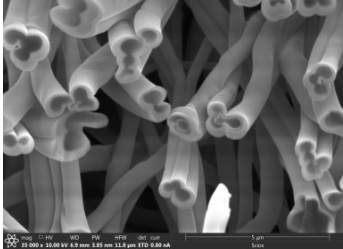
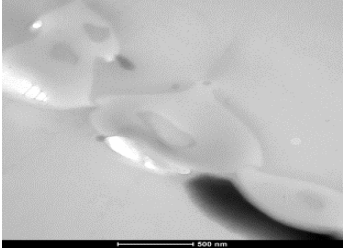
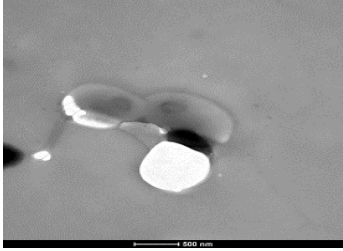


Figure 81: Schematic representation of the coaxial electrospinning setup.

Coaxial fibers were created with two different combinations: A) 300PA as shell, 1000PA as core B)300PA as shell PCL as the core. To prove the correct creation of the core/shell system were taken cross-section images at the FIB-SEM microscope and at TEM microscope.

Table 24: SEM, FIB-SEM, and TEM images of the produced coaxial fibers.

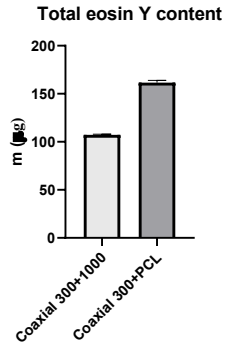
300PA shell-1000PA core	300PA shell-PCL core
 <p>Magnification: 650 x 100 µm</p>	 <p>Magnification: 1000 x Accelerating Voltage: 10 kV Spot Size: 3 50 µm</p>
FIB-SEM cross-section images	FIB-SEM cross-section images
 <p>1 µm</p>	 <p>1 µm</p>
TEM cross-section images	TEM cross-section images
 <p>500 nm</p>	 <p>500 nm</p>

Once the parameters over the black fibers were optimized, the scaffolds embedded with eosin were produced.

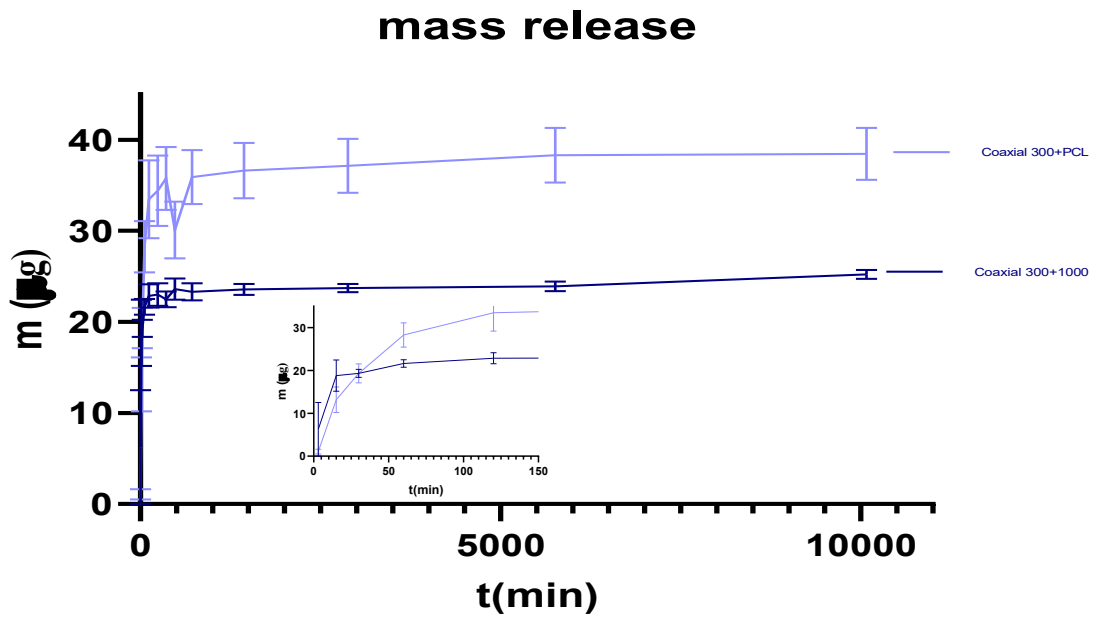
Table 25: SEM, FIB-SEM, and TEM images of the produced coaxial fibers.

300PA shell-1000PA core	300PA shell-PCL core
-------------------------	----------------------

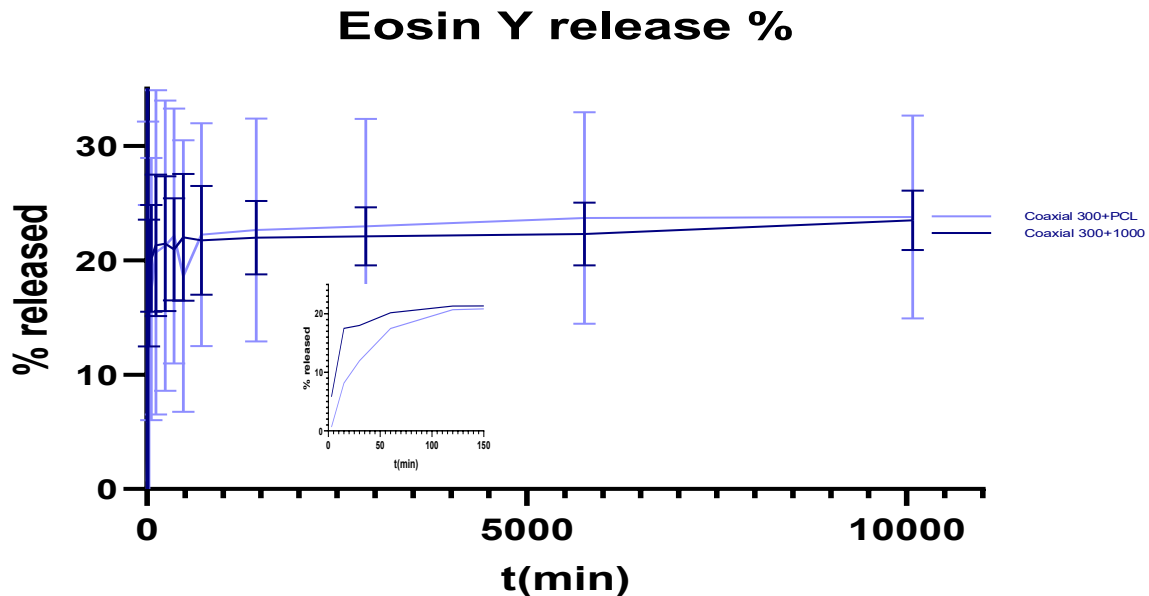




Graph 7: Total eosin Y content in 1mg of the tested the tested fibers.



Graph 8: Micrograms of eosin Y rereleased in 7 days. The zoom represent the first 150 minutes.



Graph 9: Percentage of eosin Y rereleased in 7 days. The zoom represent the first 150 minutes.

The core/shell contains less eosin than the other scaffolds, probably due to the thinner diameter of fiber in the core. Nevertheless, the presence of the shell, acting as a physical wall, greatly slows the release from the core. This situation allows a mild released quantity, with a percentage of around 20% of the total released after one week.

Summarizing all the preliminary results gained, four different system were chosen for the creation of istaroxime drug release devices: A) 300PA simple nanofiber B) blended 300PA/1000PA 50/50 nanofiber C) the two coaxial systems.

The absence of chromophore in the istaroxime structure forced us to identify a fast and reliable assay for the spectrophotometric determination of the released amount. The system identified involves the fluorescamine assay, characterized by an high selectivity towards amino groups, low detection limit and absence of background of the degraded reagent.[189]

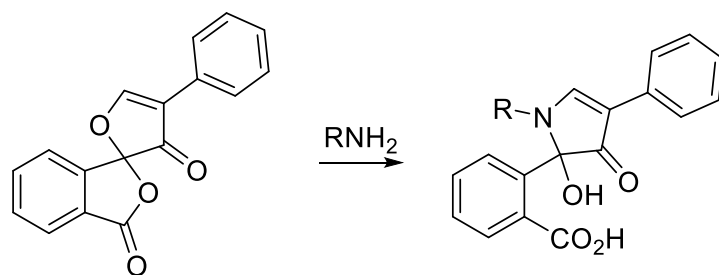


Figure 82: mechanism of fluorescamine reaction with amines.

Despite the successful creation of a calibration curve and the standardization of the protocol for the detection of istaroxime, due to the rising of COVID-19 pandemic was not possible to produce and analyze the desired fibers. However, the promising results obtained with the model compound eosin Y suggest the potential applicability of this kind of nanofibers for the local and sustained delivery of istaroxime, together with the possibility of inducing tissue regeneration in the damaged myocardium.

# 4. Conclusions

Istaroxime represents one of the most promising lead compounds for the treatment of heart failure. Still, due to its genotoxic metabolite and fast metabolism, the use for prolonged periods is remarkably limited.

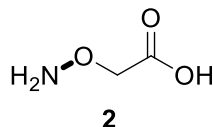


Figure 83: The genotoxic hydroxylamine.

To overcome the great limitation of the compound and to exploit the possibility of creating a new first-in-class drug, during this thesis was created a library of metabolically stable follow-on compounds of istaroxime and its metabolite PST3093.

PST3093 is the only example in literature being a pure SERCA-2a stimulator, with potential applicability as a new and unique tool for the treatment of heart failure disease.

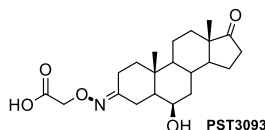


Figure 84: structure of PST3093.

Starting from this compound was rationally designed a library of metabolically stable derivatives exploiting the same mechanism of action. All the compounds synthesized and characterized demonstrated *in vitro* activity as pure SERCA-2a stimulators. Also, the two compounds **CVie214** and **CVie216** were chosen as lead compounds for the *in vivo* experiments, and their synthesis scaled-up according to the grams-quantity needed. The exiting results of *in vivo* test, in which the molecules demonstrated to be non-toxic, active, and orally administrable lead to the deposit of a European patent.

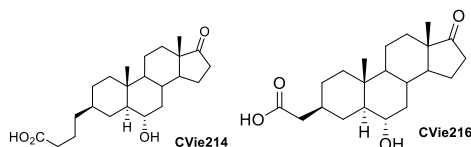


Figure 85: Structure of **CVie214** and **CVie216**.

The rationalization and the identification of the exact mechanism of action are still needed. Human SERCA-2a structure was published only in 2019 by Sitsel *et al.* allowing us to perform *in silico* studies. [27] However, the complex molecular structure of SERCA-2a led to the identification of several potential binding sites, excluding only the binding of these molecules with phospholamban, the natural inhibitor of SERCA. Additional NMR experiments are in progress. Preliminary results show the capability of **CVie216** to intercalate in simulated membranes, leading to the hypothesis that these molecules can bind in the transmembrane region of SERCA-2a disrupting the inhibitory activity of phospholamban.

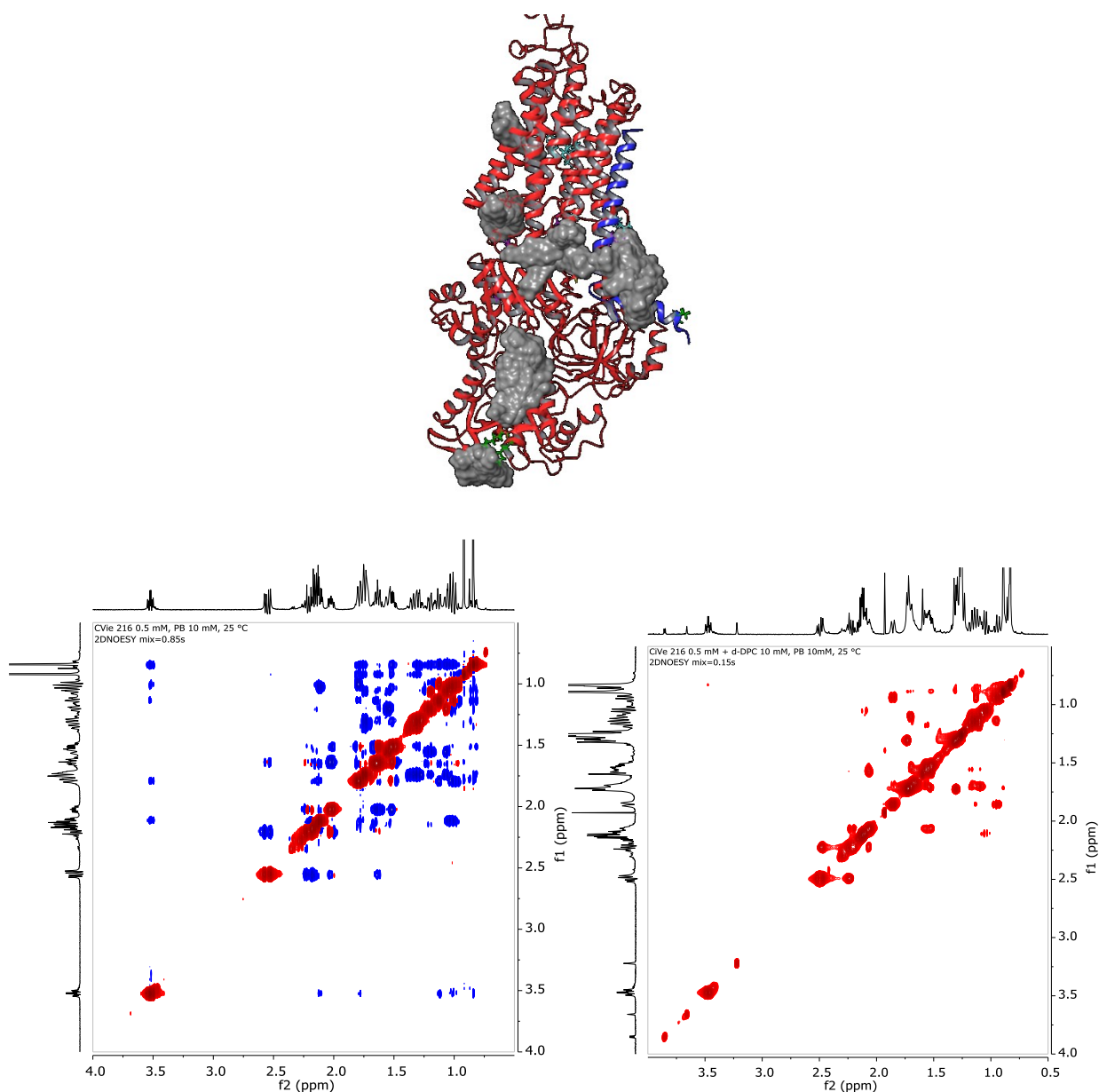


Figure 86: A) Docking between SERCA2a (red) complex with phospholamban (blue) and CVie216. Grey areas represent the possible binding sites and orientation of the molecule. B) 2DNOESY of CVie216 in PB buffer. The positive (blue) NOE cross peaks reflects short correlation times of the low molecular weight molecule in solution. C) 2DNOESY of CVie216 in PB buffer with 10mM Dodecylphosphorylcholine-d38. In this case, the signals became negative due to a rising in the correlation time, since the small molecule acquires the motional properties of the micelles during the residence time in the bound state.

Similarly, new metabolically stable Istaroxime derivatives were developed and synthesized, bearing cyclic amines. However, the challenging synthesis and the low activity as double targeting molecules, able to inhibit Na/K-ATPase and stimulate SERCA-2a action, excluded this class from the scale-up and

the *in vivo* characterization. Still, the behavior of these molecules proved to be non-predictable basing on the chemical structure, opening question marks towards their mechanism that needs clarification.

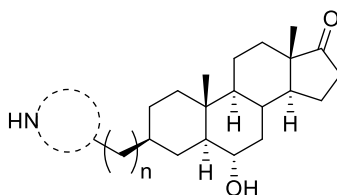


Figure 87: General structure of istaroxime follow-on compounds.

To overcome the limits observed with the cyclic amines derivatives, in collaboration with the group of prof. Moroni of Maastricht university, new drug delivery systems for istaroxime was developed.

Such systems are based on electrospun nanofibers, capable of delivering the drug directly at the site of action, and to induce the regeneration of the damaged myocardial tissue. The creation of highly aligned fibers was made with a custom electrospinning device, using three different polymers and techniques.

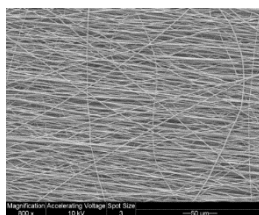


Figure 88: example of aligned electrospun nanofiber produced with 300PA.

Preliminary results of drug release were obtained embedding eosin Y, a fluorescent probe, in the polymeric matrix leading to the identification of four different scaffolds as the most promising for istaroxime delivery, showing a sustained release of the model drug for more than 7 days without noticeable burst phase.

Also, a detection method based on the derivatization of istaroxime allowed the standardization of a fast protocol for the study of the release kinetics of the molecule from the device. However, the rising of the COVID-19 pandemic did not allow the finalization of the project, involving the creation of the chosen scaffolds embedded with istaroxime and the determination of the release kinetic.

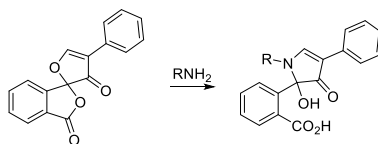


Figure 89: Fluorescamine assay for the detection of istaroxime.

In any case, preliminary release studies led to the identification of the most promising scaffolds for the future development of this drug delivery system based on electrospun nanofibers. Such composite already demonstrated the ability to induce cellular regeneration at the damaged myocardium and, in the future, could become even more powerful when combined with istaroxime. Remarkably, this approach combines two different kinds of therapies, one based on localized pharmacological treatment while the other on bio-engineered tissue regeneration. Also, once confirmed the potential of this approach, it could find a similar application in which the pure SERCA2a stimulators are embedded in the fibers, creating a unique tool for the treatment of heart failure, nevertheless pushing the therapy towards a personalized one, in which for every patient corresponds an individual pharmacological treatment with a singular dose of pharmaceutical, based on its needs.

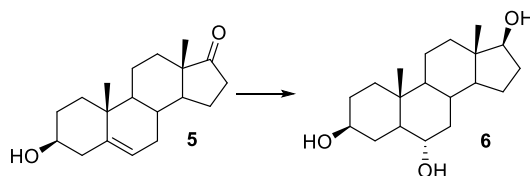
# 5. Experimental section

## 1. General

All reagents and solvents were purchased from commercial source and used without further purifications, unless stated otherwise. Reactions were monitored by thin-layer chromatography (TLC) performed over Silica Gel 60 F254 plates (Merck®). Flash chromatography purifications were performed on silica gel 60 40-63 $\mu$ m from commercial source.  $^1\text{H}$  and  $^{13}\text{C}$  NMR spectrum were recorded with Bruker Advance 400 with TopSpin® software, or with NMR Varian 400 with Vnmrj software. Chemical shifts are expressed in ppm respect  $\text{Me}_4\text{Si}$ ; coupling constants are expressed in Hz. The multiplicity in the  $^{13}\text{C}$  spectra was deduced by APT experiments. Exact masses were recorded with Orbitrap Fusion™ Tribrid™. Polyactive polymers were purchased from Polyvation®, Groningen, The Netherlands. Other polymers and solvents were buy from commercial sources and not purified unless stated otherwise. SEM images were recorded with a Philips XL 30 SEM microscope, while FIB-SEM were recorded with a Scios DualBeam.

## 2. Design of non-toxic istaroxime analogues

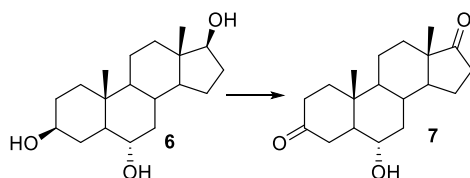
### Preparation of 5 $\alpha$ -Androstane-3 $\beta$ ,6 $\alpha$ ,17 $\beta$ -triol 6



To a stirred solution of dehydroepiandrosterone **5** (5 g, 17.5 mmol, 1 eq.) in THF (85 mL) at  $-20\text{ }^\circ\text{C}$ , under Ar, was added 1M  $\text{BH}_3\cdot\text{THF}$  complex in THF (44 mL, 44 mmol, 2.5 eq.). The resulting solution was stirred at room temperature for 3 h.  $\text{H}_2\text{O}$  (85 mL) was cautiously added dropwise followed by  $\text{NaBO}_3\cdot 4\text{H}_2\text{O}$  (5.4 g, 35 mmol, 2 eq). After stirring at room temperature overnight, the mixture was filtered. The solid was washed with THF and then discarded. The liquors were saturated with NaCl and extracted with THF (3  $\times$  40 mL). The combined organic extracts were dried over NaCl and  $\text{Na}_2\text{SO}_4$ , filtered, and evaporated to dryness. The crude product was crystallized from EtOAc/MeOH (2/1, 10 mL/g) to give a white solid (3.8 g, 70%).

$^1\text{H}$  NMR (DMSO- $d_6$ )  $\delta$  4.44 (t,  $J = 4.1$  Hz, 1H, OH), 4.24 (d,  $J = 5.6$  Hz, 1H, OH), 3.45-3.36 (m, 1H, 16-Ha), 3.26 (m, 1H, 3-H), 3.12 (m, 1H, 6-H), 0.72 (s, 3H,  $\text{CH}_3$ ), 0.60 (s, 3H,  $\text{CH}_3$ ). mp  $232\text{-}234\text{ }^\circ\text{C}$ .

### Preparation of 6 $\alpha$ -Hydroxyandrostane-3,17-dione 7

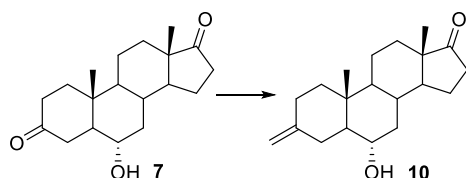


To a stirred solution of **6** (2 g, 6.5 mmol, 1 eq) in dioxane/H<sub>2</sub>O/pyridine (54/10/1 mL), NBS (3.4 g, 19.5 mmol, 3 eq) was added at 0°C. After the addition, the mixture was allowed to warm to room temperature and stirred overnight. The orange solution was diluted with water (50 mL) and quenched with Na<sub>2</sub>S<sub>2</sub>O<sub>3</sub> (350 mg). The organic solvent was evaporated under vacuum until a white solid appears. The solid was filtered and washed with water. After drying at 40 °C, was obtained a white solid 1.3g (70%).

<sup>1</sup>H NMR (acetone-d<sub>6</sub>) δ 3.61 (d, *J* = 5.7 Hz, 1H, OH), 3.48 (m, 1H, 6-H), 1.11 (s, 3H, CH<sub>3</sub>), 0.86 (s, 3H, CH<sub>3</sub>).

mp 204-206 °C lit.206-207 (Hammerschmidt & Spitteller, 1973)

#### Synthesis of adrostan-3-methylene-17-one **10**

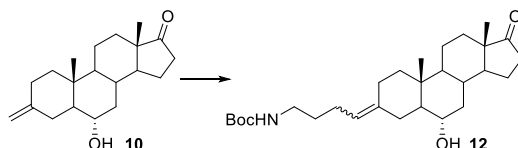


To a suspension of methyltriphenylphosphonium bromide (1,66 g, 6 mmol, 4 eq.) in THF (10 mL) was added t-BuOK (670 mg, 6 mmol, 4 eq.) at -5°C. The solution changes immediately colour to bright orange. After 10 minutes **7** (450 mg, 1.5 mmol, 1eq.) was added keeping the temperature below 0°C. Immediately after the addition the reaction was quenched by the addition of aq. 1M HCl (15 mL) and extracted with EtOAc (3x20mL). The combined organic phases were dried over Na<sub>2</sub>SO<sub>4</sub> and evaporated to dryness. Crude were purified over column chromatography (eluent EtOAc: Petroleum spirit 4:6) to give 376 mg (83%) of a white foam.

<sup>1</sup>H NMR (400 MHz, Chloroform-d) δ 4.63 (d, *J* = 5.8 Hz, 2H, 3α-CH<sub>2</sub>), 3.47 (td, *J* = 10.8, 4.6 Hz, 1H, 6-H), 2.55 (dd, *J* = 13.6, 3.6 Hz, 1H, 16Ha), 2.44 (ddd, 1H, *J* = 19.2, 9.0, 1.1 Hz, 16-Hb), 0.89 (s, 3H, CH<sub>3</sub>), 0.86 (s, 3H, CH<sub>3</sub>), 0.80 – 0.70 (m, 1H).

<sup>13</sup>C NMR (101 MHz, Chloroform-d) δ 220.79 (17-C), 148.22 (3-C), 107.40 (3-CH<sub>2</sub>), 69.85 (6-C), 13.79 (CH<sub>3</sub>), 12.91 (CH<sub>3</sub>).

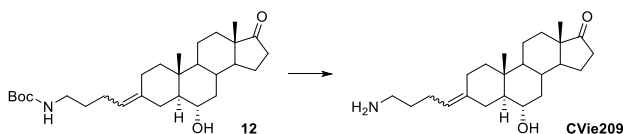
#### Cross metathesis for the synthesis of **12**



To a solution of **6** (100 mg, 0.33 mmol, 1 eq) in DCM (1 mL) was added Hoveyda-Grubbs 2<sup>nd</sup> generation catalyst (12 mg, 0.015 mmol, 0.05 eq.). The solution was heated at reflux and treated with 30  $\mu$ L of N-Boc-4-pentyne-1-amine every 20 minutes (total 610  $\mu$ L, 3.3 mmol, 10 eq.). After the end of the addition, the mixture was refluxed for additional 2h. Reaction mixture was concentrated *in vacuo* and purified by flash chromatography (Eluent Acetone: petroleum spirit 3:7) to obtain **12** as a mixture of diastereoisomers (38mg, 25%).

<sup>1</sup>H NMR (400 MHz, Chloroform-d)  $\delta$  5.18 – 5.03 (m, 1H, 3 $\alpha$ -H), 3.46 (td,  $J$  = 11.0, 5.7 Hz, 1H, 6-H), 1.44 (s, 9H, t-Bu), 0.90 (d,  $J$  = 1.8 Hz, 3H, CH<sub>3</sub>), 0.86 (s, 3H, CH<sub>3</sub>), 0.74 (m, 1H).

#### Synthesis of CVie209

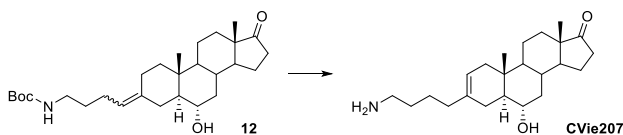


Compound **12** (50 mg, 0,1 mmol, 1 eq) was treated with 500  $\mu$ L of a 1:1 mixture TFA/DCM trifluoroacetic acid in DCM) and then stirred at room temperature. After stirring for 1 minute, the reaction was diluted with EtOAc (50mL) and washed with saturated aq. NaHCO<sub>3</sub> (3x30mL). The organic phase was dried over Na<sub>2</sub>SO<sub>4</sub>, filtered, and evaporated to dryness to produce (E $Z$ )-3-(4-aminobutylidene]-6 $\alpha$ -hydroxyandrostane-17-one (**CVie209**) as white solid (28 mg, 75%).

<sup>1</sup>H NMR (400 MHz, CD<sub>3</sub>OD)  $\delta$  5.13 (m, 1H, 3 $\alpha$ -H), 3.40 (tt, 1H,  $J$  = 10.9, 4.9 Hz, 6-H), 3.35 – 3.28 (m, 2H, 3 $\gamma$ -H), 0.96 (s, 3H, CH<sub>3</sub>), 0.87 (s, 3H, CH<sub>3</sub>), 0.83 – 0.70 (m, 1H).

<sup>13</sup>C NMR (101 MHz, CD<sub>3</sub>OD)  $\delta$  224.41 (17-C), 143.00 (3A-C), 142.68 (3 $\alpha$ B-C), 124.31 (3 $\alpha$ A-C), 124.02 (3 $\alpha$ B-C), 72.75 (C-6), 16.70 (CH<sub>3</sub>), 15.78 (CH<sub>3</sub>).

#### Synthesis of CVie207



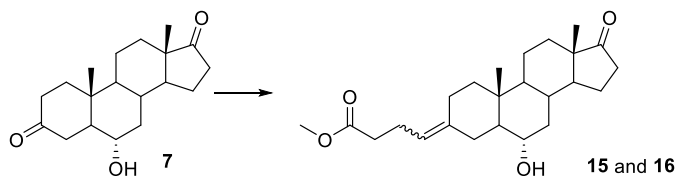
1M TMSI in DCM (100 $\mu$ L, 0,1 mmol, 1 eq.) was added to a solution of diastereoisomers **25** (50 mg, 0,1mmol, 1eq.) in 1 mL of MeOH at room temperature. After stirring 2h at the same temperature, the solvent was removed *in vacuo*. Methanol (2 mL) was added to the residue and left for 1h at room temperature. After removal of the solvent *in vacuo*, **CVie207** was obtained without further purification.

<sup>1</sup>H NMR (400 MHz, CD<sub>3</sub>OD)  $\delta$  5.36 (d,  $J$  = 5.1 Hz, 1H, H-2), 3.44 (td,  $J$  = 11.0, 4.5 Hz, 1H, 6-H), 2.94 (t,  $J$  = 7.6 Hz, 2H, 3 $\gamma$ -H), 2.45 (dd,  $J$  = 19.1, 8.7 Hz, 1H, 16-Ha), 0.88 (s, 3H, CH<sub>3</sub>), 0.79 (s, 3H, CH<sub>3</sub>).

<sup>13</sup>C NMR (101 MHz, CD<sub>3</sub>OD)  $\delta$  222.35 (17-C), 134.89 (3-C), 119.69 (2-C), 70.31 (6-H), 12.75 (CH<sub>3</sub>), 12.07 (CH<sub>3</sub>).

### 3. Section 2-Pure SERCA-2a stimulators

### Synthesis of 15 and 16 via DMSO/NaH protocol

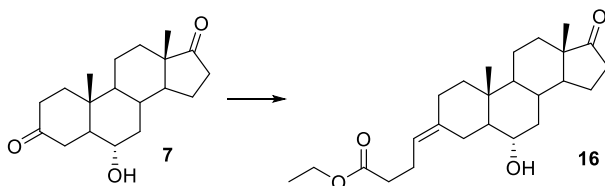


NaH 60% in mineral oil (100mg, 2.56mmol, 8 eq.) was carefully added to dry DMSO (1 mL) under Ar atmosphere, the resulting solution was stirred at 60°C for 20 minutes. After cooling at room temperature, (3-carboxypropyl)triphenylphosphonium bromide (550 mg, 1.28 mmol, 4eq.) was added. A bright orange color appears immediately. The solution was stirred for 2h then **7** (100mg, 0.32mmol, 1 eq.) was added to the mixture. The resulting solution was allowed to stir at room temperature for additional 4h. The reaction mixture diluted with EtOAc (25mL) was washed with aq. 1M HCl (3x30mL). The organic layer dried over Na<sub>2</sub>SO<sub>4</sub> was evaporated to dryness obtaining 25mg of crude material.

The crude material was dissolved in MeOH (1.5mL) then EDC hydrochloride (115mg, 0.6mmol, 2eq.) and DMAP (5mg, 0.03 mmol, 0.1 eq.) were added. The solution was stirred at room temperature for 3h. After concentration *in vacuo*. The crude solid was dissolved in EtOAc (15mL) and washed with aq. 1M HCl (3x10mL). The crude product was purified by flash chromatography over silica gel (Acetone:Pet.Sp 3:7). 25mg of a clear oil were obtained (20%).

<sup>1</sup>H NMR (Chloroform-d) mixture of 2 diastereoisomers.  $\delta$  5.16-4.96 (m, 1H, 3 $\alpha$ -H), 3.66 (s, 3H, CH<sub>3</sub>O), 3.47 (m, 1H, 6-OH), 0.89 (s, 3H, CH<sub>3</sub>), 0.86 (s, 3H, CH<sub>3</sub>), 0.74 (m, 1H).

### Synthesis of 16 via THF/LiHMDS protocol



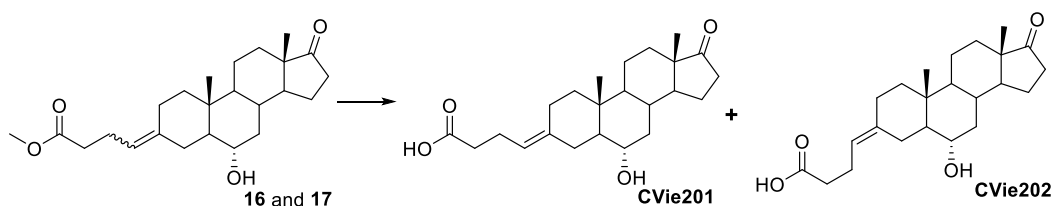
LiHMDS 1M solution in THF (40mL, 40mmol, 12 eq.) was carefully added to a dry THF (33mL) suspension of (3-carboxypropyl)triphenylphosphonium bromide (8.5 g, 20 mmol, 6eq.) under Ar atmosphere at -40°C. The solution was stirred at -40°C until a bright orange color appears then **7** (1g, 3.3mmol, 1 eq.) was added to the solution at -40°C. after stirring at room temperature overnight the reaction mixture quenched with aq. 1M HCl (300mL) was extracted with EtOAc (3x350mL). The combined organic layers were dried over Na<sub>2</sub>SO<sub>4</sub> and evaporated to dryness.

The crude material was dissolved in absolute EtOH (17mL) then EDC hydrochloride (1.26mg, 6.6mmol, 2eq.) and DMAP (50mg, 0.3 mmol, 0.1 eq.) was added. The mixture was allowed to stir at room temperature for 3h. The reaction diluted in EtOAc (150mL) was washed with aq. 1M HCl (3x100mL). The crude product was purified by flash chromatography over silica gel (Acetone:Pet.Sp 3:7). 910mg (72%).

$^1\text{H}$  NMR (Chloroform-d)  $\delta$  5.07 (d,  $J$  = 4.9 Hz, 1H, 3 $\alpha$ -H), 4.10 (q,  $J$  = 7.1, 2H, OCH<sub>2</sub>), 3.47 (td,  $J$  = 10.7, 4.5 Hz, 1H, 6-H), 2.91 (ddd,  $J$  = 13.9, 3.5, 1.7 Hz, 1H), 0.88 (s, 3H, CH<sub>3</sub>), 0.85 (s, 3H, CH<sub>3</sub>), 0.71 (m, 1H).

$^{13}\text{C}$  NMR (101 MHz, Chloroform-d)  $\delta$  173.67 (17-C), 139.60 (3 $\alpha$ -C), 119.94(3-C), 69.98 (6-C), 60.41 (OCH<sub>2</sub>), 51.33 (5-C), 40.37 (CH<sub>3</sub>), 13.92 (CH<sub>3</sub>), 13.08 (CH<sub>3</sub>).

#### Synthesis of CVie 201 and CVie202



To a solution of the methyl esters **16** and **17** (25mg, 0.06mmol, 1eq.) in THF (600 $\mu$ L) and water (200 $\mu$ L) aq. 1M LiOH (150  $\mu$ L, 2.5eq.) was added. After 2h the reaction diluted with water (10mL) and quenched by the addition of 1M HCl until pH 1. The aqueous phase was extracted with EtOAc (3x15mL). The combined organic layers were dried over Na<sub>2</sub>SO<sub>4</sub> and evaporated to dryness. Crude was purified over flash chromatography (AcOEt:Pet.Sp. 7:3 1% HCOOH). Two white solid were obtained corresponding to the E (7 mg, 31%) and Z (12 mg, 54%) diastereoisomers.

Spectroscopic data for **CVie201**:

$^1\text{H}$  NMR (Chloroform-d)  $\delta$  5.12 (d,  $J$  = 7.0 Hz, 3 $\alpha$ -H), 3.46 (td,  $J$  = 10.7, 8.9, 6-H), 2.48 (d,  $J$  = 9.4 Hz, 16-Ha), 0.90 (s, 3H, CH<sub>3</sub>), 0.86 (s, 3H, CH<sub>3</sub>), 0.80 – 0.68 (m, 1H).

$^{13}\text{C}$  NMR (101 MHz, Chloroform-d)  $\delta$  221.30 (17-C), 178.72 (CO<sub>2</sub>), 139.71 (3-C), 119.89(3 $\alpha$ -C), 69.95(6-C), 54.03 (5-C), 24.03 (16-C), 13.93(CH<sub>3</sub>), 13.06(CH<sub>3</sub>).

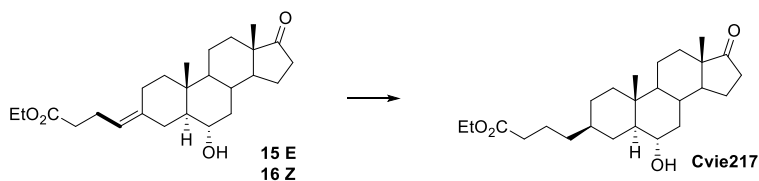
MS (ESI) calculated for C<sub>23</sub>H<sub>33</sub>O<sub>4</sub> [M] 373,2. Found: 373.4

Spectroscopic data for **CVie202**:

$^1\text{H}$  NMR (400 MHz, Chloroform-d)  $\delta$  5.10 (t,  $J$  = 7.3 Hz, 1H, 3 $\alpha$ -H), 3.50 (td,  $J$  = 10.5, 4.7 Hz, 1H, 6-H), 2.91 (d,  $J$  = 13.8 Hz, 1H, 16-Ha), 0.89 (s, 3H, CH<sub>3</sub>), 0.86 (s, 3H, CH<sub>3</sub>), 0.73 (m, 1H).

$^{13}\text{C}$  NMR (101 MHz, Chloroform-d)  $\delta$  220.86 (17-C), 177.66 (CO<sub>2</sub>), 139.84 (C-3), 119.47 (Ca), 70.08 (C-6), 13.78(CH<sub>3</sub>), 12.91 (CH<sub>3</sub>).

#### Synthesis of CVie217

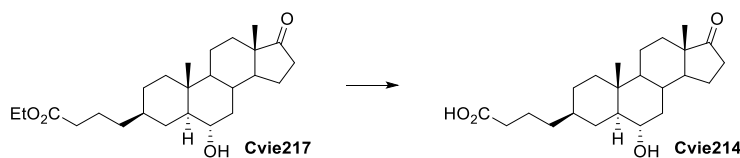


While under Ar atmosphere, 10% Pd-C (70 mg) was added to a degassed solution of diastereoisomer compounds **16** and **17** (200 mg, 0.53 mmol, 1 eq) in EtOAc (20 mL). After three cycles of vacuum/hydrogen, the reaction was allowed to stir at room temperature overnight under H<sub>2</sub> atmosphere. After removal of hydrogen by vacuum/Ar cycle, the reaction mixture was filtered over CELITE®. The filtered solution was evaporated to dryness. **CVie217** product was obtained without purification at 186 mg (90%).

<sup>1</sup>H NMR (400 MHz, Chloroform-d) δ 4.09 (q, *J* = 6.8, 2H, CH<sub>2</sub>O), 3.40 (td, 1H, td, *J* = 10.5, 5.1 Hz, 6-H), 2.42 (ddd, *J* = 19.1, 8.9, 16-Ha), 2.24 (t, *J* = 8.0, 5.4, 2.1 Hz, 2H, 3δ-H), 0.83 (s, 3H, CH<sub>3</sub>), 0.76 (s, 3H, CH<sub>3</sub>).

<sup>13</sup>C NMR (101 MHz, Chloroform-d) δ 220.91 (17-C), 173.77 (CO<sub>2</sub>), 69.63 (6-C), 60.14 (CH<sub>2</sub>O), 14.23 (CH<sub>3</sub>), 13.76 (CH<sub>3</sub>), 13.36 (CH<sub>3</sub>).

#### Synthesis of **CVie214**

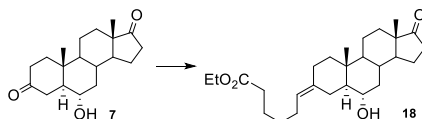


**CVie219** was synthesized following the same procedure for the synthesis of **CVie201**.

<sup>1</sup>H NMR (400 MHz, Chloroform-d) δ 3.43 (bt, 1H, 6-H), 2.44 (dd, *J* = 19.2, 8.7 Hz, 1H, 16Ha), 2.31 (bt, 2H, 3γ-H), 0.84 (s, 3H, CH<sub>3</sub>), 0.77 (s, 3H, CH<sub>3</sub>).

<sup>13</sup>C NMR (101 MHz, Chloroform-d) δ 221.35 (17-C), 179.11 (CO<sub>2</sub>), 69.90 (6-C), 13.78 (CH<sub>3</sub>), 13.37(CH<sub>3</sub>)

#### Synthesis of **18**

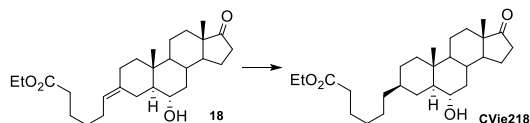


**18** was synthesized following the same procedure for the synthesis of **16** *via* THF/LiHMDS protocol.

<sup>1</sup>H NMR (400 MHz, Chloroform-d) δ 5.08 (td, *J* = 6.4, 5.6, 1.8 Hz, 1H), 3.45 (td, *J* = 10.8, 4.6 Hz, 1H), 2.87 (ddd, *J* = 14.0, 3.6, 1.8 Hz, 1H), 2.49 – 2.39 (m, 1H), 1.24 (t, *J* = 7.1 Hz, 5H), 0.89 (s, 3H), 0.86 (s, 3H), 0.79 – 0.69 (m, 1H).

<sup>13</sup>C NMR (101 MHz, Chloroform-d) δ 174.19, 138.44, 121.41, 69.92, 60.28, 54.55, 54.03, 51.21, 47.76, 40.52, 40.26, 37.46, 34.23, 33.88, 32.17, 31.43, 29.27, 26.36, 25.21, 24.35, 21.76, 20.21, 14.23, 13.78, 12.90.

### Synthesis of CVie218

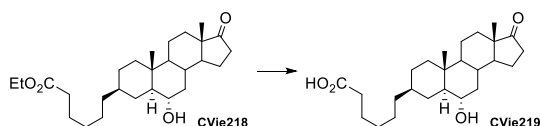


**CVie218** was synthesized following the same procedure for the synthesis of **CVie217**.

$^1\text{H}$  NMR (400 MHz, Chloroform- $d$ )  $\delta$  4.11 (q,  $J$  = 6.9 Hz, 2H,  $\text{OCH}_2$ ), 3.40 (td,  $J$  = 10.0, 4.5 Hz, 1H, 6-H), 2.43 (dd,  $J$  = 19.2, 8.9 Hz, 1H, 16-Ha), 2.26 (t,  $J$  = 7.5, 2H,  $3\epsilon\text{-H}$ ), 0.84 (s, 3H,  $\text{CH}_3$ ), 0.76 (s, 3H,  $\text{CH}_3$ ).

$^{13}\text{C}$  NMR (101 MHz, Chloroform- $d$ )  $\delta$  220.91 (17-C), 173.87 ( $\text{CO}_2$ ), 69.81 (6-C), 60.14 ( $\text{CH}_2\text{O}$ ), 14.24 ( $\text{CH}_3$ ), 13.79 ( $\text{CH}_3$ ), 13.39 ( $\text{CH}_3$ ).

### Synthesis of CVie219

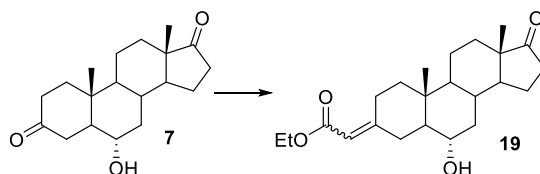


**CVie219** was synthesized following the same procedure for the synthesis of **CVie201**.

$^1\text{H}$  NMR (400 MHz, Chloroform- $d$ )  $\delta$  3.47 – 3.39 (bt, 1H, 6-H), 2.44 (dd,  $J$  = 19.2, 8.6 Hz, 1H, 17-Ha), 2.33 (t,  $J$  = 7.4 Hz, 2H,  $3\epsilon\text{-H}$ ), 0.85 (s, 3H,  $\text{CH}_3$ ), 0.77 (s, 3H,  $\text{CH}_3$ ).

$^{13}\text{C}$  NMR (101 MHz, Chloroform- $d$ )  $\delta$  221.06 (17-C), 178.93 ( $\text{CO}_2$ ), 69.91 (6-C), 13.80 ( $\text{CH}_3$ ), 13.39 ( $\text{CH}_3$ ).

### Synthesis of 19

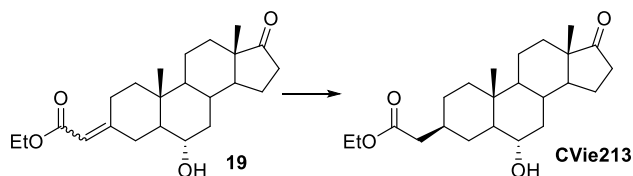


To a suspension of NaH 60% in mineral oil (1.3 g, 33 mmol, 5 eq) in DMF (200 mL) under Ar atmosphere triethylphosphonoacetate (6.5 mL, 33 mmol, 5 eq) was added carefully at 0°C. The resulting solution was warmed at room temperature and stirred for 20 minutes, then **7** (2 g, 6.5 mmol, 1 eq) was added at 0°C. After stirring overnight at room temperature the reaction was quenched by careful addition of  $\text{H}_2\text{O}$  (100mL) and extracted with  $\text{Et}_2\text{O}$  (3x150mL) the combined organic layers were dried over  $\text{Na}_2\text{SO}_4$  and evaporated *in vacuo*. Crude was purified by flash chromatography over a column of silica gel (acetone: petroleum spirit 3:7) to give 2.1g (86%) of a clear oil mixture of two diastereoisomers.

$^1\text{H}$  NMR (Chloroform-d)  $\delta$  5.60 (s, 1H, 3 $\alpha$ -H), 4.21 – 4.06 (m, 2H, CH<sub>2</sub>O), 3.45 (td,  $J$  = 10.8, 4.5 Hz, 1H, 6-H), 2.41 (dd,  $J$  = 19.3, 8.8 Hz, 1H, 16-Ha), 0.90 (s, 3H, CH<sub>3</sub>), 0.82 (s, 3H, CH<sub>3</sub>), 0.77-0.66 (m, 1H, 5-H).

$^{13}\text{C}$  NMR (101 MHz, Chloroform-d)  $\delta$  220.85 (17-C), 166.81 (CO<sub>2</sub>), 161.87 (3-C), 113.75 (3 $\alpha$ -C), 69.41 (6-C), 13.76 (CH<sub>3</sub>), 13.00 (CH<sub>3</sub>).

#### Synthesis of CVie213

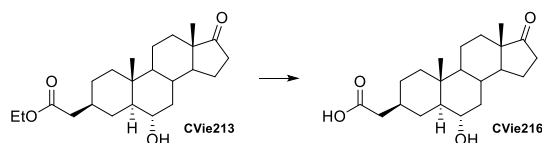


**CVie213** was synthesized following the same procedure for the synthesis of **CVie217**.

$^1\text{H}$  NMR (Chloroform-d)  $\delta$  4.12 (q,  $J$  = 7.2 Hz, 2H, OCH<sub>2</sub>), 3.38 (td,  $J$  = 10.7, 4.4 Hz, 1H, 6-H), 2.42 (dd,  $J$  = 19.2, 8.8 Hz, 1H, 16-Ha), 2.27 (t,  $J$  = 4.3 Hz, 2H, 3 $\alpha$ -CH<sub>2</sub>), 0.82 (s, 3H, CH<sub>3</sub>), 0.76 (s, 3H, CH<sub>3</sub>).

$^{13}\text{C}$  NMR (101 MHz, Chloroform-d)  $\delta$  221.03 (17-C), 172.93 (CO<sub>2</sub>), 69.43 (6-C), 13.76 (CH<sub>3</sub>), 13.32(CH<sub>3</sub>).

#### Synthesis of CVie216

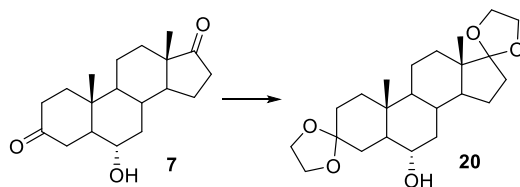


**CVie216** was synthesized following the same procedure for the synthesis of **CVie201**.

$^1\text{H}$  NMR (400 MHz, Chloroform-d)  $\delta$  3.43 (td, td,  $J$  = 10.7, 4.5 Hz, 1H, 6-H), 2.45 (dd,  $J$  = 19.3, 8.7 Hz, 1H, 16-Ha), 2.28 (t, 3 $\alpha$ -H), 0.85 (s, 3H, CH<sub>3</sub>), 0.80 (s, 3H, CH<sub>3</sub>).

$^{13}\text{C}$  NMR (101 MHz, acetone)  $\delta$  220.44 (17-C), 174.27 (CO<sub>2</sub>), 68.57 (6-C), 12.99 (CH<sub>3</sub>), 12.59 (CH<sub>3</sub>).

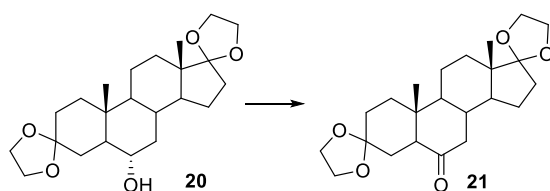
#### Preparation of 3,3:17,17-Bis(ethyldioxy)androstane-6 $\alpha$ -ol 20



A solution of **7** (1.5 g, 4.9 mmol, 1 eq), ethylene glycol (10.5 mL, 88 mmol, 36 eq) and pTSA (561 mg, 2.9 mmol, 0.6 eq) in toluene (160 mL) was stirred at reflux for 12 h with a Dean-Stark trap. After cooling to room temperature, the mixture was neutralized with aq. 5% NaHCO<sub>3</sub> solution. The organic layer was separated and washed with H<sub>2</sub>O (2 × 40 mL), dried over Na<sub>2</sub>SO<sub>4</sub> and evaporated to dryness to give a white solid (1.9 g, 98%).

<sup>1</sup>H NMR (DMSO-d<sub>6</sub>) δ 4.25 (d, *J* = 5.6 Hz, 1H, OH), 3.88-3.70 (m, 8H, OCH<sub>2</sub>), 3.11 (m, 1H, 6-H), 0.74 (s, 3H, CH<sub>3</sub>), 0.73 (s, 3H, CH<sub>3</sub>).

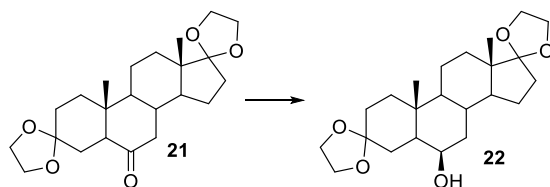
#### Preparation of 3,3:17,17-Bis(ethylenedioxy)androstane-6-one **21**



To a solution of **20** (3 g, 14 mmol, 1 eq) and sodium ascorbate (1.2 g, 14 mmol, 4 eq.) in dry CH<sub>2</sub>Cl<sub>2</sub> (87 mL) was added PCC (148 mg, 0.69 mmol, 4 eq) at 0°. The mixture was stirred overnight at room temperature. The mixture was washed with aq. 1M HCl (3 × 30 mL) and water (3 × 30 mL). The organic layer was dried over Na<sub>2</sub>SO<sub>4</sub> and evaporated to dryness. Crude was purified by flash chromatography over a column of silica gel (eluent acetone: petroleum spirit 2:8). 1.53 g (96%) of a white solid were obtained.

<sup>1</sup>H NMR (Acetone-d<sub>6</sub>) δ 3.97-3.76 (m, 8H, CH<sub>2</sub>O), 2.82 (d, *J* = 12.7 Hz, 1H), 2.54 (t, *J* = 8.1 Hz, 1H), 2.19 (dd, 1H, *J* = 13.2, 5.0 Hz, 16-Ha), 0.84 (s, 3H, CH<sub>3</sub>), 0.75 (s, 3H, CH<sub>3</sub>).

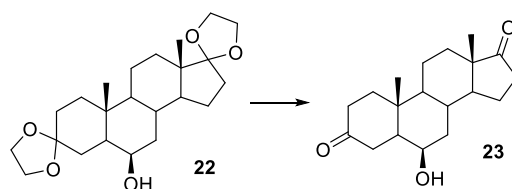
#### Preparation of 3,3:17,17-Bis(ethylenedioxy)androstane-6β-ol **22**



To a stirred **21** (1 g, 2.5 mmol, 1 eq) in MeOH (13 mL) at 0°C, NaBH<sub>4</sub> (144 mg, 3 mmol, 1.2 eq) was added. After 2 h at 0 °C, H<sub>2</sub>O (40 mL) was added dropwise. The mixture was extracted with EtOAc (3 × 40 mL). The combined organic extracts were dried over Na<sub>2</sub>SO<sub>4</sub>, filtered, and evaporated to dryness to give a white solid (915 mg, 92%).

<sup>1</sup>H NMR (acetone-d<sub>6</sub>) δ 3.95-3.75 (m, 8H, OCH<sub>2</sub>), 3.70 (m, 1H, 6-H), 3.33 (s, 1H, 6-OH), 1.05 (s, 3H, CH<sub>3</sub>), 0.84 (s, 3H, CH<sub>3</sub>).

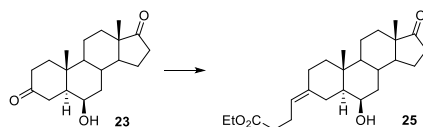
#### Preparation of 6β-Hydroxyandrostane-3,17-dione **23**



PTSA (2.26 g, 11.5 mmol, 5 eq) was added in small portion over 5 minutes to a solution of **22** (910 mg, 2.3 mmol, 1 eq) in acetone (46 mL). After stirring at room temperature for 1 h, the solution was quenched by addition of aq. 5% NaHCO<sub>3</sub> until pH 7. After stirring for 5 minutes, a white solid appears. The volatiles were removed *in vacuo*. The suspension was extracted with CH<sub>2</sub>Cl<sub>2</sub> (3x30 mL) the combined organic extracts were washed with brine (40 mL), dried over Na<sub>2</sub>SO<sub>4</sub>, filtered, and evaporated. The solid obtained was stirred with n-hexane/EtOAc 8/2 (10 mL) for 45 minutes and then collected by filtration. The solid was dried 45 °C for 3 hours. 568 mg (81%) of a white solid were obtained.

<sup>1</sup>H NMR (DMSO-d<sub>6</sub>) δ 4.47 (d, *J* = 3.9 Hz, 1H, OH), 3.57 (m, 1H, 6-H), 1.13 (s, 3H, CH<sub>3</sub>), 0.81 (s, 3H, CH<sub>3</sub>).

#### Synthesis of **25**

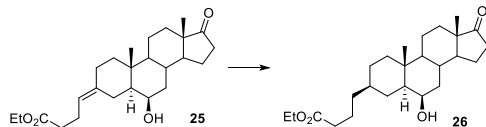


**25** was synthesized following the same procedure for the synthesis of **16** *via* THF/LiHMDS protocol.

<sup>1</sup>H NMR (400 MHz, Chloroform-d) δ 5.07 (s, 1H, 3α-H), 3.89 (dd, *J* = 5.8, 2.5 Hz, 1H, 6-H), 3.66 (s, 3H, OCH<sub>3</sub>), 2.46 (dd, *J* = 19.1, 8.7 Hz, 1H, 16-Ha), 1.10 (s, 3H, CH<sub>3</sub>), 0.89 (s, 3H, CH<sub>3</sub>), 0.79 – 0.64 (m, 1H).

<sup>13</sup>C NMR (101 MHz, Chloroform-d) δ 221.21 (17-C), 176.10 (CO<sub>2</sub>), 140.33 (3-C), 119.39 (3α-C), 71.75 (6-C), 54.49 (5-C), 51.20 (OCH<sub>3</sub>), 15.24 (CH<sub>3</sub>), 13.87 (CH<sub>3</sub>).

#### Synthesis of **26**

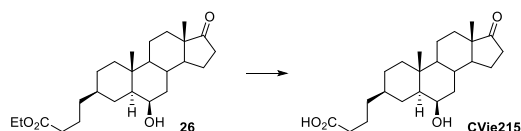


**26** was synthesized following the same procedure for the synthesis of **CVie217**.

$^1\text{H}$  NMR (400 MHz, Chloroform- $d$ )  $\delta$  3.83 (bs, 1H, 6-H), 3.66 (bs, 3H,  $\text{OCH}_3$ ), 2.44 (dd,  $J = 19.2, 8.9$  Hz, 1H, 16-Ha), 2.28 (t,  $J = 7.4$  Hz, 2H, 3 $\gamma$ -H), 0.99 (s, 3H,  $\text{CH}_3$ ), 0.88 (s, 3H,  $\text{CH}_3$ ), 0.79 – 0.70 (m, 1H).

$^{13}\text{C}$  NMR (101 MHz, Chloroform- $d$ )  $\delta$  221.43 (17-C), 174.25 ( $\text{CO}_2$ ), 71.96 (6-C), 51.25 ( $\text{OCH}_3$ ), 15.74 ( $\text{CH}_3$ ), 13.86( $\text{CH}_3$ ).

#### Synthesis of **CVie215**

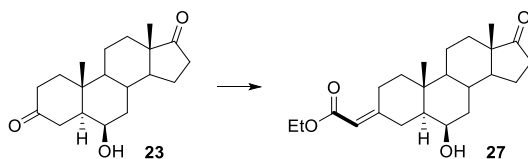


**CVie215** was synthesized following the same procedure for the synthesis of **CVie201**.

$^1\text{H}$  NMR (400 MHz, Chloroform- $d$ )  $\delta$  3.85 (s, 1H, 6-H), 2.45 (dd,  $J = 19.2, 8.9$  Hz, 1H, 16-Ha), 2.34 (t,  $J = 7.4$  Hz, 2H, 3 $\gamma$ -H), 1.00 (s, 3H,  $\text{CH}_3$ ), 0.89 (s, 3H,  $\text{CH}_3$ ), 0.74 (d, 1H).

$^{13}\text{C}$  NMR (101 MHz, Chloroform- $d$ )  $\delta$  221.50 (17-C), 179.04 ( $\text{CO}_2\text{H}$ ), 72.03 (6-C), 15.76 ( $\text{CH}_3$ ), 13.87 ( $\text{CH}_3$ ).

#### Synthesis of **27**

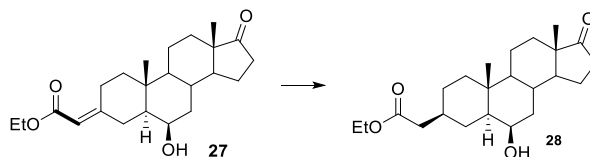


**27** was synthesized following the same procedure for the synthesis of **19** and isolated as mixture of diastereoisomers.

$^1\text{H}$  NMR (400 MHz, Chloroform- $d$ )  $\delta$  5.64 (d,  $J = 5.1$  Hz, 1H), 4.14 (q,  $J = 7.1$  Hz, 3H), 3.90 (dd,  $J = 27.4, 2.8$  Hz, 1H), 3.81 – 3.70 (m, 1H), 3.67 – 3.57 (m, 1H), 0.91 (s, 5H), 0.86 – 0.73 (m, 2H).

$^{13}\text{C}$  NMR (101 MHz, Chloroform- $d$ )  $\delta$  221.01, 166.87, 166.72, 163.06, 162.87, 128.31, 127.88, 113.51, 113.21, 71.36, 71.19, 59.55, 54.31, 54.23, 51.16, 51.12, 50.51, 49.84, 41.40, 40.83, 38.62, 38.40, 37.35, 36.30, 35.83, 35.80, 33.35, 31.47, 30.01, 29.98, 29.33, 25.36, 21.77, 20.27, 20.22, 15.31, 15.29, 14.31, 13.88.

#### Synthesis of **28**

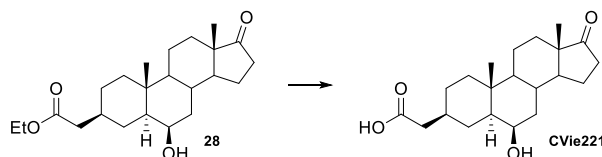


**28** was synthesized following the same procedure for the synthesis of **CVie213**.

$^1\text{H}$  NMR (400 MHz, Chloroform- $d$ )  $\delta$  4.12 (q,  $J$  = 7.1 Hz, 2H), 3.88 – 3.82 (m, 1H), 2.52 – 2.40 (m, 1H), 2.24 (dd,  $J$  = 7.0, 1.1 Hz, 2H), 2.07 (dt,  $J$  = 18.9, 9.0 Hz, 1H), 1.01 (s, 3H), 0.89 (s, 3H), 0.76 (ddd,  $J$  = 12.2, 10.1, 4.1 Hz, 1H).

$^{13}\text{C}$  NMR (101 MHz, Chloroform- $d$ )  $\delta$  221.25, 172.98, 71.78, 60.18, 54.48, 51.25, 49.00, 47.85, 41.98, 39.84, 38.32, 35.91, 35.83, 35.50, 32.17, 31.50, 30.09, 30.05, 28.41, 21.76, 21.73, 20.07, 15.69, 14.28, 13.86.

#### Synthesis of **CVie221**



**CVie221** was synthesized following the same procedure for the synthesis of **CVie201**.

$^1\text{H}$  NMR (400 MHz, Chloroform- $d$ )  $\delta$  3.78 (s, 1H), 2.44 (dd,  $J$  = 19.1, 8.8 Hz, 1H), 2.22 (d,  $J$  = 7.0 Hz, 2H), 1.02 (d,  $J$  = 1.2 Hz, 2H), 0.90 (d,  $J$  = 1.2 Hz, 3H), 0.85 – 0.76 (m, 1H).

$^{13}\text{C}$  NMR (101 MHz, Chloroform- $d$ )  $\delta$  221.33, 177.81, 77.33, 77.01, 76.69, 71.76, 54.45, 51.22, 48.96, 47.86, 41.47, 39.81, 38.33, 35.89, 35.83, 35.30, 32.08, 31.48, 30.05, 29.69, 28.39, 21.76, 21.74, 20.07, 15.69, 13.86.

## 4. Section 3-double target molecules

#### Preparation of **N-Boc-3-(2-hydroxyethyl)azetidine 30**



To a solution of *N*-Boc-azetidine-3-acetic acid (1g, 4.6 mmol) in THF (30mL), 1M  $\text{BH}_3$  THF complex (6.9 mL, 1.5 eq) was added to the solution at 0°C. After stirring 2h at the same temperature, reaction was quenched by addition of water (30mL). THF was removed by concentration *in vacuo*. The residue was extracted with EtOAc (3x 25 mL). Combined organic phases was dried over  $\text{Na}_2\text{SO}_4$  and evaporated to dryness, obtaining 1.03g (q.tive). Product was used without further purification.

$^1\text{H}$  NMR (400 MHz, Chloroform- $d$ )  $\delta$  4.02 (t,  $J$  = 8.4 Hz, 2H), 3.68 – 3.54 (m, 4H), 2.65 (tt,  $J$  = 7.9, 5.6 Hz, 1H), 1.84 (dt,  $J$  = 7.5, 6.4 Hz, 2H), 1.66 (s, 2H), 1.42 (s, 9H).

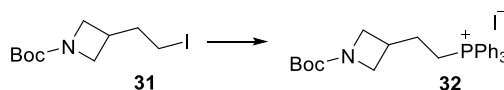
#### Preparation of N-Boc-3-(2-iodoethyl)azetidine **31**



To a solution of **30** (2.3g, 11.4 mmol), triphenylphosphine (3.3g, 12.5 mmol, 1.1 eq), and imidazole (1.2g, 17.1 mmol, 1.5 eq) in ACN (57 mL), iodine (3.1g, 12.5 mmol, 1.1 eq) was added in little portions at 0°C. The resulting solution was stirred at room temperature overnight. After addition of water (100mL) the solution was extracted with petroleum spirit (3x40mL). Combined organic phases was dried over  $\text{Na}_2\text{SO}_4$  and evaporated to dryness, obtaining 2.8 g (56%). Product was used without further purification.

$^1\text{H}$  NMR (400 MHz, Chloroform- $d$ )  $\delta$  4.08 – 3.99 (m, 2H), 3.56 (dd,  $J$  = 8.6, 5.5 Hz, 2H), 3.10 (t,  $J$  = 7.0 Hz, 2H), 2.69 – 2.57 (m, 1H), 2.13 (q,  $J$  = 7.1 Hz, 2H), 1.43 (s, 9H).

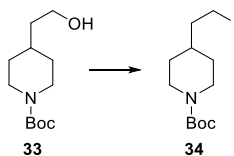
#### Preparation of N-Boc-3-(2-triphenylphosphoniumethyl)azetidine iodide **32**



To a solution of **31** (2.08g, 6.7 mmol) in DMF (13 mL), was added triphenyl phosphine (2.6g, 10mmol, 1.5 eq.). Mixture was heated overnight at 90°C. After concentration *in vacuo* crude was crystallized from toluene to obtain 3.21g (83%) of the final product, used without further purifications.

$^1\text{H}$  NMR (400 MHz, DMSO- $d_6$ )  $\delta$  7.99 – 7.50 (m, 15H), 7.32 – 7.06 (m, 1H), 4.47 – 4.01 (m, 1H), 3.74 – 3.51 (m, 2H), 3.43 – 3.04 (m, 1H), 2.48 (p,  $J$  = 1.9 Hz, 9H), 2.28 (s, 1H), 1.60 (dt,  $J$  = 16.8, 10.4 Hz, 1H).

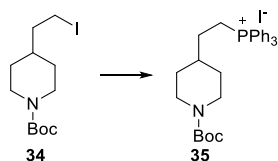
#### Preparation of N-Boc-4-(2-iodoethyl)piperidine **34**



**32** was synthesized following the same procedure for the synthesis of **31**.

$^1\text{H}$  NMR (400 MHz, DMSO- $d_6$ )  $\delta$  3.89 (d,  $J$  = 12.5 Hz, 2H), 3.35 – 3.22 (m, 3H), 2.65 (s, 2H), 2.52 – 2.44 (m, 1H), 1.69 (q,  $J$  = 7.1 Hz, 2H), 1.65 – 1.56 (m, 2H), 1.48 (ddq,  $J$  = 10.9, 7.4, 3.6, 3.1 Hz, 1H), 1.36 (s, 7H), 0.96 (qd,  $J$  = 12.5, 4.3 Hz, 2H).

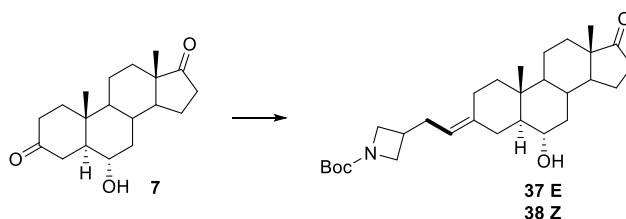
#### Preparation of N-Boc-4-(2-triphenylphosphoniumethyl)piperidine iodide **35**



**33** was synthesized following the same procedure for the synthesis of **32**.

$^1\text{H}$  NMR (400 MHz, DMSO- $d_6$ )  $\delta$  7.93 – 7.63 (m, 16H), 3.89 (s, 2H), 3.59 (d,  $J$  = 14.4 Hz, 2H), 2.64 (s, 2H), 1.68 (d,  $J$  = 12.7 Hz, 2H), 1.46 (d,  $J$  = 7.8 Hz, 1H), 1.35 (s, 11H), 0.96 (q,  $J$  = 10.6, 10.1 Hz, 2H).

#### Synthesis of **37** and **38**



**36** and **37** was synthesized following the same procedure for the synthesis of **16** *via* NaH/DMSO protocol.

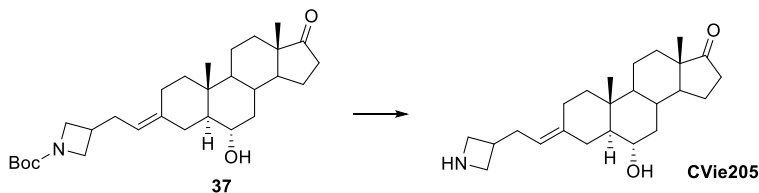
Spectroscopic data for **37**

$^1\text{H}$  NMR (400 MHz, Chloroform- $d$ )  $\delta$  5.03 (t,  $J$  = 7.4 Hz, 1H, 3 $\alpha$ -H), 3.95 (td,  $J$  = 8.2, 2.9 Hz, 2H, CH<sub>2</sub>A-azetidine), 3.49 (m, 3H, CH<sub>2</sub>B-azetidine and 6-H), 1.43 (s, 9H), 0.90 (s, 3H, CH<sub>3</sub>), 0.87 (s, 3H, CH<sub>3</sub>).

Spectroscopic data for **38**

$^1\text{H}$  NMR (400 MHz, Chloroform- $d$ )  $\delta$  5.01 (bt, 1H, 3 $\alpha$ -H), 3.95 (q,  $J$  = 8.7 Hz, 2H, CH<sub>2</sub>A-azetidine), 3.58 – 3.41 (m, 3H, CH<sub>2</sub>B-azetidine and 6-H), 2.90 (d,  $J$  = 13.9 Hz, 1H), 2.53 – 2.37 (m, 2H, 16-H), 1.43 (s, 9H, t-Bu), 0.90 (s, 3H, CH<sub>3</sub>), 0.86 (s, 3H, CH<sub>3</sub>), 0.75 (t, 1H).

#### Synthesis of **CVie205**

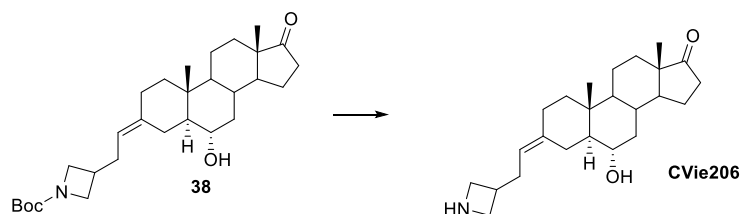


**CVie205** was synthesized following the same procedure for the synthesis of **CVie209**.

$^1\text{H}$  NMR (400 MHz, CD<sub>3</sub>OD)  $\delta$  5.05 (t,  $J$  = 7.6 Hz, 1H, 3 $\alpha$ -H), 3.82 (t,  $J$  = 9.0 Hz, 1H), 3.53 – 3.47 (m, 2H), 3.44 – 3.34 (m, 1H, 6-H), 2.86 – 2.72 (m, 1H), 0.95 (s, 3H, CH<sub>3</sub>), 0.88 (s, 3H, CH<sub>3</sub>).

$^{13}\text{C}$  NMR (101 MHz, CD<sub>3</sub>OD)  $\delta$  222.68 (17-C), 141.87 (3-C), 116.34 (3 $\alpha$ -C), 69.15 (6-C), 13.62 (CH<sub>3</sub>), 12.74 (CH<sub>3</sub>).

#### Synthesis of **CVie206**

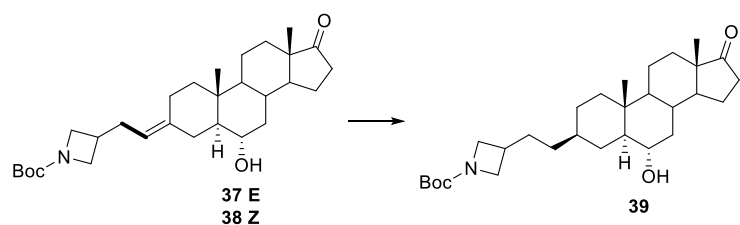


**CVie206** was synthesized following the same procedure for the synthesis of **CVie209**.

$^1\text{H}$  NMR (400 MHz,  $\text{CD}_3\text{OD}$ )  $\delta$  5.04 (t,  $J = 7.5$  Hz, 1H, 3 $\alpha$ -H), 4.06 – 3.91 (m, 2H), 3.72 – 3.61 (m, 2H), 3.47 (qd,  $J = 10.8, 6.5$  Hz, 1H, 6-H), 0.95 (s, 3H,  $\text{CH}_3$ ), 0.88 (s, 3H,  $\text{CH}_3$ ), 0.75 (m, 1H).

$^{13}\text{C}$  NMR (101 MHz,  $\text{CD}_3\text{OD}$ )  $\delta$  226.09 (17-C), 145.65 (3-C), 120.09 (3 $\alpha$ -C), 72.87 (6-C), 16.69 ( $\text{CH}_3$ ), 15.82 ( $\text{CH}_3$ ).

#### Synthesis of **39**

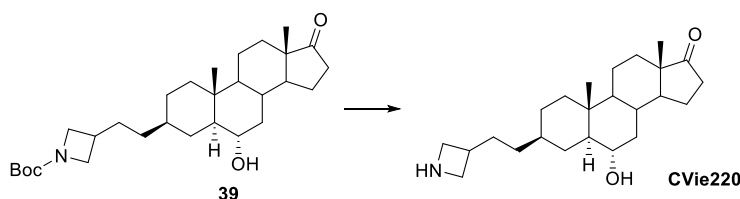


**39** was synthesized following the same procedure for the synthesis of **CVie213**.

$^1\text{H}$  NMR (400 MHz, Chloroform- $d$ )  $\delta$  3.97 (t,  $J = 8.3$  Hz, 2H), 3.50 (dd,  $J = 8.5, 5.4$  Hz, 2H), 3.43 (td,  $J = 10.7, 4.5$  Hz, 1H), 2.52 – 2.39 (m, 2H), 1.28 – 1.43 (s, 9H), 0.87 – 0.84 (s, 3H).

$^{13}\text{C}$  NMR (101 MHz, Chloroform- $d$ )  $\delta$  220.98, 156.48, 79.16, 69.79, 54.50, 54.17, 53.38, 51.23, 47.79, 40.42, 38.74, 37.26, 36.96, 35.80, 34.53, 33.85, 31.91, 31.74, 31.43, 29.69, 29.65, 29.33, 29.24, 29.05, 28.42, 22.68, 21.75, 20.18, 13.79, 13.39.

#### Synthesis of **CVie220**

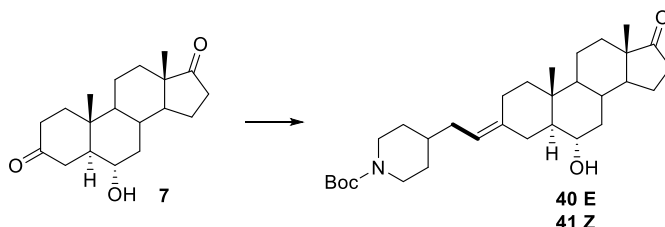


**CVie220** was synthesized following the same procedure for the synthesis of **CVie209**.

$^1\text{H}$  NMR (400 MHz,  $\text{CD}_3\text{OD}$ )  $\delta$  3.98 – 3.88 (m, 1H), 3.64 – 3.52 (m, 1H), 2.35 (dd,  $J = 19.1, 8.7$  Hz, 1H), 0.77 (s, 4H), 0.73 (s, 3H).

$^{13}\text{C}$  NMR (101 MHz,  $\text{CD}_3\text{OD}$ )  $\delta$  216.48, 68.88, 54.30, 51.22, 48.23, 48.02, 47.81, 47.60, 47.39, 47.17, 46.96, 40.02, 36.64, 35.25, 33.77, 31.33, 29.38, 21.32, 19.92, 12.77, 12.33, -0.27.

#### Synthesis of **40** and **41**



**40** and **41** was synthesized following the same procedure for the synthesis of **16** *via* NaH/DMSO protocol.

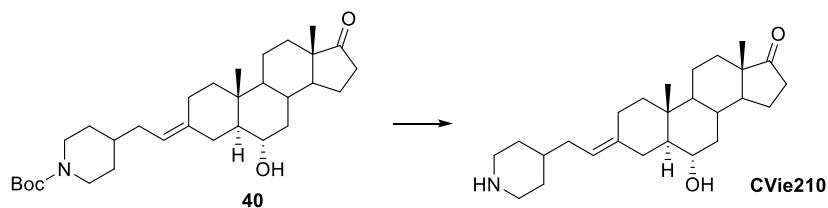
Spectroscopic data for **40**

$^1\text{H}$  NMR (400 MHz, Chloroform- $d$ )  $\delta$  5.10 (t,  $J = 7.6$  Hz, 1H,  $3\alpha\text{-H}$ ), 4.05 (d,  $J = 13.2$  Hz, 2H), 3.48 (td,  $J = 10.7$ , 4.5 Hz, 1H, 6-H), 2.84 (dd,  $J = 13.5$ , 3.1 Hz, 1H), 2.64 (td,  $J = 12.9$ , 2.7 Hz, 2H), 2.45 (dd,  $J = 19.2$ , 8.8 Hz, 1H, 16-Ha), 1.44 (s, 9H, t-Bu), 0.89 (s, 3H,  $\text{CH}_3$ ), 0.86 (s, 3H,  $\text{CH}_3$ ), 0.74 (t,  $J = 11.2$  Hz, 1H).

Spectroscopic data for **41**

$^1\text{H}$  NMR (400 MHz, Chloroform- $d$ )  $\delta$  5.14 (t,  $J = 7.6$  Hz, 1H,  $3\alpha\text{-H}$ ), 4.06 (d,  $J = 12.9$  Hz, 2H), 3.48 (td,  $J = 10.8$ , 4.6 Hz, 1H, 6-H), 2.65 (t,  $J = 13.0$  Hz, 2H), 1.45 (s, 9H, t-Bu), 0.90 (s, 3H,  $\text{CH}_3$ ), 0.87 (s, 3H,  $\text{CH}_3$ ), 0.76 (s, 1H).

#### Synthesis of **CVie210**

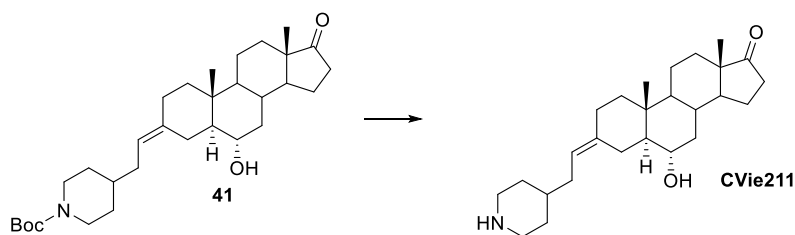


**CVie210** was synthesized following the same procedure for the synthesis of **CVie209**.

$^1\text{H}$  NMR (400 MHz,  $\text{CD}_3\text{OD}$ )  $\delta$  5.12 (t,  $J = 7.6$  Hz, 1H,  $3\alpha\text{-H}$ ), 3.43 (td,  $J = 10.8$ , 4.5 Hz, 1H, 6-H), 3.08 (dt,  $J = 12.8$ , 3.2 Hz, 2H), 2.99 – 2.87 (m, 1H), 2.62 (td,  $J = 12.3$ , 2.7 Hz, 2H), 2.44 (dd,  $J = 19.1$ , 8.7 Hz, 1H, 17-Ha), 0.94 (s, 3H,  $\text{CH}_3$ ), 0.88 (s, 3H,  $\text{CH}_3$ ), 0.75 (td, 1H).

$^{13}\text{C}$  NMR (101 MHz,  $\text{CD}_3\text{OD}$ )  $\delta$  222.13 (17-C), 139.45 (3-C), 118.90 ( $3\alpha\text{-C}$ ), 68.99 (6-C), 12.78 ( $\text{CH}_3$ ), 11.90 ( $\text{CH}_3$ ).

#### Synthesis of **CVie211**

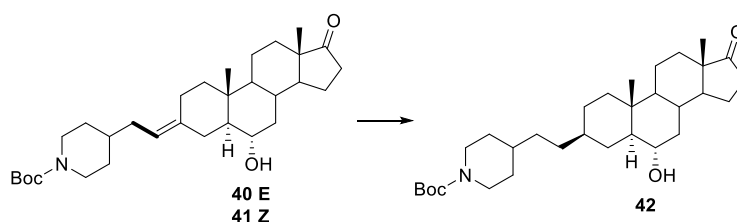


**CVie211** was synthesized following the same procedure for the synthesis of **CVie209**.

$^1\text{H}$  NMR (400 MHz,  $\text{CD}_3\text{OD}$ )  $\delta$  5.13 (d,  $J = 8.1$  Hz, 1H,  $3\alpha\text{-H}$ ), 3.46 – 3.37 (m, 1H, 6-H), 3.23 (d,  $J = 12.6$  Hz, 2H), 2.77 (d,  $J = 12.9$  Hz, 3H), 2.53 – 2.39 (m, 3H), 0.95 (s, 3H,  $\text{CH}_3$ ), 0.88 (s, 3H,  $\text{CH}_3$ ).

$^{13}\text{C}$  NMR (101 MHz,  $\text{CD}_3\text{OD}$ )  $\delta$  191.64 (17-C), 144.10 (3-C), 122.44 ( $3\alpha\text{-C}$ ), 73.08 (6-C), 16.68 ( $\text{CH}_3$ ), 15.77 ( $\text{CH}_3$ ).

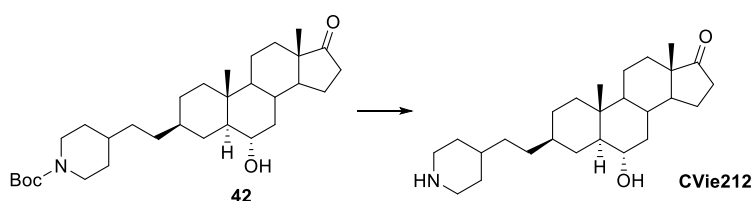
#### Synthesis of **42**



**42** was synthesized following the same procedure for the synthesis of **CVie213**.

$^1\text{H}$  NMR (400 MHz, Chloroform- $d$ )  $\delta$  4.09 – 3.99 (m, 2H), 3.42 (td,  $J = 10.8, 4.5$  Hz, 1H, 6-H), 2.65 (t,  $J = 12.6$  Hz, 3H), 2.44 (dd,  $J = 19.2, 8.8$  Hz, 1H, 16-Ha), 1.44 (s, 9H, t-Bu), 0.85 (s, 3H,  $\text{CH}_3$ ), 0.77 (s, 3H,  $\text{CH}_3$ ).

#### Synthesis of **CVie212**



**CVie212** was synthesized following the same procedure for the synthesis of **CVie209**.

$^1\text{H}$  NMR (400 MHz,  $\text{CD}_3\text{OD}$ )  $\delta$  3.43 (d,  $J = 12.7$  Hz, 3H), 2.85 (s, 2H), 2.45 (dd,  $J = 19.2, 8.8$  Hz, 1H, 16-Ha), 0.86 (s, 3H,  $\text{CH}_3$ ), 0.78 (s, 3H,  $\text{CH}_3$ ).

## 5. Section 4-drug delivery platform

### Production of the nanofibers

Polymers was dissolved in the solvent system and concentration as reported in the table 25, and stirred overnight at room temperature. For eosin Y embedded fibers, 2% of eosin was added directly to the polymer solution and stirred together overnight.

Electrospun nanofibers was created using a custom electrospinning device equipped with a single needle or with a coaxial needle, which diameters are respectively 0.7 mm for the single axial and 0,8 and 0,5 mm for the coaxial. Voltage, flow rate, humidity, and temperature are indicated in the table 25.

SCAFFOLD	300PA	1000PA	PCL	Blend 1000PA-300PA 75/25	Blend 1000PA-300PA 50/50	Blend 1000PA-300PA 25/75	Coaxial 300 shell-1000 core	Coaxial 300 shell-PCL core
Blank	20% CHCl <sub>3</sub> /HFIP 7:3	10% CHCl <sub>3</sub> /HFIP 9:1	10% HFIP	20% CHCl <sub>3</sub> /HFIP 7:3	20% CHCl <sub>3</sub> /HFIP 7:3	20% CHCl <sub>3</sub> /HFIP 7:3	300:20% CHCl <sub>3</sub> /HFIP 7:3	300:20% CHCl <sub>3</sub> /HFIP 7:3
							1000:10% CHCl <sub>3</sub>	PCL:5% HFIP
	1,0 mL/h	0,9 mL/h	1,0 mL/h	1,2 mL/h	1,0 mL/h	0,8 mL/h	300: 1,2mL/h	300: 1,2mL/h
							1000: 0,2 mL/h	PCL: 0,2 mL/h
	22-24 KV	20-22 KV	12-14 KV	18-20 KV	20-22 KV	21-23 KV	12-13KV	14-15 KV
	19-21 °C	19-21 °C	19-21 °C	19-21 °C	19-21 °C	19-21 °C	19-21 °C	19-21 °C
38-45%	38-45%	38-45%	38-45%	38-45%	38-45%	38-45%	40-45%	
Eosyn Y embeded	20% CHCl <sub>3</sub> /HFIP 7:3	10% CHCl <sub>3</sub> /HFIP 9:1	10% HFIP	20% CHCl <sub>3</sub> /HFIP 7:3	20% CHCl <sub>3</sub> /HFIP 7:3	20% CHCl <sub>3</sub> /HFIP 7:3	300:20% CHCl <sub>3</sub> /HFIP 7:3	300:20% CHCl <sub>3</sub> /HFIP 7:3
							1000:10% CHCl <sub>3</sub> /HFIP 9:1	1000:10% CHCl <sub>3</sub> /HFIP 9:1
	1,0 mL/h	0,8 mL/h	0,9 mL/h	1,1 mL/h	1,0 mL/h	0,7 mL/h	300: 1,2mL/h	300: 1,2mL/h
							1000: 0,2 mL/h	PCL: 0,2 mL/h
	22-24 KV	20-22 KV	13-15 KV	19-21 KV	20-22 KV	22-24 KV	12-13KV	14-15 KV
	19-21 °C	19-21 °C	19-21 °C	19-21 °C	19-21 °C	19-21 °C	19-20 °C	19-20 °C
38-45%	38-45%	38-45%	38-45%	38-45%	38-45%	38-45%	40-45%	

Fibers were collected over a rotating mandrel at 3000 rpm equipped with an aluminum foil.

### SEM images of nanofibers

A disk of  $\varnothing 12\text{mm}$  of the sample was mounted over a commercial  $\varnothing 12.5\text{ mm}$  SAM stub equipped with conductive carbon tape. Samples was sputter coated with gold before record of the image. The diameter of the fibers was calculated from the SEM images by using the ImageJ Software (National Institutes of Health) to measure the fibers at more than 100 points in the images.

### FIB-SEM images of nanofibers

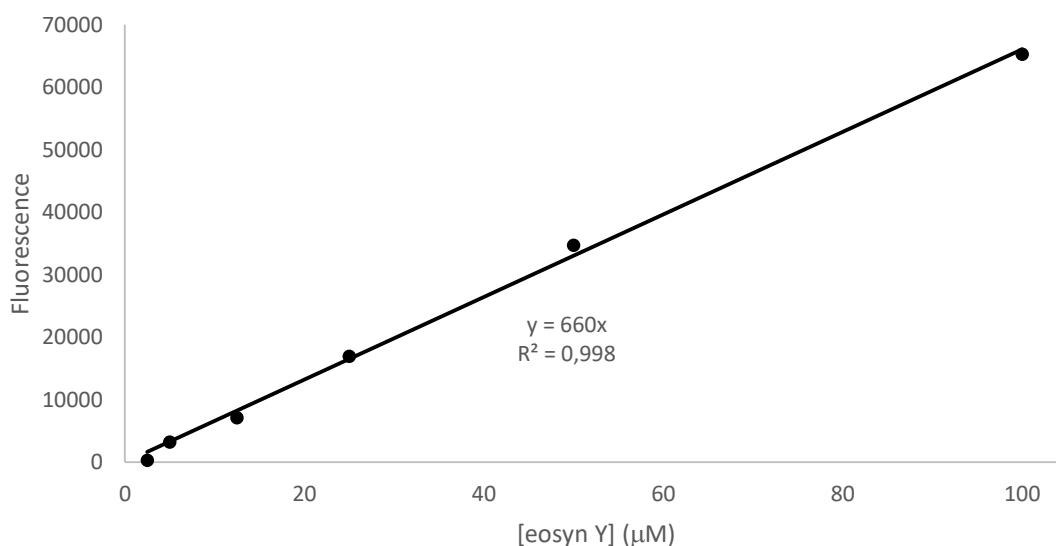
A disk of  $\varnothing 12\text{mm}$  of the sample was mounted over a commercial  $\varnothing 12.5\text{ mm}$  SAM stub equipped with conductive carbon tape. Samples was sputter coated with gold before record of the image. A non-aligned filament of the fiber was coated with a thin deposition of platinum, then the area in front was sectioned using the ion beam.

### TEM images of nanofibers

A disk of  $\varnothing 12\text{mm}$  of the sample was embedded with epoxy resin in a test tube. Sample was sectioned rith a Ultramicrotome Leica EM UC7 and images retrieved with a FEI Tecnai F30 Twin 300kV TEM.

### Protocol for the quantification of the total amount of eosin Y embedded

Calibration curve was built in the range  $2\mu\text{M}$ - $100\mu\text{M}$ . Eosin Y was first dissolved in water and then diluted in order to obtain the final solutions in 1:10 HFIP: $\text{H}_2\text{O}$ . Fluorencence was recorded over a CLARIOstar Plus<sup>®</sup> plate reader using Greiner 96 F-bottom plates. Excitation was settled at 450nm while emission was recorded at 530nm with fixed focal height of 7 mm and gain.

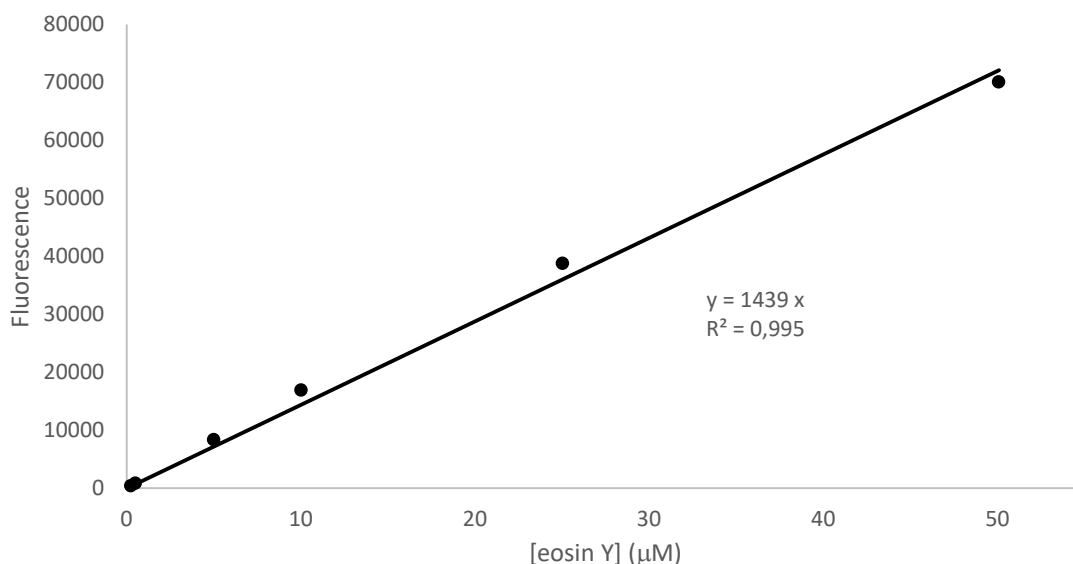


1 mg of the eosin Y embedded fiber was dissolved in HFIP. The solution was diluted 1:10 in water. Fluorescence was recorded with a plate reader, in the same conditions reported above, and the concentration retrieved by calculation over the reported calibration curve.

All the measurement was made in 3 independent experiments and confronted with the non-embedded scaffold as blank.

#### Protocol for the release studies

Calibration curve was built in the range 0.25 $\mu$ M-50 $\mu$ M. Eosin Y was dissolved in pH 7.4 PBS buffer and then diluted with the same solvent. Fluorecence was recorded over a CLARIOstar Plus<sup>®</sup> plate reader using Greiner 96 F-bottom plates. Excitation was settled at 450nm while emission was recorded at 530nm with fixed focal height of 7 mm and gain.



1mg of the test sample was fixed in a test tube using a rubber ring. 1 mL pH 7.4 PBS buffer solution was added to the reaction tube and gently mixed. 100 $\mu$ L of the test media was retrieved and substituted with 100 $\mu$ L of fresh pH 7.4 PBS buffer.

Fluorescent was read in the same condition reported above. Value was kept in the linearity range with appropriate dilution of the samples with pH 7.4 PBS buffer when needed.

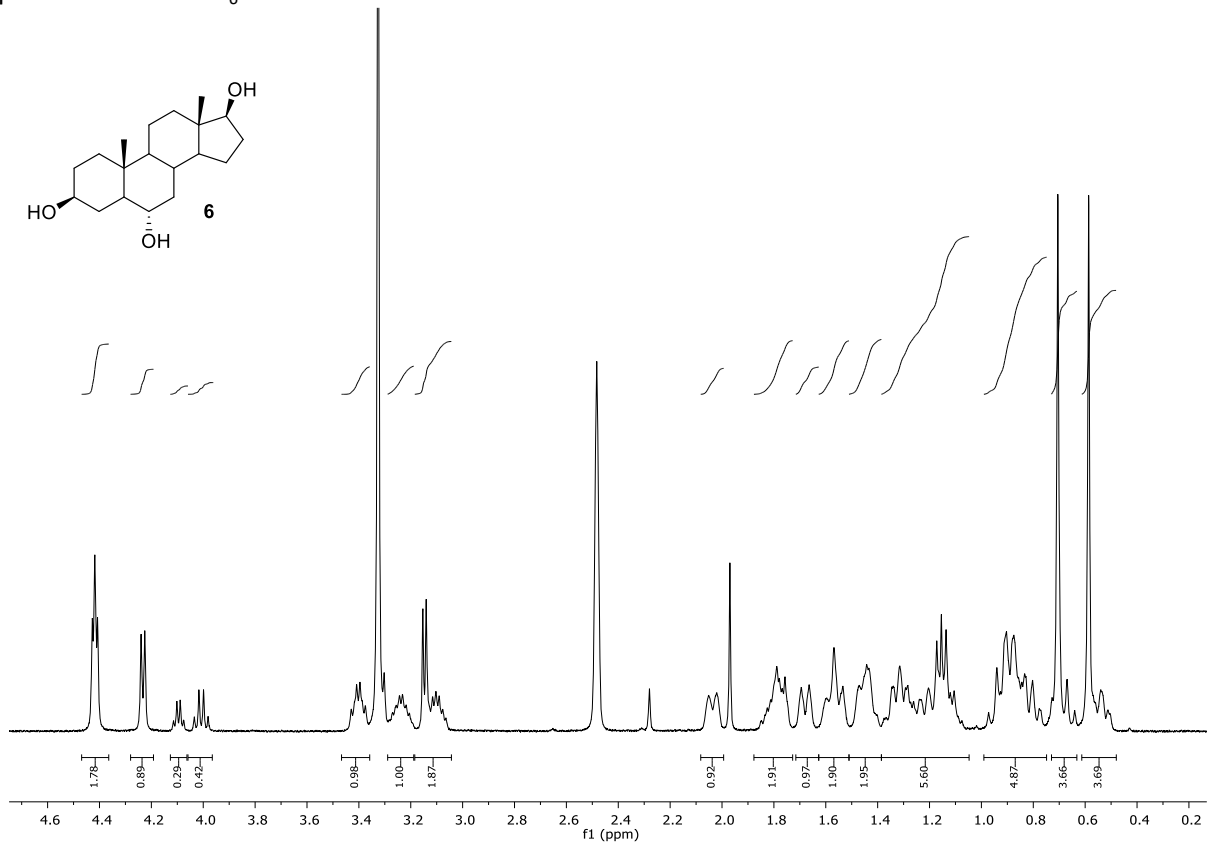
All the measurement was made in 3 independent experiments and confronted with the non-embedded scaffold.

#### Protocol for the fluorescamine assay

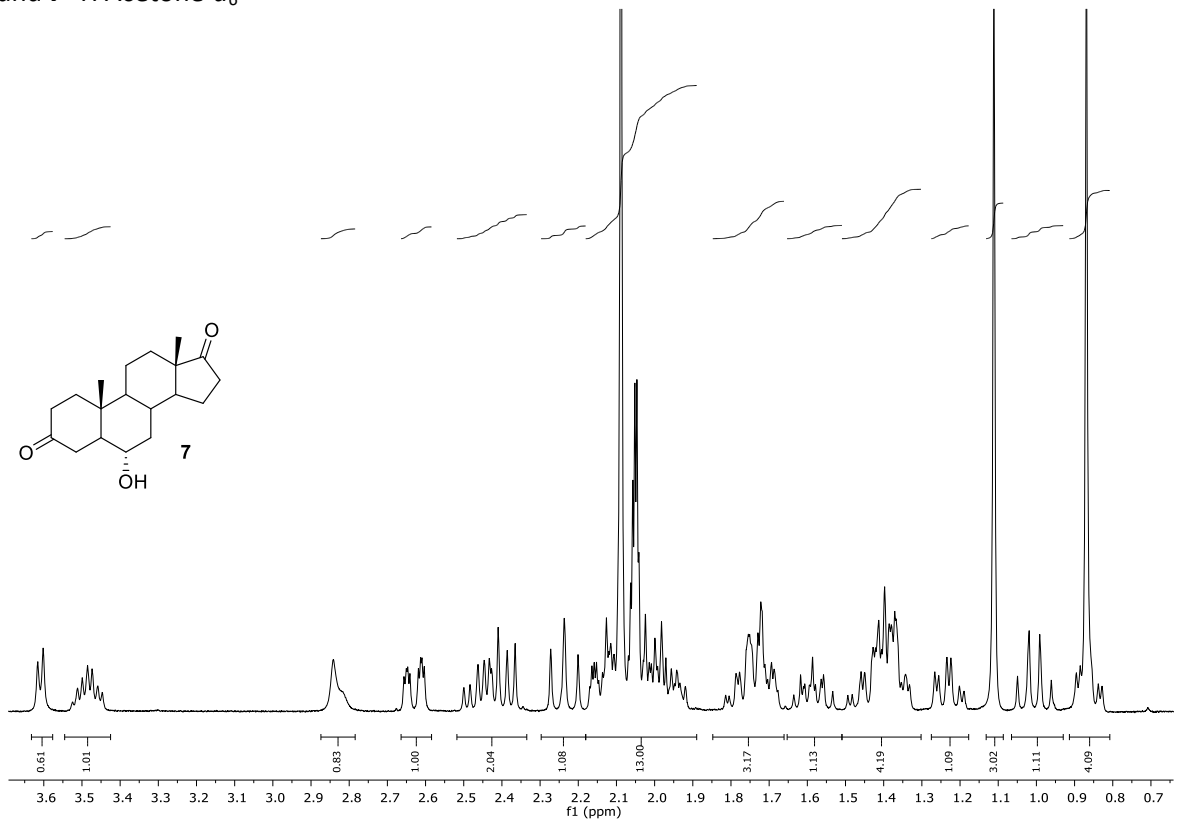
Fluorescamine assay was made with a Imai modified protocol.[189] Was prepared a stock solution at concentration 5mg/mL solution of fluorescamine in DMSO. 500  $\mu$ L of the test sample was diluted with 500  $\mu$ L of pH 7.4 PBS buffer. To the above solution was added 500  $\mu$ L of the stock solution. The mixture was vortexed for 1 minute. Fluorecence was recorded over a CLARIOstar Plus<sup>®</sup> plate reader using Greiner 96 F-bottom plates. Excitation was settled at 375-390nm while emission was recorded at 475nm with fixed focal height of 7 mm and gain.

## 6. Supporting informations

Compound **6**  $^1\text{H}$  DMSO- $d_6$

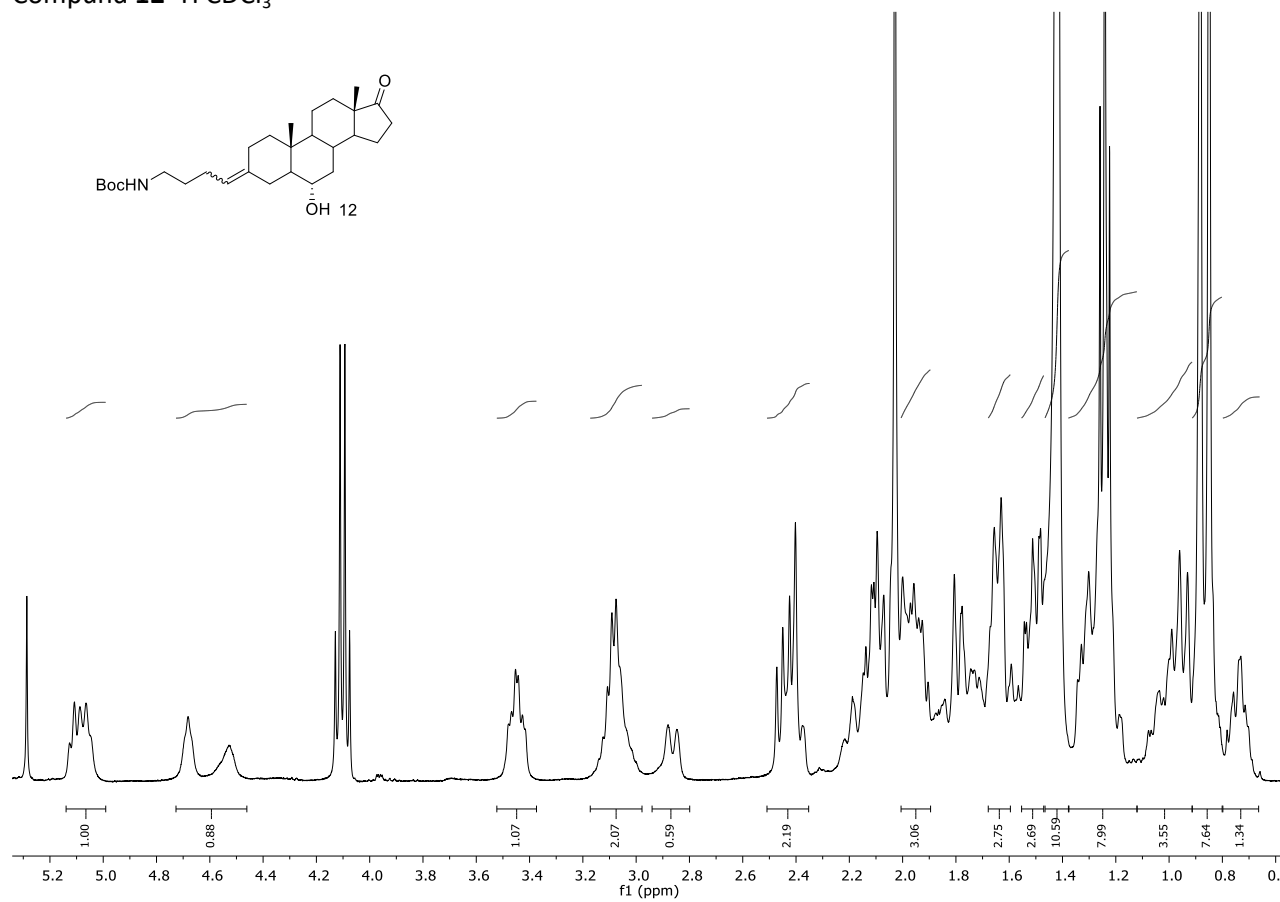
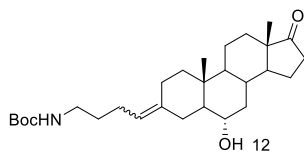


Compound **7**  $^1\text{H}$  Acetone- $d_6$

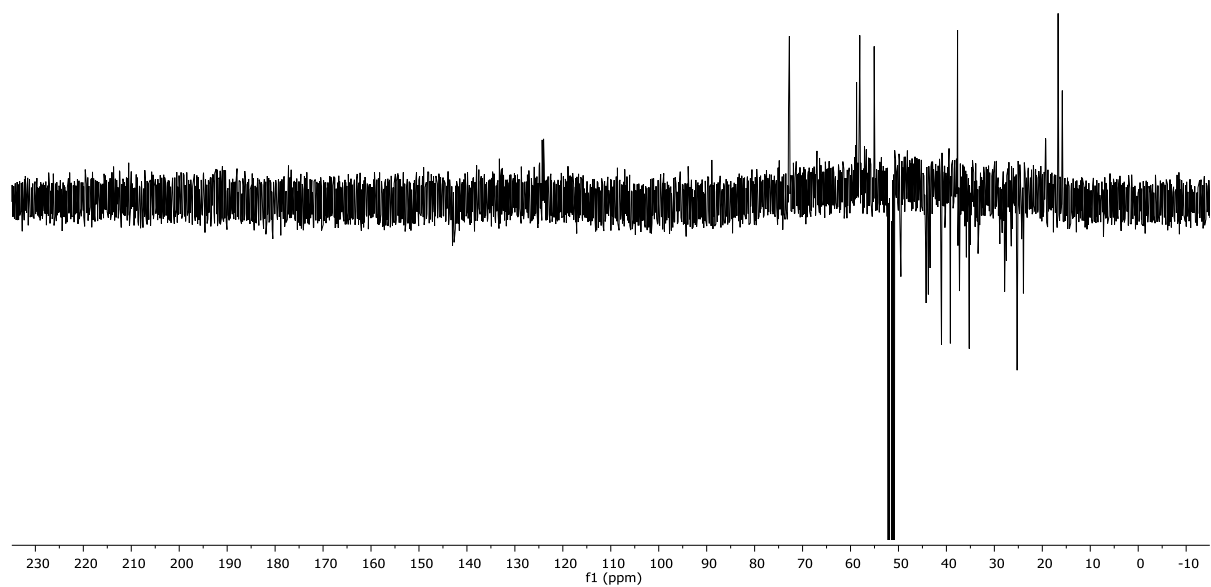
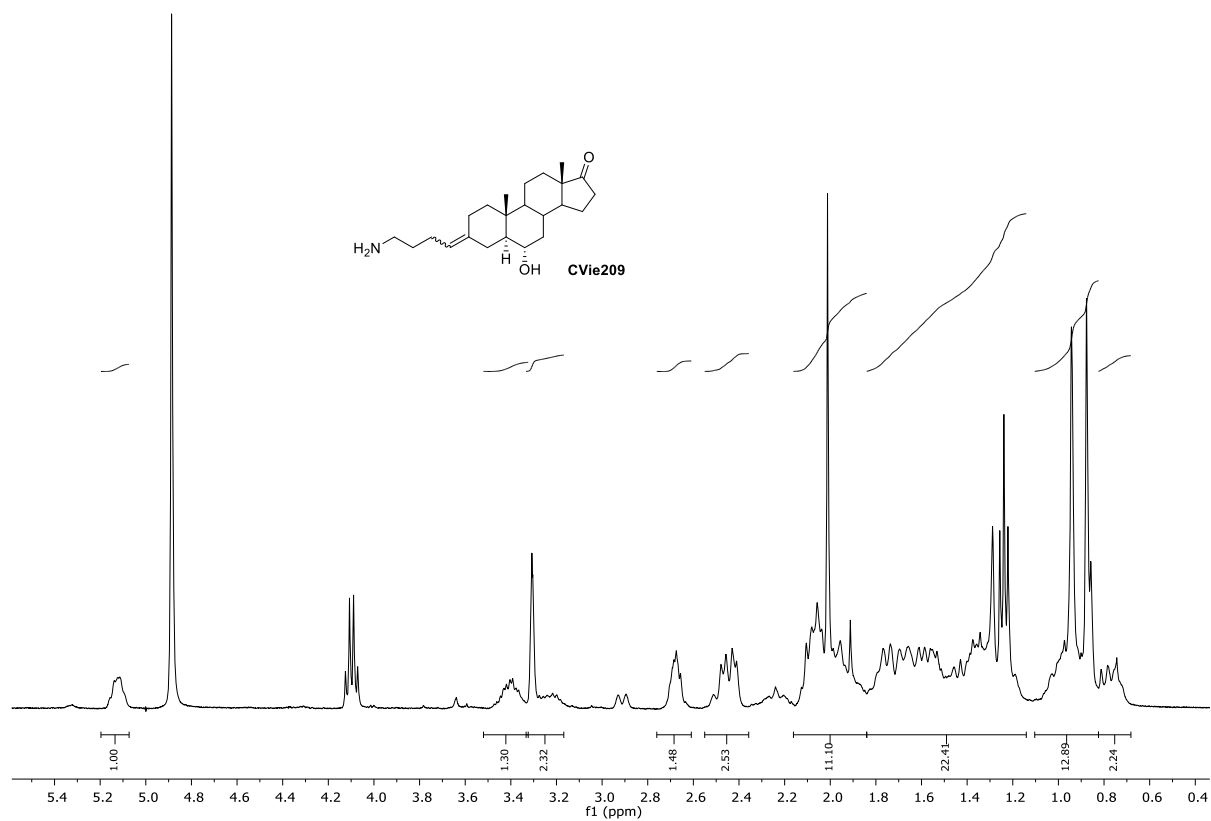




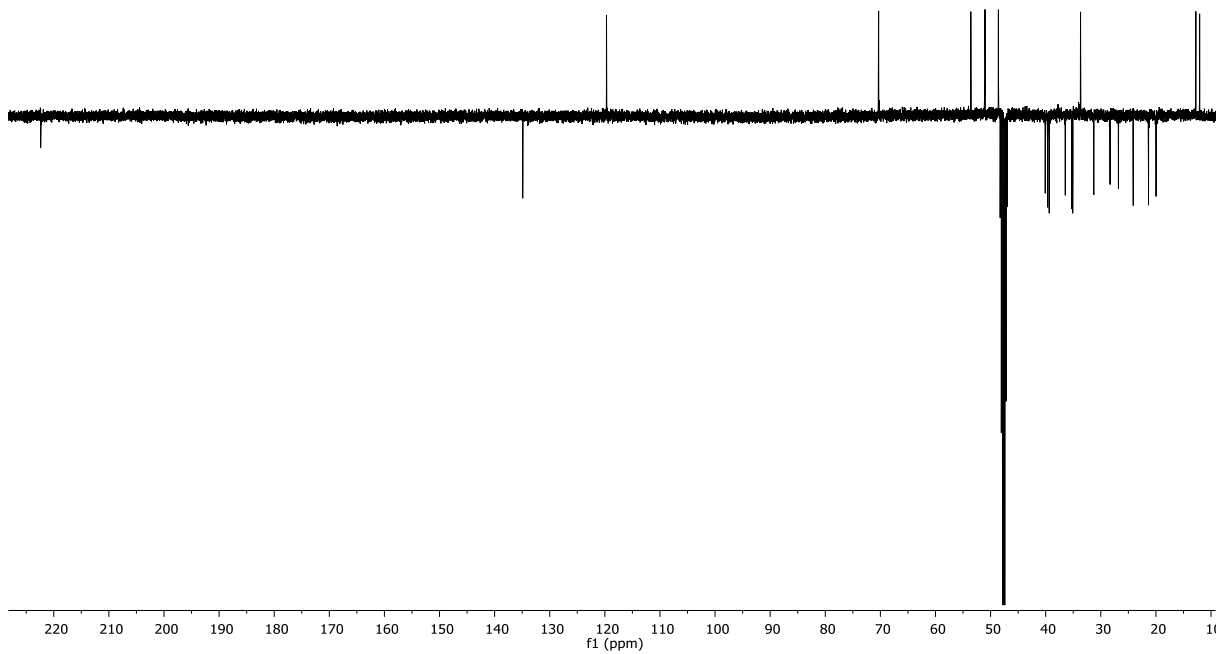
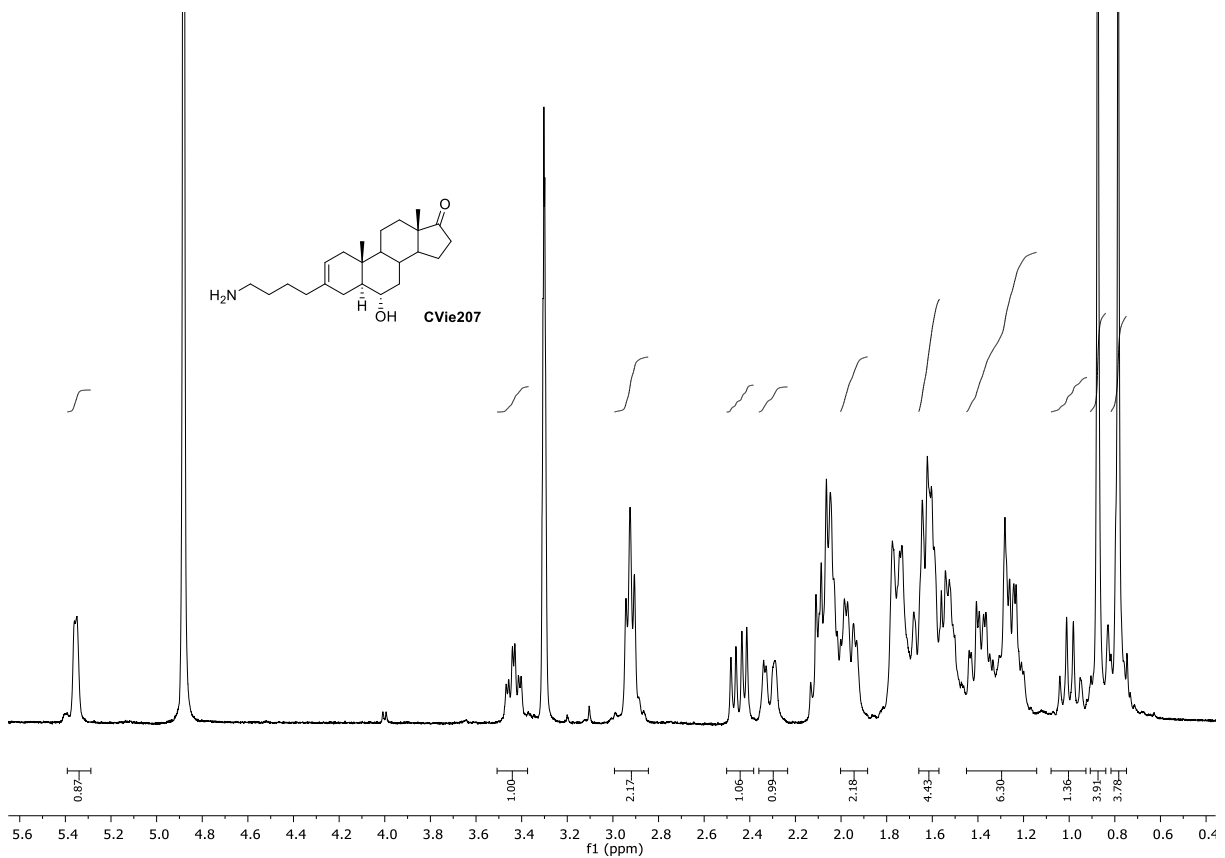
Compound **12**  $^1\text{H}$   $\text{CDCl}_3$



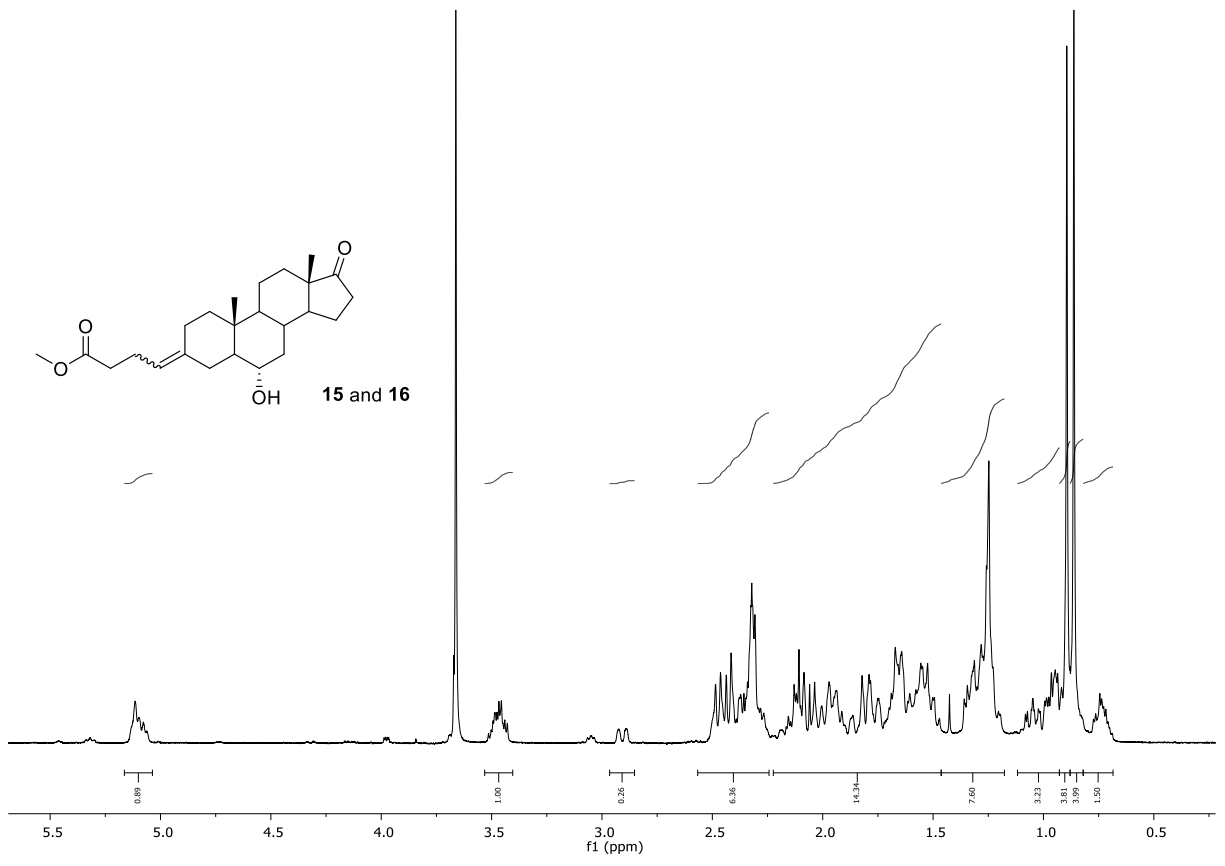
CVie209  $^1\text{H}$  and  $^{13}\text{C}$   $\text{CD}_3\text{OD}$



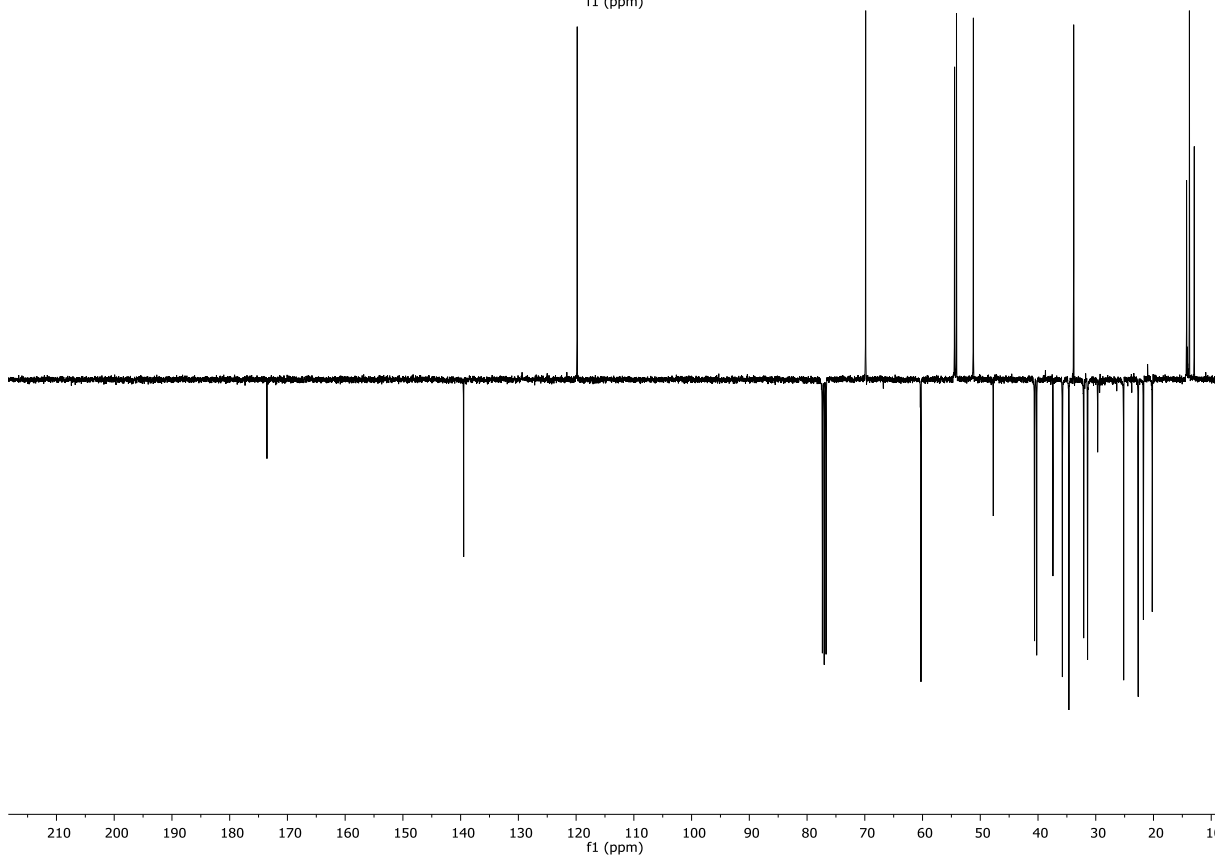
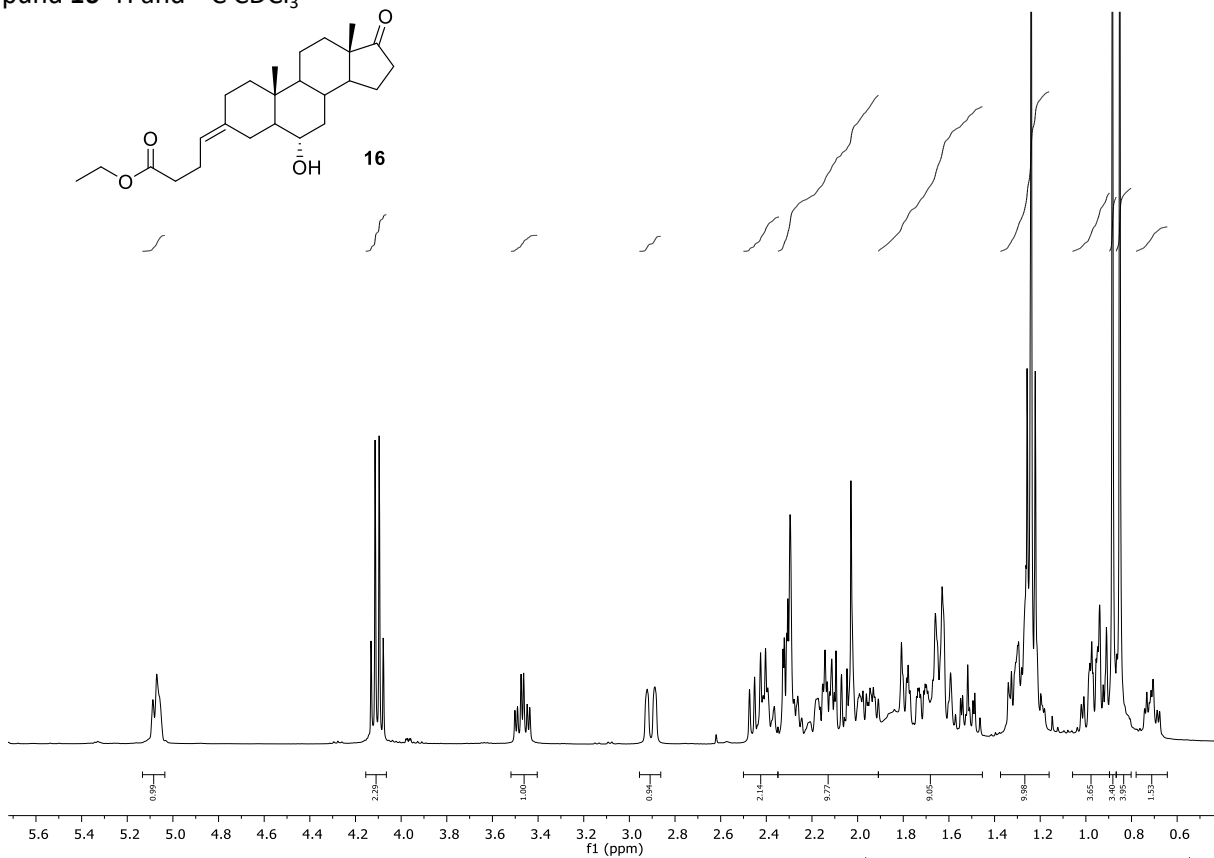
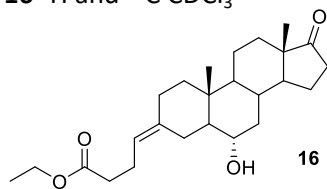
CVie207  $^1\text{H}$  and  $^{13}\text{C}$   $\text{CD}_3\text{OD}$



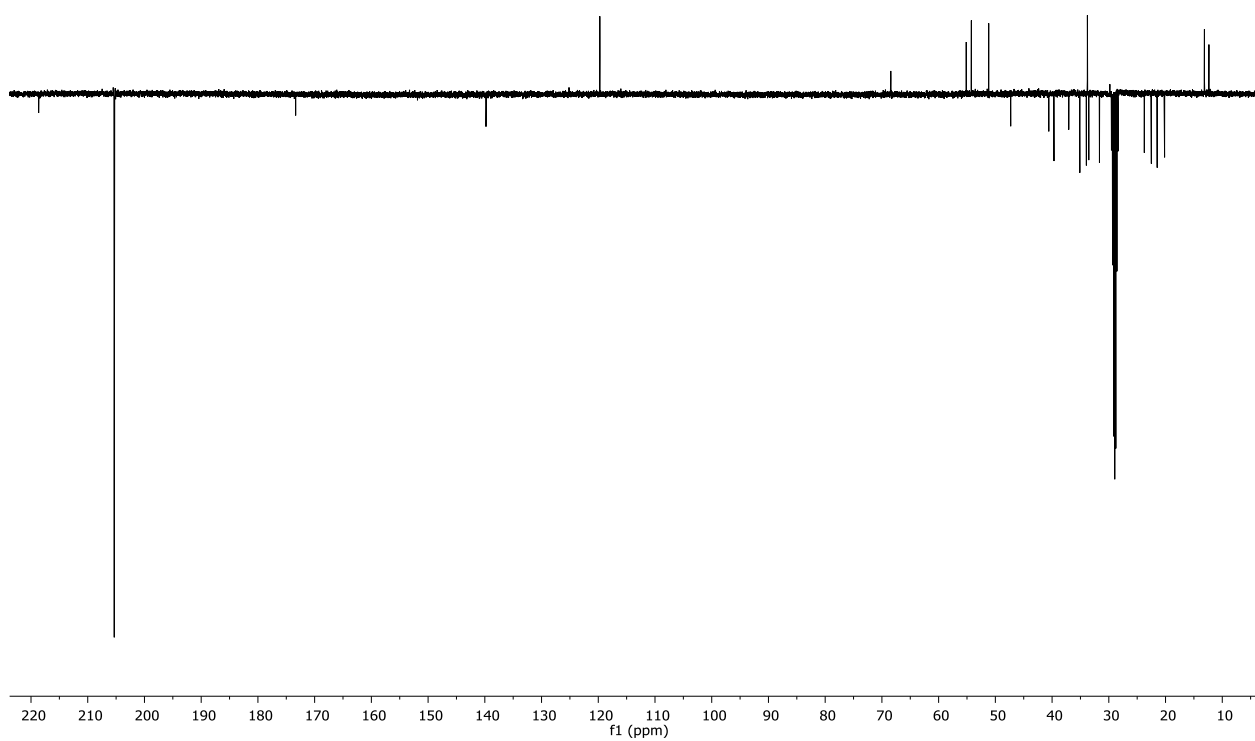
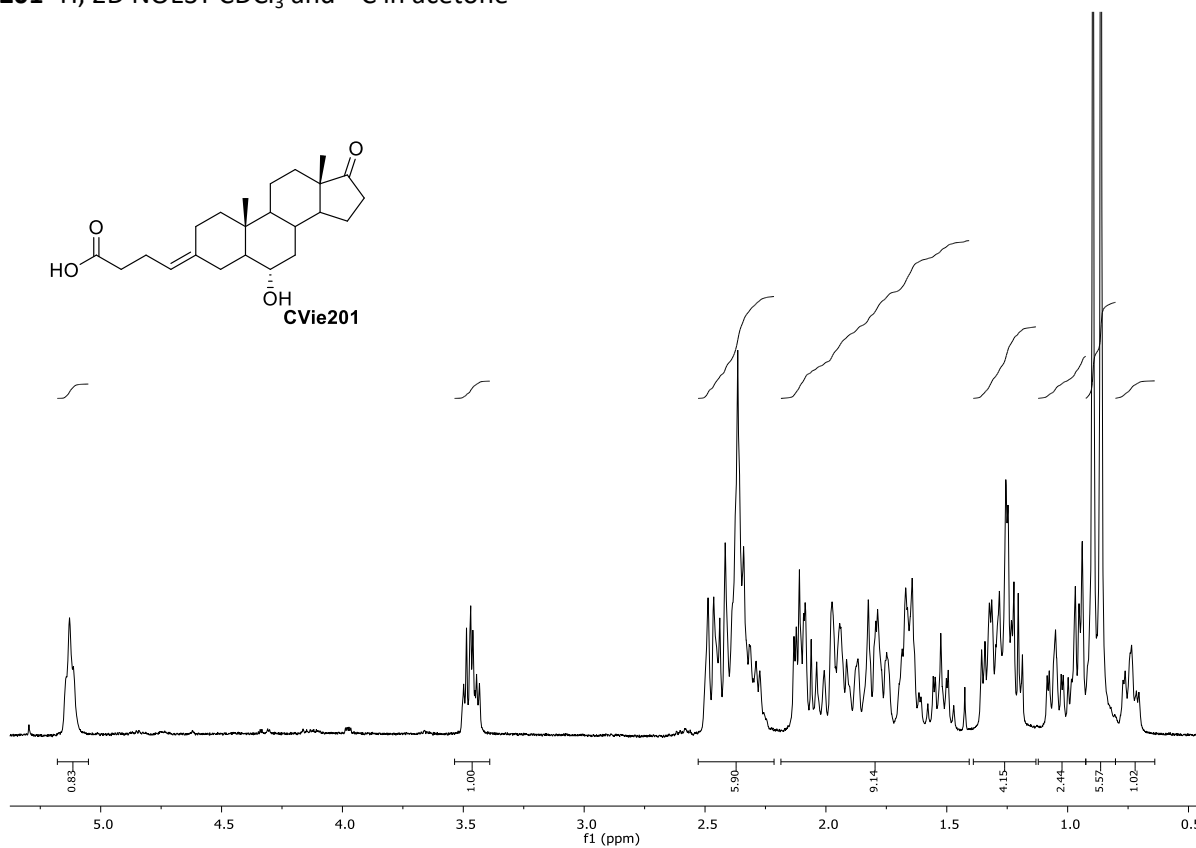
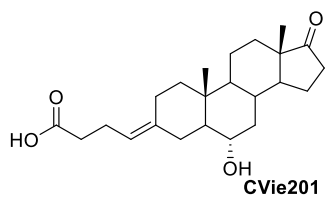
Compound **15** and **16** (mixture of diastereoisomers)  $^1\text{H}$   $\text{CDCl}_3$

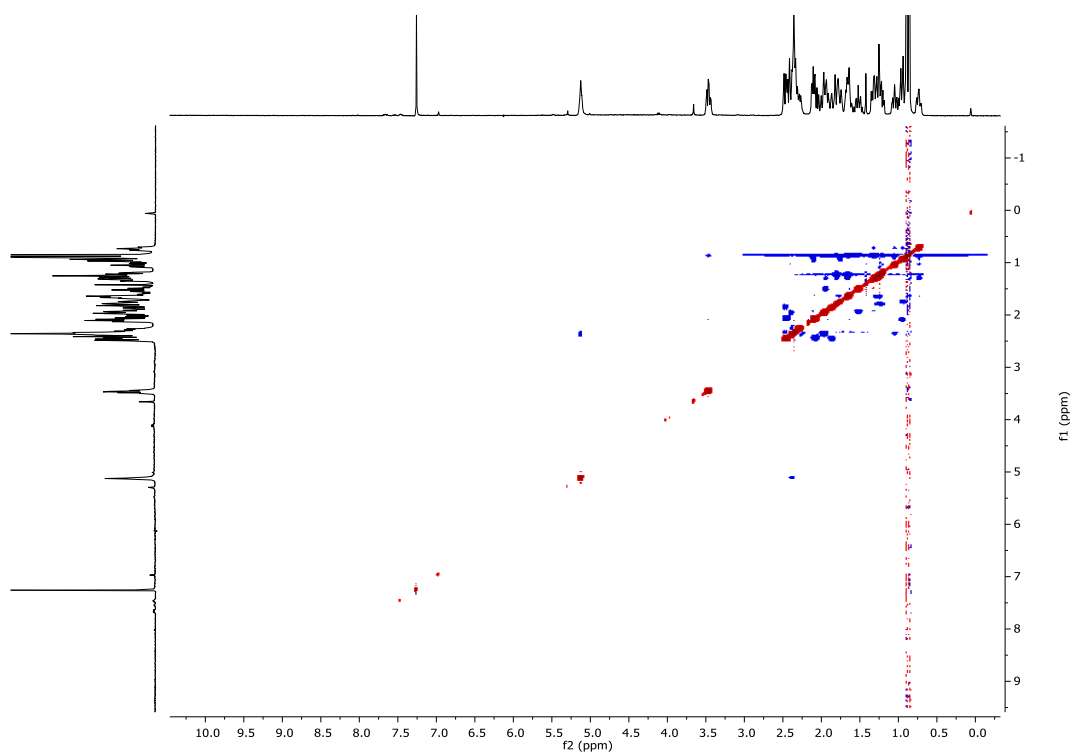


Compound **16**  $^1\text{H}$  and  $^{13}\text{C}$   $\text{CDCl}_3$

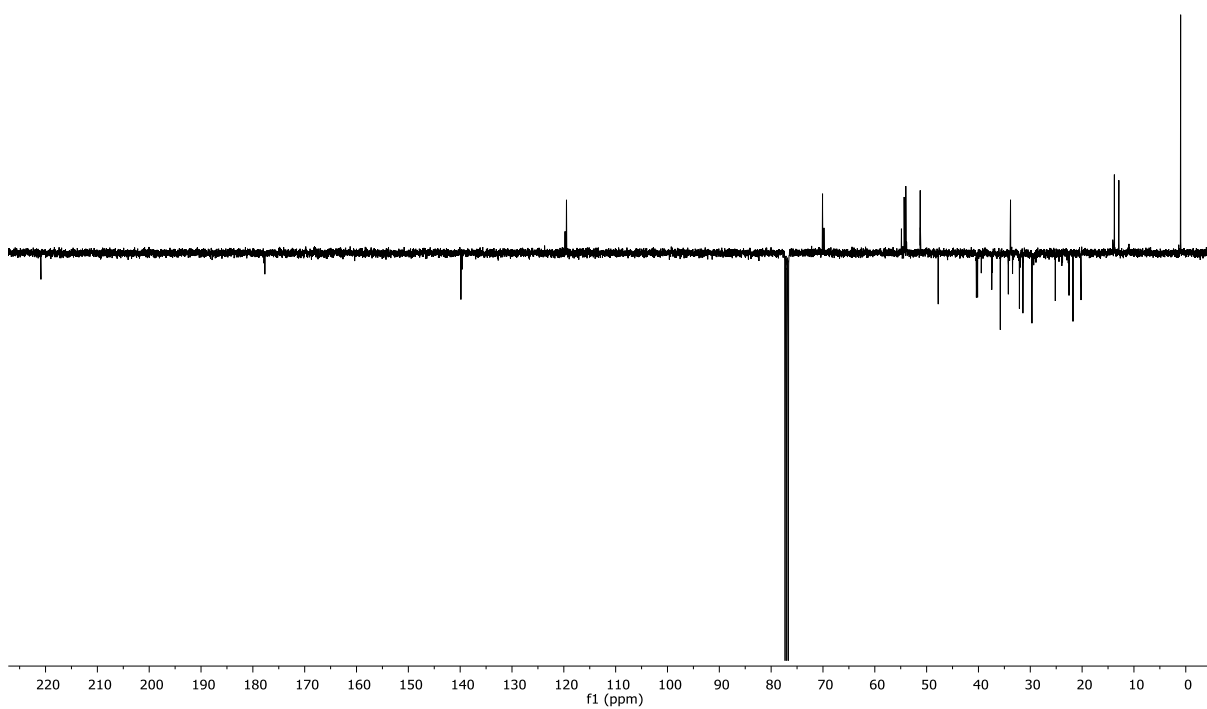
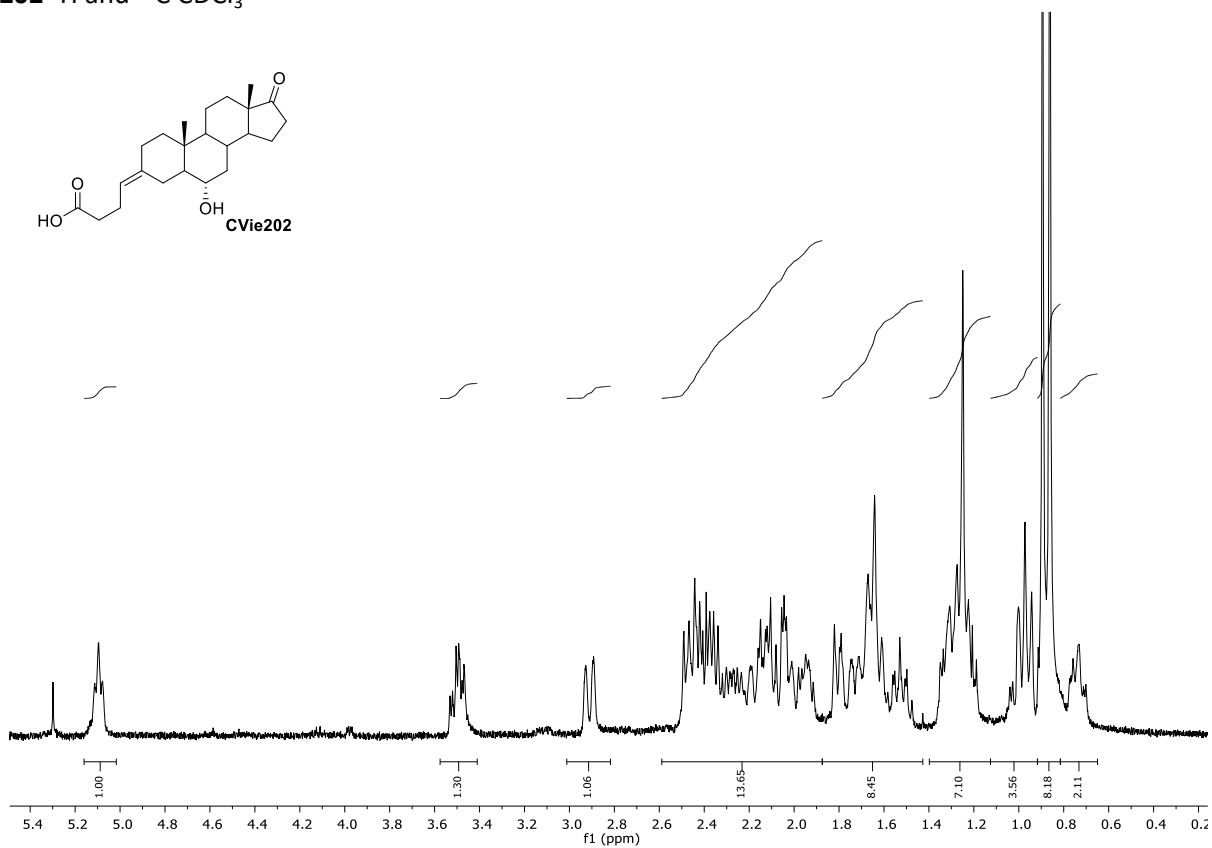
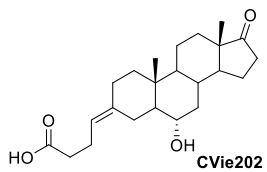


CVie201  $^1\text{H}$ , 2D NOESY  $\text{CDCl}_3$  and  $^{13}\text{C}$  in acetone

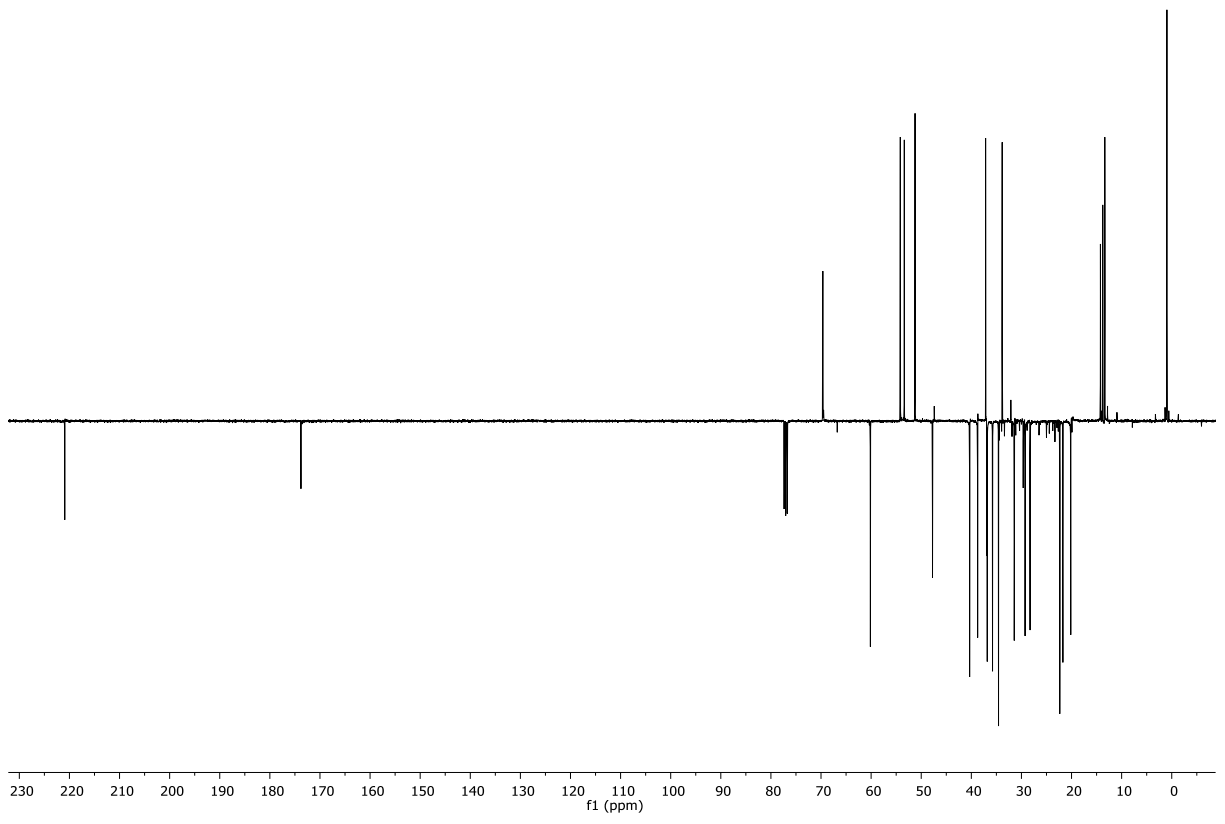
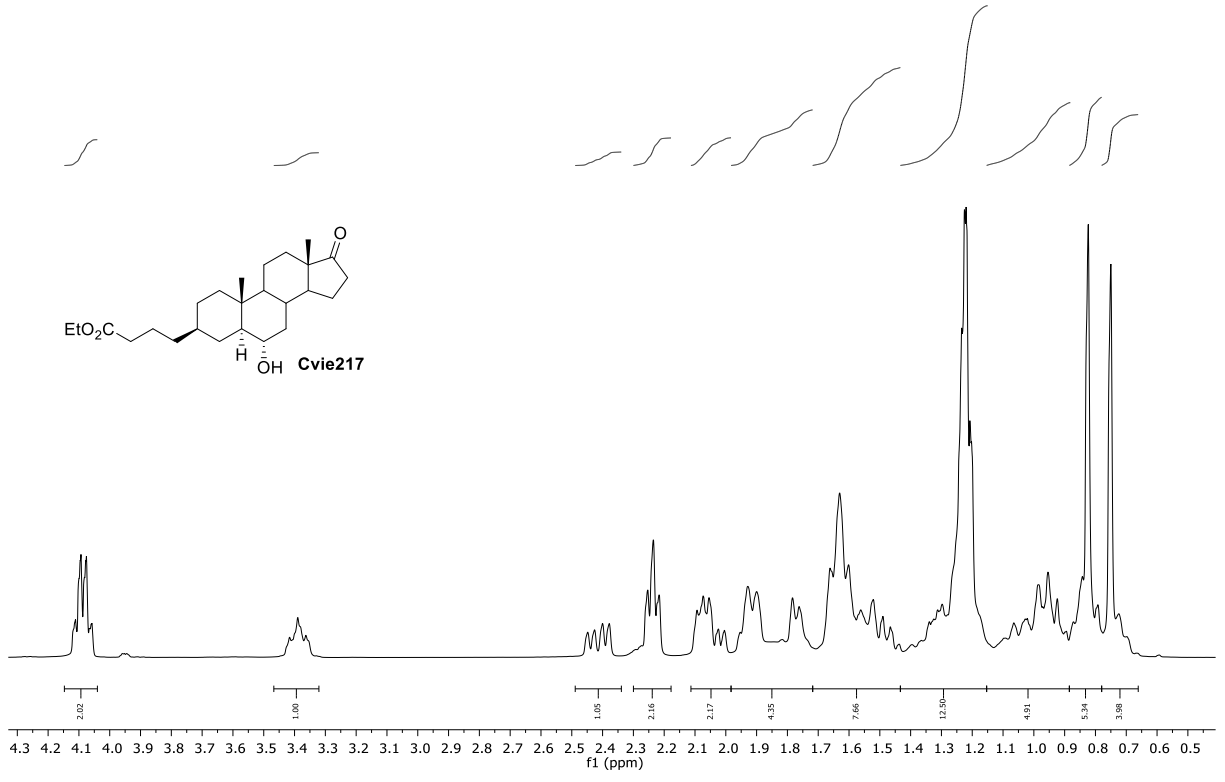




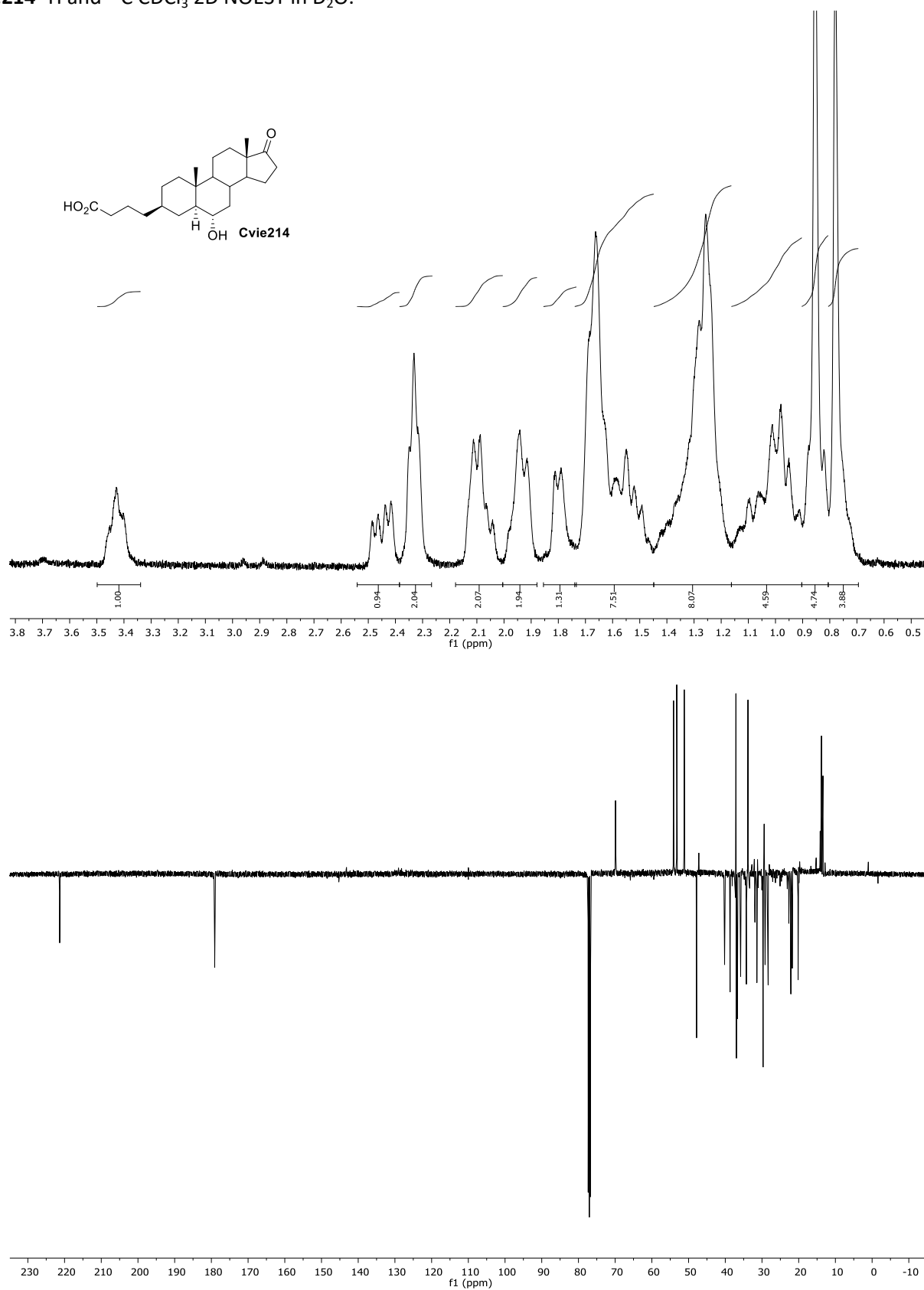
CVie202  $^1\text{H}$  and  $^{13}\text{C}$   $\text{CDCl}_3$

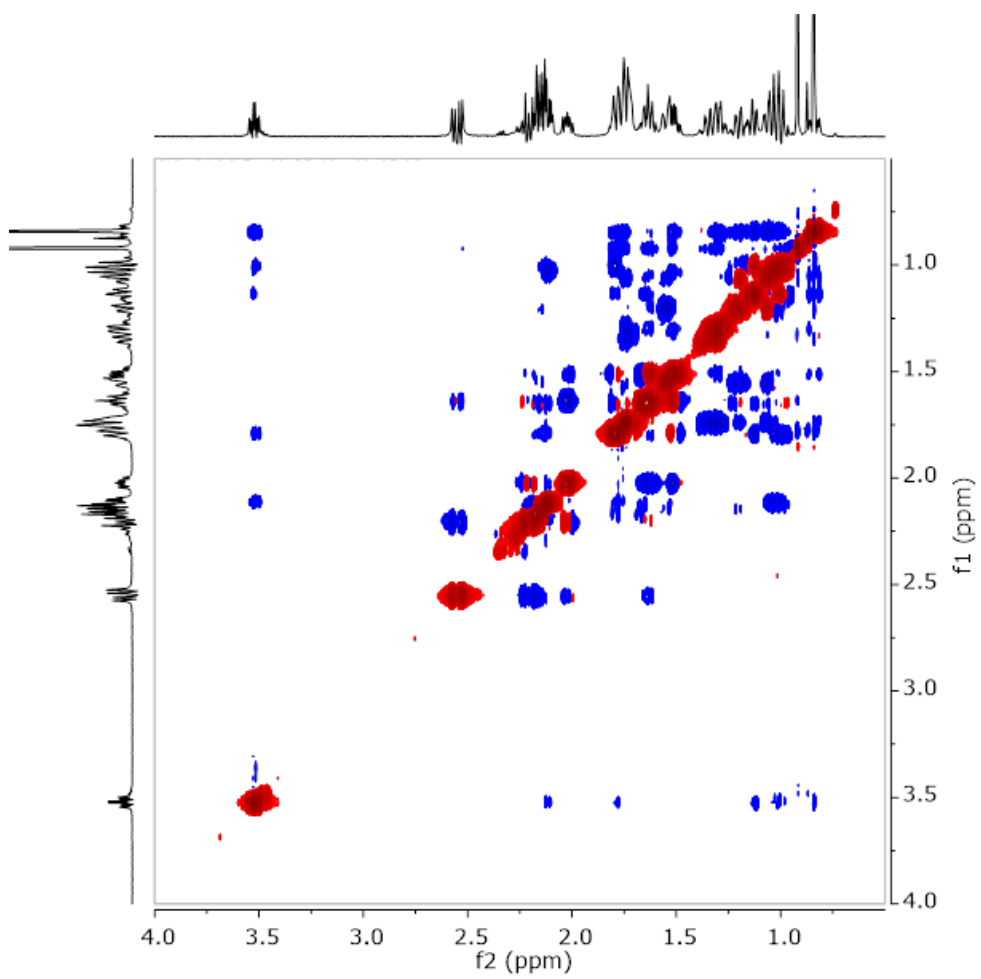


CVie217  $^1\text{H}$  and  $^{13}\text{C}$   $\text{CDCl}_3$

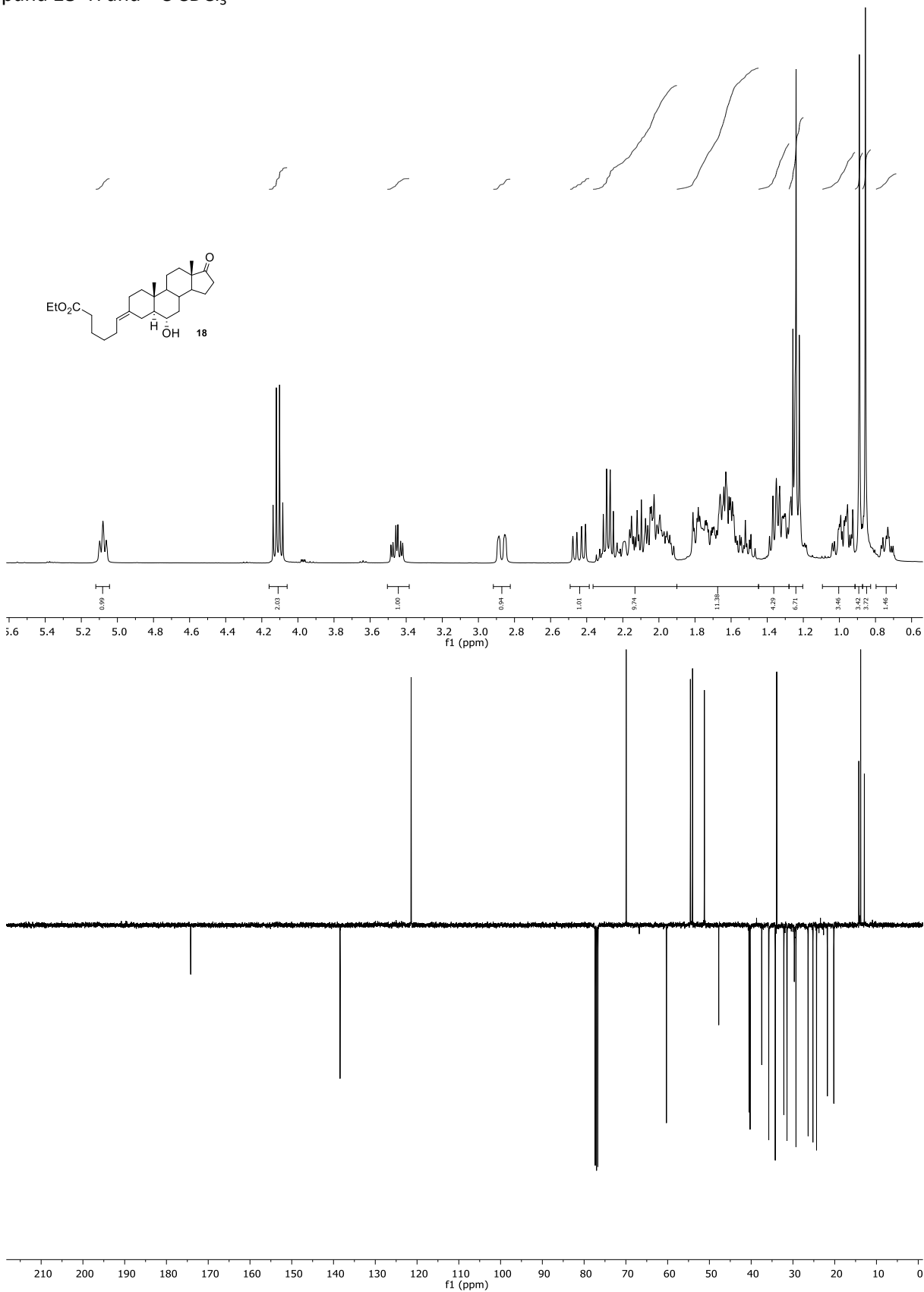


CVie214  $^1\text{H}$  and  $^{13}\text{C}$   $\text{CDCl}_3$  2D NOESY in  $\text{D}_2\text{O}$ .

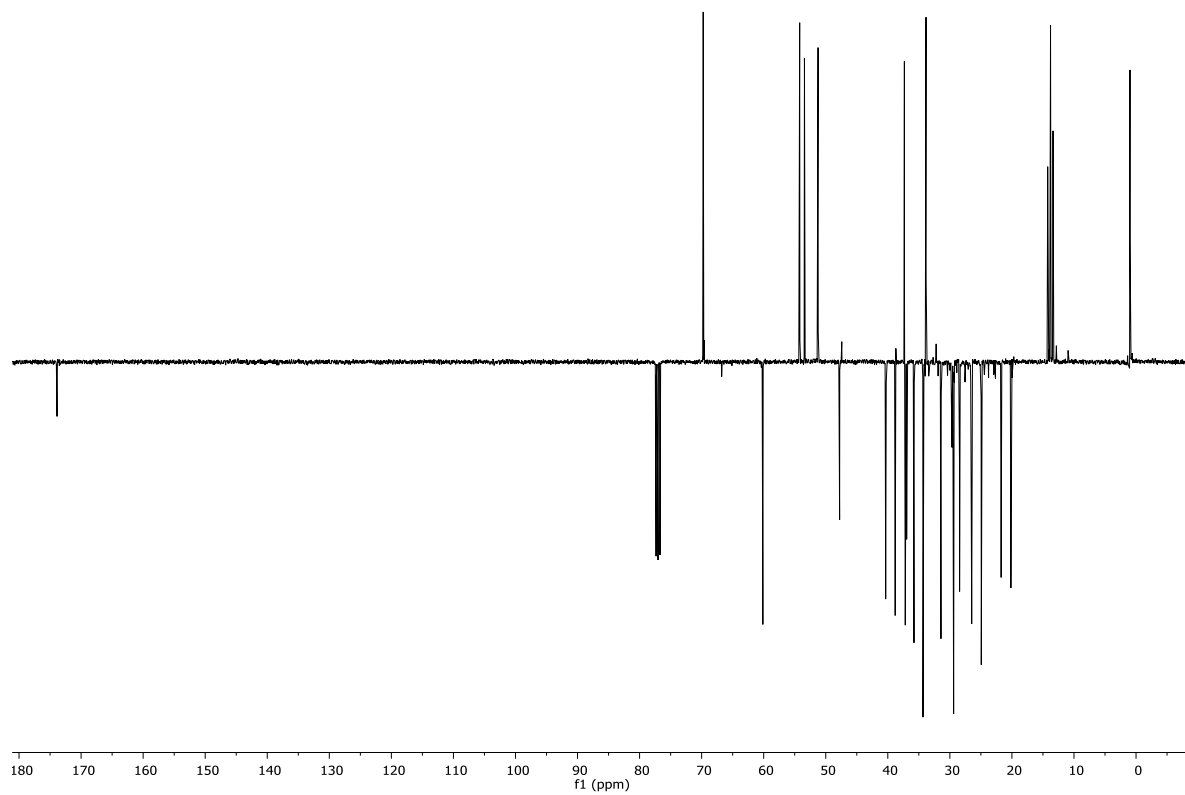
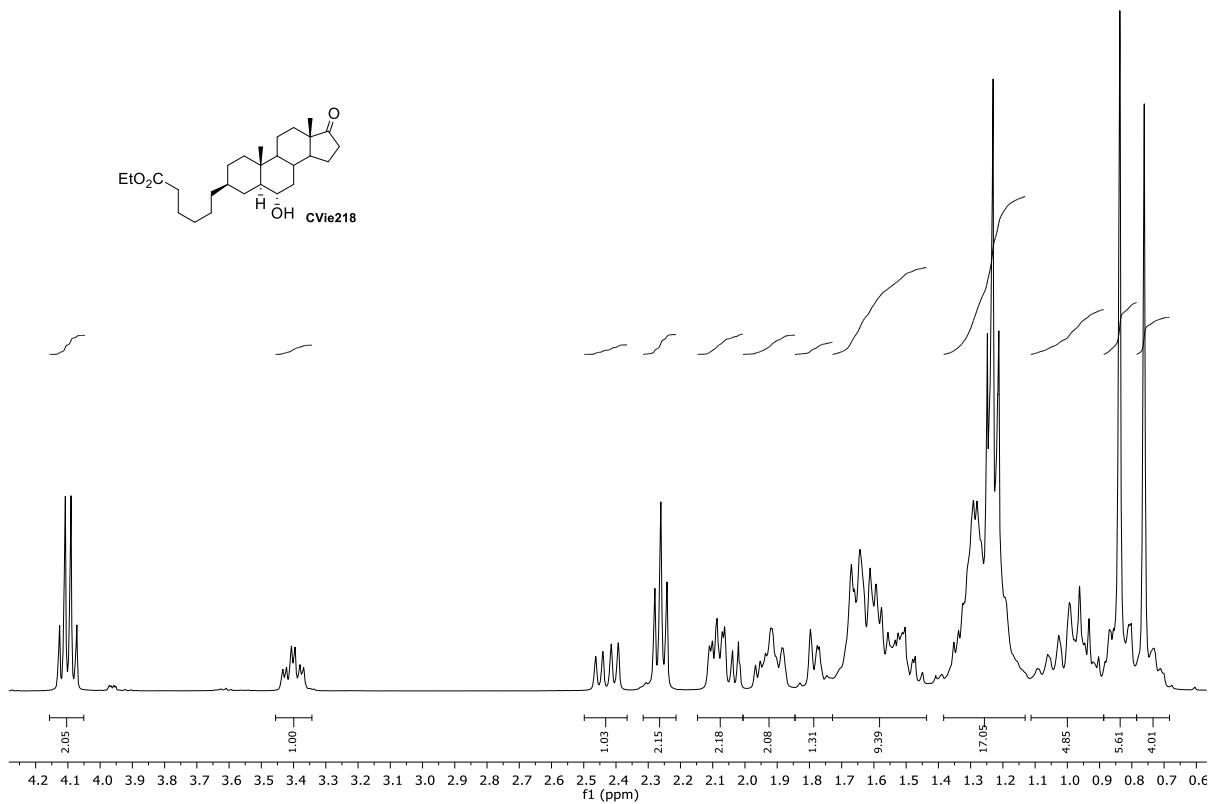
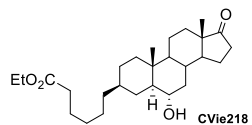




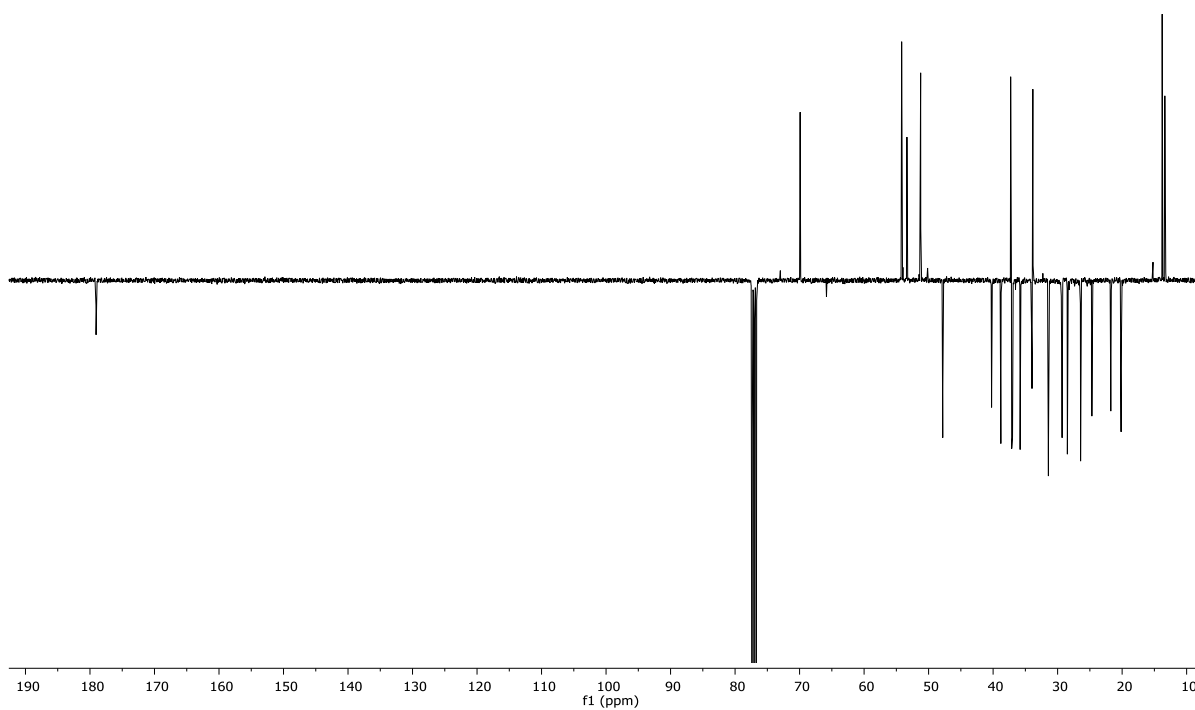
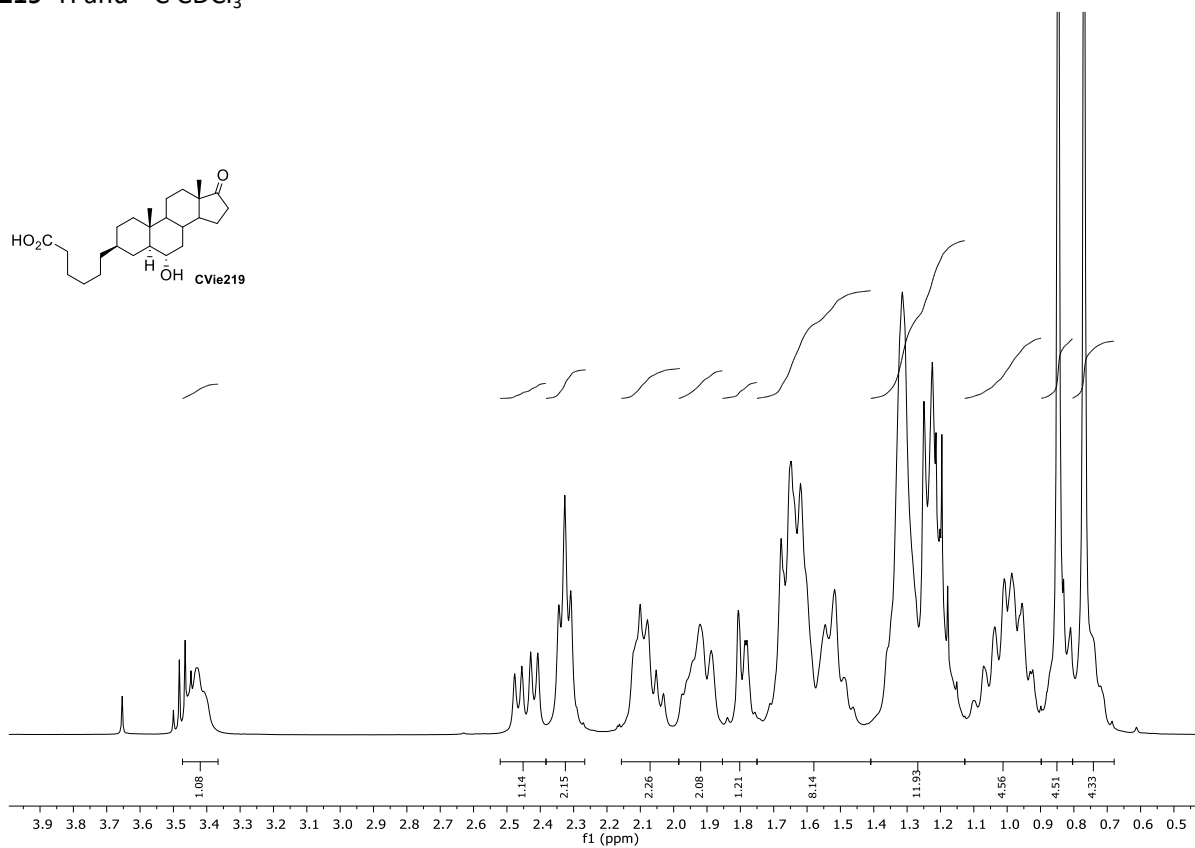
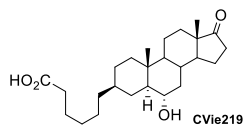
Compound **18**  $^1\text{H}$  and  $^{13}\text{C}$   $\text{CDCl}_3$



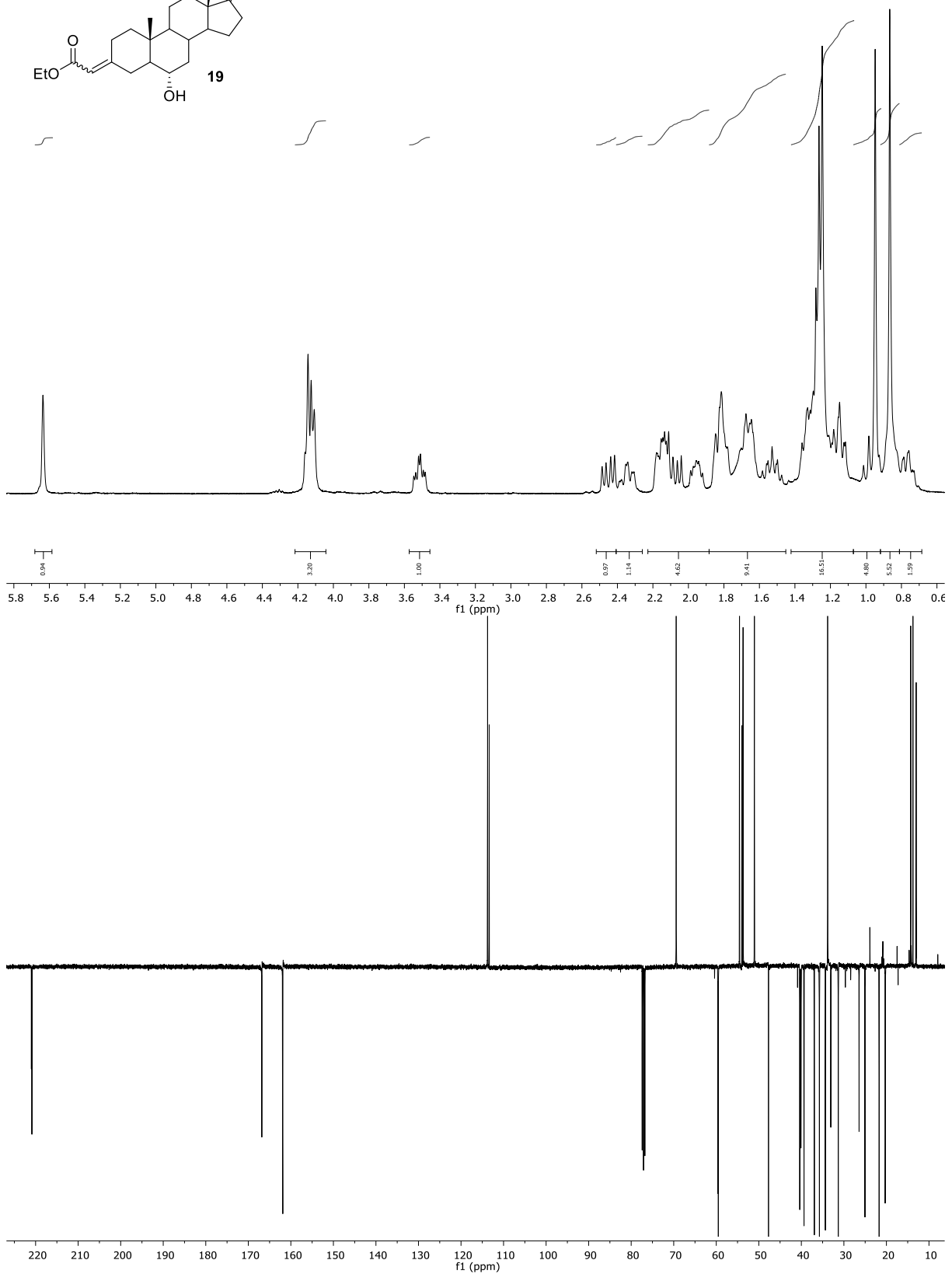
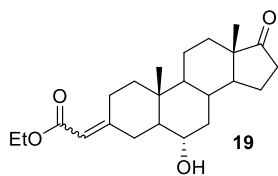
CVie218  $^1\text{H}$  and  $^{13}\text{C}$   $\text{CDCl}_3$



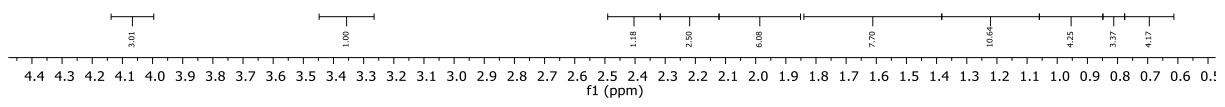
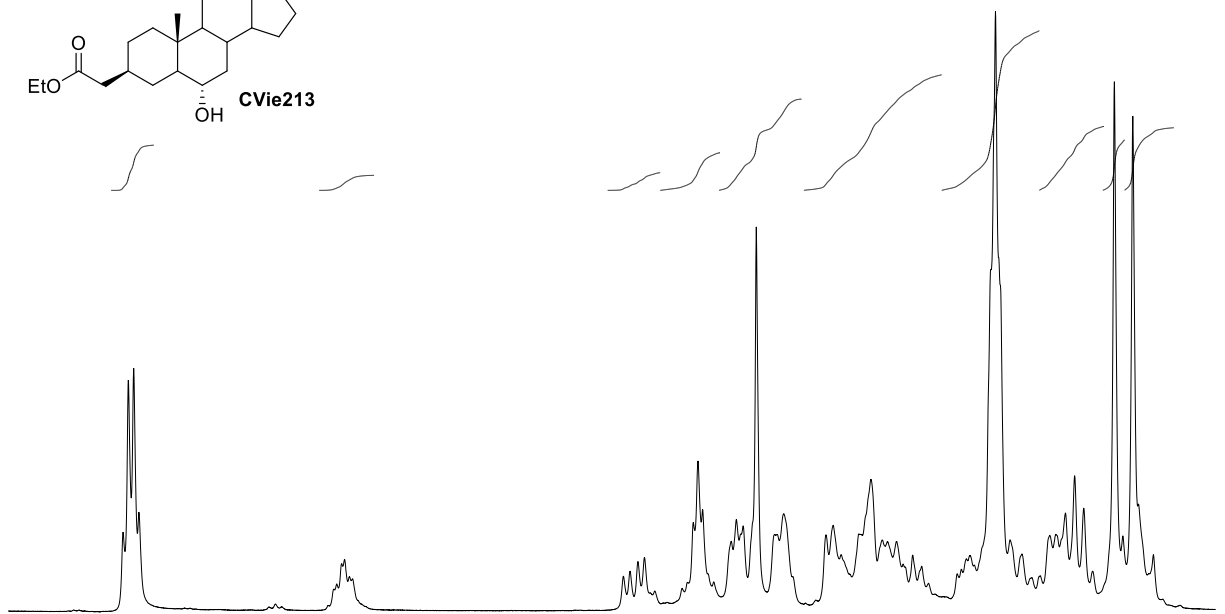
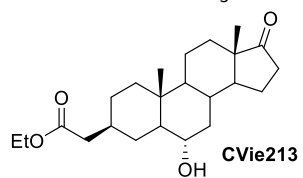
CVie219  $^1\text{H}$  and  $^{13}\text{C}$   $\text{CDCl}_3$



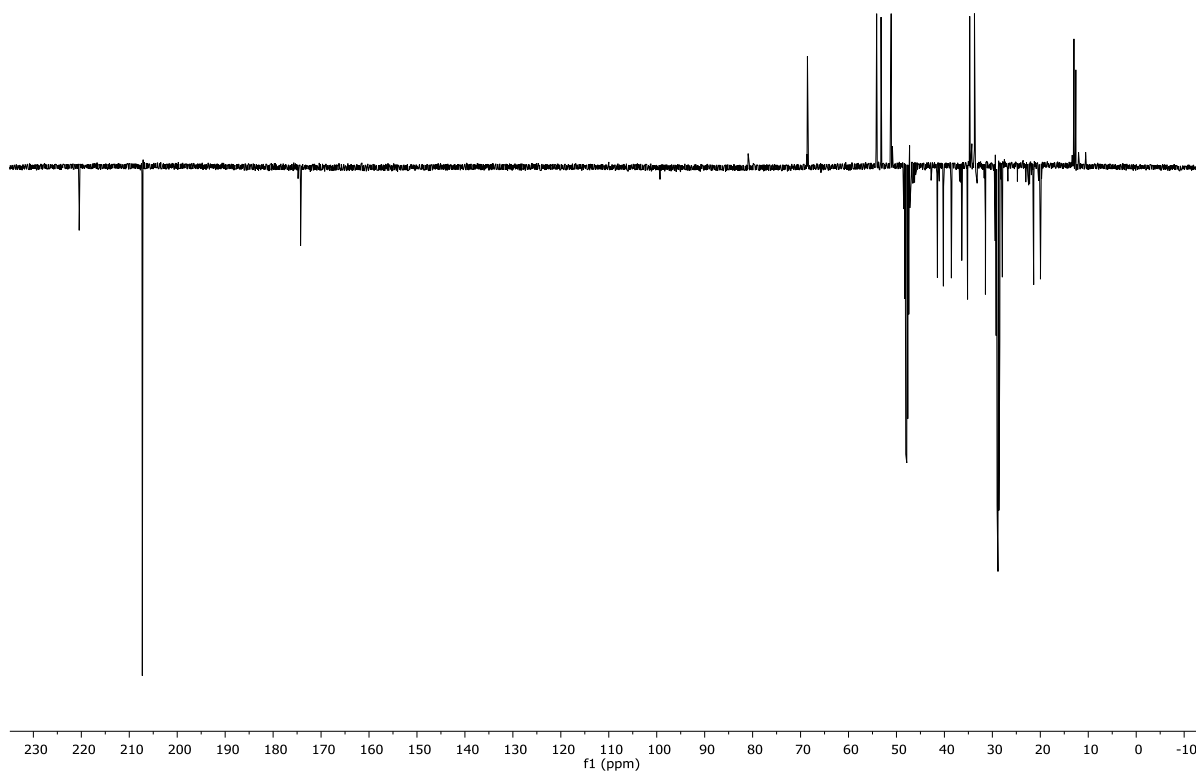
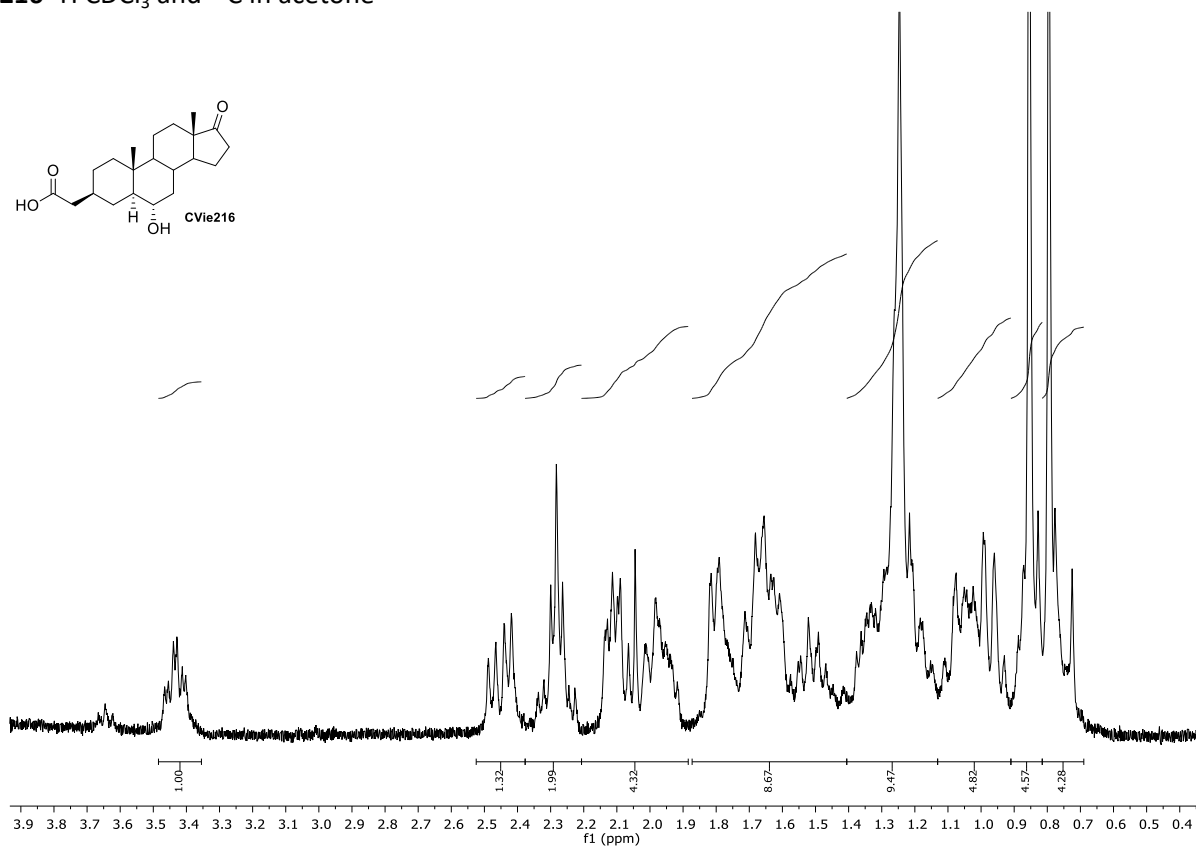
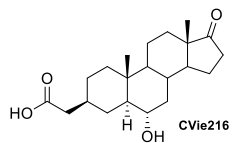
Compound **19**  $^1\text{H}$  and  $^{13}\text{C}$   $\text{CDCl}_3$



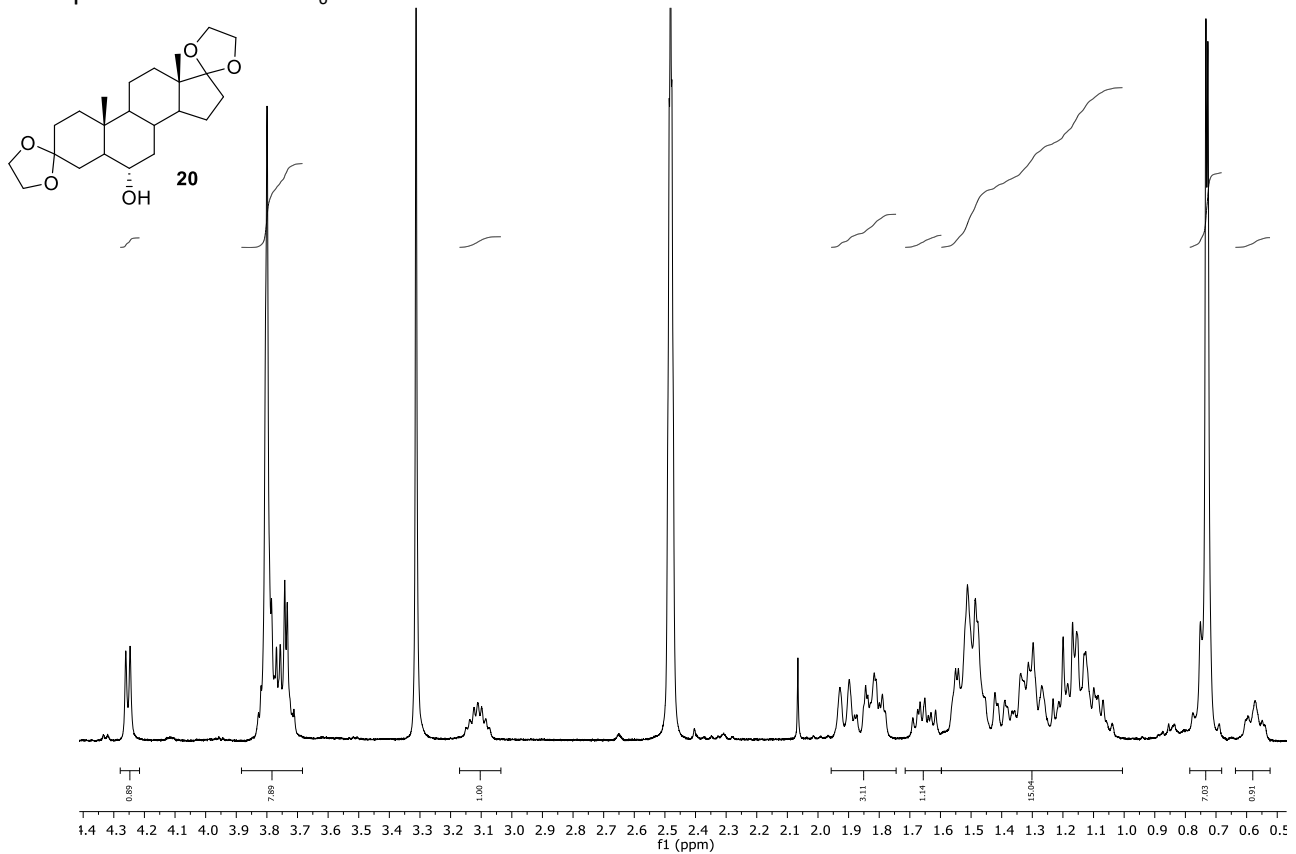
CVie213  $^1\text{H}$  and  $^{13}\text{C}$   $\text{CDCl}_3$



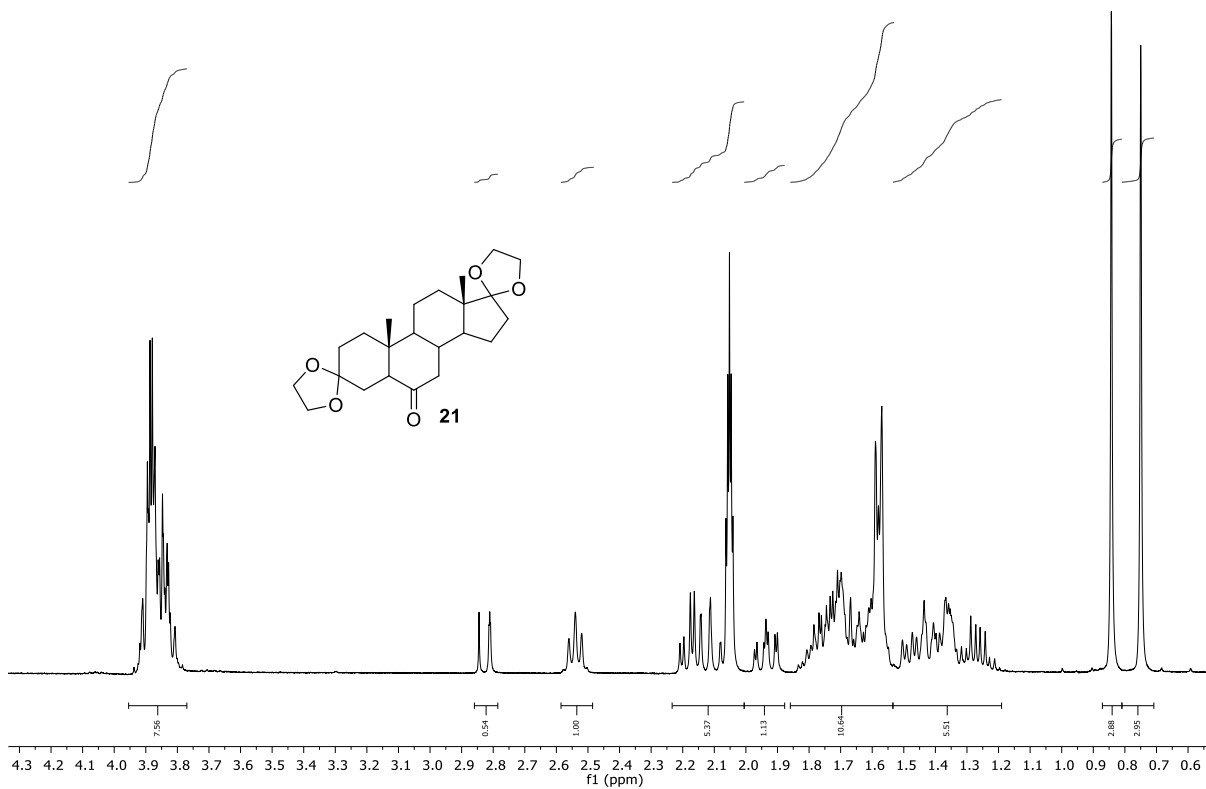
CVie216  $^1\text{H}$   $\text{CDCl}_3$  and  $^{13}\text{C}$  in acetone



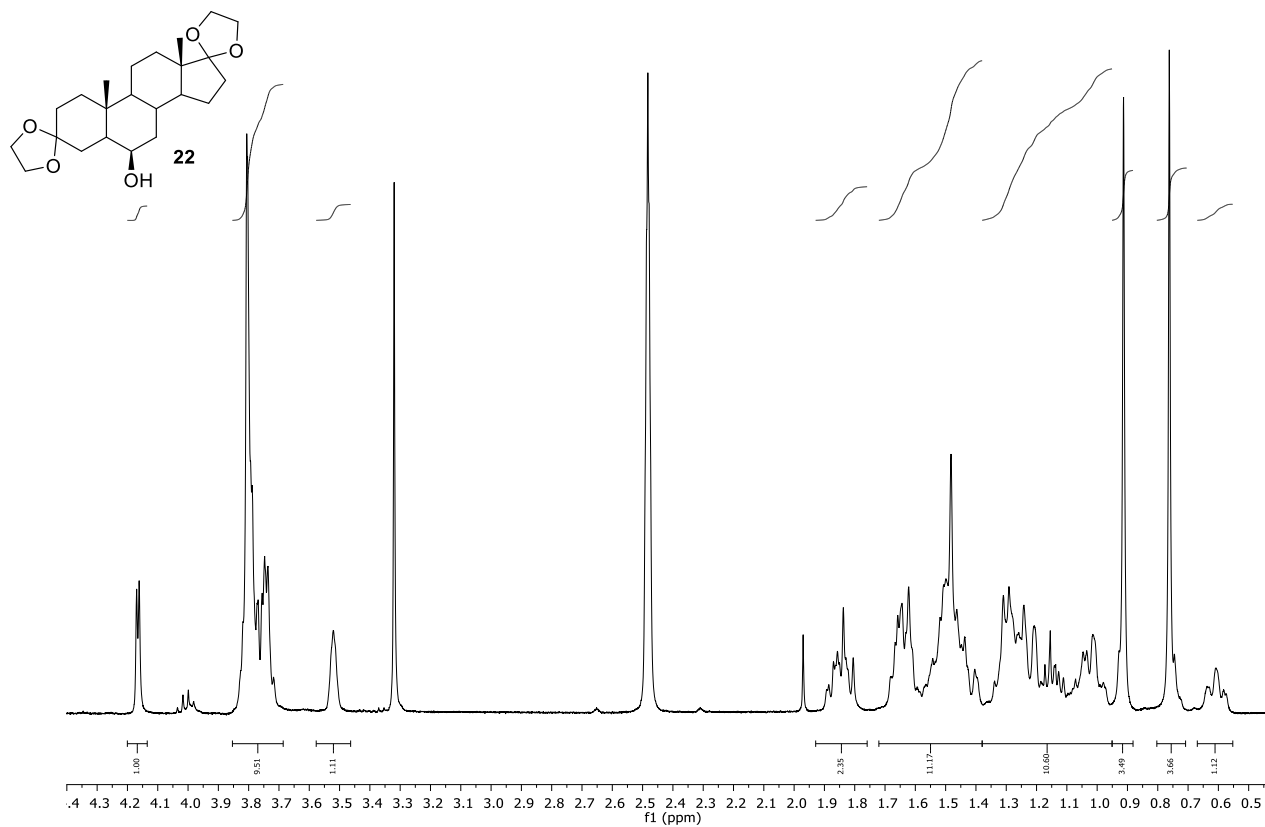
Compound **20**  $^1\text{H}$  DMSO- $d_6$



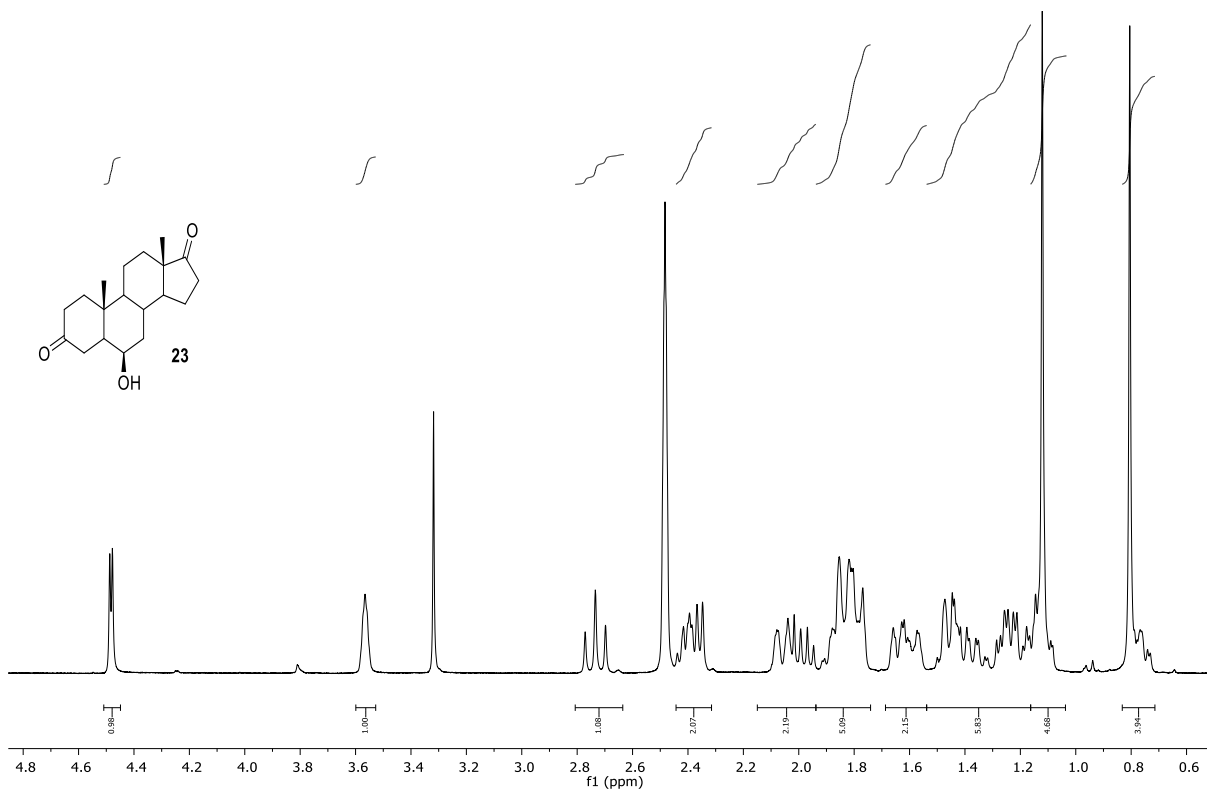
Compound **21**  $^1\text{H}$  Acetone- $d_6$



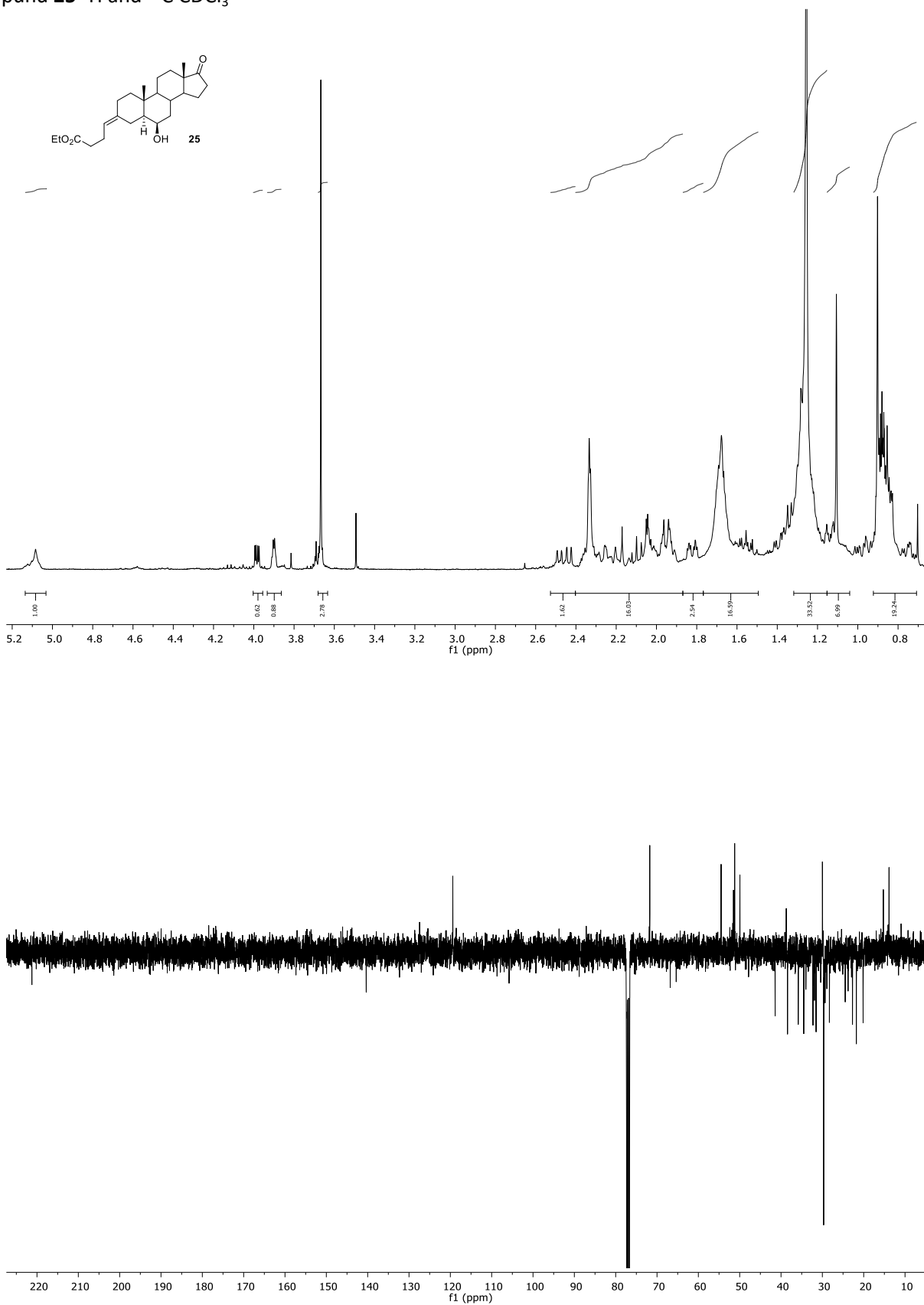
Compound **22**  $^1\text{H}$  Acetone- $d_6$



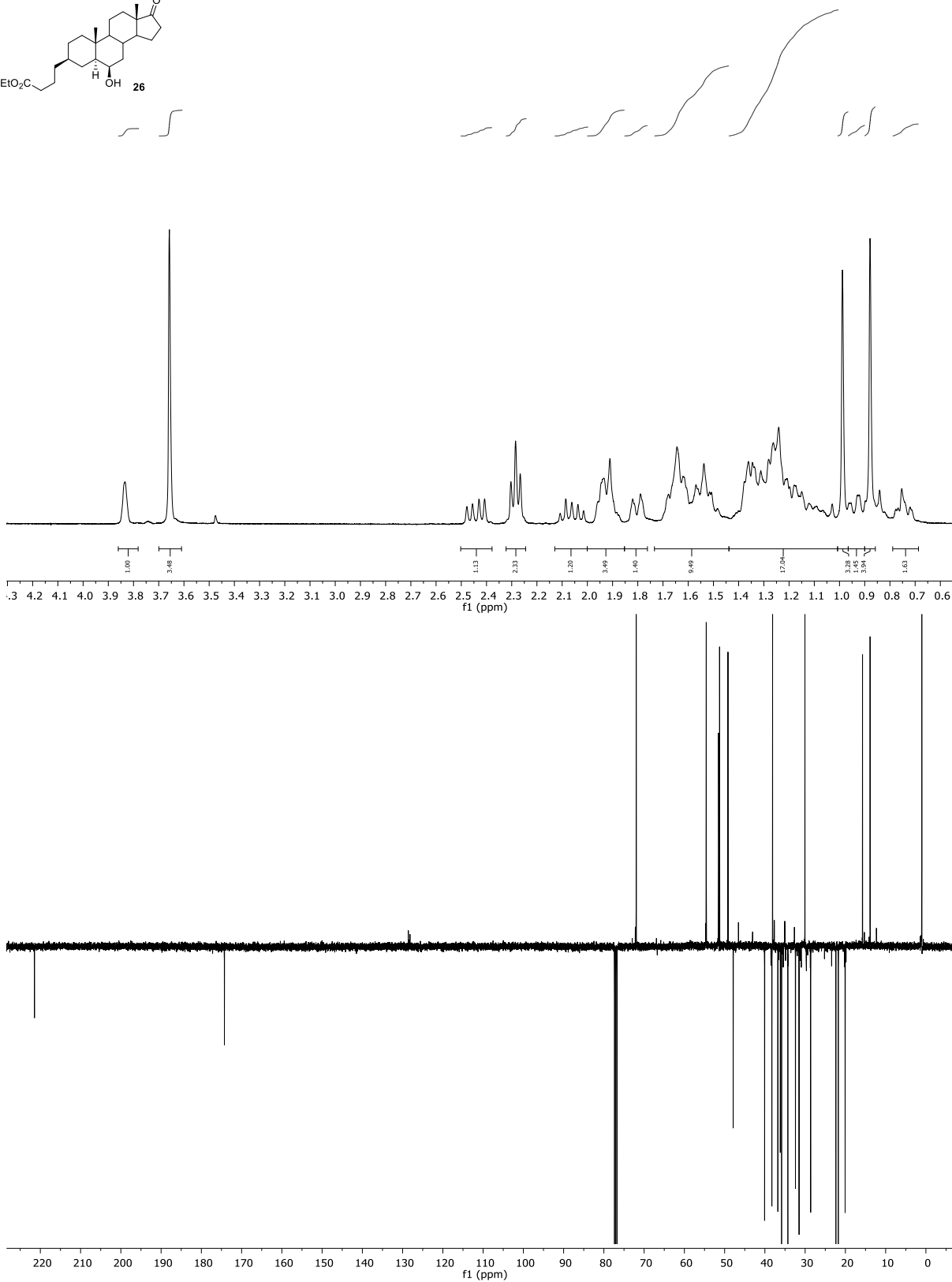
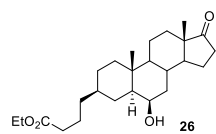
Compound **23**  $^1\text{H}$  DMSO- $d_6$



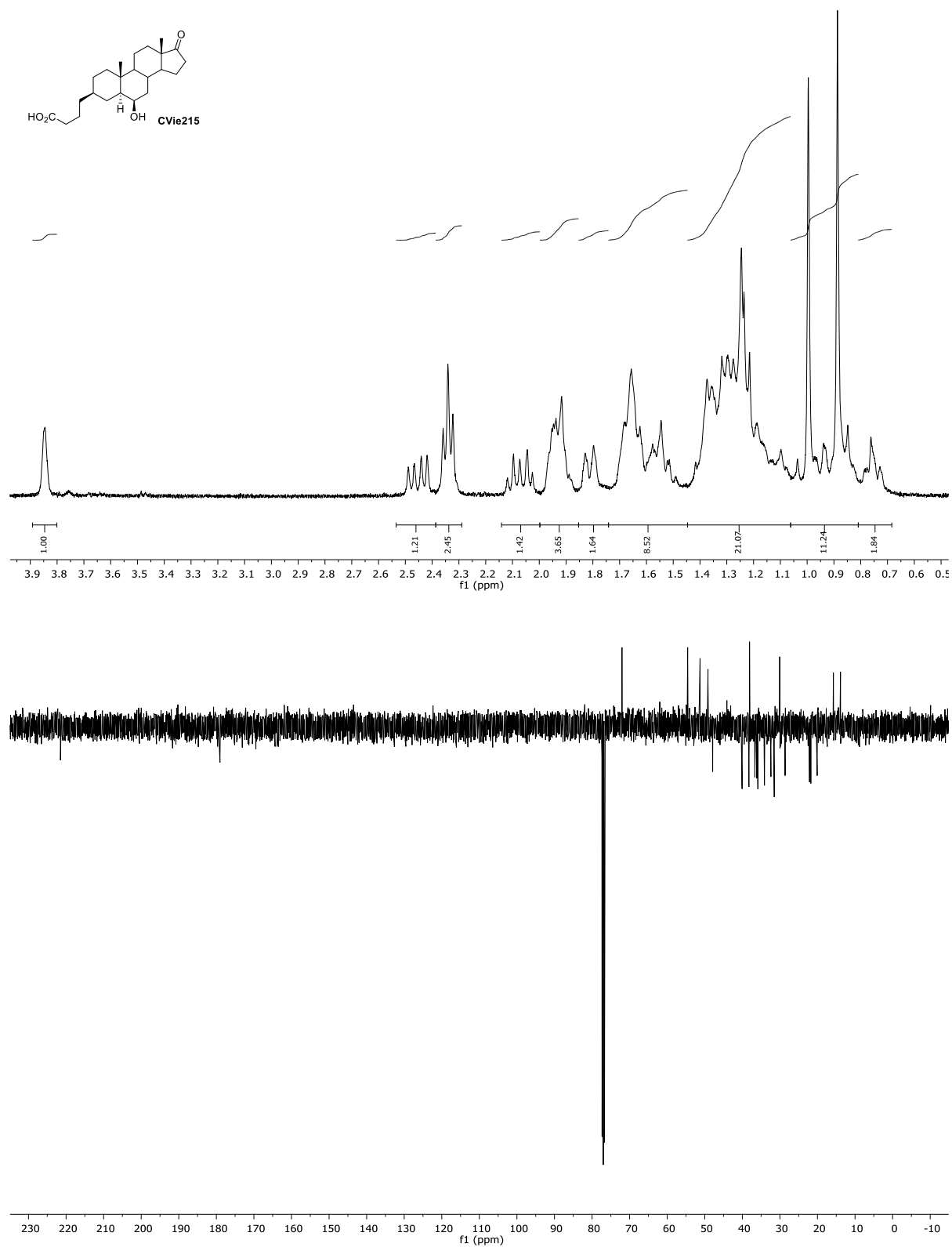
Compound **25**  $^1\text{H}$  and  $^{13}\text{C}$   $\text{CDCl}_3$



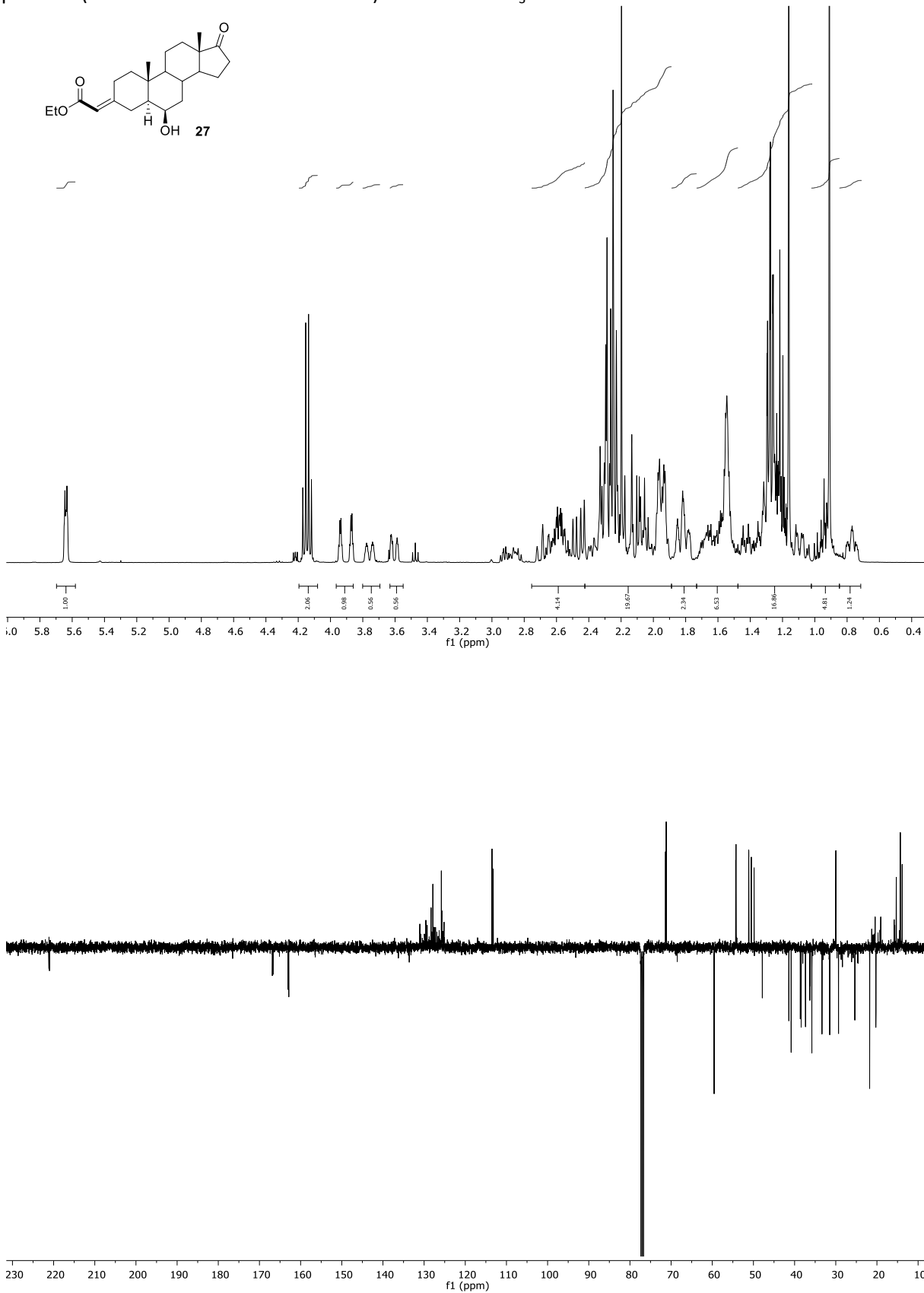
Compound **26**  $^1\text{H}$  and  $^{13}\text{C}$   $\text{CDCl}_3$



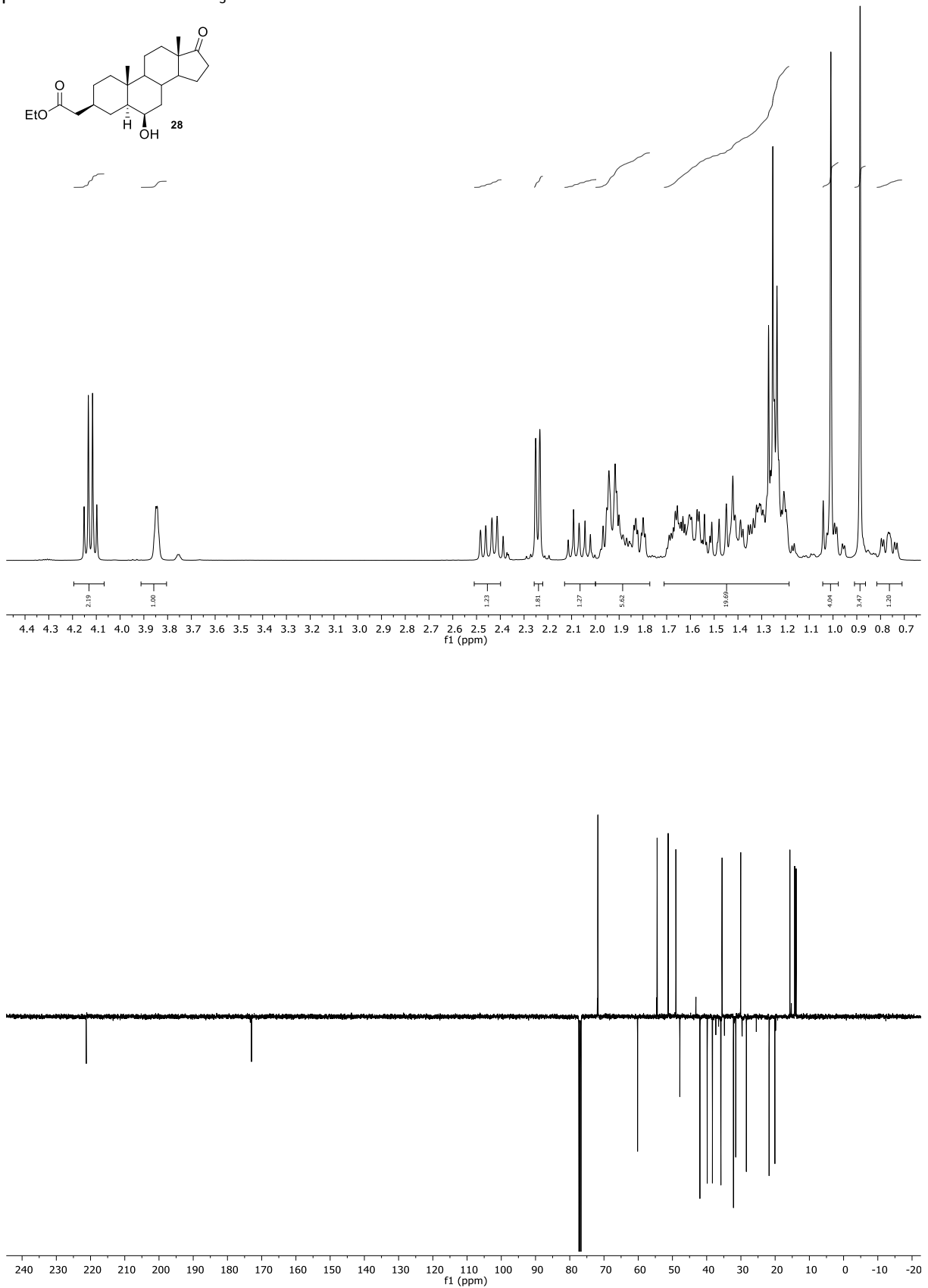
CVie215  $^1\text{H}$  and  $^{13}\text{C}$   $\text{CDCl}_3$



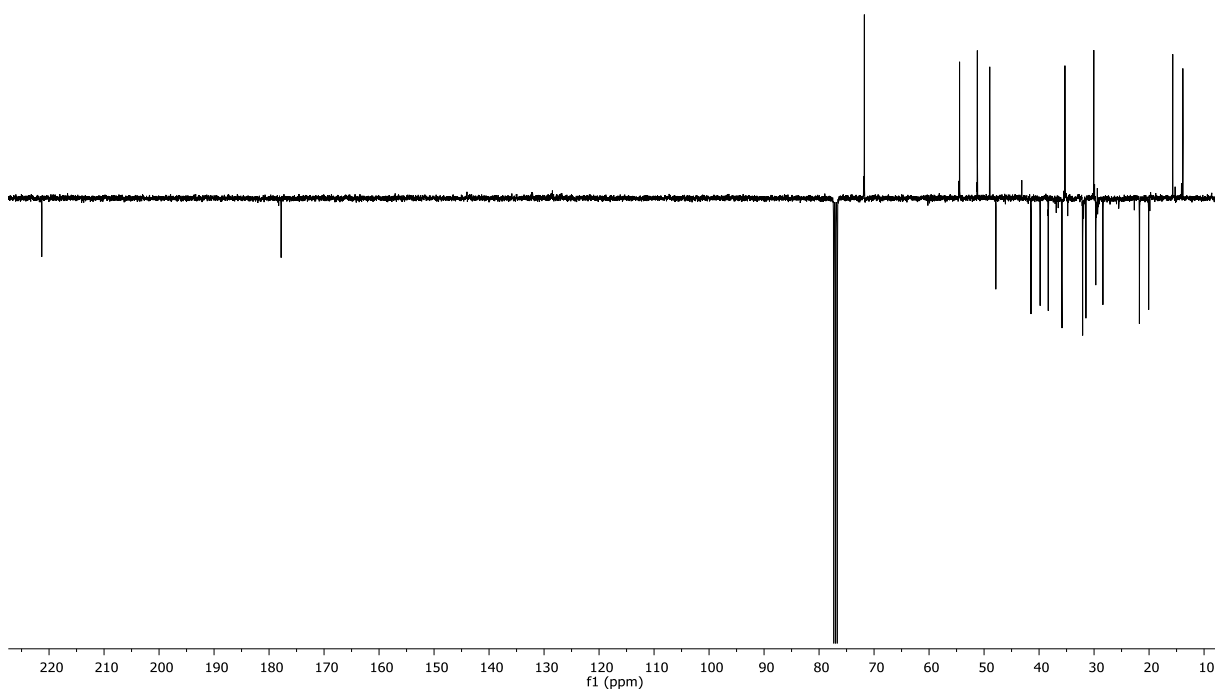
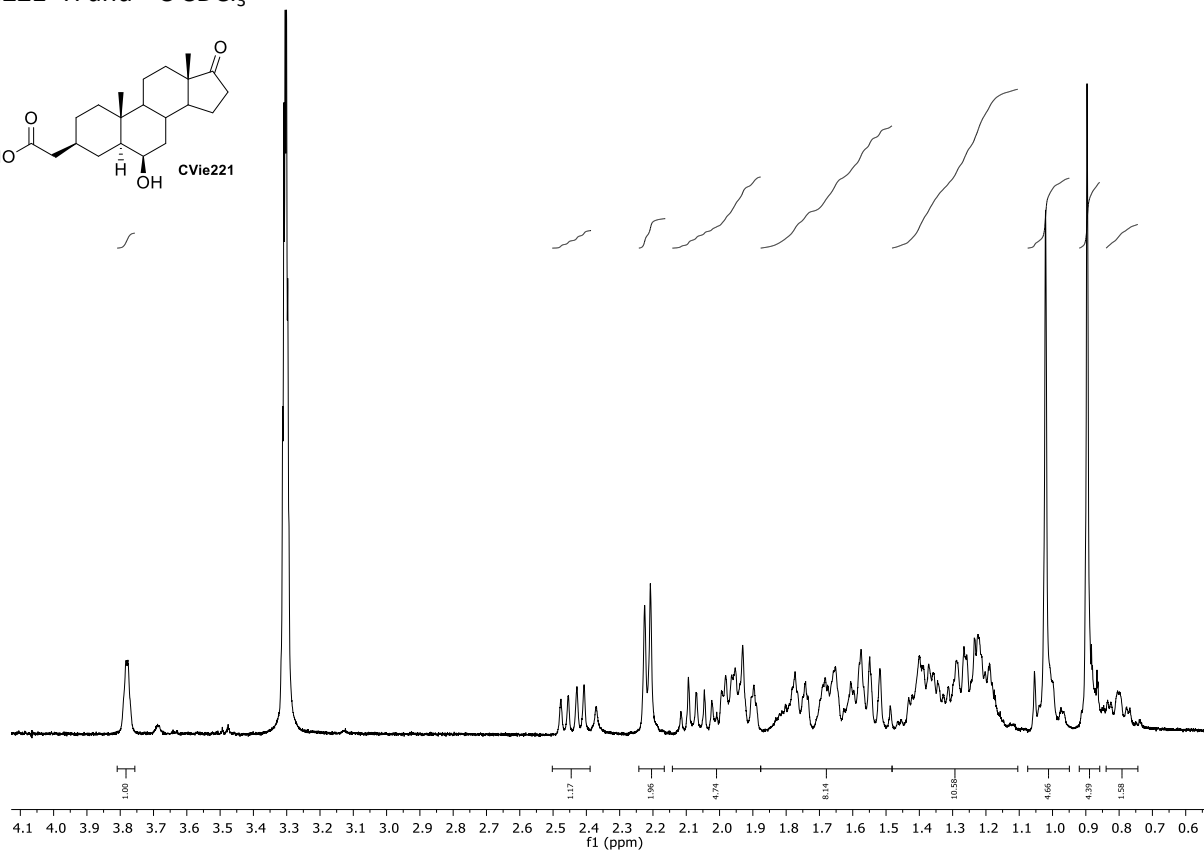
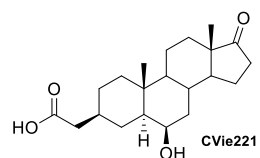
Compound **27** (mixture of two diastereoisomers)  $^1\text{H}$  and  $^{13}\text{C}$   $\text{CDCl}_3$



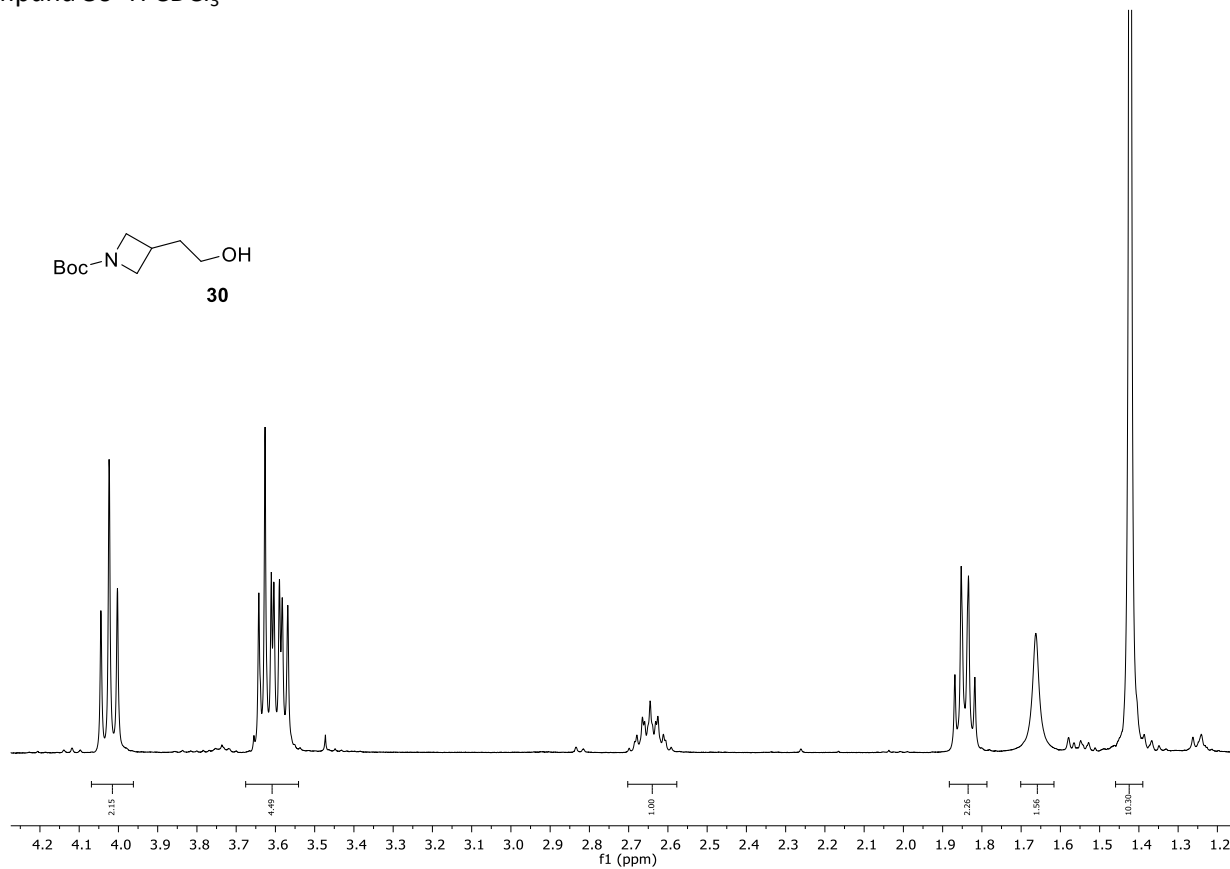
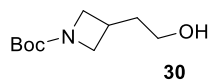
Compound **28**  $^1\text{H}$  and  $^{13}\text{C}$   $\text{CDCl}_3$



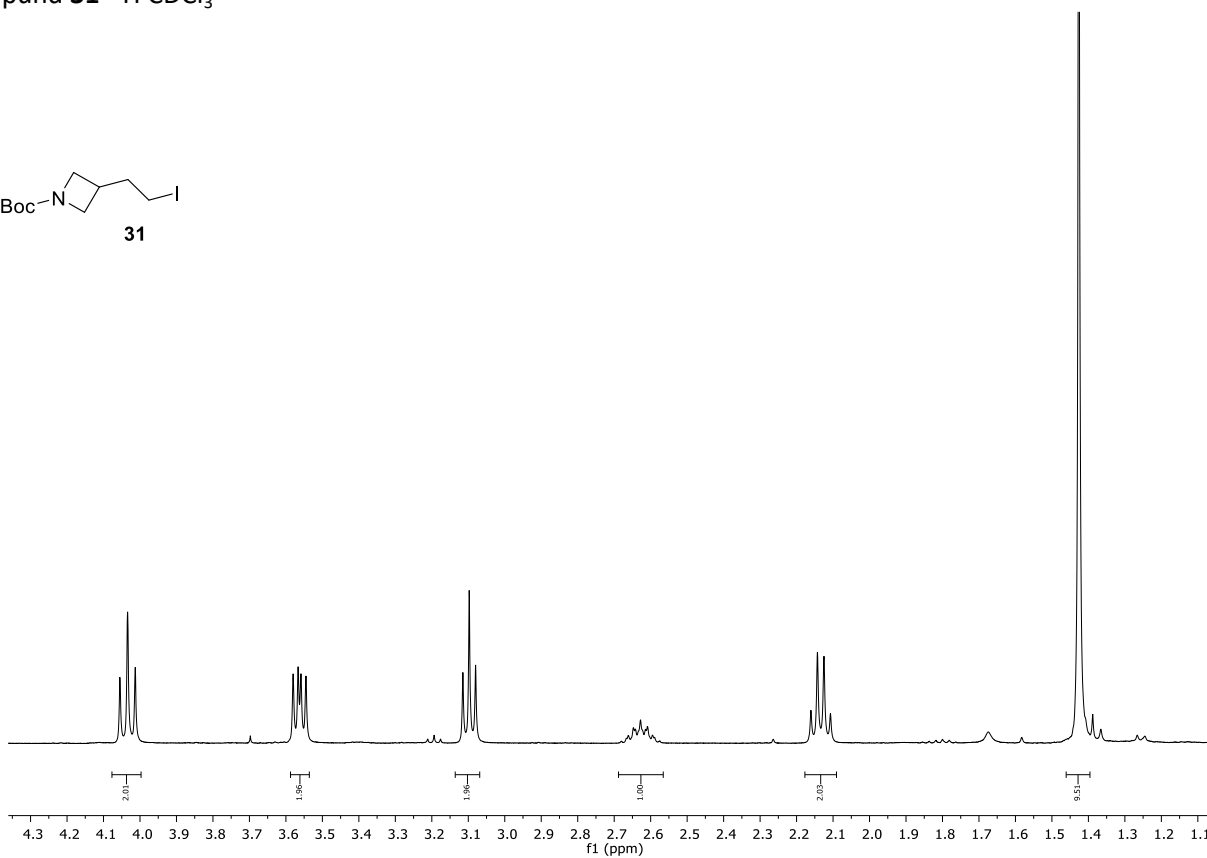
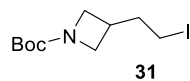
CVie221  $^1\text{H}$  and  $^{13}\text{C}$   $\text{CDCl}_3$



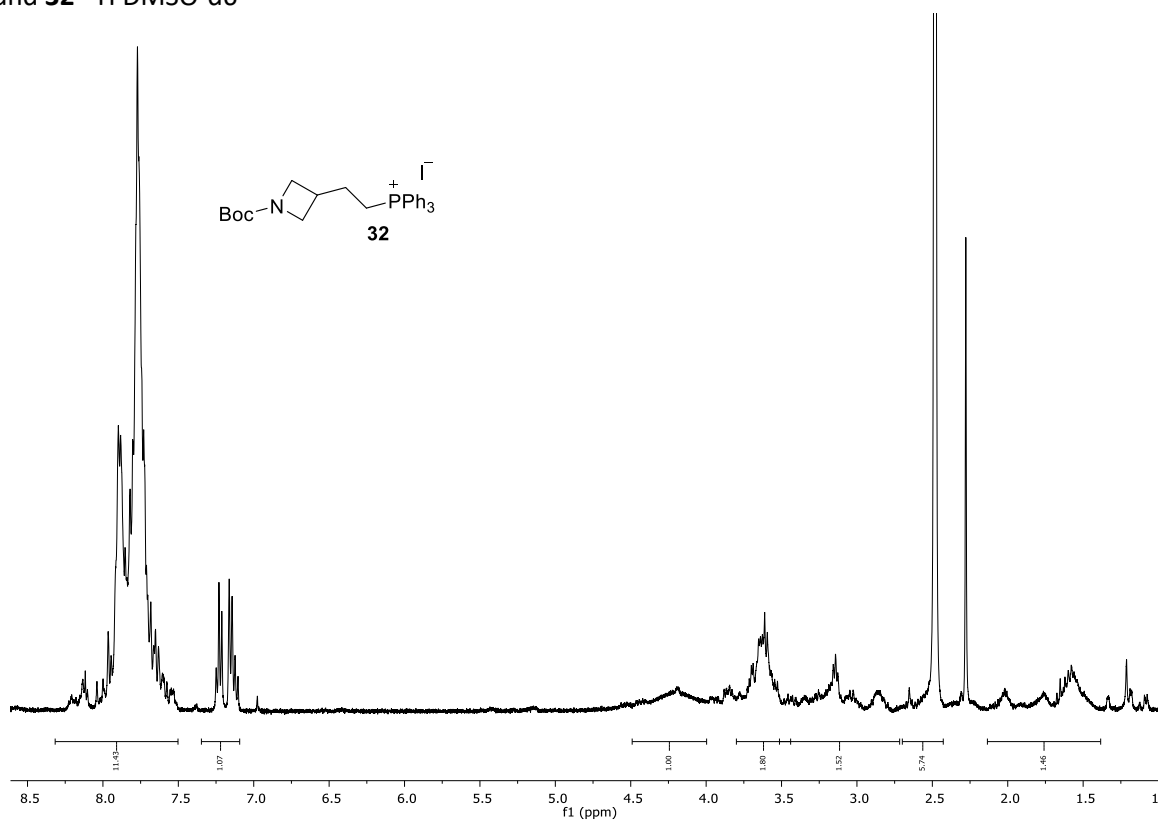
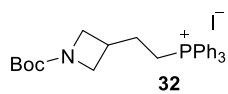
Compound **30**  $^1\text{H}$   $\text{CDCl}_3$



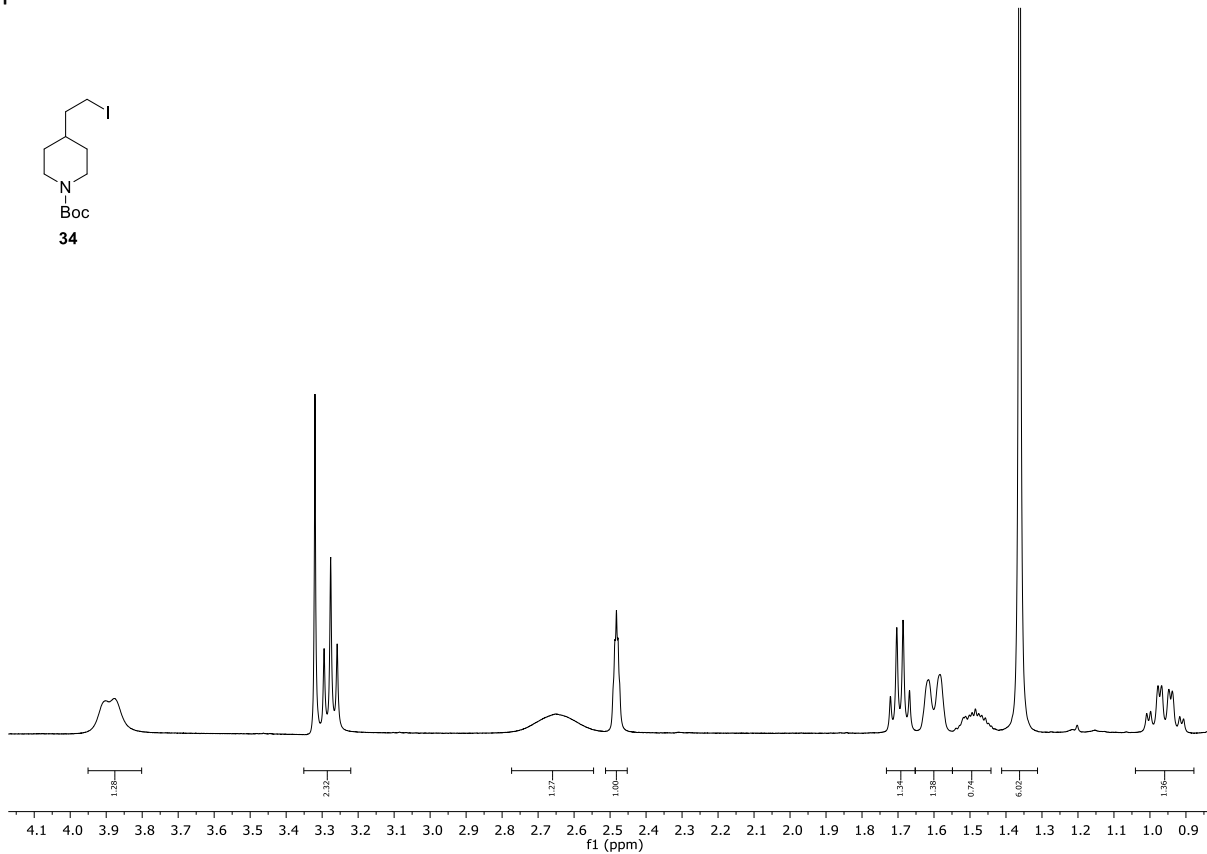
Compound **31**  $^1\text{H}$   $\text{CDCl}_3$



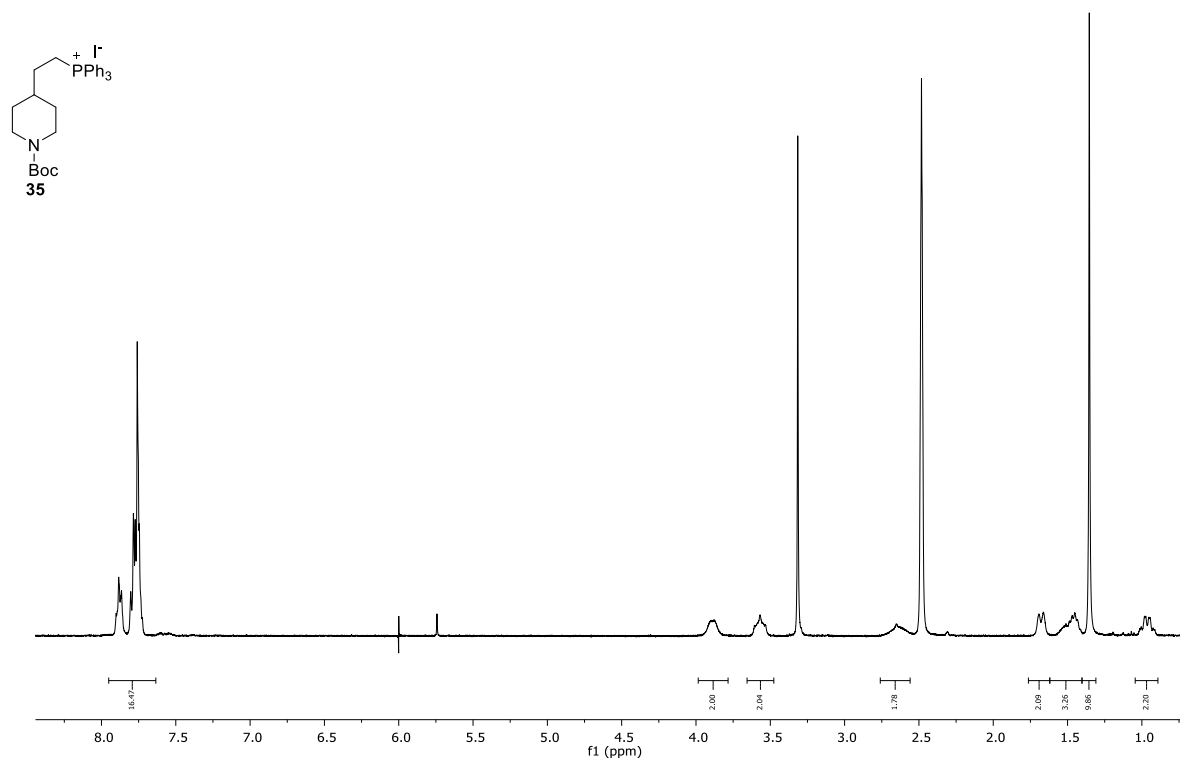
Compound **32**  $^1\text{H}$   $\text{DMSO-d}_6$



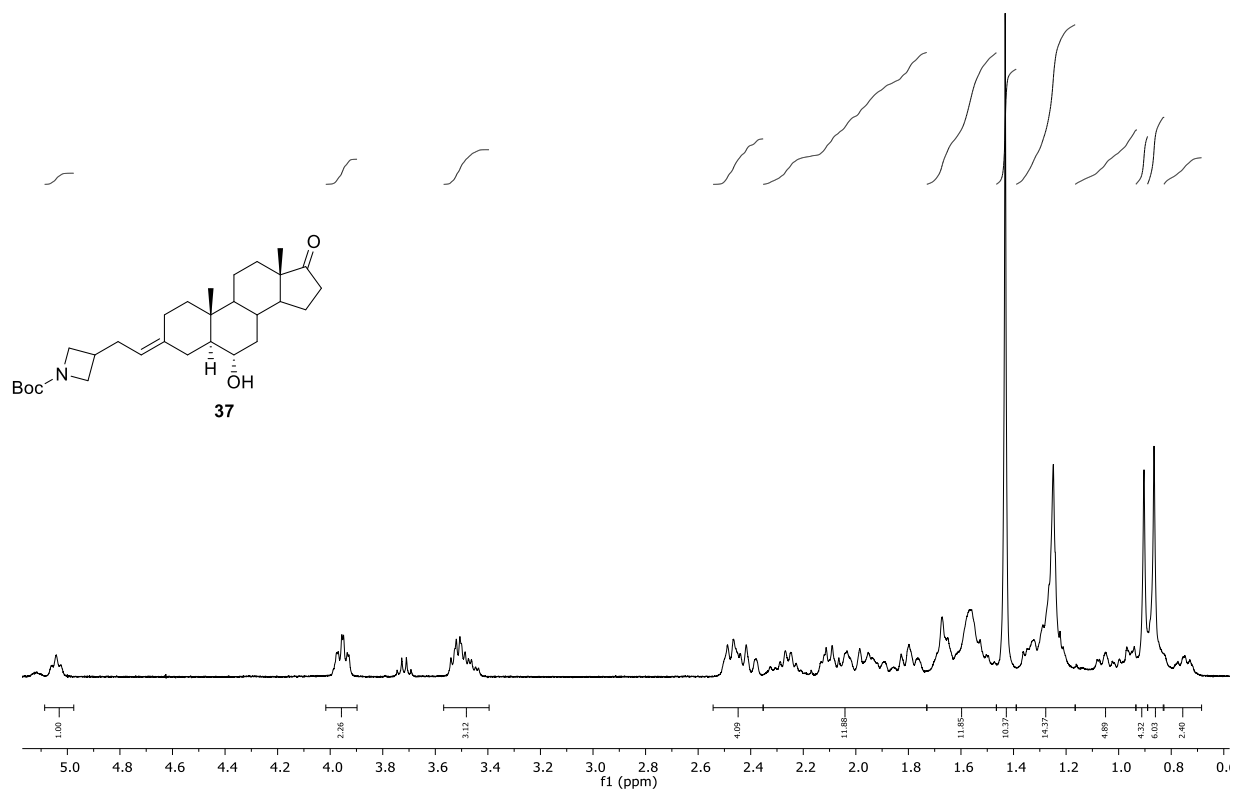
Compound **34**  $^1\text{H}$  DMSO-d6



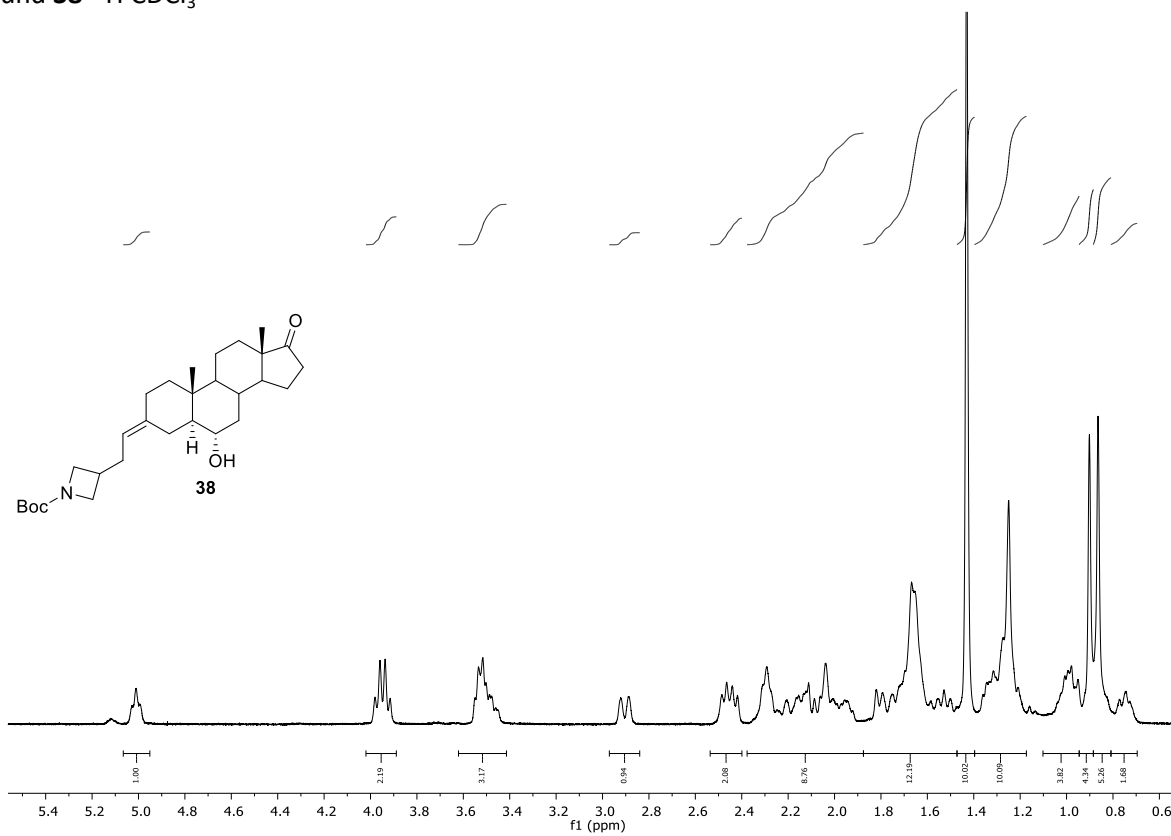
Compound **35**  $^1\text{H}$  DMSO-d6



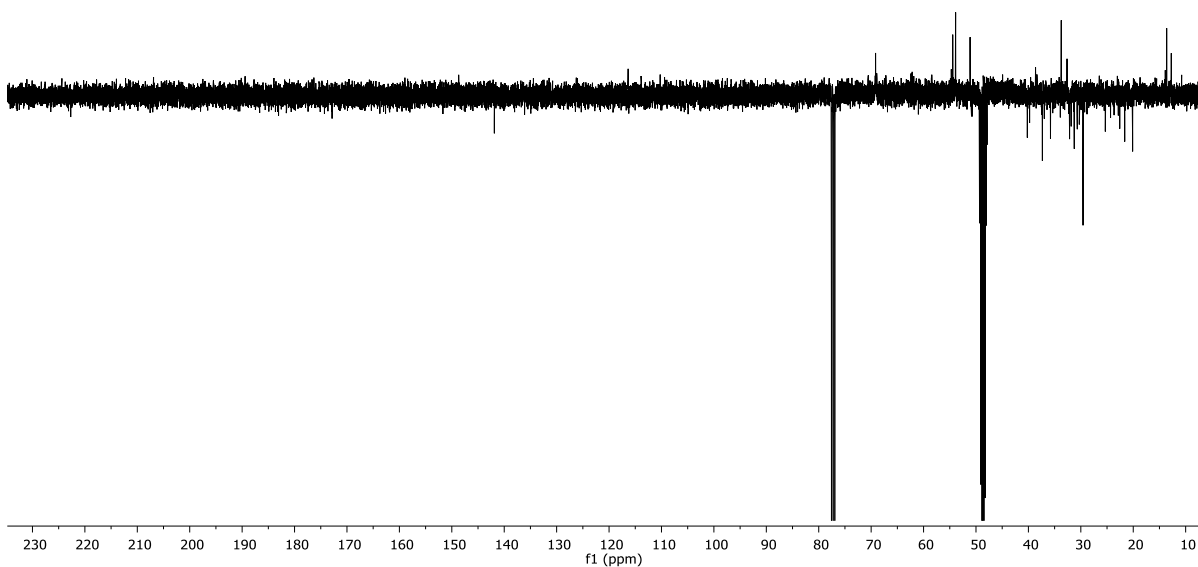
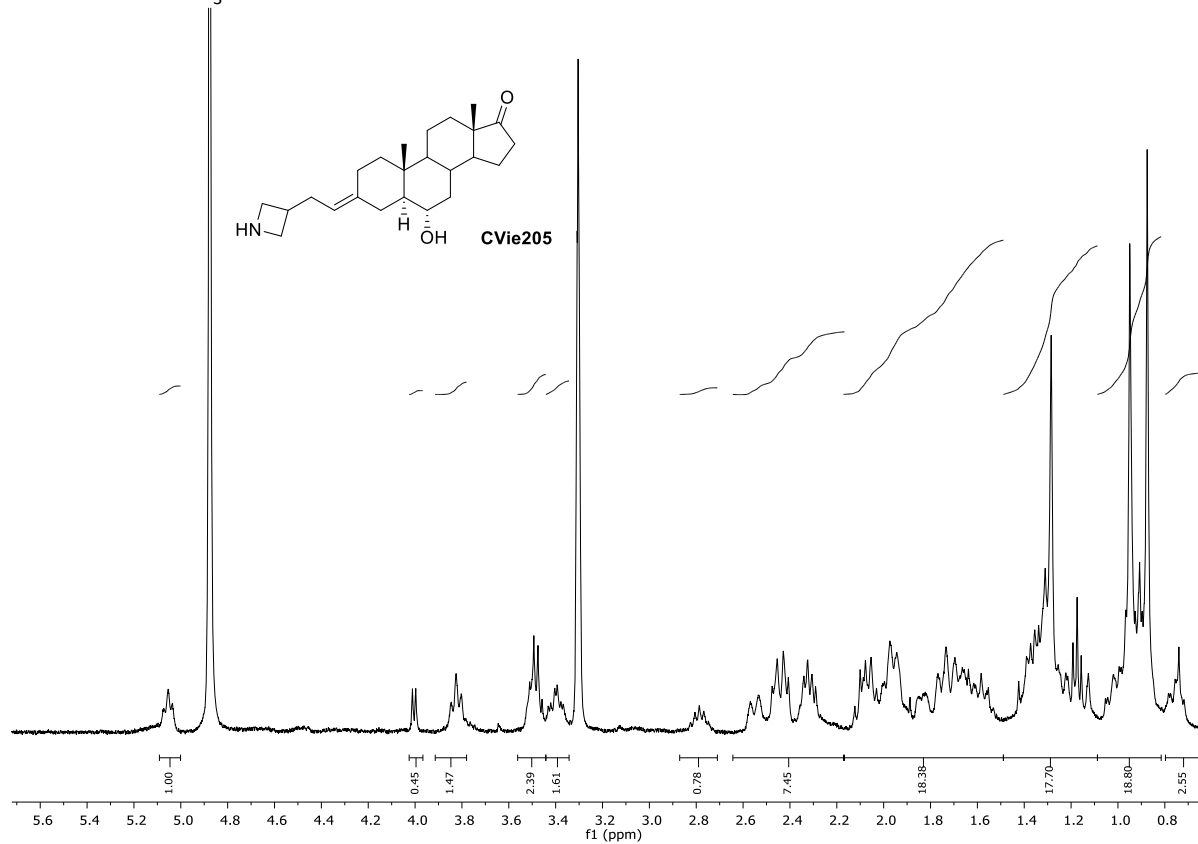
Compound **37**  $^1\text{H}$   $\text{CDCl}_3$



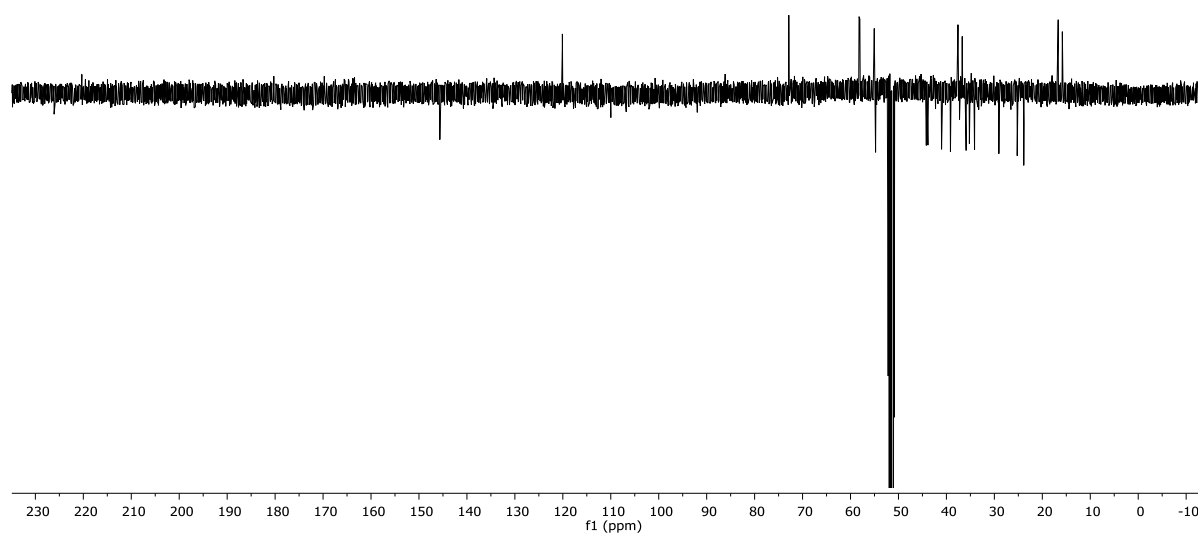
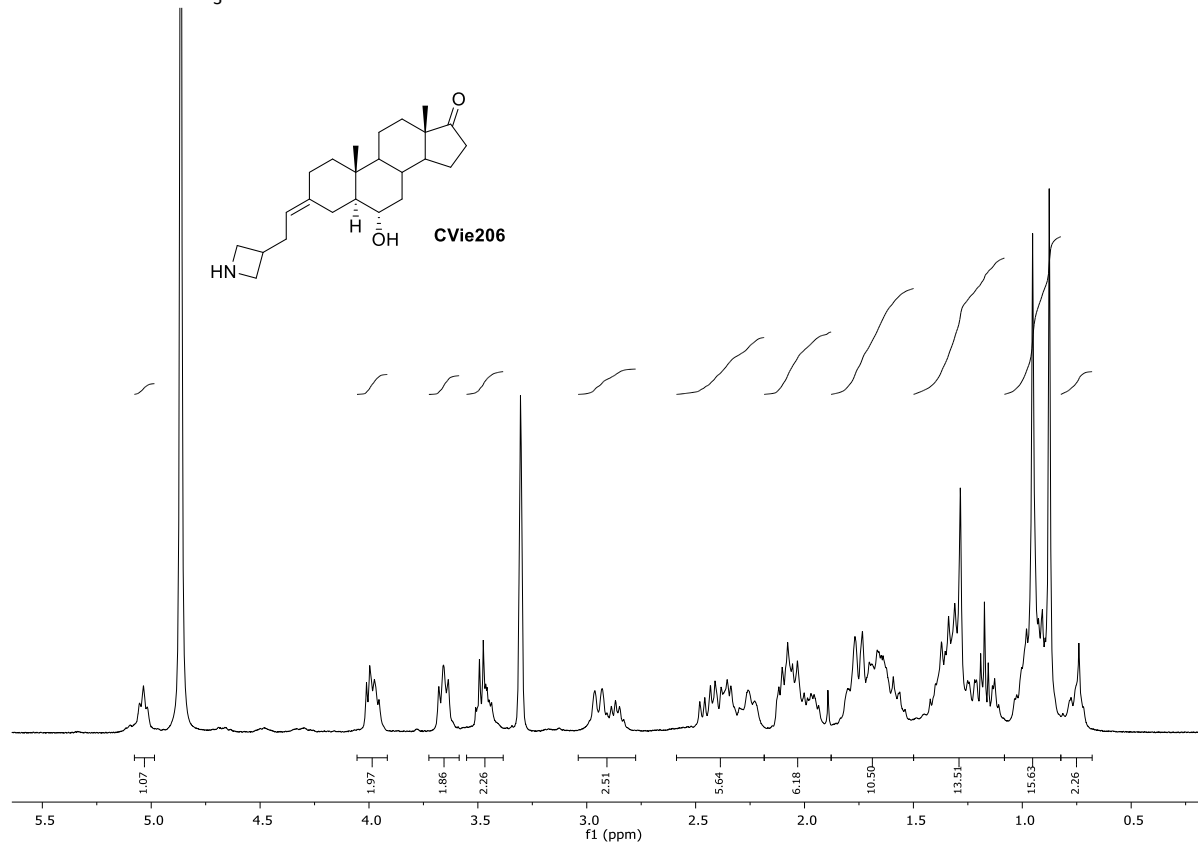
Compound **38**  $^1\text{H}$   $\text{CDCl}_3$



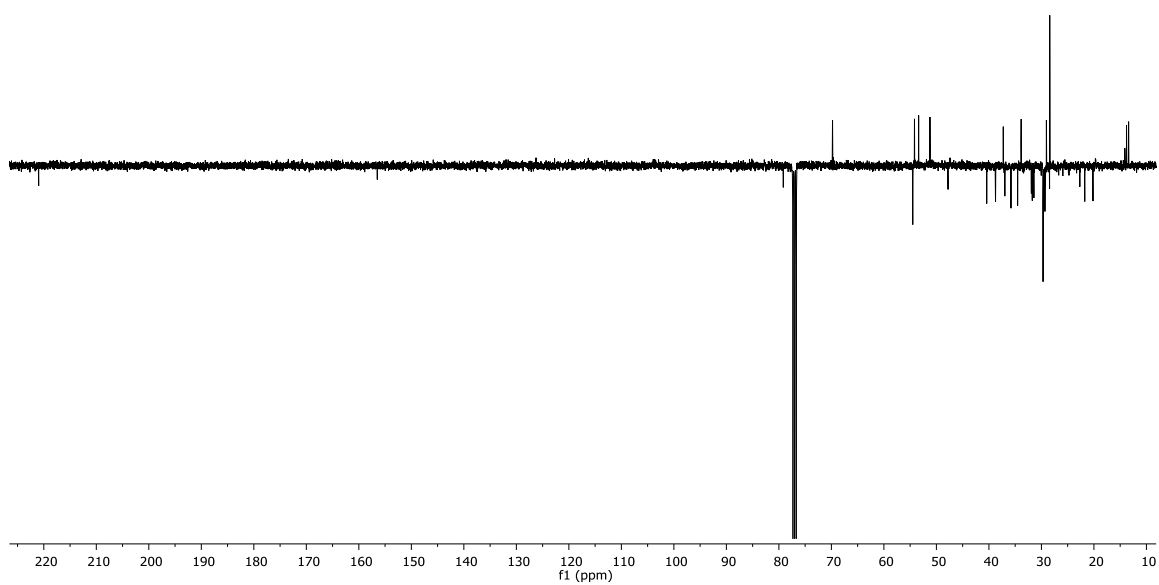
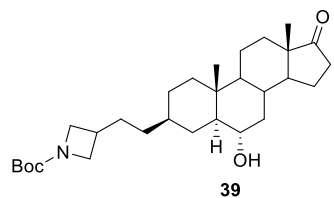
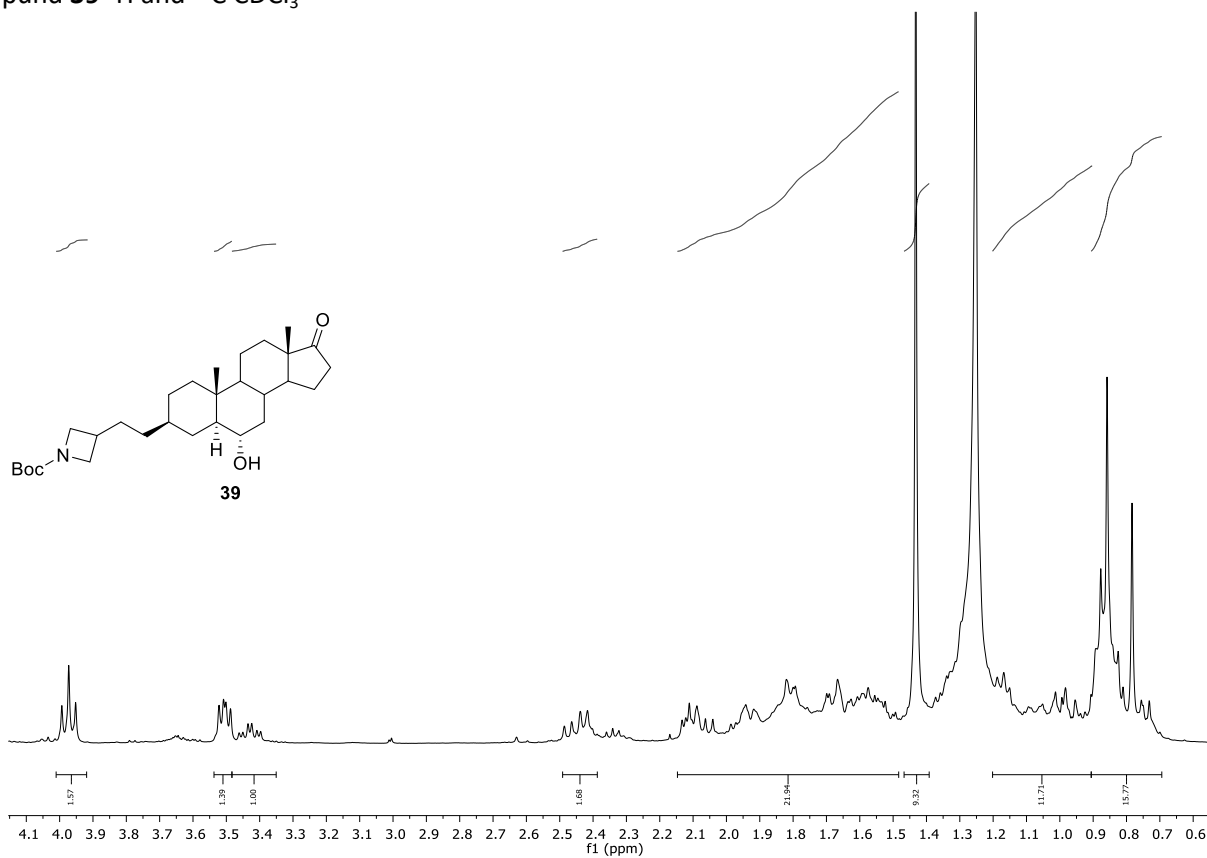
CVie205 <sup>1</sup>H and <sup>13</sup>C CD<sub>3</sub>OD



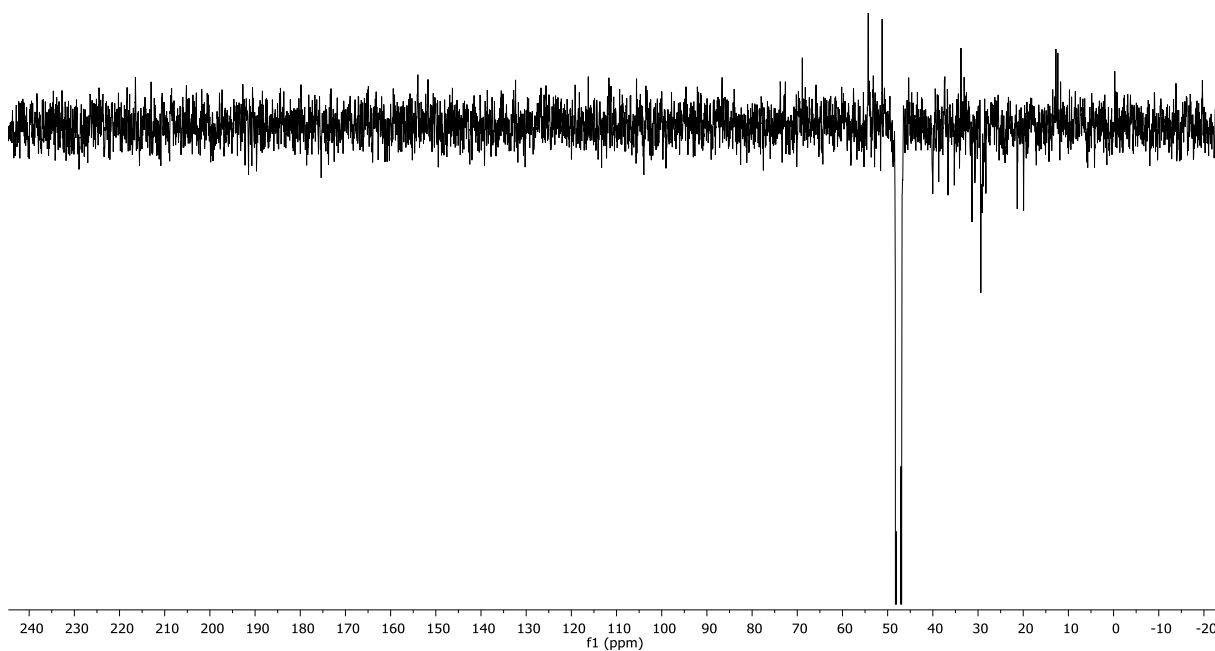
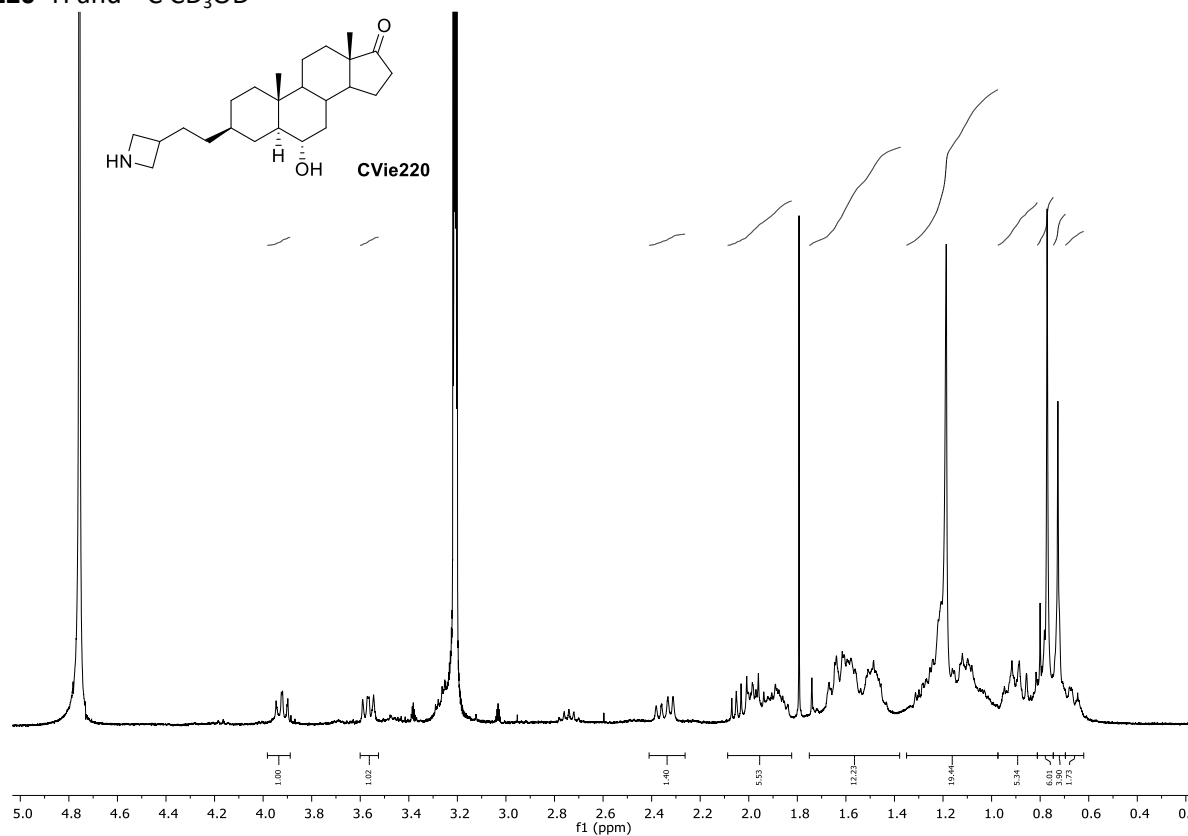
CVie206 <sup>1</sup>H and <sup>13</sup>C CD<sub>3</sub>OD



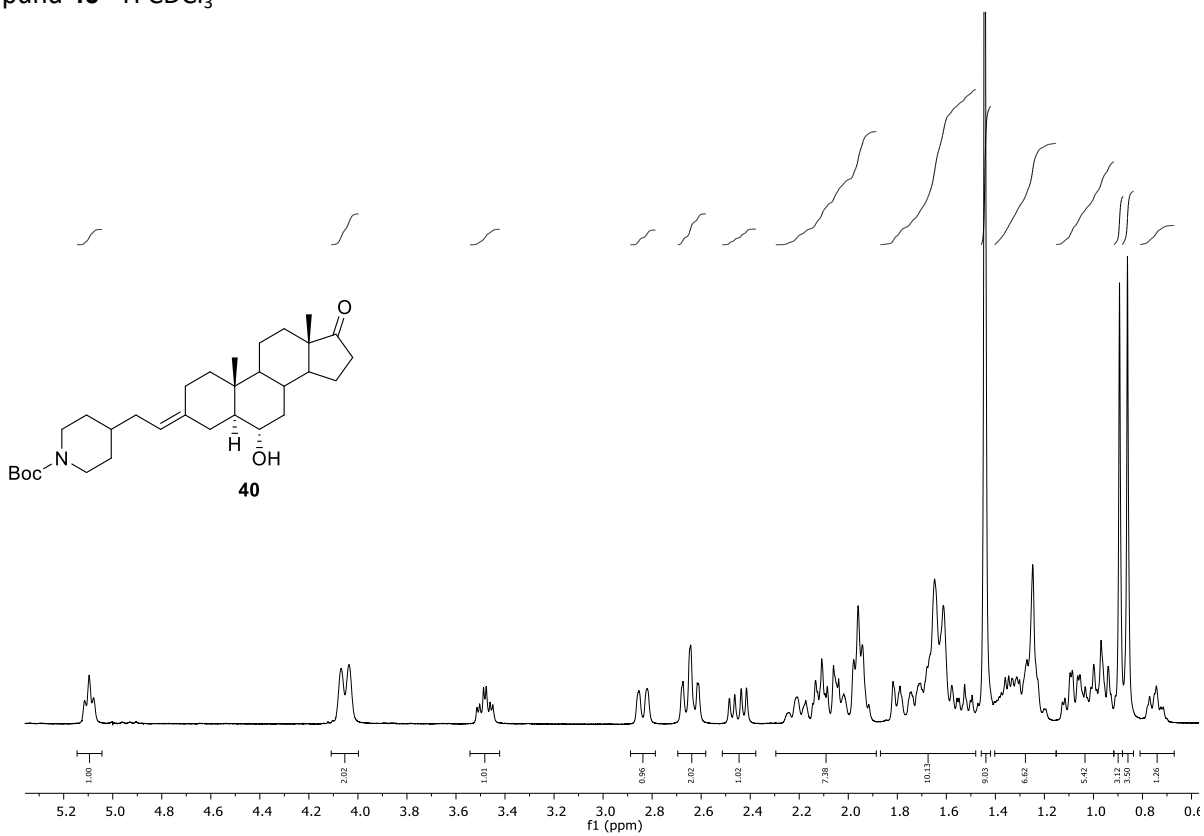
Compound **39**  $^1\text{H}$  and  $^{13}\text{C}$   $\text{CDCl}_3$



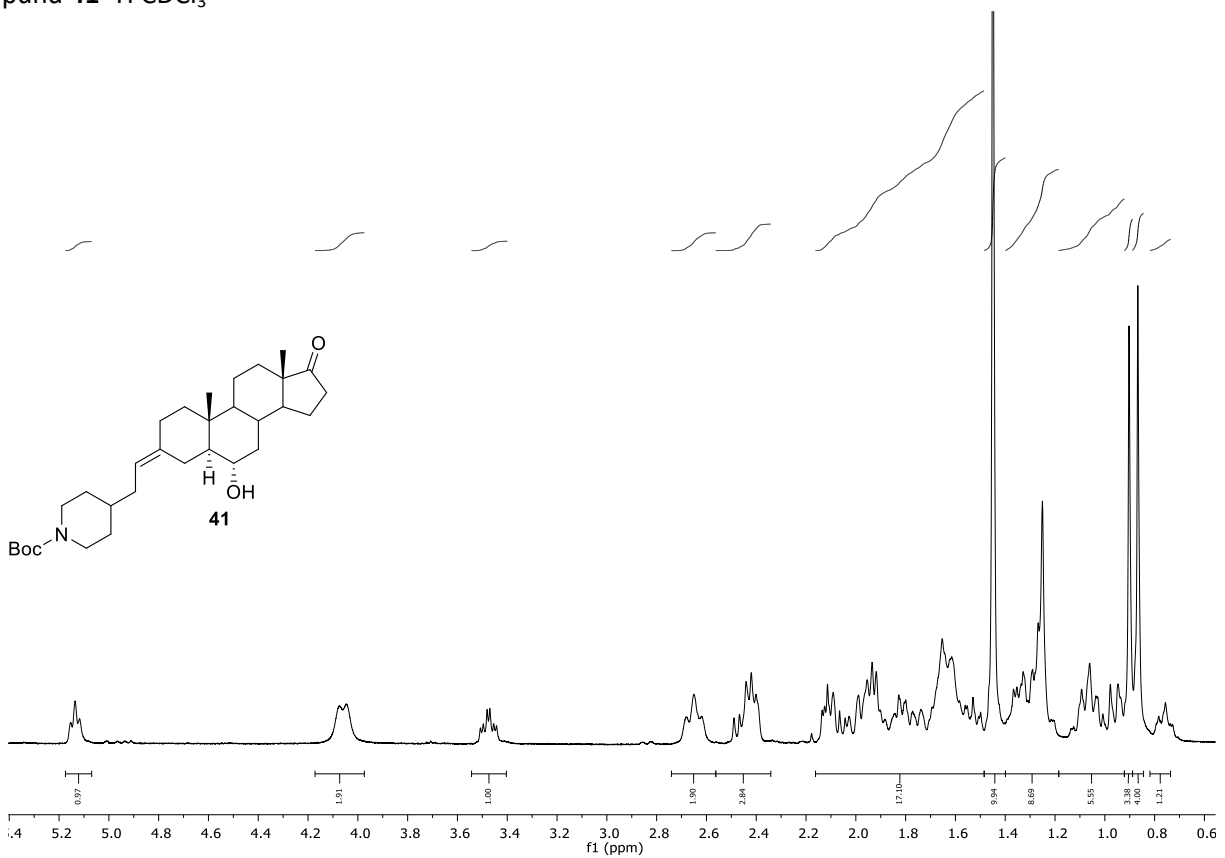
CVie220 <sup>1</sup>H and <sup>13</sup>C CD<sub>3</sub>OD



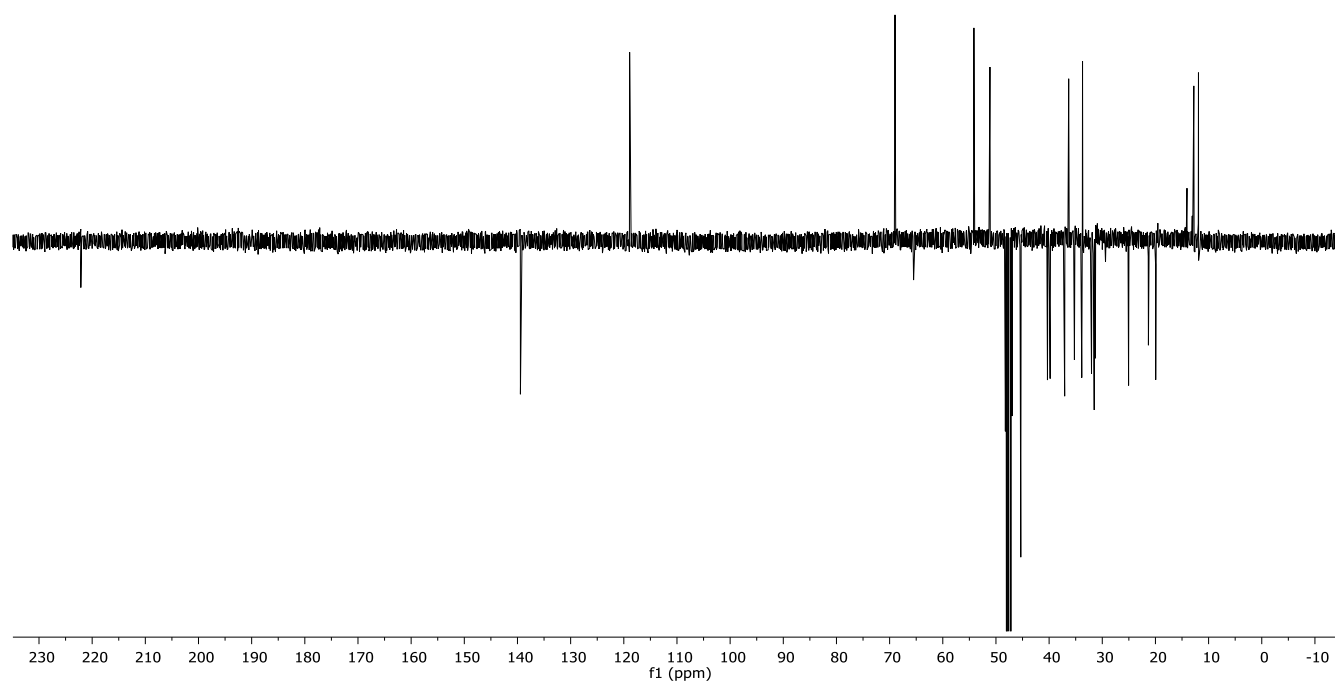
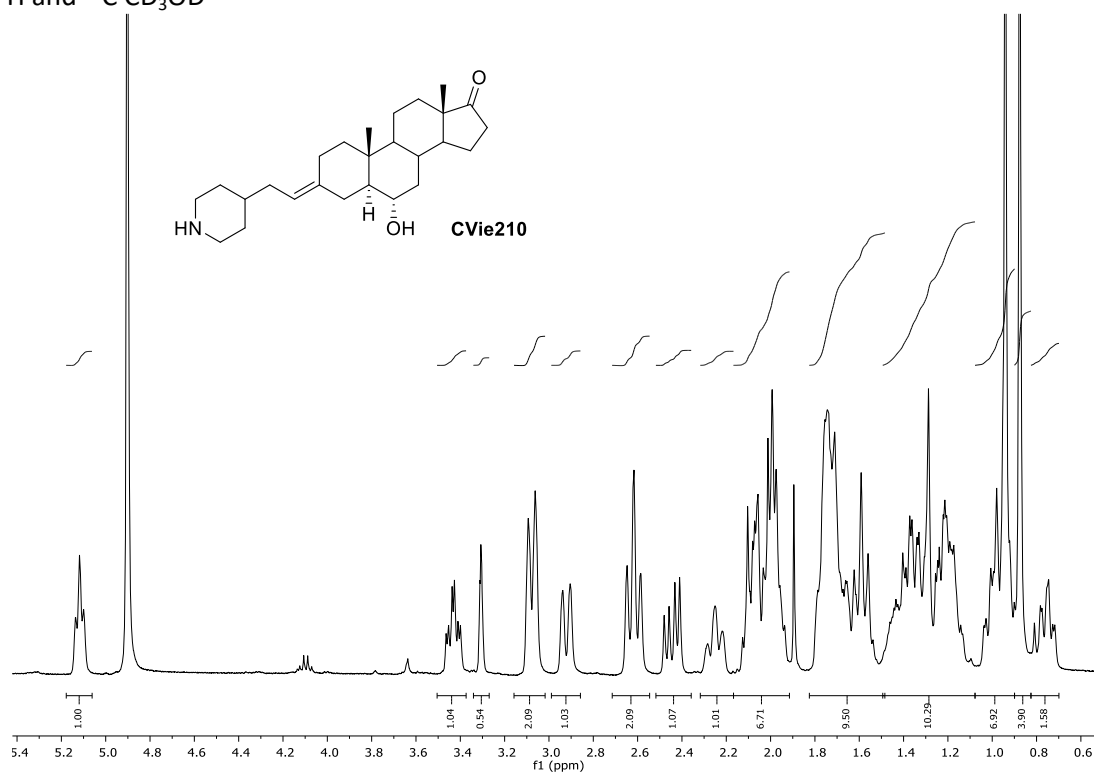
Compound **40**  $^1\text{H}$   $\text{CDCl}_3$



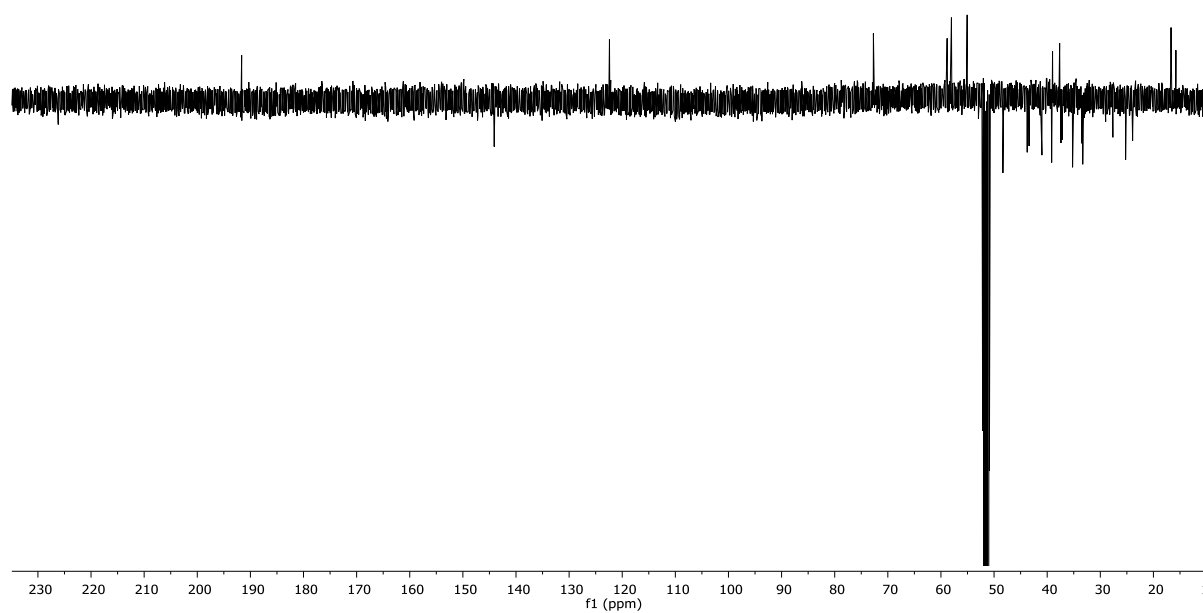
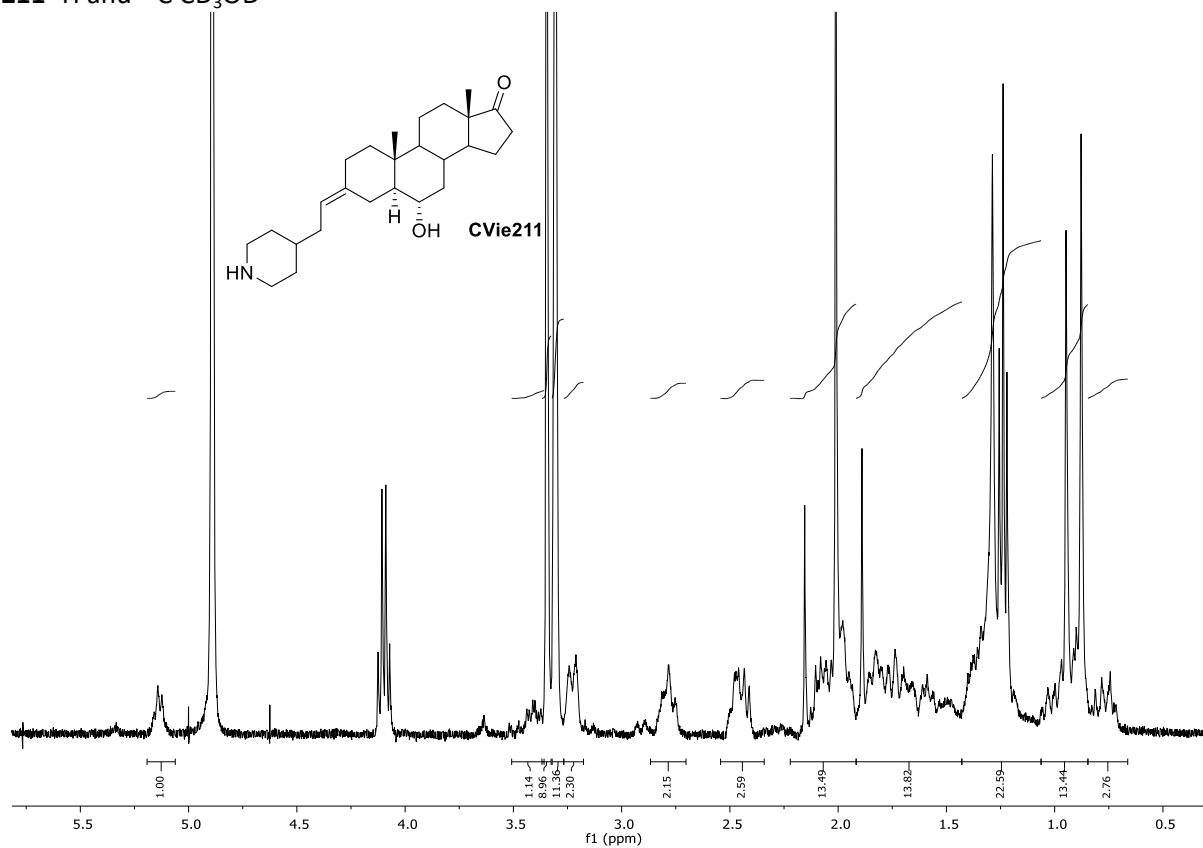
Compound **41**  $^1\text{H}$   $\text{CDCl}_3$



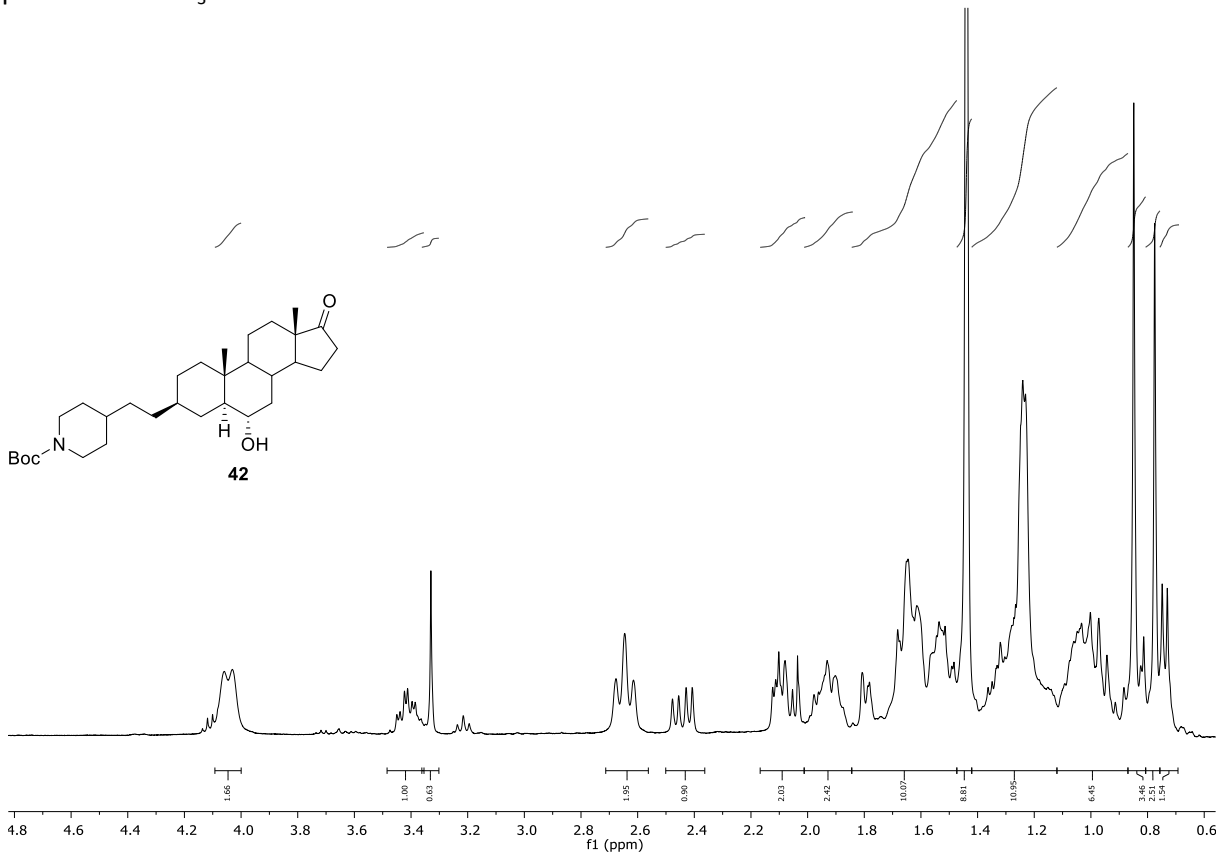
CVie210  $^1\text{H}$  and  $^{13}\text{C}$   $\text{CD}_3\text{OD}$



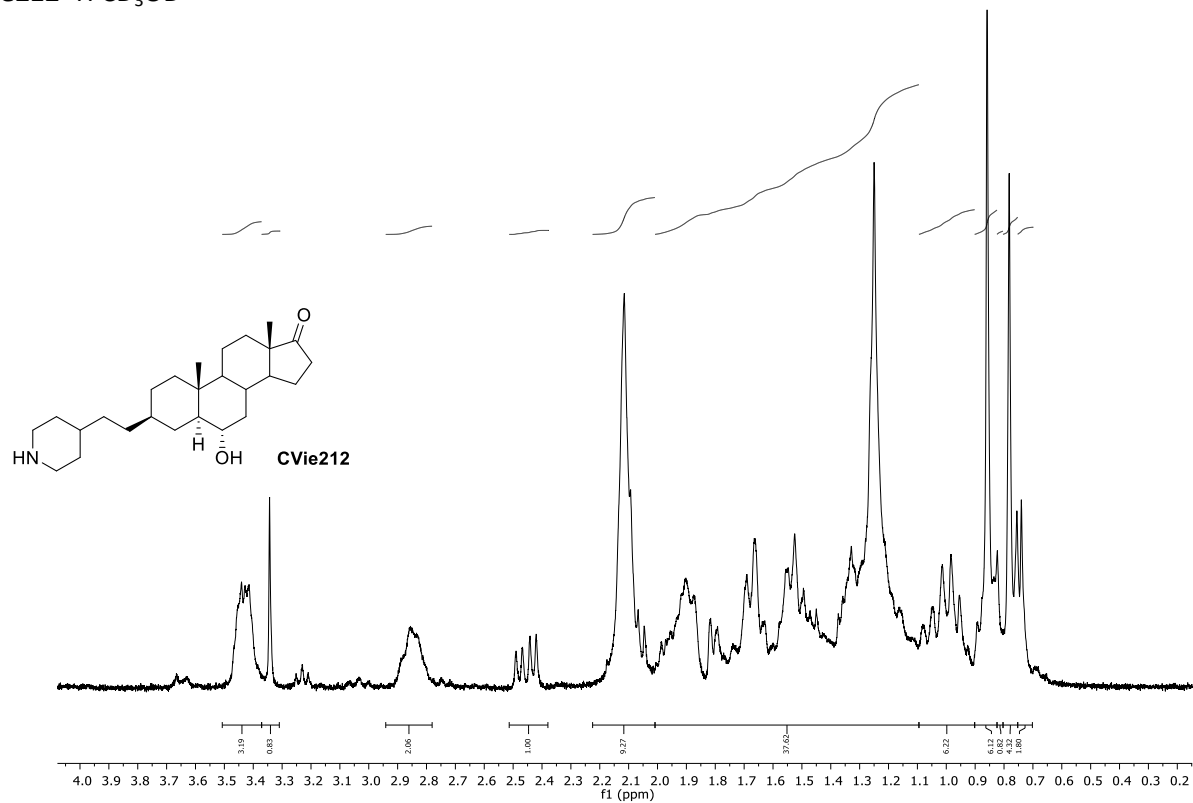
CVie211  $^1\text{H}$  and  $^{13}\text{C}$   $\text{CD}_3\text{OD}$



Compound **42**  $^1\text{H}$   $\text{CDCl}_3$



CVie212 <sup>1</sup>H CD<sub>3</sub>OD



# 7. Bibliography

- [1] Guyton AC. Guyton and Hall textbook of medical physiology. 2016.
- [2] J. GORDON BETTS, PETER DESAIX, EDDIE JOHNSON, JODY E. JOHNSON, OKSANA KOROL, DEAN KRUSE, BRANDON POE, JAMES A. WISE, MARK WOMBLE KAY. Anatomy & Physiology. 2016.
- [3] Anatomy. The Anatomical Basis of Clinical Pracrice. 2018.
- [4] Olivetti G, Cigola E, Maestri R, Corradi D, Lagrasta C, Gambert SR, et al. Aging, cardiac hypertrophy and ischemic cardiomyopathy do not affect the proportion of mononucleated and multinucleated myocytes in the human heart. *J Mol Cell Cardiol* 1996;28:1463–77. <https://doi.org/10.1006/jmcc.1996.0137>.
- [5] Mitchell JR, Wang JJ. Expanding application of the Wiggers diagram to teach cardiovascular physiology. *Adv Physiol Educ* 2015;38:170–5. <https://doi.org/10.1152/advan.00123.2013>.
- [6] World Health Organization (WHO). Core medical equipment. *Core Med Equip* 2011;2011:16488.
- [7] Rice WJ, Young HS, Martin DW, Sachs JR, Stokes DL. Structure of Na<sup>+</sup>,K<sup>+</sup>-ATPase at 11-Å resolution: Comparison with Ca<sup>2+</sup>-ATPase in E1 and E2 states. *Biophys J* 2001;80:2187–97. [https://doi.org/10.1016/S0006-3495\(01\)76191-7](https://doi.org/10.1016/S0006-3495(01)76191-7).
- [8] Skou JC. Nobel Lecture:The Identification of the Sodium-Potassium Pump n.d.
- [9] Axelsen KB, Palmgren MG. Evolution of substrate specificities in the P-type ATPase superfamily. *J Mol Evol* 1998;46:84–101. <https://doi.org/10.1007/PL00006286>.
- [10] Morth JP, Pedersen BP, Toustrup-Jensen MS, Sørensen TLM, Petersen J, Andersen JP, et al. Crystal structure of the sodium-potassium pump. *Nature* 2007;450:1043–9. <https://doi.org/10.1038/nature06419>.
- [11] Sachs JR. The order of release of sodium and addition of potassium in the sodium-potassium pump reaction mechanism. *J Physiol* 1980;302:219–40. <https://doi.org/10.1113/jphysiol.1980.sp013239>.
- [12] Liao J, Li H, Zeng W, Sauer DB, Belmares R, Jiang Y. Structural Insight into the Sodium / Calcium Exchanger. *Science (80- )* 2012;335:686. <https://doi.org/10.1126/science.1215759>.
- [13] Xu L, Chen J, Li XY, Ren S, Huang CX, Wu G, et al. Analysis of Na<sup>+</sup>/Ca<sup>2+</sup> exchanger (NCX) function and current in murine cardiac myocytes during heart failure. *Mol Biol Rep* 2012;39:3847–52. <https://doi.org/10.1007/s11033-011-1163-x>.
- [14] Blaustein MP, Lederer WJ, Annunziato L. Sodium / Calcium Exchange : Its Physiological Implications. *Society* 2008;79:763–854.
- [15] Eisner DA, Sipido KR. Sodium calcium exchange in heart: Necessity or luxury? *Circ Res* 2004;95:549–51. <https://doi.org/10.1161/01.RES.0000143419.87518.9e>.
- [16] Grant AO. Cardiac ion channels. *Circ Arrhythmia Electrophysiol* 2009;2:185–94. <https://doi.org/10.1161/CIRCEP.108.789081>.
- [17] Hasan S, Bove C, Silvestri G, Mantuano E, Modoni A, Veneziano L, et al. A channelopathy mutation in the voltage-sensor discloses contributions of a conserved phenylalanine to gating properties of Kv1.1 channels and ataxia. *Sci Rep* 2017;7:1–13. <https://doi.org/10.1038/s41598-017-03041-z>.

- [18] Payandeh J, Scheuer T, Zheng N, Catterall WA. The crystal structure of a voltage-gated sodium channel. *Nature* 2011;475:353–9. <https://doi.org/10.1038/nature10238>.
- [19] Shattock MJ, Ottolia M, Bers DM, Blaustein MP, Boguslavskiy A, Bossuyt J, et al. Na<sup>+</sup>/Ca<sup>2+</sup> exchange and Na<sup>+</sup>/K<sup>+</sup>-ATPase in the heart. *J Physiol* 2015;593:1361–82. <https://doi.org/10.1113/jphysiol.2014.282319>.
- [20] Kadir LA, Stacey M, Barrett-Jolley R. Emerging roles of the membrane potential: Action beyond the action potential. *Front Physiol* 2018;9:1–10. <https://doi.org/10.3389/fphys.2018.01661>.
- [21] Rossier MF. T-type calcium channel: A privileged gate for calcium entry and control of adrenal steroidogenesis. *Front Endocrinol (Lausanne)* 2016;7:1–17. <https://doi.org/10.3389/fendo.2016.00043>.
- [22] Bronner F. Extracellular and intracellular regulation of calcium homeostasis. *ScientificWorldJournal* 2001;1:919–25. <https://doi.org/10.1100/tsw.2001.489>.
- [23] Endo M. Calcium-induced release of calcium from the sarcoplasmic reticulum. *Adv Exp Med Biol* 2007;592:275–85. [https://doi.org/10.1007/978-4-431-38453-3\\_23](https://doi.org/10.1007/978-4-431-38453-3_23).
- [24] Yan Z, Bai XC, Yan C, Wu J, Li Z, Xie T, et al. Structure of the rabbit ryanodine receptor RyR1 at near-atomic resolution. *Nature* 2015;517:50–5. <https://doi.org/10.1038/nature14063>.
- [25] Zhihao L, Jingyu N, Lan L, Michael S, Rui G, Xiyun B, et al. SERCA2a: a key protein in the Ca<sup>2+</sup> cycle of the heart failure. *Heart Fail Rev* 2020;25:523–35. <https://doi.org/10.1007/s10741-019-09873-3>.
- [26] Periasamy M, Kalyanasundaram A. SERCA pump isoforms: Their role in calcium transport and disease. *Muscle and Nerve* 2007;35:430–42. <https://doi.org/10.1002/mus.20745>.
- [27] Sitsel A, De Raeymaecker J, Drachmann ND, Derua R, Smaardijk S, Andersen JL, et al. Structures of the heart specific SERCA 2a Ca<sup>2+</sup> - ATPase. *EMBO J* 2019;38:1–17. <https://doi.org/10.15252/embj.2018100020>.
- [28] Inoue M, Sakuta N, Watanabe S, Zhang Y, Yoshikaie K, Tanaka Y, et al. Structural Basis of Sarco/Endoplasmic Reticulum Ca<sup>2+</sup> -ATPase 2b Regulation via Transmembrane Helix Interplay. *Cell Rep* 2019;27:1221–1230.e3. <https://doi.org/10.1016/j.celrep.2019.03.106>.
- [29] Haghghi K, Gregory KN, Kranias EG. Sarcoplasmic reticulum Ca-ATPase–phospholamban interactions and dilated cardiomyopathy. *Biochem Biophys Res Commun* 2004;322:1214–22. <https://doi.org/10.1016/j.bbrc.2004.07.164>.
- [30] MacLennan DH, Kranias EG. Phospholamban: A crucial regulator of cardiac contractility. *Nat Rev Mol Cell Biol* 2003;4:566–77. <https://doi.org/10.1038/nrm1151>.
- [31] Akin BL, Hurley TD, Chen Z, Jones LR. The structural basis for phospholamban inhibition of the calcium pump in sarcoplasmic reticulum. *J Biol Chem* 2013;288:30181–91. <https://doi.org/10.1074/jbc.M113.501585>.
- [32] Kranias EG, Hajjar RJ. Modulation of cardiac contractility by the phospholamban/SERCA2a regulome. *Circ Res* 2012;110:1646–60. <https://doi.org/10.1161/CIRCRESAHA.111.259754>.
- [33] Santana LF, Cheng EP, Lederer WJ. How does the shape of the cardiac action potential control calcium signaling and contraction in the heart? *J Mol Cell Cardiol* 2010;49:901–3.

<https://doi.org/10.1016/j.yjmcc.2010.09.005>.

- [34] Morad M, Tung L. Ionic events responsible for the cardiac resting and action potential. *Am J Cardiol* 1982;49:584–94. [https://doi.org/10.1016/S0002-9149\(82\)80016-7](https://doi.org/10.1016/S0002-9149(82)80016-7).
- [35] Grunnet M, Neurosearch AS. *Acta Physiologica*. *Acta Physiol* 2010;198.
- [36] Rudy Y. Molecular basis of cardiac action potential repolarization. *Ann N Y Acad Sci* 2008;1123:113–8. <https://doi.org/10.1196/annals.1420.013>.
- [37] Braunwald E. Cardiovascular Medicine at the Turn of the Millennium: Triumphs, Concerns, and Opportunities. *N Engl J Med* 1997;337:1360–9. <https://doi.org/10.1056/NEJM199711063371906>.
- [38] Breslow JL. Cardiovascular disease burden increases, NIH funding decreases. *Nat Med* 1997;3:600–1. <https://doi.org/10.1038/nm0697-600>.
- [39] Kearney PM, Whelton M, Reynolds K, Muntner P, Whelton PK, He J. Global burden of hypertension: analysis of worldwide data. *Lancet* 2005;365:217–23. [https://doi.org/10.1016/S0140-6736\(05\)17741-1](https://doi.org/10.1016/S0140-6736(05)17741-1).
- [40] PICKERING GW. THE NATUTAL HISTORY OF HYPERTENSION. *Br Med Bull* 1952;8:305–9. <https://doi.org/10.1093/oxfordjournals.bmb.a074193>.
- [41] Lackland DT, Roccella EJ, Deutsch AF, Fornage M, George MG, Howard G, et al. Factors influencing the decline in stroke mortality a statement from the american heart association/american stroke association. *Stroke* 2014;45:315–53. <https://doi.org/10.1161/01.str.0000437068.30550.cf>.
- [42] Lackland DT, Weber MA. Global burden of cardiovascular disease and stroke: Hypertension at the core. *Can J Cardiol* 2015;31:569–71. <https://doi.org/10.1016/j.cjca.2015.01.009>.
- [43] “What Is Atherosclerosis? - NHLBI, NIH” n.d. <https://www.nhlbi.nih.gov/health-topics/atherosclerosis>.
- [44] Ross R. The Pathogenesis of Atherosclerosis — An Update. *N Engl J Med* 1986;314:488–500. <https://doi.org/10.1056/NEJM198602203140806>.
- [45] Ross R. Atherosclerosis — An Inflammatory Disease. *N Engl J Med* 1999;340:115–26. <https://doi.org/10.1056/NEJM199901143400207>.
- [46] Davis NE. Atherosclerosis--an inflammatory process. *J Insur Med* 2005;37:72–5.
- [47] Global, regional, and national age–sex specific all-cause and cause-specific mortality for 240 causes of death, 1990–2013: a systematic analysis for the Global Burden of Disease Study 2013. *Lancet* 2015;385:117–71. [https://doi.org/10.1016/S0140-6736\(14\)61682-2](https://doi.org/10.1016/S0140-6736(14)61682-2).
- [48] Libby P, Theroux P. Pathophysiology of coronary artery disease. *Circulation* 2005;111:3481–8. <https://doi.org/10.1161/CIRCULATIONAHA.105.537878>.
- [49] McMahon CJ, Ganame J. Hypertrophic Cardiomyopathy. *Echocardiogr Pediatr Congenit Hear Dis From Fetus to Adult* 2009;287:581–96. <https://doi.org/10.1002/9781444306309.ch34>.
- [50] Abboud J, Murad Y, Chen-Scarabelli C, Saravolatz L, Scarabelli TM. Peripartum cardiomyopathy: A comprehensive review. *Int J Cardiol* 2007;118:295–303. <https://doi.org/10.1016/j.ijcard.2006.08.005>.

- [51] MARCUS FI, FONTAINE G. Arrhythmogenic Right Ventricular Dysplasia/Cardiomyopathy: A Review. *Pacing Clin Electrophysiol* 1995;18:1298–314. <https://doi.org/10.1111/j.1540-8159.1995.tb06971.x>.
- [52] Luk A, Ahn E, Soor GS, Butany J. Dilated cardiomyopathy: A review. *J Clin Pathol* 2009;62:219–25. <https://doi.org/10.1136/jcp.2008.060731>.
- [53] Sharpe N, Doughty R. Epidemiology of heart failure and ventricular dysfunction. *Lancet* 1998;352:3–7. [https://doi.org/10.1016/s0140-6736\(98\)90012-5](https://doi.org/10.1016/s0140-6736(98)90012-5).
- [54] Metra M, Teerlink JR. Heart failure. *Lancet* 2017;390:1981–95. [https://doi.org/10.1016/S0140-6736\(17\)31071-1](https://doi.org/10.1016/S0140-6736(17)31071-1).
- [55] COLUCCI, WS. Pathophysiology of heart failure. *Hear Dis A Textb Cardiovasc Med* 2001.
- [56] Yancy CW, Jessup M, Bozkurt B, Butler J, Casey DE, Drazner MH, et al. 2013 ACCF/AHA guideline for the management of heart failure: Executive summary: A report of the American college of cardiology foundation/American Heart Association task force on practice guidelines. *Circulation* 2013;128:1810–52. <https://doi.org/10.1161/CIR.0b013e31829e8807>.
- [57] Mebazaa A, Birhan Yilmaz M, Levy P, Ponikowski P, Peacock WF, Laribi S, et al. 26 CURRENT OPINION Recommendations on pre-hospital and early hospital management of acute heart failure: a consensus paper from the Heart Failure-short version. *Eur Heart J* 2015;36:1958–66. <https://doi.org/10.1002/ejhf.289/full>.
- [58] Ponikowski P, Voors AA, Anker SD, Bueno H, Cleland JGF, Coats AJS, et al. 2016 ESC Guidelines for the diagnosis and treatment of acute and chronic heart failure. *Eur Heart J* 2016;37:2129-2200m. <https://doi.org/10.1093/eurheartj/ehw128>.
- [59] McMurray JJV, Stewart S. The burden of heart failure. *Eur Hear Journal, Suppl* 2004;6:50–8. [https://doi.org/10.1016/S1520-765X\(04\)80002-6](https://doi.org/10.1016/S1520-765X(04)80002-6).
- [60] Long L, Mordi IR, Bridges C, Sagar VA, Davies EJ, Coats AJ, et al. Exercise-based cardiac rehabilitation for adults with heart failure. *Cochrane Database Syst Rev* 2019;1. <https://doi.org/10.1002/14651858.CD003331.pub5>.
- [61] Yancy CW, Jessup M, Bozkurt B, Butler J, Casey DE, Colvin MM, et al. 2016 ACC/AHA/HFSA focused update on new pharmacological therapy for heart failure: An update of the 2013 ACCF/AHA guideline for the management of heart failure: A report of the American College of Cardiology/American Heart Association Task Force on Clinic. *Circulation* 2016;134:e282–93. <https://doi.org/10.1161/CIR.0000000000000435>.
- [62] Bonow RO, Louis S, Mann DL, Libby P. Braunwald’s Heart Disease 9th edition. vol. I. 2011.
- [63] Wassmuth R. Heart failure in patients with normal coronary anatomy: diagnostic algorithm and disease pattern of various etiologies as defined by cardiac MRI. *Cardiovasc Diagn Ther* 2012;2:128–12837. <https://doi.org/10.3978/j.issn.2223-3652.2012.04.04>.
- [64] Casu G, Merella P. Diuretic therapy in heart failure - Current approaches. *Eur Cardiol Rev* 2015;10:42–7. <https://doi.org/10.15420/ecr.2015.10.01.42>.
- [65] Cohn JAYN, Pw A, Dc W, Jr B, Jo P. KEY REFERENCES Vasodilators in Congestive Heart Failure 1979:1979–81.

- [66] Vallotton MB. The renin-angiotensin system 1987;81.
- [67] Dzau VJ, Colucci WS, Hollenberg NK, Williams GH. Relation of the renin-angiotensin-aldosterone system to clinical state in congestive heart failure. *Circulation* 1981;63:645–51. <https://doi.org/10.1161/01.CIR.63.3.645>.
- [68] Ouwerkerk W, Teng THK, Tromp J, Tay WT, Cleland JG, van Veldhuisen DJ, et al. Effects of combined renin–angiotensin–aldosterone system inhibitor and beta-blocker treatment on outcomes in heart failure with reduced ejection fraction: insights from BIOSTAT-CHF and ASIAN-HF registries. *Eur J Heart Fail* 2020;472–82. <https://doi.org/10.1002/ejhf.1869>.
- [69] Dickstein K, Gottlieb S, Fleck E, Kostis J, Levine B, DeKock M, et al. Hemodynamic and neurohumoral effects of the angiotensin II antagonist losartan in patients with heart failure. *J Hypertens Suppl* 1994;12:1602–9.
- [70] Rocca HPB La, Vaddadi G, Esler MD. Recent insight into therapy of congestive heart failure: Focus on ACE inhibition and angiotensin-II antagonism. *J Am Coll Cardiol* 1999;33:1163–73. [https://doi.org/10.1016/S0735-1097\(99\)00025-X](https://doi.org/10.1016/S0735-1097(99)00025-X).
- [71] Thottan MK, Chuanyi J. Patent Application Publication ( 10 ) Pub . No . : US 2004 / 0231417 A1 2004;1:12–7.
- [72] Abrams J. The Role of Nitrates in Coronary Heart Disease. *Arch Intern Med* 1995;155:357. <https://doi.org/10.1001/archinte.1995.00430040023003>.
- [73] Pautz A, Rauschkolb P, Schmidt N, Art J, Oelze M, Wenzel P, et al. Effects of nitroglycerin or pentaerythryl tetranitrate treatment on the gene expression in rat hearts: Evidence for cardiotoxic and cardioprotective effects. *Physiol Genomics* 2009;38:176–85. <https://doi.org/10.1152/physiolgenomics.00035.2009>.
- [74] Zobel LR, Finkelstein SM, Carlyle PF, Cohn JN. Pressure pulse contour analysis in determining the effect of vasodilator drugs on vascular hemodynamic impedance characteristics in dogs. *Am Heart J* 1980;100:81–8. [https://doi.org/10.1016/0002-8703\(80\)90282-3](https://doi.org/10.1016/0002-8703(80)90282-3).
- [75] Francis GS. Calcium channel blockers and congestive heart failure. *Circulation* 1991;83:336–8. <https://doi.org/10.1161/01.CIR.83.1.336>.
- [76] Elkayam U, Weber L, McKay CR, Rahimtoola SH. Differences in hemodynamic response to vasodilation due to calcium channel antagonism with nifedipine and direct-acting agonism with hydralazine in chronic refractory congestive heart failure. *Am J Cardiol* 1984;54:126–31. [https://doi.org/10.1016/0002-9149\(84\)90316-3](https://doi.org/10.1016/0002-9149(84)90316-3).
- [77] Brum PC, Rolim NPL, Bacurau AVN, Medeiros A. Neurohumoral activation in heart failure: The role of adrenergic receptors. *An Acad Bras Cienc* 2006;78:485–503. <https://doi.org/10.1590/s0001-37652006000300009>.
- [78] Stiles GL, Caron MG, Lefkowitz RJ.  $\beta$ -Adrenergic receptors: Biochemical mechanisms of physiological regulation. *Physiol Rev* 1984;64:661–743. <https://doi.org/10.1152/physrev.1984.64.2.661>.
- [79] Ahlquist RP. A STUDY OF THE ADRENOTROPIC RECEPTORS. *Am J Physiol Content* 1948;153:586–600. <https://doi.org/10.1152/ajplegacy.1948.153.3.586>.
- [80] Parker JD, Landzberg JS, Bittl JA, Mirsky I, Colucci WS. Effects of  $\beta$ -adrenergic stimulation with

- dobutamine on isovolumic relaxation in the normal and failing human left ventricle. *Circulation* 1991;84:1040–8. <https://doi.org/10.1161/01.CIR.84.3.1040>.
- [81] Velez-Roa S, Renard M, Degaute JP, Van De Borne P. Peripheral Sympathetic Control during Dobutamine Infusion: Effects of Aging and Heart Failure. *J Am Coll Cardiol* 2003;42:1605–10. <https://doi.org/10.1016/j.jacc.2003.07.004>.
- [82] Bristow MR. Treatment of chronic heart failure with  $\beta$ -adrenergic receptor antagonists: A convergence of receptor pharmacology and clinical cardiology. *Circ Res* 2011;109:1176–94. <https://doi.org/10.1161/CIRCRESAHA.111.245092>.
- [83] Ho D, Yan L, Iwatsubo K, Vatner DE, Vatner SF. Modulation of  $\beta$ -adrenergic receptor signaling in heart failure and longevity: targeting adenylyl cyclase type 5. *Heart Fail Rev* 2010;15:495–512. <https://doi.org/10.1007/s10741-010-9183-5>.
- [84] Fröhlich H, Torres L, Täger T, Schellberg D, Corletto A, Kazmi S, et al. Bisoprolol compared with carvedilol and metoprolol succinate in the treatment of patients with chronic heart failure. *Clin Res Cardiol* 2017;106:711–21. <https://doi.org/10.1007/s00392-017-1115-0>.
- [85] Hamaad A, Lip GYH, Nicholls D, MacFadyen RJ. Comparative dose titration responses to the introduction of bisoprolol or carvedilol in stable chronic systolic heart failure. *Cardiovasc Drugs Ther* 2007;21:437–44. <https://doi.org/10.1007/s10557-007-6055-x>.
- [86] Graffagnino JP, Avant LC, Calkins BC, Swetz KM. Home Therapies in Advanced Heart Failure: Inotropes and Diuretics. *Curr Heart Fail Rep* 2020;17:314–23. <https://doi.org/10.1007/s11897-020-00482-y>.
- [87] Yancy CW, Jessup M, Bozkurt B, Butler J, Casey DE, Drazner MH, et al. 2013 ACCF/AHA guideline for the management of heart failure: A report of the American college of cardiology foundation/american heart association task force on practice guidelines. *J Am Coll Cardiol* 2013;62. <https://doi.org/10.1016/j.jacc.2013.05.019>.
- [88] Floh AA, Jean-St.-Michel E, Schwartz SM. The Use of Inotropic Agents in Acute Decompensated Heart Failure. Elsevier Inc.; 2018. <https://doi.org/10.1016/B978-0-12-802393-8.00039-9>.
- [89] Goldhaber JL, Hamilton MA. Role of Inotropic Agents in the Treatment of Heart Failure. *Circulation* 2010;121:1655–60. <https://doi.org/10.1161/CIRCULATIONAHA.109.899294>.
- [90] Bardal SK, Waechter JE, Martin DS. Chapter 11 - Cardiology. In: Bardal SK, Waechter JE, Martin DSBT-AP, editors., Philadelphia: Content Repository Only!; 2011, p. 99–126. <https://doi.org/https://doi.org/10.1016/B978-1-4377-0310-8.00011-7>.
- [91] Haikala Heimo; Lindén I-B. Mechanisms of Action of Calcium-Sensitizing Drugs. *J Cardiovasc Pharmacol* 1995:10–9.
- [92] Perrone S V., Kaplinsky EJ. Calcium sensitizer agents: A new class of inotropic agents in the treatment of decompensated heart failure. *Int J Cardiol* 2005;103:248–55. <https://doi.org/10.1016/j.ijcard.2004.12.012>.
- [93] Yatime L, Laursen M, Morth JP, Esmann M, Nissen P, Fedosova NU. Structural insights into the high affinity binding of cardiotonic steroids to the Na<sup>+</sup>,K<sup>+</sup>-ATPase. *J Struct Biol* 2011;174:296–306. <https://doi.org/10.1016/j.jsb.2010.12.004>.
- [94] Schönfeld W, Weiland J, Lindig C, Masnyk M, Kabat MM, Kurek A, et al. The lead structure in

- cardiac glycosides is 5  $\beta$ ,14  $\beta$ -androstane-3  $\beta$ ,14-diol. *Naunyn Schmiedebergs Arch Pharmacol* 1985;329:414–26. <https://doi.org/10.1007/BF00496377>.
- [95] Canessa M, Jaimovich E, de la Fuente M. Harmaline: A competitive inhibitor of Na Ion in the (Na<sup>++</sup>K<sup>+</sup>)-ATPase system. *J Membr Biol* 1973;13:263–82. <https://doi.org/10.1007/BF01868232>.
- [96] Cerri A, Gobbini M. Simplified digitalis-like compounds acting on Na<sup>+</sup>, K<sup>+</sup>-ATPase. *J Enzyme Inhib Med Chem* 2003;18:289–95. <https://doi.org/10.1080/1475636031000138750>.
- [97] Digoxin Drug Usage Statistics, United States, 2007 - 2017 n.d. <https://clincalc.com/DrugStats/Drugs/Digoxin>.
- [98] Hollman A. Digoxin comes from Digitalis lanata. *BMJ* 1996;312:912–912. <https://doi.org/10.1136/bmj.312.7035.912>.
- [99] Hollman A. Digoxin comes from Digitalis lanata. *BMJ* 1996;312:912–912. <https://doi.org/10.1136/bmj.312.7035.912>.
- [100] Cornelius F, Kanai R, Toyoshima C. A structural view on the functional importance of the sugar moiety and steroid hydroxyls of cardiotonic steroids in binding to Na,K-ATPase. *J Biol Chem* 2013;288:6602–16. <https://doi.org/10.1074/jbc.M112.442137>.
- [101] Laursen M, Gregersen JL, Yatime L, Nissen P, Fedosova NU. Structures and characterization of digoxin- And bufalin-bound Na<sup>+</sup>,K<sup>+</sup>-ATPase compared with the ouabain-bound complex. *Proc Natl Acad Sci U S A* 2015;112:1755–60. <https://doi.org/10.1073/pnas.1422997112>.
- [102] Dobler S, Dalla S, Wagschal V, Agrawal AA. Community-wide convergent evolution in insect adaptation to toxic cardenolides by substitutions in the Na,K-ATPase. *Proc Natl Acad Sci U S A* 2012;109:13040–5. <https://doi.org/10.1073/pnas.1202111109>.
- [103] Zhang H, Sridhar Reddy M, Phoenix S, Deslongchamps P. Total Synthesis of Ouabagenin and Ouabain. *Angew Chemie* 2008;120:1292–5. <https://doi.org/10.1002/ange.200704959>.
- [104] Laursen M, Yatime L, Nissen P, Fedosova NU. Crystal structure of the high-affinity Na<sup>+</sup>,K<sup>+</sup>-ATPase- ouabain complex with Mg<sup>2+</sup> bound in the cation binding site. *Proc Natl Acad Sci U S A* 2013;110:10958–63. <https://doi.org/10.1073/pnas.1222308110>.
- [105] Hamlyn JM, Blaustein MP, Bova S, DuCharme DW, Harris DW, Mandel F, et al. Identification and characterization of a ouabain-like compound from human plasma. *Proc Natl Acad Sci* 1991;88:6259–63. <https://doi.org/10.1073/pnas.88.14.6259>.
- [106] Ferrandi M, Manunta P, Balzan S, Hamlyn JM, Bianchi G, Ferrari P. Ouabain-like Factor Quantification in Mammalian Tissues and Plasma. *Hypertension* 1997;30:886–96. <https://doi.org/10.1161/01.HYP.30.4.886>.
- [107] Balzan S, Neglia D, Ghione S, D'Urso G, Baldacchino MC, Montali U, et al. Increased circulating levels of ouabain-like factor in patients with asymptomatic left ventricular dysfunction. *Eur J Heart Fail* 2001;3:165–71. [https://doi.org/10.1016/S1388-9842\(00\)00132-X](https://doi.org/10.1016/S1388-9842(00)00132-X).
- [108] Garg R, Gorlin R, Smith T, Yusuf S. The effect of digoxin on mortality and morbidity in patients with heart failure. *N Engl J Med* 1997;336:525–33. <https://doi.org/10.1056/NEJM199702203360801>.
- [109] THOMAS R, GRAY P, ANDREWS J. Digitalis: Its Mode of Action, Receptor, and Structure–Activity

Relationships, 1990, p. 311–562. <https://doi.org/10.1016/B978-0-12-013319-2.50009-7>.

- [110] Gobbin M, Almirante N, Cerri A, Padoani G, Melloni P. Synthesis and Biological Evaluation of 14-Methoxy Digitalis Derivatives. *Molecules* 1998;3:20–5. <https://doi.org/10.3390/30100020>.
- [111] Cerri A. Digitalis-Like Compounds: The Discovery of the O-Aminoalkyloxime Group as a Very Powerful Substitute for the Unsaturated  $\gamma$ -Butyrolactone Moiety. *Front Med Chem - (Volume 4)* 2012:214–36. <https://doi.org/10.2174/978160805207310904010214>.
- [112] Gobbin M, Marazzi G, Padoani G, Quadri L, Valentino L, Zappavigna M., et al. Synthesis and biological evaluation of 2-Hydroxy derivatives of digitoxigenin and 3-Epidigitoxigenin 1A preliminary account of this work has been presented at the First International Electronic Conference on Synthetic Organic Chemistry (ECSOC-1), A0012, 1. *Bioorg Med Chem* 1998;6:1889–94. [https://doi.org/10.1016/S0968-0896\(98\)00119-9](https://doi.org/10.1016/S0968-0896(98)00119-9).
- [113] Gobbin M, Armaroli S, Banfi L, Benicchio A, Carzana G, Ferrari P, et al. Novel analogues of Istaroxime, a potent inhibitor of Na<sup>+</sup>,K<sup>+</sup>-ATPase: Synthesis, structure–activity relationship and 3D-quantitative structure–activity relationship of derivatives at position 6 on the androstane scaffold. *Bioorg Med Chem* 2010;18:4275–99. <https://doi.org/10.1016/j.bmc.2010.04.095>.
- [114] Ferrari P, Ferrandi M, Valentini G, Bianchi G. Rostafuroxin: an ouabain antagonist that corrects renal and vascular Na<sup>+</sup>-K<sup>+</sup>-ATPase alterations in ouabain and adducin-dependent hypertension. *Am J Physiol Integr Comp Physiol* 2006;290:R529–35. <https://doi.org/10.1152/ajpregu.00518.2005>.
- [115] Ferrari P. Rostafuroxin: An ouabain-inhibitor counteracting specific forms of hypertension. *Biochim Biophys Acta - Mol Basis Dis* 2010;1802:1254–8. <https://doi.org/10.1016/j.bbadis.2010.01.009>.
- [116] Byrne MJ, Power JM, Prevolos A, Mariani JA, Hajjar RJ, Kaye DM. Recirculating cardiac delivery of AAV2/1SERCA2a improves myocardial function in an experimental model of heart failure in large animals. *Gene Ther* 2008;15:1550–7. <https://doi.org/10.1038/gt.2008.120>.
- [117] Hoshijima M, Ikeda Y, Iwanaga Y, Minamisawa S, Date MO, Gu Y, et al. Chronic suppression of heart-failure progression by a pseudophosphorylated mutant of phospholamban via in vivo cardiac rAAV gene delivery. *Nat Med* 2002;8:864–71. <https://doi.org/10.1038/nm739>.
- [118] Iwanaga Y, Hoshijima M, Gu Y, Iwatate M, Dieterle T, Ikeda Y, et al. Chronic phospholamban inhibition prevents progressive cardiac dysfunction and pathological remodeling after infarction in rats. *J Clin Invest* 2004;113:727–36. <https://doi.org/10.1172/JCI18716>.
- [119] Lohse MJ, Engelhardt S, Eschenhagen T. What Is the Role of  $\beta$ -Adrenergic Signaling in Heart Failure? *Circ Res* 2003;93:896–906. <https://doi.org/10.1161/01.RES.0000102042.83024.CA>.
- [120] Rocchetti M, Besana A, Mostacciuolo G, Micheletti R, Ferrari P, Sarkozi S, et al. Modulation of sarcoplasmic reticulum function by Na<sup>+</sup>/K<sup>+</sup> pump inhibitors with different toxicity: Digoxin and PST2744 [(E,Z)-3-((2-aminoethoxy)imino)androstane-6,17-dione hydrochloride]. *J Pharmacol Exp Ther* 2005;313:207–15. <https://doi.org/10.1124/jpet.104.077933>.
- [121] Kaneko M, Yamamoto H, Sakai H, Kamada Y, Tanaka T, Fujiwara S, et al. A pyridone derivative activates SERCA2a by attenuating the inhibitory effect of phospholamban. *Eur J Pharmacol* 2017;814:1–8. <https://doi.org/10.1016/j.ejphar.2017.07.035>.

- [122] Dalma G. Chapter 36 The Erythrophleum Alkaloids, 1954, p. 265–73. [https://doi.org/10.1016/S1876-0813\(08\)60163-3](https://doi.org/10.1016/S1876-0813(08)60163-3).
- [123] Gensler WJ, Sherman GM. Location of Ketone and Hydroxyl Functions of Cassaic Acid. *J Am Chem Soc* 1959;81:5217–22. <https://doi.org/10.1021/ja01528a049>.
- [124] Ravindar K, Caron PY, Deslongchamps P. Total synthesis of (+)-cassaine utilizing an anionic polycyclization strategy. *Org Lett* 2013;15:6270–3. <https://doi.org/10.1021/ol4030937>.
- [125] De Munari S, Cerri A, Gobbin M, Almirante N, Banfi L, Carzana G, et al. Structure-based design and synthesis of novel potent Na<sup>+</sup>,K<sup>+</sup>-ATPase inhibitors derived from a 5 $\alpha$ ,14 $\alpha$ -androstane scaffold as positive inotropic compounds. *J Med Chem* 2003;46:3644–54. <https://doi.org/10.1021/jm030830y>.
- [126] Ferrandi M, Barassi P, Tadini-Buoninsegni F, Bartolommei G, Molinari I, Tripodi MG, et al. Istaroxime stimulates SERCA2a and accelerates calcium cycling in heart failure by relieving phospholamban inhibition. *Br J Pharmacol* 2013;169:1849–61. <https://doi.org/10.1111/bph.12278>.
- [127] Zaza A, Rocchetti M. Calcium Store Stability as an Antiarrhythmic Endpoint. *Curr Pharm Des* 2014;21:1053–61. <https://doi.org/10.2174/1381612820666141029100650>.
- [128] Gheorghide M, Blair JEA, Filippatos GS, Macarie C, Ruzylo W, Korewicki J, et al. Hemodynamic, Echocardiographic, and Neurohormonal Effects of Istaroxime, a Novel Intravenous Inotropic and Lusitropic Agent. A Randomized Controlled Trial in Patients Hospitalized With Heart Failure. *J Am Coll Cardiol* 2008;51:2276–85. <https://doi.org/10.1016/j.jacc.2008.03.015>.
- [129] Alemanni M, Rocchetti M, Re D, Zaza A. Role and mechanism of subcellular Ca<sup>2+</sup> distribution in the action of two inotropic agents with different toxicity. *J Mol Cell Cardiol* 2011;50:910–8. <https://doi.org/10.1016/j.yjmcc.2011.02.008>.
- [130] Derivatives I, Plant D, Medicinals H, Vera P. Chapter 16 Hydrazines, Hydroxylamines, Carbamates, Acetamides, Thioacetamides and Thioureas, 1979, p. 307–30. [https://doi.org/10.1016/S0166-1116\(08\)71327-X](https://doi.org/10.1016/S0166-1116(08)71327-X).
- [131] Carubelli V, Zhang Y, Metra M, Lombardi C, Felker GM, Filippatos G, et al. Treatment with 24 hour istaroxime infusion in patients hospitalised for acute heart failure: a randomised, placebo-controlled trial. *Eur J Heart Fail* 2020;1–10. <https://doi.org/10.1002/ejhf.1743>.
- [132] Khanna I. Drug discovery in pharmaceutical industry: Productivity challenges and trends. *Drug Discov Today* 2012;17:1088–102. <https://doi.org/10.1016/j.drudis.2012.05.007>.
- [133] No Title n.d. <https://www.statista.com/statistics/309466/global-r-and-d-expenditure-for-pharmaceuticals/>.
- [134] Van Norman GA. Drugs, Devices, and the FDA: Part 1: An Overview of Approval Processes for Drugs. *JACC Basic to Transl Sci* 2016;1:170–9. <https://doi.org/10.1016/j.jacbts.2016.03.002>.
- [135] Van Norman GA. Phase II Trials in Drug Development and Adaptive Trial Design. *JACC Basic to Transl Sci* 2019;4:428–37. <https://doi.org/10.1016/j.jacbts.2019.02.005>.
- [136] Fenton OS, Olafson KN, Pillai PS, Mitchell MJ, Langer R. Advances in Biomaterials for Drug Delivery. *Adv Mater* 2018;30:1–29. <https://doi.org/10.1002/adma.201705328>.

- [137] Pant B, Park M, Park SJ. Drug delivery applications of core-sheath nanofibers prepared by coaxial electrospinning: A review. *Pharmaceutics* 2019;11. <https://doi.org/10.3390/pharmaceutics11070305>.
- [138] Sykes EA, Chen J, Zheng G, Chan WCW. Investigating the impact of nanoparticle size on active and passive tumor targeting efficiency. *ACS Nano* 2014;8:5696–706. <https://doi.org/10.1021/nn500299p>.
- [139] Dogra P, Butner JD, Chuang Y li, Caserta S, Goel S, Brinker CJ, et al. Mathematical modeling in cancer nanomedicine: a review. *Biomed Microdevices* 2019;21. <https://doi.org/10.1007/s10544-019-0380-2>.
- [140] Wang C, Wang J, Zeng L, Qiao Z, Liu X, Liu H, et al. Fabrication of electrospun polymer nanofibers with diverse morphologies. *Molecules* 2019;24. <https://doi.org/10.3390/molecules24050834>.
- [141] Feng X, Li J, Zhang X, Liu T, Ding J, Chen X. Electrospun polymer micro/nanofibers as pharmaceutical repositories for healthcare. *J Control Release* 2019;302:19–41. <https://doi.org/10.1016/j.jconrel.2019.03.020>.
- [142] Narayanaswamy R, Torchilin VP. Hydrogels and their applications in targeted drug delivery. *Molecules* 2019;24. <https://doi.org/10.3390/molecules24030603>.
- [143] Maleki Dizaj S, Sharifi S, Jahangiri A. Electrospun nanofibers as versatile platform in antimicrobial delivery: current state and perspectives. *Pharm Dev Technol* 2019;24:1187–99. <https://doi.org/10.1080/10837450.2019.1656238>.
- [144] Kurtz IS, Schiffman JD. Current and emerging approaches to engineer antibacterial and antifouling electrospun nanofibers. *Materials (Basel)* 2018;11. <https://doi.org/10.3390/ma11071059>.
- [145] Poláková L, Širc J, Hobzová R, Cocârță AI, Heřmánková E. Electrospun nanofibers for local anticancer therapy: Review of in vivo activity. *Int J Pharm* 2019;558:268–83. <https://doi.org/10.1016/j.ijpharm.2018.12.059>.
- [146] Jain R, Shetty S, Yadav KS. Unfolding the electrospinning potential of biopolymers for preparation of nanofibers. *J Drug Deliv Sci Technol* 2020;57:101604. <https://doi.org/10.1016/j.jddst.2020.101604>.
- [147] Islam MS, Ang BC, Andriyana A, Afifi AM. A review on fabrication of nanofibers via electrospinning and their applications. *SN Appl Sci* 2019;1:1–16. <https://doi.org/10.1007/s42452-019-1288-4>.
- [148] Barhoum A. *Handbook of Nanofibers*. 2019. <https://doi.org/10.1007/978-3-319-53655-2>.
- [149] Contreras-Cáceres R, Cabeza L, Perazzoli G, Díaz A, López-Romero JM, Melguizo C, et al. Electrospun nanofibers: Recent applications in drug delivery and cancer therapy. *Nanomaterials* 2019;9:1–24. <https://doi.org/10.3390/nano9040656>.
- [150] Calori IR, Braga G, de Jesus P da CC, Bi H, Tedesco AC. Polymer scaffolds as drug delivery systems. *Eur Polym J* 2020;129:109621. <https://doi.org/10.1016/j.eurpolymj.2020.109621>.
- [151] Zelkó R, Lamprou DA, Sebe I. Recent development of electrospinning for drug delivery. *Pharmaceutics* 2020;12:1–5. <https://doi.org/10.3390/pharmaceutics12010005>.

- [152] Sandri G, Rossi S, Bonferoni MC, Caramella C, Ferrari F. Electrospinning Technologies in Wound Dressing Applications. *Ther Dressings Wound Heal Appl* 2020;315–36. <https://doi.org/10.1002/9781119433316.ch14>.
- [153] Dong Y, Zheng Y, Zhang K, Yao Y, Wang L, Li X, et al. Electrospun Nanofibrous Materials for Wound Healing. *Adv Fiber Mater* 2020. <https://doi.org/10.1007/s42765-020-00034-y>.
- [154] Tan GZ, Zhou Y. Electrospinning of biomimetic fibrous scaffolds for tissue engineering: a review. *Int J Polym Mater Polym Biomater* 2019;0:1–14. <https://doi.org/10.1080/00914037.2019.1636248>.
- [155] Chahal S, Kumar A, Hussian FSJ. Development of biomimetic electrospun polymeric biomaterials for bone tissue engineering. A review. *J Biomater Sci Polym Ed* 2019;30:1308–55. <https://doi.org/10.1080/09205063.2019.1630699>.
- [156] Mirjalili M, Zohoori S. Review for application of electrospinning and electrospun nanofibers technology in textile industry. *J Nanostructure Chem* 2016;6:207–13. <https://doi.org/10.1007/s40097-016-0189-y>.
- [157] Han WH, Wang YZ, Su JM, Xin X, Guo Y Da, Long YZ, et al. Fabrication of nanofibrous sensors by electrospinning. *Sci China Technol Sci* 2019;62:886–94. <https://doi.org/10.1007/s11431-018-9405-5>.
- [158] Miletić A, Pavlić B, Ristić I, Zeković Z, Pilić B. Encapsulation of fatty oils into electrospun nanofibers for cosmetic products with antioxidant activity. *Appl Sci* 2019;9. <https://doi.org/10.3390/app9152955>.
- [159] Zhang C, Li Y, Wang P, Zhang H. Electrospinning of nanofibers: Potentials and perspectives for active food packaging. *Compr Rev Food Sci Food Saf* 2020;19:479–502. <https://doi.org/10.1111/1541-4337.12536>.
- [160] Ding Y, Li W, Zhang F, Liu Z, Zanjanzadeh Ezazi N, Liu D, et al. Electrospun Fibrous Architectures for Drug Delivery, Tissue Engineering and Cancer Therapy. *Adv Funct Mater* 2019;29:1–35. <https://doi.org/10.1002/adfm.201802852>.
- [161] Tijing LD, Yao M, Ren J, Park C-H, Kim CS, Shon HK. Nanofibers for Water and Wastewater Treatment: Recent Advances and Developments. 2019. [https://doi.org/10.1007/978-981-13-3259-3\\_20](https://doi.org/10.1007/978-981-13-3259-3_20).
- [162] Zong X, Kim K, Fang D, Ran S, Hsiao BS, Chu B. Structure and process relationship of electrospun bioabsorbable nanofiber membranes. *Polymer (Guildf)* 2002;43:4403–12. [https://doi.org/10.1016/S0032-3861\(02\)00275-6](https://doi.org/10.1016/S0032-3861(02)00275-6).
- [163] Unnithan AR, Arathyram RS, Kim CS. *Electrospinning of Polymers for Tissue Engineering*. Elsevier Inc.; 2015. <https://doi.org/10.1016/B978-0-323-32889-0.00003-0>.
- [164] Litovitz TA. Temperature dependence of the viscosity of associated liquids. *J Chem Phys* 1952;20:1088–9. <https://doi.org/10.1063/1.1700671>.
- [165] Yang Q, Zhenyu LI, Hong Y, Zhao Y, Qiu S, Wang CE, et al. Influence of solvents on the formation of ultrathin uniform poly(vinyl pyrrolidone) nanofibers with electrospinning. *J Polym Sci Part B Polym Phys* 2004;42:3721–6. <https://doi.org/10.1002/polb.20222>.
- [166] Shahreen L, Chase GG. Effects of electrospinning solution properties on formation of beads in

- TiO<sub>2</sub> fibers with PdO particles. *J Eng Fiber Fabr* 2015;10:136–45.  
<https://doi.org/10.1177/155892501501000308>.
- [167] Yang GZ, Li HP, Yang JH, Wan J, Yu DG. Influence of Working Temperature on The Formation of Electrospun Polymer Nanofibers. *Nanoscale Res Lett* 2017;12. <https://doi.org/10.1186/s11671-016-1824-8>.
- [168] Casper CL, Stephens JS, Tassi NG, Chase DB, Rabolt JF. Controlling surface morphology of electrospun polystyrene fibers: Effect of humidity and molecular weight in the electrospinning process. *Macromolecules* 2004;37:573–8. <https://doi.org/10.1021/ma0351975>.
- [169] Nagarajan S, Bechelany M, Kalkura NS, Miele P, Bohatier CP, Balme S. *Electrospun Nanofibers for Drug Delivery in Regenerative Medicine*. Elsevier Inc.; 2019. <https://doi.org/10.1016/b978-0-12-814029-1.00020-x>.
- [170] Ye K, Kuang H, You Z, Morsi Y, Mo X. Electrospun nanofibers for tissue engineering with drug loading and release. *Pharmaceutics* 2019;11:1–17.  
<https://doi.org/10.3390/pharmaceutics11040182>.
- [171] Ulery BD, Nair LS, Laurencin CT. Biomedical applications of biodegradable polymers. *J Polym Sci Part B Polym Phys* 2011;49:832–64. <https://doi.org/10.1002/polb.22259>.
- [172] Zhang C, Feng F, Zhang H. Emulsion electrospinning: Fundamentals, food applications and prospects. *Trends Food Sci Technol* 2018;80:175–86.  
<https://doi.org/10.1016/j.tifs.2018.08.005>.
- [173] Buzgo M, Mickova A, Rampichova M, Doupnik M. Blend electrospinning, coaxial electrospinning, and emulsion electrospinning techniques. Elsevier Ltd; 2018.  
<https://doi.org/10.1016/b978-0-08-102198-9.00011-9>.
- [174] Salas C. *Solution electrospinning of nanofibers*. Elsevier Ltd.; 2017.  
<https://doi.org/10.1016/B978-0-08-100907-9.00004-0>.
- [175] Wang J, Windbergs M. Controlled dual drug release by coaxial electrospun fibers – Impact of the core fluid on drug encapsulation and release. *Int J Pharm* 2019;556:363–71.  
<https://doi.org/10.1016/j.ijpharm.2018.12.026>.
- [176] Cianci E, Trubiani O, Diomede F, Merciaro I, Meschini I, Bruni P, et al. Immobilization and delivery of biologically active Lipoxin A4 using electrospinning technology. *Int J Pharm* 2016;515:254–61. <https://doi.org/10.1016/j.ijpharm.2016.09.077>.
- [177] Zeng J, Aigner A, Czubayko F, Kissel T, Wendorff JH, Greiner A. Poly(vinyl alcohol) Nanofibers by Electrospinning as a Protein Delivery System and the Retardation of Enzyme Release by Additional Polymer Coatings. *Biomacromolecules* 2005;6:1484–8.  
<https://doi.org/10.1021/bm0492576>.
- [178] Laha A, Sharma CS, Majumdar S. Electrospun gelatin nanofibers as drug carrier: Effect of crosslinking on sustained release. *Mater Today Proc* 2016;3:3484–91.  
<https://doi.org/10.1016/j.matpr.2016.10.031>.
- [179] Ruvinov E, Shandalov Y, Levenberg S, Cohen S. *Principles of Cardiovascular Tissue Engineering*. 2014. <https://doi.org/10.1016/B978-0-12-420145-3.00018-3>.
- [180] Zaza A, Rocchetti M. Calcium Store Stability as an Antiarrhythmic Endpoint. *Curr Pharm Des*

2014;21:1053–61. <https://doi.org/10.2174/1381612820666141029100650>.

- [181] Neumann RA, Berger S. Observation of a betaine lithium salt adduct during the course of a Wittig reaction. *European J Org Chem* 1998;1085–7. [https://doi.org/10.1002/\(sici\)1099-0690\(199806\)1998:6<1085::aid-ejoc1085>3.0.co;2-g](https://doi.org/10.1002/(sici)1099-0690(199806)1998:6<1085::aid-ejoc1085>3.0.co;2-g).
- [182] Takatsuto S, Gotoh C, Noguchi T, Nomura T, Fujioka S, Yokota T. Synthesis of Deuterio-labelled 24-Methylenecholesterol and Related Steroids. *J Chem Res - Part S* 1998;206–7. <https://doi.org/10.1039/a707402f>.
- [183] Murali VP, Fujiwara T, Gallop C, Wang Y, Wilson JA, Atwill MT, et al. Modified electrospun chitosan membranes for controlled release of simvastatin. *Int J Pharm* 2020;584:119438. <https://doi.org/10.1016/j.ijpharm.2020.119438>.
- [184] Vanzanella V, Scatto M, Zant E, Sisani M, Bastianini M, Grizzuti N. The rheology of PEOT/PBT block copolymers in the melt state and in the thermally-induced sol/gel transition. Implications on the 3D-printing bio-scaffold process. *Materials (Basel)* 2019;12. <https://doi.org/10.3390/ma12020226>.
- [185] Hendrikson WJ, Zeng X, Rouwkema J, van Blitterswijk CA, van der Heide E, Moroni L. Biological and Tribological Assessment of Poly(Ethylene Oxide Terephthalate)/Poly(Butylene Terephthalate), Polycaprolactone, and Poly(L/DL) Lactic Acid Plotted Scaffolds for Skeletal Tissue Regeneration. *Adv Healthc Mater* 2016;5:232–43. <https://doi.org/10.1002/adhm.201500067>.
- [186] Sackers RJB, De Wijn JR, Dalmeyer RAJ, Brand R, Van Blitterswijk CA. Evaluation of copolymers of polyethylene oxide and polybutylene terephthalate (polyactive): Mechanical behaviour. *J Mater Sci Mater Med* 1998;9:375–9. <https://doi.org/10.1023/A:1013227428530>.
- [187] Hajiali F, Tajbakhsh S, Shojaei A. Fabrication and Properties of Polycaprolactone Composites Containing Calcium Phosphate-Based Ceramics and Bioactive Glasses in Bone Tissue Engineering: A Review. *Polym Rev* 2018;58:164–207. <https://doi.org/10.1080/15583724.2017.1332640>.
- [188] Deshmukh K, Basheer Ahamed M, Deshmukh RR, Khadheer Pasha SK, Bhagat PR, Chidambaram K. Biopolymer Composites with High Dielectric Performance: Interface Engineering. Elsevier Inc.; 2017. <https://doi.org/10.1016/B978-0-12-809261-3.00003-6>.
- [189] Imai K. Fluorimetric assay of dopamine, norepinephrine and their 3-o-methyl metabolites by using fluorecamine. *J Chromatogr A* 1975. [https://doi.org/10.1016/S0021-9673\(01\)81097-9](https://doi.org/10.1016/S0021-9673(01)81097-9).

# 8. Patent application

# Androstane derivatives with activity as pure or predominantly pure stimulators of SERCA2a for the treatment of heart failure

## Field

[1] The present invention relates to the field of pharmaceuticals, in particular, to androstane derivatives for use in the treatment of acute heart failure.

## Background of the invention

[2] The prevalence of heart failure (HF) is age-dependent, ranging from less than 2% of people younger than 60 years to more than 10% of individuals older than 75 years (Metra M & Teerlink JR, *Lancet* 2017, 390:1981-1995). Most patients with HF have a history of hypertension, coronary artery disease, cardiomyopathies, valve disease, or a combination of these disorders (Metra M & Teerlink JR, *Lancet* 2017, 390:1981-1995). The calculated lifetime risk of developing HF is expected to increase, and those with hypertension are at higher risk (Lloyd-Jones DM *et al.*, *Circulation* 2002,106:3068-3072). Patients with HF have a poor prognosis with high rates of hospital admission and mortality.

[3] Clinical symptoms in HF are caused by a cardiac double pathological feature that consists in an inotropic abnormality, resulting in diminished systolic emptying (systolic dysfunction), and a compliance abnormality in which the ability of the ventricles to suck blood from the venous system is impaired (diastolic dysfunction). This, in turn, causes a reduction in the amount of blood available for systolic contraction (impairment of left ventricle (LV) filling). The impaired contractility and relaxation are the consequence of an abnormal distribution of intracellular  $\text{Ca}^{2+}$ , resulting from reduced  $\text{Ca}^{2+}$  uptake by the sarcoplasmic reticulum (SR), which is the intracellular  $\text{Ca}^{2+}$  store (Bers DM *et al.*, *Ann N.Y. Acad Sci* 2006, 1080:165-177). The latter is operated by the  $\text{Ca}^{2+}$  ATPase of the SR membrane (SERCA2a), which is an active membrane transport. SERCA2a activity is physiologically limited by its interaction with phospholamban (PLN) (Bers DM., *Annu Rev Physiol* 2008, 70:23-49; MacLennan DH & Kranias EG, *Nat Rev Mol Cell Biol* 2003, 4(7): 566-577); such a restriction is normally relieved by PLN phosphorylation by protein kinase A (PKA), which is a signaling pathway that is severely depressed as a consequence of HF remodeling (Lohse M *et al.*, *Circ Res* 2003, 93:896-906). Thus, SERCA2a function is impaired in the failing myocardium (Bers DM *et al.*, *Ann N.Y. Acad Sci* 2006, 1080:165-177) and is thus primarily responsible for reduced  $\text{Ca}^{2+}$  uptake by the SR. In addition to its consequences on myocyte contractility and relaxation, abnormal  $\text{Ca}^{2+}$  distribution also facilitates cardiac arrhythmias (Zaza & Rocchetti, *Curr Pharm Des* 2015, 21:1053-1061) and, on the long term, it accelerates myocytes loss by apoptosis

(Nakayama H *et al.*, J Clin Invest 2007, 117:2431-44). Reduced SERCA2a function also increases the energy cost of contraction because it requires a compensatory increase in Ca<sup>2+</sup> extrusion through the Na-Ca exchanger (NCX), which is less energy efficient (Lipskaya L *et al.*, Expert Opin Biol Ther 2010, 10:29-41). Substantial evidence indicates that normalization of SERCA2a function restores intracellular Ca<sup>2+</sup> homeostasis and improves contractility and relaxation of cardiomyocytes and of the heart *in situ* (Byrne MJ *et al.*, Gene Therapy 2008, 15:1550-1557; Sato *et al.*, JBC 2001, 276:9392-99). To summarize, recovery of SERCA2a function in HF may improve cardiac relaxation and, possibly, contractility while minimizing arrhythmias, myocardial oxygen consumption, and myocyte death (Lipskaya L *et al.*, Expert Opin Biol Ther. 2010, 10:29-41). This highlights a need for “pure” SERCA2a activators. Indeed, SERCA2a activation, because of improved Ca<sup>2+</sup> sequestration, can elevate the intra-SR threshold for the generation of Ca<sup>2+</sup> waves exerting a negative feedback on the Ca<sup>2+</sup>-induced-Ca<sup>2+</sup> release sustaining the waves (Fernandez-Tenorio M & Niggli E J, Mol Cell Cardiol 2018, 119:87-95). Hence, a pure or predominantly pure SERCA2a activation might afford a reduced arrhythmogenic risk and, therefore, justifies an interest for compounds with SERCA2a-stimulating action.

[4] In conclusion, novel molecules able to enhance SERCA2a function alone might improve overall cardiac function in HF. This provides a strong motivation for the search of new compounds with such a pharmacodynamic profile.

[5] Current long-term therapy of HF is aimed at prevention of “myocardial remodeling” (*e.g.*, beta-blockers, ACE inhibitors, and aldosterone antagonists), which is a chronic maladaptive response to reduced contractility that amplifies the initial damage and underlies disease evolution (Heineke J & Molkentin D, Nat Rev 2006, 7:589-600). While this approach has indisputable merit, it does not target impaired “contractility” and “relaxation”, which are the functional derangements that define HF and are responsible for its symptoms. Indeed, particularly in the advanced disease stages, drugs that increase myocardial contractility/relaxation (“inotropic/lusitropic agents”) are still widely used and crucial for patient’s management (Metra M & Teerlink JR, Lancet 2017, 390:1981-1995). These include sympathomimetic amines (dobutamine) and levosimendan, which is a Ca<sup>2+</sup>-sensitizer with a strong vasodilator effect. Unfortunately, these agents act by mechanisms with potentially harmful components, such as facilitation of life-threatening arrhythmias, increased myocardial oxygen consumption, and impairment of an already insufficient coronary blood flow due to the fall in blood pressure caused by vasodilation (Ashkar H, Makaryus AN StatPearls. Treasure Island (FL): StatPearls Publishing, 2018 Jan-2017 Dec 19 (<https://www.ncbi.nlm.nih.gov/books/NBK470431/>); Gong B. *et al.*, J Cardiothorac Vasc Anesth 2015, 29: 1415-25 EDITORIAL). This limits the use of inotropic agents to late

disease stages, thus losing the potential benefits of increasing contractility early in the disease course. Furthermore, these agents do not improve patient's prognosis and survival, and their therapeutic use must be carefully monitored (Ashkar H & Makaryus AN, StatPearls. Treasure Island (FL): StatPearls Publishing, 2018 Jan-2017 Dec 19) (Gong B. *et al.*, J Cardiothorac Vasc Anesth 2015, 29: 1415-25 EDITORIAL).

[6] Among positive inotropes, the cardiac glycoside Digoxin, an inhibitor of the Na<sup>+</sup>/K<sup>+</sup> ATPase enzymatic activity, has been one of the most commonly prescribed medications in the past. However, its use has been decreasing over the last few decades because of the difficulty in maintaining Digoxin within serum concentration ranges (0.5-0.7 ng/ml) at which Digoxin displays its beneficial effects without reaching the threshold level of 0.9 ng/ml, above which increased risk of death, mainly due to arrhythmias, has been observed (Packer M, Journal of Cardiac Failure 2016, 22:726-730; Packer M, Eur J Heart Failure 2018, 20:851-852).

[7] Intensive research is also in progress for the development of HF drugs with mechanisms of action other than positive inotropy. Among many, the agents most investigated and under clinical development are: SERELAXIN-recombinant relaxin 2 mediator; ULARITIDE-recombinant natriuretic peptide; OMECANTIV MECARBIL-cardiac myosin activator; BMS986231-NO donor; ADRECIZUMAB-Adrenomedullin inhibitor; ANX-042-spliced variant of NP; TD1439-Neprylisin (NEP) inhibitor. However, when evaluated in clinical phase 2-3 trials, none of these new agents has met the primary end-point without safety concern.

[8] The clinical course and prognosis of a patient with chronic HF (CHF) is much worse after an episode of acute HF (AHF) (Solomon SD *et al.*, Circulation 2007, 116:1482-87). AHFS can be defined as the new onset or recurrence of symptoms and signs of HF, requiring urgent evaluation and treatment and resulting in unscheduled care or hospital admission. Half of the patients with AHFS have reduced systolic function (HFrEF), representing a target for potential future therapies (Braunwald E. Lancet 2015; 385:812-24). Therapies for AHFS in patients with reduced ejection fraction (rEF) have focused on alleviating congestion with vasodilators, diuretics, or ultrafiltration or by increasing cardiac output with positive inotropes. Although this therapeutic strategy has reduced the risk of sudden cardiac death, the post-discharge event rate remains unacceptably high in patients hospitalized for AHFS. Many unwanted cardiovascular side effects can be caused by the available therapy, such as myocardial ischemia, cardiac injury, and arrhythmias consequent to the inotropic therapy, particularly in patients with coronary artery disease (CAD) (Abraham WT *et al.*, J Am Coll Cardiol 2005, 46:57-64; Flaherty JD *et al.*, J Am Coll Cardiol. 2009, 53(3):254-63), hypotension, and low perfusion of the peripheral

organs (kidney) caused by vasodilators, particularly in HF patients with low blood pressure. Accordingly, the main goal during hospitalization is to improve cardiac output without causing cardiac and/or kidney injury. Moreover, there has been little focus on examining or treating an impaired left ventricular (LV) diastolic relaxation that, in the remaining 50% of patients with HF but preserved EF, is responsible for the symptoms of HF. In addition, patients with AHFS with reduced EF also have an impairment of ventricular relaxation that contributes to the overall failure of cardiac function. A variety of echocardiographic indexes have been developed to measure the cardiac relaxation capacity both in animal models and patients with HF (e.g., decreased early mitral annular tissue velocity [ $e'$ ] and decreased early mitral inflow [E] deceleration time [DT]), along with echocardiographic parameters of increased LV filling pressure (e.g., E/ $e'$  ratio). Even though the correspondence of the single index changes is not perfectly superimposable in some animal models and patients, their overall changes in animal models of ventricular relaxation impairment are certainly translatable to the human condition and used to study the drug effect in AHFS (Shah SA *et al.*, *Am Heart J* 2009, 157:1035-41).

[9] Various therapeutic approaches that increase SERCA2a function have been recently investigated. These include SERCA2a overexpression by gene transfer (Byrne *et al.*, *Gene Therapy* 2008, 15:1550-1557), PLN inactivation through expression of mutants with negative dominance (Hoshijima M *et al.*, *Nat. Med.* 2002, 8: 864-871; Iwanaga Y *et al.*, *J Clin Invest* 2004, 113: 727-736), AdV-shRNA (Suckau L *et al.*, *Circulation* 2009, 119: 1241-1252), microRNA (Gröbl *et al.*, *PLoS One* 2014, 9: e92188), or antibodies (Kaye DM *et al.*, *J. Am. Coll. Cardiol.* 2007, 50:253-260). As highlighted by the negative results of the largest phase IIb clinical trial applying SERCA2a gene delivery in HF (CUPID 2), these approaches suffer from major problems in construct delivery (viral vectors etc.) and dose adjustment that are far from being solved (Hulot JS, *Eur Heart J* 2016, 19:1534-1541). A small-molecule (pyridone derivative) inhibiting PLN, which is structurally different from Istaroxime, has been recently described (Kaneko M. *et al.*, *Eur J Pharmacol* 2017, 814:1-7).

[10] Hence, the development of a small-molecule SERCA2a activator would be advantageous for treating HF and still represents a very promising strategy.

[11] Istaroxime is a new small-molecule drug under clinical development for the treatment of AHFS. Istaroxime is disclosed in EP0825197 and in S. De Munari *et al.* (*J. Med. Chem.* 2003, 64:3644-3654) and is compound (3Z,5 $\alpha$ )-3-[(2-aminoethoxy)imino] androstane-6,17-dione. Istaroxime is endowed of the double mechanism of action of inhibiting the Na<sup>+</sup>/K<sup>+</sup> pump (Micheletti *et al.*, *J Pharmacol Exp Ther* 2002, 303:592-600) while activating SERCA2a (Rocchetti M *et al.*, *J Pharmacol Exp Ther.* 2005, 313:207-15).

At the same level of inotropy, the proarrhythmic effect of Istaroxime is considerably lower than that of Digoxin, which is a pure Na<sup>+</sup>/K<sup>+</sup> pump inhibitor (Rocchetti M *et al.*, *J Pharmacol Exp Ther.* 2005, 313:207-15). This suggests that by improving Ca<sup>2+</sup> clearance from the cytosol (Alemanni, *J Mol Cell Cardiol* 2011, 50:910-8), SERCA2a stimulation may also minimize the proarrhythmic effect of Na<sup>+</sup>/K<sup>+</sup> pump blockade (Rocchetti M *et al.*, *J Pharmacol Exp Ther.* 2005, 313:207-15; Zaza & Rocchetti, *Curr Pharm Des* 2015, 21:1053-1061) while preserving its inotropic effect. The reduction of the proarrhythmic effect by Istaroxime has been confirmed in clinical studies (Gheorghiade M *et al.*, *J Am Coll Cardiol* 2008, 51:2276-85).

[12] In HF patients, Istaroxime infusion improved both systolic and diastolic functions (Horizon study) (Gheorghiade M *et al.*, *J Am Coll Cardiol* 2008, 51:2276-85; Shah SA *et al.*, *Am Heart J* 2009, 157:1035-41). Amelioration of systolic function was detected as an increase in systolic tissue velocity (*s'*) and in the slope of end-systolic elastance (ESPVR slope); increased diastolic compliance was revealed by an increment in diastolic tissue velocity (*e'*); and decreased end-diastolic elastance (EDPVR slope) (Shah SA *et al.*, *Am Heart J* 2009, 157:1035-41).

[13] While it is endowed with an excellent pharmacodynamic profile, Istaroxime is not optimal for chronic administration because of its poor gastrointestinal (GI) absorption and high clearance rate. Istaroxime, therefore, has been developed for intravenous infusion in hospitalized patients with AHFS only, and its administration requires well-trained medical personnel (Dec GW, *J Am Coll Cardiol.* 2008, 51:2286-88; Shah SA *et al.*, *Am Heart J* 2009, 157:1035-41).

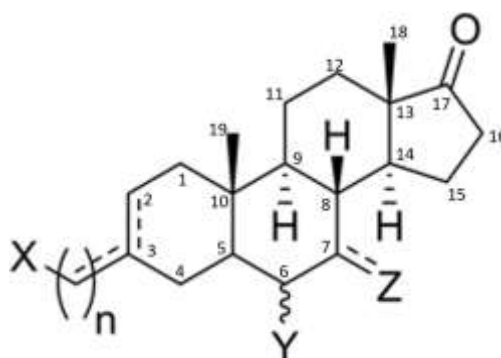
[14] Accordingly, there is a long-felt need for a compound for use in the treatment of HF endowed with a positive lusitropic effect and that can be administered preferably by oral route (Butler J *et al.*, *Eur J Heart Failure* 2018, 20:839-841; Wagner S *et al.*, *Circ Res* 2015, 116:1956-1970; Hasenfuss G & Teerlink JR., *Eur Heart J.* 2011, 32(15):1838-45).

[15] It is possible that an improved diastolic function may be achieved by a "pure" SERCA2a activator. However, notwithstanding the intense research on discovering small molecules or gene therapy aimed at selectively activating SERCA2a, no promising clinical outcomes have been reached so far.

[16] The present invention satisfies the above needs and overcomes the problem of prior art.

## Summary of the invention

[17] It has now been found that certain androstane derivatives exhibit pure or predominantly pure SERCA2a activation. In other words, the androstane derivatives provided herein significantly activate SERCA2a, but do not, or only moderately, inhibit the Na<sup>+</sup>/K<sup>+</sup> ATPase pump. In general, these androstane derivatives contain a functional group attached through a carbon linker at Carbon-3 (C3) and functional groups at C6 and/or C7. The structure of these pure or predominantly pure SERCA2a activators has the general formula (I) as shown here:



Wherein X is any one of a carboxylic acid, carboxylic ester and their bioisosters (e.g., sulfate, sulfonic acid, phosphate, phosphonate, and nitrogen-containing etherocyclic rings such as triazoles and tetrazoles), primary alcohol, ethers, or an amine group (e.g., primary amine, secondary amine, or cyclic amine);

n is 1, 2, 3, 4, or 5;

the C3-C1' dashed line represents an optional exocyclic double bond C=C;

the C2-C3 dashed line represents an optional endocyclic double bond C=C;

Y at C6 is a hydroxyl (OH) in the  $\alpha$ - or  $\beta$ -configuration or a hydroxymethyl (CH<sub>2</sub>OH) in the  $\alpha$ -configuration;

Z at C7 could be either -H or -OH in an  $\alpha$ -configuration or a ketone. The dashed line represents an optional carbonyl group (C=O) in such position.

The compounds disclosed herein may include enantiomeric and/or diastereomeric mixtures; their pharmaceutically acceptable salts, solvates, or hydrates; or their metabolite and metabolic precursors.

[18] In the context of the present invention, metabolite and metabolic precursor means a compound of formula (**I**) which has been transformed by a metabolic reaction, but substantially maintains or increases the pharmacological activity.

[19] Examples of metabolites or metabolic precursors are hydroxylated, carboxylated, sulphonated, glycosylated, methylated or demethylated, acetylated, covalently linked to glucuronic acid, glycine and other amino acids, glutathione, oxidized or reduced derivatives of the compounds of formula (**I**).

[20] Some compounds of formula (**I**), especially esters, can also be prodrugs of the active forms.

[21] Where the compounds of formula (**I**) can exhibit tautomerism, the formula is intended to cover all tautomers; the invention includes within its scope all the possible stereoisomers, Z and E isomers, optical isomers, enantiomers and their mixtures.

[22] Also the pharmaceutical acceptable salts are included in the scope of the invention. Pharmaceutical acceptable salts are salts which retain the biological activity of the base compound and are derived from such known pharmacologically acceptable acids such as, e. g., hydrochloric, hydrobromic, sulfuric, phosphoric, nitric, fumaric, succinic, oxalic, malic, tartaric, maleic, citric, methanesulfonic or benzoic acid and others commonly used in the art, see for example Pharmaceutical Salts and Co-crystals, Editors: Johan Wouters, Luc Quéré, RSC Publishing, 2011.

[23] Further object of the present invention are the said compounds of general formula (**I**) for use as medicaments, in particular for the treatment of HF.

[24] In some embodiments, the compound of claim 1 is selected from the group consisting of: (E)-4-(6 $\alpha$ -hydroxy-17-oxoandrostane-3-ylidene)butyric acid; (Z)-4-(6 $\alpha$ -hydroxy-17-oxoandrostane-3-ylidene) butyric acid; (E)-4-(6 $\beta$ -hydroxy-17-oxoandrostane-3-ylidene) butyric acid; (Z)-4-(6 $\beta$ -hydroxy-17-oxoandrostane-3-ylidene) butyric acid; (E)-3-[2-(azetidin-3-yl)ethylidene]-6 $\alpha$ -hydroxyandrostane-17-one; (Z)-3-[2-(azetidin-3-yl)ethylidene]-6 $\alpha$ -hydroxyandrostane-17-one; (E)-3-(4-aminobutyl)-6 $\alpha$ -hydroxyandrost-2-ene-17-one hydroiodide; 3-[2-(piperidin-4-yl)ethyl]-6 $\alpha$ -hydroxyandrost-2-ene-17-one hydroiodide; (EZ)-3-(4-aminobutylidene)-6 $\alpha$ -hydroxyandrostane-17-one; (E)-3-[2-(piperidin-4-yl)ethylidene]-6 $\alpha$ -hydroxyandrostane-17-one; (Z)-3-[2-(piperidin-4-yl)ethylidene]-6 $\alpha$ -hydroxyandrostane-17-one; 3 $\beta$ -[2-(piperidin-4-yl)ethyl]-6 $\alpha$ -hydroxyandrostane-17-one; Ethyl (6 $\alpha$ -hydroxy-17-ketoandrostane-3 $\beta$ -yl) acetate; 4-(6 $\alpha$ -hydroxy-17-oxoandrostane-3-yl) butyric acid; 4-(6 $\beta$ -hydroxy-17-oxoandrostane-3-yl)

butyric acid; 2-(6beta-hydroxy-17-oxoandrostane-3-yl) acetic acid; 4-(6alpha-hydroxy-17-oxoandrostane-3-yl) ethylbutyrate; 4-(6alpha-hydroxy-17-oxoandrostane-3-yl) ethylcaproate; 4-(6beta-hydroxy-17-oxoandrostane-3-yl) caproic acid; (E)-3-(5-N-methylaminopentylidene)-6alpha-hydroxymethylandrosterone-7,17-dione; (E)-3-[2-(pyrrolidin-3-yl)ethylidene]-6alpha-hydroxymethylandrosterone-7,17-dione; (E)-3-[2-(azetidin-2-yl)ethylidene]-6alpha-hydroxymethylandrosterone-7,17-dione; (E)-3-[2-(piperidin-4-yl)ethylidene]-6alpha-hydroxymethylandrosterone-7,17-dione; (E)-3-(5-N-methylaminopentylidene)-6alpha-hydroxymethyl-7alpha-hydroxyandrostane-17-one; 3beta-[2-(azetidin-2-yl)ethynyl]-6alpha-hydroxymethylandrosterone-7,17-dione; 3beta-[2-(azetidin-2-yl)ethynyl]-6alpha-hydroxymethyl-7alpha-hydroxyandrostane-17-one; 3beta-[2-(pyrrolidin-3-yl)ethynyl]-6alpha-hydroxymethylandrosterone-7,17-dione; 3beta-[2-(pyrrolidin-3-yl)ethynyl]-6alpha-hydroxymethyl-7alpha-hydroxyandrostane-17-one; 3beta-[2-(piperidin-4-yl)ethynyl]-6alpha-hydroxymethylandrosterone-7,17-dione; and 3beta-[2-(piperidin-4-yl)ethynyl]-6alpha-hydroxymethyl-7alpha-hydroxyandrostane-17-one.

[25] A further object of the present invention are pharmaceutical compositions comprising one or more of the compounds of formula (I), optionally in combination with other therapeutically active ingredients. In turn, these pharmaceutical compositions may be formulated for oral administration, intravenous or intramuscular injection, inhalation, intravitreal injection, and the like. In particular embodiments, the pharmaceutical compositions disclosed herein are used in treating HF.

[26] The above and other objects of the present invention will be now disclosed in detail also by means of examples and Figures.

### **Brief description of the drawings**

[27] **Figure 1** shows the effects of 1  $\mu$ M CVie216 on sarcoplasmic reticulum (SR)  $\text{Ca}^{2+}$  uptake parameters in rat ventricular myocytes isolated from STZ rats (loading protocol). The SR  $\text{Ca}^{2+}$  uptake parameters included  $\text{Ca}^{2+}$  transient (CaT) amplitude (Panel A);  $\text{Ca}^{2+}$ -induced  $\text{Ca}^{2+}$  release (CICR) gain (Panel B) and the time constant ( $\tau$ ) of  $\text{Ca}^{2+}$  decay (Panel C). Differences between curves in control (N=16-18) and CVie216 (N=20-23) were statistically significant ( $p < 0.05$ , two-way ANOVA) in panels A-C.

[28] **Figure 2** shows the effects of 1  $\mu$ M CVie214 on sarcoplasmic reticulum (SR)  $\text{Ca}^{2+}$  uptake parameters in rat ventricular myocytes isolated from STZ rats (loading protocol). The SR  $\text{Ca}^{2+}$  uptake parameters included  $\text{Ca}^{2+}$  transient (CaT) amplitude (Panel A);  $\text{Ca}^{2+}$ -induced  $\text{Ca}^{2+}$  release (CICR) gain (Panel B) and the time constant ( $\tau$ ) of  $\text{Ca}^{2+}$  decay (Panel C). Differences between curves in control (N=14) and CVie214 (N=11) were statistically significant in panel B ( $p < 0.05$ ) and close to significance in panel C ( $p = 0.05$ ).

[29] **Figure 3** shows the effect of CVie216 on action potential (AP) and short term variability (STV) of action potential duration (APD) at various stimulation rates (Hz) in guinea-pig ventricular myocytes. Shown in panels A, left to right, are the rate-dependency of action potential duration at 90% repolarization ( $APD_{90}$ ) (left panel), diastolic membrane potential ( $E_{diast}$ ) (middle panel), and maximum depolarization velocity ( $dV/dt_{max}$ ) (right panel) under basal condition (CTR, closed circles;  $N > 13$ ) or in the presence of 1  $\mu$ M CVie216 (open circles;  $N > 11$ ). The differences measured between the control group and the CVie216 group were not statistically significant for all parameters. In panel B, the linear correlation between STV and the mean  $APD_{90}$  is shown for control (CTR, closed circles) and CVie216 (open circles) group. The data from all pacing rates were pooled in each group to extend STV evaluation to a wide APD range. Solid lines are linear fits of data points (control slope = 0.013 vs CVie216 slope = 0.009, NS) to indicate that CVie216 did not alter STV sensitivity to APD prolongation.

[30] **Figure 4** shows the effect of CVie214 on action potential (AP) and short term variability (STV) of action potential duration (APD) at various stimulation rates (Hz) in guinea-pig ventricular myocytes. Shown in panels A, left to right, are the rate-dependency of action potential duration at 90% repolarization ( $APD_{90}$ ) (left panel), diastolic membrane potential ( $E_{diast}$ ) (middle panel), and maximum depolarization velocity ( $dV/dt_{max}$ ) (right panel) under basal condition (CTR, closed circles;  $N > 17$ ) or in the presence of 1  $\mu$ M CVie214 (open circles;  $N > 17$ ). The differences measured between the control group and the CVie214 group were not statistically significant for all parameters. In panel B, the linear correlation between STV and the mean  $APD_{90}$  is shown for control (CTR, closed circles) and CVie214 (open circles) group. The data from all pacing rates were pooled in each group to extend STV evaluation to a wide APD range. Solid lines are linear fits of data points (control slope = 0.012 vs CVie214 slope = 0.014, NS) to indicate that CVie214 did not alter STV sensitivity to APD prolongation.

### **Detailed description of the invention**

[31] Disclosed herein are compositions and methods useful for the treatment of heart failure. In particular, provided herein are compositions comprising novel androstane derivatives. Further, there is one group of novel androstane derivatives described herein that activate SERCA2a, while only moderately inhibiting the  $Na^+/K^+$  ATPase pump. This group of androstane derivatives, referred to as "predominantly pure" SERCA2a stimulators, have the general formula (I) with an amine-containing functional group at the C3 carbon. Another group of novel androstane derivatives described herein exhibit strong SERCA2a activation without any significant  $Na^+/K^+$  ATPase pump inhibition. This group of androstane derivatives, referred to as "pure" SERCA2a stimulators, have the general formula (I) with a carboxylic acid/ester-containing functional group lined through

a spacer at the C3 carbon. In other embodiments, the predominantly pure or pure SERCA2a stimulators of general formula (I) may include an alcohol-, sulphate-, or phosphate-containing functional group at the C3 carbon. As such, these compositions are endowed with positive lusitropic characteristics and can be used to selectively activate SERCA2a while avoiding the proarrhythmic effect of Na<sup>+</sup>/K<sup>+</sup> ATPase pump inhibition. The compositions and methods disclosed herein will now be described in more detail below.

### Definitions

[32] Unless defined otherwise, all technical and scientific terms used herein have the same meaning as those commonly understood by one of ordinary skill in the art to which this invention belongs. Standard techniques are used unless otherwise specified. Although methods and materials similar or equivalent to those described herein can be used in the practice or testing of the present disclosure, suitable methods and materials are described below. The materials, methods and examples are illustrative only, and are not intended to be limiting. All publications, patents and other documents mentioned herein are incorporated by reference in their entirety.

[33] As used herein, the singular forms "a," "an," and "the" include the plural referents unless the context clearly indicates otherwise.

[34] The term "about" refers to the variation in the numerical value of a measurement, *e.g.*, volume, time, pressure, concentration, etc., due to typical error rates of the device used to obtain that measure. In one embodiment, the term "about" means within 5% of the reported numerical value, preferably, the term "about" means within 3% of the reported numerical value.

[35] The term "heart failure" refers to a clinical syndrome characterized by typical symptoms (*e.g.*, breathlessness, ankle swelling and fatigue) that may be accompanied by signs (*e.g.*, elevated jugular venous pressure, pulmonary crackles and peripheral edema) caused by a structural and/or functional cardiac abnormality, resulting in a reduced cardiac output and/or elevated intracardiac pressures at rest or during stress.

[36] The terms "acute heart failure" or "AHF" are used interchangeably herein and refer generally to a rapid onset or worsening of symptoms and/or signs of HF requiring immediate treatment and hospitalization. The current definition of "acute heart failure" is rather nonspecific and may include a broad spectrum of conditions with several phenotypes characterized by different clinical presentation, etiology, precipitating factors, therapeutic approach, and prognosis. In addition, a large proportion of patients have a

subacute course of the disease with a progressive worsening of signs and symptoms of HF which could develop days before hospital admission.

[37] The terms "chronic heart failure" or "CHF" are used interchangeably herein and refer to the current clinical classification of chronic HF based on the presence of signs and symptoms of HF and left ventricular ejection fraction (LVEF), recognizing three categories: "heart failure with reduced ejection fraction" or "HFrEF," which is characterized by an LVEF of less than about 40%; "heart failure with mid-range ejection fraction" or "HFmEF" or "HFmrEF," which is characterized by an LVEF from about 40% to about 49%; and "heart failure with preserved ejection fraction" or "HFpEF," which is characterized by an LVEF of equal to or greater than about 50%. The terms "HFmrEF" and "HFpEF" include two additional criteria; namely, increased natriuretic peptides levels (BNP >35 pg/ml and/or NT-proBNP >125 pg/mL) associated with the evidence of structural and/or functional heart disease (left ventricular hypertrophy and/or left atrium enlargement and/or evidence of diastolic dysfunction). The efficacy of HF evidence-based medications have been confirmed only in patients with "HFrEF," whereas in "HfpEF" no treatment demonstrated a significant improvement of outcomes.

[38] The terms "metabolite" and "metabolic precursor" refer to compounds that have been transformed/modified by a metabolic reaction, but which substantially maintain or exhibit an increase in their pharmacological activity.

[39] The term "treating" refers to any indicia of success in the treatment or amelioration of the disease or condition. Treating can include, for example, reducing or alleviating the severity of one or more symptoms of the disease or condition, or it can include reducing the frequency with which symptoms of a disease, defect, disorder, or adverse condition, and the like, are experienced by an individual, such as a human patient.

[40] The term "preventing" refers to the prevention of the disease or condition, *e.g.*, acute heart failure, in an individual, such as a human patient. For example, if an individual at risk of developing heart failure is treated with the methods of the present invention and does not later develop heart failure, then the disease has been prevented in that individual.

[41] The term "treat or prevent" is sometimes used herein to refer to a method that results in some level of treatment or amelioration of the disease or condition, and contemplates a range of results directed to that end, including, but not restricted to, prevention of the condition entirely.

[42] As used herein, the term "pharmaceutically acceptable carrier" means a chemical composition with which an active compound, such as an androstane derivative having the general formula (I) or a metabolite of thereof, may be combined and which, following the combination, can be used to administer the compound to a mammal.

[43] As used herein, the term "pharmaceutically acceptable" salt, solvate, hydrate, or ester means a salt, solvate, hydrate, or ester form of the active ingredient which is compatible with any other ingredients of the pharmaceutical composition, which is not deleterious to the subject to which the composition is to be administered. The term "pharmaceutical acceptable salt" further refers to a salt form of a compound which retains the biological activity of the base compound and which is derived from a pharmacologically acceptable acid.

[44] The term "parameter" as used herein to refer to measuring heart function means any heart function that is observable or measurable using suitable measuring techniques available in the art. A non-limiting list of exemplary "parameters" of heart function include calcium transient amplitude (CaT), calcium-induced calcium release (CICR), time constant of calcium decay, rate-dependency of action potential duration at 90% repolarization (APD<sub>90</sub>), diastolic membrane potential (E<sub>diast</sub>), maximum depolarization velocity (dV/dt<sub>max</sub>), heart rate, blood pressure, diastolic relaxation, systolic contraction, left ventricular ejection fraction (LVEF), diastolic blood pressure, systolic blood pressure, cardiac output, stroke volume, contraction velocity (s'), early relaxation velocity (e'), late relaxation velocity (a'), index of left ventricular filling pressure (E/e'), deceleration time of E wave (DT), mitral deceleration index (DT/E), deceleration slope (E/DT), cardiac index, mitral inflow velocity, and the like. As one having ordinary skill in the art will appreciate, measuring one or more "parameters" of heart function can be used to detect heart dysfunction as compared to the average normal "parameters" and can also be used to determine whether heart function has improved following or during treatment.

[45] The term "predominantly pure" as it relates to SERCA2a activation or stimulation refers to a compound, such as an androstane derivative, that has the ability to stimulate in a statistically significant way SERCA2a activity in a cell-free system (SR cardiac microsomes from guinea pig, dog, rat, etc.) while only moderately inhibiting the purified dog kidney Na<sup>+</sup>/K<sup>+</sup> ATPase in the cell-free system (*i.e.*, having an IC<sub>50</sub> greater than about 0.5 μM, preferably greater than about 1 μM).

[46] The term "pure" as it relates to SERCA2a activation or stimulation refers to a compound, such as an androstane derivative, that has the ability to stimulate in a statistically significant way SERCA2a activity in a cell-free system (SR cardiac

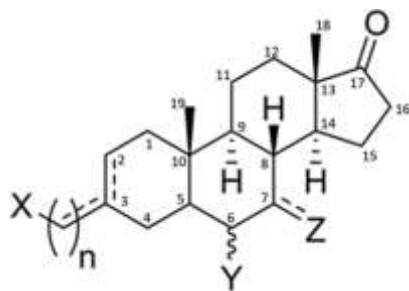
microsomes from guinea pig, dog, rat, etc.) without exhibiting significant inhibition of the Na<sup>+</sup>/K<sup>+</sup> ATPase pump (*i.e.*, having an IC<sub>50</sub> greater than about 100 μM).

[47] The terms “therapeutically active” or “active” ingredient or compound refer to a substance that provides a beneficial effect to the individual to whom the substance is administered. A “therapeutically effective amount” or “therapeutically effective dose” is the amount of a composition or active ingredient sufficient to provide a beneficial effect to the individual to whom the composition or active ingredient is administered.

#### Androstane derivatives with predominantly pure or pure SERCA2a stimulatory activity

[48] The present invention is based on the discovery of androstane derivatives with predominantly pure or pure SERCA2a stimulatory activity. In other words, these are derivatives that exhibit stimulation of SERCA2a with only moderate or no Na<sup>+</sup>/K<sup>+</sup> ATPase pump inhibition.

[49] These novel androstane derivatives are functionalized at the C-3 carbon with a carbon linker bearing a variety of functional groups, such as amine-containing or carboxylic acid/ester-containing functional group. Further, these novel androstane derivatives are also functionalized at the C-6 and/or C-7 carbons, such as with a hydroxyl, hydroxymethyl, or ketone group. Preferably, each of the novel androstane derivatives suitable for use herein will have the general formula (**I**):



[50] Wherein X is any one of a carboxylic acid, carboxylic ester and their bioisosters (*e.g.*, sulfate, sulfonic acid, phosphate, phosphonate, and nitrogen-containing etherocyclic rings such as triazoles and tetrazoles), primary alcohol, ethers, or an amine group (*e.g.*, primary amine, secondary amine, or cyclic amine);

[51] the carbon linker at C6 will have one or more carbons represented by n, which is an integer between 1 and 5 (*e.g.*, 1, 2, 3, 4, or 5);

[52] the dashed line represents an optional double bond (C=C at C3-C1' or C2-C3) and C=O at C7;

[53] the Y group at C6 is a hydroxyl (OH) in the alpha- or beta-configuration or a hydroxymethyl (CH<sub>2</sub>OH) in the alpha-configuration; and

[54] the Z group at C7 could be either -H or -OH in an  $\alpha$ -configuration or a ketone (C=O).

[55] In certain embodiments, a predominantly pure SERCA2a stimulator may be desired. As such, the androstane derivatives suitable for use herein may include those having the general formula (**I**) wherein X is an amine functional group (e.g., primary amine, secondary amine, or cyclic amine). However, in some embodiments, it may be desirable to select a pure SERCA2a stimulator. As such, the androstane derivatives suitable for use may include those having the general formula (**I**), except that the X is not an amine function group (e.g., primary amine, secondary amine, or cyclic amine). In a preferred embodiment, the pure SERCA2a stimulator will have the general formula (**I**) with a carboxylic acid or a carboxylic ester at X.

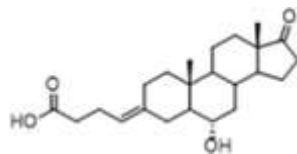
[56] It is preferable that the androstane derivatives disclosed herein contain an oxygen-containing functional group at either Z or Y or both.

[57] Also suitable for use herein are the enantiomeric and/or diastereomeric mixtures of the compounds represented by general formula (**I**) as well as their pharmaceutically acceptable salts, solvates, and/or hydrates and their metabolite and/or metabolic precursors. Examples of metabolites or metabolic precursors include the hydroxylated, carboxylated, sulfonated, acetylated, glycosylated, glucuronated, methylated or demethylated, covalently linked to glutathione, glycine or other amino acids, oxidized or reduced derivatives of the compounds of formula (**I**). Moreover, some compounds of formula (**I**), especially esters, can also be prodrugs of the active forms. Examples of pharmaceutical acceptable salts include, but are not limited to, hydrochloric, hydrobromic, sulfuric, phosphoric, nitric, fumaric, succinic, oxalic, malic, tartaric, maleic, citric, methanesulfonic or benzoic acid and others commonly used in the art (see, for example, *Pharmaceutical Salts and Co-crystals*, Editors: Johan Wouters, Luc Quéré, RSC Publishing, 2011, the entire content of which is hereby incorporated by reference).

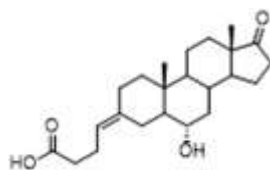
[58] Where the compounds of formula (**I**) can exhibit tautomerism, the formula is intended to cover all tautomers, including, but not limited to, all the possible stereoisomers, Z and E isomers, optical isomers, enantiomers and their mixtures.

[59] Particular androstane derivatives suitable for use herein include:

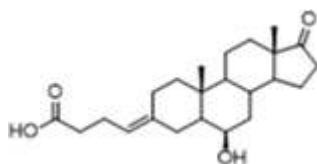
[60] (E)-4-(6 $\alpha$ -hydroxy-17-oxoandrostane-3-ylidene)butyric acid (**CVie201**)



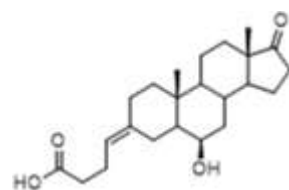
[61] (Z)-4-(6alpha-hydroxy-17-oxoandrostane-3-ylidene)butyric acid (**CVie202**)



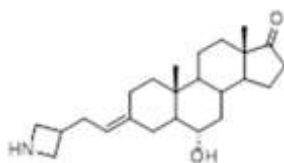
[62] (E)-4-(6beta-hydroxy-17-oxoandrostane-3-ylidene)butyric acid (**CVie203**)



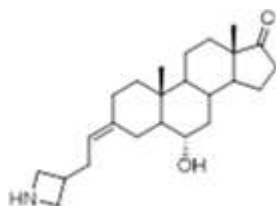
[63] (Z)-4-(6beta-hydroxy-17-oxoandrostane-3-ylidene)butyric acid (**CVie204**)



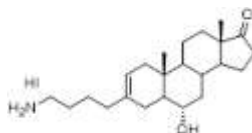
[64] (E)-3-[2-(azetidin-3-yl)ethylidene]-6alpha-hydroxyandrostane-17-one (**CVie205**)



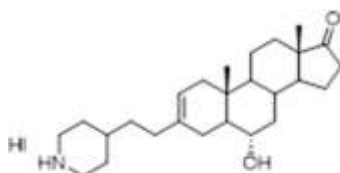
[65] (Z)-3-[2-(azetidin-3-yl)ethyliden]-6alpha-hydroxyandrostane-17-one (**CVie206**)



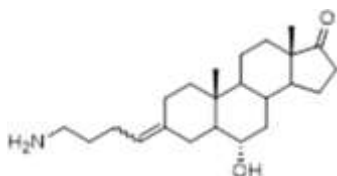
[66] (E)-3-(4-aminobutyl)-6alpha-hydroxyandrost-2-ene-17-one hydroiodide (**CVie207**)



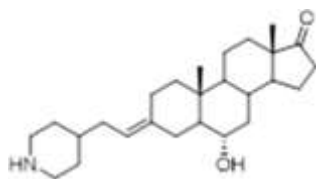
[67] 3-[2-(piperidin-4-yl)ethyl]-6alpha-hydroxyandrost-2-ene-17-one hydroiodide (**CVie208**)



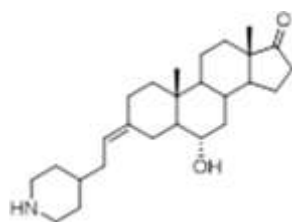
[68] (EZ)-3-(4-aminobutyliden)-6alpha-hydroxyandrostane-17-one (**CVie209**)



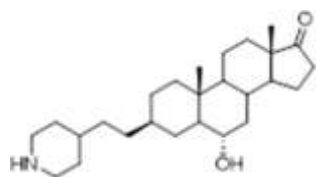
[69] (E)-3-[2-(piperidin-4-yl)ethyliden]-6alpha-hydroxyandrostane-17-one (**CVie210**)



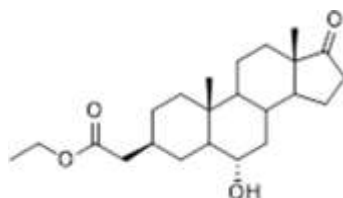
[70] (Z)-3-[2-(piperidin-4-yl)ethyliden]-6alpha-hydroxyandrostane-17-one (**CVie211**)



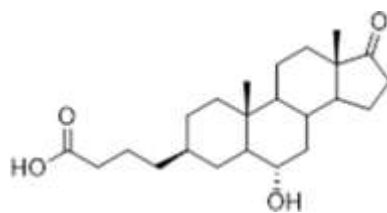
[71] 3beta-[2-(piperidin-4-yl)ethyl]-6alpha-hydroxyandrostane-17-one (**CVie212**)



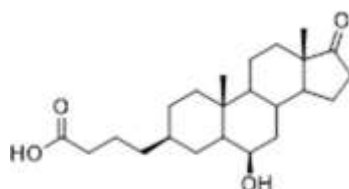
[72] Ethyl (6alpha-hydroxy-17-ketoandrostane-3beta-yl) acetate (**CVie213**)



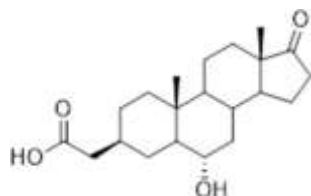
[73] 4-(6alpha-hydroxy-17-oxoandrostane-3-yl) butyric acid (**CVie214**)



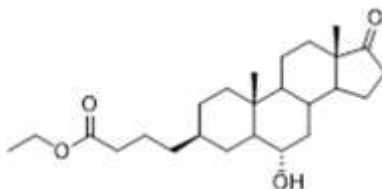
[74] 4-(6beta-hydroxy-17-oxoandrosterane-3-yl) butyric acid (**CVie215**)



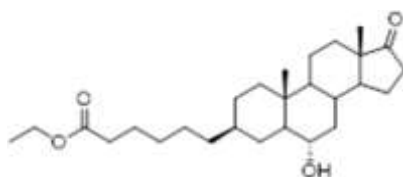
[75] 2-(6beta-hydroxy-17-oxoandrosterane-3-yl) acetic acid (**CVie216**)



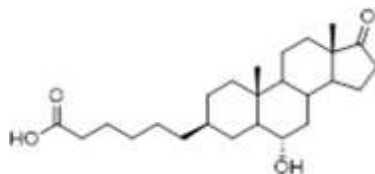
[76] 4-(6alpha-hydroxy-17-oxoandrosterane-3-yl) ethylbutyrate (**CVie217**)



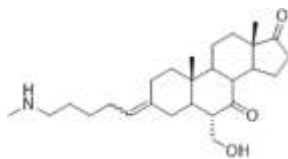
[77] 4-(6alpha-hydroxy-17-oxoandrosterane-3-yl) ethylcaproate (**CVie218**)



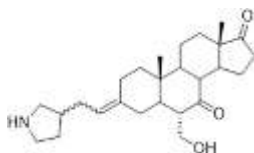
[78] 4-(6beta-hydroxy-17-oxoandrosterane-3-yl) caproic acid (**CVie219**)



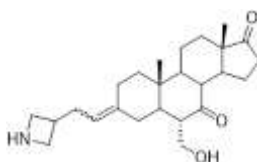
[79] (E,Z)-3-(5-N-methylaminopentyliden)-6alpha-hydroxymethylandrostande-7,17-dione (**CVie401**)



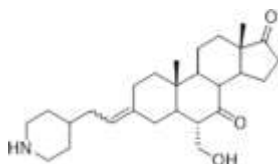
[80] (E,Z)-3-[2-(pirrolidin-3yl)ethyliden]-6alpha-hydroxymethylandrostande-7,17-dione (**CVie402**)



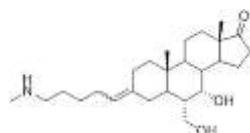
[81] (E,Z)-3-[2-(azetidin-2-yl)ethyliden]-6alpha-hydroxymethylandrostande-7,17-dione (**CVie403**)



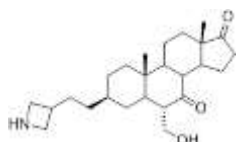
[82] (E,Z)-3-[2-(piperidin-4-yl)ethyliden]-6alpha-hydroxymethylandrostande-7,17-dione (**CVie405**)



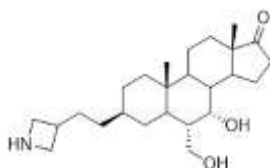
[83] (E,Z)-3-(5-N-methylaminopentyliden)-6alpha-hydroxymethyl-7alpha-hydroxyandrostande-17-one (**CVie406**)



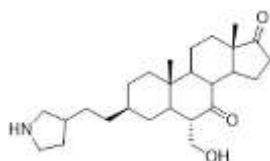
[84] 3beta-[2-(azetidin-2-yl)ethynyl]-6alpha-hydroxymethylandrostande-7,17-dione  
(**CVie407**)



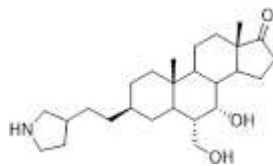
[85] 3beta-[2-(azetidin-2-yl)ethynyl]-6alpha-hydroxymethyl-7alpha-hydroxyandrostande-17-one (**CVie408**)



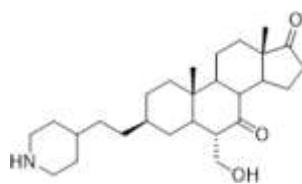
[86] 3beta-[2-(pirrolidin-3-yl)ethynyl]-6alpha-hydroxymethylandrostande-7,17-dione  
(**CVie409**)



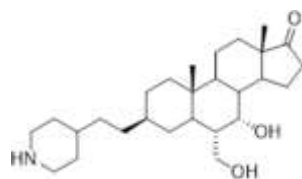
[87] 3beta-[2-(pirrolidin-3-yl)ethynyl]-6alpha-hydroxymethyl-7alpha-hydroxyandrostande-17-one (**CVie410**)



[88] 3beta-[2-(piperidin-4-yl)ethynyl]-6alpha-hydroxymethylandrostande-7,17-dione  
(**CVie411**)



[89] 3beta-[2-(piperidin-4-yl)ethynyl]-6alpha-hydroxymethyl-7alpha-hydroxyandrostande-17-one (**CVie412**)



[90] It is also an object of the present invention to utilize the SERCA2a-activation properties of the compound of formula (**I**) for treating, ameliorating, reversing, or abating or diminishing the symptoms of, or preventing diseases associated with diminished SERCA2a activation, such as heart failure (AHF and/or CHF). Because defective intracellular  $\text{Ca}^{2+}$  distribution has a role in the myocardial remodeling process, its correction by SERCA2a stimulation may counter it. Thus, evolution of an initial and compensated derangement in contractility to overt heart failure may be prevented.

[91] As mentioned above, the androstane derivatives disclosed herein act as pure or predominantly pure SERCA2a activators. As shown in the examples below, these compounds exhibit SERCA2a activation. The pure SERCA2a activators, such as CVie201-204 and CVie213-219 do not significantly inhibit  $\text{Na}^+/\text{K}^+$  ATPase. For instance, these compounds displayed  $\text{IC}_{50}$  values of greater than  $100 \mu\text{M}$  on isolated canine renal  $\text{Na}^+/\text{K}^+$  ATPase (see **Example 3**). On the other hand, the predominantly pure SERCA2a

activators, such as CVie205-212 and CVie401-412, only moderately inhibit Na<sup>+</sup>/K<sup>+</sup> ATPase. For instance, these compounds display IC<sub>50</sub> values of at least 0.8 μM on isolated canine renal Na<sup>+</sup>/K<sup>+</sup> ATPase; preferably, they will have IC<sub>50</sub> values of at least 1 μM on isolated canine renal Na<sup>+</sup>/K<sup>+</sup> ATPase (**Example 3**). Moreover, the predominantly pure SERCA2a activators exhibit about 6-fold to about 170-fold less Na<sup>+</sup>/K<sup>+</sup> ATPase inhibition as compared to istaroxime.

[92] In some embodiments, the predominantly pure and pure SERCA2a activators can be differentiated by their respective functional groups attached to the C3 carbon linker (*i.e.*, X in formula **(I)**). In some embodiments, the pure SERCA2a activators will have a carboxylic acid or a carboxylic ester at the C3 carbon linker. In other embodiments, the predominantly pure SERCA2a activators will have an amine functional group (e.g., primary amine, secondary amine, or cyclic amine) at the C3 carbon linker.

[93] The pure or predominantly pure SERCA2a activator compounds provided herein can be used to treat heart failure. This ability to activate SERCA2a without significantly inhibiting the Na<sup>+</sup>/K<sup>+</sup> ATPase allows these compounds to provide a lusitropic effect on the heart to improve heart function without increasing the risk of arrhythmias or cardiomyocyte damage associated with Na<sup>+</sup>/K<sup>+</sup> ATPase inhibition. As such, these compounds can be used as a medicament for the treatment of heart failure (acute or chronic) and in methods of treatment or prevention of heart failure. As such, they can be included in pharmaceutical compositions formulated for different routes of administration using synthesis and formulation techniques well within the purview of one having ordinary skill in the art. The pharmaceutical compositions and methods of therapeutic treatment utilizing the pure or predominantly pure SERCA2a activators disclosed herein will now be discussed in further detail.

#### Pharmaceutical Compositions

[94] The compounds of formula **(I)** as therapeutic agents can be administered alone or as a component of a pharmaceutical formulation (composition). As such, disclosed herein is a pharmaceutical composition comprising the compound of formula **(I)**, or any of the particular derivatives disclosed herein, in an admixture with at least one pharmaceutically acceptable vehicle and/or excipient. The pharmaceutical composition may be formulated for administering to an individual parenterally, topically, subcutaneously, intramuscularly, orally or by local administration, such as by aerosol or transdermally. In a particular embodiment, the route of administration is oral.

[95] The pharmaceutical compositions can be formulated in any way and can be administered in a variety of unit dosage forms depending upon the condition or disease

and the degree of illness, the general medical condition of each patient, the resulting preferred method of administration and the like. Details on techniques for formulation and administration are well described in the scientific and patent literature, *see, e.g.*, the latest edition of Remington's Pharmaceutical Sciences, Mack Publishing Co, Easton PA.

[96] The compounds may be formulated for administration in any convenient way for use in human or veterinary medicine. Wetting agents, emulsifiers, and lubricants, such as sodium lauryl sulfate and magnesium stearate, as well as coloring agents, release agents, coating agents, sweetening, flavoring and perfuming agents, buffers, preservatives, and antioxidants can also be present in the compositions.

[97] Formulations of the compositions according to the present invention include those suitable for oral, nasal, topical, parenteral – for example by intramuscular or intravenous injection - rectal, subcutaneous, and/or intravaginal administration. The formulations may conveniently be presented in unit dosage form and may be prepared by any methods well known in the art of pharmacy. The amount of active ingredient which can be combined with a carrier material to produce a single dosage form will vary depending upon the subject being treated and/or the particular mode of administration. The amount of active ingredient which can be combined with a carrier material to produce a single dosage form will generally be that amount of the compound which produces a therapeutic effect.

[98] Pharmaceutical formulations as provided herein can be prepared according to any method known to the art for the manufacture of pharmaceuticals. Such formulations can contain sweetening agents, flavoring agents, coloring agents, and preserving agents. A formulation can be admixed with nontoxic pharmaceutically acceptable excipients which are suitable for manufacture. Formulations may comprise one or more diluents, emulsifiers, preservatives, buffers, excipients, etc. and may be provided in such forms as liquids, powders, emulsions, lyophilized powders, sprays, creams, lotions, controlled release formulations, tablets, pills, gels, on patches, in implants, etc.

[99] Pharmaceutical formulations for oral administration can be formulated using pharmaceutically acceptable carriers well known in the art in appropriate and suitable dosages. Such carriers enable the pharmaceuticals to be formulated in unit dosage forms as tablets, gel tabs, pills, powder, dragees, capsules, liquids, lozenges, gels, syrups, slurries, suspensions, etc., suitable for ingestion by the patient. Pharmaceutical preparations for oral use can be formulated as a solid excipient, optionally grinding a resulting mixture, and processing the mixture of granules after adding suitable additional compounds, if desired, to obtain tablets or dragee cores. Suitable solid excipients are carbohydrate or protein fillers include, *e.g.*, sugars, including lactose, sucrose, mannitol,

or sorbitol; starch from corn, wheat, rice, potato, or other plants; cellulose, such as methyl cellulose, hydroxypropylmethyl-cellulose, or sodium carboxymethylcellulose; gums, including arabic and tragacanth; and proteins, such as gelatin and collagen. Disintegrating or solubilizing agents may be added, such as the cross-linked polyvinyl pyrrolidone, agar, alginic acid, or a salt thereof (*e.g.*, sodium alginate).

[100] Dragee cores are provided with suitable coatings, such as concentrated sugar solutions, which may also contain gum arabic, talc, polyvinylpyrrolidone, carbopol gel, polyethylene glycol, titanium dioxide, lacquer solutions, and/or suitable organic solvents or solvent mixtures. Dyestuffs or pigments may be added to the tablets or dragee coatings for product identification or to characterize the quantity of active compound (*i.e.*, dosage). Pharmaceutical preparations used to practice the uses and methods as provided herein can also be used orally using, *e.g.*, push-fit capsules made of gelatin, as well as soft, sealed capsules made of gelatin and a coating such as glycerol or sorbitol. Push-fit capsules can contain active agents mixed with a filler or binders such as lactose or starches, lubricants such as talc or magnesium stearate, and, optionally, stabilizers. In soft capsules, the active agents can be dissolved or suspended in suitable liquids, such as fatty oils, liquid paraffin, or liquid polyethylene glycol with or without stabilizers.

[101] Aqueous suspensions can contain an active agent (*e.g.*, a composition used to practice the uses and methods as provided herein) in admixture with excipients suitable for the manufacture of aqueous suspensions. Such excipients include a suspending agent, such as sodium carboxymethylcellulose, methylcellulose, hydroxypropylmethylcellulose, sodium alginate, polyvinylpyrrolidone, gum tragacanth and gum acacia; and dispersing or wetting agents such as a naturally occurring phosphatide (*e.g.*, lecithin), a condensation product of an alkylene oxide with a fatty acid (*e.g.*, polyoxyethylene stearate), a condensation product of ethylene oxide with a long chain aliphatic alcohol (*e.g.*, heptadecaethylene oxycetanol), a condensation product of ethylene oxide with a partial ester derived from a fatty acid and a hexitol (*e.g.*, polyoxyethylene sorbitol mono-oleate), or a condensation product of ethylene oxide with a partial ester derived from fatty acid and a hexitol anhydride (*e.g.*, polyoxyethylene sorbitan mono-oleate). The aqueous suspension can also contain one or more preservatives such as ethyl or n-propyl p-hydroxybenzoate, one or more coloring agents, one or more flavoring agents, and one or more sweetening agents, such as sucrose, aspartame or saccharin, or erythritol, or rebaudioside A. Formulations can be adjusted for osmolarity.

[102] Oil-based pharmaceuticals are particularly useful for administering hydrophobic active agents suitable in the uses and methods as provided herein. Oil-based suspensions

can be formulated by suspending an active agent in a vegetable oil, such as arachis oil, olive oil, sesame oil or coconut oil, or in a mineral oil such as liquid paraffin; or a mixture of these. See, e.g., U.S. Patent No. 5,716,928 describing using essential oils or essential oil components for increasing bioavailability and reducing inter- and intra-individual variability of orally administered hydrophobic pharmaceutical compounds; see *also* U.S. Patent No. 5,858,401. The oil suspensions can contain a thickening agent, such as beeswax, hard paraffin, or cetyl alcohol. Sweetening agents can be added to provide a palatable oral preparation, such as glycerol, sorbitol or sucrose, erythritol, or rebaudioside A. These formulations can be preserved by the addition of an antioxidant, such as ascorbic acid. As an example of an injectable oil vehicle, see Minto J., *Pharmacol. Exp. Ther.* 1997, 281:93-102. The pharmaceutical formulations as provided herein can also be in the form of oil-in-water emulsions. The oily phase can be a vegetable oil or a mineral oil, as described above, or a mixture of these. Suitable emulsifying agents include naturally-occurring gums, such as gum acacia and gum tragacanth; naturally occurring phosphatides, such as soybean lecithin; esters; or partial esters derived from fatty acids and hexitol anhydrides, such as sorbitan mono-oleate, and condensation products of these partial esters with ethylene oxide, such as polyoxyethylene sorbitan mono-oleate. The emulsion can also contain sweetening agents and flavoring agents, as in the formulation of syrups and elixirs. Such formulations can also contain a demulcent, a preservative, or a coloring agent.

[103] According to the present invention, the pharmaceutical compounds can also be administered by intranasal, intraocular and intravaginal routes including suppositories, insufflation, powders and aerosol formulations (for examples of steroid inhalants, see Rohatagi, *J. Clin. Pharmacol.* 1995, 35:1187-1193; Tjwa, *Ann. Allergy Asthma Immunol.* 1995, 75:107-111, the contents of each of which are incorporated herein by reference in their entireties). Suppositories formulations can be prepared by mixing the drug with a suitable non-irritating excipient which is solid at ordinary temperatures but liquid at body temperatures and will therefore melt in the body to release the drug. Such materials are cocoa butter and polyethylene glycols.

[104] According to the present invention, the pharmaceutical compounds can be delivered by transdermally, by a topical route, formulated as applicator sticks, solutions, suspensions, emulsions, gels, creams, ointments, pastes, jellies, paints, powders, and aerosols.

[105] According to the present invention, the pharmaceutical compounds of formula **(I)** can be delivered by inhalation; for example, in alternative embodiments the compounds of formula **(I)** for inhalation are prepared for dry dispersal, for example, by spray drying

a solution containing the active ingredient, *i.e.* the compound of formula (**I**), *e.g.*, using methods as described in U.S. Patent Nos 6,509,006; 6,592,904; 7,097,827; and 6,358,530, the contents of each of which are incorporated herein by reference in their entireties. Exemplary dry powder excipients include a low molecular weight carbohydrates or polypeptides to be mixed with the compound of formula (**I**) to aid in dispersal. In alternative embodiments, types of pharmaceutical excipients that are useful as carriers for dry powder dispersal include stabilizers such as human serum albumin (HSA), that is also a useful dispersing agent, bulking agents such as carbohydrates, amino acids and polypeptides; pH adjusters or buffers; salts such as sodium chloride; and the like. These carriers may be in a crystalline or amorphous form or may be a mixture of the two. Devices that can be used to deliver powder or aerosol formulations include those as described *e.g.*, in U.S. Patent Nos 5,605,674 and 7,097,827.

[106] According to the present invention, the pharmaceutical compounds can also be delivered as nanoparticles or microspheres for slow release in the body. For example, nanoparticles or microspheres can be administered via intradermal or subcutaneous injection of drug which slowly release subcutaneously; see Rao J., *Biomater*, *Sci. Polym. Ed.* 1995, 7:623-645; as biodegradable and injectable gel formulations, see, *e.g.*, Gao, *Pharm. Res.* 1995, 12:857-863; or, as microspheres for oral administration, see, *e.g.*, Eyles, *J. Pharm. Pharmacol.* 1997, 49:669-674, the entire contents of each of which are incorporated herein by reference in their entireties.

[107] According to the present invention, the pharmaceutical compounds of formula (**I**) can be parenterally administered, such as by intramuscular (IM) or intravenous (IV) administration or administration into a body cavity or lumen of an organ. These formulations can comprise a solution of active agent dissolved in a pharmaceutically acceptable carrier. Acceptable vehicles and solvents that can be employed are water, dextrose in water, and Ringer's solution, which is an isotonic sodium chloride. In addition, sterile fixed oils can be employed as a solvent or suspending medium. For this purpose, any bland fixed oil can be employed including synthetic mono- or diglycerides. In addition, fatty acids such as oleic acid can likewise be used in the preparation of injectables. These solutions are sterile and generally free of undesirable matter. These formulations may be sterilized by conventional, well known sterilization techniques. The formulations may contain pharmaceutically acceptable auxiliary substances as required to approximate physiological conditions such as pH adjusting and buffering agents, toxicity adjusting agents, *e.g.*, sodium acetate, sodium chloride, potassium chloride, calcium chloride, sodium lactate, and the like. The concentration of active agent in these formulations can vary widely, and will be selected primarily based on fluid volumes, viscosities, body weight, and the like, in accordance with the particular mode of

administration selected and the patient's needs. For IV administration, the formulation can be a sterile injectable preparation, such as a sterile injectable aqueous or oleaginous suspension. This suspension can be formulated using those suitable dispersing or wetting agents and suspending agents. The sterile injectable preparation can also be a suspension in a nontoxic parenterally-acceptable diluent or solvent, such as a solution of 1,3-butanediol. The administration can be by bolus or continuous infusion (*e.g.*, substantially uninterrupted introduction into a blood vessel for a specified period of time).

[108] The pharmaceutical compounds and formulations as provided herein can be lyophilized. Provided are a stable lyophilized formulation comprising a composition as provided herein, which can be made by lyophilizing a solution comprising a pharmaceutical as provided herein and a bulking agent, *e.g.*, mannitol, trehalose, raffinose, and sucrose or mixtures thereof. There are many other conventional lyophilizing agents. Among the sugars, lactose is the most common. Also used are citric acid, sodium carbonate, EDTA, benzyl alcohol, glycine, sodium chloride, etc. (see, for example, *Journal of Excipients and Food Chemistry* Vol. 1, Issue 1 (2010) pp 41-54; U.S. patent app. pub. no. 20040028670).

#### Methods of Treatment

[109] According to the present invention, the compounds of formula (**I**) as provided herein can be for use for prophylactic and/or therapeutic treatments. In therapeutic applications, the pharmaceutical compositions are administered to a subject already suffering from a condition or disease in a therapeutically effective amount. In other embodiments, the pharmaceutical compositions provided herein are administered in an amount sufficient to treat, prevent, or ameliorate the condition or disease in an individual in need thereof. The dosage schedule and amounts effective for this use, *i.e.*, the "dosing regimen," will depend upon a variety of factors, including the stage of the disease or condition, the severity of the disease or condition, the general state of the patient's health, the patient's physical status, age, and the like. In calculating the dosage regimen for a patient, the mode of administration also is taken into consideration.

[110] In particular embodiments, the compounds of formula (**I**) are for use for the treatment of an individual with heart failure. In preferred embodiments, the individual exhibits symptoms of, or has been diagnosed with, acute heart failure. While the individual can be a non-human animal, in a preferred embodiment, the individual is a human patient, such as a human patient suffering from heart failure. In other embodiments, the compounds provided herein are for use for the stimulation of SERCA2a in an individual.

[111] In general, the compounds of formula (**I**) and pharmaceutical compositions described herein can be for use for the treatment of heart failure or acute heart failure. A method of therapy includes providing or presenting the individual having heart failure or acute heart failure. In some cases, a measuring step is first carried out to determine the baseline heart function of the individual. The measuring step may include measuring one or more parameters of heart function, such as, but not limited to, heart rate, blood pressure, diastolic relaxation, systolic contraction, left ventricular ejection fraction (LVEF), diastolic blood pressure, systolic blood pressure, cardiac output, stroke volume, deceleration slope (E/DT), contraction velocity ( $s'$ ), early relaxation velocity ( $e'$ ), late relaxation velocity ( $a'$ ), index of left ventricular filling pressure (E/ $e'$ ), E/Ea or E/A ratios, Ea ratio, deceleration time of E wave (DT), mitral deceleration index (DT/E), deceleration slope (E/DT), cardiac index, mitral inflow velocity, and the like. In an individual with heart failure or impaired heart function, the measured parameters may include one or more of decreased heart rate, decreased heart pressure, decreased systolic and/or diastolic blood pressure, reduced left ventricular end-diastolic/systolic volume and function (LVEF), or increased E/Ea or E/A ratios reduced Ea ratio decreased stroke volume. The measuring step can also be used to determine the effectiveness of the administration of the pharmaceutical compositions (*i.e.*, restoration or partial restoration of heart function) and/or to monitor the individual's condition during treatment. As such, the measuring step can be performed prior to, during, or subsequent to the administering of the pharmaceutical composition. As one having ordinary skill in the art will appreciate, any suitable measuring technique available in the art at the time of the measuring step is suitable for use herein, and it is well within the purview of such skilled artisan to select an appropriate measuring technique corresponding to the parameter of interest. A non-limiting list of suitable measuring equipment/techniques includes blood test, echocardiography (including tissue doppler imaging), cardiac catheterization, nuclear stress test, CAT scan, radionuclide ventriculography scan, stethoscope, sphygmomanometer, and the like. For instance, the diastolic relaxation can be measured by echocardiography or PCWP.

[112] The methods disclosed herein also include administering to the individual a therapeutically effective amount of a compound of general formula (**I**). In preferred embodiments, the compound is in a pharmaceutical composition, such as any one of the combinations discussed above. The compound is administered in a therapeutically effective dose as disclosed elsewhere herein, *e.g.*, between about 1 mg/kg and about 20 mg/kg. In a more preferred embodiment, the route of administration is oral. The measuring step can be performed before, during, or after the administering step. For instance, it may be desired to continually monitor one or more of the parameters of heart function during treatment and for a period of time thereafter.

[113] The dosage regimen also takes into consideration pharmacokinetics parameters well known in the art, *i.e.*, the active agents' rate of absorption, bioavailability, metabolism, clearance, and the like (see, e.g., Hidalgo-Aragones (1996) *J. Steroid Biochem. Mol. Biol.* 58:611-617; Groning (1996) *Pharmazie* 51:337-341; Fotherby (1996) *Contraception* 54:59-69; Johnson (1995) *J. Pharm. Sci.* 84:1144-1146; Rohatagi (1995) *Pharmazie* 50:610-613; Brophy (1983) *Eur. J. Clin. Pharmacol.* 24:103-108; the latest Remington's, *supra*). The state of the art allows the clinician to determine the dosage regimen for each individual patient, active agent and disease or condition treated. Guidelines provided for similar compositions used as pharmaceuticals can be used as guidance to determine the dosage regimen, *i.e.*, dose schedule and dosage levels, administered practicing the methods as provided herein are correct and appropriate.

[114] Single or multiple administrations of formulations can be given depending on the dosage and frequency as required and tolerated by the patient. The formulations should provide a sufficient quantity of active agent to effectively treat, prevent, or ameliorate a conditions, diseases or symptoms as described herein. For example, an exemplary pharmaceutical formulation for oral administration of compositions used to practice the methods and uses as provided herein can be in a daily amount of between about 1 to about 20, 50, 100 or 1000 or more  $\mu\text{g}/\text{kg}$  of body weight per day or an equivalent of a pharmaceutically acceptable salt, solvate or hydrate thereof.

[115] In alternative embodiments, an effective amount of a compound of formula (**I**) or an equivalent of a pharmaceutically acceptable salt, solvate or hydrate thereof, administered to an individual in need thereof comprises use of various dosaging schedules, *e.g.*: A) in case of AHFS, to rescue hospitalized patient, a compound of formula (**I**) can be administered by intravenous infusion over 12h, 24h, 48h, 72h, or more, and at doses ranging from 0,1 to 0,5 to about 10, 50 or 100 or more  $\mu\text{g}/\text{kg}$  of body weight per minute; B) in patients rescued from AHFS and discharged from the hospital, the dosage schedule for the maintenance of the therapeutic effect can be in the daily amount of between 1, 10, 50 or 100 or 1000 or more  $\mu\text{g}/\text{kg}$  of body weight.

[116] The compounds of formula (**I**) useful for practicing the invention may be administered to deliver a dose of between 1 ng/kg and 50 mg/kg body weight as a single bolus, or an oral or intravenous dose of between 1  $\mu\text{g}$  and about 20 mg, or in a repeated regimen, or a combination thereof as readily determined by the skilled artisan. In certain embodiments, the dosage comprises at least 0.05 mg/kg, 0.1 mg/kg, or at least 0.2 mg/kg, or at least 0.3 mg/kg, or at least 0.4 mg/kg, or at least 0.5 mg/kg, or at least 0.6 mg/kg, or at least 0.7 mg/kg, or at least 0.8 mg/kg, or at least 0.9 mg/kg, or at

least 1 mg/kg, or at least 2 mg/kg, or at least 3 mg/kg, or at least 4 mg/kg, or at least 5 mg/kg, or at least 6 mg/kg, or at least 7 mg/kg, or at least 8 mg/kg, or at least 9 mg/kg, or at least 10 mg/kg, or at least 15 mg/kg, or at least 20 mg/kg, or at least 25 mg/kg, or at least 30 mg/kg, or at least 35 mg/kg, or at least 40 mg/kg, or at least 45 mg/kg, or at least 50 mg/kg, on a daily basis or on another suitable periodic regimen.

[117] In one embodiment, the invention envisions intravenous or subcutaneous administration of a compound of general formula (I), as described herein, at a therapeutically effective dose that is between about 0.125 mg/kg and about 10 mg/kg, e.g., 0.125 mg/kg, 0.25 mg/kg, 0.5 mg/kg, 0.75 mg/kg, 1 mg/kg, 1.25 mg/kg, 1.5 mg/kg, 1.75 mg/kg, 2 mg/kg, 2.25 mg/kg, 2.5 mg/kg, 2.75 mg/kg, 3 mg/kg, 3.25 mg/kg, 3.5 mg/kg, 3.75 mg/kg, 4 mg/kg, 4.25 mg/kg, 4.5 mg/kg, 4.75 mg/kg, 5 mg/kg, 5.25 mg/kg, 5.5 mg/kg, 5.75 mg/kg, 6 mg/kg, 6.25 mg/kg, 6.5 mg/kg, 6.75 mg/kg, 7 mg/kg, 7.25 mg/kg, 7.5 mg/kg, 7.75 mg/kg, 8 mg/kg, 8.25 mg/kg, 8.5 mg/kg, 8.75 mg/kg, 9 mg/kg, 9.25 mg/kg, 9.5 mg/kg, 9.75 mg/kg, or 10 mg/kg. In a preferred embodiment, the compound is administered via intravenous or subcutaneous delivery (e.g., injection or infusion) at a therapeutically effective dose that is between about 0.25 mg/kg and about 5 mg/kg. In another embodiment, the therapeutically effective dose is between about 0.5 mg/kg and about 5 mg/kg. In yet another embodiment, the therapeutically effective dose is between about 0.5 mg/kg and 4 mg/kg or between about 0.5 mg/kg and about 3 mg/kg.

[118] In another embodiment, the invention envisions intramuscular administration of a compound with general formula (I), as described herein, at a therapeutically effective dose that is between about 0.25 mg/kg and about 50 mg/kg, e.g., 0.25 mg/kg, 0.5 mg/kg, 1 mg/kg, 1.5 mg/kg, 2 mg/kg, 2.5 mg/kg, 3 mg/kg, 3.5 mg/kg, 4 mg/kg, 4.5 mg/kg, 5 mg/kg, 5.5 mg/kg, 6 mg/kg, 6.5 mg/kg, 7 mg/kg, 7.5 mg/kg, 8 mg/kg, 8.5 mg/kg, 9 mg/kg, 9.5 mg/kg, 10 mg/kg, 10.5 mg/kg, 11 mg/kg, 11.5 mg/kg, 12 mg/kg, 12.5 mg/kg, 13 mg/kg, 13.5 mg/kg, 14 mg/kg, 14.5 mg/kg, 15 mg/kg, 15.5 mg/kg, 16 mg/kg, 16.5 mg/kg, 17 mg/kg, 17.5 mg/kg, 18 mg/kg, 18.5 mg/kg, 19 mg/kg, 19.5 mg/kg, 20 mg/kg, 20.5 mg/kg, 21 mg/kg, 21.5 mg/kg, 22 mg/kg, 22.5 mg/kg, 23 mg/kg, 23.5 mg/kg, 24 mg/kg, 24.5 mg/kg, 25 mg/kg, 26 mg/kg, 27 mg/kg, 28 mg/kg, 29 mg/kg, 30 mg/kg, 31 mg/kg, 32 mg/kg, 33 mg/kg, 34 mg/kg, 35 mg/kg, 36 mg/kg, 37 mg/kg, 38 mg/kg, 39 mg/kg, 40 mg/kg, 41 mg/kg, 42 mg/kg, 43 mg/kg, 44 mg/kg, 45 mg/kg, 46 mg/kg, 47 mg/kg, 48 mg/kg, 49 mg/kg, or 50 mg/kg. In a preferred embodiment, the androstane derivative is administered via intramuscular delivery (e.g., injection) at a therapeutically effective dose that is between about 0.25 mg/kg and about 35 mg/kg. In another embodiment, the therapeutically effective dose is between about 0.25 mg/kg and 30 mg/kg. In yet another embodiment, the therapeutically effective

dose is between about 0.25 mg/kg and 10 mg/kg. In still other embodiments, the therapeutically effective dose is between about 0.25 mg/kg and 5 mg/kg.

[119] In yet another embodiment, the invention envisions intravitreal administration of a compound with general formula (**I**), as described herein, at a therapeutically effective dose that is between about 1  $\mu$ g and about 10 mg, *e.g.*, 1  $\mu$ g, 1.25  $\mu$ g, 1.5  $\mu$ g, 1.75  $\mu$ g, 2  $\mu$ g, 2.25  $\mu$ g, 2.5  $\mu$ g, 2.75  $\mu$ g, 3  $\mu$ g, 3.25  $\mu$ g, 3.5  $\mu$ g, 3.75  $\mu$ g, 4  $\mu$ g, 4.25  $\mu$ g, 4.5  $\mu$ g, 4.75  $\mu$ g, 5  $\mu$ g, 5.25  $\mu$ g, 5.5  $\mu$ g, 5.75  $\mu$ g, 6  $\mu$ g, 6.25  $\mu$ g, 6.5  $\mu$ g, 6.75  $\mu$ g, 7  $\mu$ g, 7.25  $\mu$ g, 7.5  $\mu$ g, 7.75  $\mu$ g, 8  $\mu$ g, 8.25  $\mu$ g, 8.5  $\mu$ g, 8.75  $\mu$ g, 9  $\mu$ g, 9.25  $\mu$ g, 9.5  $\mu$ g, 9.75  $\mu$ g, 10  $\mu$ g, 20  $\mu$ g, 30  $\mu$ g, 40  $\mu$ g, 50  $\mu$ g, 60  $\mu$ g, 70  $\mu$ g, 80  $\mu$ g, 90  $\mu$ g, 100  $\mu$ g, 150  $\mu$ g, 200  $\mu$ g, 250  $\mu$ g, 300  $\mu$ g, 350  $\mu$ g, 400  $\mu$ g, 450  $\mu$ g, 500  $\mu$ g, 550  $\mu$ g, 600  $\mu$ g, 650  $\mu$ g, 700  $\mu$ g, 750  $\mu$ g, 800  $\mu$ g, 850  $\mu$ g, 900  $\mu$ g, 950  $\mu$ g, 1 mg, 1.1 mg, 1.2 mg, 1.3 mg, 1.4 mg, 1.5 mg, 1.6 mg, 1.7 mg, 1.8 mg, 1.9 mg, 2 mg, 2.1 mg, 2.2 mg, 2.3 mg, 2.4 mg, 2.5 mg, 2.6 mg, 2.7 mg, 2.8 mg, 2.9 mg, 3 mg, 3.5 mg, 4 mg, 4.5 mg, 5 mg, 5.5 mg, 6 mg, 6.5 mg, 7 mg, 7.5 mg, 8 mg, 8.5 mg, 9 mg, 9.5 mg, or 10 mg; preferably, the dose is between about 1  $\mu$ g and about 2,000  $\mu$ g, *e.g.*, about 1  $\mu$ g to about 2,000  $\mu$ g or about 100  $\mu$ g to about 1,500  $\mu$ g, or about 500  $\mu$ g to about 1,200  $\mu$ g, or about 500  $\mu$ g to about 1,000  $\mu$ g. In some embodiments, the therapeutically effective dose of the compound is delivered via intravitreal administration is at least about 0.02 mg, *e.g.*, at least about 0.02 mg, 0.03 mg, 0.04 mg, 0.05 mg, 0.06 mg, 0.07 mg, 0.08 mg, 0.09 mg, 0.1 mg, 0.15 mg, 0.2 mg, 0.25 mg, 0.3 mg, 0.35 mg, 0.4 mg, 0.45 mg, 0.5 mg, 0.55 mg, 0.6 mg, 0.65 mg, 0.7 mg, 0.75 mg, 0.8 mg, 0.85 mg, 0.9 mg, 0.95 mg, or 1 mg.

[120] In another embodiment, the invention envisions oral administration of a compound with general formula (**I**), as described herein, at a therapeutically effective dose that is between about 1 mg/kg and about 20 mg/kg, *e.g.*, 1 mg/kg, 1.5 mg/kg, 2 mg/kg, 2.5 mg/kg, 3 mg/kg, 3.5 mg/kg, 4 mg/kg, 4.5 mg/kg, 5 mg/kg, 5.5 mg/kg, 6 mg/kg, 6.5 mg/kg, 7 mg/kg, 7.5 mg/kg, 8 mg/kg, 8.5 mg/kg, 9 mg/kg, 9.5 mg/kg, 10 mg/kg, 10.5 mg/kg, 11 mg/kg, 11.5 mg/kg, 12 mg/kg, 12.5 mg/kg, 13 mg/kg, 13.5 mg/kg, 14 mg/kg, 14.5 mg/kg, 15 mg/kg, 15.5 mg/kg, 16 mg/kg, 16.5 mg/kg, 17 mg/kg, 17.5 mg/kg, 18 mg/kg, 18.5 mg/kg, 19 mg/kg, 19.5 mg/kg, or 20 mg/kg. In a preferred embodiment, the compound is administered via oral delivery at a therapeutically effective dose that is between about 1 mg/kg and about 10 mg/kg. For instance, in one particular embodiment, a compound with general formula (**I**) is delivered orally to a human at a dose of about 1 and 5 mg/kg. In some embodiments, the oral dose described herein is administered once. In other embodiments, it is administered daily.

[121] In another embodiment, a therapeutically effective amount of a compound with general formula **(I)**, as described herein, is administered to an individual by infusion according to dosing schedules, such as, from about 0.1 to about 5.0  $\mu\text{g}/\text{kg}/\text{min}$ , *e.g.*, 0.1  $\mu\text{g}/\text{kg}/\text{min}$ , 0.2  $\mu\text{g}/\text{kg}/\text{min}$ , 0.3  $\mu\text{g}/\text{kg}/\text{min}$ , 0.4  $\mu\text{g}/\text{kg}/\text{min}$ , 0.5  $\mu\text{g}/\text{kg}/\text{min}$ , 0.6  $\mu\text{g}/\text{kg}/\text{min}$ , 0.7  $\mu\text{g}/\text{kg}/\text{min}$ , 0.8  $\mu\text{g}/\text{kg}/\text{min}$ , 0.9  $\mu\text{g}/\text{kg}/\text{min}$ , 1.0  $\mu\text{g}/\text{kg}/\text{min}$ , 1.1  $\mu\text{g}/\text{kg}/\text{min}$ , 1.2  $\mu\text{g}/\text{kg}/\text{min}$ , 1.3  $\mu\text{g}/\text{kg}/\text{min}$ , 1.4  $\mu\text{g}/\text{kg}/\text{min}$ , 1.5  $\mu\text{g}/\text{kg}/\text{min}$ , 1.6  $\mu\text{g}/\text{kg}/\text{min}$ , 1.7  $\mu\text{g}/\text{kg}/\text{min}$ , 1.8  $\mu\text{g}/\text{kg}/\text{min}$ , 1.9  $\mu\text{g}/\text{kg}/\text{min}$ , 2.0  $\mu\text{g}/\text{kg}/\text{min}$ , 2.1  $\mu\text{g}/\text{kg}/\text{min}$ , 2.2  $\mu\text{g}/\text{kg}/\text{min}$ , 2.3  $\mu\text{g}/\text{kg}/\text{min}$ , 2.4  $\mu\text{g}/\text{kg}/\text{min}$ , 2.5  $\mu\text{g}/\text{kg}/\text{min}$ , 2.6  $\mu\text{g}/\text{kg}/\text{min}$ , 2.7  $\mu\text{g}/\text{kg}/\text{min}$ , 2.8  $\mu\text{g}/\text{kg}/\text{min}$ , 2.9  $\mu\text{g}/\text{kg}/\text{min}$ , 3.0  $\mu\text{g}/\text{kg}/\text{min}$ , 3.1  $\mu\text{g}/\text{kg}/\text{min}$ , 3.2  $\mu\text{g}/\text{kg}/\text{min}$ , 3.3  $\mu\text{g}/\text{kg}/\text{min}$ , 3.4  $\mu\text{g}/\text{kg}/\text{min}$ , 3.5  $\mu\text{g}/\text{kg}/\text{min}$ , 3.6  $\mu\text{g}/\text{kg}/\text{min}$ , 3.7  $\mu\text{g}/\text{kg}/\text{min}$ , 3.8  $\mu\text{g}/\text{kg}/\text{min}$ , 3.9  $\mu\text{g}/\text{kg}/\text{min}$ , 4.0  $\mu\text{g}/\text{kg}/\text{min}$ , 4.1  $\mu\text{g}/\text{kg}/\text{min}$ , 4.2  $\mu\text{g}/\text{kg}/\text{min}$ , 4.3  $\mu\text{g}/\text{kg}/\text{min}$ , 4.4  $\mu\text{g}/\text{kg}/\text{min}$ , 4.5  $\mu\text{g}/\text{kg}/\text{min}$ , 4.6  $\mu\text{g}/\text{kg}/\text{min}$ , 4.7  $\mu\text{g}/\text{kg}/\text{min}$ , 4.8  $\mu\text{g}/\text{kg}/\text{min}$ , 4.9  $\mu\text{g}/\text{kg}/\text{min}$ , or 5.0  $\mu\text{g}/\text{kg}/\text{min}$ . For instance, in some embodiments, the compound is administered by infusion at an effective dose from about 0.2  $\mu\text{g}/\text{kg}/\text{min}$  to about 2.0  $\mu\text{g}/\text{kg}/\text{min}$ , or from about 0.2  $\mu\text{g}/\text{kg}/\text{min}$  to about 1.5  $\mu\text{g}/\text{kg}/\text{min}$ , or from about 0.25  $\mu\text{g}/\text{kg}/\text{min}$  to about 1.0  $\mu\text{g}/\text{kg}/\text{min}$ , or from about 0.5  $\mu\text{g}/\text{kg}/\text{min}$  to about 1.0  $\mu\text{g}/\text{kg}/\text{min}$ .

[122] In alternative embodiments, an effective amount of a compound of formula **(I)**, or an equivalent of a pharmaceutically acceptable salt, solvate, or hydrate thereof, administered to an individual in need thereof is individualized based on monitoring of Pulmonary Capillary Wedge Pressure (PCWP), Tissue Doppler Imaging (TDI) measurements, dyspnea, peripheral and pulmonary venous congestion, urinary volume, exercise capacity, serum biomarkers such as NT-proBNP, and high sensitive cardiac Troponin (hs-cTnT).

[123] In alternative embodiments, a compound of formula **(I)**, or an equivalent of a pharmaceutically acceptable salt, solvate, or hydrate thereof, administered to an individual in need thereof is an amount sufficient to maintain normal exercise tolerance without breathlessness.

[124] In alternative embodiments, an effective amount is demonstrated by reduction of PCWP, orthopnea, paroxysmal nocturnal dyspnea, increase of exercise tolerance, reduction of peripheral and pulmonary venous congestion, such as pulmonary crepitations or rales, reduction of ankle swelling, reduction of biomarkers urinary output such as NT-proBNP, and high sensitive cardiac Troponin (hs-cTnT).

[125] In alternative embodiments, lower dosages of a compound of formula **(I)**, or an equivalent of a pharmaceutically acceptable salt, solvate, or hydrate thereof, are used when administered in the bloodstream or IV or IM (in contrast to administration *e.g.*, orally, by inhalation or subcutaneously) *e.g.*, as an IV or an IM administration, or into a

body cavity or into a lumen of an organ. Substantially higher dosages can be used in topical, spray, inhalation or oral administration or administering by powders, spray or inhalation. Actual methods for preparing parenterally or non-parenterally administrable formulations will be known or apparent to those skilled in the art and are described in more detail in such publications as Remington's (see Remington's Pharmaceutical Sciences, Mack Publishing Co, Easton PA).

[126] In particular embodiments, a compound of formula **(I)**, or an equivalent of a pharmaceutically acceptable salt, solvate or hydrate thereof, are given chronically, *e.g.*, from day of diagnosis and until the last day of a patient's life or until the disease has abated. In alternative embodiments, dose adjustments are required moving from a treatment phase to a maintenance period through the periodic monitoring of specific, conventionally known biomarkers or clinical signs of the disease.

[127] In alternative embodiments, in evaluating the efficacy of a treatment, a treatment regimen or a particular dosage, or to determine if a treatment versus a maintenance dosage should be given, individuals, *e.g.*, patients affected by AHF or CHF, are subject to regular periodic screening for the presence and extent of organ and tissue involvement or damage, *e.g.*, heart (ventricle dilatation, third heart sound cardiac hypertrophy), fatigue, tiredness, reduced exercise tolerance, increased time to recover after exercise, kidney (renal insufficiency, oliguria), lung (orthopnea, paroxysmal nocturnal dyspnea, tachypnea), ankle swelling, elevated jugular venous pressure. A thorough physical examination should be done at a time interval chosen by those experts in the treatment of a cardiovascular disease, in particular AHF or CHF which would concentrate on cardiac, pulmonary and peripheral circulation functions. Accordingly, in alternative embodiments, therapy with a compound of formula **(I)**, or an equivalent of a pharmaceutically acceptable salt, solvate or hydrate thereof, is instituted as early as possible, preferably in emergency, to prevent the rapid evolution of symptoms and continued after patient's discharge for years, preferably during the whole life of the patient or at least a period consistent with the way other drugs are used in HF.

[128] According to the present invention, uses and methods as provided herein can further comprise co-administration with other drugs or pharmaceuticals. In fact, the present invention selectively corrects a depressed cardiac biochemical function (namely the SERCA2a activity). This certainly contributes to relieving the existing HF clinical symptoms, with less unwanted side effects than those of the available therapies (just because the selectivity mentioned above). However, as CHF and AHF are complex clinical syndromes the present invention is potentially associable to existing and future drug classes and /or specific drugs such as: a) drug classes such as, ACE inhibitors, AIRBs,

diuretics, Ca<sup>2+</sup> channel blockers,  $\beta$ -blockers, digitalis, NO donors, vasodilators, SERCA2a stimulators, neprilysin (NEP) inhibitors, myosin filament activators, recombinant relaxin-2 mediators, recombinant NP protein, activators of the soluble guanylate cyclase (sGC), beta-arrestin ligand of angiotensin II receptor; b) specific drugs: hydrochlorothiazide, furosemide, verapamil, diltiazem, carvedilol, metoprolol, hydralazine, eplerenone, spironolactone, lisinopril, ramipril, nitroglycerin, nitrates, digoxin, valsartan, olmesartan, telmisartan, candesartan, losartan, entresto, omecamtiv, sacubitril, serelaxin, ularitide, levosimendan, cinaciguat.

[129] The compounds of the present invention, as used as therapeutic agents, in particular for treating HF, can be combined with other therapeutic agents used in the treatment of the same disease. Exemplary other therapeutic agents are diuretics, for example furosemide, bumetanide, and torasemide. Metolazone, an aldosterone antagonist, such as spironolactone or eplerenone; thiazide diuretics, such as hydrochlorothiazide, metolazone, and chlorthalidone. Other agents are ACE inhibitors, for example lisinopril and ramipril. Also Angiotensin II receptor blockers (ARBs), such as valsartan, candesartan and losartan can be taken into consideration. Angiotensin receptor/neprilysin inhibitor (ARNI), sacubitril for example, are comprised. Other agents can be selected from beta-blockers, such as carvedilol and metoprolol for example, or vasodilators, for example hydralazine, optionally combined with isosorbide dinitrate, hydralazine, nitrates, as nitroglycerin, amlodipine and felodipine nondihydropyridines such as diltiazem or verapamil. The compounds of the present invention can also be combined with digoxin, if needed. Other drugs, as ivabradine and other anticoagulant may be considered. Still, other drugs may include OMECAMTRIV MECARBIL.

[130] The compounds of the present invention can be combined with other therapeutic agents, in particular agents useful for treating cardiovascular diseases, more in particular in the combination therapy of HF. The combined active ingredients can be administered according to different protocols, decided by the medical doctor. According to an embodiment of the present invention, combination therapy can be carried out by administering the compounds of formula **(I)** both at the same time or at different time of the further therapeutically active ingredient or ingredients. In case of concomitant administration, the compound of the present invention and the further active ingredient or ingredients can be each formulated in a respective pharmaceutical composition. In this case, the present invention provides a kit, in particular for the treatment of heart failure, comprising separate pharmaceutical compositions containing the compound of the present invention and the further active ingredient or ingredients, respectively. In another embodiment, the present invention provides a pharmaceutical unit dosage form

kit, in particular for the treatment of HF, comprising compound of the present invention and the further active ingredient or ingredients.

#### Nanoparticles, Nanolipoparticles and Liposomes.

[131] Also provided are nanoparticles, nanolipoparticles, vesicles, and liposomal membranes comprising the compounds provided herein, *e.g.*, to deliver pharmaceutically active compounds and compositions as provided herein (a compound of formula **(I)** or an equivalent of a pharmaceutically acceptable salt, solvate or hydrate thereof) to a subject in need thereof. In alternative embodiments, these compositions are designed to target specific molecules, including biologic molecules, such as polypeptides, including cell surface polypeptides, *e.g.*, for targeting a desired cell type, *e.g.*, a myocyte or heart cell, an endothelial cell, and the like.

[132] Provided are multilayered liposomes comprising compounds used to practice the methods of the present disclosure, *e.g.*, as described in Park *et al.*, U.S. Pat. Pub. No. 20070082042, the content of which is incorporated by reference herein in its entirety. The multilayered liposomes can be prepared using a mixture of oil-phase components comprising squalene, sterols, ceramides, neutral lipids or oils, fatty acids and lecithins, to about 200 to 5000 nm in particle size, to entrap a composition used to practice uses and methods as provided herein.

[133] Liposomes can be made using any method, *e.g.*, as described in U.S. Pat. No.4,534,899; U.S. Pat. Pub. No. 20070042031, including method of producing a liposome by encapsulating an active agent according to the present invention (or a combination of active agents), the method comprising providing an aqueous solution in a first reservoir; providing an organic lipid solution in a second reservoir, and then mixing the aqueous solution with the organic lipid solution in a first mixing region to produce a liposome solution, where the organic lipid solution mixes with the aqueous solution to substantially instantaneously produce a liposome encapsulating the active agent; and immediately then mixing the liposome solution with a buffer solution to produce a diluted liposome solution.

[134] In one embodiment, liposome compositions used to practice uses and methods as provided herein comprise a substituted ammonium and/or polyanions, *e.g.*, for targeting delivery of a compound a compound of formula **(I)** or an equivalent of a pharmaceutically acceptable salt, solvate or hydrate thereof used to practice methods as provided herein to a desired cell type, as described *e.g.*, in U.S. Pat. Pub. No. 20070110798.

[135] Provided are nanoparticles comprising compounds according to the present invention used to practice uses and methods as provided herein in the form of active agent-containing nanoparticles (*e.g.*, a secondary nanoparticle), as described, *e.g.*, in U.S. Pat. Pub. No. 20070077286. In one embodiment, provided are nanoparticles comprising a fat-soluble active agent used to practice a use and method as provided herein or a fat-solubilized water-soluble active agent to act with a bivalent or trivalent metal salt.

[136] In one embodiment, solid lipid suspensions can be used to formulate and to deliver compositions used to practice uses and methods as provided herein to mammalian cells *in vivo*, *in vitro*, or *ex vivo*, as described, *e.g.*, in U.S. Pat. Pub. No. 20050136121.

[137] The compositions and formulations used to practice the uses and methods as provided herein can be delivered by the use of liposomes or nanoliposomes. By using liposomes, particularly where the liposome surface carries ligands specific for target cells, or are otherwise preferentially directed to a specific organ, one can focus the delivery of the active agent into target cells *in vivo*. See, *e.g.*, U.S. Patent Nos. 6,063,400; 6,007,839; Al-Muhammed, J. Microencapsul. 1996, 13:293-306; Chonn, Curr. Opin. Biotechnol. 1995, 6:698-708; Ostro, Am. J. Hosp. Pharm. 1989, 46:1576-1587.

#### Delivery vehicles

[138] In alternative embodiments, any delivery vehicle can be used to practice the uses and methods provided herein, *e.g.*, to deliver the compounds provided herein to a subject in need thereof. For example, delivery vehicles comprising polycations, cationic polymers and/or cationic peptides, such as polyethyleneimine derivatives, can be used as described, *e.g.*, in U.S. Pat. Pub. No. 20060083737.

[139] In one embodiment, a dried polypeptide-surfactant complex is used to formulate a composition used to practice a use and method as provided herein as described, *e.g.*, in U.S. Pat. Pub. No. 20040151766.

[140] In one embodiment, a composition used to practice uses and methods as provided herein can be applied to cells using vehicles with cell membrane-permeant peptide conjugates, *e.g.*, as described in U.S. Patent Nos. 7,306,783; 6,589,503. In one aspect, the composition to be delivered is conjugated to a cell membrane-permeant peptide. In one embodiment, the composition to be delivered and/or the delivery vehicle are conjugated to a transport-mediating peptide, *e.g.*, as described in U.S. Patent No.

5,846,743, describing transport-mediating peptides that are highly basic and bind to poly-phosphoinositides.

[141] In one embodiment, electro-permeabilization is used as a primary or adjunctive means to deliver the composition to a cell using any electroporation system as, for example, as described in U.S. Patent Nos. 7,109,034; 6,261,815; 5,874,268.

#### Preparation of the compounds of formula (I)

[142] The compounds of the present invention can be synthesized by many methods available to those skilled in the art of organic chemistry. General and exemplary synthetic schemes for preparing compounds of the present invention are described below. These schemes are illustrative and are not meant to limit the possible techniques one skilled in the art may use to prepare the compounds disclosed herein. Different methods to prepare the compounds of the present invention will be evident to those skilled in the art. Additionally, the various steps in the synthesis may be performed in an alternate sequence in order to give the desired compound or compounds.

[143] Examples of compounds of the present invention prepared according to methods described in the general schemes are given in the examples section set out hereinafter.

[144] The compounds of the present invention can be synthesized using the methods described below, together with synthetic methods known in the art of synthetic organic chemistry, or by variations thereon as appreciated by those skilled in the art. The reactions are performed in a solvent or solvent mixture appropriate to the reagents and materials employed and suitable for the transformations being effected. It will be understood by those skilled in the art of organic synthesis that the functionality present on the molecule should be consistent with the transformations proposed.

[145] Also, the skilled in the art can easily alter the reagents and reaction conditions exemplified in the schemes below to include any combination of substituents as defined above. Also, the skilled artisan can easily use interchangeable steps for each synthetic process and incorporate isolation and/or purification steps as deemed necessary.

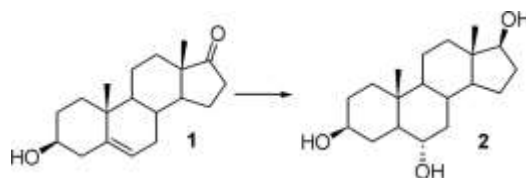
[146] Starting materials and intermediates useful for preparing compounds of the invention are commercially available or can be prepared by well known synthetic procedures.

[147] The final products obtained by the synthesis described below may be purified using techniques commonly known to one skilled in the art such as preparatory chromatography, thin-layer chromatography, HPLC, or crystallization.

[148] Exemplary processes for the synthesis of the compounds of the invention are herein described.

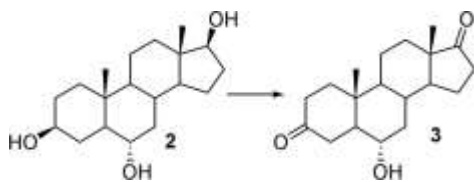
[149] In the following preparations, chemical compounds, solvents, reactants and any other material are from commercial sources, except where otherwise stated. Generally, compounds of formula (**I**) can be prepared by multistep synthesis starting from dehydroepiandrosterone (prasterone). Dehydroepiandrosterone is a commercial product or can be prepared according to well-known methods starting from 4-androsten-3,17-dione (androstenedione).

*Preparation of 5 $\alpha$ -Androstane-3 $\beta$ ,6 $\alpha$ ,17 $\beta$ -triol*



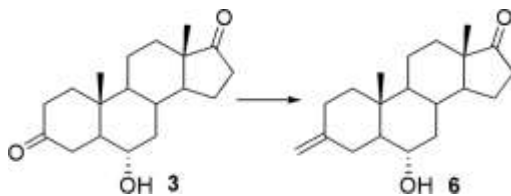
[150] A suitable intermediate for the synthesis of 6- $\alpha$ -3,17 androstanedione (**2**) was produced from dehydroepiandrosterone **1** by hydroboration followed by oxidation as described in De Munari, *et al.* (J. Med. Chem., 2003, 46(17):3644-54). Briefly, a solution of dehydroepiandrosterone **1** (5 g, 17.5 mmol, 1 eq.) in THF (85 mL) was stirred at -20 °C under Ar. Then, 1M BH<sub>3</sub>·THF complex in THF was added to the stirred solution (44 mL, 44 mmol, 2.5 eq.), and stirring was continued at room temperature for 3 hours. H<sub>2</sub>O (85 mL) was cautiously added dropwise and followed by the dropwise addition of NaBO<sub>3</sub>·4H<sub>2</sub>O (5.4 g, 35 mmol, 2 eq). After stirring at room temperature overnight, the mixture was filtered. The solid was washed with THF and then discarded. The liquors were saturated with NaCl and extracted with THF (3 × 40 mL). The combined organic extracts were dried over NaCl and Na<sub>2</sub>SO<sub>4</sub>, filtered, and evaporated to dryness. The crude 5 $\alpha$ -Androstane-3 $\beta$ ,6 $\alpha$ ,17 $\beta$ -triol **2** product was crystallized from EtOAc/MeOH (2/1, 10 mL/g) to give a white solid (3.8 g, 70%).

### Preparation of 6 $\alpha$ -Hydroxyandrostane-3,17-dione



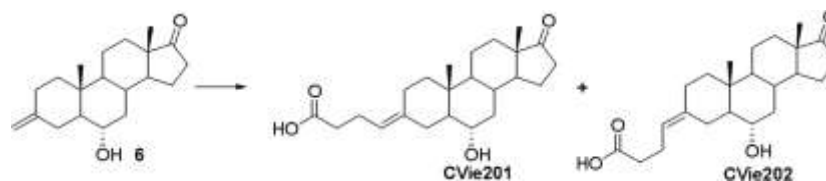
[151] Intermediate **3** was obtained from **2** by selective oxidation at C3 and C17 positions. NBS (3.4 g, 19.5 mmol, 3 eq) was added to a stirred solution of 5 $\alpha$ -Androstane-3 $\beta$ ,6 $\alpha$ ,17 $\beta$ -triol **2** (2 g, 6.5 mmol, 1 eq) in dioxane/H<sub>2</sub>O/pyridine (54/10/1 mL) at 0°C. After the addition, the mixture was allowed to warm to room temperature and was stirred overnight. The orange solution was diluted with water (50 mL) and quenched with Na<sub>2</sub>S<sub>2</sub>O<sub>3</sub> (350 mg). The organic solvent was evaporated under vacuum until a white solid appears. The solid was filtered and washed with water. After drying at 40 °C, 6 $\alpha$ -hydroxyandrostane-3,17-dione **3** was obtained as a white solid (1.3 g, 70%).

### Synthesis of adrostan-3-methylene-17-one



[152] 6 $\alpha$ -3,17 androstanedione **3** was then converted to the exo-methane derivative **6** (adrostan-3-methylene-17-one) via a Wittig reaction selective on the C3 carbonyl followed by the cross-metathesis coupling with 5-pentenoic acid. *t*-BuOK (670 mg, 6 mmol, 4 eq.) was added to a suspension of methyltriphenylphosphonium bromide (1,66 g, 6 mmol, 4 eq.) in THF (10 mL) at -5°C. The solution immediately changed colour to bright orange. After 10 minutes, 6 $\alpha$ -hydroxy androstane-3,17-dione **3** (450 mg, 1.5 mmol, 1eq.) was added while the temperature was kept below 0°C. Immediately after the addition, the reaction was quenched by the addition of aq. 1M HCl (15 mL) and extracted with EtOAc (3x20mL). The combined organic phases were dried over Na<sub>2</sub>SO<sub>4</sub> and evaporated to dryness. The crude extracts were purified over column chromatography (eluent EtOAc: Petroleum spirit 4:6) to produce 376 mg (83%) of adrostan-3-methylene-17-one **6** as a white foam.

*Direct synthesis of CVie 201 and 202 from precursor 6 by cross-metathesis*

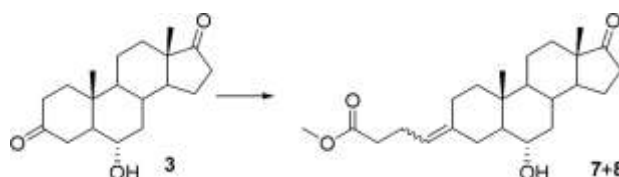


[153] Hoveyda-Grubbs 2<sup>nd</sup> generation catalyst (12 mg, 0.015 mmol, 0.05 eq.) was added to a solution of androstan-3-methylene-17-one **6** (100 mg, 0.33 mmol, 1 eq) in DCM (1 mL). The solution was then heated at reflux and treated with 10  $\mu$ L of 4-pentenoic acid every 20 minutes (total 330  $\mu$ L, 3.3 mmol, 10 eq.). After the end of the addition, the mixture was refluxed for additional 2h. The reaction mixture was concentrated *in vacuo* and purified by flash chromatography (Eluent Acetone: petroleum spirit 3:7+0.1% HCO<sub>2</sub>H) to obtain two different white solids (E)-4-(6 $\alpha$ -hydroxy-17-oxoandrostan-3-yliden)butyric acid (4.8 mg, 4%) (**CVie201**) and (Z)-4-(6 $\alpha$ -hydroxy-17-oxoandrostan-3-yliden)butyric acid (7.2 mg, 6%) (**CVie202**).

[154] Alternatively, **CVie201** and **CVie202** were obtained by varying the Wittig reaction. In one method (Route A), a betaine intermediate was stabilized by the use of a polar solvent, such as DMSO, and a base, such as NaH. The second approach (Route B) allowed for the stabilization of a cyclo-oxaphosphetane intermediate using an aprotic solvent, such as THF, as the base. Route A produced a mixture of diastereomers (60% of Z/syn **CVie202**; 30% E/anti **CVie201**), whereas Route B provided **CVie202** derived from the cyclo-oxaphosphate intermediate. Either procedure requires the production of diastereomers **7** and/or **8** as described below.

*Alternative synthesis of CVie 201 and 202 via Wittig reaction*

*Route A*

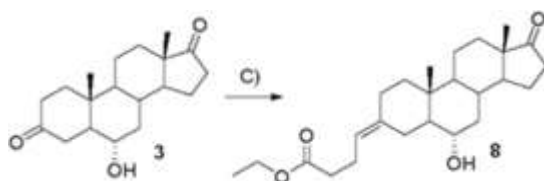


[155] NaH 60% in mineral oil (100 mg, 2.56 mmol, 8 eq.) was carefully added to dry DMSO (1 mL) under Ar atmosphere. The resulting solution was stirred at 60°C for 20

minutes. After cooling at room temperature, (3-carboxypropyl)triphenylphosphonium bromide (550 mg, 1.28 mmol, 4eq.) was added. A bright orange color appeared immediately. The solution was stirred for 2h. Then, 6 $\alpha$ -hydroxyandrostane-3,17 dione **3** (100 mg, 0.32 mmol, 1 eq.) was added to the mixture. The resulting solution was allowed to stir at room temperature for additional 4h. The reaction mixture diluted with EtOAc (25mL) was washed with aq. 1M HCl (3 x 30mL). The organic layer dried over Na<sub>2</sub>SO<sub>4</sub> was evaporated to dryness obtaining 25mg of crude material.

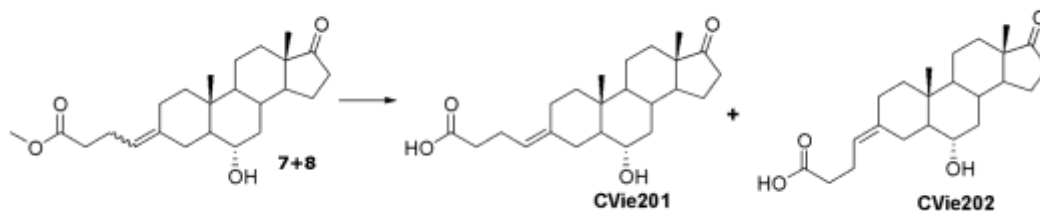
[156] The crude material was first dissolved in MeOH (1.5mL), followed by the addition of EDC hydrochloride (115mg, 0.6mmol, 2eq.) and DMAP (5mg, 0.03 mmol, 0.1 eq.). The solution was stirred at room temperature for 3h. After concentration *in vacuo*. The crude solid was dissolved in EtOAc (15 mL) and washed with aq. 1M HCl (3 x 10mL). The crude product was purified by flash chromatography over silica gel (Acetone:Pet.Sp 3:7) to obtain 25 mg of a clear oil (20%) comprising a mixture of diastereoisomers **7** and **8**.

*Route B*



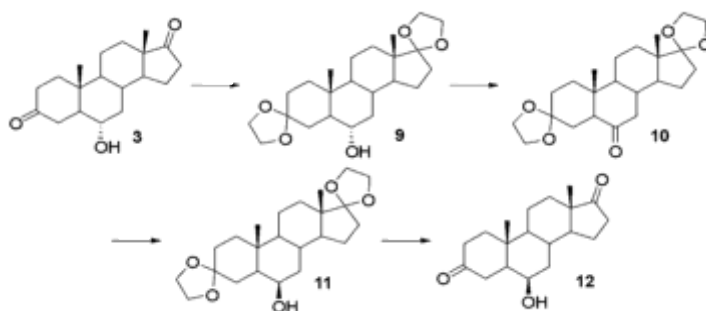
[157] LiHMDS 1M solution in THF (40 mL, 40mmol, 12 eq.) was carefully added to a dry THF (33 mL) suspension of (3-carboxypropyl)triphenylphosphonium bromide (8.5 g, 20 mmol, 6eq.) under Ar atmosphere at -40°C. The solution was stirred at -40°C until a bright orange color appears. Then, 6 $\alpha$ -hydroxyandrostane-3,17 dione **3** (1g, 3.3mmol, 1 eq.) was added to the solution at -40°C. after stirring at room temperature overnight the reaction mixture quenched with aq. 1M HCl (300mL) was extracted with EtOAc (3 x3 50mL). The combined organic layers were dried over Na<sub>2</sub>SO<sub>4</sub> and evaporated to dryness.

[158] The crude material was dissolved in absolute EtOH (17 mL) then EDC hydrochloride (1.26mg, 6.6mmol, 2eq.) and DMAP (50mg, 0.3 mmol, 0.1 eq.) were added. The mixture was allowed to stir at room temperature for 3h. The reaction diluted in EtOAc (150mL) was washed with aq. 1M HCl (3 x 100mL). The crude product was purified by flash chromatography over silica gel (Acetone:Pet.Sp 3:7) to obtain 910mg (72%) of compound **8**.



*Final hydrolysis of methyl (or ethyl) esters*

[159] An aqueous solution of 1M LiOH (150  $\mu$ L, 2.5eq.) was added to a solution of the methyl esters **7** and **8** (25 mg, 0.06 mmol, 1eq.) in THF (600  $\mu$ L) and water (200  $\mu$ L). After 2h, the reaction was diluted with water (10 mL) and quenched by the addition of 1M HCl until the solution reached pH 1. The aqueous phase was extracted with EtOAc (3 x 15mL). The combined organic layers were dried over Na<sub>2</sub>SO<sub>4</sub> and evaporated to dryness. Crude was purified over flash chromatography (AcOEt:Pet.Sp. 7:3 1% HCOOH). Two white solid were obtained corresponding to the E (7 mg, 31%) and Z (12 mg, 54%) diastereoisomers (**CVie201** and **CVie202**, respectively).



*Synthetic way to CVie 203 and 204: synthesis of intermediate compound 12*

[160] To prepare **CVie203** and **CVie204**, the precursor **12** was first produced from 6- $\alpha$ -3,17 androstanedione **3**. The carbonyls of 6- $\alpha$ -3,17 androstanedione **3** were protected as diketals by reaction with ethylene glycol in combination with acid catalysis (p-tSA or camphorsulfonic acid) in toluene, obtaining compound **9**. Oxidation of compound **9** with PCC or other oxidants gave compound **10**, which was then reduced with NaBH<sub>4</sub> or KBH<sub>4</sub> to produce the protected alcohol **11** with the C6-hydroxyl group selectively in the  $\beta$ -configuration. Final cleavage of the cyclic diketals by acidic treatment as described in De Munari *et al.* (J. Med. Chem., 2003, 46(17):3644-54) in acetone afforded precursor **12**.

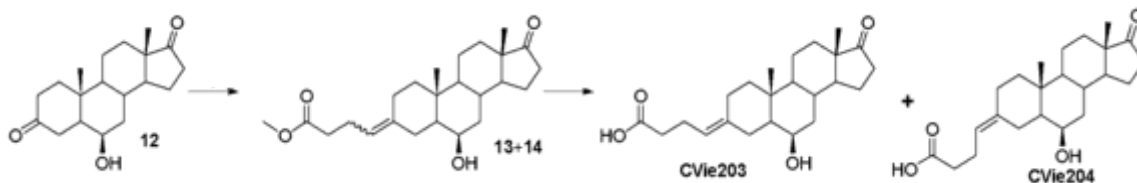
[161] Briefly, a solution of 6 $\alpha$ -hydroxyandrostane-3,17-dione (1.5 g, 4.9 mmol, 1 eq), ethylene glycol (10.5 mL, 88 mmol, 36eq) and PTSA (561 mg, 2.9 mmol, 0.6 eq) in toluene (160 mL) was stirred at reflux for 12 h with a Dean-Stark trap. After cooling to room temperature, the mixture was neutralized with aq. 5% NaHCO<sub>3</sub> solution. The organic layer was separated and washed with H<sub>2</sub>O (2  $\times$  40 mL), dried over Na<sub>2</sub>SO<sub>4</sub>, and evaporated to dryness to produce 3,3:17,17-Bis(ethylendioxy)androstane-6 $\alpha$ -ol **9** as a white solid compound (1.9 g, 98%).

[162] PCC (148 mg, 0.69 mmol, 4 eq) was added to a solution of 3,3:17,17-bis(ethylendioxy)androstane-6 $\alpha$ -ol (3 g, 14 mmol, 1 eq) **9** and sodium ascorbate (1.2 g, 14 mmol, 4eq.) in dry CH<sub>2</sub>Cl<sub>2</sub> (87 mL) at 0°. The mixture was stirred overnight at room temperature. The mixture was washed with aq. 1M HCl (3  $\times$  30mL) and water (3  $\times$  30 mL). The organic layer was dried over Na<sub>2</sub>SO<sub>4</sub> and evaporated to dryness. Crude was purified by flash chromatography over a column of silica gel (eluent acetone: petroleum spirit 2:8). 3,3:17,17-Bis(ethylendioxy)androstane-6-one **10** was obtained as a white solid (1.53 g (96%)).

[163] NaBH<sub>4</sub> (144 mg, 3 mmol, 1.2 eq) was added to a stirred suspension of 3,3:17,17-bis(ethylendioxy)androstane-6-one **10** (1 g, 2.5 mmol, 1 eq) in MeOH (13 mL) at 0°C. After 2 h at 0 °C, H<sub>2</sub>O (40 mL) was added dropwise. The mixture was extracted with EtOAc (3  $\times$  40 mL). The combined organic extracts were dried over Na<sub>2</sub>SO<sub>4</sub>, filtered, and evaporated to dryness to give a white solid, which was 3,3:17,17-Bis(ethylendioxy)androstane-6 $\beta$ -ol **11** (915 mg, 92%).

[164] PTSA (2.26 g, 11.5 mmol, 5 eq) was added in small portion over 5 minutes to a solution of 3,3:17,17-bis(ethylendioxy)androstane-6 $\beta$ -ol **11** (910 mg, 2.3 mmol, 1 eq) in acetone (46 mL). After stirring at room temperature for 1 h, the solution was quenched by addition of aq. 5% NaHCO<sub>3</sub> until pH 7. After stirring for 5 minutes, a white solid appeared. The volatiles were removed *in vacuo*. The suspension was extracted with CH<sub>2</sub>Cl<sub>2</sub> (3  $\times$  30 mL) and the combined organic extracts were washed with brine (40 mL), dried over Na<sub>2</sub>SO<sub>4</sub>, filtered, and evaporated. The obtained solid was stirred with n-hexane/EtOAc 8/2 (10 mL) for 45 minutes and then collected by filtration. The solid was dried 45 °C for 3 hours. 568 mg (81%) of a white solid was obtained (*i.e.*, 6 $\beta$ -hydroxyandrostane-3,17-dione **12**).

Conversion of **12** into final CVie 203 and 204



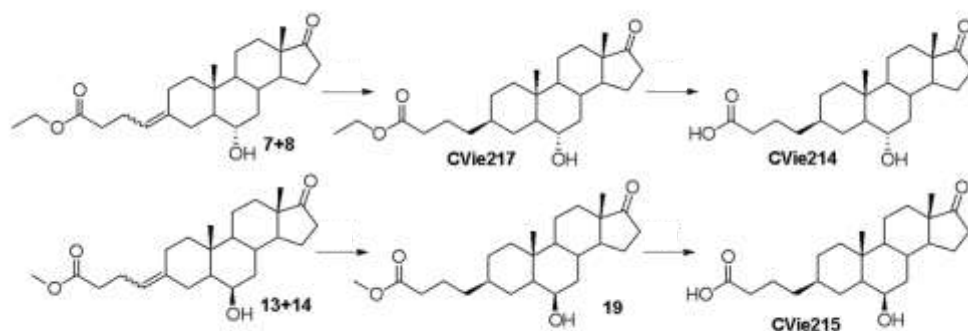
[165] **CVie203** and **CVie204** were then obtained from precursor **12** via the Wittig reaction using the same procedures described above for **CVie201** and **CVie202**. The configurations at the C3-C1' double bond were identified in the two isomers by means of NOESY experiments.

[166] Briefly, NaH 60% in mineral oil (100 mg, 2.56 mmol, 8 eq.) was carefully added to dry DMSO (1 mL) under Ar atmosphere. The resulting solution was stirred at 60°C for 20 minutes. After cooling at room temperature, (3-carboxypropyl)triphenylphosphonium bromide (550 mg, 1.28 mmol, 4eq.) was added. A bright orange color appeared immediately. The solution was stirred for 2h. Then, 6 $\beta$ -hydroxyandrostane-3,17-dione **12** (100 mg, 0.32 mmol, 1 eq.) was added to the mixture. The resulting solution was allowed to stir at room temperature for additional 4h. The reaction mixture was diluted with EtOAc (25mL) and washed with aq. 1M HCl (3 x 30mL). The organic layer was dried over Na<sub>2</sub>SO<sub>4</sub> and evaporated to dryness to obtain 25mg of crude material.

[167] The crude material was then dissolved in MeOH (1.5mL). EDC hydrochloride (115mg, 0.6mmol, 2eq.) and DMAP (5mg, 0.03 mmol, 0.1 eq.) were added. The solution was stirred at room temperature for 3h. After concentration *in vacuo*. The crude solid was dissolved in EtOAc (15 mL) and washed with aq. 1M HCl (3 x 10mL). The crude product was purified by flash chromatography over silica gel (Acetone:Pet.Sp 3:7) to obtain a mixture of diastereoisomers **13** and **14** at 17% yield and 30% yield, respectively.

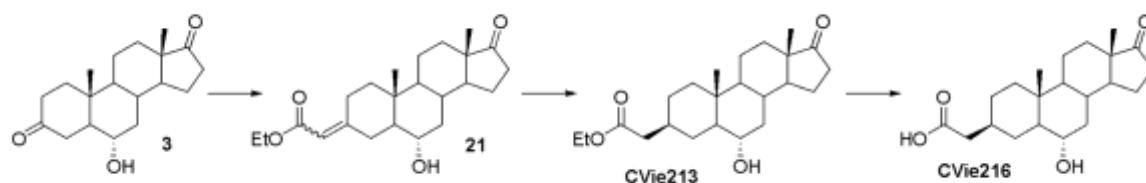
[168] The reaction mixture was concentrated *in vacuo* and purified by flash chromatography (Eluent Acetone: petroleum spirit 3:7+0.1% HCO<sub>2</sub>H) to obtain two different white solids (E)-4-(6beta-hydroxy-17-oxoandrostane-3-ylidene)butyric acid (**CVie203**) and (Z)-4-(6beta-hydroxy-17-oxoandrostane-3-ylidene)butyric acid (**CVie204**).

*Production of **CVie214**, **CVie215**, and **CVie217** via hydrogenation and ester hydrolysis*



[169] Compound **CVie217** was produced from the mixture of diastereomers **7+8** described above. Briefly, hydrogenation of the C3-C1' double bonds of the diastereomers was carried out in EtOAc using Pd-C catalysis. The resulting compound was **CVie217**. The configuration of the stereogenic center formed at C3 was identified by NOESY experiments. Compound **CVie217** was then hydrolyzed with 1M LiOH or NaOH in THF to produce **CVie214**. Similarly, diastereomers **13+14** were hydrogenated in EtOAc using Pd-C catalysis to produce the ester compound **19**, which was then hydrolyzed with 1M LiOH or NaOH in THF to produce **CVie215**.

*Production of **CVie213** and **CVie216** by via Wittig reaction followed by C=C hydrogenation and ester hydrolysis*

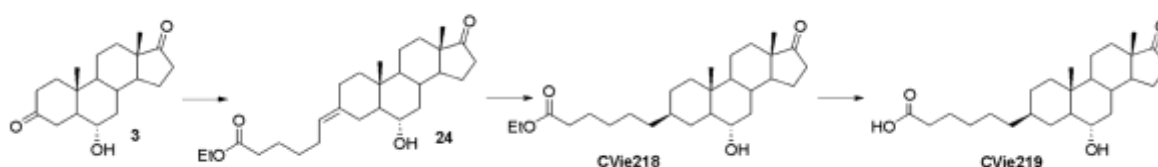


[170] Compound 6- $\alpha$ -3,17 androstenedione **3** was also used as the starting point for the synthesis of **CVie213** and **CVie216** via a Horner-Emmons reaction. First, triethylphosphonoacetate (6.5 mL, 33 mmol, 5 eq) was added carefully to a suspension of NaH 60% in mineral oil (1.3 g, 33 mmol, 5 eq) in DMF (200 mL) under Ar atmosphere at 0°C. The resulting solution was warmed at room temperature and stirred for 20 minutes. Then, 6- $\alpha$ -3,17 androstenedione **3** (2 g, 6.5 mmol, 1 eq) was added at 0°C. After stirring overnight at room temperature, the reaction was quenched by careful addition of H<sub>2</sub>O (100 mL) and extracted with Et<sub>2</sub>O (3 x 150mL). The combined organic layers were dried over Na<sub>2</sub>SO<sub>4</sub> and evaporated *in vacuo*. Crude was purified by flash

chromatography over a column of silica gel (acetone: petroleum spirit 3:7) to produce 2.1g (86%) of a clear oil mixture of two diastereoisomers (compounds **21**).

[171] While under Ar atmosphere, 10% Pd-C (700 mg) was added to a degassed solution of diastereoisomer compounds **21** (2g, 5.3 mmol, 1 eq) in EtOAc (200 mL). After three cycles of vacuum/hydrogen, the reaction was allowed to stir at room temperature overnight under H<sub>2</sub> atmosphere. After removal of hydrogen by vacuum/Ar cycle, the reaction mixture was filtered over CELITE®. The filtered solution was evaporated to dryness. The **CVie213** product was obtained without purification at 1.8 g (90%). Further hydrolysis of **CVie213** with 1M LiOH or NaOH in THF produced **CVie216**.

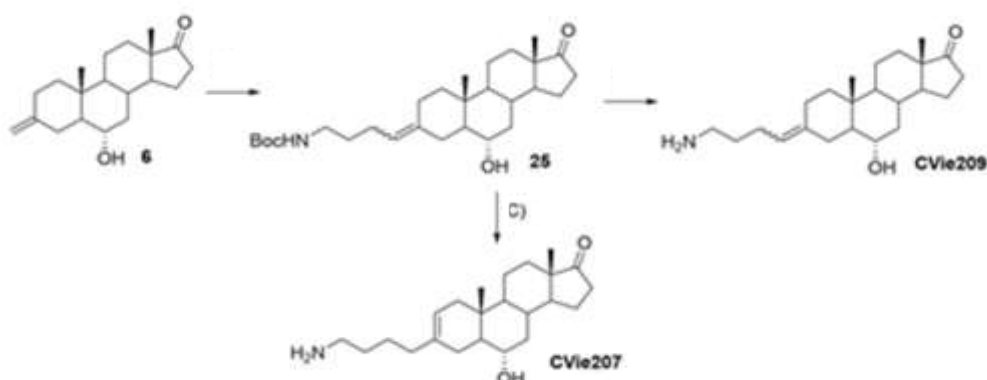
*Production of **CVie218** and **CVie219** via Wittig reaction followed by C=C hydrogenation and ester hydrolysis*



[172] Similarly, reacting 6- $\alpha$ -3,17 androstanedione **3** with the proper triphenylphosphonium salt (e.g., 5-carboxytriphenylphosphonium bromide, LiHMDS, THF then EtOH (or MeOH)) produced compound **24**. Next, catalytic hydrogenation of compound **24** using Pd-C catalysis in the presence of hydrogen produced **CVie218**, which included a C<sub>6</sub> chain at the C-3 position. Hydrolysis of **CVie218** with 1M LiOH or NaOH in THF produced **CVie219**.

*Synthesis of derivatives with primary amine groups from precursor **6** by metathesis reaction with Boc-protected amines followed by Boc deprotection*

For the synthesis of the derivatives with a primary amine group as the X substituent in formula

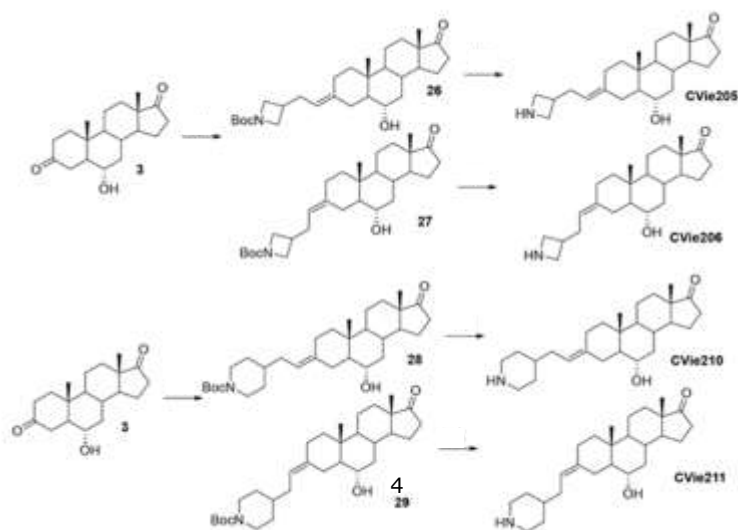


(I), a cross metathesis reaction was carried out on precursor **6** using the same experimental conditions described above for the synthesis of **CVie201** and **CVie202**.

[173] Briefly, a Hoveyda-Grubbs 2<sup>nd</sup> generation catalyst was added to a solution of androstan-3-methylene-17-one **6** in DCM. Androstan-3-methylene-17-one **6** was then combined with an exo-methylene group with the appropriate Boc-protected amine (e.g., tert-butyl pent-4-en-1-yl carbamate or *N*-Boc-4-pentyne-1-amine) to produce diastereoisomers **25** (25% yield). Compound **25** (50 mg, 0,1 mmol, 1 eq) was treated with 500  $\mu$ L of a 1:1 mixture TFA/DCM trifluoroacetic acid in DCM) and then stirred at room temperature to directly cleave the Boc group. After stirring at room temperature for 1 minute, the reaction was diluted with EtOAc (50mL) and washed with saturated aq. NaHCO<sub>3</sub> (3x30mL). The organic phase was dried over Na<sub>2</sub>SO<sub>4</sub>, filtered, and evaporated to dryness to produce (E*Z*)-3-(4-aminobutyliden]-6 $\alpha$ -hydroxyandrostande-17-one (**CVie209**) as white solid (28 mg, 75%)

[174] Alternatively, reacting compound **25** with trimethylsilyl iodide in alcoholic solvent (e.g., MeOH) resulted in Boc cleavage accompanied by migration of the exocyclic double bond to produce **CVie207**, which has an endocyclic double bond between C2 and C3. Briefly, 1M TMSI in DCM (100 $\mu$ L, 0,1 mmol, 1 eq.) was added to a solution of diastereoisomers **25** (50 mg, 0,1mmol, 1eq.) at room temperature. After stirring 2h at the same temperature, the solvent was removed *in vacuo*. Methanol (2 mL) was added to the residue and left for 1h at room temperature. After removal of the solvent *in vacuo*, **CVie207** was obtained without further purification.

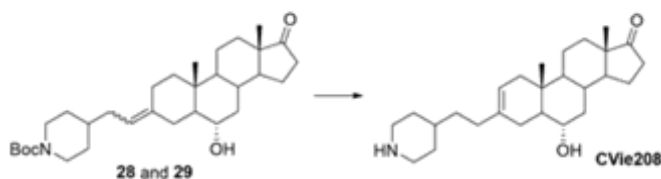
*Synthesis of Cyclic Amine Derivatives with exocyclic insaturations: CVie205, CVie206, CVie210 and CVie211*



[175] Cyclic amine derivatives were synthesized by a sodium hydride (NaH)-DMSO Wittig reaction as described above for **CVie203** and **CVie204** while utilizing an

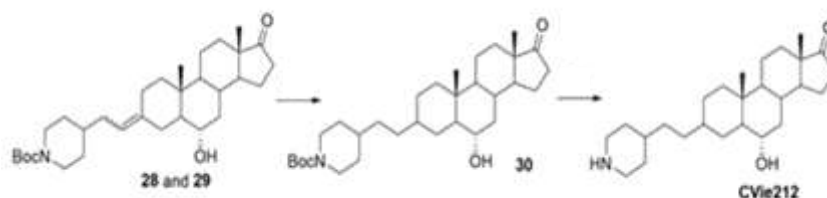
appropriate N-protected phosphonium salt, such as *N*-Boc-4-(2-triphenylphosphoniummethyl)azetidine iodide to produce compounds **26** and **27** or *N*-Boc-3-(2-triphenylphosphoniummethyl)piperidin iodide to produce compounds **28** and **29**. After purification of the diastereomeric mixture, the *N*-Boc group was cleaved by acidic hydrolysis with TFA to produce **CVie205**, **CVie206**, **CVie210** and **CVie211**.

*Synthesis of CVie208 with an endocyclic insaturation (C=C double bond migration during Boc deprotection)*



[176] Further treatment of compounds **28** and **29** with TMSI as described above for the synthesis of **CVie207** produced **CVie208**.

*Hydrogenation and Boc-cleavage with TFA to produce CVie212*

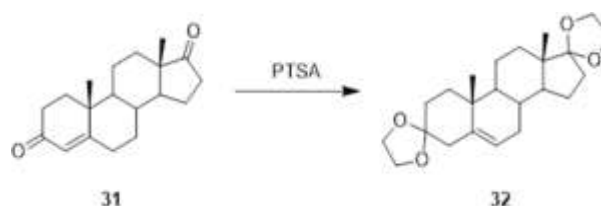


[177] Alternatively, catalytic hydrogenation ( $H_2$ , Pd-C, EtOAc) of the double bonds of compounds **28** and **29** to synthesize compound **30** followed by Boc cleavage with TFA in DCM produced **CVie212**.

[178] Synthesis of compounds bearing a 6 $\alpha$ -hydroxymethylandrostande-7,17-dione was achieved starting from the common intermediate **37**. Compound **37** itself was

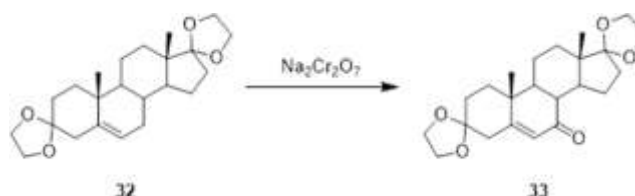
synthesized starting from 4-androsten-3,17-dione **31**, by protection of the two ketone moiety by cyclic acetal **32** and simultaneous migration of the double bond, oxidation of the allylic position by sodium dichromate **33**, formation of the silyl enol ether **35**, hydroxymethylation with  $\text{Me}_3\text{Al}$  and formaldehyde (**36**), and final cleavage of acetals in acidic conditions. The synthesis is described in more detail in the following passages.

*Synthesis of compound **32**: (20S,7R)-7,20-dimethyldispiro[1,3-dioxolane-2,5'-tetracyclo[8.7.0.0<2,7>.0<11,15>]heptadecane-14',2''-1,3-dioxolane]-12-ene*



[179] A mixture of androst-4-ene-3,17-dione **31** (400.0 g, 1.4 mol) and  $\text{PTSA}\cdot\text{H}_2\text{O}$  (13.3 g, 70.0 mmol) in ethylene glycol (8.0 L) was stirred at 100 °C until the reaction was clear. About 5.0 L of glycol was distilled under vacuum so that the boiling temperature was around 80-85 °C. The mixture was cooled down to room temperature. The mixture was adjusted to  $\text{pH}\sim 9$ . Then, the mixture was poured into ice-water. The mixture was filtered, and the solid was washed with water, collected, and triturated with acetone to get crude compound **32** (469.0 g, 89%) as a yellow solid.

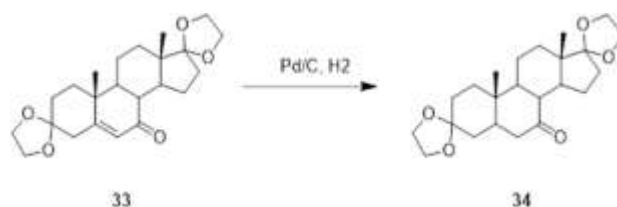
*Synthesis of compound **33**: (20S,7R)-7,20-dimethyldispiro[1,3-dioxolane-2,5'-tetracyclo[8.7.0.0<2,7>.0<11,15>]heptadecane-14',2''-1,3-dioxolane]-12-en-14-one*



[180] A mixture of compound **32** (440.0 g, 1.2 mol), HOSU (541.2 g, 4.7 mol) and  $\text{Na}_2\text{Cr}_2\text{O}_7\cdot\text{H}_2\text{O}$  (527.5 g, 1.8 mol) in acetone (8.0 L) was vigorously stirred at 50 °C for 2 days. After cooling down to room temperature, the mixture was quenched with aq.  $\text{Na}_2\text{SO}_3$  and stirred for 20 min. The mixture was poured into ice-water. The resulting

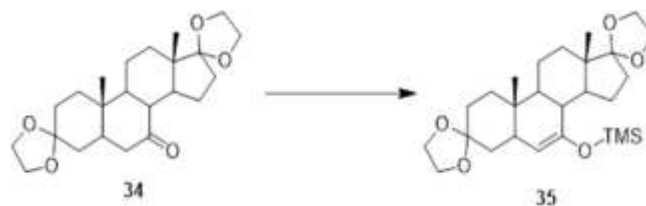
mixture was stirred for 20 min and then filtered. The solid filtrate was washed with water, collected, and dried in vacuum to get crude compound **33** (390.0 g, 85%) as a yellow solid.

*Synthesis of compound **34**: (7S,20S)-7,20-dimethyldispiro[1,3-dioxolane-2,5'-tetracyclo[8.7.0.0<2,7>.0<11,15>]heptadecane-14',2''-1,3-dioxolane]-14-one*



[181] A mixture of compound **33** (50.0 g, 128.9 mmol) in EtOAc (1250 mL) was added to Pd/C (16.0 g). Then the mixture was stirred at room temperature overnight under H<sub>2</sub>. TLC showed the reaction was completed. The mixture was filtered, concentrated, and purified by flash chromatography (PE/EA = 2/1) to obtain compound **34** (25.0 g, 50.0%) as a white solid.

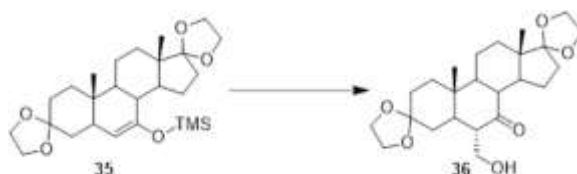
*Synthesis of compound **35**: 1-((20S,7R)-7,20-dimethyldispiro[1,3-dioxolane-2,5'-tetracyclo[8.7.0.0<2,7>.0<11,15>]heptadecane-14',2''-1,3-dioxolane]-13-en-14-yloxy)-1,1-dimethyl-1-silaethane*



[182] A mixture of compound **34** (20.0 g, 51.3 mmol) in dry THF (100.0 mL) was stirred at -78 °C, and then 1.5 M LDA in toluene (205.2 mL, 307.8 mmol) was added dropwise. After stirring at the same temperature for 1 hr, Me<sub>3</sub>SiCl (50.0 mL, 400.1 mmol) was added dropwise. After stirring at -70 °C for 3 hrs, the temperature was raised to -30 °C and triethylamine (33.5 g, 331.5 mmol) was added. After stirring at the same temperature for 1 hr, the mixture was warmed up to room temperature and water (200.0 mL) and EtOAc (100.0 mL) were added. The separated aqueous phase was extracted with EtOAc. The combined organic layers were washed with brine, dried over Na<sub>2</sub>SO<sub>4</sub>,

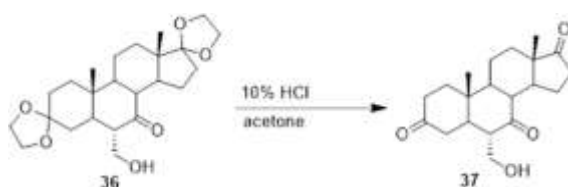
filtered, and evaporated to dryness. The residue was purified by flash chromatography (PE/EA = 2/1) to obtain compound **35** (14.3 g, 60.3 %) as a white solid.

*Synthesis of compound 36: (13S,20S,7R)-13-(hydroxymethyl)-7,20-dimethyldispiro[1,3-dioxolane-2,5'-tetracyclo[8.7.0.0<2,7>.0<11,15>]heptadecane-14',2''-1,3-dioxolane]-14-one*



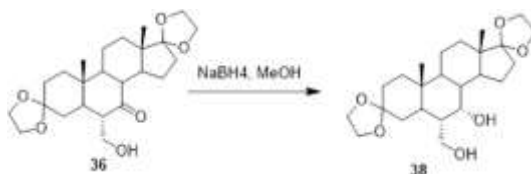
[183] A mixture of 2,6-diphenylphenol (10.0 g, 27.6 mmol) in dry DCM (450.0 mL) was added dropwise to a solution of Me<sub>3</sub>Al in toluene (41.4 mL, 82.9 mmol) while cooling with a ice/water bath so that the temperature did not exceed room temperature. After stirring at room temperature for 1 hr, the solution was cooled at 0 °C, and a solution of trioxane (24.8 g, 276.0 mmol) in dry DCM (100.0 mL) was added dropwise. The light yellow solution was stirred for another 1 hr at 0 °C and then the temperature was cooled down to -78 °C. A solution of compound **35** (10.0 g, 27.6 mmol) in dry DCM (125 mL) was added. After stirring at -78 °C for 1 h, the temperature was raised to -20 °C and the reaction mixture was stirred at that temperature overnight. 5% aq. NaHCO<sub>3</sub> (85.0 mL) was added at room temperature. The jelly mixture was filtered through a CELITE® pad washing thoroughly with DCM. The separated organic layer was washed with water and evaporated. About 1M TBAF in THF (24.0 mL) was added to the residue and the solution was stirred at room temperature for 1.5 h. The solution was washed with water, dried over Na<sub>2</sub>SO<sub>4</sub>, filtered, and evaporated to dryness. The residue was purified by flash chromatography to give compound **36** (6.5 g, 71.4%) as a yellow solid.

*Synthesis of compound 37: (6S,10R,13S)-6-(hydroxymethyl)-10,13-dimethyldecahydro-1H-cyclopenta[a]phenanthrene-3,7,17(2H,4H,8H)-trione*



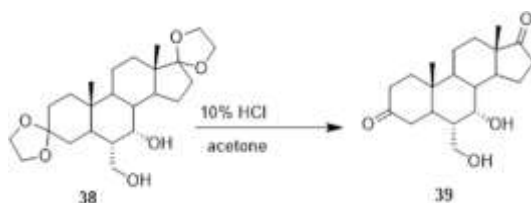
[184] A mixture of compound **36** (8.0 g, 19.0 mmol) in acetone (100.0 mL) was added to 10% aq. HCl (50.0 mL). Then the mixture was heated to 70 °C for 1 h. TLC showed the reaction was completed. The mixture was quenched with 5% aq. NaOH and extracted with DCM (50.0 mL \* 2). The combined organic phases were washed with brine (50.0 mL), dried over Na<sub>2</sub>SO<sub>4</sub>, filtered, concentrated, and purified by flash chromatography (DCM/EA = 4/1) to get the crude product, which was triturated with ether to get the pure product **37** (3.3 g, 52.4 %) as a white solid.

*Synthesis of compound **38**: (13S,14S,20S,7R)-13-(hydroxymethyl)-7,20-dimethyldispiro[1,3-dioxolane-2,5'-tetracyclo[8.7.0.0<2,7>.0<11,15>]heptadecane-14',2''-1,3-dioxolane]-14-ol*



[185] NaBH<sub>4</sub> (4.0 g, 104.8 mmol) was added slowly to a mixture of compound **36** (22.0 g, 52.4 mmol) in MeOH (1000.0 mL) at 0 °C. Then the mixture was stirred at rt for 1 h. TLC showed the reaction was completed. The mixture was quenched with 5% aq. NaH<sub>2</sub>PO<sub>4</sub> (220.0 mL) and extracted with DCM (300.0 mL \* 3). The combined organic phases were washed with brine (200.0 mL), dried over Na<sub>2</sub>SO<sub>4</sub>, filtered, concentrated, and purified by flash chromatography (DCM/EA = 4/1) to get the crude product, which was triturated with ether to obtain the compound **38** (7.5 g, 34.1 %) as a white solid.

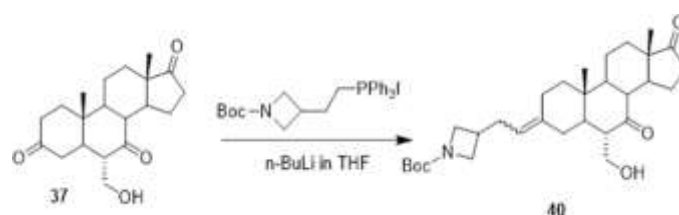
*Synthesis of compound **39**: (8S,9S,15S,2R)-9-hydroxy-8-(hydroxymethyl)-2,15-dimethyltetracyclo[8.7.0.0<2,7>.0<11,15>]heptadecane-5,14-dione*



[186] 10% aq. HCl (35.0 mL) was added to a mixture of compound **38** (5.7 g, 13.5 mmol) in acetone (70.0 mL). Then, the mixture was heated to 70 °C for 1 h. TLC showed the reaction was completed. The mixture was quenched with 5% aq. NaOH and extracted

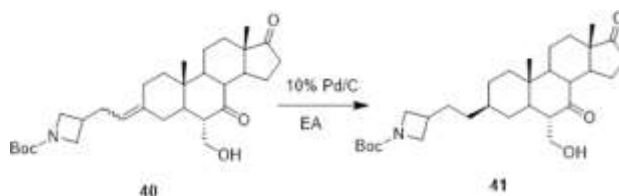
with DCM (50.0 mL \* 2). The combined organic phases were washed with brine (50 mL), dried over Na<sub>2</sub>SO<sub>4</sub>, filtered, and concentrated. The residue was purified by flash chromatography (DCM/EA = 4/1) to get the crude product, which was triturated with ether to obtain the pure product **39** (1.8 g, 40.0 %) as a white solid.

*Synthesis of compound 40: tert-butyl-(2-((6S,10R,13S)-6-(hydroxymethyl)-10,13-dimethyl-7,17-dioxododecahydro-1H-cyclopenta[a]phenanthren-3(2H,4H,10H)-ylidene)ethyl)azetidine-1-carboxylate*



[187] To a solution of phosphonium salt (2.57 g, 4.5 mmol) in THF (25 mL), a solution of n-BuLi in THF (2.5 M, 3.6 mL, 9.0 mmol) was added at -78 °C. The mixture was stirred at 30 °C for 1 hour. Next, the compound **37** (500 mg, 1.5 mmol) was added to the mixture at -20 °C and then warmed to 30°C for 2 hours. The mixture was quenched with sat.NH<sub>4</sub>Cl (25 mL) and extracted with EtOAc (25 mL \* 3). The combined organic layers were concentrated and the residue was purified by column chromatography on silica gel (hexane/EtOAc = 1/1) to give the crude compound. The compound was purified by reverse column to obtain pure compound **40** (60 mg, 8%) as a white solid.

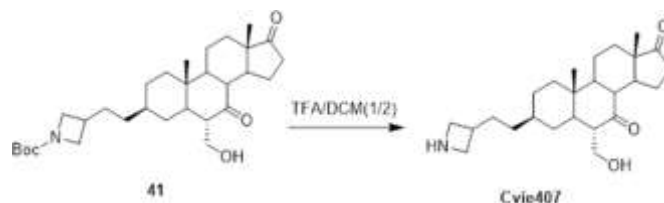
*Synthesis of compound 41: tert-butyl-3-(2-((3S,6S,10R,13S)-6-(hydroxymethyl)-10,13-dimethyl-7,17-dioxohexadeca-hydro-1H-cyclopenta[a]phenanthren-3-yl)ethyl)azetidine-1-carboxylate*



[188] Pd/C (60 mg) was added to the solution of compound **40** (60 mg, 0.12 mmol) in EA (3 mL). Then, the mixture was stirred at room temperature overnight under H<sub>2</sub>. The

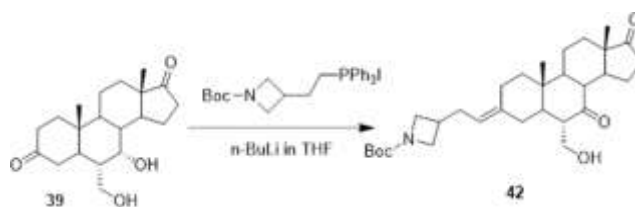
mixture was filtered and the filtrate was concentrated to produce compound **41** (52 mg, 86%) as a white solid.

*Synthesis of CVie407: (3S,6S,10R,13S)-3-(2-(azetidin-3-yl)ethyl)-6-(hydroxymethyl)-10,13-dimethyldodecahydro-1H-cyclopenta[a]phenanthrene-7,17(2H,8H)-dione*



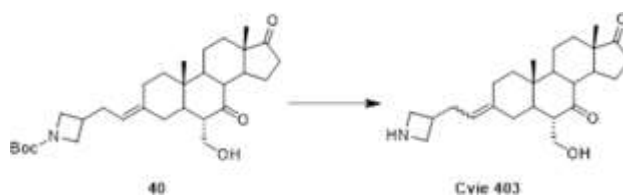
[189] A solution of compound **41** (52 mg, 0.10 mmol) in TFA/DCM (1 mL/2 mL) was stirred at room temperature for 1 hour. The mixture was diluted with *sat.*NaHCO<sub>3</sub> to adjust to pH 8-9. The mixture was extracted with DCM (25 mL \* 3). The combined organic layers were concentrated and the residue was purified by prep-HPLC to produce compound **CVie407** (13 mg, 32%) as a white solid.

*Synthesis of compound 42: tert-butyl-3-((E)-2-((6S,10R,13S)-6-(hydroxymethyl)-10,13-dimethyl-7,17-dioxododecahydro-1H-cyclopenta[a]phenanthren-3(2H,4H,10H)-ylidene)ethyl)azetidine-1-carboxylate*



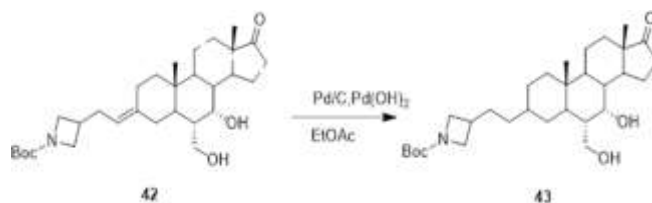
[190] A solution of n-BuLi in THF (2.5 M, 0.7 mL, 1.80 mmol) was added to a solution of compound phosphonium salt (514 mg, 0.90 mmol) in THF (5 mL) at -78 °C. The mixture was stirred at 40 °C for 1 hour. Then, compound **39** (100 mg, 0.30 mmol) was added to the mixture at 0 °C and then warmed to 40 °C overnight. The reaction was repeated for nine times. The mixture was quenched with *sat.*NH<sub>4</sub>Cl (80 mL) and extracted with EtOAc (100 mL \* 3). The combined organic layers were concentrated and the residue was purified by prep-HPLC to produce compound **42** (20 mg, 1%) as a yellow solid.

Synthesis of **CVie403**: (6*S*,10*R*,13*S*)-3-(2-(azetidin-3-yl)ethylidene)-6-(hydroxymethyl)-10,13-dimethyldodecahydro-1*H*-cyclopenta[*a*]phenanthrene-7,17(2*H*,8*H*)-dione



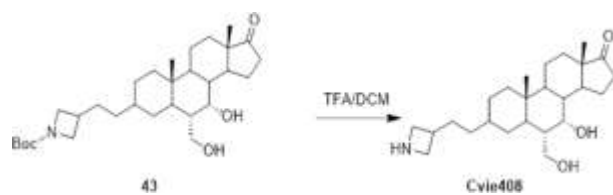
[191] The solution of compound **40** (130 mg, 0.26 mmol) in TFA/DCM (1 mL/2 mL) was stirred at room temperature for 1 hour. The mixture was basified with sat.NaHCO<sub>3</sub> to pH 8-9. The mixture was extracted with DCM (30 mL \*3). The combined organic layer was concentrated and the residue was purified by prep-HPLC to produce compound **CVie403** (13 mg, yield 13%) as a yellow solid.

Synthesis of compound **43**: 3-(2-((6*S*,7*S*,10*R*,13*S*)-7-hydroxy-6-(hydroxymethyl)-10,13-dimethyl-17-oxohexadecahydro-1*H*-cyclopenta[*a*]phenanthren-3-yl)ethyl)azetidine-1-carboxylate



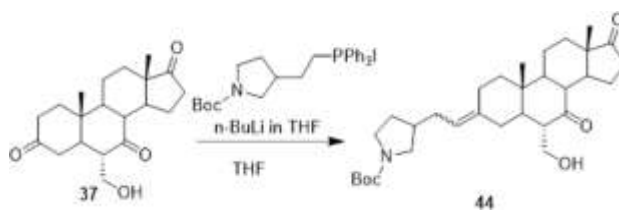
[192] A mixture of compound **42** (20 mg, 0.04 mmol), Pd/C (10%, 20 mg), and Pd(OH)<sub>2</sub> (20%, 20 mg) in EtOAc (2 mL) was stirred at room temperature overnight under H<sub>2</sub> (in balloon). The mixture was filtered and the filtrate was concentrated to give the crude compound **43** (20 mg, 100%) as a brown solid.

Synthesis of **CVie408**: (6*S*,7*S*,10*R*,13*S*)-3-(2-(azetidin-3-yl)ethyl)-7-hydroxy-6-(hydroxymethyl)-10,13-dimethyltetradecahydro-1*H*-cyclopenta[*a*]phenanthren-17(2*H*)-one



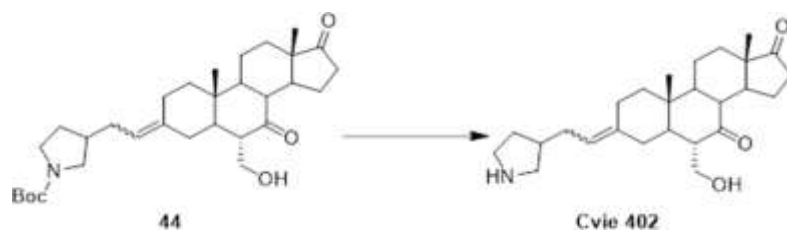
[193] A mixture of compound **43** (20 mg, 0.04 mmol) in TFA/DCM (1:1, 2 mL) was stirred at 0 °C for 30 minutes. The mixture was diluted with *sat.*NaHCO<sub>3</sub> to adjust to pH 8-9. The mixture was extracted with DCM (25 mL \* 3). The combined organic layers were dried over Na<sub>2</sub>SO<sub>4</sub>, filtered and concentrated. The residue was purified by prep-HPLC to produce compound **CVie408** (6.4 mg, 40%) as a yellow solid.

*Synthesis of compound 44: tert-butyl-3-(2-((6S,10R,13S)-6-(hydroxymethyl)-10,13-dimethyl-7,17-dioxododecahydro-1H-cyclopenta[a]phenanthren-3(2H,4H,10H)-ylidene)ethyl)pyrrolidine-1-carboxylate*



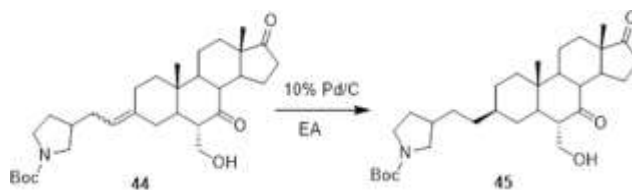
[194] A solution of *n*-BuLi in THF (2.5M, 1.57 mL, 3.94 mmol) was added to a solution of compound phosphonium salt (1.5 g, 2.62 mmol) in THF (15 mL) at -78 °C. The reaction mixture was stirred at 35 °C for 1 hour. Then, a solution of compound **37** (350 mg, 1.05 mmol) was added to the mixture at -20 °C and warmed to room temperature for 2 hours. The mixture was quenched with *sat.*NH<sub>4</sub>Cl (25 mL) and extracted with EtOAc (25 mL \* 3). The combined organic layers were concentrated and the residue was purified by flash chromatography (hexane:EA = 1:1) to give crude compound. Then the compound was purified by reverse column to obtain pure compound **44** (53 mg, 10%) as a white solid.

*Synthesis of CVie402: (6S,10R,13S)-6-(hydroxymethyl)-10,13-dimethyl-3-(2-(pyrrolidin-3-yl)ethylidene)dodecahydro-1H-cyclopenta[a]phenanthrene-7,17(2H,8H)-dione*



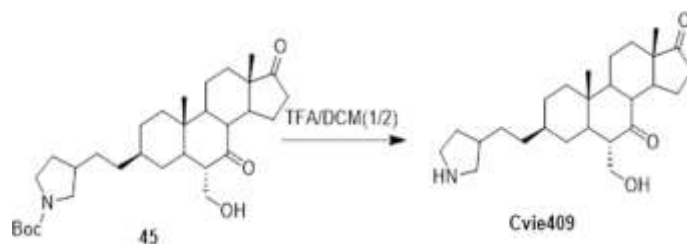
[195] A solution of compound **44** (89 mg, 0.173 mmol) in TFA/DCM (1 mL/2 mL) was stirred at room temperature for 1 hour. The mixture was diluted with sat.NaHCO<sub>3</sub> to adjust pH = 8-9. The mixture was extracted with DCM (25 mL \*3). The combined organic layer was concentrated and the residue was purified by prep-HPLC to produce compound **CVie402** (38 mg, 53%) as a white solid.

*Synthesis of compound 45: tert-butyl-3-(2-((3S,6S,10R,13S)-6-(hydroxymethyl)-10,13-dimethyl-7,17-dioxohexadecahydro-1H-cyclopenta[a]phenanthren-3-yl)ethyl)pyrrolidine-1-carboxylate*



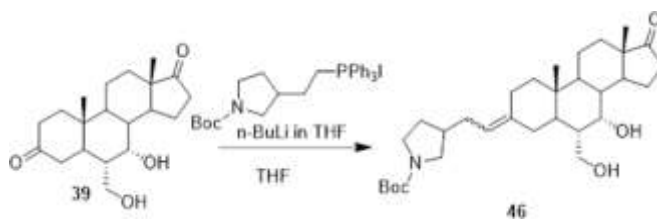
[196] A solution of compound **44** (53 mg, 0.103 mmol) in EA (3 mL) was added to Pd/C (60 mg). Then, the mixture was stirred at room temperature overnight under H<sub>2</sub>. The mixture was filtered and the filtrate was concentrated to produce compound **45** (50 mg, 94%) as a white solid.

Synthesis of **CVie409**: (3*S*,6*S*,10*R*,13*S*)-6-(hydroxymethyl)-10,13-dimethyl-3-(2-(pyrrolidin-3-yl)ethyl)dodecahydro-1*H*-cyclopenta[*a*]phenanthrene-7,17(2*H*,8*H*)-dione



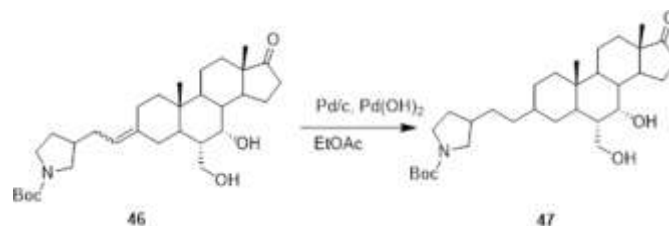
[197] A solution of compound **45** (50 mg, 0.09 mmol) in TFA/DCM (1 mL/2 mL) was stirred at room temperature for 1 hour. The mixture was diluted with *sat.*NaHCO<sub>3</sub> to adjust to pH 8-9. The mixture was extracted with DCM (25 mL \* 3). The combined organic layers were concentrated and the residue was purified by prep-HPLC to produce compound **CVie409** (12 mg, 32%) as a white solid.

Synthesis of compound **46**: *tert*-butyl-3-(2-((6*S*,7*S*,10*R*,13*S*)-7-hydroxy-6-(hydroxymethyl)-10,13-dimethyl-17-oxododecahydro-1*H*-cyclopenta[*a*]phenanthren-3(2*H*,4*H*,10*H*)-ylidene)ethyl)pyrrolidine-1-carboxylate



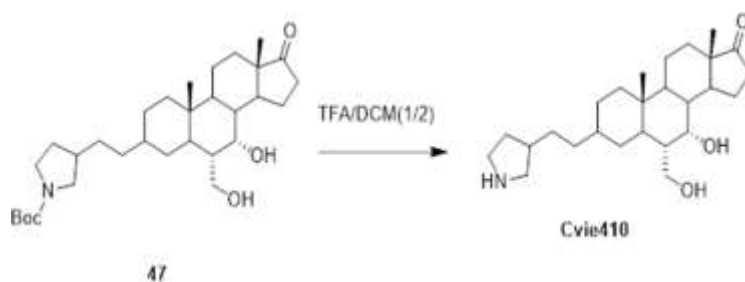
[198] A solution of *n*-BuLi in THF (2.5M, 0.7 mL, 1.80 mmol) was added to a solution of compound phosphonium salt (527 mg, 0.90 mmol) in THF (5 mL) at -78 °C. The reaction mixture was stirred at 35 °C for 1 hour. Then compound **39** (100 mg, 0.30 mmol) was added to the mixture at 0 °C and then warmed to 35 °C overnight. The reaction was repeated for four times. The mixture was quenched with *sat.*NH<sub>4</sub>Cl (80 mL) and extracted with EtOAc (100 mL \* 3). The combined organic layers were concentrated and the residue was purified by prep-HPLC to give compound **46** (26 mg, 3%) as a white solid.

Synthesis of compound **47**: *tert*-butyl-3-(2-((6*S*,7*S*,10*R*,13*S*)-7-hydroxy-6-(hydroxymethyl)-10,13-dimethyl-17-oxohexadecahydro-1*H*-cyclopenta[*a*]phenanthren-3-yl)ethyl)pyrrolidine-1-carboxylate



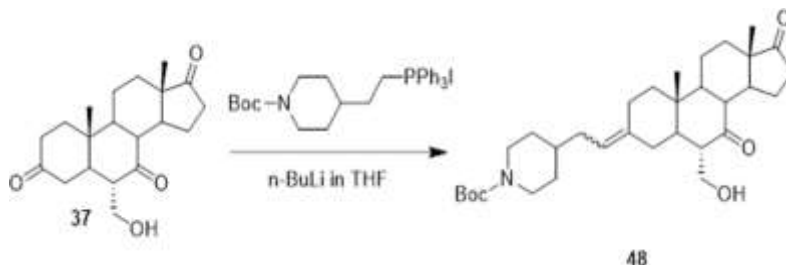
[199] A mixture of compound **46** (26 mg, 0.05 mmol), Pd/C (10%, 30 mg), and Pd(OH)<sub>2</sub> (20%, 30 mg) in EtOAc (3 mL) was stirred at room temperature overnight under H<sub>2</sub> (in balloon). The mixture was filtered and filtrate was concentrated to give the crude compound **47** (26 mg, 100%) as a yellow solid.

*Synthesis of CVie410: (6S,7S,10R,13S)-7-hydroxy-6-(hydroxymethyl)-10,13-dimethyl-3-(2-(pyrrolidin-3-yl)ethyl)tetradecahydro-1H-cyclopenta[a]phenanthren-17(2H)-one*



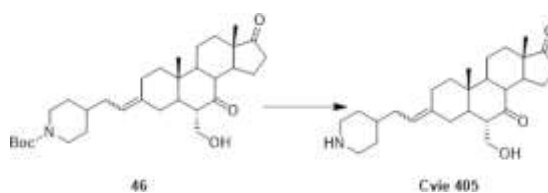
[200] A solution of compound **47** (26 mg, 0.05 mmol) in TFA/DCM (1:2, 2 mL) was stirred at 0 °C for 1 hour. The mixture was diluted with sat. NaHCO<sub>3</sub> to adjust to pH 8-9. The mixture was extracted with DCM (20 mL \* 3). The combined organic layers were dried over Na<sub>2</sub>SO<sub>4</sub>, filtered and concentrated. The residue was purified by prep-HPLC to produce compound **CVie410** (9 mg, 43%) as a yellow solid.

Synthesis of compound **48**: *tert*-butyl-4-(2-((6*S*,10*R*,13*S*)-6-(hydroxymethyl)-10,13-dimethyl-7,17-dioxododecahydro-1*H*-cyclopenta[*a*]phenanthren-3(2*H*,4*H*,10*H*)-ylidene)ethyl)piperidine-1-carboxylate



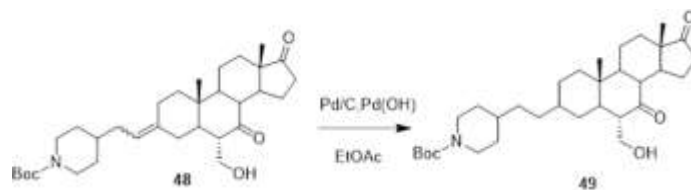
[201] A solution of *n*-BuLi in THF (2.5 M, 2.90 mL, 7.20 mmol) was added to a mixture of compound phosphonium salt (2.16 g, 3.60 mmol) in THF (16 mL) at -78 °C. The reaction mixture was stirred at 30 °C for 1 hour. Then compound **37** (400 mg, 1.20 mmol) was added to the mixture at -20 °C. The mixture was stirred at -20 °C for 30 minutes and then warmed to 30 °C for 2 hours. The mixture was quenched with sat.NH<sub>4</sub>Cl (15 mL) and extracted with EtOAc (30 mL \* 3). The combined organic layers were concentrated and the residue was purified by prep-HPLC to give the compound **48** (28 mg, 4%) as a yellow solid.

Synthesis of **CVie405**: (6*S*,10*R*,13*S*)-6-(hydroxymethyl)-10,13-dimethyl-3-(2-(piperidin-4-yl)ethylidene)dodecahydro-1*H*-cyclopenta[*a*]phenanthrene-7,17(2*H*,8*H*)-dione



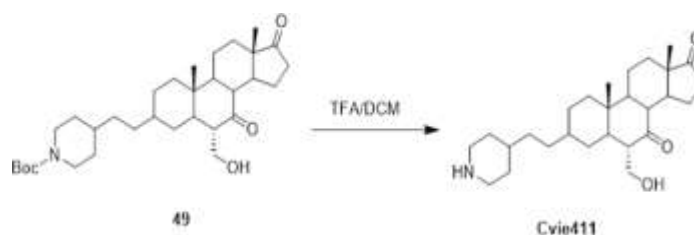
[202] A solution of compound **46** (80 mg, 0.152 mmol) in TFA/DCM (1 mL/2 mL) was stirred at room temperature for 30 minutes. The mixture was basified with sat.NaHCO<sub>3</sub> to pH = 8-9. The mixture was extracted with DCM (25 mL \*3). The combined organic layer was dried over Na<sub>2</sub>SO<sub>4</sub>, filtered and concentrated. The residue was purified by prep-HPLC to produce compound **CVie405** (30 mg, 46%) as a yellow solid.

*Synthesis of compound **49**: tert-butyl-4-(2-((6S,10R,13S)-6-(hydroxymethyl)-10,13-dimethyl-7,17-dioxohexadecahydro-1H-cyclopenta[a]phenanthren-3-yl)ethyl)piperidine-1-carboxylate*



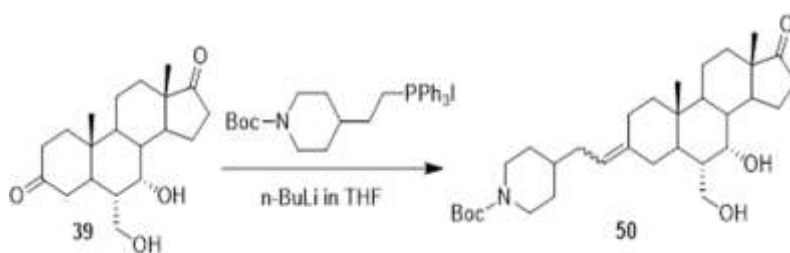
[203] A mixture of compound **48** (28 mg, 0.05 mmol) and Pd/C (10%, 50 mg) in EtOAc (2 mL) was stirred at room temperature overnight under H<sub>2</sub> (in balloon). The mixture was filtered and the filtrate was concentrated to give the crude compound **49** (28 mg, 100%) as a yellow solid.

*Synthesis of **CVie411**: (6S,10R,13S)-6-(hydroxymethyl)-10,13-dimethyl-3-(2-(piperidin-4-yl)ethyl)dodecahydro-1H-cyclopenta[a]phenanthrene-7,17(2H,8H)-dione*



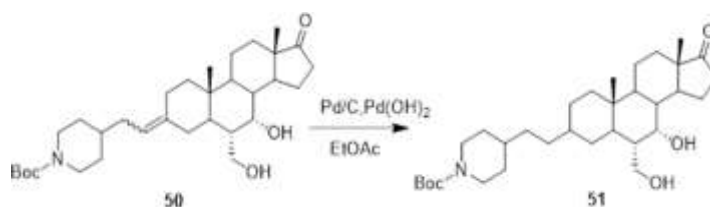
[204] A solution of compound **49** (28 mg, 0.05 mmol) in TFA/DCM (1mL/2 mL) was stirred at room temperature for 30 minutes. The mixture was diluted with sat. NaHCO<sub>3</sub> to adjust to pH 8-9. The mixture was extracted with DCM (25 mL \* 3). The combined organic layers were dried over Na<sub>2</sub>SO<sub>4</sub>, filtered and concentrated. The residue was purified by prep-HPLC to produce compound **CVie411** (10 mg, 43%) as a yellow solid.

*Synthesis of compound **50**: tert-butyl-4-(2-((6S,10R,13S)-6-(hydroxymethyl)-10,13-dimethyl-7,17-dioxododecahydro-1H-cyclopenta[a]phenanthren-3(2H,4H,10H)-ylidene)ethyl)piperidine-1-carboxylate*



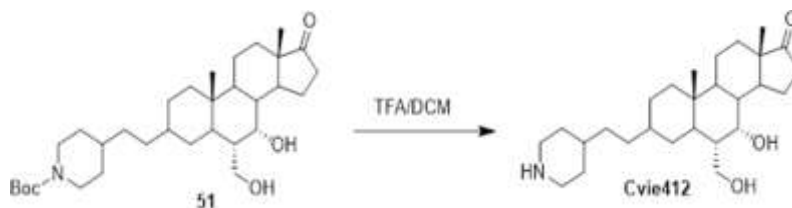
[205] n-BuLi in THF (2.5 M, 0.70 mL, 1.80 mmol) was added to a solution of phosphonium salt (540 mg, 0.90 mmol) in THF (5 mL) at -78 °C. The reaction mixture was stirred at 40 °C for 1 hour. Then, compound **39** (100 mg, 0.30 mmol) was added to the mixture at 0 °C and then warmed to 40 °C for 2 hours. The reaction was repeated for five times. The mixture was quenched with sat.NH<sub>4</sub>Cl (80 mL) and extracted with EtOAc (100 mL \* 3). The combined organic layers were concentrated and the residue was purified by prep-HPLC to give the crude compound **50** (35 mg, 4%) as a white solid.

*Synthesis of compound **51**: tert-butyl-4-(2-((6S,7S,10R,13S)-7-hydroxy-6-(hydroxymethyl)-10,13-dimethyl-17-oxohexadecahydro-1H-cyclopenta[a]phenanthren-3-yl)ethyl)piperidine-1-carboxylate*



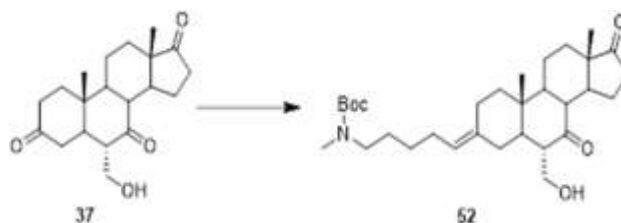
[206] A mixture of compound **50** (35 mg, 0.07 mmol), Pd/C (10%, 40 mg), and Pd(OH)<sub>2</sub> (20%, 40 mg) in EtOAc (2 mL) was stirred at room temperature overnight under H<sub>2</sub> (in balloon). The mixture was filtered and the filtrate was concentrated to give the crude compound **51** (35 mg, 100%) as a brown solid.

Synthesis of **CVie412**: (6*S*,7*S*,10*R*,13*S*)-7-hydroxy-6-(hydroxymethyl)-10,13-dimethyl-3-(2-(piperidin-4-yl)ethyl)tetradecahydro-1*H*-cyclopenta[*a*]phenanthren-17(2*H*)-one



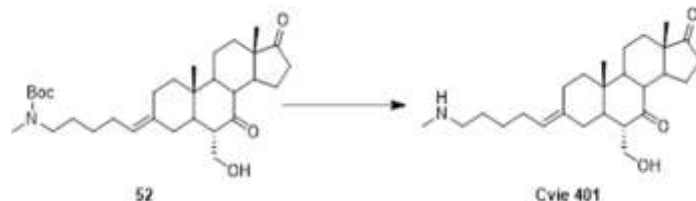
[207] The solution of compound **51** (35 mg, 0.07 mmol) in TFA/DCM (1:2, 2 mL) was stirred at room temperature for 30 minutes. The mixture was diluted with sat. NaHCO<sub>3</sub> to adjust to pH 8-9. The mixture was extracted with DCM (25 mL \* 3). The combined organic layers were dried over Na<sub>2</sub>SO<sub>4</sub>, filtered and concentrated. The residue was purified by prep-HPLC to produce compound **CVie412** (13 mg, 46%) as a yellow solid.

Synthesis of compound **52**: tert-butyl((*E*)-5-((6*S*,10*R*,13*S*)-6-(hydroxymethyl)-10,13-dimethyl-7,17-dioxododecahydro-1*H*-cyclopenta[*a*]phenanthren-3(2*H*,4*H*,10*H*)-ylidene)pentyl)(methyl)carbamate



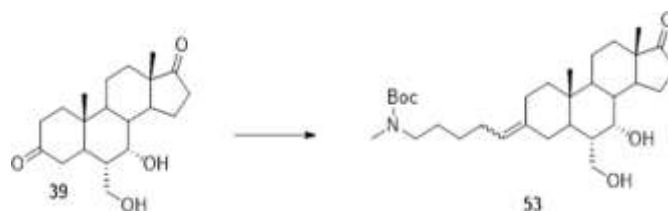
[208] To a mixture of N-Boc-N-methyl-5-triphenylphosphoniumpentenamine iodide (4.26 g, 7.23 mmol) in THF (50 mL), *n*-BuLi (3.18 mL, 7.95 mmol) was added dropwise at -78 °C. The mixture was stirred at 0 °C for 20 min. Then, the mixture was cooled to -30 °C. Compound **37** (800 mg, 2.41 mmol) was then added to the reaction mixture. The mixture was stirred at r.t overnight. The reaction mixture was quenched with H<sub>2</sub>O and concentrated. The residue was purified by column chromatography on silica gel (PE/EtOAc = 1/2) and then purified by prep-HPLC to produce compound **52** (36 mg, 200 mg) as colorless oil.

Synthesis of **CVie401**: (6*S*,10*R*,13*S*,*E*)-6-(hydroxymethyl)-10,13-dimethyl-3-(5-(methylamino)pentylidene)dodecahydro-1*H*-cyclopenta[*a*]phenanthrene-7,17(2*H*,8*H*)-dione



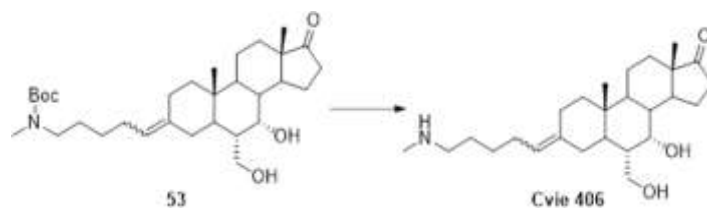
[209] A mixture of compound **52** (60 mg, 0.116 mmol) in TFA/DCM (1 mL/2 mL) was stirred at room temperature overnight. Then, the mixture was concentrated and diluted with EtOAc, washed with sat. Na<sub>2</sub>CO<sub>3</sub>, dried over Na<sub>2</sub>SO<sub>4</sub>, filtered, and concentrated to produce compound **CVie401** (38 mg, 79%) as yellow oil.

Synthesis of compound **53**: tert-butyl(5-((6*S*,7*S*,10*R*,13*S*)-7-hydroxy-6-(hydroxymethyl)-10,13-dimethyl-17-oxododecahydro-1*H*-cyclopenta[*a*]phenanthren-3(2*H*,4*H*,10*H*)-ylidene)pentyl)(methyl)carbamate



[210] To a mixture of N-Boc-N-methyl-5-triphenylphosphoniumpentenamine iodide (4.39 g, 7.45 mmol) in THF (45 mL), a solution of nBuLi in THF (4.46 mL, 2.5 N, 11.16 mmol) was added dropwise at -78°C. Then, the mixture was stirred at 0°C for 20 min. The mixture was cooled to -50°C and compound **39** (830 mg, 2.48 mmol) was added. The mixture was stirred at r.t overnight. The mixture was quenched with H<sub>2</sub>O, concentrated and purified by column chromatography (PE/EtOAc = 1/1) and then purified by prep-HPLC to give compound **53** (80 mg, 300 mg) as white solid.

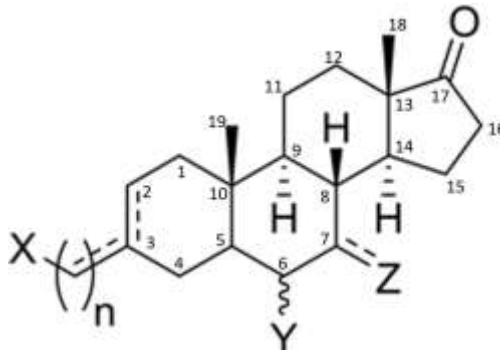
Synthesis of **CVie406**: (6*S*,7*S*,10*R*,13*S*)-7-hydroxy-6-(hydroxymethyl)-10,13-dimethyl-3-(5-(methylamino)pentylidene)tetradecahydro-1*H*-cyclopenta[*a*]phenanthren-17(2*H*)-one



[211] A solution of compound **53** (80 mg, 0.155 mmol) in TFA/DCM (1 mL/2 mL) was stirred at room temperature for 10 minutes. The mixture was basified with sat. NaHCO<sub>3</sub> to pH = 8-9. The mixture was extracted with DCM (25 mL\*2). The combined organic layer was dried over Na<sub>2</sub>SO<sub>4</sub>, filtered and concentrated. The residue was purified by prep-HPLC to give the compound **Cvie406** (60 mg, 94%) as a yellow solid.

[212] The present invention can be described in one or more of the following aspects or combinations thereof:

[213] Aspect 1: A compound having a formula (**I**)



Wherein X is any one of a carboxylic acid, carboxylic ester and their bioisosters (*e.g.*, sulfate, sulfonic acid, phosphate, phosphonate, and nitrogen-containing etherocyclic rings such as triazoles and tetrazoles), primary alcohol, ethers, or an amine group (*e.g.*, primary amine, secondary amine, or cyclic amine);

n is 1, 2, 3, 4, or 5;

the C3-C1' dashed line represents an optional exocyclic double bond C=C;

the C2-C3 dashed line represents an optional endocyclic double bond C=C;

Y at C6 is a hydroxyl (OH) in the  $\alpha$ - or  $\beta$ -configuration or a hydroxymethyl (CH<sub>2</sub>OH) in the  $\alpha$ -configuration;

Z at C7 could be either -H or -OH in an  $\alpha$ -configuration or a ketone. The dashed line represents an optional carbonyl group (C=O) in such position.

or a pharmaceutically acceptable salt, solvate, or hydrate thereof.

[214] Aspect 2: The compound of aspect 1, wherein X is selected from the group consisting of a carboxylic acid, carboxylic ester, primary amine, secondary amine, and cyclic amine.

[215] Aspect 3: The compound of aspect 1, wherein X is a carboxylic acid or a carboxylic ester.

[216] Aspect 4: The compound of aspect 1, wherein X is not a primary amine, secondary amine, or cyclic amine.

[217] Aspect 5: The compound of aspect 1, selected from the group consisting of: (E)-4-(6 $\alpha$ -hydroxy-17-oxoandrostane-3-yliden) butyric acid; (Z)-4-(6 $\alpha$ -hydroxy-17-oxoandrostane-3-yliden) butyric acid; (E)-4-(6 $\beta$ -hydroxy-17-oxoandrostane-3-yliden)butyric acid; (Z)-4-(6 $\beta$ -hydroxy-17-oxoandrostane-3-yliden) butyric acid; (E)-3-[2-(azetidin-3-yl)ethyliden]-6 $\alpha$ -hydroxyandrostane-17-one; (Z)-3-[2-(azetidin-3-yl)ethyliden]-6 $\alpha$ -hydroxyandrostane-17-one; (E)-3-(4-aminobutyl)-6 $\alpha$ -hydroxyandrost-2-ene-17-one hydroiodide; 3-[2-(piperidin-4-yl)ethyl]-6 $\alpha$ -hydroxyandrost-2-ene-17-one hydroiodide; (EZ)-3-(4-aminobutyliden)-6 $\alpha$ -hydroxyandrostane-17-one; (E)-3-[2-(piperidin-4-yl)ethyliden]-6 $\alpha$ -hydroxyandrostane-17-one; (Z)-3-[2-(piperidin-4-yl)ethyliden]-6 $\alpha$ -hydroxyandrostane-17-one; 3 $\beta$ -[2-(piperidin-4-yl)ethyl]-6 $\alpha$ -hydroxyandrostane-17-one; Ethyl (6 $\alpha$ -hydroxy-17-ketoandrostane-3 $\beta$ -yl) acetate; 4-(6 $\alpha$ -hydroxy-17-oxoandrostane-3-yl) butyric acid; 4-(6 $\beta$ -hydroxy-17-oxoandrostane-3-yl) butyric acid; 2-(6 $\beta$ -hydroxy-17-oxoandrostane-3-yl) acetic acid; 4-(6 $\alpha$ -hydroxy-17-oxoandrostane-3-yl) ethylbutyrate; 4-(6 $\alpha$ -hydroxy-17-oxoandrostane-3-yl) ethylcaproate; 4-(6 $\beta$ -hydroxy-17-oxoandrostane-3-yl) caproic acid; (E,Z)-3-(5-N-methylaminopentyliden)-6 $\alpha$ -hydroxymethylandrostane-7,17-dione; (E,Z)-3-[2-(piperidin-3-yl)ethyliden]-6 $\alpha$ -hydroxymethylandrostane-7,17-dione; (E,Z)-3-[2-(azetidin-2-yl)ethyliden]-6 $\alpha$ -hydroxymethylandrostane-7,17-dione; (E,Z)-3-[2-(piperidin-4-yl)ethyliden]-6 $\alpha$ -hydroxymethylandrostane-7,17-dione; (E,Z)-3-(5-N-methylaminopentyliden)-6 $\alpha$ -hydroxymethyl-7 $\alpha$ -hydroxyandrostane-17-one; 3 $\beta$ -[2-(azetidin-2-yl)ethynyl]-6 $\alpha$ -hydroxymethylandrostane-7,17-dione; 3 $\beta$ -[2-

(azetidin-2-yl) ethynyl]-6alpha-hydroxymethyl-7alpha-hydroxyandrostane-17-one; 3beta-[2-(pirrolidin-3yl) ethynyl]-6alpha-hydroxymethylandrostane-7,17-dione; 3beta-[2-(pirrolidin-3yl)ethynyl] 6alpha-hydroxymethyl-7alpha-hydroxyandrostane-17-one; 3beta-[2-(piperidin-4-yl) ethynyl]-6alpha-hydroxymethylandrostane-7,17-dione; and 3beta-[2-(piperidin-4-yl) ethynyl]-6alpha-hydroxymethyl-7alpha-hydroxyandrostane-17-one.

[218] Aspect 6: The compound of aspect 1, selected from the group consisting of: (E)-4-(6alpha-hydroxy-17-oxoandrostane-3-yliden) butyric acid; (Z)-4-(6alpha-hydroxy-17-oxoandrostane-3-yliden) butyric acid; (E)-4-(6beta-hydroxy-17-oxoandrostane-3-yliden) butyric acid; (Z)-4-(6beta-hydroxy-17-oxoandrostane-3-yliden) butyric acid; Ethyl (6alpha-hydroxy-17-ketoandrostane-3beta-yl) acetate; 4-(6alpha-hydroxy-17-oxoandrostane-3-yl) butyric acid; 4-(6beta-hydroxy-17-oxoandrostane-3-yl) butyric acid; 2-(6beta-hydroxy-17-oxoandrostane-3-yl) acetic acid; 4-(6alpha-hydroxy-17-oxoandrostane-3-yl) ethylbutyrate; 4-(6alpha-hydroxy-17-oxoandrostane-3-yl) ethylcaproate; and 4-(6beta-hydroxy-17-oxoandrostane-3-yl) caproic acid.

[219] Aspect 7: The compound of aspect 1, selected from the group consisting of 4-(6alpha-hydroxy-17-oxoandrostane-3-yl) butyric acid and 2-(6beta-hydroxy-17-oxoandrostane-3-yl) acetic acid.

[220] Aspect 8: The compound of any one of aspects 1-7, wherein the pharmaceutically acceptable salt is selected from chloride, bromide, sulfate, phosphate, nitrate, fumarate, succinate, oxalate, malate, tartrate, maleate, citrate, methanesulfate, and benzoate.

[221] Aspect 9: A pharmaceutical composition for use in a method for the treatment of heart failure comprising a therapeutically effective amount of one or more of the compounds of any one of aspects 1-8, in combination with at least one pharmaceutically acceptable vehicle and/or excipient.

[222] Aspect 10: The pharmaceutical composition of aspect 9, formulated for enteral administration, parenteral administration, or inhalation.

[223] Aspect 11: The pharmaceutical composition of aspect 10, formulated for oral administration.

[224] Aspect 12: The pharmaceutical composition of aspect 11, administered at a dose of between about 1 mg/kg and about 20 mg/kg, optionally, the dose is between about 1 mg/kg and about 10 mg/kg.

[225] Aspect 13: The pharmaceutical composition of aspect 9, formulated for intravenous injection.

[226] Aspect 14: The pharmaceutical composition of aspect 13, administered at a dose of between about 0.125 mg/kg and about 10 mg/kg, optionally, the dose is between about 0.25 mg/kg and about 5 mg/kg.

[227] Aspect 15: The pharmaceutical composition of aspect 9, formulated for intramuscular injection.

[228] Aspect 16: The pharmaceutical composition of aspect 15, administered at a dose of between about 0.25 mg/kg and about 50 mg/kg, optionally, the dose is between about 0.25 mg/kg and about 35 mg/kg.

[229] Aspect 17: The pharmaceutical composition of any one of aspects 9-16, administered at least once per day.

[230] Aspect 18: The pharmaceutical composition of any one of aspects 9-17, further comprising one or more additional therapeutically active ingredients.

[231] Aspect 19: The pharmaceutical composition of aspect 18, wherein said one or more additional therapeutically active ingredients are selected from the group consisting of ACE inhibitors, AIRBs, diuretics, Ca<sup>2+</sup> channel blockers,  $\beta$  blockers, digitalis, NO donors, vasodilators, SERCA2a stimulators, neprilysin (NEP) inhibitors, myosin filament activators, recombinant relaxin-2 mediators, recombinant NP protein, activators of the soluble guanylate cyclase (sGC), and beta-arrestin ligand of angiotensin II receptor.

[232] Aspect 20: The pharmaceutical composition of aspect 19, wherein said diuretic is selected from the group consisting of furosemide, bumetanide, torasemide, metolazone, an aldosterone antagonist, thiazide diuretics.

[233] Aspect 21: The pharmaceutical composition of aspect 19, wherein said ACE inhibitor is lisinopril or ramipril.

[234] Aspect 22: The pharmaceutical composition of aspect 18, wherein said one or more additional therapeutically active ingredients are selected from the group consisting of valsartan, candesartan, olmesartan, telmisartan, losartan, sacubitril, carvedilol, omecamtiv, and metoprolol.

[235] Aspect 23: A compound of any one of aspects 1-8 for use as a medicament.

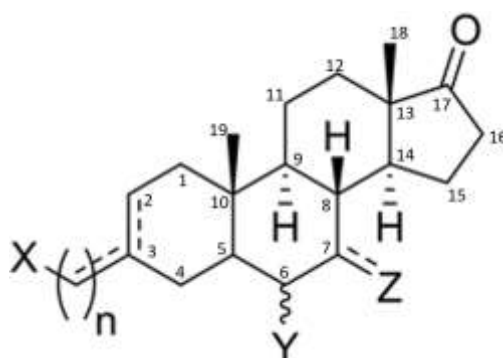
[236] Aspect 24: The compound of aspect 23, for use in treating heart failure.

[237] Aspect 25: The compound of aspect 24, for use in treating acute heart failure.

[238] Aspect 26: The compound of aspect 24, for use in treating chronic heart failure.

[239] Aspect 27: A method of treating an individual having heart failure, the method comprising the steps of: (1) providing an individual having heart failure; (2) administering to the individual a therapeutically effective amount of a pharmaceutical composition comprising (i) a pharmaceutically acceptable carrier and (ii) a predominantly pure SERCA2a stimulator or a pharmaceutically acceptable salt, solvate, or hydrate thereof; and (3) measuring one or more parameters of heart function; wherein the administering of the pharmaceutical composition results in an improvement in heart function.

[240] Aspect 28: The method of aspect 27, wherein the predominantly pure SERCA2a stimulator has the general formula (**I**):



wherein:

X is selected from the group consisting of a carboxylic acid, carboxylic ester, bio-isoster of a carboxylic acid or carboxylic ester (e.g., sulfate, sulfonic acid, phosphate, phosphonate, and nitrogen-containing etherocyclic rings such as triazoles and tetrazoles), primary alcohol, ether, or an amine group (e.g., primary amine, secondary amine, or cyclic amine);

Y is a hydroxyl (OH) in an  $\alpha$ -configuration, a hydroxyl (OH) in a  $\beta$ -configuration, or a hydroxymethyl (CH<sub>2</sub>OH) in an  $\alpha$ -configuration;

Z is selected from the group consisting of a hydrogen (H), a hydroxyl (OH) in an  $\alpha$ -configuration, and a ketone (O);

n is between 1 and 5; and

a dotted line represents an optional double bond (C=C).

[241] Aspect 29: The method of aspect 28, wherein X is selected from the group consisting of a carboxylic acid, carboxylic ester, primary amine, secondary amine, and cyclic amine.

[242] Aspect 30: The method of aspect 28, wherein X is a carboxylic acid or a carboxylic ester.

[243] Aspect 31: The method of aspect 28, wherein X is not a primary amine, secondary amine, or cyclic amine.

[244] Aspect 32: The method of aspect 28, wherein the predominantly pure SERCA2a stimulator is selected from the group consisting of: (E)-4-(6alpha-hydroxy-17-oxoandrostane-3-yliden)butyric acid; (Z)-4-(6alpha-hydroxy-17-oxoandrostane-3-yliden) butyric acid; (E)-4-(6beta-hydroxy-17-oxoandrostane-3-yliden) butyric acid; (Z)-4-(6beta-hydroxy-17-oxoandrostane-3-yliden) butyric acid; (E)-3-[2-(azetid-3-yl)ethyliden]-6alpha-hydroxyandrostane-17-one; (Z)-3-[2-(azetid-3-yl)ethyliden]-6alpha-hydroxyandrostane-17-one; (E)-3-(4-aminobutyl)-6alpha-hydroxyandrost-2-ene-17-one hydroiodide; 3-[2-(piperidin-4-yl)ethyl]-6alpha-hydroxyandrost-2-ene-17-one hydroiodide; (E,Z)-3-(4-aminobutyliden)-6alpha-hydroxyandrostane-17-one; (E)-3-[2-(piperidin-4-yl)ethyliden]-6alpha-hydroxyandrostane-17-one; (Z)-3-[2-(piperidin-4-yl)ethyliden]-6alpha-hydroxyandrostane-17-one; 3beta-[2-(piperidin-4-yl)ethyl]-6alpha-hydroxyandrostane-17-one; Ethyl (6alpha-hydroxy-17-ketoandrostane-3beta-yl) acetate; 4-(6alpha-hydroxy-17-oxoandrostane-3-yl) butyric acid; 4-(6beta-hydroxy-17-oxoandrostane-3-yl) butyric acid; 2-(6beta-hydroxy-17-oxoandrostane-3-yl) acetic acid; 4-(6alpha-hydroxy-17-oxoandrostane-3-yl) ethylbutyrate; 4-(6alpha-hydroxy-17-oxoandrostane-3-yl) ethylcaproate; 4-(6beta-hydroxy-17-oxoandrostane-3-yl) caproic acid; (E,Z)-3-(5-N-methylaminopentyliden)-6alpha-hydroxymethylandrostane-7,17-dione; (E,Z)-3-[2-(pirrolidin-3yl)ethyliden]-6alpha-hydroxymethylandrostane-7,17-dione; (E,Z)-3-[2-(azetid-2-yl)ethyliden]-6alpha-hydroxymethylandrostane-7,17-dione; (E,Z)-3-[2-(piperidin-4-yl)ethyliden]-6alpha-hydroxymethylandrostane-7,17-dione; (E,Z)-3-(5-N-methylaminopentyliden)-6alpha-hydroxymethyl-7alpha-hydroxyandrostane-17-one; 3beta-[2-(azetid-2-yl)ethynyl]-6alpha-hydroxymethylandrostane-7,17-dione; 3beta-[2-(azetid-2-yl)ethynyl]-6alpha-hydroxymethyl-7alpha-hydroxyandrostane-17-one; 3beta-[2-(pirrolidin-3yl)ethynyl]-6alpha-hydroxymethyl-7alpha-hydroxyandrostane-7,17-dione; 3beta-[2-(pirrolidin-3yl)ethynyl]-6alpha-hydroxymethyl-7alpha-hydroxyandrostane-17-one; 3beta-[2-(piperidin-4-yl)ethynyl]-6alpha-hydroxymethylandrostane-7,17-dione; and 3beta-[2-(piperidin-4-yl)ethynyl]-6alpha-hydroxymethyl-7alpha-hydroxyandrostane-17-one.

[245] Aspect 33: The method of aspect 28, wherein the predominantly pure SERCA2a stimulator is selected from the group consisting of: (E)-4-(6alpha-hydroxy-17-oxoandrostane-3-yliden) butyric acid; (Z)-4-(6alpha-hydroxy-17-oxoandrostane-3-yliden) butyric acid; (E)-4-(6beta-hydroxy-17-oxoandrostane-3-yliden) butyric acid; (Z)-4-(6beta-hydroxy-17-oxoandrostane-3-yliden) butyric acid; Ethyl (6alpha-hydroxy-17-ketoandrostane-3beta-yl)acetate; 4-(6alpha-hydroxy-17-oxoandrostane-3-yl) butyric acid; 4-(6beta-hydroxy-17-oxoandrostane-3-yl) butyric acid; 2-(6beta-hydroxy-17-oxoandrostane-3-yl) acetic acid; 4-(6alpha-hydroxy-17-oxoandrostane-3-yl) ethylbutyrate; 4-(6alpha-hydroxy-17-oxoandrostane-3-yl) ethylcaproate; and 4-(6beta-hydroxy-17-oxoandrostane-3-yl) caproic acid.

[246] Aspect 34: The method of aspect 28, wherein the predominantly pure SERCA2a stimulator is selected from the group consisting of 4-(6alpha-hydroxy-17-oxoandrostane-3-yl) butyric acid and 2-(6beta-hydroxy-17-oxoandrostane-3-yl) acetic acid.

[247] Aspect 35: The method of any one of aspects 28-34, wherein the pharmaceutically acceptable salt is selected from chloride, bromide, sulfate, phosphate, nitrate, fumarate, succinate, oxalate, malate, tartrate, maleate, citrate, methanesulfate, and benzoate.

[248] Aspect 36: The method of any one of aspects 28-35, wherein the pharmaceutical composition is administered orally.

[249] Aspect 37: The method of aspect 36, wherein the pharmaceutical composition is administered at a dose of between about 1 mg/kg and about 20 mg/kg, optionally, the dose is between about 1 mg/kg and about 10 mg/kg.

[250] Aspect 38: The method of any one of aspects 28-35, wherein the pharmaceutical composition is administered intravenously.

[251] Aspect 39: The method of aspect 38, wherein the pharmaceutical composition is administered at a dose of between about 0.125 mg/kg and about 10 mg/kg, optionally, the dose is between about 0.25 mg/kg and about 5 mg/kg.

[252] Aspect 40: The method of any one of aspects 28-35, wherein the pharmaceutical composition is administered intramuscularly.

[253] Aspect 41: The method of aspect 40, wherein the pharmaceutical composition is administered at a dose of between about 0.25 mg/kg and about 50 mg/kg, optionally, the dose is between about 0.25 mg/kg and about 35 mg/kg.

[254] Aspect 42: The method of any one of aspects 28-41, wherein the pharmaceutical composition comprises one or more additional therapeutically active ingredients.

[255] Aspect 43: The method of aspect 42, wherein said one or more additional therapeutically active ingredients are selected from the group consisting of ACE inhibitors, AIRBs, diuretics, Ca<sup>2+</sup> channel blockers,  $\beta$  blockers, digitalis, NO donors, vasodilators, SERCA2a stimulators, neprilysin (NEP) inhibitors, myosin filament activators, recombinant relaxin-2 mediators, recombinant NP protein, activators of the soluble guanylate cyclase (sGC), and beta-arrestin ligand of angiotensin II receptor.

[256] Aspect 44: The method of aspect 43, wherein said diuretic is selected from the group consisting of furosemide, bumetanide, torasemide, metolazone, an aldosterone antagonist, thiazide diuretics.

[257] Aspect 45: The method of aspect 43, wherein said ACE inhibitor is lisinopril or ramipril.

[258] Aspect 46: The method of aspect 42, wherein said one or more additional therapeutically active ingredients are selected from the group consisting of valsartan, candesartan, olmesartan, telmisartan, losartan, sacubitril, carvedilol, omecamtiv, and metoprolol.

[259] Aspect 47: The method of any one of aspects 28-46, wherein the individual is human.

[260] Aspect 48: The method of any one of aspect 28-47, wherein the one or more parameters of heart function are selected from the group consisting of Ca<sup>2+</sup> transient (CaT) amplitude, Ca<sup>2+</sup>-induced Ca<sup>2+</sup> release (CICR), rate-dependency of action potential duration at 90% repolarization (APD90), diastolic membrane potential ( $E_{diast}$ ), maximum depolarization velocity ( $dV/dt_{max}$ ), heart rate, heart pressure, systolic blood pressure, diastolic blood pressure, LVEF, E/e' ration, E/Ea ratio, E/A ratio, and stroke volume.

[261] Aspect 49: The method of any one of aspects 28-48, wherein the measuring step is carried out before, during, and/or after the administering step.

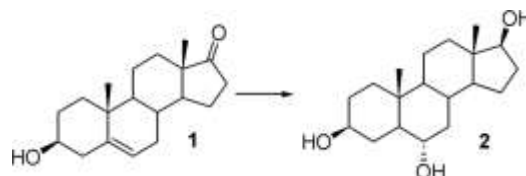
[262] The following examples further illustrate the present invention.

### **Example 1: Preparation of the compounds of formula (I)**

[263] In the following examples, chemical compounds, solvents, reactants and any other material are from commercial sources, except where otherwise stated. Generally, compounds of formula (I) were prepared by multistep synthesis starting from

dehydroepiandrosterone (prasterone). Dehydroepiandrosterone is a commercial product or can be prepared according to well-known methods starting from 4-androsten-3,17-dione (androstenedione).

*Preparation of 5 $\alpha$ -Androstane-3 $\beta$ ,6 $\alpha$ ,17 $\beta$ -triol*

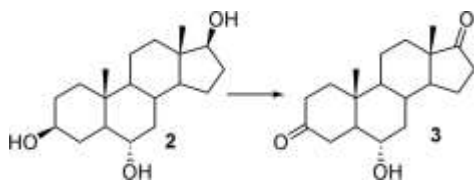


[264] A suitable intermediate for the synthesis of 6- $\alpha$ -3,17 androstanedione (**2**) was produced from dehydroepiandrosterone **1** by hydroboration followed by oxidation as described in De Munari, *et al.* (J. Med. Chem., 2003, 46(17):3644-54), the entire content of which is incorporated by reference herein. Briefly, a solution of dehydroepiandrosterone **1** (5 g, 17.5 mmol, 1 eq.) in THF (85 mL) was stirred at -20 °C under Ar. Then, 1M BH<sub>3</sub>·THF complex in THF was added to the stirred solution (44 mL, 44 mmol, 2.5 eq.), and stirring was continued at room temperature for 3 hours. H<sub>2</sub>O (85 mL) was cautiously added dropwise and followed by the dropwise addition of NaBO<sub>3</sub>·4H<sub>2</sub>O (5.4 g, 35 mmol, 2 eq). After stirring at room temperature overnight, the mixture was filtered. The solid was washed with THF and then discarded. The liquors were saturated with NaCl and extracted with THF (3 × 40 mL). The combined organic extracts were dried over NaCl and Na<sub>2</sub>SO<sub>4</sub>, filtered, and evaporated to dryness. The crude 5 $\alpha$ -Androstane-3 $\beta$ ,6 $\alpha$ ,17 $\beta$ -triol **2** product was crystallized from EtOAc/MeOH (2/1, 10 mL/g) to give a white solid (3.8 g, 70%).

[265] Spectroscopic data for 5 $\alpha$ -Androstane-3 $\beta$ ,6 $\alpha$ ,17 $\beta$ -triol **2**:

[267] <sup>1</sup>H NMR (DMSO-d<sub>6</sub>)  $\delta$  4.44 (m, 1H, OH), 4.42 (m, 1H, OH), 4.24 (d, 1H, OH), 3.42 (dt, 1H, 16-Ha), 3.26 (m, 1H, 3-H), 3.12 (m, 1H, 6-H), 0.72 (s, 3H, CH<sub>3</sub>), 0.60 (s, 3H, CH<sub>3</sub>). mp 232-234 °C.

### Preparation of 6 $\alpha$ -Hydroxyandrostane-3,17-dione

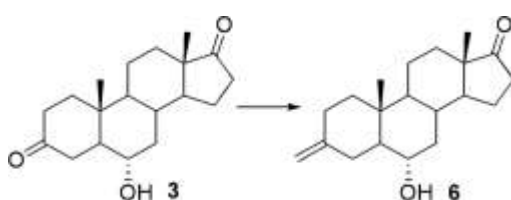


[268] Intermediate **3** was obtained from **2** by selective oxidation at C3 and C17 positions. NBS (3.4 g, 19.5 mmol, 3 eq) was added to a stirred solution of 5 $\alpha$ -Androstane-3 $\beta$ ,6 $\alpha$ ,17 $\beta$ -triol **2** (2 g, 6.5 mmol, 1 eq) in dioxane/H<sub>2</sub>O/pyridine (54/10/1 mL) at 0°C. After the addition, the mixture was allowed to warm to room temperature and was stirred overnight. The orange solution was diluted with water (50 mL) and quenched with Na<sub>2</sub>S<sub>2</sub>O<sub>3</sub> (350 mg). The organic solvent was evaporated under vacuum until a white solid appears. The solid was filtered and washed with water. After drying at 40 °C, 6 $\alpha$ -hydroxyandrostane-3,17-dione **3** was obtained as a white solid (1.3 g, 70%).

[269] Spectroscopic data for 6 $\alpha$ -hydroxyandrostane-3,17-dione **3**:

[270] <sup>1</sup>H NMR (acetone-d<sub>6</sub>)  $\delta$  3.61 (d, 1H, OH), 3.48 (m, 1H, 6-H), 1.11 (s, 3H, CH<sub>3</sub>), 0.86 (s, 3H, CH<sub>3</sub>). mp 204-206 °C lit. 206-207 (Hammerschmidt & Spitteller, 1973)

### Synthesis of adrostan-3-methylene-17-one



[271] 6- $\alpha$ -3,17 androstanedione **3** was then converted to the exo-methane derivative **6** (adrostan-3-methylene-17-one) via a Wittig reaction selective on the C3 carbonyl followed by the cross-metathesis coupling with 5-pentenoic acid. t-BuOK (670 mg, 6 mmol, 4 eq.) was added to a suspension of methyltriphenylphosphonium bromide (1,66 g, 6 mmol, 4 eq.) in THF (10 mL) at -5°C. The solution immediately changed colour to bright orange. After 10 minutes, 6 $\alpha$ -hydroxy androstane-3,17-dione **3** (450 mg, 1.5 mmol, 1eq.) was added while the temperature was kept below 0°C. Immediately after the addition, the reaction was quenched by the addition of aq. 1M HCl (15 mL) and

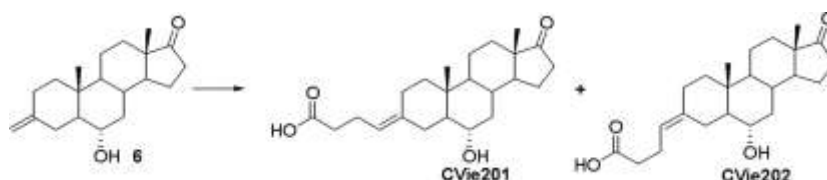
extracted with EtOAc (3x20mL). The combined organic phases were dried over Na<sub>2</sub>SO<sub>4</sub> and evaporated to dryness. The crude extracts were purified over column chromatography (eluent EtOAc: Petroleum spirit 4:6) to produce 376 mg (83%) of adrostane-3-methylene-17-one **6** as a white foam.

[272] Spectroscopic data for adrostane-3-methylene-17-one **6**:

[273] <sup>1</sup>H NMR (400 MHz, Chloroform-d) δ 4.63 (dt, 2H, 3 $\alpha$ -CH<sub>2</sub>), 3.47 (td, 1H, 6-H), 2.55 (ddd, 1H, 16Ha), 2.44 (ddd, 1H, 16-Hb), 0.89 (s, 3H, CH<sub>3</sub>), 0.86 (s, 3H, CH<sub>3</sub>), 0.80 – 0.70 (m, 1H, 5-H).

[274] <sup>13</sup>C NMR (101 MHz, Chloroform-d) δ 220.79 (17-C), 148.22 (3-C), 107.40 (3-CH<sub>2</sub>), 69.85 (6-C), 13.79 (CH<sub>3</sub>), 12.91 (CH<sub>3</sub>).

*Direct synthesis of CVie 201 and 202 from precursor 6 by cross-metathesis*



[275] Hoveyda-Grubbs 2<sup>nd</sup> generation catalyst (12 mg, 0.015 mmol, 0.05 eq.) was added to a solution of androstan-3-methylene-17-one **6** (100 mg, 0.33 mmol, 1 eq) in DCM (1 mL). The solution was then heated at reflux and treated with 10  $\mu$ L of 4-pentenoic acid every 20 minutes (total 330  $\mu$ L, 3.3 mmol, 10 eq.). After the end of the addition, the mixture was refluxed for additional 2h. The reaction mixture was concentrated *in vacuo* and purified by flash chromatography (Eluent Acetone: petroleum spirit 3:7+0.1% HCO<sub>2</sub>H) to obtain two different white solids (E)-4-(6 $\alpha$ -hydroxy-17-oxoandrostane-3-ylidene)butyric acid (4.8 mg, 4%) (**CVie201**) and (Z)-4-(6 $\alpha$ -hydroxy-17-oxoandrostane-3-ylidene)butyric acid (7.2 mg, 6%) (**CVie202**).

[276] Spectroscopic data for **CVie201**:

[277] <sup>1</sup>H NMR (Chloroform-d) δ 5.10 (t, J = 7.3 Hz, 1H, 3 $\alpha$ -H), 3.50 (td, J = 10.3, 9.8, 6.0 Hz, 1H, 6-H), 2.91 (d, 1H, 16-Ha), 0.89 (s, 3H, CH<sub>3</sub>), 0.86 (s, 3H, CH<sub>3</sub>), 0.73 (m, 1H, 5-H).

[278] <sup>13</sup>C NMR (101 MHz, Chloroform-d) δ 221.30 (17-C), 178.72 (CO<sub>2</sub>), 139.71 (3-C), 119.89(3 $\alpha$ -C), 69.95(6-C), 54.03 (5-C), 24.03 (16-C), 13.93(CH<sub>3</sub>), 13.06(CH<sub>3</sub>).

[279] MS (ESI) calculated for  $C_{23}H_{33}O_4^- [M^-]$  373.2. Found: 373.4

[280] Spectroscopic data for **CVie202**:

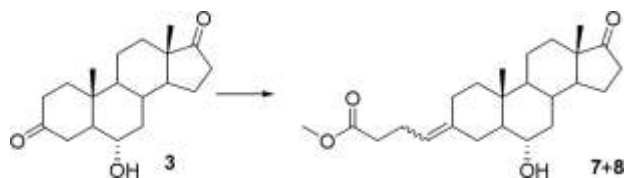
[281]  $^1H$  NMR (400 MHz, Chloroform- $d$ )  $\delta$  5.10 (t, 1H,  $3\alpha$ -H), 3.50 (td, 1H, 6-H), 2.91 (d, 1H, 16-Ha), 0.89 (s, 3H,  $CH_3$ ), 0.86 (s, 3H,  $CH_3$ ), 0.73 (t, 1H, 5-H).

[282]  $^{13}C$  NMR (101 MHz, Chloroform- $d$ )  $\delta$  220.86 (17-C), 177.66 ( $CO_2$ ), 139.84 (C-3), 119.47 (Ca), 70.08 (C-6), 13.78( $CH_3$ ), 12.91 ( $CH_3$ ).

[283] Alternatively, **CVie201** and **CVie202** were obtained by varying the Wittig reaction. In one method (Route A), a betaine intermediate was stabilized by the use of a polar solvent, such as DMSO, and a base, such as NaH. The second approach (Route B) allowed for the stabilization of a cyclo-oxaphosphetane intermediate using an aprotic solvent, such as THF, as the base. Route A produced a mixture of diastereomers (60% of Z/syn **CVie202**; 30% E/anti **CVie201**), whereas Route B provided **CVie202** derived from the cyclo-oxaphosphate intermediate. Either procedure requires the production of diastereomers **7** and/or **8** as described below.

*Alternative synthesis of CVie 201 and 202 via Wittig reaction*

*Route A*



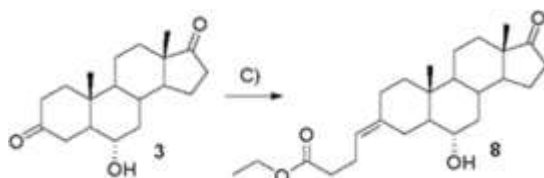
[284] NaH 60% in mineral oil (100 mg, 2.56 mmol, 8 eq.) was carefully added to dry DMSO (1 mL) under Ar atmosphere. The resulting solution was stirred at 60°C for 20 minutes. After cooling at room temperature, (3-carboxypropyl)triphenylphosphonium bromide (550 mg, 1.28 mmol, 4eq.) was added. A bright orange color appeared immediately. The solution was stirred for 2h. Then, 6 $\alpha$ -hydroxyandrostane-3,17 dione **3** (100 mg, 0.32 mmol, 1 eq.) was added to the mixture. The resulting solution was allowed to stir at room temperature for additional 4h. The reaction mixture diluted with EtOAc (25mL) was washed with aq. 1M HCl (3 x 30mL). The organic layer dried over  $Na_2SO_4$  was evaporated to dryness obtaining 25mg of crude material.

[285] The crude material was first dissolved in MeOH (1.5mL), followed by the addition of EDC hydrochloride (115mg, 0.6mmol, 2eq.) and DMAP (5mg, 0.03 mmol, 0.1 eq.). The solution was stirred at room temperature for 3h. After concentration *in vacuo*. The crude solid was dissolved in EtOAc (15 mL) and washed with aq. 1M HCl (3 x 10mL). The crude product was purified by flash chromatography over silica gel (Acetone:Pet.Sp 3:7) to obtain 25 mg of a clear oil (20%) comprising a mixture of diastereoisomers **7** and **8**.

[286] Spectroscopic data for the two diastereoisomers **7** and **8**:

[287] <sup>1</sup>H NMR (Chloroform-d) δ 5.16-4.96 (m, 1H, 3 $\alpha$ -H), 3.66 (s, 3H, CH<sub>3</sub>O), 3.47 (m, 1H, 6-OH), 0.89 (s, 3H,CH<sub>3</sub>), 0.86 (s, 3H, CH<sub>3</sub>), 0.74 (m, 1H, 5-H).

*Route B*



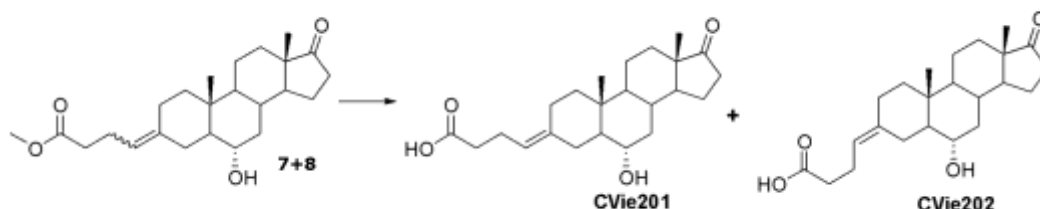
[288] LiHMDS 1M solution in THF (40 mL, 40mmol, 12 eq.) was carefully added to a dry THF (33 mL) suspension of (3-carboxypropyl)triphenylphosphonium bromide (8.5 g, 20 mmol, 6eq.) under Ar atmosphere at -40°C. The solution was stirred at -40°C until a bright orange color appears. Then, 6 $\alpha$ -hydroxyandrostane-3,17 dione **3** (1g, 3.3mmol, 1 eq.) was added to the solution at -40°C. after stirring at room temperature overnight the reaction mixture quenched with aq. 1M HCl (300mL) was extracted with EtOAc (3 x 3 50mL). The combined organic layers were dried over Na<sub>2</sub>SO<sub>4</sub> and evaporated to dryness.

[289] The crude material was dissolved in absolute EtOH (17 mL) then EDC hydrochloride (1.26mg, 6.6mmol, 2eq.) and DMAP (50mg, 0.3 mmol, 0.1 eq.) were added. The mixture was allowed to stir at room temperature for 3h. The reaction diluted in EtOAc (150mL) was washed with aq. 1M HCl (3 x 100mL). The crude product was purified by flash chromatography over silica gel (Acetone:Pet.Sp 3:7) to obtain 910mg (72%) of compound **8**.

[290] Spectroscopic data for compound **8**:

[291] <sup>1</sup>H NMR (Chloroform-d) δ 5.07 (t, 1H, 3 $\alpha$ -H), 4.10 (q, 2H, OCH<sub>2</sub>), 3.47 (td, 1H, 6-H), 2.91 (d, 1H), 0.88 (s, 3H, CH<sub>3</sub>), 0.85 (s, 3H, CH<sub>3</sub>), 0.71 (m, 1H, 5-H).

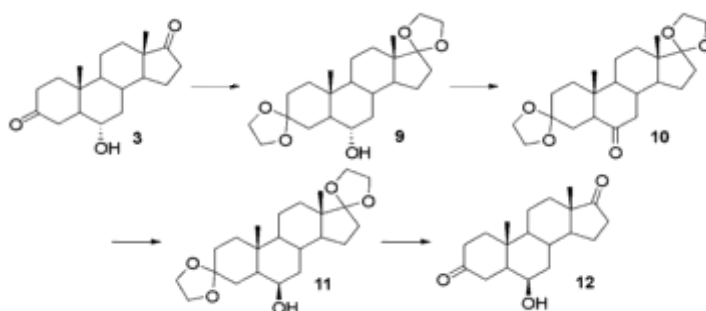
[292]  $^{13}\text{C}$  NMR (101 MHz, Chloroform-d)  $\delta$  173.67 (17-C), 139.60 (3 $\alpha$ -C), 119.94(3-C), 69.98 (6-C), 60.41 (OCH<sub>2</sub>), 51.33 (5-C), 40.37 (CH<sub>3</sub>), 13.92 (CH<sub>3</sub>), 13.08 (CH<sub>3</sub>).



*Final hydrolysis of methyl (or ethyl) esters*

[293] An aqueous solution of 1M LiOH (150  $\mu\text{L}$ , 2.5eq.) was added to a solution of the methyl esters **7** and **8** (25 mg, 0.06 mmol, 1eq.) in THF (600  $\mu\text{L}$ ) and water (200  $\mu\text{L}$ ). After 2h, the reaction was diluted with water (10 mL) and quenched by the addition of 1M HCl until the solution reached pH 1. The aqueous phase was extracted with EtOAc (3 x 15mL). The combined organic layers were dried over Na<sub>2</sub>SO<sub>4</sub> and evaporated to dryness. Crude was purified over flash chromatography (AcOEt:Pet.Sp. 7:3 1% HCOOH). Two white solid were obtained corresponding to the E (7 mg, 31%) and Z (12 mg, 54%) diastereoisomers (**CVie201** and **CVie202**, respectively).

[294]  $^1\text{H}$  NMR (Chloroform-d)  $\delta$  5.12 (bt, 1H, 3 $\alpha$ -H), 3.51-3.42 (m, 1H, 6-H), 0.90 (s, 3H, CH<sub>3</sub>), 0.86 (s, 3H, CH<sub>3</sub>), 0.79-0.69 (m, 1H, 5-H).



*Synthetic way to CVie 203 and 204: synthesis of intermediate compound 12*

[295] To prepare **CVie203** and **CVie204**, the precursor **12** was first produced from 6- $\alpha$ -3,17 androstenedione **3**. The carbonyls of 6- $\alpha$ -3,17 androstenedione **3** were protected as

diketals by reaction with ethylene glycol in combination with acid catalysis (p-tSA or camphosulfonic acid) in toluene, obtaining compound **9**. Oxidation of compound **9** with PCC or other oxidants gave compound **10**, which was then reduced with NaBH<sub>4</sub> or KBH<sub>4</sub> to produce the protected alcohol **11** with the C6-hydroxyl group selectively in the  $\beta$ -configuration. Final cleavage of the cyclic diketals by acidic treatment as described in De Munari *et al.* (J. Med. Chem., 2003, 46(17):3644-54) in acetone afforded precursor **12**.

[296] Briefly, a solution of 6 $\alpha$ -hydroxyandrostane-3,17-dione (1.5 g, 4.9 mmol, 1 eq), ethylene glycol (10.5 mL, 88 mmol, 36eq) and PTSA (561 mg, 2.9 mmol, 0.6 eq) in toluene (160 mL) was stirred at reflux for 12 h with a Dean-Stark trap. After cooling to room temperature, the mixture was neutralized with aq. 5% NaHCO<sub>3</sub> solution. The organic layer was separated and washed with H<sub>2</sub>O (2  $\times$  40 mL), dried over Na<sub>2</sub>SO<sub>4</sub>, and evaporated to dryness to produce 3,3:17,17-Bis(ethylendioxy)androstane-6 $\alpha$ -ol **9** as a white solid compound (1.9 g, 98%).

[297] Spectroscopic data for 3,3:17,17-Bis(ethylendioxy)androstane-6 $\alpha$ -ol **9**:

[298] <sup>1</sup>H NMR (DMSO-d<sub>6</sub>)  $\delta$  4.25 (d, 1H, OH), 3.88-3.70 (m, 8H, OCH<sub>2</sub>), 3.11 (m, 1H, 6-H), 0.74 (s, 3H, CH<sub>3</sub>), 0.73 (s, 3H, CH<sub>3</sub>).

[299] PCC (148 mg, 0.69 mmol, 4 eq) was added to a solution of 3,3:17,17-bis(ethylendioxy)androstane-6 $\alpha$ -ol (3 g, 14 mmol, 1 eq) **9** and sodium ascorbate (1.2 g, 14 mmol, 4eq.) in dry CH<sub>2</sub>Cl<sub>2</sub> (87 mL) at 0°. The mixture was stirred overnight at room temperature. The mixture was washed with aq. 1M HCl (3  $\times$  30mL) and water (3  $\times$  30 mL). The organic layer was dried over Na<sub>2</sub>SO<sub>4</sub> and evaporated to dryness. Crude was purified by flash chromatography over a column of silica gel (eluent acetone: petroleum spirit 2:8). 3,3:17,17-Bis(ethylendioxy)androstane-6-one **10** was obtained as a white solid (1.53 g (96%)).

**[300]** Spectroscopic data for 3,3:17,17-Bis(ethylendioxy)androstane-6-one **10**

[301] <sup>1</sup>H NMR (Acetone-d<sub>6</sub>)  $\delta$  3.97-3.76 (m, 8H, CH<sub>2</sub>O), 2.19 (dd, 1H, 16-Ha), 0.84 (s, 3H, CH<sub>3</sub>), 0.75 (s, 3H, CH<sub>3</sub>).

[302] NaBH<sub>4</sub> (144 mg, 3 mmol, 1.2 eq) was added to a stirred suspension of 3,3:17,17-bis(ethylendioxy)androstane-6-one **10** (1 g, 2.5 mmol, 1 eq) in MeOH (13 mL) at 0°C. After 2 h at 0 °C, H<sub>2</sub>O (40 mL) was added dropwise. The mixture was extracted with EtOAc (3  $\times$  40 mL). The combined organic extracts were dried over Na<sub>2</sub>SO<sub>4</sub>, filtered, and evaporated to dryness to give a white solid, which was 3,3:17,17-Bis(ethylendioxy)androstane-6 $\beta$ -ol **11** (915 mg, 92%).

[303] Spectroscopic data for 3,3:17,17-Bis(ethyendioxy)androstane-6 $\beta$ -ol **11**:

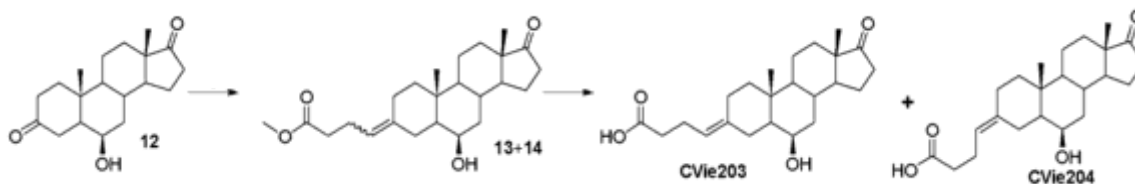
[304]  $^1\text{H}$  NMR (acetone- $d_6$ )  $\delta$  3.95-3.75 (m, 8H, OCH $_2$ ), 3.70 (m, 1H, 6-H), 3.33 (d, 1H, 6-OH), 1.05 (s, 3H, CH $_3$ ), 0.84 (s, 3H, CH $_3$ ).

[305] PTSA (2.26 g, 11.5 mmol, 5 eq) was added in small portion over 5 minutes to a solution of 3,3:17,17-bis(ethyendioxy)androstane-6 $\beta$ -ol **11** (910 mg, 2.3 mmol, 1 eq) in acetone (46 mL). After stirring at room temperature for 1 h, the solution was quenched by addition of aq. 5% NaHCO $_3$  until pH 7. After stirring for 5 minutes, a white solid appeared. The volatiles were removed *in vacuo*. The suspension was extracted with CH $_2$ Cl $_2$  (3 x 30 mL) and the combined organic extracts were washed with brine (40 mL), dried over Na $_2$ SO $_4$ , filtered, and evaporated. The obtained solid was stirred with n-hexane/EtOAc 8/2 (10 mL) for 45 minutes and then collected by filtration. The solid was dried 45  $^\circ\text{C}$  for 3 hours. 568 mg (81%) of a white solid was obtained (*i.e.*, 6 $\beta$ -hydroxyandrostane-3,17-dione **12**).

[306] Spectroscopic data for 6 $\beta$ -hydroxyandrostane-3,17-dione **12**:

[307]  $^1\text{H}$  NMR (DMSO- $d_6$ )  $\delta$  4.47 (d, 1H, OH), 3.57 (m, 1H, 6-H), 1.13 (s, 3H, CH $_3$ ), 0.81 (s, 3H, CH $_3$ ).

Conversion of **12** into final CVie 203 and 204



[308] **CVie203** and **CVie204** were then obtained from precursor **12** via the Wittig reaction using the same procedures described above for **CVie201** and **CVie202**. The configurations at the C3-C1' double bond were identified in the two isomers by means of NOESY experiments.

[309] Briefly, NaH 60% in mineral oil (100 mg, 2.56 mmol, 8 eq.) was carefully added to dry DMSO (1 mL) under Ar atmosphere. The resulting solution was stirred at 60 $^\circ\text{C}$  for 20 minutes. After cooling at room temperature, (3-carboxypropyl)triphenylphosphonium bromide (550 mg, 1.28 mmol, 4eq.) was added. A bright orange color appeared immediately. The solution was stirred for 2h. Then, 6 $\beta$ -hydroxyandrostane-3,17-dione **12** (100 mg, 0.32 mmol, 1 eq.) was added to the mixture. The resulting solution was allowed to stir at room temperature for additional 4h. The reaction mixture was diluted

with EtOAc (25mL) and washed with aq. 1M HCl (3 x 30mL). The organic layer was dried over Na<sub>2</sub>SO<sub>4</sub> and evaporated to dryness to obtain 25mg of crude material.

[310] The crude material was then dissolved in MeOH (1.5mL). EDC hydrochloride (115mg, 0.6mmol, 2eq.) and DMAP (5mg, 0.03 mmol, 0.1 eq.) were added. The solution was stirred at room temperature for 3h. After concentration *in vacuo*. The crude solid was dissolved in EtOAc (15 mL) and washed with aq. 1M HCl (3 x 10mL). The crude product was purified by flash chromatography over silica gel (Acetone:Pet.Sp 3:7) to obtain a mixture of diastereoisomers **13** and **14** at 17% yield and 30% yield, respectively.

[311] Spectroscopic data for the compound **13**:

[312] <sup>1</sup>H NMR (400 MHz, Chloroform-d) δ 5.07 (bs, 1H, 3 $\alpha$ -H), 3.85 (d, 1H, 6-H), 3.66 (s, 3H, OCH<sub>3</sub>), 2.54 – 2.39 (m, 2H, 3 $\gamma$ -H), 1.10 (s, 3H, CH<sub>3</sub>), 0.89 (s, 3H, CH<sub>3</sub>), 0.80 – 0.69 (m, 1H, 5-H).

[313] <sup>13</sup>C NMR (101 MHz, Chloroform-d) δ 219.74 (17-C), 167.24 (CO<sub>2</sub>), 140.38 (3-C), 119.60 (3 $\alpha$ -C), 71.52 (6-C), 54.45 (5-C), 51.22 (OCH<sub>3</sub>), 14.09 (CH<sub>3</sub>), 13.86 (CH<sub>3</sub>).

[314] Spectroscopic data for compound **14**

[315] <sup>1</sup>H NMR (400 MHz, Chloroform-d) δ 5.07 (s, 1H, 3 $\alpha$ -H), 3.89 (d, 1H, 6-H), 3.66 (s, 3H, OCH<sub>3</sub>), 2.46 (dd, 1H, 16-Ha), 1.10 (s, 3H, CH<sub>3</sub>), 0.89 (s, 3H, CH<sub>3</sub>), 0.79 – 0.64 (m, 1H, 5-H).

[316] <sup>13</sup>C NMR (101 MHz, Chloroform-d) δ 221.21 (17-C), 176.10 (CO<sub>2</sub>), 140.33 (3-C), 119.39 (3 $\alpha$ -C), 71.75 (6-C), 54.49 (5-C), 51.20 (OCH<sub>3</sub>), 15.24 (CH<sub>3</sub>), 13.87 (CH<sub>3</sub>).

[317] The reaction mixture was concentrated *in vacuo* and purified by flash chromatography (Eluent Acetone: petroleum spirit 3:7+0.1% HCO<sub>2</sub>H) to obtain two different white solids (E)-4-(6 $\beta$ -hydroxy-17-oxoandrostane-3-yliden)butyric acid (**CVie203**) and (Z)-4-(6 $\beta$ -hydroxy-17-oxoandrostane-3-yliden)butyric acid (**CVie204**).

[318] Spectroscopic data for compound **CVie203**:

[319] <sup>1</sup>H NMR (400 MHz, Acetone-d<sub>6</sub>) δ 4.84 (bt, 1H, 3 $\alpha$ -H), 3.55 (d, 1H, 6-H), 0.90 (s, 3H, CH<sub>3</sub>), 0.61 (s, 3H, CH<sub>3</sub>), 0.51 (ddd, 1H, 5-H).

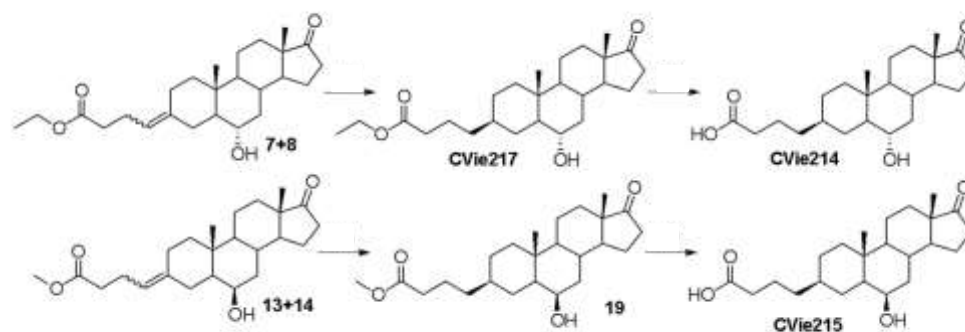
[320] <sup>13</sup>C NMR (101 MHz, acetone-d<sub>6</sub>) δ 218.86 (17-C), 173.42(CO<sub>2</sub>), 140.74 (3-C), 119.29(3 $\alpha$ -C), 70.18 (6-C), 14.74 (CH<sub>3</sub>), 13.18 (CH<sub>3</sub>).

[321] Spectroscopic data for compound **CVie204**:

[322]  $^1\text{H}$  NMR (400 MHz, Chloroform- $d$ )  $\delta$  5.07 (s, 1H, 3 $\alpha$ -H), 3.88 (s, 1H, 6-H), 1.08 (s, 3H, CH<sub>3</sub>), 0.88 (s, 3H, CH<sub>3</sub>), 0.72 (s, 1H, 5-H).

[323]  $^{13}\text{C}$  NMR (101 MHz, acetone)  $\delta$  216.39 (17-C), 173.80 (CO<sub>2</sub>), 135.48(3-C), 113.80 (3 $\alpha$ -C), 66.52 (6-C), 10.07 (CH<sub>3</sub>), 8.70 (CH<sub>3</sub>).

*Production of **CVie214**, **CVie215**, and **CVie217** via hydrogenation and ester hydrolysis*



[324] Compound **CVie217** was produced from the mixture of diastereomers **7+8** described above. Briefly, hydrogenation of the C3-C1' double bonds of the diastereomers was carried out in EtOAc using Pd-C catalysis. The resulting compound was **CVie217**. The configuration of the stereogenic center formed at C3 was identified by NOESY experiments. Compound **CVie217** was then hydrolyzed with 1M LiOH or NaOH in THF to produce **CVie214**. Similarly, diastereomers **13+14** were hydrogenated in EtOAc using Pd-C catalysis to produce the ester compound **19**, which was then hydrolyzed with 1M LiOH or NaOH in THF to produce **CVie215**.

[325] Spectroscopic data for compound **19**:

[326]  $^1\text{H}$  NMR (400 MHz, Chloroform- $d$ )  $\delta$  3.83 (bs, 1H, 6-H), 3.66 (bs, 3H, OCH<sub>3</sub>), 2.44 (dd, 1H, 16-Ha), 2.28 (t, 2H, 3 $\gamma$ -H), 0.99 (s, 3H, CH<sub>3</sub>), 0.88 (s, 3H, CH<sub>3</sub>), 0.79 – 0.70 (m, 1H, 5-H).

[327]  $^{13}\text{C}$  NMR (101 MHz, Chloroform- $d$ )  $\delta$  221.43 (17-C), 174.25 (CO<sub>2</sub>), 71.96 (6-C), 51.25 (OCH<sub>3</sub>), 15.74 (CH<sub>3</sub>), 13.86(CH<sub>3</sub>).

[328] Spectroscopic data for compound **CVie214**:

[329]  $^1\text{H}$  NMR (400 MHz, Chloroform- $d$ )  $\delta$  3.43 (bt, 1H, 6-H), 2.44 (dd, 1H, 16Ha), 2.31 (t, 2H, 3 $\gamma$ -H), 0.84 (s, 3H, CH<sub>3</sub>), 0.77 (s, 3H, CH<sub>3</sub>).

[330]  $^{13}\text{C}$  NMR (101 MHz, Chloroform-d)  $\delta$  221.35 (17-C), 179.11 ( $\text{CO}_2$ ), 69.90 (6-C), 13.78 ( $\text{CH}_3$ ), 13.37( $\text{CH}_3$ )

[331] Spectroscopic data for compound **CVie215**:

[332]  $^1\text{H}$  NMR (400 MHz, Chloroform-d)  $\delta$  3.85 (s, 1H, 6-H), 2.45 (dd, 1H, 16-Ha), 2.34 (t, 2H, 3 $\gamma$ -H), 1.00 (s, 3H,  $\text{CH}_3$ ), 0.89 (s, 3H,  $\text{CH}_3$ ), 0.74 (d, 1H, 5-H).

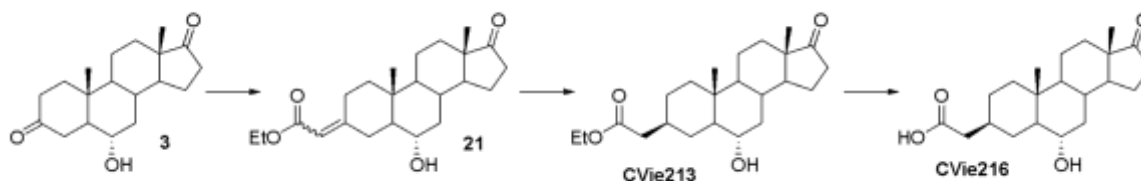
[333]  $^{13}\text{C}$  NMR (101 MHz, Chloroform-d)  $\delta$  221.50 (17-C), 179.04 ( $\text{CO}_2\text{H}$ ), 72.03 (6-C), 15.76 ( $\text{CH}_3$ ), 13.87 ( $\text{CH}_3$ ).

[334] Spectroscopic data for compound **CVie217**:

[335]  $^1\text{H}$  NMR (400 MHz, Chloroform-d)  $\delta$  4.09 (q, 2H,  $\text{CH}_2\text{O}$ ), 3.40 (td, 1H, 6-H), 2.49 – 2.36 (dd, 1H, 16-Ha), 2.24 (t, 2H, 3 $\delta$ -H), 0.83 (s, 3H,  $\text{CH}_3$ ), 0.76 (s, 3H,  $\text{CH}_3$ ).

[336]  $^{13}\text{C}$  NMR (101 MHz, Chloroform-d)  $\delta$  220.91 (17-C), 173.77 ( $\text{CO}_2$ ), 69.63 (6-C), 60.14 ( $\text{CH}_2\text{O}$ ), 14.23 ( $\text{CH}_3$ ), 13.76 ( $\text{CH}_3$ ), 13.36 ( $\text{CH}_3$ ).

*Production of **CVie213** and **CVie216** by via Wittig reaction followed by C=C hydrogenation and ester hydrolysis*



[337] Compound 6- $\alpha$ -3,17 androstenedione **3** was also used as the starting point for the synthesis of **CVie213** and **CVie216** via a Horner-Emmons reaction. First, triethylphosphonoacetate (6.5 mL, 33 mmol, 5 eq) was added carefully to a suspension of NaH 60% in mineral oil (1.3 g, 33 mmol, 5 eq) in DMF (200 mL) under Ar atmosphere at 0°C. The resulting solution was warmed at room temperature and stirred for 20 minutes. Then, 6- $\alpha$ -3,17 androstenedione **3** (2 g, 6.5 mmol, 1 eq) was added at 0°C. After stirring overnight at room temperature, the reaction was quenched by careful addition of  $\text{H}_2\text{O}$  (100 mL) and extracted with  $\text{Et}_2\text{O}$  (3 x 150mL). The combined organic layers were dried over  $\text{Na}_2\text{SO}_4$  and evaporated *in vacuo*. Crude was purified by flash chromatography over a column of silica gel (acetone: petroleum spirit 3:7) to produce 2.1g (86%) of a clear oil mixture of two diastereoisomers (compounds **21**).

[338] Spectroscopic data for diastereoisomer compounds **21**:

[339]  $^1\text{H}$  NMR (Chloroform- $d$ )  $\delta$  5.60 (d, Hz, 1H,  $3\alpha$ -H), 4.08 (q, 2H,  $\text{CH}_2\text{O}$ ), 3.45 (dq, 1H, 6-H), 2.41 (dd, 1H, 16-Ha), 0.90 (s, 3H,  $\text{CH}_3$ ), 0.82 (s, 3H,  $\text{CH}_3$ ), 0.77-0.66 (m, 1H, 5-H).

[340]  $^{13}\text{C}$  NMR (101 MHz, Chloroform- $d$ )  $\delta$  220.85 (17-C), 166.81 ( $\text{CO}_2$ ), 161.87 (3-C), 113.75 ( $3\alpha$ -C), 69.41 (6-C), 13.76 ( $\text{CH}_3$ ), 13.00 ( $\text{CH}_3$ ).

[341] While under Ar atmosphere, 10% Pd-C (700 mg) was added to a degassed solution of diastereoisomer compounds **21** (2g, 5.3 mmol, 1 eq) in EtOAc (200 mL). After three cycles of vacuum/hydrogen, the reaction was allowed to stir at room temperature overnight under  $\text{H}_2$  atmosphere. After removal of hydrogen by vacuum/Ar cycle, the reaction mixture was filtered over CELITE<sup>®</sup>. The filtered solution was evaporated to dryness. The **CVie213** product was obtained without purification at 1.8 g (90%). Further hydrolysis of **CVie213** with 1M LiOH or NaOH in THF produced **CVie216**.

[342] Spectroscopic data for compound **CVie213**:

[343]  $^1\text{H}$  NMR (Chloroform- $d$ )  $\delta$  4.12 (q, 2H,  $\text{OCH}_2$ ), 3.38 (td, 1H, 6-H), 2.42 (dd, 1H, 16-Ha), 2.27 (t, 2H,  $3\alpha$ - $\text{CH}_2$ ), 0.82 (s, 3H,  $\text{CH}_3$ ), 0.76 (s, 3H,  $\text{CH}_3$ ).

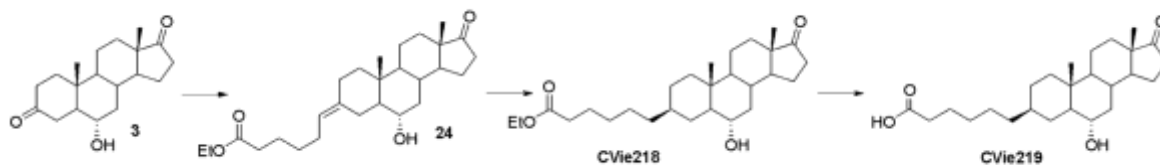
[344]  $^{13}\text{C}$  NMR (101 MHz, Chloroform- $d$ )  $\delta$  221.03 (17-C), 172.93 ( $\text{CO}_2$ ), 69.43 (6-C), 13.76 ( $\text{CH}_3$ ), 13.32( $\text{CH}_3$ ).

[345] Spectroscopic data for compound **CVie216**:

[346]  $^1\text{H}$  NMR (400 MHz, Chloroform- $d$ )  $\delta$  3.43 (td, 1H, 6-H), 2.45 (dd, 1H, 16-Ha), 2.28 (t,  $3\alpha$ -H), 0.85 (s, 3H,  $\text{CH}_3$ ), 0.80 (s, 3H,  $\text{CH}_3$ ).

[347]  $^{13}\text{C}$  NMR (101 MHz, acetone)  $\delta$  220.44 (17-C), 174.27 ( $\text{CO}_2$ ), 68.57 (6-C), 12.99 ( $\text{CH}_3$ ), 12.59 ( $\text{CH}_3$ ).

*Production of **CVie218** and **CVie219** via Wittig reaction followed by C=C hydrogenation and ester hydrolysis*



[348] Similarly, reacting 6- $\alpha$ -3,17 androstane-3,17-dione **3** with the proper triphenylphosphonium salt (e.g., 5-carboxytriphenylphosphonium bromide, LiHMDS, THF

then EtOH (or MeOH)) produced compound **24**. Next, catalytic hydrogenation of compound **24** using Pd-C catalysis in the presence of hydrogen produced **CVie218**, which included a C<sub>6</sub> chain at the C-3 position. Hydrolysis of **CVie218** with 1M LiOH or NaOH in THF produced **CVie219**.

[349] Spectroscopic data for compound **CVie218**:

[350] <sup>1</sup>H NMR (400 MHz, Chloroform-d) δ 4.15 – 4.05 (m, 2H, OCH<sub>2</sub>), 3.40 (td, 1H, 6-H), 2.43 (dd, 1H, 16-Ha), 2.26 (td, 2H, 3ε-H), 0.84 (s, 3H, CH<sub>3</sub>), 0.76 (s, 3H, CH<sub>3</sub>).

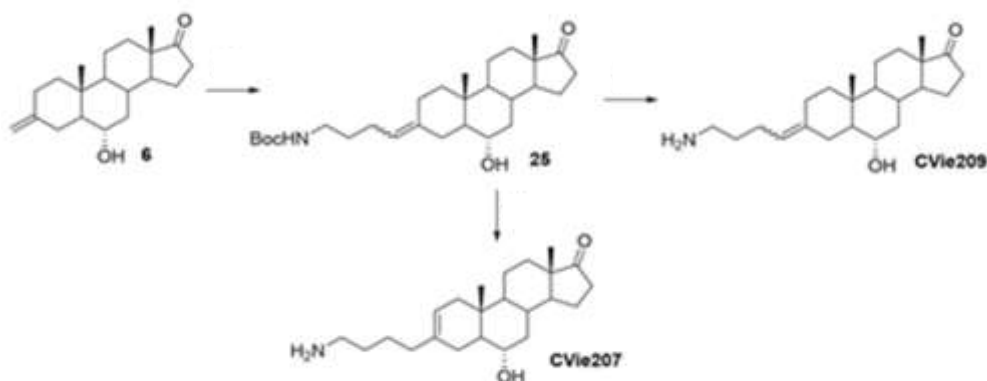
[351] <sup>13</sup>C NMR (101 MHz, Chloroform-d) δ 220.91 (17-C), 173.87 (CO<sub>2</sub>), 69.81 (6-C), 60.14 (CH<sub>2</sub>O), 14.24 (CH<sub>3</sub>), 13.79 (CH<sub>3</sub>), 13.39 (CH<sub>3</sub>).

[352] Spectroscopic data for compound **CVie219**:

[353] <sup>1</sup>H NMR (400 MHz, Chloroform-d) δ 3.47 – 3.39 (bt, 1H, 6-H), 2.44 (dd, 1H, 17-Ha), 2.33 (t, 2H, 3ε-H), 0.85 (s, 3H, CH<sub>3</sub>), 0.77 (s, 3H, CH<sub>3</sub>).

[354] <sup>13</sup>C NMR (101 MHz, Chloroform-d) δ 221.06 (17-C), 178.93 (CO<sub>2</sub>), 69.91 (6-C), 13.80 (CH<sub>3</sub>), 13.39 (CH<sub>3</sub>).

*Synthesis of derivatives with primary amine groups from precursor **6** by metathesis reaction with Boc-protected amines followed by Boc deprotection*



[355] For the synthesis of the derivatives with a primary amine group as the X substituent in formula (I), a cross metathesis reaction was carried out on precursor **6** using the same experimental conditions described above for the synthesis of **CVie201** and **CVie202**.

[356] Briefly, a Hoveyda-Grubbs 2<sup>nd</sup> generation catalyst was added to a solution of androstan-3-methylene-17-one **6** in DCM. Androstan-3-methylene-17-one **6** was then combined with an exo-methylene group with the appropriate Boc-protected amine (e.g., tert-butyl pent-4-en-1-yl carbamate or *N*-Boc-4-pentyne-1-amine) to produce diastereoisomers **25** (25% yield). Compound **25** (50 mg, 0,1 mmol, 1 eq) was treated with 500  $\mu$ L of a 1:1 mixture TFA/DCM trifluoroacetic acid in DCM) and then stirred at room temperature to directly cleave the Boc group. After stirring at room temperature for 1 minute, the reaction was diluted with EtOAc (50mL) and washed with saturated aq. NaHCO<sub>3</sub> (3x30mL). The organic phase was dried over Na<sub>2</sub>SO<sub>4</sub>, filtered, and evaporated to dryness to produce (EZ)-3-(4-aminobutyliden]-6 $\alpha$ -hydroxyandrostane-17-one (**CVie209**) as white solid (28 mg, 75%)

[357] Spectroscopic data for diastereoisomer mixture **25**:

[358] <sup>1</sup>H NMR (400 MHz, Chloroform-d)  $\delta$  5.18 – 5.03 (m, 1H, 3 $\alpha$ -H), 3.46 (td, 1H, 6-H), 1.44 (s, 9H, t-Bu), 0.90 (d, J = 1.8 Hz, 3H, CH<sub>3</sub>), 0.86 (s, 3H, CH<sub>3</sub>), 0.74 (m, 1H, 5-H).

[359] Spectroscopic data for **CVie209**:

[360] <sup>1</sup>H NMR (400 MHz, CD<sub>3</sub>OD)  $\delta$  5.13 (d, 1H, 3 $\alpha$ -H), 3.40 (tt, 1H, 6-H), 3.35 – 3.28 (m, 2H, 3 $\gamma$ -H), 0.96 (s, 3H, CH<sub>3</sub>), 0.87 (s, 3H, CH<sub>3</sub>), 0.83 – 0.70 (m, 1H, 5-H).

[361] <sup>13</sup>C NMR (101 MHz, CD<sub>3</sub>OD)  $\delta$  224.41 (17-C), 143.00 (3A-C), 142.68 (3 $\alpha$ B-C), 124.31 (3 $\alpha$ A-C), 124.02 (3 $\alpha$ B-C), 72.75 (C-6), 16.70 (CH<sub>3</sub>), 15.78 (CH<sub>3</sub>).

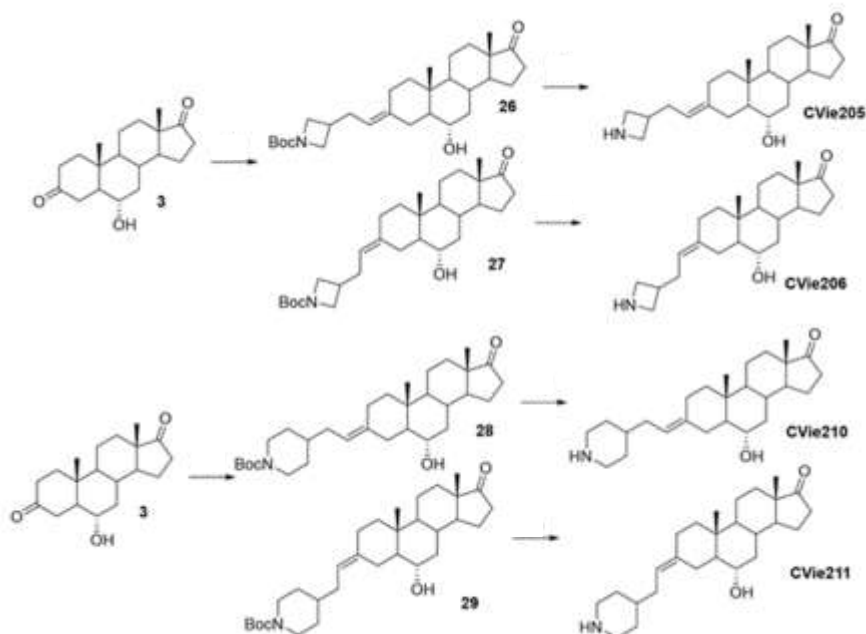
[362] Alternatively, reacting compound **25** with trimethylsilyl iodide in alcoholic solvent (e.g., MeOH) resulted in Boc cleavage accompanied by migration of the exocyclic double bond to produce **CVie207**, which has an endocyclic double bond between C2 and C3. Briefly, 1M TMSI in DCM (100 $\mu$ L, 0,1 mmol, 1 eq.) was added to a solution of diastereoisomers **25** (50 mg, 0,1mmol, 1eq.) at room temperature. After stirring 2h at the same temperature, the solvent was removed *in vacuo*. Methanol (2 mL) was added to the residue and left for 1h at room temperature. After removal of the solvent *in vacuo*, **CVie207** was obtained without further purification.

[363] Spectroscopic data for **CVie207**:

[364] <sup>1</sup>H NMR (400 MHz, CD<sub>3</sub>OD)  $\delta$  5.36 (d, 1H, H-2), 3.44 (td, 1H, 6-H), 2.94 (t, 2H, 3 $\gamma$ -H), 2.45 (dd, 1H, 16-Ha), 0.88 (s, 3H, CH<sub>3</sub>), 0.79 (s, 3H, CH<sub>3</sub>).

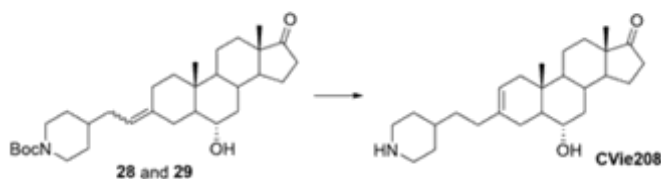
[365]  $^{13}\text{C}$  NMR (101 MHz,  $\text{CD}_3\text{OD}$ )  $\delta$  222.35 (17-C), 134.89 (3-C), 119.69 (2-C), 70.31 (6-H), 12.75 ( $\text{CH}_3$ ), 12.07 ( $\text{CH}_3$ ).

*Synthesis of Cyclic Amine Derivatives with exocyclic insaturations: CVie205, CVie206, CVie210 and CVie211*



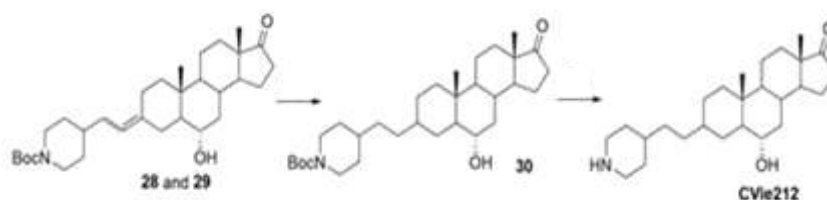
[366] Cyclic amine derivatives were synthesized by a sodium hydride (NaH)-DMSO Wittig reaction as described above for **CVie203** and **CVie204** while utilizing an appropriate N-protected phosphonium salt, such as *N*-Boc-4-(2-triphenylphosphoniummethyl)azetidine iodide to produce compounds **26** and **27** or *N*-Boc-3-(2-triphenylphosphoniummethyl)piperidin iodide to produce compounds **28** and **29**. After purification of the diastereoisomeric mixture, the *N*-Boc group was cleaved by acidic hydrolysis with TFA to produce **CVie205**, **CVie206**, **CVie210** and **CVie211**.

*Synthesis of CVie208 with an endocyclic insaturation (C=C double bond migration during Boc deprotection)*



[367] Further treatment of compounds **28** and **29** with TMSI as described above for the synthesis of **CVie207** produced **CVie208**.

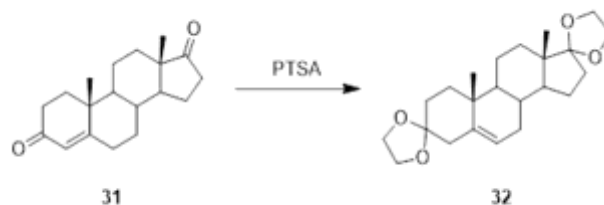
*Hydrogenation and Boc-cleavage with TFA to produce **CVie212***



[368] Alternatively, catalytic hydrogenation ( $H_2$ , Pd-C, EtOAc) of the double bonds of compounds **28** and **29** to synthesize compound **30** followed by Boc cleavage with TFA in DCM produced **CVie212**.

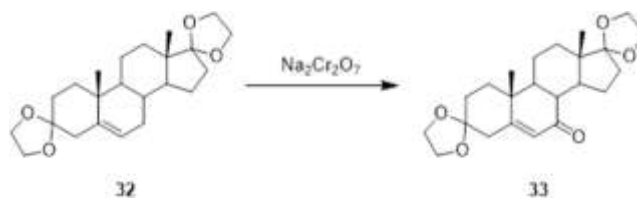
[369] Synthesis of compounds bearing a 6 $\alpha$ -hydroxymethylandrostan-7,17-dione was achieved starting from the common intermediate **37**. Compound **37** itself was synthesized starting from 4-androsten-3,17-dione **31**, by protection of the two ketone moiety by cyclic acetal **32** and simultaneous migration of the double bond, oxidation of the allylic position by sodium dichromate **33**, formation of the silyl enol ether **35**, hydroxymethylation with  $Me_3Al$  and formaldehyde (**36**), and final cleavage of acetals in acidic conditions. The synthesis is described in more detail in the following passages.

*Synthesis of compound **32**: (20S,7R)-7,20-dimethyldispiro[1,3-dioxolane-2,5'-tetracyclo[8.7.0.0<2,7>.0<11,15>]heptadecane-14',2''-1,3-dioxolane]-12-ene*



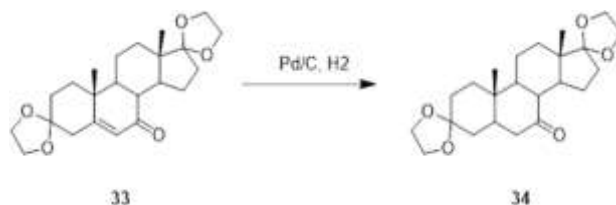
[370] A mixture of androst-4-ene-3,17-dione **31** (400.0 g, 1.4 mol) and PTSA·H<sub>2</sub>O (13.3 g, 70.0 mmol) in ethylene glycol (8.0 L) was stirred at 100 °C until the reaction was clear. About 5.0 L of glycol was distilled under vacuum so that the boiling temperature was around 80-85 °C. The mixture was cooled down to room temperature. The mixture was adjusted to pH~9. Then, the mixture was poured into ice-water. The mixture was filtered, and the solid was washed with water, collected, and triturated with acetone to get crude compound **32** (469.0 g, 89%) as a yellow solid.

*Synthesis of compound **33**: (20S,7R)-7,20-dimethyldispiro[1,3-dioxolane-2,5'-tetracyclo[8.7.0.0<2,7>.0<11,15>]heptadecane-14',2''-1,3-dioxolane]-12-en-14-one*



[371] A mixture of compound **32** (440.0 g, 1.2 mol), HOSU (541.2 g, 4.7 mol) and Na<sub>2</sub>Cr<sub>2</sub>O<sub>7</sub>·H<sub>2</sub>O (527.5 g, 1.8 mol) in acetone (8.0 L) was vigorously stirred at 50 °C for 2 days. After cooling down to room temperature, the mixture was quenched with aq. Na<sub>2</sub>SO<sub>3</sub> and stirred for 20 min. The mixture was poured into ice-water. The resulting mixture was stirred for 20 min and then filtered. The solid filtrate was washed with water, collected, and dried in vacuum to get crude compound **33** (390.0 g, 85%) as a yellow solid.

*Synthesis of compound **34**: (7S,20S)-7,20-dimethyldispiro[1,3-dioxolane-2,5'-tetracyclo[8.7.0.0<2,7>.0<11,15>]heptadecane-14',2''-1,3-dioxolane]-14-one*



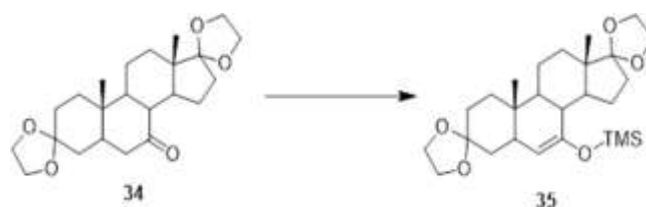
[372] A mixture of compound **33** (50.0 g, 128.9 mmol) in EtOAc (1250 mL) was added to Pd/C (16.0 g). Then the mixture was stirred at room temperature overnight under H<sub>2</sub>.

TLC showed the reaction was completed. The mixture was filtered, concentrated, and purified by flash chromatography (PE/EA = 2/1) to obtain compound **34** (25.0 g, 50.0%) as a white solid.

[373] Spectroscopic data for (7S,20S)-7,20-dimethyldispiro[1,3-dioxolane-2,5'-tetracyclo[8.7.0.0<2,7>.0<11,15>]heptadecane-14',2''-1,3-dioxolane]-14-one **34**:

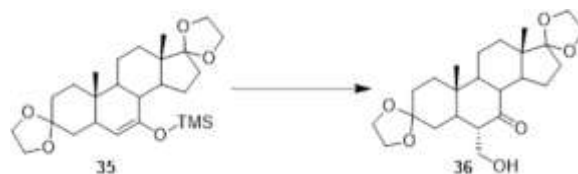
[374] <sup>1</sup>H NMR (400 MHz, DMSO-*d*<sub>6</sub>): δ 3.85-3.75 (m, 8H), 2.44-2.35 (m, 2H), 2.08-2.03 (m, 1H), 1.87-1.79 (m, 2H), 1.70-1.49 (m, 8H), 1.41-1.28 (m, 4H), 1.17-1.10 (m, 2H), 1.03 (s, 3H), 1.00-0.97 (m, 1H), 0.76 (s, 3H).

*Synthesis of compound 35: 1-((20S,7R)-7,20-dimethyldispiro[1,3-dioxolane-2,5'-tetracyclo[8.7.0.0<2,7>.0<11,15>]heptadecane-14',2''-1,3-dioxolane]-13-en-14-yloxy)-1,1-dimethyl-1-silaethane*



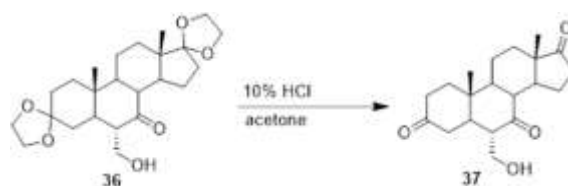
[375] A mixture of compound **34** (20.0 g, 51.3 mmol) in dry THF (100.0 mL) was stirred at -78 °C, and then 1.5 M LDA in toluene (205.2 mL, 307.8 mmol) was added dropwise. After stirring at the same temperature for 1 hr, Me<sub>3</sub>SiCl (50.0 mL, 400.1 mmol) was added dropwise. After stirring at -70 °C for 3 hrs, the temperature was raised to -30 °C and triethylamine (33.5 g, 331.5 mmol) was added. After stirring at the same temperature for 1 hr, the mixture was warmed up to room temperature and water (200.0 mL) and EtOAc (100.0 mL) were added. The separated aqueous phase was extracted with EtOAc. The combined organic layers were washed with brine, dried over Na<sub>2</sub>SO<sub>4</sub>, filtered, and evaporated to dryness. The residue was purified by flash chromatography (PE/EA = 2/1) to obtain compound **35** (14.3 g, 60.3 %) as a white solid.

*Synthesis of compound 36: (13S,20S,7R)-13-(hydroxymethyl)-7,20-dimethyldispiro[1,3-dioxolane-2,5'-tetracyclo[8.7.0.0<2,7>.0<11,15>]heptadecane-14',2''-1,3-dioxolane]-14-one*



[376] A mixture of 2,6-diphenylphenol (10.0 g, 27.6 mmol) in dry DCM (450.0 mL) was added dropwise to a solution of  $\text{Me}_3\text{Al}$  in toluene (41.4 mL, 82.9 mmol) while cooling with a ice/water bath so that the temperature did not exceed room temperature. After stirring at room temperature for 1 hr, the solution was cooled at 0 °C, and a solution of trioxane (24.8 g, 276.0 mmol) in dry DCM (100.0 mL) was added dropwise. The light yellow solution was stirred for another 1 hr at 0 °C and then the temperature was cooled down to -78 °C. A solution of compound **35** (10.0 g, 27.6 mmol) in dry DCM (125 mL) was added. After stirring at -78 °C for 1 h, the temperature was raised to -20 °C and the reaction mixture was stirred at that temperature overnight. 5% aq.  $\text{NaHCO}_3$  (85.0 mL) was added at room temperature. The jelly mixture was filtered through a CELITE® pad washing thoroughly with DCM. The separated organic layer was washed with water and evaporated. About 1M TBAF in THF (24.0 mL) was added to the residue and the solution was stirred at room temperature for 1.5 h. The solution was washed with water, dried over  $\text{Na}_2\text{SO}_4$ , filtered, and evaporated to dryness. The residue was purified by flash chromatography to give compound **36** (6.5 g, 71.4%) as a yellow solid.

*Synthesis of compound 37: (6S,10R,13S)-6-(hydroxymethyl)-10,13-dimethyldecahydro-1H-cyclopenta[a]phenanthrene-3,7,17(2H,4H,8H)-trione*



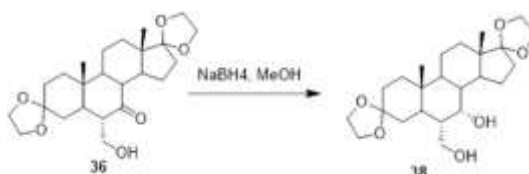
[377] A mixture of compound **36** (8.0 g, 19.0 mmol) in acetone (100.0 mL) was added to 10% aq. HCl (50.0 mL). Then the mixture was heated to 70 °C for 1 h. TLC showed the reaction was completed. The mixture was quenched with 5% aq. NaOH and extracted with DCM (50.0 mL \* 2). The combined organic phases were washed with brine (50.0 mL), dried over  $\text{Na}_2\text{SO}_4$ , filtered, concentrated, and purified by flash chromatography (DCM/EA = 4/1) to get the crude product, which was triturated with ether to get the pure product **37** (3.3 g, 52.4 %) as a white solid.

[378] Spectroscopic data for (6S,10R,13S)-6-(hydroxymethyl)-10,13-dimethyldecahydro-1H-cyclopenta[a]phenanthrene-3,7,17(2H,4H,8H)-trione **37**:

[379]  $^1\text{H}$  NMR (400 MHz,  $\text{DMSO-}d_6$ ):  $\delta$  4.14 (t, 1H), 3.63-3.59 (m, 1H), 3.50-3.47 (m, 1H), 2.74-2.69 (m, 1H), 2.42-2.27 (m, 5H), 2.15-1.93 (m, 3H), 1.87-1.79 (m, 1H), 1.68-1.59 (m, 3H), 1.54-1.44 (m, 2H), 1.32-1.06 (m, 7H), 0.81 (s, 3H).

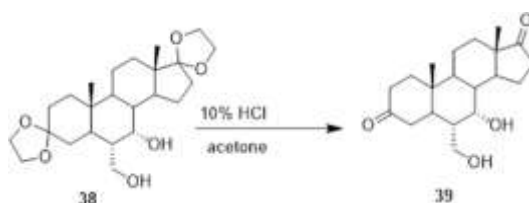
[380] LCMS [mobile phase: from 55% water (0.05% FA) and 45%  $\text{CH}_3\text{CN}$  (0.05% FA) to 55% water (0.05% FA) and 45%  $\text{CH}_3\text{CN}$  (0.05% FA) in 6.0 min, finally under these conditions for 0.5 min], purity is >90%,  $R_t = 2.514$  min; MS Calcd.: 332.2; MS Found: 333.2  $[\text{M}+1]^+$ .

*Synthesis of compound **38**: (13S,14S,20S,7R)-13-(hydroxymethyl)-7,20-dimethyldispiro[1,3-dioxolane-2,5'-tetracyclo[8.7.0.0<2,7>.0<11,15>]heptadecane-14',2''-1,3-dioxolane]-14-ol*



[381]  $\text{NaBH}_4$  (4.0 g, 104.8 mmol) was added slowly to a mixture of compound **36** (22.0 g, 52.4 mmol) in MeOH (1000.0 mL) at 0 °C. Then the mixture was stirred at rt for 1 h. TLC showed the reaction was completed. The mixture was quenched with 5% aq.  $\text{NaH}_2\text{PO}_4$  (220.0 mL) and extracted with DCM (300.0 mL \* 3). The combined organic phases were washed with brine (200.0 mL), dried over  $\text{Na}_2\text{SO}_4$ , filtered, concentrated, and purified by flash chromatography (DCM/EA = 4/1) to get the crude product, which was triturated with ether to obtain the compound **38** (7.5 g, 34.1 %) as a white solid.

*Synthesis of compound **39**: (8S,9S,15S,2R)-9-hydroxy-8-(hydroxymethyl)-2,15-dimethyltetracyclo[8.7.0.0<2,7>.0<11,15>]heptadecane-5,14-dione*



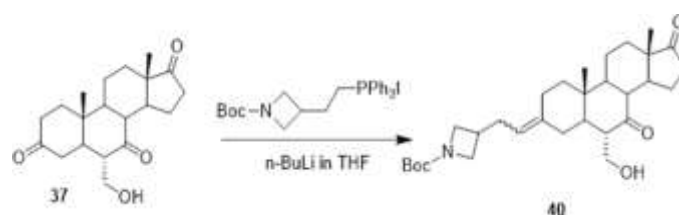
[382] 10% aq. HCl (35.0 mL) was added to a mixture of compound **38** (5.7 g, 13.5 mmol) in acetone (70.0 mL). Then, the mixture was heated to 70 °C for 1 h. TLC showed the reaction was completed. The mixture was quenched with 5% aq. NaOH and extracted with DCM (50.0 mL \* 2). The combined organic phases were washed with brine (50 mL), dried over Na<sub>2</sub>SO<sub>4</sub>, filtered, and concentrated. The residue was purified by flash chromatography (DCM/EA = 4/1) to get the crude product, which was triturated with ether to obtain the pure product **39** (1.8 g, 40.0 %) as a white solid.

[383] Spectroscopic data for (8*S*,9*S*,15*S*,2*R*)-9-hydroxy-8-(hydroxymethyl)-2,15-dimethyl tetracyclo[8.7.0.0.<2,7>.0<11,15>]heptadecane-5,14-dione **39**:

[384] <sup>1</sup>H NMR (400 MHz, DMSO-*d*<sub>6</sub>): δ4.37 (brs, 1H), 4.27 (d, *J* = 4.8 Hz, 1H), 3.87-3.86 (m, 1H), 3.44-3.42 (m, 2H), 2.45-1.87 (m, 10H), 1.63-1.23 (m, 9H), 0.99 (s, 3H), 0.81 (s, 3H).

[385] LCMS [mobile phase: from 55% water (0.05% FA) and 45% CH<sub>3</sub>CN (0.05% FA) to 55% water (0.05% FA) and 45% CH<sub>3</sub>CN (0.05% FA) in 6.0 min, finally under these conditions for 0.5 min], purity is >90%, Rt = 2.515 min; MS Calcd.: 334.2; MS Found: 352.2 [M+18]<sup>+</sup>.

*Synthesis of compound 40: tert-butyl-(2-((6*S*,10*R*,13*S*)-6-(hydroxymethyl)-10,13-dimethyl-7,17-dioxododecahydro-1*H*-cyclopenta[*a*]phenanthren-3(2*H*,4*H*,10*H*)-ylidene)ethyl)azetidine-1-carboxylate*

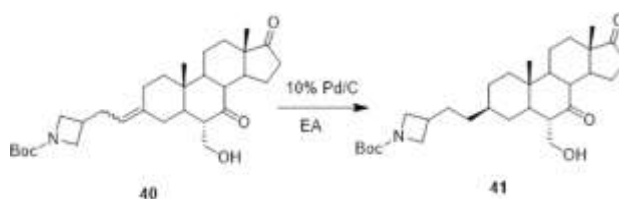


[386] To a solution of phosphonium salt (2.57 g, 4.5 mmol) in THF (25 mL), a solution of n-BuLi in THF (2.5 M, 3.6 mL, 9.0 mmol) was added at -78 °C. The mixture was stirred at 30 °C for 1 hour. Next, the compound **37** (500 mg, 1.5 mmol) was added to the mixture at -20 °C and then warmed to 30°C for 2 hours. The mixture was quenched with sat.NH<sub>4</sub>Cl (25 mL) and extracted with EtOAc (25 mL \* 3). The combined organic layers were concentrated and the residue was purified by column chromatography on silica gel (hexane/EtOAc = 1/1) to give the crude compound. The compound was purified by reverse column to obtain pure compound **40** (60 mg, 8%) as a white solid.

[387] Data for compound **40**:

[388] LCMS column: C18; column size: 4.6\*30 mm 5  $\mu$ m; Dikwa Diamonsil plus; mobile phase: B(ACN) : A (0.02%NH<sub>4</sub>Ac+5%ACN); gradient (B%) in 3 min-5-95-POS; flow 1.5 mL/min, stop time 3mins. Rt = 1.820 min; MS Calcd.: 499, MS Found: 400 [M+H-Boc]<sup>+</sup>.

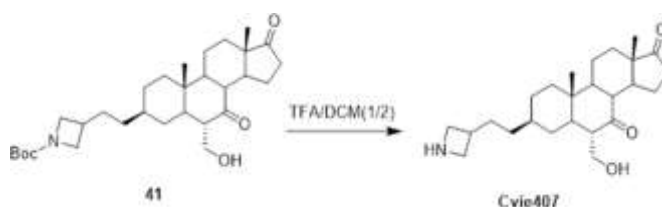
*Synthesis of compound **41**: tert-butyl-3-(2-((3S,6S,10R,13S)-6-(hydroxymethyl)-10,13-dimethyl-7,17-dioxohexadecahydro-1H-cyclopenta[a]phenanthren-3-yl)ethyl)azetidine-1-carboxylate*



[389] Pd/C (60 mg) was added to the solution of compound **40** (60 mg, 0.12 mmol) in EA (3 mL). Then, the mixture was stirred at room temperature overnight under H<sub>2</sub>. The mixture was filtered and the filtrate was concentrated to produce compound **41** (52 mg, 86%) as a white solid.

[390] LCMS column: C18; column size: 4.6\*30 mm 5  $\mu$ m,; Dikma Diamonsil plus; mobile phase: B(ACN) : A (0.02%NH<sub>4</sub>Ac+5%ACN); gradient (B%) in 3 min-5-95-POS; flow 1.5 mL/min, stop time 3mins. Rt = 1.911 min; MS Calcd.: 501, MS Found: 402 [M+H-Boc]<sup>+</sup>.

*Synthesis of **Cvie407**: (3S,6S,10R,13S)-3-(2-(azetidin-3-yl)ethyl)-6-(hydroxymethyl)-10,13-dimethyldodecahydro-1H-cyclopenta[a]phenanthrene-7,17(2H,8H)-dione*



[391] A solution of compound **41** (52 mg, 0.10 mmol) in TFA/DCM (1 mL/2 mL) was stirred at room temperature for 1 hour. The mixture was diluted with sat. NaHCO<sub>3</sub> to

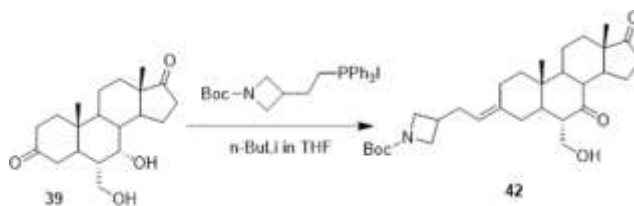
adjust to pH 8-9. The mixture was extracted with DCM (25 mL \* 3). The combined organic layers were concentrated and the residue was purified by prep-HPLC to produce compound **Cvie407** (13 mg, 32%) as a white solid.

[392] Spectroscopic data for **Cvie407**:

[393]  $^1\text{H}$  NMR ( $\text{CD}_3\text{OD}$ , 400 MHz):  $\delta$  3.86-3.82 (m, 2H), 3.71-3.67 (m, 1H), 3.54-3.47 (m, 2H), 2.78-2.67 (m, 2H), 2.56-2.39 (m, 3H), 2.15-2.06 (m, 1H), 1.85-1.50 (m, 12H), 1.21-1.14 (m, 9H), 1.07-1.01 (m, 2H), 0.88 (s, 3H).

[394] LCMS column: column: C18; column size: 4.6\*50 mm; mobile phase: B (ACN) : A (0.02% $\text{NH}_4\text{Ac}$ ); gradient (B%) in 6.5 min-5-95-POS;  $R_t$  = 3.114 min; MS Calcd.: 401, MS Found: 402  $[\text{M}+\text{H}]^+$ .

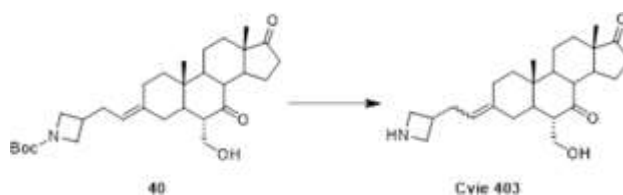
*Synthesis of compound 42: tert-butyl-3-((E)-2-((6S,10R,13S)-6-(hydroxymethyl)-10,13-dimethyl-7,17-dioxododecahydro-1H-cyclopenta[a]phenanthren-3(2H,4H,10H)-ylidene)ethyl)azetidine-1-carboxylate*



[395] A solution of n-BuLi in THF (2.5 M, 0.7 mL, 1.80 mmol) was added to a solution of compound phosphonium salt (514 mg, 0.90 mmol) in THF (5 mL) at -78 °C. The mixture was stirred at 40 °C for 1 hour. Then, compound **39** (100 mg, 0.30 mmol) was added to the mixture at 0 °C and then warmed to 40 °C overnight. The reaction was repeated for nine times. The mixture was quenched with sat. $\text{NH}_4\text{Cl}$  (80 mL) and extracted with EtOAc (100 mL \* 3). The combined organic layers were concentrated and the residue was purified by prep-HPLC to produce compound **42** (20 mg, 1%) as a yellow solid.

[396] LCMS column: C18; column size: 4.6\*30 mm 5  $\mu\text{m}$ ; Dikwa Diamonsil plus; mobile phase: B (ACN) : A (0.02% $\text{NH}_4\text{Ac}$ +5%ACN); gradient (B%) in 3 min-5-95-POS; flow 1.5 mL/min, stop time 3mins.  $R_t$  = 1.945 min; MS Calcd.: 501, MS Found: 402  $[\text{M}+\text{H}-\text{Boc}]^+$ .

Synthesis of **CVie403**: (6*S*,10*R*,13*S*)-3-(2-(azetidin-3-yl)ethylidene)-6-(hydroxymethyl)-10,13-dimethyldodecahydro-1*H*-cyclopenta[*a*]phenanthrene-7,17(2*H*,8*H*)-dione



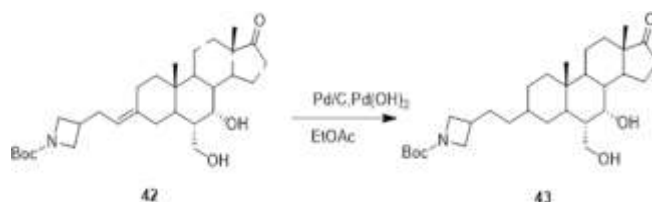
[397] The solution of compound **40** (130 mg, 0.26 mmol) in TFA/DCM (1 mL/2 mL) was stirred at room temperature for 1 hour. The mixture was basified with sat.NaHCO<sub>3</sub> to pH 8-9. The mixture was extracted with DCM (30 mL \*3). The combined organic layer was concentrated and the residue was purified by prep-HPLC to produce compound **CVie403** (13 mg, yield 13%) as a yellow solid.

[398] Spectroscopic data for **CVie403**:

[399] <sup>1</sup>H NMR (CD<sub>3</sub>OD, 400 MHz): δ 5.00-4.96 (m, 1H), 3.92-3.81 (m, 3H), 3.66-3.62 (m, 1H), 3.54-3.52 (m, 2H), 2.77-2.73 (m, 1H), 2.67-2.61 (m, 2H), 2.49-2.43 (m, 2H), 2.38-2.29 (m, 2H), 2.23-2.18 (m, 2H), 2.06-1.96 (m, 2H), 1.83-1.76 (m, 2H), 1.71-1.61 (m, 3H), 1.51-1.35 (m, 3H), 1.18 (s, 3H), 1.12-1.05 (m, 2H), 0.98-0.90 (m, 1H), 0.80 (s, 3H).

[400] LCMS column: Rt = 3.964 min; MS Calcd.:399, MS Found: 400 [M+H]<sup>+</sup>.

Synthesis of compound **43**: 3-(2-((6*S*,7*S*,10*R*,13*S*)-7-hydroxy-6-(hydroxymethyl)-10,13-dimethyl-17-oxohexadecahydro-1*H*-cyclopenta[*a*]phenanthren-3-yl)ethyl)azetidine-1-carboxylate

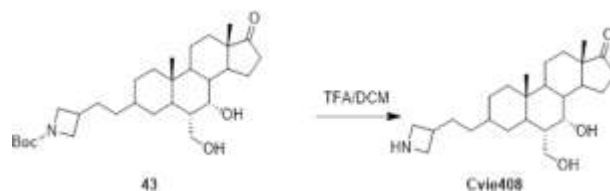


[401] A mixture of compound **42** (20 mg, 0.04 mmol), Pd/C (10%, 20 mg), and Pd(OH)<sub>2</sub> (20%, 20 mg) in EtOAc (2 mL) was stirred at room temperature overnight under

H<sub>2</sub> (in balloon). The mixture was filtered and the filtrate was concentrated to give the crude compound **43** (20 mg, 100%) as a brown solid.

[402] LCMS column: C18; column size: 4.6\*30 mm 5 μm,; Dikma Diamonsil plus; mobile phase: B(ACN) : A (0.02%NH<sub>4</sub>Ac+5%ACN); gradient (B%) in 3 min-5-95-POS; flow 1.5 mL/min, stop time 3mins. Rt = 1.978 min; MS Calcd.:503, MS Found: 404 [M+H-Boc]<sup>+</sup>.

*Synthesis of CVie408: (6S,7S,10R,13S)-3-(2-(azetidin-3-yl)ethyl)-7-hydroxy-6-(hydroxymethyl)-10,13-dimethyltetradecahydro-1H-cyclopenta[a]phenanthren-17(2H)-one*



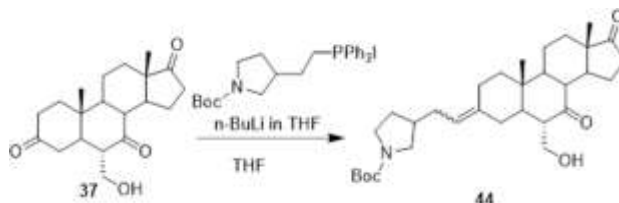
[403] A mixture of compound **43** (20 mg, 0.04 mmol) in TFA/DCM (1:1, 2 mL) was stirred at 0 °C for 30 minutes. The mixture was diluted with *sat.* NaHCO<sub>3</sub> to adjust to pH 8-9. The mixture was extracted with DCM (25 mL \* 3). The combined organic layers were dried over Na<sub>2</sub>SO<sub>4</sub>, filtered and concentrated. The residue was purified by prep-HPLC to produce compound **CVie408** (6.4 mg, 40%) as a yellow solid.

[404] Spectroscopic data for **CVie408**:

[405] <sup>1</sup>H NMR (CD<sub>3</sub>OD, 400 MHz): δ 4.08 (s, 1H), 3.84 (t, *J* = 8.4 Hz, 1H), 3.77-3.68 (m, 2H), 3.52-3.48 (m, 2H), 2.81-2.73 (m, 1H), 2.52-2.44 (m, 1H), 2.18-2.06 (m, 2H), 1.86-1.71 (m, 4H), 1.69-1.59 (m, 6H), 1.52-1.43 (m, 2H), 1.39-1.30 (m, 4H), 1.24-1.15 (m, 4H), 1.12-1.04 (m, 1H), 0.95-0.92 (m, 1H), 0.90(s, 3H), 0.87 (s, 3H).

[406] LCMS column: column: C18;column size:4.6\*50 mm ;mobile phase: B (ACN) : A (0.02%NH<sub>4</sub>Ac); gradient (B%) in 6.5 min-5-95-POS; Rt = 3.078 min; MS Calcd.:403, MS Found: 404 [M+H]<sup>+</sup>.

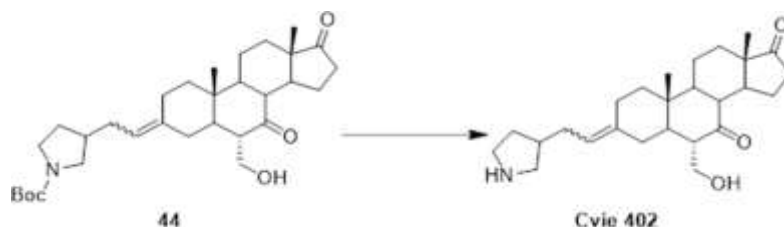
Synthesis of compound **44**: *tert*-butyl-3-(2-((6*S*,10*R*,13*S*)-6-(hydroxymethyl)-10,13-dimethyl-7,17-dioxododecahydro-1*H*-cyclopenta[*a*]phenanthren-3(2*H*,4*H*,10*H*)-ylidene)ethyl)pyrrolidine-1-carboxylate



[407] A solution of *n*-BuLi in THF (2.5M, 1.57 mL, 3.94 mmol) was added to a solution of compound phosphonium salt (1.5 g, 2.62 mmol) in THF (15 mL) at -78 °C. The reaction mixture was stirred at 35 °C for 1 hour. Then, a solution of compound **37** (350 mg, 1.05 mmol) was added to the mixture at -20 °C and warmed to room temperature for 2 hours. The mixture was quenched with *sat.*NH<sub>4</sub>Cl (25 mL) and extracted with EtOAc (25 mL \* 3). The combined organic layers were concentrated and the residue was purified by flash chromatography (hexane:EA = 1:1) to give crude compound. Then the compound was purified by reverse column to obtain pure compound **44** (53 mg, 10%) as a white solid.

[408] LCMS column: C18; column size: 4.6\*30 mm 5 μm; Dikma Diamonsil plus; mobile phase: B (ACN) : A (0.02%NH<sub>4</sub>Ac+5%ACN); gradient (B%) in 3 min-5-95-POS; flow 1.5 mL/min, stop time 3mins. Rt = 2.017 min; MS Calcd.: 513, MS Found: 414 [M+H-Boc]<sup>+</sup>.

Synthesis of **CVie402**: (6*S*,10*R*,13*S*)-6-(hydroxymethyl)-10,13-dimethyl-3-(2-(pyrrolidin-3-yl)ethylidene)dodecahydro-1*H*-cyclopenta[*a*]phenanthrene-7,17(2*H*,8*H*)-dione



[409] A solution of compound **44** (89 mg, 0.173 mmol) in TFA/DCM (1 mL/2 mL) was stirred at room temperature for 1 hour. The mixture was diluted with *sat.*NaHCO<sub>3</sub> to

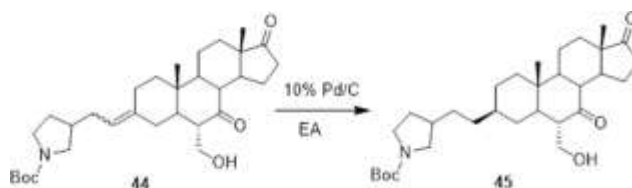
adjust pH = 8-9. The mixture was extracted with DCM (25 mL \*3). The combined organic layer was concentrated and the residue was purified by prep-HPLC to produce compound **CVie402** (38 mg, 53%) as a white solid.

[410] Spectroscopic data for **CVie402**:

[411]  $^1\text{H}$  NMR ( $\text{CD}_3\text{OD}$ , 400 MHz):  $\delta$  5.08-5.05 (m, 1H), 3.88-3.82 (m, 1H), 3.63-3.59 (m, 1H), 3.12-3.02 (m, 2H), 2.99-2.92 (m, 1H), 2.66-2.55 (m, 3H), 2.48-2.42 (m, 2H), 2.37-2.30 (m, 1H), 2.23-2.19 (m, 1H), 2.15-2.04 (m, 2H), 2.03-1.91 (m, 4H), 1.83-1.78 (m, 2H), 1.75-1.61 (m, 3H), 1.51-1.34 (m, 4H), 1.19-1.17 (m, 3H), 1.12-1.03 (m, 2H), 0.97-0.90 (m, 1H), 0.80 (s, 3H).

[412] LCMS column:  $R_t$  = 3.060 min; MS Calcd.:413, MS Found: 414[M+H] $^+$ .

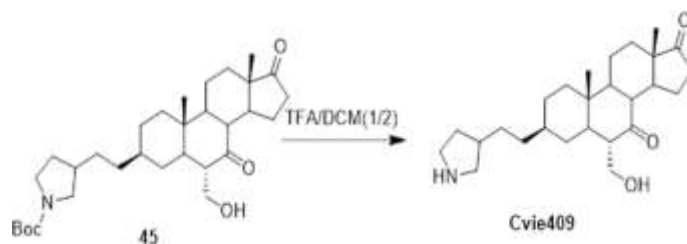
*Synthesis of compound **45**: tert-butyl-3-(2-((3S,6S,10R,13S)-6-(hydroxymethyl)-10,13-dimethyl-7,17-dioxohexadecahydro-1H-cyclopenta[a]phenanthren-3-yl)ethyl)pyrrolidine-1-carboxylate*



[413] A solution of compound **44** (53 mg, 0.103 mmol) in EA (3 mL) was added to Pd/C (60 mg). Then, the mixture was stirred at room temperature overnight under  $\text{H}_2$ . The mixture was filtered and the filtrate was concentrated to produce compound **45** (50 mg, 94%) as a white solid.

[414] LCMS column: C18; column size: 4.6\*30 mm 5  $\mu\text{m}$ ; Dikma Diamonsil plus; mobile phase: B (ACN) : A (0.02% $\text{NH}_4\text{Ac}$ +5%ACN); gradient (B%) in 3 min-5-95-POS; flow 1.5 mL/min, stop time 3mins.  $R_t$  = 1.984 min; MS Calcd.: 515, MS Found: 416 [M+H-Boc] $^+$ .

Synthesis of **CVie409**: (3*S*,6*S*,10*R*,13*S*)-6-(hydroxymethyl)-10,13-dimethyl-3-(2-(pyrrolidin-3-yl)ethyl)dodecahydro-1*H*-cyclopenta[*a*]phenanthrene-7,17(2*H*,8*H*)-dione



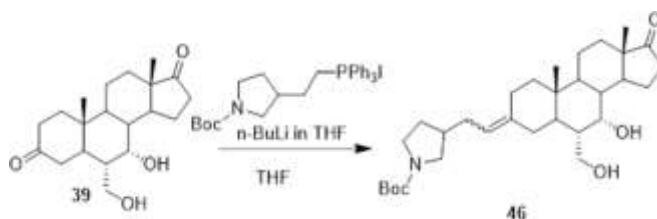
[415] A solution of compound **45** (50 mg, 0.09 mmol) in TFA/DCM (1 mL/2 mL) was stirred at room temperature for 1 hour. The mixture was diluted with *sat.*NaHCO<sub>3</sub> to adjust to pH 8-9. The mixture was extracted with DCM (25 mL \* 3). The combined organic layers were concentrated and the residue was purified by prep-HPLC to produce compound **CVie409** (12 mg, 32%) as a white solid.

[416] Spectroscopic data for **CVie409**:

[417] <sup>1</sup>H NMR (CD<sub>3</sub>OD, 400 MHz): δ 3.87-3.82 (m, 1H), 3.70-3.64 (m, 1H), 3.28-3.24 (m, 1H), 3.21-3.16 (m, 1H), 3.11-3.04 (m, 1H), 2.72-2.62 (m, 2H), 2.57-2.51 (m, 1H), 2.47-2.39 (m, 2H), 2.17-2.05 (m, 3H), 1.85-1.70 (m, 5H), 1.66-1.49 (m, 8H), 1.38-1.34 (m, 2H), 1.25-1.19 (m, 6H), 1.14-1.10 (m, 2H), 0.88 (s, 3H).

[418] LCMS column: column:C18; column size: 4.6\*50 mm; mobile phase: B(ACN) : A(0.02%NH<sub>4</sub>Ac); gradient(B%) in 6.5 min-5-95-POS; Rt = 3.180 min; MS Calcd.:415, MS Found: 416 [M+H]<sup>+</sup>

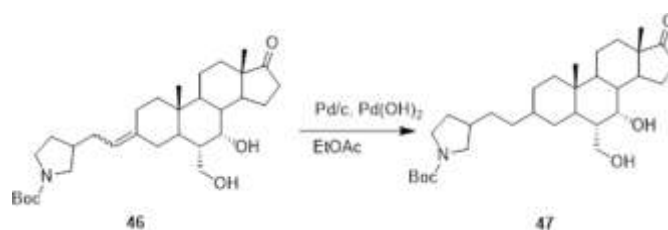
Synthesis of compound **46**: *tert*-butyl-3-(2-((6*S*,7*S*,10*R*,13*S*)-7-hydroxy-6-(hydroxymethyl)-10,13-dimethyl-17-oxododecahydro-1*H*-cyclopenta[*a*]phenanthren-3(2*H*,4*H*,10*H*)-ylidene)ethyl)pyrrolidine-1-carboxylate



[419] A solution of n-BuLi in THF (2.5M, 0.7 mL, 1.80 mmol) was added to a solution of compound phosphonium salt (527 mg, 0.90 mmol) in THF (5 mL) at -78 °C. The reaction mixture was stirred at 35 °C for 1 hour. Then compound **39** (100 mg, 0.30 mmol) was added to the mixture at 0 °C and then warmed to 35 °C overnight. The reaction was repeated for four times. The mixture was quenched with sat.NH<sub>4</sub>Cl (80 mL) and extracted with EtOAc (100 mL \* 3). The combined organic layers were concentrated and the residue was purified by prep-HPLC to give compound **46** (26 mg, 3%) as a white solid.

[420] LCMS column: C18; column size: 4.6\*30 mm 5 μm; Dikma Diamonsil plus; mobile phase: B (ACN) : A (0.02%NH<sub>4</sub>Ac+5%ACN); gradient (B%) in 3 min-5-95-POS; flow 1.5 mL/min, stop time 3mins. Rt = 2.000 min; MS Calcd.:515, MS Found: 416 [M+H-Boc]<sup>+</sup>.

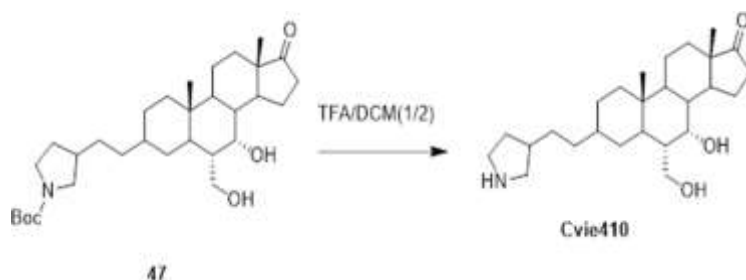
*Synthesis of compound **47**: tert-butyl-3-(2-((6S,7S,10R,13S)-7-hydroxy-6-(hydroxymethyl)-10,13-dimethyl-17-oxohexadecahydro-1H-cyclopenta[a]phenanthren-3-yl)ethyl)pyrrolidine-1-carboxylate*



[421] A mixture of compound **46** (26 mg, 0.05 mmol), Pd/C (10%, 30 mg), and Pd(OH)<sub>2</sub> (20%, 30 mg) in EtOAc (3 mL) was stirred at room temperature overnight under H<sub>2</sub> (in balloon). The mixture was filtered and filtrate was concentrated to give the crude compound **47** (26 mg, 100%) as a yellow solid.

[422] LCMS column: C18; column size: 4.6\*30 mm 5 μm; Dikma Diamonsil plus; mobile phase: B (ACN) : A (0.02%NH<sub>4</sub>Ac+5%ACN); gradient (B%) in 3 min-5-95-POS; flow 1.5 mL/min, stop time 3mins. Rt =2.059 min; MS Calcd.:517, MS Found: 418 [M+H-Boc]<sup>+</sup>.

Synthesis of **CVie410**: (6*S*,7*S*,10*R*,13*S*)-7-hydroxy-6-(hydroxymethyl)-10,13-dimethyl-3-(2-(pyrrolidin-3-yl)ethyl)tetradecahydro-1*H*-cyclopenta[*a*]phenanthren-17(2*H*)-one



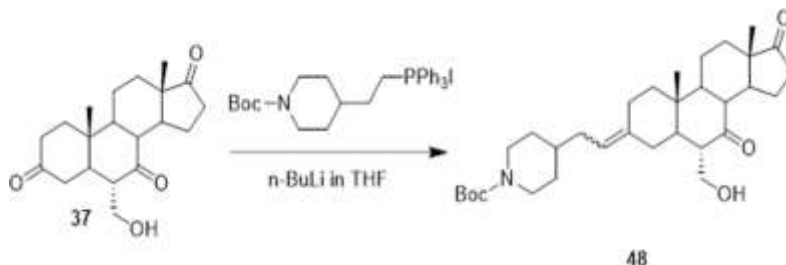
[423] A solution of compound **47** (26 mg, 0.05 mmol) in TFA/DCM (1:2, 2 mL) was stirred at 0 °C for 1 hour. The mixture was diluted with *sat.*NaHCO<sub>3</sub> to adjust to pH 8-9. The mixture was extracted with DCM (20 mL \* 3). The combined organic layers were dried over Na<sub>2</sub>SO<sub>4</sub>, filtered and concentrated. The residue was purified by prep-HPLC to produce compound **CVie410** (9 mg, 43%) as a yellow solid.

[424] Spectroscopic data for **CVie410**:

[425] <sup>1</sup>H NMR (CD<sub>3</sub>OD, 400 MHz): δ 3.95 (s, 1H), 3.64-3.57 (m, 2H), 3.12-3.07 (m, 1H), 3.04-2.96 (m, 1H), 2.93-2.89 (m, 1H), 2.48-2.44 (m, 1H), 2.38-2.32 (m, 1H), 2.05-1.93 (m, 4H), 1.69-1.57 (m, 5H), 1.55-1.46 (m, 4H), 1.37-1.33 (m, 4H), 1.25-1.18 (m, 5H), 1.08-0.90 (m, 3H), 0.82-0.80 (m, 1H), 0.77 (s, 3H), 0.75 (s, 3H).

[426] LCMS column: column: C18;column size:4.6\*50 mm ; mobile phase: B(ACN) : A(0.02%NH<sub>4</sub>Ac); gradient (B%) in 6.5 min-5-95-POS; Rt = 3.139 min; MS Calcd.:417, MS Found: 418 [M+H]<sup>+</sup>.

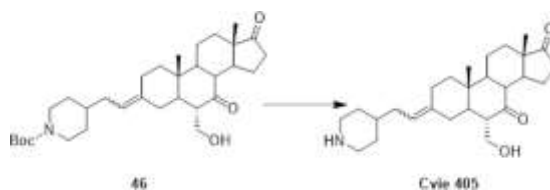
Synthesis of compound **48**: *tert*-butyl-4-(2-((6*S*,10*R*,13*S*)-6-(hydroxymethyl)-10,13-dimethyl-7,17-dioxododecahydro-1*H*-cyclopenta[*a*]phenanthren-3(2*H*,4*H*,10*H*)-ylidene)ethyl)piperidine-1-carboxylate



[427] A solution of *n*-BuLi in THF (2.5 M, 2.90 mL, 7.20 mmol) was added to a mixture of compound phosphonium salt (2.16 g, 3.60 mmol) in THF (16 mL) at -78 °C. The reaction mixture was stirred at 30 °C for 1 hour. Then compound **37** (400 mg, 1.20 mmol) was added to the mixture at -20 °C. The mixture was stirred at -20 °C for 30 minutes and then warmed to 30 °C for 2 hours. The mixture was quenched with *sat.*NH<sub>4</sub>Cl (15 mL) and extracted with EtOAc (30 mL \* 3). The combined organic layers were concentrated and the residue was purified by prep-HPLC to give the compound **48** (28 mg, 4%) as a yellow solid.

[428] LCMS column: C18; column size: 4.6\*30 mm 5 μm; Dikma Diamonsil plus; mobile phase: B (ACN) : A (0.02%NH<sub>4</sub>Ac+5%ACN); gradient (B%) in 3 min-30-95-POS; flow 1.5 mL/min, stop time 3mins. Rt = 2.013 min; MS Calcd.: 527, MS Found: 428 [M+H-Boc]<sup>+</sup>.

Synthesis of **CVie405**: (6*S*,10*R*,13*S*)-6-(hydroxymethyl)-10,13-dimethyl-3-(2-(piperidin-4-yl)ethylidene)dodecahydro-1*H*-cyclopenta[*a*]phenanthrene-7,17(2*H*,8*H*)-dione



[429] A solution of compound **46** (80 mg, 0.152 mmol) in TFA/DCM (1 mL/2 mL) was stirred at room temperature for 30 minutes. The mixture was basified with *sat.*NaHCO<sub>3</sub> to pH = 8-9. The mixture was extracted with DCM (25 mL \*3). The combined organic layer

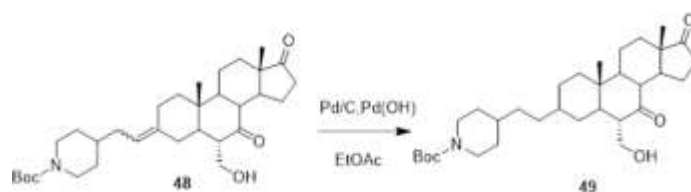
was dried over Na<sub>2</sub>SO<sub>4</sub>, filtered and concentrated. The residue was purified by prep-HPLC to produce compound **CVie405** (30 mg, 46%) as a yellow solid.

[430] Spectroscopic data for **CVie405**:

[431] <sup>1</sup>H NMR (CD<sub>3</sub>OD, 400 MHz): δ 5.14 (t, J = 7.2 Hz, 1H), 3.88-3.80 (m, 1H), 3.74-3.66 (m, 1H), 3.09-3.06 (m, 2H), 2.67-2.49 (m, 6H), 2.45-2.38 (m, 1H), 2.33-2.26 (m, 1H), 2.19-2.04 (m, 2H), 2.01-1.83(m, 3H), 1.80-1.69 (m, 6H), 1.61-1.47 (m, 2H), 1.45-1.34 (m, 2H), 1.30-1.25 (m, 5H), 1.19-1.08(m, 4H), 1.04-0.90 (m, 1H), 0.88 (s, 3H).

[432] LCMS column: Rt = 3.219 min; MS Calcd.:427, MS Found: 428 [M+H]<sup>+</sup>.

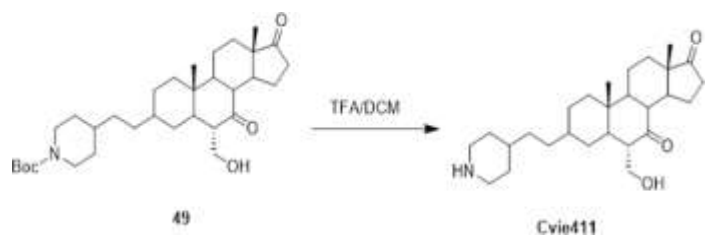
*Synthesis of compound 49: tert-butyl-4-(2-((6S,10R,13S)-6-(hydroxymethyl)-10,13-dimethyl-7,17-dioxohexadecahydro-1H-cyclopenta[a]phenanthren-3-yl)ethyl)piperidine-1-carboxylate*



[433] A mixture of compound **48** (28 mg, 0.05 mmol) and Pd/C (10%, 50 mg) in EtOAc (2 mL) was stirred at room temperature overnight under H<sub>2</sub> (in balloon). The mixture was filtered and the filtrate was concentrated to give the crude compound **49** (28 mg, 100%) as a yellow solid.

[434] LCMS column: C18; column size: 4.6\*30 mm 5 μm;; Dikwa Diamonsil plus; mobile phase: B(ACN) : A (0.02%NH<sub>4</sub>Ac+5%ACN); gradient (B%) in 3 min-5-95-POS; flow 1.5 mL/min, stop time 3mins.Rt = 2.109 min; MS Calcd.:529, MS Found: 430 [M+H-Boc]<sup>+</sup>.

Synthesis of **CVie411**: (6*S*,10*R*,13*S*)-6-(hydroxymethyl)-10,13-dimethyl-3-(2-(piperidin-4-yl)ethyl)dodecahydro-1*H*-cyclopenta[*a*]phenanthrene-7,17(2*H*,8*H*)-dione



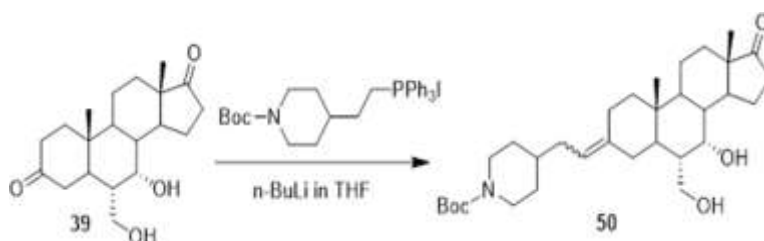
[435] A solution of compound **49** (28 mg, 0.05 mmol) in TFA/DCM (1mL/2 mL) was stirred at room temperature for 30 minutes. The mixture was diluted with sat. NaHCO<sub>3</sub> to adjust to pH 8-9. The mixture was extracted with DCM (25 mL \* 3). The combined organic layers were dried over Na<sub>2</sub>SO<sub>4</sub>, filtered and concentrated. The residue was purified by prep-HPLC to produce compound **CVie411** (10 mg, 43%) as a yellow solid.

[436] Spectroscopic data for **CVie411**:

[437] <sup>1</sup>H NMR (CD<sub>3</sub>OD, 400 MHz): δ 3.85-3.81 (m, 1H), 3.71-3.66 (m, 1H), 3.07-3.04 (m, 2H), 2.69 (t, *J* = 11.2 Hz, 1H), 2.63-2.51 (m, 3H), 2.48-2.39 (m, 2H), 2.15-2.05 (m, 1H), 1.84-1.72 (m, 7H), 1.63-1.46 (m, 4H), 1.37-1.33 (m, 6H), 1.28-1.14 (m, 7H), 1.09-0.98 (m, 3H), 0.88 (s, 3H).

[438] LCMS column: column:C18; column size:4.6\*50 mm; mobile phase: B (ACN) : A (0.02%NH<sub>4</sub>Ac); gradient (B%) in 6.5 min-5-95-POS; Rt = 4.188 min; MS Calcd.:429, MS Found: 430 [M+H]<sup>+</sup>.

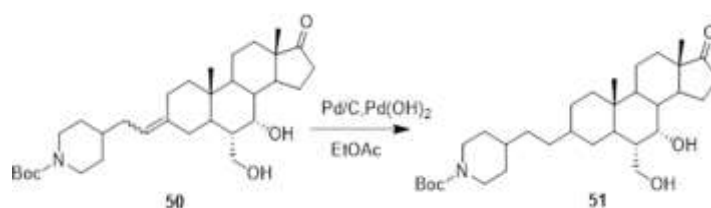
Synthesis of compound **50**: tert-butyl-4-(2-((6*S*,10*R*,13*S*)-6-(hydroxymethyl)-10,13-dimethyl-7,17-dioxododecahydro-1*H*-cyclopenta[*a*]phenanthren-3(2*H*,4*H*,10*H*)-ylidene)ethyl)piperidine-1-carboxylate



[439] n-BuLi in THF (2.5 M, 0.70 mL, 1.80 mmol) was added to a solution of phosphonium salt (540 mg, 0.90 mmol) in THF (5 mL) at -78 °C. The reaction mixture was stirred at 40 °C for 1 hour. Then, compound **39** (100 mg, 0.30 mmol) was added to the mixture at 0 °C and then warmed to 40 °C for 2 hours. The reaction was repeated for five times. The mixture was quenched with sat.NH<sub>4</sub>Cl (80 mL) and extracted with EtOAc (100 mL \* 3). The combined organic layers were concentrated and the residue was purified by prep-HPLC to give the crude compound **50** (35 mg, 4%) as a white solid.

[440] LCMS column: C18; column size: 4.6\*30 mm 5 μm; Dikma Diamonsil plus; mobile phase: B(ACN) : A (0.02%NH<sub>4</sub>Ac+5%ACN); gradient (B%) in 3 min-5-95-POS; flow 1.5 mL/min, stop time 3mins. Rt = 2.104 min; MS Calcd.: 529, MS Found: 430 [M+H-Boc]<sup>+</sup>.

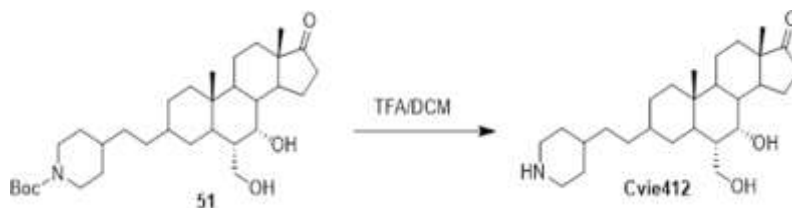
*Synthesis of compound **51**: tert-butyl-4-(2-((6S,7S,10R,13S)-7-hydroxy-6-(hydroxymethyl)-10,13-dimethyl-17-oxohexadecahydro-1H-cyclopenta[a]phenanthren-3-yl)ethyl)piperidine-1-carboxylate*



[441] A mixture of compound **50** (35 mg, 0.07 mmol), Pd/C (10%, 40 mg), and Pd(OH)<sub>2</sub> (20%, 40 mg) in EtOAc (2 mL) was stirred at room temperature overnight under H<sub>2</sub> (in balloon). The mixture was filtered and the filtrate was concentrated to give the crude compound **51** (35 mg, 100%) as a brown solid.

[442] LCMS column: C18; column size: 4.6\*30 mm 5 μm; Dikma Diamonsil plus; mobile phase: B(ACN) : A (0.02%NH<sub>4</sub>Ac+5%ACN); gradient (B%) in 3 min-5-95-POS; flow 1.5 mL/min, stop time 3mins. Rt = 2.126 min; MS Calcd.:531, MS Found: 432 [M+H-Boc]<sup>+</sup>.

Synthesis of **CVie412**: (6*S*,7*S*,10*R*,13*S*)-7-hydroxy-6-(hydroxymethyl)-10,13-dimethyl-3-(2-(piperidin-4-yl)ethyl)tetradecahydro-1*H*-cyclopenta[*a*]phenanthren-17(2*H*)-one



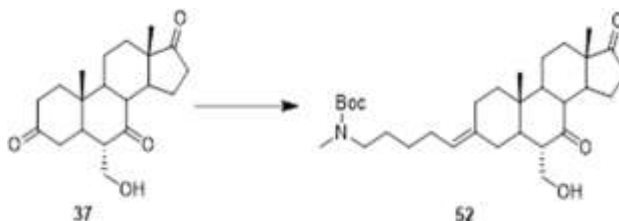
[443] The solution of compound **51** (35 mg, 0.07 mmol) in TFA/DCM (1:2, 2 mL) was stirred at room temperature for 30 minutes. The mixture was diluted with *sat.*NaHCO<sub>3</sub> to adjust to pH 8-9. The mixture was extracted with DCM (25 mL \* 3). The combined organic layers were dried over Na<sub>2</sub>SO<sub>4</sub>, filtered and concentrated. The residue was purified by prep-HPLC to produce compound **CVie412** (13 mg, 46%) as a yellow solid.

[444] Spectroscopic data for **CVie412**:

[445] <sup>1</sup>H NMR (CD<sub>3</sub>OD, 400 MHz): δ 4.04 (s, 1H), 3.72-3.61 (m, 2H), 3.09-3.06 (m, 2H), 2.63 (t, *J* = 11.6 Hz, 2H), 2.48-2.41 (m, 1H), 2.13-2.03 (m, 2H), 1.75-1.66 (m, 5H), 1.63-1.55 (m, 5H), 1.45-1.35 (m, 3H), 1.31-1.17 (m, 10H), 1.10-1.03 (m, 2H), 0.89 (s, 1H), 0.87 (s, 3H), 0.84 (s, 3H).

[446] LCMS column: column: C18; column size:4.6\*50 mm; mobile phase: B(ACN) : A (0.02%NH<sub>4</sub>Ac); gradient (B%) in 6.5 min-5-95-POS; Rt = 3.203 min; MS Calcd.:431, MS Found: 432 [M+H]<sup>+</sup>.

Synthesis of compound **52**: *tert*-butyl((*E*)-5-((6*S*,10*R*,13*S*)-6-(hydroxymethyl)-10,13-dimethyl-7,17-dioxododecahydro-1*H*-cyclopenta[*a*]phenanthren-3(2*H*,4*H*,10*H*)-ylidene)pentyl)(methyl)carbamate

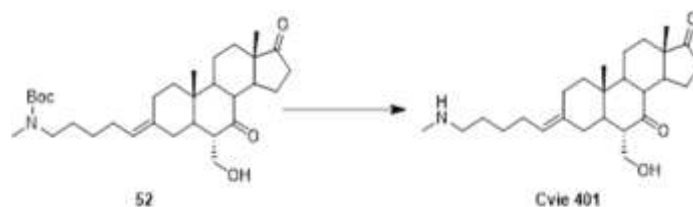


[447] To a mixture of N-Boc-N-methyl-5-triphenylphosphoniumpentenamine iodide (4.26 g, 7.23 mmol) in THF (50 mL), n-BuLi (3.18 mL, 7.95 mmol) was added dropwise at -78 °C. The mixture was stirred at 0 °C for 20 min. Then, the mixture was cooled to -30 °C. Compound **37** (800 mg, 2.41 mmol) was then added to the reaction mixture. The mixture was stirred at r.t overnight. The reaction mixture was quenched with H<sub>2</sub>O and concentrated. The residue was purified by column chromatography on silica gel (PE/EtOAc = 1/2) and then purified by prep-HPLC to produce compound **52** (36 mg, 200 mg) as colorless oil.

[448] Spectroscopic data for compound **52**:

[449] <sup>1</sup>H NMR (CD<sub>3</sub>OD, 400 MHz): 5.16-5.12 (m, 1H), 3.89-3.85 (m, 1H), 3.77-3.73 (m, 1H), 3.22-3.19 (m, 2H), 2.83 (s, 3H), 2.75-2.60 (m, 2H), 2.60-2.50 (m, 2H), 2.46-2.41 (m, 1H), 2.33-2.27 (m, 1H), 2.15-2.02 (m, 4H), 1.90-1.79 (m, 2H), 1.77-1.71 (m, 3H), 1.60-1.52 (m, 4H), 1.50 (s, 9H), 1.45-1.42 (m, 1H), 1.34-1.29 (m, 2H), 1.26 (s, 3H), 1.24-1.21 (m, 1H), 1.19-1.05 (m, 2H), 1.05-0.99 (m, 1H).

*Synthesis of CVie401: (6S,10R,13S,E)-6-(hydroxymethyl)-10,13-dimethyl-3-(5-(methylamino)pentylidene)dodecahydro-1H-cyclopenta[a]phenanthrene-7,17(2H,8H)-dione*



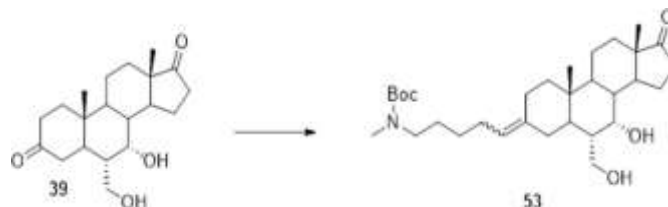
[450] A mixture of compound **52** (60 mg, 0.116 mmol) in TFA/DCM (1 mL/2 mL) was stirred at room temperature overnight. Then, the mixture was concentrated and diluted with EtOAc, washed with sat. Na<sub>2</sub>CO<sub>3</sub>, dried over Na<sub>2</sub>SO<sub>4</sub>, filtered, and concentrated to produce compound **CVie401** (38 mg, 79%) as yellow oil.

[451] Spectroscopic data for **CVie401**:

[452] <sup>1</sup>H NMR (CD<sub>3</sub>OD, 400 MHz): 5.36 (s, 1H), 3.89-3.86 (m, 1H), 3.71-3.67 (m, 1H), 2.80-2.77 (m, 2H), 2.73-2.67 (m, 1H), 2.55-2.39 (m, 6H), 2.15-2.01 (m, 4H), 1.92-1.85 (m, 1H), 1.77-1.69 (m, 4H), 1.65-1.45 (m, 7H), 1.38-1.25 (m, 6H), 1.19 (s, 3H), 0.89 (s, 4H).

[453] LCMS: Rt = 2.128 min, [M+1]<sup>+</sup> = 416.

*Synthesis of compound 53: tert-butyl(5-((6S,7S,10R,13S)-7-hydroxy-6-(hydroxymethyl)-10,13-dimethyl-17-oxododecahydro-1H-cyclopenta[a]phenanthren-3(2H,4H,10H)-ylidene)pentyl)(methyl)carbamate*

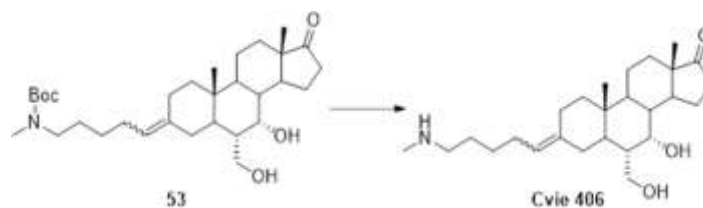


[454] To a mixture of N-Boc-N-methyl-5-triphenylphosphoniumpentenamine iodide (4.39 g, 7.45 mmol) in THF (45 mL), a solution of nBuLi in THF (4.46 mL, 2.5 N, 11.16 mmol) was added dropwise at -78°C. Then, the mixture was stirred at 0°C for 20 min. The mixture was cooled to -50°C and compound **39** (830 mg, 2.48 mmol) was added. The mixture was stirred at r.t overnight. The mixture was quenched with H<sub>2</sub>O, concentrated and purified by column chromatography (PE/EtOAc = 1/1) and then purified by prep-HPLC to give compound **53** (80 mg, 300 mg) as white solid.

[455] Spectroscopic data for compound **53**:

[456] <sup>1</sup>H NMR (CD<sub>3</sub>OD, 400 MHz): 5.10-5.08 (m, 1H), 4.05 (s, 1H), 3.78-3.72 (m, 1H), 3.23-3.20 (m, 2H), 2.83 (s, 3H), 2.56-2.53 (m, 1H), 2.48-2.41 (m, 1H), 2.12-2.10 (m, 1H), 2.07-2.00 (m, 5H), 1.85-1.81 (m, 1H), 1.74-1.51 (m, 10H), 1.49 (s, 9H), 1.39-1.30 (m, 4H), 1.21-1.18 (m, 1H), 1.08-1.04 (m, 1H), 0.96 (s, 3H), 0.88 (s, 3H).

*Synthesis of CVie406: (6S,7S,10R,13S)-7-hydroxy-6-(hydroxymethyl)-10,13-dimethyl-3-(5-(methylamino)pentylidene)tetradecahydro-1H-cyclopenta[a]phenanthren-17(2H)-one*



[457] A solution of compound **53** (80 mg, 0.155 mmol) in TFA/DCM (1 mL/2 mL) was stirred at room temperature for 10 minutes. The mixture was basified with sat. NaHCO<sub>3</sub> to pH = 8-9. The mixture was extracted with DCM (25 mL\*2). The combined organic layer was dried over Na<sub>2</sub>SO<sub>4</sub>, filtered and concentrated. The residue was purified by prep-HPLC to give the compound **CVie406** (60 mg, 94%) as a yellow solid.

[458] LCMS column: Rt = 0.370 min; MS Calcd.: 417, MS Found: 418[M+H]<sup>+</sup>.

## **Example 2. General procedures for measuring biological activity.**

### Example Animal care

[459] The investigation attains to the Guide of the Care and Use of Laboratory Animals published by the National Institute of Health (NIH publication no. 85-23, revised 1996) and to the guidelines for animal care endorsed by the participating institutions.

### Measurements in isolated left ventricular cardiomyocytes

[460] The compounds were characterized for their effect on (i) SR Ca<sup>2+</sup> uptake function and (ii) action potential (AP) in myocytes freshly dissociated from rat and guinea-pig ventricles, respectively, by retrograde coronary perfusion with enzymatic solution (Rocchetti M *et al.*, J Pharmacol Exper Therap 2005, 313(1):207–215).

### Statistical analysis

[461] *Whole animal experiments*: Data reported as mean ± SD. Statistical analysis was performed by Student's t-test (paired t test).

[462] *Isolated myocyte experiments*: Data are reported as mean ± SE. Curves including multiple means were compared by two-way ANOVA for repeated measurements; drug-induced changes in overall curve steepness were defined according to significance of the "factor X group" interaction. Due to inadequate mono-exponential fit of Ca<sup>2+</sup> decay,  $\tau_{\text{decay}}$  was not estimated in a few cells for which CaT data are reported; the sample size (N) reported in the corresponding figures. STV dependency on mean APD was quantified by linear regression. P<0.05 was regarded as statistically significant in all comparisons.

## **Example 3. In vitro screening of compounds of Formula (I)**

### Inhibition of dog renal Na<sup>+</sup>/K<sup>+</sup> ATPase activity

[463] As noted elsewhere herein, the compounds of the present invention are pure or predominantly pure SERCA2a stimulators. As such, these compounds will exhibit little

to no inhibition of the enzymatic activity of the Na<sup>+</sup>/K<sup>+</sup> ATPase. The compounds were thus tested for their inhibitory effect on the canine renal Na<sup>+</sup>/K<sup>+</sup> ATPase enzyme.

[464] Purification of renal Na<sup>+</sup>/K<sup>+</sup> ATPase was performed according to the method described by Jørgensen (Methods Enzymol. 1988, 156:29-43). Kidneys were excised from 1-3 year-old male beagle dogs (WuXi AppTec, Suzhou Co., Ltd. 1318 Wuzhong Ave., Wuzhong District Suzhou, 215104 P.R. China) under pentobarbital anesthesia (Import Authorization from Italian Health Ministry 0009171-09/04/2015-DGSAF-COD\_UO-P, 2015). Kidneys were sliced and the outer medulla was dissected and suspended (1g/10 ml) in a sucrose-histidine solution containing 250 mM sucrose, 30 mM histidine, and 5 mM EDTA, pH 7.2. The tissue was homogenized by using an Ultra Turrax homogenizer. The sample was centrifuged at 6,000 g for 15 min. Next, the supernatant was decanted and centrifuged at 48,000 g for 30 min. The pellet was suspended in the sucrose-histidine buffer and incubated for 20 min with a sodium-dodecyl-sulphate (SDS) solution dissolved in a gradient buffer containing 25 mM imidazole and 1 mM EDTA, pH 7.5. The sample was layered on the top of a sucrose discontinuous gradient (10, 15, and 29.4 %) and centrifuged at 60,000 g for 115 min. The pellet was suspended in the gradient buffer.

[465] Na<sup>+</sup>/K<sup>+</sup> ATPase activity was assayed *in vitro* by measuring the release of <sup>32</sup>P from <sup>32</sup>P-ATP, as described (Ferrandi M. *et al.*, Hypertension 1996, 28:1018-25). Increasing concentrations of the standard ouabain, or tested compound, were incubated with 0.3 µg of purified dog kidney enzyme for 10 min at 37°C in 120 µl final volume of a medium containing 140 mM NaCl, 3 mM MgCl<sub>2</sub>, 50 mM HEPES-Tris, 3 mM ATP, pH 7.5. Then, 10 µl of a solution containing 10 mM KCl and 20 nCi of <sup>32</sup>P-ATP (3-10 Ci/mmol, Perkin Elmer) were added. The reaction was allowed to continue for 15 min at 37°C and then stopped by acidification with 20% v/v ice-cold perchloric acid. <sup>32</sup>P was separated by centrifugation with activated Charcoal (Norit A, Serva) and the radioactivity was counted. The inhibitory activity was expressed as percent of the control samples carried out in the absence of ouabain, or tested compound. The concentration of compound causing 50% inhibition of the Na<sup>+</sup>/K<sup>+</sup> ATPase activity (IC<sub>50</sub>) was calculated by using a multiple parameter non-linear regression best fitting program (Kaleidagraph™, Sinergy Software).

[466] Compounds CVie201, CVie202, CVie203, CVie204, CVie213, CVie214, CVie215, CVie216, CVie217, CVie218, and CVie219 did not inhibit the enzymatic activity of the purified Na<sup>+</sup>/K<sup>+</sup> ATPase and the IC<sub>50</sub>, expressed in µM, resulted > 100 µM, as shown in Table 1. Compounds CVie205, CVie206, CVie207, CVie208, CVie209, CVie210, CVie211, CVie212, CVie401, CVie402, CVie403, CVie404, CVie405, CVie406, CVie407,

CVie408, CVie409, CVie410, CVie411, and CVie412 only modestly inhibited Na<sup>+</sup>/K<sup>+</sup> ATPase (range of IC<sub>50</sub> between 0.8 and 24 μM) (**Table 1**).

[467] Compounds have been compared with the reference drugs Digoxin (IC<sub>50</sub> 0.18 μM) and Istaroxime (IC<sub>50</sub> 0.14 μM) (**Table 1**).

**Table 1. Inhibition of dog renal Na<sup>+</sup>/K<sup>+</sup> ATPase**

Compound	IC <sub>50</sub> , μM
Digoxin	0.18
Istaroxime	0.14
CVie201	> 100
CVie202	> 100
CVie203	> 100
CVie204	> 100
CVie205	7
CVie206	5.9
CVie207	3.9
CVie208	10.4
CVie209	0.8
CVie210	13.1
CVie211	8.3
CVie212	3.5
CVie213	> 100
CVie214	> 100
CVie215	> 100
CVie216	> 100
CVie217	> 100
CVie218	> 100
CVie219	> 100
CVie401	24.0
CVie402	4.6
CVie403	2.9
CVie405	7.9
CVie406	1.9
CVie407	3.5
CVie408	3.3
CVie409	3.4
CVie410	3.7
CVie411	1.9
CVie412	3.0

SERCA2a ATPase activity in heart-derived SR microsomes from normal guinea-pig

[468] The compounds disclosed herein were also tested for their ability to stimulate SERCA2a activity in SR microsomes derived from normal guinea-pig heart tissue over a range of concentrations from 1-200 nM. Two month-old guinea-pigs (350-450 g from Envigo, Udine, Italy) were used for the preparation of cardiac SERCA2a microsomes. Guinea-pigs were sacrificed under pentobarbital anesthesia. Left ventricles (LV) were quickly dissected and immediately frozen in liquid nitrogen. LV tissues were processed following the method described by Nediani C. *et al.* (J Biol Chem. 1996, 271:19066-7).

The tissue was suspended in 4 x volumes of a buffer containing 10 mM NaHCO<sub>3</sub>, pH 7, 1 mM PMSF, 10 µg/ml aprotinin and leupeptin and then homogenized using an Ultra Turrax homogenizer. The sample was centrifuged at 12,000g for 15 minutes. The obtained supernatant was filtered and centrifuged at 100,000g for 30 min. Contractile proteins were extracted by suspending the pellet with 0.6 M KCl, 30 mM histidine, pH 7 and by further centrifugation at 100,000g for 30 min. The final pellet was reconstituted with 0.3 M sucrose, 30 mM histidine, pH 7 and stored in aliquots at -80°C until use.

[469] SERCA2a activity was measured *in vitro* as <sup>32</sup>P-ATP hydrolysis at different Ca<sup>2+</sup> concentrations (100-4000 nM) in the absence and presence of the tested compounds, as described (Micheletti R. *et al.*, Am J Card 2007, 99:24A-32A). Increasing concentrations of each compound (ranging from 1 to 200 nM) were pre-incubated with 2 µg of SERCA2a enriched microsomes for 5 min at 4°C in 80 µl of a solution containing 100 mM KCl, 5 mM MgCl<sub>2</sub>, 1 µM A23187, 20 mM Tris, pH 7.5. Then, 20 µl of 5 mM Tris-ATP containing 50 nCi of <sup>32</sup>P-ATP (3-10 Ci/mmol, Perkin Elmer) were added. The ATP hydrolysis was continued for 15 min at 37°C and the reaction was stopped by acidification with 100 µl of 20% v/v ice-cold perchloric acid. <sup>32</sup>P was separated by centrifugation with activated charcoal (Norit A, SERVA) and the radioactivity was measured. SERCA2a-dependent activity was identified as the portion of total hydrolytic activity inhibited by 10 µM cyclopiazonic acid (Seidler NW *et al.*, J Biol Chem. 1989, 264:17816-23).

[470] Dose-response curves were fitted by using a sigmoidal equation and the activity at the maximal velocity (V<sub>max</sub>) and the K<sub>d</sub> for Ca<sup>2+</sup> were calculated (Synergy Software KaleidaGraph 3.6). The effect of the compounds in normal guinea-pig preparations was expressed as % decrease of K<sub>d</sub> Ca<sup>2+</sup> (implying an increase of affinity for Ca<sup>2+</sup>) of a control sample run in the absence of compound (**Table 2**). This effect indicates that the compounds increase SERCA2a activity in a physiological range of Ca<sup>2+</sup> concentrations (Rocchetti M *et al.*, J Pharmacol Exp Ther. 2005, 313:207-15; Rocchetti M *et al.*, J Pharmacol Exp Ther. 2008, 326:957-65; Ferrandi M *et al.*, Br J Pharmacol 2013, 169:1849-1861). Data are mean ± SD, n = number of experiments, \*at least p < 0.05.

[471] At nanomolar concentrations, the tested compounds decreased SERCA2a K<sub>d</sub> Ca<sup>2+</sup> of Ca<sup>2+</sup>-dose response curves in microsomes from guinea-pig heart preparations (**Table 2**). These results indicated that the compounds increased SERCA2a activity in a physiological range of Ca<sup>2+</sup> concentrations and suggested a lusitropic effect. Istaroxime has been used as comparator indicating its ability to stimulate SERCA2a (**Table 2**). At variance with this, Digoxin failed to stimulate SERCA2a activity (Ferrandi M *et al.*, Br J

Pharmacol 2013, 169:1849-61; Rocchetti M *et al.*, J Pharmacol Exp Ther 2005, 313:207-215).

**Table 2. Effect of the tested compounds on SERCA2a Kd Ca<sup>2+</sup> in heart-derived SR microsomes from normal guinea-pig**

Compound	Concentration nM	Kd Ca <sup>2+</sup> (nM) mean ± SD	% decrease Kd vs control *p<0.05
Istaroxime	0	562.9 ± 68.12 (n=12)	0
	1 nM	524.1 ± 57.41 (n=9)	-7%
	10 nM	464.3 ± 52.35 (n=13)	-18%*
	100 nM	462.35 ± 59.12 (n=13)	-18%*
CVie201	0	533.7 ± 51.4 (n=7)	0
	10 nM	459.4 ± 57.1 (n=6)	-14%*
	100 nM	454.1 ± 53.2 (n=5)	-15%*
CVie202	0	466.3 ± 18.7 (n=4)	0
	10 nM	448.0 ± 9.4 (n=4)	-4%
	100 nM	435.6 ± 24.9 (n=4)	-7%
	200 nM	437.0 ± 26.4 (n=3)	-6%
CVie203	0	454.8 ± 27.9 (n=5)	0
	10 nM	418.3 ± 36.5 (n=5)	-8%
	100 nM	385.8 ± 33.3 (n=5)	-15%*
	200 nM	392.9 ± 31.3 (n=5)	-14%*
CVie204	0	435.3 ± 20.7 (n=5)	0
	100 nM	493.4 ± 106.6 (n=5)	+13%
	200 nM	423.8 ± 82.7 (n=5)	-3%
CVie205	0	786.2 ± 56.9 (n=5)	0
	100 nM	655.8 ± 56.6 (n=5)	-16.7%*
	200 nM	683.1 ± 46.4 (n=5)	-13.1%*
CVie206	0	786.2 ± 56.94 (n=5)	0
	100 nM	678.2 ± 86.7 (n=5)	-13.7%*
	200 nM	667.3 ± 55.57 (n=5)	-15.1%*
CVie208	0	447.3 ± 62.9 (n=5)	0
	100 nM	361.8 ± 72.2 (n=5)	-19.1%*
	200 nM	350.1 ± 109.2 (n=5)	-21.7%
CVie212	0	508.9 ± 123 (n=11)	0
	10 nM	409 ± 121 (n=7)	-19.6%*
	100 nM	406.1 ± 82.9 (n=11)	-20.2%*
CVie213	0	490.6 ± 118.9 (n=13)	0
	10 nM	431.5 ± 128.9 (n=8)	-12%
	100 nM	377.9 ± 113.5 (n=13)	-23%*
	200 nM	406.6 ± 123.5 (n=9)	-17%*
CVie214	0	541.1 ± 45.7 (n=5)	0
	1 nM	473.5 ± 40.4 (n=5)	-13%*
	10 nM	466.5 ± 62.4 (n=5)	-14%*
	100 nM	427.1 ± 48.9 (n=5)	-21%*
	200 nM	408.7 ± 60.1 (n=5)	-24%*
CVie215	0	568.4 ± 46.2 (n=5)	0
	1 nM	530.0 ± 47.9 (n=5)	-7%
	10 nM	459.2 ± 80.3 (n=5)	-19%*
	100 nM	436.9 ± 74.1 (n=5)	-23%*
CVie216	0	587.9 ± 54.0 (n=5)	0
	1 nM	529.0 ± 75.8 (n=5)	-10%

	10 nM	465.4 ± 73.4 (n=5)	-21%*
	100 nM	442.9 ± 85.1 (n=5)	-25%*
	200 nM	462.7 ± 76.3 (n=5)	-21%*
CVie217	0	954.1 ± 145.99 (n=7)	0
	1 nM	763.1 ± 102.57 (n=5)	-20%
	10 nM	718.6 ± 141.93 (n=5)	-24.7%*
	100 nM	763.8 ± 119.89 (n=5)	-20%*
	200 nM	673.6 ± 150.44 (n=5)	-29.4%*
CVie218	0	725.15 ± 76.09 (n=5)	0
	1 nM	705.13 ± 88.79 (n=4)	-3%
	10 nM	676.84 ± 13.75 (n=4)	-7%*
	100 nM	586.51 ± 50.49 (n=5)	-19.1%*
	200 nM	618.51 ± 48.01 (n=5)	-15%*
CVie219	0	577.87 ± 92.8 (n=6)	0
	1 nM	517.1 ± 100.76 (n=6)	-10.5%
	10 nM	485.25 ± 81.17 (n=6)	-16%*
	100 nM	465.4 ± 61.14 (n=6)	-19.5%*
	200 nM	478.73 ± 109.21 (n=6)	-17.2%*
CVie407	0	428.4 ± 104.9 (n=5)	0
	100 nM	390.3 ± 91.45 (n=5)	-8.9%
	200 nM	428.3 ± 87.27 (n=5)	0%
CVie408	0	449.2 ± 67.99 (n=4)	0
	100 M	356.3 ± 33.84 (n=4)	-20.7%*
	200 nM	354.8 ± 66.94 (n=4)	-21%*
CVie411	0	428.4 ± 104.8 (n=5)	0
	100 nM	427.7 ± 76.59 (n=5)	0%
	200 nM	407.3 ± 111.03 (n=5)	-4.9%
CVie412	0	449.2 ± 67.9 (n=4)	0
	100 nM	363.5 ± 74.13 (n=4)	-19.1%
	200 nM	361 ± 76.3 (n=4)	-19.6%*

#### Example 4. Studies on CVie214 and CVie216 in isolated ventricular myocytes

##### SR Ca<sup>2+</sup> uptake function in rat ventricular myocytes

[472] To test the effects of the compounds in a model of diastolic dysfunction, Sprague Dawley male rats (150-175 g) were made diabetic by a single tail vein injection of streptozotocin (STZ 50 mg/kg, Sigma-Aldrich). STZ was freshly prepared in 0.1 M sodium citrate buffer at pH 4.5. Fasting glycaemia was measured after 1 week and rats with values > 300 mg/dl were considered diabetic. Drug effects on SR Ca<sup>2+</sup> uptake function were evaluated in isolated left ventricular myocytes 9 weeks after STZ injection. Myocytes were incubated for at least 30 min in the presence of a specific drug to guarantee its cell membrane permeation. Statistical analysis was performed by a "group comparison" model.

[473] Drug effects on SR Ca<sup>2+</sup> uptake rate were evaluated with a SR "loading protocol" specifically devised to rule out the contribution of the Na/Ca exchanger (NCX) and to assess the uptake rate starting at low levels of SR Ca<sup>2+</sup> loading. Under voltage-clamp conditions, intracellular Ca<sup>2+</sup> concentration was dynamically measured by epifluorescence (Fluo4-AM). Membrane current, whose time-dependent component mainly reflected I<sub>CaL</sub>, was simultaneously recorded. The SR loading protocol consisted in

emptying the SR by a brief caffeine pulse and then progressively refilling it by voltage steps activating  $\text{Ca}^{2+}$  influx through the sarcolemmal  $\text{Ca}^{2+}$  channel ( $I_{\text{CaL}}$ ). NCX was blocked by omission of  $\text{Na}^+$  from intracellular and extracellular solutions. The procedure is in agreement with published methods, with minor modifications (Rocchetti M *et al.*, *J Pharmacol Exper Therap* 2005, 313:207–215).

[474] Drug effects on SR  $\text{Ca}^{2+}$  uptake were analyzed by considering multiple parameters: the rate at which 1)  $\text{Ca}^{2+}$  transient (CaT) amplitude and 2) the  $\text{Ca}^{2+}$  induced  $\text{Ca}^{2+}$  release (CICR) gain increased during the loading protocol, reflecting the rate at which the SR refilled and the gain of the system, 3) the time constant of cytosolic  $\text{Ca}^{2+}$  decay ( $\tau_{\text{decay}}$ ) within each pulse, reflecting net  $\text{Ca}^{2+}$  transport rate (by SERCA2a) across the SR membrane (a decrease in  $\tau_{\text{decay}}$  corresponds to enhanced SR  $\text{Ca}^{2+}$  uptake).

[475] Specificity of the "loading protocol" in detecting SERCA2a activation was supported by the observation that it did not detect any effect of Digoxin, an inotropic agent blocking the  $\text{Na}^+/\text{K}^+$  ATPase pump, but devoid of SERCA2a stimulatory effect (Rocchetti M *et al.*, *J Pharmacol Exp Ther* 2005, 313:207-215; Alemanni M *et al.*, *JMCC* 2011, 50:910-918).

[476] CVie216 (1  $\mu\text{M}$ ) increased the rate of  $\text{Ca}^{2+}$  transient (CaT) increment during SR reloading (Fig 1A); this was associated with an increase in CICR gain (Fig 1B) and a reduction in  $\tau_{\text{decay}}$  (Fig 1C).

[477] CVie214 (1  $\mu\text{M}$ ) changed CaT parameters during SR loading protocol in a similar way to CVie216 (Fig. 2). CICR gain (Fig. 2B) and  $\tau_{\text{decay}}$  (Fig. 2C) were affected by the drug as expected from SERCA2a enhancement. CVie214 failed to significantly increase the rate of CaT increment during SR reloading (Fig. 2A). However, the increment in CICR gain suggested that this may reflect concomitant  $I_{\text{CaL}}$  inhibition, rather than negating the effect on SERCA2a.

[478] The results in Fig. 1 and 2 converge to indicate that CVie216 and CVie214 significantly increased  $\text{Ca}^{2+}$  uptake by the SR. Under the experimental conditions applied, SR  $\text{Ca}^{2+}$  uptake was entirely supported by SERCA2a; therefore, the results are consistent with SERCA2a activation by the two agents.

#### Action potential measurements

[479] Cvie216 and Cvie214 effects on action potential parameters were evaluated at the concentration of 1  $\mu\text{M}$  modulating SERCA2a in guinea-pig myocytes. The action potential (AP) contour provides a first-line estimate of the integrated function of membrane ion channels, and its changes may disclose ancillary actions - potentially

resulting in untoward effects of the compound. To increase sensitivity of the AP contour as a reporter, effects on the rate-dependency of AP parameters were also tested, thus providing a multiparametric (more stringent) approach. AP were recorded in guinea-pig ventricular myocytes because the AP contour reproduces the human AP. Myocytes were incubated for at least 30 min in the presence of the drug to guarantee that effects were absent even after long exposure times. Statistical analysis was performed by a "group comparison" model.

[480] APs were recorded in normal Tyrode's solution at 36.5°C in guinea-pig ventricular myocytes. The following parameters were measured at 4 stimulation rates (0.5-1-2-4 Hz): diastolic membrane potential ( $E_{\text{diast}}$ ), maximum depolarization velocity ( $dV/dt_{\text{max}}$ ), action potential duration (APD at 90% of repolarization). Short term APD variability (STV) during steady-state pacing, an index of repolarization stability, was measured as the sum of absolute orthogonal deviations from the identity line in the  $APD_n/APD_{n+1}$  plot (Poincare plot) (Altomare C *et al.*, Circulation A&E 2015, 8:1265-1275).

[481] CVie216 (Fig 3A) and CVie214 (Fig 4A) at 1  $\mu\text{M}$  did not affect action potential duration ( $APD_{90}$ ), diastolic membrane potential ( $E_{\text{diast}}$ ), the maximum depolarization velocity ( $dV/dt_{\text{max}}$ ) and the rate-dependency of each AP parameter.

[482] Short term APD variability (STV) is a marker of electrical instability and correlates with arrhythmogenic risk. STV is a function of mean APD; therefore, STV was measured at multiple pacing rates (0.5-1-2 and 4 Hz) to extend its evaluation to a wide APD range. STV and its dependency on mean APD were not significantly affected by both CVie216 (Fig 3B) and CVie214 (Fig 4B).

[483] Altogether, the multiparametric approach used for action potential analysis stands for the absence of undesired drug effects on cardiac electrical activity. Thus, according to this analysis, CVie216 and CVie214 exert SERCA2a modulation selectively (positive lusitropic drug), *i.e.* without affecting electrical activity and the membrane currents involved.

## **Example 5. *In vivo* studies on CVie214 and CVie216**

### Bioavailability in rats

[484] Bioavailability in rats was measured by Sundia MediTech Service, China. In particular, the bioavailability of CVie214-salt and CVie216-salt was measured in rats after an intravenous injection (i.v.) at 1 mg/kg and an oral administration (os) at 10 mg/kg. Plasma concentrations of the tested compounds CVie214-salt and CVie216-salt were measured at intervals from time 0 to time 24h and detected by LC-MS method. F value

(%) has been calculated and resulted to be 41.5% and 16.9% for CVie214-salt and CVie216-salt, respectively.

#### Acute toxicity in the mouse

[485] The acute toxicity of the tested compound CVie214-salt and CVie216-salt have been determined in the mouse (Albino Swiss CD-1, body weight 30 g). Compounds have been orally administered or intravenously injected at increasing doses to identify the dose causing 50% mortality. Mortality occurred within 30 min after the administration and survival after 24h.

[486] The results for CVie214-salt and CVie216-salt acute toxicity are reported in **Table 3**. As comparison, the acute toxicity for the reference compounds Digoxin and Istaroxime were also included. Digoxin refers to literature data (www.lookchem.com, Reference for Digoxin intravenous: Afifi AM, Ammar EM. Pharmacological Research Communications. Vol. 6, Pg. 417, 1974; Reference for Digoxin oral: Archives Internationales de Pharmacodynamie et de Therapie. Vol. 153, Pg. 436, 1965) (**Table 3**).

**Table 3. Acute toxicity (LD<sub>50</sub>) of CVie214-salt and CVie216-salt in the mouse**

Acute toxicity (mouse)		
Compound	LD <sub>50</sub> mg/kg	
Digoxin iv	7.7	data from literature
Digoxin os	17.8	
Istaroxime iv	29-32	
Istaroxime os	200	
CVie214-salt iv	300	
CVie214-salt os	>800	
CVie216-salt iv	>300	
CVie216-salt os	>700	

Haemodynamics in streptozotocin diabetic rats (echocardiography 2M-Doppler-Tissue Doppler)

[487] CVie214 and CVie216 were tested in a diabetic rat model. Briefly, rats were injected with streptozotocin (STZ). After 7-9 weeks from STZ injection, rats were submitted to transthoracic echocardiographic and Doppler evaluation performed under urethane anesthesia. Two-dimensionally guided M-mode recordings were used to obtain short-axis measurements of left ventricular end-diastolic diameter (LVEDD), left ventricular end-systolic diameter (LVESD), posterior (PW) and septal (SW) diastolic wall thickness according to the American Society of Echocardiography guidelines (Lang RM *et al.*, Eur J Echocardiography 2006, 7:79-108). Fractional shortening was calculated as  $FS=(LVEDD-LVESD)/LVEDD$ . Relative wall thickness was calculated as  $PWTd+IVSTd/LVEDD$ . Mitral inflow was measured by pulsed Doppler at the tips of mitral leaflets from an apical 4-chamber view to obtain early and late filling velocities (E, A) and deceleration time of early filling velocity (DT). The deceleration slope was calculated as E/DT ratio. The mitral deceleration index was calculated as DT/E ratio. Tissue Doppler Imaging (TDI) was evaluated from the apical 4-chamber view to record septal mitral annular movements, i.e., peak myocardial systolic ( $s'$ ) and early and late diastolic velocity ( $e'$  and  $a'$ ).

[488] After baseline hemodynamic measurements were taken, the rats were administered Digoxin, CVie214, CVie216 and compared to control. Digoxin, used as reference drug, was intravenously infused at 0.11 mg/kg/min for 15 min and echocardiographic parameters measured after 1h. CVie214-salt and CVie216-salt were intravenously infused in STZ diabetic rats at 0.2 mg/kg/min and echocardiographic parameters were measured after 15 min and 30 min.

[489] **Tables 4-6** show the haemodynamic parameters in STZ diabetic rats for Digoxin, CVie214-salt, and CVie216-salt. Data shown in **Tables 4-6** are mean  $\pm$  SD; values with asterisk are statistically significant with at least  $p < 0,05$ .

[490] The data indicate that the streptozotocin diabetic rat model is characterized by a diastolic dysfunction compared to healthy control rats (control  $n=18$  rats; STZ  $n=20$  rats) (**Table 4**). In particular, STZ rats showed increased DT, DT/E and reduced E, DT/E,  $e'$ , HR. CVie214-salt and CVie216-salt ameliorated diastolic function, deteriorated in STZ vs controls (**Table 4**), inducing a significant decrease of DT, DT/E and an increase of E/DT and  $e'$  associated with an improvement of SV and CO (**Table 5-6**). E/ $e'$  was significantly reduced after 30 min from CVie216-salt infusion (**Table 6**). Only CVie214 modestly, but significantly, increased  $s'$  and HR after 15 min (**Table 5**). Digoxin, taken as reference compound, ameliorated diastolic function, decreasing DT, DT/E and increasing E/DT,  $e'$  and systolic function (FS,  $s'$ ), but did not affect overall cardiac function, such as SV and CO (**Table 4**).

**Table 4. Hemodynamic parameters in control and STZ diabetic rats and effect of Digoxin IV infusion in STZ rats**

Function	Echo Parameters	control rats (n=18)	STZ rats (n=20)	STZ Before DIGO (n=10)	STZ after 15 min DIGO 0.11 mg/kg/min (n=10)
Systolic	FS	53.1±4.96	55.12±7.02	47,62±6,26	53.1±5.6*6
	s'	29.59±4.9	21.74±1.92*	23,45±2,98	26.03±4.66*
Diastolic	E	0.93±0.06	0.84±0.12*	0,83±0,09	0.92±0.19
	A	0.65±0.17	0.599±0.123	0,59±0,15	0.79±0.19*
	E/A	1.5±0.35	1.44±0.25	1,48±0,36	1.20±0.21*
	DT	54.6±8.95	59.3±5.32*	53,4±11,97	44.1±10.29*
	DT/E	59.23±10.24	70.61±14.02*	65,21±16,8	50.18±17.05*
	E/DT	17.41±3.29	14.63±2.64*	16,53±5,33	22.66±9.56*
	E/e'	40.1±5.67	40.75±4.84	39,64±2,85	38.95±7.31
	e'	23.46±3.27	20.74±2.22*	20,96±1,66	23.82±2.87*
OVERALL	a'	24.54±5.86	22.9±4.42	25,86±6,29	29.78±6.17*
	CO	178.9±43.52	172.55±45.53	138,5±35,6	155.6±45.7
	HR	305.5±43.3	244±44.9*	236±39	257±36
	SV	0.59±0.14	0.611±0.17	0,59±0,1	0.6±0.12

FS %: fractional shortening, systolic function; E m/s : early filling velocity of mitral inflow; A m/s : late filling velocity of mitral inflow; E/A : index of LV function; DT ms : deceleration time of E wave; DT/E s<sup>2</sup>/m : mitral deceleration index; E/DT m/s<sup>2</sup> : deceleration slope; s' cm/s TDI : contraction velocity; e' cm/s TDI : early relaxation velocity; a' cm/s TDI : late relaxation velocity; E/e' : index of LV filling pressure; CO ml/min : cardiac output; HR beat/min : heart rate; SV ml/beat : stroke volume. \*at least p<0.05 control vs STZ or STZ plus drug vs STZ before

**Table 5. Hemodynamic parameters after CVie214-salt IV infusion of STZ diabetic rats**

Function	Echo Parameters	STZ Before CVie214 (n=13)	STZ after 15 min CVie214 0.2 mg/kg/min (n=13)	STZ after 30 min CVie214 0.2 mg/kg/min (n=13)
Systolic	FS	57.96±7.25	58.1±8.59	60.69±8.36
	s'	21.34±2.16	22.45±3.12*	21.82±2.81
Diastolic	E	0.78±0.11	0.88±0.15*	0.91±0.16*
	A	0.55±0.12	0.65±0.13*	0.69±0.11*
	E/A	1.46±0.37	1.36±0.17	1.34±0.21
	DT	53.9±9.82	42.5±10.19*	42.15±9.88*
	DT/E	71.42±19.17	49.52±12.41*	48.51±16.44*
	E/DT	15.14±5.1	21.49±5.8*	23.18±8.37*
	E/e'	38.03±3.58	37.49±4.34	37.47±4.48
	e'	20.38±2.32	23.33±2.62*	24.24±2.34*
OVERALL	a'	22.99±5.68	29.13±6.56*	28.94±5.32*
	CO	151.5±29.32	177.23±40.64*	175.15±33.96*
	HR	241±47	268±54*	252±49
	SV	0.64±0.14	0.68±0.19	0.71±0.16*

**Table 6. Hemodynamic parameters after CVie216-salt IV infusion of STZ diabetic rats**

Function	Echo Parameters	STZ Before CVie216 (n=11)	STZ after 15 min CVie216 0.2 mg/kg/min (n=11)	STZ after 30 min CVie216 0.2 mg/kg/min (n=11)
Systolic	FS	55.45±9.96	56.29±9.95	55.19±7.32
	s'	21.83±3.6	22.47±2.45	22.68±3.18
Diastolic	E	0.84±0.15	0.90±0.13*	0.87±0.09
	A	0.56±0.14	0.66±0.17*	0.68±0.15*
	E/A	1.59±0.4	1.42±0.28*	1.34±0.27*
	DT	58.45±11.18	49.72±12.56*	47.46±10.17*
	DT/E	71.9±19.32	56.52±16.45*	54.8±12.84*
	E/DT	15.51±6.96	19.76±8.27*	19.38±5.39*
	E/e'	40.66±5.48	39.08±5.04	35.82±3.92*
	e'	20.71±1.89	23.1±1.96*	24.48±2.1*
OVERALL	a'	23.54±6.03	25.85±6.98*	26.66±6.94*
	CO	149.36±33.4	165.45±30.9*	181.82±23.75*
	HR	223±61	221±50	225±50
	SV	0.68±0.09	0.76±0.12*	0.83±0.15*

### Receptor binding assay

[491] Radioligand binding to a panel of receptors was carried out by Eurofins on crude membrane preparations according to published procedures and by using appropriate reference standard (Eurofin, Taiwan, compound code CVie216-3 (1226840), study # TW04-0004235, quote # TW04-0004235-Q04, for Cvie Therapeutics Limited, Taiwan). CVie216-salt was tested at the concentration of 10 µM. No significant interaction was documented on a panel of receptors, as shown in **Table 7**.

**Table 7 Receptor binding assay for Cvie216-salt**

Cat #	Assay name	Batch	Species	Rep	Conc	% inhib
107480	ATPase, Ca2+, skeletal muscle	438642	pig	2	10 µM	-1
118040	CYP450, 19	438644	hum	2	10 µM	0
124010	HMG-CoA Reductase	438610	hum	2	10 µM	-4
140010	Monoamine Oxidase MAO-A	438645	hum	2	10 µM	1
140120	Monoamine Oxidase MAO-B	438647	hum	2	10 µM	-2
143000	Nitric Oxide Synthase, Endothelial (eNOS)	438568	bov	2	10 µM	2

107300	Peptidase, Angiotensin Converting Enzyme	438641	rabbit	2	10 $\mu$ M	7
164610	Peptidase, Renin	438648	hum	2	10 $\mu$ M	7
152000	Phosphodiesterase PDE3	438611	hum	2	10 $\mu$ M	-25
171601	Protein Tyrosine Kinase, ABL1	438612	hum	2	10 $\mu$ M	13
176810	Protein Tyrosine Kinase, Src	438613	hum	2	10 $\mu$ M	2
200510	Adenosine A1	438614	hum	2	10 $\mu$ M	-1
200610	Adenosine A2A	438614	hum	2	10 $\mu$ M	-1
203100	Adrenergic $\alpha$ 1A	438615	rat	2	10 $\mu$ M	5
203200	Adrenergic $\alpha$ 1B	438615	rat	2	10 $\mu$ M	6
203630	Adrenergic $\alpha$ 2A	438616	hum	2	10 $\mu$ M	-2
204010	Adrenergic $\beta$ 1	438652	hum	2	10 $\mu$ M	2
204110	Adrenergic $\beta$ 2	438571	hum	2	10 $\mu$ M	-6
204600	Aldosterone	438617	rat	2	10 $\mu$ M	-3
206000	Androgen (Testosterone)	438618	hum	2	10 $\mu$ M	6
210030	Angiotensin AT1	438653	hum	2	10 $\mu$ M	1
210120	Angiotensin AT2	438653	hum	2	10 $\mu$ M	-6
214600	Calcium Channel L-type, Dihydropyridine	438620	rat	2	10 $\mu$ M	-20
219500	Dopamine D1	438660	hum	2	10 $\mu$ M	13
219700	Dopamine D2s	439024	hum	2	10 $\mu$ M	-4
219800	Dopamine D3	438660	hum	2	10 $\mu$ M	0
226010	Estrogen ER $\alpha$	438622	hum	2	10 $\mu$ M	-3